2004 USNC/URSI National Radio Science Meeting

URSI 2004 Digest

June 20-25, 2004
Monterey, California

STUTZMAN

VING papers
6, 8, 103

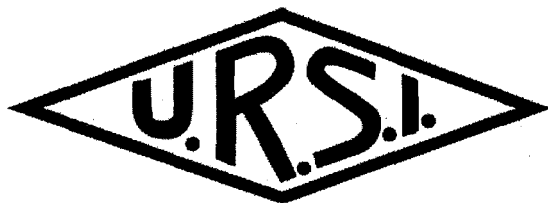58, 59 (mujex)
71, 15
153, 155

USNC/URSI
National Radio Science Meeting

June 20-25, 2004
Monterey, California

2004 Digest

IEEE Antennas and Propagation Society International Symposium 2004

◆IEEE

For information about purchasing this four-volume set, write to the following address:
IEEE Operations Center, 445 Hoes Lane, P.O. Box 1331, Piscataway, NJ 08855-1331

2004 IEEE AP-S International Symposium and USNC / URSI National Radio Science Meeting

June 20-26, 2004 Monterey, California
http://aps2004.llnl.gov/index.htm

Welcome!

On behalf of the 2004 Steering Committee, I would like to offer the warmest welcome to all of you to Monterey, California, and to the 2004 IEEE AP-S USNC/URSI Symposium.

The theme of this year's conference "The Next Wave" reflects the re-thinking of future technology directions after the fading of the internet boom and the roller coaster ride in the stock market. Insightful views and predictions on the next big developments will be presented and discussed. This year's steering committee includes representatives from prestigious national laboratories and Silicon Valley hi-tech companies. Our carefully selected team is at the forefront of IT and wireless technology, defense electronics, and homeland security. Their perspectives and insights represent tremendous value and influence to this year's conference. Your participation will add more value, improvements, and knowledge as well. We have prepared a full technical program with several special sessions and a comprehensive array of exhibitors.

Monterey, conveniently located close to the heart of Silicon Valley, is one of the most diverse and beautiful areas in Northern California. Get acquainted with Monterey Fisherman's Wharf, Cannery Row, Monterey Bay Aquarium, Monterey wine country, Carmel-by-the-Sea, Big Sur, Point Lobos, miles of beaches, Ocean Avenue, Carmel Mission, and a variety of art and photography galleries in the area. Monterey also features an array of fine restaurants, boutiques, inns and recreational opportunities. Monterey is a wonderful host to a wide variety of festivals and world-class events.

Our conference occupies the Monterey Meeting Connection of the Portola Plaza Hotel (formerly the Doubletree Hotel), the Monterey Marriott, and the Monterey Conference Center. As resort hotels, Portola Plaza and Monterey Marriott are conveniently located in the heart of the historic downtown on Monterey Bay, just steps from Fisherman's Wharf. You will be surrounded by the attractions of the spectacular Monterey Peninsula. An array of social events has been planned to make your experience during the Symposium more memorable. The steering committee and I look forward to seeing you and hope that you will have a fun and memorable time as well as a scientifically productive week in Monterey.

Hsueh-Yuan Pao
Chair, 2004 IEEE AP-S USNC/URSI Joint Symposia

IEEE 2004 Awards

2004 IEEE Electromagnetics Award

Jin Au Kong

For contributions to fundamental electromagnetic theory and its advanced applications, especially to remote sensing and geophysical probing.
This award is sponsored by the IEEE Antennas and Propagation, Electromagnetic Compatibility. Microwave Theory and Techniques, and Geoscience and Remote Sensing Societies.

Antennas and Propagation Society 2004 Awards

2004 Distinguished Achievement Award

Allan W. Love

For his many contributions in the field of antennas, and particularly for his creative development of the line source feed for the Arecibo spherical reflector antenna.

2004 Chen-To Tai Distinguished Educator Award

Raj Mittra

For outstanding contributions to electromagnetics education in the classroom, in graduate student supervision, and in research leadership.

2004 John Kraus Antenna Award

Victor H. Rumsey

For his creative and innovative development of frequency-independent antennas.

2004 S. A. Schelkunoff Transactions Prize Paper Award

David M. Pozar

For the paper titled "Waveform Optimizations for Ultrawideband Radio Systems," published in the IEEE Transactions on Antennas and Propagation , Volume 51, September 2003, pp. 2335-2345.

2004 H. A. Wheeler Applications Prize Paper Award

Steven Weigand, Greg H. Huff, Kankan H. Pan, and Jennifer T. Bernhard

For the paper titled "Analysis and Design of Broad-Band Single-Layer Rectangular U-Slot Microstrip Patch Antennas," published in the IEEE Transactions on Antennas and Propagation , Volume 51, March 2003, pp. 457-468.

2004 R.W. P. King Award

Thorsten W. Hertel

For the paper "On the Dispersive Properties of the Conical Spiral Antenna and Its Use for Pulsed Radiation", co-authored with Glenn S. Smith and published in the IEEE Transactions on Antennas and Propagation, Volume 51, July 2003, pp. 1426-1433.

2004 IEEE Fellows

JAN I. H. ASKNE
Chalmers University of Technology
Gothenburg, Sweden
For contributions to microwave remote sensing
applications and education.

DAU-CHYRH CHANG★
De Yeh University
Da-Tsuen, Taiwan, China
For technical leadership in antenna design and
measurement systems.

THOMAS ALLEN CWIK★
NASA Jet Propulsion Laboratory
Pasadena, CA, USA
For contributions to computational techniques in
large-scale electromagnetic modeling and
analysis

ALY E. FATHY
University of Tennessee
Knoxville, TN, USA
For contributions to advanced antenna concepts
and implementations.

VINCENT FRANCIS FUSCO★
The Queens University of Belfast
Belfast, Antrim, Northern Ireland
For contributions to the design of active and
self-tracking antenna technology.

STEPHEN D. GEDNEY★
University of Kentucky
Lexington, KY, USA
For contributions to computational
electromagnetics.

ROBERT T. HILL
Chula Vista, CA
For contributions to shipborne phased array
radar.

NATHAN IDA
University of Akron
Akron, OH, USA
For contributions to electromagnetic
nondestructive testing, computational
electromagnetics and engineering education.

YA-QIU JIN
Fudan University
Shanghai, China
For contributions to an electromagnetic
scattering model for remote sensing applications

YASUO KUGA
University of Washington
Seattle, WA, USA
For contributions to backscattering enhancement
and imaging in geophysical sensing

J. J. LEE★
Raytheon Electronics Systems
El Segundo, CA, USA
For contributions to wide band array antennas
for radars and communication systems

STEFANO MACI★
University of Siena
Siena, Italy
For contributions to the diffraction theory of
planar periodic printed phased array antennas.

GIULIANO MANARA★
University of Pisa
Pisa, Italy
For contributions to the uniform geometrical
theory of diffraction and its applications.

JURGEN NITSCH
Otto-von-Guericke University
Magdeburg, Saxony-Anhalt, Germany
For contributions to the analysis of complex
systems for electromagnetic pulse and high-
power microwave applications.

ALEXANDER NOSICH*
IRE NASU
Kharkov, Ukraine
For contributions to the applications of
computational electromagnetics to antennas and
open waveguides.

BJORN ERIK OTTERSTEN
KTH, Royal Institute of Technology
Stockholm, Sweden
For contributions to antenna signal processing
and wireless communications.

SURENDRA PAL
ISRO Satellite Centre
Bangalore, Karnataka, India
For contributions to space-borne communication
systems

DANIEL DEAN STANCIL
Carnegie Mellon University
Pittsburgh, PA, USA
For contributions to the theory and development
of microwave and optical devices using
magnetic garnet thin films and patterned
ferroelectric domains.

PAUL GREGORY STEFFES
Georgia Institute of Technology
Atlanta, GA, USA
For contributions to the understanding of
planetary atmospheres

HARRY BRUCE WALLACE
US Army Research Laboratory
Adelphia, MD, USA
For contributions to millimeter wave devices,
sensors, and technologies.

* evaluated by the IEEE AP-S Fellow Committee

Conference Steering Committee

General Chair
Hsueh-yuan Pao
Lawrence Livermore National
Laboratory
Phone: (925) 424-9744
pao2@llnl.gov

Vice Chair
Robert Sharpe
Lawrence Livermore
National Laboratory
Phone: (925) 422-0581
rsharpe@llnl.gov

Secretary
Michael Thorbum
Space System/Loral
Phone: (650) 852-5520
m.a.thorburn@ieee.org

Symposium Coordinator
Ann Tyler
Lawrence Livermore
National Laboratory
Phone: (925) 422-4380
tyler8@llnl.gov

Technical Program
Andrew J. Poggio
Lawrence Livermore
National Laboratory
Phone: (925) 422-8557
apoggio@llnl.gov

Technical Program
Vice Chair
Kendall F. Casey,
SRI International
Phone: (650) 859-4725
kendall.casey@sri.com

Registration
Daniel White
Lawrence Livermore
National Laboratory
Phone: (925) 422-9870
dwhite@llnl.gov

Treasurer
David Steich
Lawrence Livermore
National Laboratory
Phone: (925) 422-6978
Steich1@llnl.gov

URSI Liaison
Gerald Burke
Lawrence Livermore
National Laboratory
Phone: (925) 422-8414
burke2@llnl.gov

Publications
Nathan Champagne
Lawrence Livermore
National Laboratory
Phone: (925) 422-1612
nchampagne@llnl.gov

Binh Tran
Lawrence Livermore
National Laboratory
Phone: (925) 422-0452
tran24@llnl.gov

Short Courses/Workshops
Lawrence I. Williams
Ansoft Corporation
Phone: (714) 528-9358
williams@ansoft.com

Michael Brenneman
Ansoft Corporation
Phone: (408) 261-9095 x201
meb@ansoft.com

Student Paper Contest
Kathleen L. Melde
University of Arizona
Phone: (520) 626-2538
melde@ece.arizona.edu

Special Sessions
J. Brian Grant
ANT-S
Phone: (925) 337-0104
grant.04@ant-s.com

Local Arrangements
Don Rucker
Northrop Grumman
Mission Systems
Phone: (916) 570-4063
don.rucker@ngc.com

Anthony Jennetti
Northrop Grumman
Mission Systems
Phone: (408) 531-2026
anthony.jennetti@ngc.com

Richard Adler
Naval Post Graduate School
Phone: (831) 646-1111
rwa@attglobal.net

Spouse Program
Sharron Rucker
sharr7@attbi.com

Exhibitors
Jian-X. Zheng
Zeland Software, Inc.
Phone: (510) 623-7162
jian@zeland.com

Publicity
Ronald Kane
Lawrence Livermore
National Laboratory
Phone: (925) 422-7393
kane@ieee.org

Sponsors

Sponsors of the 2004 IEEE International Antennas and Propagation Society Symposium and USNC / URSI National Radio Science Meeting

On behalf of the IEEE Antennas and Propagation Society and the United States National Committee (USNC) of the International Union of Radio Science (URSI), the steering committee gratefully acknowledges the support of the following sponsors for this conference:

<u>Platinum</u> Level

University of California

Lawrence Livermore National Laboratory

<u>Gold</u> Level

NORTHROP GRUMMAN
Mission Systems
Electronic Systems
Space Technology

ITT Industries

ANSOFT

APS/URSI 2004 CONTENTS

MONDAY

Array Design and Analysis

Co-Chairs: Vakur Erturk, *Bilkent University, Turkey*
               William Davis, *Virginia Polytechnic Institute and State University, USA*

EBG Surfaces I

Organizers: Per-Simon Kildal, *Chalmers University of Technology, Sweden*
             Nader Engheta, *University of Pennsylvania, USA*

Co-Chairs: Per-Simon Kildal, *Chalmers University of Technology, Sweden*
             Nader Engheta, *University of Pennsylvania, USA*

AP/URSI B   Joint Special Session   Session: 11

Smart Electromagnetic Materials, Devices and Applications

Organizers: Thomas X. Wu, *University of Central Florida, USA*
              Vasundara Varadan, *Pennsylvania State University, USA*

Co-Chairs: Thomas X. Wu, *University of Central Florida, USA*
              Vasundara Varadan, *Pennsylvania State University, USA*

Inroads of Multigrid and Domain Decomposition Methods

Organizers: Romanus Dyczij-Edlinger, *Universitat des Saarlandes, Germany*
Jin-Fa Lee, *The Ohio State University, USA*

Co-Chairs: Romanus Dyczij-Edlinger, *Universitat des Saarlandes, Germany*
Jin-Fa Lee, *The Ohio State University, USA*

EMI/EMC Modeling/Validation Part I

Organizers: Danilo Erricolo, *University of Illinois at Chicago, USA*
                Michael Lockard, *Clemson University, USA*

Co-Chairs: Danilo Erricolo, *University of Illinois at Chicago, USA*
                Michael Lockard, *Clemson University, USA*

Applications of Novel Analysis Methods

Co-Chairs: William Johnson, *Sandia National Laboratories, USA*
              John S. Asvestas, *NAVAIR, USA*

Analysis and Diagnosis of Propagation and Coupling

Co-Chairs: Gianluca Lazzi, *North Carolina State University, USA*
              Robert Paknys, *Concordia University, Canada*

Wave Guiding Structures

Co-Chairs: Yehuda Leviatan, *Technion, Israel*
              Jiming Song, *Iowa State University, USA*

URSI B   Session: 24

Antennas for Wireless Communications

Co-Chairs: Zhijun Zhang, *Amphenol T&M Antennas, USA*
              Cornelius F. Du Toit, *Paratek Microwave, Inc., USA*

AP/URSI B   Session: 30

Wide Bandwidth and Multiband Antenna

Co-Chairs: Vaughn Cable, *Jet Propulsion Laboratory, USA*
              Peter S. Hall, *University of Birmingham, Unitred Kingdom*

AP/URSI B   Joint Special Session   Session: 31

EBG Surfaces II

Organizers: Nader Engheta, *University of Pennsylvania, USA*
              Per-Simon Kildal, *Chalmers University of Technology, Sweden*
Co-Chairs: Nader Engheta, *University of Pennsylvania, USA*
              Per-Simon Kildal, *Chalmers University of Technology, Sweden*

AP/URSI B&E   Joint Special Session   Session: 34

EMI/EMC Modeling/Validation Part II

Organizers: Danilo Erricolo, *University of Illinois at Chicago, USA*
              Robert Gardner, *Consultant, USA*

Co-Chairs: Danilo Erricolo, *University of Illinois at Chicago, USA*
              Robert Gardner, *Consultant, USA*

URSI F   Session: 37

Propagation Modeling

Co-Chairs: Stephen Burk, *Naval Research Laboratory-Monterey, USA*
              Paul Frederickson, *Naval Postgraduate School, USA*

URSI B   Session: 43

Reconfigurable Apertures and Novel Beamsteering Techniques

Co-Chairs: Jennifer T. Bernhard, *University of Illinois at Urbana-Champaign, USA*
                James Schaffner, *HRL Laboratories LLC, USA*

AP/URSI A — Session: 45

Planar Structures - EMI & Filters

Co-Chairs: Nemai C. Karmakar, *Nanyang Technological University, Singapore*
              Thomas X. Wu, *University of Central Florida, USA*

TUESDAY

Fundamental Properties of Source-Excited Field at the Interface of a 2D EBG Material..APS
F. Capolino, *University of Siena, Italy*; D. R. Jackson, D. R. Wilton, *University of Houston, USA*

A Microstrip Phase Shifter Using Ferroelectric Electromagnetic Bandgap Ground Plane...APS
D. Kim, M. Kim, S.-W. Kim, *Korea University, Korea*

AP/URSI A   Session: 50

Antenna, Chamber, and Array Characterization

Co-Chairs: William Davis, *Virginia Polytechnic Institute and State University, USA*
                Amir Zaghloul, *Virginia Polytechnic Institute and State University, USA*

URSI D   Session: 51

Optical and RF Devices

Co-Chairs: Wilson Pearson, *Clemson University, USA*
                Mostafa Abdulla, *Intel Corporation, USA*

AP/URSI K   Session: 52

Implanted Antennas

Chair: Rainee N. Simons, *NASA Glenn Research Center, USA*

AP/URSI B   Session: 53

High Frequency Techniques

Co-Chairs: Robert J. Burkholder, *The Ohio State University, USA*
              Paul Hussar, *Alion Science and Technology, USA*

AP/URSI B   Joint Special Session   Session: 55

Metamaterials for Electromagnetic Applications

Organizers: George V. Eleftheriades, *University of Toronto, Canada*
             John L. Volakis, *The Ohio State University, USA*

Co-Chairs: George V. Eleftheriades, *University of Toronto, Canada*
            John L. Volakis, *The Ohio State University, USA*

AP/URSI B&D   Joint Special Session   Session: 56

Integration of Antennas in RF/Wireless Packages

Organizers: Manos M. Tentzeris, *Georgia Institute of Technology, USA*
             Jennifer Bernhard, *University of Illinois at Urbana-Champaign, USA*

Co-Chairs: Manos M. Tentzeris, *Georgia Institute of Technology, USA*
             Jennifer Bernhard, *University of Illinois at Urbana-Champaign, USA*

URSI B   Session: 58

Electromagnetic Theory II

Co-Chairs: S.R. Seshadri, *Unaffiliated; Madison, WI, USA*
             Ehud Heyman, *Tel Aviv University, Israel*

URSI F   Session: 59

Propagation Measurements

Co-Chairs: Amalia Barrios, *SPAWAR SYSCEN, USA*
              Kamal Sarabandi, *University of Michigan, USA*

URSI B   Session: 60

Reflectors, Lenses, and Frequency Selective Surfaces

Co-Chairs: Sembiam Rengarajan, *California State University Northridge, USA*
                  Mario Orefice, *Politecnico di Torino, Italy*

AP/URSI B&D   Session: 62

Nonlinear Electromagnetics for Devices and Waves

Co-Chairs: Mauricio Silveira, *National Institute of Telecom - INATEL, Brazil*
             Vikram Jandhyala, *University of Washington, USA*

Enhancing & Hybridizing the FDTD

Organizers: Massimiliano Marrone, *Pennsylvania State University, USA*
               Raj Mittra, *Pennsylvania State University, USA*

Co-Chairs: Massimiliano Marrone, *Pennsylvania State University, USA*
               Raj Mittra, *Pennsylvania State University, USA*

Novel Radiating Elements and Antennas

Co-Chairs:　Michael Hamid, *University of South Alabama, USA*
　　　　　　M.F. Iskander, *University of Hawaii, USA*

Dosimetry and Medical Applications

Co-Chairs: Om P. Gandhi, *University of Utah, USA*
              Koichi Ito, *Chiba University, Japan*

URSI B   Session: 72

Numerical Method Enhancements

Co-Chairs: Amir Boag, *Tel Aviv University, Israel*
              Frank Olyslager, *Ghent University, Belgium*

AP/URSI B   Joint Special Session   Session: 74

Microscale and Nanoscale Electromagnetics

Organizers: Douglas Werner, *Pennsylvania State University, USA*
               Alkim Akyurtlu, *University of Massachusetts Lowell, USA*

Co-Chairs: Douglas Werner, *Pennsylvania State University, USA*
               Alkim Akyurtlu, *University of Massachusetts Lowell, USA*

AP/URSI B   Session: 77

Electromagnetic Theory

Co-Chairs: Robert Nevels, *Texas A&M University, USA*
              Edmund K. Miller, *Los Alamos National Laboratory (retired), USA*

AP/URSI B   Session: 78

EBG Antenna Applications

Co-Chairs: Daniel Sievenpiper, *HRL Laboratories LLC, USA*
            Constantin Simovski, *Helsinki University of Technology, Finland*

AP/URSI B   Session: 79

Radar Imagery

Co-Chairs: David Chambers, *Lawrence Livermore National Laboratory, USA*
            Michael Fiddy, *University of North Carolina, USA*

WEDNESDAY

Microwave Imaging and Reconstruction

Co-Chairs: Susan C. Hagness, *University of Wisconsin, USA*
                         Gianluca Lazzi, *North Carolina State University, USA*

Metamaterials I

Organizers: Richard Ziolkowski, *University of Arizona, USA*
              Nader Engheta, *University of Pennsylvania, USA*

Co-Chairs: Richard Ziolkowski, *University of Arizona, USA*
              Nader Engheta, *University of Pennsylvania, USA*

Hybrid and Reduced Order Numerical Methods

Co-Chairs: Jin-Fa Lee, *The Ohio State University, USA*
              Ronald Marhefka, *The Ohio State University, USA*

Finite Difference Time Domain Techniques

Co-Chairs: Lawrence Carin, *Duke University, USA*
             Jian-Ming Jin, *University of Illinois at Urbana-Champaign, USA*

MEMS and Periodic Structures

Co-Chairs: John Volakis, *The Ohio State University, USA*
              Abbas Omar, *University of Magdeburg, Germany*

Design and Optimization of Radiating Systems

Co-Chairs: Tadashi Takano, *Institute of Space & Astronautical Science, JAXA, Japan*
             Hao Ling, *University of Texas, USA*

Through Wall Microwave Sensing and Imaging

Organizers: Ahmad Hoorfar, *Villanova Unoversity, USA*
             Nader Engheta, *University of Pennsylvania, USA*

Co-Chairs: Ahmad Hoorfar, *Villanova Unoversity, USA*
             Nader Engheta, *University of Pennsylvania, USA*

AP/URSI B   Joint Special Session   Session: 109

Metamaterials II

Organizers: Nader Engheta, *University of Pennsylvania, USA*
                Richard Ziolkowski, *University of Arizona, USA*

Co-Chairs: Nader Engheta, *University of Pennsylvania, USA*
                Richard Ziolkowski, *University of Arizona, USA*

AP/URSI B   Session: 112

Array Beamforming and Tracking

Chair: Robert B. Dybdal, *The Aerospace Corp., USA*

URSI B   Session: 113

Analysis and Evaluation of Numerical Techniques

Co-Chairs: Giuseppe Vecchi, *Politecnico di Torino, Italy*
              Roberto Graglia, *Politecnico di Torino, Italy*

URSI B   Session: 114

Transients: Studies and Systems

Co-Chairs: E.K. Miller, *Los Alamos National Laboratory (retired), USA*
             Le-Wei Li, *National University of Singapore, Singapore*

THURSDAY

Electromagnetic Band-Gap Structures for Multiband Mitigation of Resonant Modes in Parallel-Plate Waveguides .... APS

T. Kamgaing[1,2], O. M. Ramahi[2]
[1]Motorola Inc., USA; [2]University of Maryland, USA

A Novel Hybrid Defected Ground Structure as Low Pass Filter .... APS

M. N. Mollah, N. C. Karmakar, Nanyang Technological University, Singapore

Advanced Methods to Improve Compactness in EBG Design and Utilization ...... APS

L. Yang, Z. Feng, Tsinghua University, China

AP/URSI B   Joint Special Session   Session: 127

Propagation Modeling for New and Challenging Wireless Communications Environments

Organizers: Zhengqing Yun, University of Hawaii, USA
               Magdy Iskander, University of Hawaii, USA

Co-Chairs: Zhengqing Yun, University of Hawaii, USA
               Magdy Iskander, University of Hawaii, USA

Progress in Modeling Challenging Propagation Environments .... APS

Z. Yun, M. F. Iskander, University of Hawaii, USA

Indoor Wireless Channel Modeling from 2.4 to 24GHz Using a Combined E/H-Plane 2D Ray Tracing Method .... APS

D. Lu, D. Rutledge, California Institute of Technology, USA

Efficient Ray-Tracing Techniques for Outdoors and Indoors Propagation Analysis 291

F. Catedra, O. Gutierrez, I. Gonzalez, C. Delgado, F. Saez de Adana, Universidad de Alcala, Spain

Wideband Mobile Propagation Measurements at 3.7 GHz in an Urban Environment .... APS

J. W. Porter, I. Lisica, G. Buchwald, Motorola, USA

Path Loss Correlation Between PCS and MMDS/ISM Bands in Suburban Morphology - An Empirical Model .... APS

O. W. Ata, H. Garg, Sprint PCS, USA

Experimental Verification of a 3-D Propagation Model Based on Fresnel-Kirchhoff Integral .... APS

Y. Xu, Q. Tan, D. Erricolo, P. L. E. Uslenghi, University of Illinois at Chicago, USA

Indoor Directional Channel Modelling for Future Wireless Communications ..... APS

Z. Tang, A. S. Mohan, University of Technology, Sydney, Australia

Prediction Model for the Characteristics of Non-Specular Wave Scattered from Building Surface .... APS

H. Budiarto, K. Haneda, J.-I. Takada, Tokyo Institute of Technology, Japan

AP/URSI F   Session: 132

Remote Sensing of Earth's Surface & Atmosphere

Co-Chairs: Kultegin Aydin, *Pennsylvania State University, USA*
              Kamal Sarabandi, *University of Michigan, USA*

AP/URSI E&B   Session: 133

Commission E: EMI Topics

Co-Chairs: Radian Belu, *Wayne State University, USA*
              Ross Speciale, *Research and Development, Inc., USA*

URSI B   Session: 135

Electromagnetic Scattering Analysis and Effects

Co-Chairs: Danai Torrungrueng, *Asian University of Science and Technology, Thailand*
                Agostino Monorchio, *University of Pisa, Italy*

URSI B   Session: 136

Inverse Scattering

Co-Chairs: Gary Brown, *Virginia Polytechnic Institute and State University, USA*
              Rene Marklein, *University of Kassel, Germany*

AP/URSI B   Session: 145

Finite Elements in the Frequency and Time Domains

Co-Chairs: Andreas Cangellaris, *University of Illinois at Urbana-Champaign, USA*
               Daniel A. White, *Lawrence Livermore National Laboratory, USA*

URSI B   Session: 153

Time-Domain Numerical Methods

Co-Chairs: Eric Michielssen, *University of Illinois at Urbana-Champaign, USA*
Nathan Champagne, *Louisiana Technical University, USA*

AP/URSI B   Session: 154

Random Media, Rough Surfaces and Chaos

Co-Chairs: Shira Broschat, *Washington State University, USA*
              Akira Ishmaru, *University of Washington, USA*

URSI A   Session: 155

Biological Effects & Material Characterization

Co-Chairs: William Davis, *Virginia Polytechnic Institute and State University, USA*
                Susan Hagness, *University of Wisconsin, USA*

Planar Structures & Remote Measurements

Co-Chairs: Sedki Riad, *Virginia Polytechnic Institute and State University, USA*
              Aly Fathy, *University of Tennessee - Knoxville, USA*

Complex Media and Metamaterials

Co-Chairs: Sergei A. Tretyakov, *Helsinki University of Technology, Finland*
              John L. Volakis, *The Ohio State University, USA*

AP/URSI B   Session: 162

Scattering from Particles, Slabs and Apertures

Co-Chairs: Glenn S. Smith, Georgia Institute of Technology, USA
               Robert H. MacPhie, University of Waterloo, USA

Dielectric Spectroscopy of Breast Tissue at Microwave Frequencies: A Review of Recent Progress

S. C. Hagness*, C. Beasley, M. Lazebnik, M. Converse, J. Booske
Department of Electrical and Computer Engineering, University of Wisconsin-Madison
1415 Engineering Dr., Madison, WI 53706-1691 (email: hagness@engr.wisc.edu)

M. Okoniewski, D. Popovic, L. McCartney
Department of Electrical and Computer Engineering, University of Calgary
2500 University Dr., Calgary N.W., Alberta, T2N 1N4 (email: michal@enel.ucalgary.ca)

T. M. Breslin[1], J. Harter[2], S. Sewall[2], M. J. Lindstrom[3]
Departments of (1) Surgery, (2) Pathology, and (3) Biostatistics and Medical Informatics
University of Wisconsin-Madison, 600 Highland Ave., Madison, WI 53792

W. Temple[4], D.Mew[4], A. Magliocco[5], T. Ogilvie[5]
(4) Department of Surgery and Oncology, (5) Department of Pathology
University of Calgary, 1331 29th St NW, Calgary N.W., Alberta, T2N-4N2

The University of Wisconsin (UW) and University of Calgary (UC) are conducting a comprehensive NIH-funded prospective study of the dielectric properties of healthy and diseased breast tissue at microwave frequencies (up to 20 GHz). The goal of this study is to expand our knowledge about the nature and extent of the dielectric-properties contrast between malignant and normal breast tissue. The existence of this contrast has been hypothesized based on measurements reported in the literature at RF and lower microwave frequencies. The existing data in the literature has motivated ongoing development of non-ionizing electromagnetic breast cancer detection and treatment technologies, particularly in the RF/microwave frequency regime.

Towards this goal, we are characterizing freshly excised normal and diseased tissue specimens from excisional biopsy, mastectomy, lumpectomy, and reduction mammoplasty surgeries at the UW and UC, as well as normal breast tissue in vivo during open surgery at the UW. The dielectric properties of selected regions of each tissue specimen are measured using an open-ended coaxial probe technique with a special-purpose probe and Agilent vector network analyzer. Each ex vivo measurement is carefully correlated with the histopathology of the tissue region "sensed" by the probe.

In this talk, we will highlight recent accomplishments related to the precision stainless-steel/borosilicate-glass coaxial probe developed for use in these hospital measurements. We will present improved calibration techniques for de-embedding the desired reflection coefficient from the complex reflection phenomena created by the multi-section construction of the probe and extracting the unknown permittivity of the tissue from the de-embedded reflection coefficient. The acquisition of very accurate dielectric-properties data for reference liquids has improved the overall accuracy of the calibration techniques. We will also summarize what can be concluded from our growing database of breast tissue dielectric properties. Our preliminary measurements have revealed that the heterogeneity of breast tissue is significant and the dielectric properties are strongly dependent on the tissue composition within the probe's sensing volume. Our protocol for ensuring careful correlation between dielectric characterization and histopathology has proven essential for ensuring the accurate interpretation of the dielectric measurements.

Probes for the Measurement of the Dielectric and Magnetic Properties of Building Materials

James Baker-Jarvis[*] and Richard G. Geyer
National Institute of Standards and Technology, Boulder, Colorado 80305, USA.

The purpose of this paper is to evaluate various probes that can be used to characterize the dielectric and magnetic properties of commonly used building materials. In this paper we measure the properties of solids and liquids with a number of methods, which when combined, can yield broadband, high-accuracy measurement results. These methods include the coaxial probe, dielectric resonators, the shielded open-circuited holder, and coaxial line. A detailed uncertainty analysis has been performed on the various methods. The shielded open-circuited holder has a frequency window of approximately 1 MHz to 10 GHz and can be used to measure dielectric and magnetic properties of liquids and powders. The coaxial probe can be used from 300 MHz to 26 GHz to measure liquids and powders, however air gaps at the sample-probe interface can present a real problem. Dielectric resonator methods have been designed to operate at frequencies greater than 700 MHz for both liquids and solids. We use the high-accuracy measurement capability of dielectric resonators on liquids at single frequencies to test the accuracy of the coaxial line, shielded open circuit, and coaxial probe methods and then use these fixtures to obtain broadband measurements.

Investigating Measurements of the Dielectric Properties of Granular Materials with Microstrip Antennas

Samir Trabelsi[1,2] and Stuart O. Nelson[2]

[1]Department of Biological and Agricultural Engineering, Driftmier Engineering Center, The University of Georgia, Athens, GA, U.S.A.

[2]U. S. Department of Agriculture, Agricultural Research Service, Richard B. Russell Agricultural Research Center, P. O. Box 5677, Athens, GA 30604-5677, U.S.A

Abstract: Indirect dielectric-based methods for bulk density and moisture content determination in granular materials have the advantage of being nondestructive and instantaneous. Success of these methods relies in the first place on the accuracy with which the dielectric properties are measured and the reliability of the relationships established between the dielectric properties and the desired physical properties. Furthermore, to move from the research stage to a commercial, stage the cost of the measuring system is another factor that needs to be addressed. Antennas often constitute a sensitive and important part of the system. Microstrip antennas have the advantages of being small, lightweight and inexpensive. They can be easily integrated into hand-held sensors or on-line sensing systems. In this study, a pair of microstrip antennas operating at 5.8 GHz was used to measure the dielectric properties of cereal grains and oilseeds in the near field. The microstrip antennas were placed directly against a Styrofoam box containing the sample to be tested. The antennas were connected to a Hewlett-Packard 8510C vector network analyzer (VNA) with high quality coaxial cables. The dielectric properties were calculated from free-space measurements of the scattering transmission coefficient S_{21}. For better measurement accuracy, the sample thickness was selected to minimize the effect of multiple reflections and keep the measured attenuation within the VNA dynamic range. Also, the sample was placed in a tunnel shaped enclosure to minimize interference from the surroundings and time-domain gating was applied to the sample response to filter out undesirable effects (S. Trabelsi and S. O. Nelson, Meas. Sci. Technol., 14, 589-600, 2003). The dielectric properties of samples of cereal grains and oilseeds of different bulk densities and moisture contents obtained in the near field with the microstrip antennas compare very well with those obtained at 6.0 GHz under the same experimental conditions with a pair of linearly polarized ultrabroadband horn/lens antennas. With these findings, efforts need to concentrate on the wave excitation and signal detection parts of the system for a viable commercial sensor.

Scan Blindness of Conformal Phased Arrays of Printed Dipoles

V. B. Ertürk[1], R. G. Rojas[2] and B. Güner[1]
[1] Dept. of Electrical and Electronics Engineering,
Bilkent University, 06800, Bilkent, Ankara, Turkey
E-mail: vakur@ee.bilkent.edu.tr, Tel: ++90 312 290 3154
[2] Dept. of Electrical Engineering, ElectroScience Laboratory
The Ohio State University, Columbus, Ohio 43212-1191, USA
E-mail: rojas-teran.1@osu.edu, Tel: 614 292 2530

Arrays of printed antenna elements have been successfully implemented in the past for beam scanning and other applications. Therefore, several design tools and numerical techniques have been developed and implemented in CAD packages for the analysis and design of planar printed finite and infinite arrays. However, the analysis of electrically large planar finite arrays is difficult and it is still being investigated by many researchers. Lately, many practical applications ranging from satellite and wireless communications to military systems require conformal phased arrays because conformality is required for aerodynamic reasons, or to reduce the array's radar cross section. Such arrays (planar or curved) may contain hundreds to thousands of elements, and may operate at microwave and millimeter wave frequencies on dielectric substrates (or free space) where electromagnetic coupling can lead to scan blindness; when no effective power is transmitted or received by the array. The blindness mechanism has been variously explained as a forced surface wave or as a leaky wave resonant response in the phased array. This phenomenon has been previously investigated for planar structures (finite and infinite phased arrays of printed dipoles). However, to the best of our knowledge, a similar investigation has not been presented for phased arrays of printed dipoles on curved surfaces, where the curvature affects various performance metrics of the array.

In this paper, scan blindness phenomenon is investigated for several arrays consisting of finite number of axially or circumferentially oriented printed dipoles on electrically large, dielectric coated, circular cylinders. Furthermore, a one-to-one comparison between an array of printed dipoles on the aforementioned cylinder and an array of printed dipoles on grounded planar dielectric slabs is made in terms of the scan blindness phenomenon. To achieve this goal, a hybrid Method of Moments (MoM)/Green's function technique in the spatial domain is used. It is basically an element by element approach in which the mutual coupling between dipoles through space wave as well as the surface wave is incorporated. This method is very efficient due to the computation of the Green's function, where three types of spatial domain Green's function representations are used interchangeably, based on their computational efficiency and regions where they remain accurate. Consequently, it is suitable for the analysis of relatively large arrays of printed dipoles on electrically large, dielectric coated circular cylinders.

Initial results have revealed that the curvature affects the mutual coupling between array elements and can significantly change the array current distribution of arrays mounted on coated cylinders when compared to their planar counterparts. Furthermore, axial and circumferential printed dipoles on the coated cylinder show different behavior in terms of scan blindness. Several numerical examples for relatively large arrays as well as the effect of various cylinder parameters (radius of cylinder, substrate thickness, etc.) on the scan blindness phenomenon will be presented.

Scanning properties in fracton-mode microstrip arrays using elements inspired on the Sierpinski fractal

Jaume Anguera*[(1)], Sergio Prieto[(2)], Carles Puente[(2)], Carmen Borja[(2)], and Jordi Soler[(2)]

(1) Technology Department, 358-2, Yatap-Dong, Bundang-Gu, Sungnam-Si, Kyunggi-Do, 463-828: Korea. jaume.anguera@fractus.com
(2) Technology Department, Alcalde Barnils 64-68, Edificio Testa, Barcelona, Spain

It has been shown in [*J.Anguera, G.Montesinos, C.Puente, C.Borja, and J.Soler, "An Under-Sampled High Directivity Microstrip Patch Array with a Reduced Number of Radiating elements Inspired on the Sierpinski Fractal", Microwave and Optical Technology Letters, vol.37, n°2, pp.100-103, April 2000*] that when using fractal-inspired microstrip elements in an array configuration, the number of radiating elements can be reduced with regard to classical arrays where the radiating elements operates at the fundamental mode. The idea behind is to use a multilevel antenna [*"Multilevel Antennas", patent app. WO0122528*] based on a fractal geometry which operates at a higher-order mode while exhibiting a broadside radiation pattern with high-directivity [*J.Anguera, C.Puente, C.Borja, R..Montero, and J.Soler, "Small and High Directivity Bowtie Patch Antenna based on the Sierpinski Fractal", Microwave and Optical Technology Letters, vol.31, n°3, pp.239-241, Nov 2001*].

The authors demonstrated that an under-sampled array with multilevel radiating elements operating at fracton modes achieves the same directivity but using almost 3 less number of elements within the same electrical area than a classical microstrip array. The reduction of radiating elements results in a simpler feeding network, that allows an easier integration of other microwave components as for example, phase-shifters, matching networks, and amplifiers [*"Undersampled Microstrip Array Using Multilevel and Space-Filling Shaped Elements", patent app. N° PCT/EP02/07835*].

Previous authors' research was developed for a fixed-beam arrays. This work continues the previous one analyzing the scanning properties of the under-sampled array composed by multilevel antennas operating at fracton radiating modes. The application presented here may be useful for satellite applications where space and weight is a big constraint.
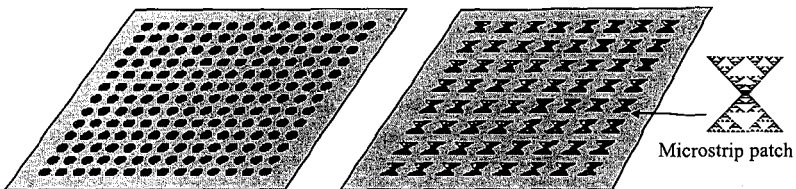
Fig.1 Bidimensional microstrip arrays. a) basic radiating element is a circular patch operating at the fundamental mode; b) basic radiating element is a multilevel antenna based on the Sierpinski structure. Such a element is operating at a higher order mode, called fracton mode. Both arrays achieve the same directivity within the same electric area. However, the array using elements inspired on the Sierpinski fractal uses a less number of elements

Showed arrays with grating lobe cancellation, but admitted this is only at selected frequencies over the band

5

Impedance Bandwidth Characterization of Highly Coupled Antenna Arrays Using Scattering Parameter Network Models

Koichiro Takamizawa*, William A. Davis, and Warren L. Stutzman
Virginia Tech Antenna Group
The Bradley Department of Electrical and Computer Engineering
Virginia Polytechnic Institute and State University

In this paper, we present a new technique for determining the impedance bandwidth of highly coupled broadband antenna arrays. There are many ways to define frequency bandwidth of an antenna. A popular definition of antenna bandwidth is based on the input impedance characteristics of the antenna. A typical definition of impedance bandwidth is a range of frequencies where voltage standing wave ratio (VSWR) is less than a reference value. Maximum VSWR values of 2 or 3 for the reference impedance of 50 Ohms are often used to define a impedance bandwidth.

Unlike single antenna, the input impedance of an array is a function of the element excitation. In addition, input impedances of the elements in an excited array may be different from each other. Thus, the elements in the array may have different impedance bandwidths. The differences are most noticeable when mutual coupling among the array elements are significant such as in the case of highly coupled broadband arrays. It would be useful to define a single array bandwidth value to characterize the array system performance.

We propose a new method to compute overall array system impedance bandwidth based on the array mismatch factor. The array mismatch factor is determined using a scattering parameter based network model of array antennas and associated feed network. The model is completely general, and it can be applied to array and feed network in any configuration. The array mismatch factor is a real number between 0 and 1. Similar to the mismatch factor of a single antenna, the array mismatch factor represents a ratio between the realized gain and the gain of the array radiation patterns.

We will demonstrate the derivation and the computation of impedance bandwidths for array antennas. The technique will be applied specifically for a conventional low-coupling dipole array and a highly coupled broadband Foursquare array to compute array bandwidths. In addition, the individual element impedance bandwidth will also be computed, and the results will be compared to the array bandwidth results.

A METHOD OF ARRAY PATTERN SYNTHESIS BY PHASE CONTROL

Roberto Vescovo

Dipartimento di Elettrotecnica Elettronica ed Informatica - Università di Trieste
Via A. Valerio 10 - 34127 Trieste - Italy
E-mail: vescovo@univ.trieste.it

A well-known synthesis problem for antenna arrays is that of modifying the excitation phases so as to produce a radiation pattern satisfying prescribed requirements such as, for example, null steering or side lobe reduction. Here we describe a technique to solve problems of this kind, which is based on the method of projections (O.M. Bucci, G. D'Elia, G. Mazzarella, and G. Panariello, " Antenna Pattern Synthesis: A New General Approach," *Proceedings of the IEEE*, Vol. 82, No. 3, pp. 358-371, March 1994).

Consider a linear array of N elements and an array pattern $F(\mathbf{I}_0;\theta)$, where $\mathbf{I}_0 = [I_{01},..,I_{0N}]$ is the vector of the element excitations and θ the angle from broadside. Furthermore let us introduce a proper mask K_0, defined as the set of all complex functions $f(\theta)$ such that $k_{01}(\theta) \le |f(\theta)| \le k_{02}(\theta)$, $-\pi/2 \le \theta \le \pi/2$, where $k_{01}(\theta)$ and $k_{02}(\theta)$ are assigned non-negative functions. We select $k_{01}(\theta)$ and $k_{02}(\theta)$ in such a way that $F(\mathbf{I}_0;\theta) \in K_0$. Consider now a new mask $K= \{f(\theta): k_1(\theta) \le |f(\theta)| \le k_2(\theta)\}$ obtained by modifying K_0. For example it might be $k_2(\theta) < k_{02}(\theta)$ in an interval $[\theta_1,\theta_2]$ of the side lobe region and $k_2(\theta) = k_{02}(\theta)$ elsewhere, while $k_1(\theta) = k_{01}(\theta)$. Thus K has a reduced sidelobe level in $[\theta_1,\theta_2]$.

We want to determine a new pattern $F(\mathbf{I};\theta)$, $\mathbf{I} = [I_1,..,I_N]$, such that: (a) $F(\mathbf{I};\theta) \in K$; (b) $|I_n| = |I_{0n}|$, $n=1,..,N$. That is, we want to modify only the excitation phases of the original pattern $F(\mathbf{I}_0;\theta)$ (condition (b)) in such a way that the modified pattern $F(\mathbf{I};\theta)$ belongs to the new mask K (condition (a)). (In the above example, solving this problem leads to reduce the side lobe level of $F(\mathbf{I}_0;\theta)$ in $[\theta_1,\theta_2]$ by phase-only control). Denote by A the space of all patterns $F(\mathbf{I};\theta)$ and by B the set of the patterns satisfying condition (b). The problem reduces then to find a pattern of $K \cap B$. If $K \cap B$ is empty we search for a pattern of B closest to K. To solve this problem we introduce the projectors T_K and T_B which associate with any function $F(\theta)$ a point of K and B, respectively, minimizing the mean-square distance from $F(\theta)$. We first project $F_0 = F(\mathbf{I}_0;\theta)$ onto B obtaining $F_1 = T_B(F_0)$. Subsequently we construct the sequence $\{F_n\}$ by the iteration $F_{n+1} = T_B T_K (F_n)$, $n \ge 1$. Each point F_n of the sequence is a pattern of B, thus it satisfies condition (b). Furthermore, denoting by d_n the distance between F_n and K, it can be shown that $d_n \ge d_{n+1}$, that is, the patterns F_n are closer and closer to K. A pattern F_n sufficiently close to K is a solution to our synthesis problem.

This method gave good results and can be extended so as to scan a shaped-beam over an angular sector by phase-only control.

Beamforming with a Dual-Polarized Array for Reception of Satellite Signals

C.B. Dietrich Jr.*[†], K. Takamizawa[†], W.A. Davis[†], D. Colatosti[‡]
(cdietric@vt.edu, kotak@vt.edu, wadavis@vt.edu,
colatostid@lunainnovations.com)
[†]Virginia Tech Antenna Group (VTAG), Bradley Dept. of Electrical and
Computer Engineering, 340 Whittemore Hall, Blacksburg, VA 24061-0111
[‡]Luna Innovations, P.O. Box 11704, 2851 Commerce Street,
Blacksburg, VA 24062-1704

Unintentional interference or deliberate jamming can hinder reception of satellite signals by terrestrial and airborne receivers. An investigation of beamforming with dual polarized arrays to mitigate interference/jamming for mobile or airborne satellite reception is presented. Beamforming approaches, antenna elements, and array architectures are considered, and simulations of several interference/jamming scenarios are performed for a planar array.

First, a review of several beamforming approaches shows that baseband digital beamforming is desirable because of its flexibility and precision. However, baseband techniques alone cannot overcome strong jammers because strong signals can saturate the receiver front end. Second, a trade study of available planar and other antenna elements for use in a receiving array shows the compact, dual-polarized foursquare element to be a suitable antenna for the application.

Beamforming simulations were performed based on three-dimensional active-element pattern measurements of a 3x3 planar array of dual-polarized foursquare elements. This simulation study indicates that 18 crossed element pairs can easily reject six jammers when the signal of interest is at least 10 degrees from the nearest jammer. Even the worst case of dual- or randmomly-polarized jammers can be handled successfully. Jamming rejection using sub-elements from a smaller 2x2 foursquare array is also simulated. It is within 3 dB of the non-jamming, single receiving antenna case for angular separations of 20 degrees or greater between the desired signal and the nearest jammer.

In addition, a conformal array design and beamforming architecture are proposed to improve low-elevation coverage. Preliminary simulations of beamforming using the conformal array are also presented. Progress in fabrication and measurement of the array is also reported.

Microstrip Implementation of Decoupling Networks for Multi-Port Arrays with Reduced Element Spacing

Ping Tyng Chua and Jacob Carl Coetzee*
Dept. of Electrical and Computer Engineering, National University of Singapore
4 Engineering Drive 3, Singapore 117576.

H.J. Chaloupka
Dept. of Electrical Engineering and Information Technology, University of Wuppertal
Rainer-Gruenter Str. 21, D-42119 Wuppertal, Germany.

An array of three monopole elements with reduced element spacing on the order of $\lambda/20$ to $\lambda/6$ is considered for application in digital beam forming and direction finding. The small element spacing introduces strong mutual coupling between the array elements. The mutual coupling affects the signal-to-noise-ratio performance of the array. Hence, there is a need for a decoupling network to compensate the mutual coupling effects so that simultaneous matching can be achieved at all the ports.

Simple decoupling and matching networks are proposed. The decoupling network consists of a series and a parallel section. The matching network is a L-network that has a series and a shunt element. In both the decoupling and matching networks, each component is either an inductor or a capacitor. The value of each element is obtained by applying a synthesis procedure.

In the design of the decoupling network, eigenmode analysis is applied to the array. In general, for a N-port network, there exists N different eigenmodes. The properties of the three-element array can be obtained from its admittance matrix **Y**. For a generalized admittance matrix, the decoupling network can be obtained by solving for the condition that all mode admittances are matched. Another way of computing the values of the components in the decoupling network is through network analysis. In this analysis, the decoupling network is obtained by reducing the mutual admittance to zero. In both the eigenmode and network analyses, the individual element values are computed analytically. Numerical values of the Y-matrix of the array are then substituted to evaluate the values of the inductances or capacitances in the decoupling and matching networks.

For a practical realization of the decoupling and matching networks, the ideal lumped capacitors or inductors are converted to microstrip components. Kuroda's identities are applied to realize the microstrip network with short-circuited microstrip stubs.

Modelling of the array and decoupling and matching networks is done using commercial software. Simulation results and measured results indicate that the structure is indeed decoupled and matched. The decoupled array has a bandwidth of 1% and a superdirective radiation pattern. This narrowband and superdirective antenna is suitable for filtering out unwanted signals and applicable for frequency selectivity in digital beam forming and direction finding.

9

Understanding STOP and GO characteristics of EBG surfaces in terms of current fences and current lanes

Per-Simon Kildal, Fellow IEEE
simon@kildal.se, www.kildal.se, Department of Electromagnetics
Chalmers University of Technology, 41296 Gothenburg, SWEDEN

Sometimes electromagnetic bandgap (EBG) surfaces are used to reduce coupling or remove surface waves, which we may refer to as a STOP characteristic. In many such cases the performance will be better if the EBG instead was made anisotropic like a soft surface, because the soft surface has STOP characteristics for all polarizations. Other times opposite walls of a rectangular waveguide are made of EBG surfaces to make them support quasi-TEM waves, which we refer to as a GO characteristic. In such cases the performance will be better if the EBG walls (or preferably all walls) were made like hard surfaces, because the hard surface has GO characteristics for all polarizations. In both these two cases the EBG is normally behaving like an artificial magnetic conductor, whereas the soft or hard surface always can be represented by a PEC/PMC strip grid oriented transversely or longitudinally, respectively, with respect to the propagation direction of the wave along the surface. In daily work it may be difficult to remember whether or not it is the transverse or longitudinal corrugations that stop waves or let them go, respectively. Therefore, we introduce the terms electric and magnetic current fences and electric and magnetic current lanes, to distinguish these two cases. It is evident that the transverse PEC/PMC strips are fences that stop the waves, and that the longitudinal PEC/PMC strips are lanes that let the waves go. In this way we will also understand that a PEC provides a fence for horizontal polarization (transverse electric currents) and a lane for vertical polarization (longitudinal electric currents), whereas a PMC provides a fence for vertical polarization (transverse magnetic currents) and a lane for horizontal polarization (longitudinal magnetic current).

The presentation will review the conceptual parts and origins of the soft and hard surfaces, the ideal PEC/PMC strip grid, and the AMC, as well as realizations in terms of classical corrugations, strip-loaded grounded slabs, strips with vias, periodically loaded strips, pin surfaces (bed of nails), patch grids, and patch grids with vias. The presentation will be spiced with applications, w-k diagrams, measured and computed results. In particular, the presentation will go through different ways of characterizing the different surface, and point out the need for numerical full wave results to obtain useful and realistic results for bandwidths, in particular of finite structures and waveguides.

The presentation will contain both previously published and unpublished material.

Incident-Angle Dependence of Electromagnetic Crystal (EMXT) Surface Impedance (Z_S)

Hao Xin, Raytheon Company, Tucson, AZ 85718

Electromagnetic crystals (EMXT) are periodic structures that have unique and interesting electromagnetic properties. It can provide a high impedance surface at some resonance frequency, a capacitive or inductive impedance surface above or below the resonance frequency, respectively. Such impedance surfaces can be very useful in many microwave and millimeter wave components and systems, such as low-profile antenna ground plane, TEM waveguide, phase shifter, band-pass and band-stop filters.

EMXT surfaces can be analyzed by using various methods including equivalent circuit model, asymptotic boundary condition, effective surface impedance model, and full-wave finite-element simulation of the entire structure. Since the unit cell size of typical EMXT impedance surface is usually much smaller than a wavelength (< 0.1λ), the effective surface impedance model is an easy and accurate approach to approximate the entire structure. However, similar to the angular dependence of the FSS surfaces, the EMXT surface impedance varies with the angle and polarization of an incident wave. In many applications, TE polarized incident wave is of great interest, for example, TEM waveguides, phase shifters, and low-profile antenna ground planes. This work focuses on the angular dependence of EMXT surface impedance for a TE incident wave. A method similar to the waveguide simulator for analyzing the scanning impedance of an infinite phased array is applied. Our results show that for small incident angles, the angular dependence of EMXT surface impedance is rather insignificant, while for larger incident angles, the angular dependence tends to increase nonlinearly, especially near the EMXT resonance frequency. The simulated angular response of an EMXT surface is compared with an analytical model and verified by measured data with waveguides of difference sizes (WR28 and WR22). A case study of a TEM waveguide with EMXT sidewalls will be presented. Excellent agreement between the effective surface impedance model using $Z_S(\theta, f)$ (θ is incident angle, f is frequency) obtained with the waveguide simulator approach and the full-wave simulation of the entire structure validates the accuracy of this approach. This method can be generalized to accurately and efficiently model other EMXT based structures and components.

(a)   (b)
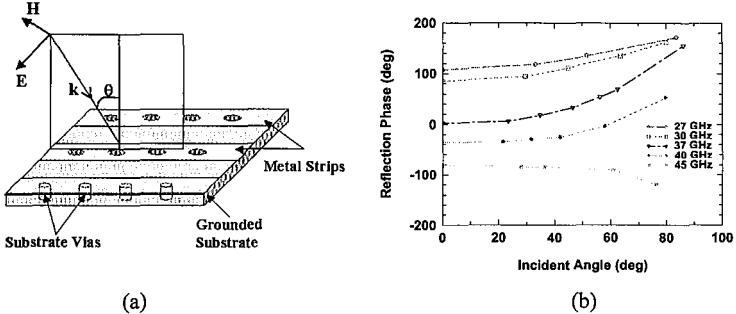
Figure 1. (a) TE plane wave incident on a strip-type EMXT surface at an angle θ. E-field is perpendicular to the metal strips. (b) Reflection phase of an EMXT surface versus incident angle at various frequencies ranging from 27 to 45 GHz using waveguide simulator method.

11

Full wave analysis of mutual coupling between dipoles over different EBG surfaces: AMC, soft and hard surfaces

*Zvonimir Sipus[1], Per-Simon Kildal[2] (Fellow IEEE)

[1]University of Zagreb, Faculty of Electrical Engineering and Computing
Unska 3, HR-10000 Zagreb, Croatia; E-mail: zvonimir.sipus@fer.hr
[2]Chalmers University of Technology, Department of Electromagnetics
SE-41296 Gothenburg, Sweden; E-mail: simon@kildal.se, www.kildal.se

We present a full wave analysis model of an EBG surface, realized as resonant patches with via holes on a grounded dielectric substrate. The via holes are treated as a wire medium with asymptotically small spacing between the wires, also referred to as a pin surface or a bed of nails, and the patches are treated by a grid impedance (low frequency approximation), as originally proposed by Tretyakov (MOTL, 2003). We have derived the spectral Green's function of the wire medium and implemented this as well as the grid impedance in our software for analyzing multilayer structures (G1DMULT algorithm). The software has also been modified to obtain the mutual coupling between dipoles located above this surface. The inverse spectral integral is solved by making use of asymptote extraction.

The computed dispersion diagrams (ω-k diagram) are very similar to those obtained with a FEM model presented by others, in particular if we make a known correction to the Green's function of the wire medium which accounts to first order for a finite wire spacing.

The results for the mutual coupling illustrate how the STOP and GO characteristics of EBG surfaces vary with frequency and polarization, depending on the thickness and permittivity of the substrate and the dimensions of the patches. We implement also a wire grid that replaces the patches (but keep the vias). The results illustrate then how the STOP characteristics of the surface is improved when the strips are located transverse to the direction of propagation between the two dipoles (corresponding to a soft surface), and how the GO characteristics are improved with longitudinal strips (corresponding to a hard surface).

LASER-METALLIZED SILICON CARBIDE ANTENNA COUPLED DIODES FOR MILLIMETER WAVE DETECTION AND FREQUENCY MIXING

A. Kar[1][*] and N. R.Quick[2]

[1]University of Central Florida, School of Optics, Center for Research and Education in Optics and Lasers (CREOL), Orlando, Florida, 32816, USA.

[2]Applicote Associates LLC, 3259 Progress Drive A, Orlando, Florida 32826, USA.

A silicon carbide antenna-coupled Schottky diode fabricated using laser direct write technologies is presented. 4H-SiC (lightly-doped n-type single crystal, (0001) Si face with an epitaxial layer of 10 μm and a donor concentration in the range of 8×10^{15} to 5×10^{18} cm^{-3}) and 6H-SiC (semi insulating single crystal, (0001) Si face, V-doped) samples were used in this study. The laser beam irradiation process selectively converts the silicon carbide to a carbon rich electrically conductive phase that behaves as an Ohmic contact and is imbedded in the substrate (N. R. Quick, US Patent No. 6,670,693, December 30, 2003). Both Nd:YAG and Excimer lasers were used. The Nd:YAG laser source was operated in the fundamental (1064 nm wavelength) as well as frequency-doubled (532 nm wavelength) modes and two types of excimer lasers, ArF (193 nm wavelength) and KrF (248 nm wavelength), were used. In the case of 1064 nm wavelength Nd:YAG laser, silicon carbide samples were irradiated with both continuous wave (CW) lasers with powers ranging from 10 to 170 W and Q-switched pulsed lasers with a repetition rate varying from 1 to 35 kHz. The non-irradiated areas maintain the 4H-SiC semiconductor properties. Laser doping technology can be used to further enhance semiconductor properties by selective p-type and n-type doping from gas-phase dopant sources [I.A. Salama, N.R. Quick and A. Kar, J. of Elec. Mat., 31, 200 (2002)].

A Schottky diode was fabricated by using a laser-metallized Ohmic contact and a magnetron sputter-deposited Ti Schottky contact.. The Ti contact can also be used as an antenna resulting in an antenna-coupled Schottky diode. The frequency response of this antenna-coupled Schottky diode was investigated through antenna polarization measurements. A 92.5-GHz (millimeter (mm) wave) source was modulated at 3 kHz in front of the antenna. The diode was biased at 820 mV and the output was observed on a lock-in amplifier. The angle between the Ti contact width direction and the electric field vector of the incident mm wave was varied by rotating the Ti contact and the output voltage of the antenna-coupled diode was measured. Since the millimeter-wave source was linearly polarized the observed polarization dependence demonstrates that the antenna-coupled diode is capable of detecting electromagnetic radiation in the range of millimeter waves. This capability of the SiC device can be used for mm wave imaging. In future work, the Ti contact will be replaced by laser metallized contacts.

Experimental Studies of Negative Refractive Index in Ordered and Random Chiral Composites

Vasundara V. Varadan[*] and Anilkumar Tellakula[+]
[*]Center for the Engineering of Electromagnetic and Acoustic Materials & Devices, The Pennsylvanaia State University, University Park, PA 16802
[+]HVS Technologies, Inc., 309 Science Park Road, State College, PA 16803

In the recent literature, electromagnetic materials that can exhibit a frequency region in which either the real part of permittivity is negative or the real part of permeability is negative or both, are referred to as metamaterials. They are structured composites formed either from periodic or random arrays of scattering elements. The interesting aspect of metamaterials is that the index of refraction can be negative in these materials (V. G. Veselago, Sov. Phys. Usp. 10, 509, 1968.) The unique electromagnetic and optical properties of these materials may be used to develop novel antennas and perfect lenses for communication and radar applications. Although there are abundant theoretical studies conducted on metamaterials made of periodic array of scatterers in the literature, experimental studies of the frequency dependent properties of metamaterials are very few. An ordered arrangement of split ring resonator is often used as the canonical model that results in negative refractive index behavior. However, there is no theoretical basis that requires periodicity or order to result in such properties. Recent literature has also often ignored the large body of work published in the 80s and 90s on chiral or biisotropic EM materials. These materials also showed very interesting frequency dependent properties. In this paper, a comprehensive experimental study of the electrical, magnetic and chiral properties of ordered and random chiral composite materials is presented. It is shown that both ordered and random composites can display negative material properties.

Chiral metamaterials are experimentally evaluated using a free space microwave measurement system, which is suitable for electromagnetic property measurements in the frequency range of 5.8 to 40 GHz (and extendible to 110 GHz). Using two spot focused antennas we can illuminate planar samples with a well defined plane wave with a well defined polarization and measure both the reflected and transmitted signals from the sample. Rotation of the receiving antenna about its axis allows us to measure depolarization effects if any. A single sample can be characterized over the entire frequency range, unlike other techniques that are limited to a narrow frequency band. A TRL calibration technique is used for completely calibrating the free space system and to define a reference plane for phase measurements. The reflection and transmission coefficients (S-parameters) of the samples are measured and inverted using closed form expressions to determine the complex permittivity and permeability. We will use the experimental data to discuss the role of order/disorder, chirality and racemicity and geometry on the observed properties. Such studies can lead to meaningful design applications.

FDTD Analysis of the Performance of Patch Antennas with Metamaterial Substrates

Andrey Semichaevsky* and Alkim Akyurtlu
Department of Electrical and Computer Engineering, University of Massachusetts
Lowell, MA 01854

Metamaterials are artificially constructed structures with electromagnetic properties which cannot be found among natural materials. Their examples include artificial bi-anisotropic materials, photonic bandgaps, and double negative materials (DNG). The frequency response and material properties of the latter may be tailored to fit the desired characteristics. Applications of metamaterials include smart antennas, absorbers and reflectors, frequency selective surfaces, and resonant structures which can be used for manufacturing non-cavity lasers and low-loss optical waveguides. As material and structure complexities increase, the limitations of analytical methods used for their analysis become more apparent and more versatile numerical techniques are necessary to study the possible applications of these materials.

The main objective of this paper is to design more efficient and wideband patch antennas by using metamaterial substrates. In order to achieve these goals, we will use the finite difference time domain method (FDTD) to model patch antennas with various metamaterials including double negative and chiral metamaterials. Recently, it has been shown that chiral media also exhibit negative ε and μ within the same frequency region (J.K. Abraham, R. Tellakula, K.J. Vinoy, Y. Sha, V.K. Varadan, *Microwave Symposium Digest, 2003 IEEE MTT-S*, Vol. 3, pp. 1837 –1840, June 2003). The FDTD technique can be used to predict scattering matrix coefficients of antennas, antenna elements such as transmission lines and their discontinuities, and antenna parameters including frequency responses and radiation patterns. Because of the resonant characteristics of microstrip antenna structures, mutual coupling, and the dispersive nature of patch antenna structures and substrate materials, this method is preferred over traditional time-harmonic methods.

In this study, the metamaterial substrates will be modeled as bulk materials and as periodic structures with individual scatterers. For the former, conventional dispersive formulations and a novel scheme for dispersive bi-isotropic media can be used (A. Akyurtlu and D. H. Werner, *2003 IEEE Ant. and Prop. Soc. Int. Symp.*,Vol. 3, pp. 371-374, 2003). Substrates with inclusions are treated as finitely periodic structures by applying periodic boundary conditions (W. Tsay and D. M. Pozar, *IEEE Microwave and Guided Wave Letters*, Vol. 3, pp. 250-252, Aug. 1993). FDTD results for the radiation patterns and the reflection parameters of the patch antennas will be presented and compared with analytical results for validation purposes. Our preliminary electromagnetic modeling results show that by introducing a planar metamaterial structure on conventional dielectric substrate next to a radiating patch, the reflection loss of an antenna can be reduced while the bandwidth is increased.

Smart Soft Electromagnetic Materials and Applications

Thomas X. Wu[1], Shin-Tson Wu[2], Jiyu Fang[3] and Vasundara Varadan[4]

[1]Department of Electrical and Computer Engineering,
University of Central Florida, Orlando, FL 32816
[2]School of Optics, University of Central Florida, Orlando, FL 32816
[3]Advanced Materials Processing and Analysis Center,
University of Central Florida, Orlando, FL 32816
[4]National Science Foundation, Arlington, VA 22230

Smart electromagnetic materials can be defined as those whose electromagnetic properties, such as permittivity, permeability, and/or conductivity can be tuned or controlled electrically, magnetically, mechanically, thermally, optically, chemically and/or biologically.

Soft materials are those materials that are neither crystallian solids (such as metal, semiconductor and ceramics which are often defined as hard materials) nor simple liquids. In our everyday life, we are familiar with some of them, such as glue, soap and food. Our human bodies are soft machines. Other examples of soft materials include liquid crystal, polymer, protein, DNA, bacteriorhodopsin, bioobject, biocolloid, and so on. In soft materials, the degree of molecular ordering is between complete positional order of crystal and full positional disorder of liquid or gas. Since typical structures in soft materials are small enough for Brownian motion, soft matter state should be visualized as a constant state of random motion. Besides, self-assembly can take place at the level of molecules (R. A. Jones, *Soft Condensed Matter*, Oxford University Press, 2002; M. Doi, *Introduction to Polymer Physics*, Clarendon Press, 1995).

In this presentation, we will overview examples of soft materials. After that, we will discuss how electromagnetic properties of some soft materials can be tuned so that they can become smart materials. We will use liquid crystal as an example to show different smart liquid crystal devices, such as liquid crystal display (LCD), optical phased array (OPA), variable optical attenuator, switchable polarization rotator, tunable microwave phase shifter and liquid crystal electronic lens. Applications of other smart soft electromagnetic materials will also be discussed.

16

Asymptotic Conditions on Transmission Line Models for Parameter Adjustable Waveguiding Structures on a Semiconductor Substrate

Mohamed El-Dessouki and Thomas Wong*
Department of Electrical and Computer Engineering
Illinois Institute of Technology
Chicago, Illinois 60616

Equivalent circuits can provide an effective means for characterizing wave propagation in a complex environment, a typical example being the interconnects found in circuits and systems where the space charge effect in the semiconductor substrate can have significant influence on the field within the guiding structure. The effects of space charge in a semiconductor can be employed to perform parametric control, via an external bias or otherwise, of the propagation properties of the guided signal. Transmission line models developed from solutions of the wave equations that incorporate the carrier transport interactions can serve as a link between circuit-based simulation tools and the full-wave solution for the constituents of a functional circuit where propagation effects need to be accounted for.

The development of a distributed equivalent circuit usually begins with the propagation constant and the wave impedance, which are obtained from the secular equations derived from the equations for the field and the charge carriers. It often occurs that more than one equivalent circuit can satisfy the requirement that the propagation characteristics within these circuits agree with those implied by the wave parameters. Additional constraints may be introduced to select the model for intended applications. Besides requiring the elements in the distributed circuit to be physically realizable, asymptotic behavior of the model in the static limit, high-frequency limit, and over the range of carrier concentration may be employed to discriminate among the candidates.

The rationale for the selection of possible transmission line models will be presented in the context of charge-field interactions. Examples of the development process will be delineated for the cases of a surface wave guided along a semiconductor surface and the quasi-TEM wave in a canonic metal-insulator-semiconductor structure.

17

FDTD Simulation of Tunneling and "Growing Exponential" in a Pair of ε-negative and μ-negative Slabs

Andrea Alù[1,*], Nader Engheta[2], and Richard W. Ziolkowski[3]

[1]Università di Roma Tre
Department of Applied Electronics, Rome, Italy
alu@uniroma3.it, http://www.dea.uniroma3.it/lema/people/andrea_alù.htm

[2]University of Pennsylvania
Department of Electrical and Systems Engineering
Philadelphia, Pennsylvania 19104, U.S.A.
engheta@ee.upenn.edu, http://www.ee.upenn.edu/~engheta

[3]University of Arizona
Electrical and Computer Engineering Department, Tucson, Arizona, U.S.A.
ziolkowski@ece.arizona.edu

Pairing together material slabs with opposite signs for the real parts of their constitutive parameters has been shown to lead to interesting and unconventional properties that are not otherwise available for single slabs. One such case was demonstrated analytically for the "conjugate" pairing of infinite planar slabs of negative-epsilon (ENG) and negative-mu (MNG) media (A. Alù, and N. Engheta, IEEE Trans. AP, vol. 51, no. 10, pp. 2558-2570). There it was shown that when these two slabs are juxtaposed, resonance, complete tunneling, total transparency and reconstruction of evanescent wave may occur, even though each of the two slabs by themselves are essentially opaque to the incoming radiation.

That study, however, was performed analytically for the time-harmonic steady-state regime. However, it is important to explore how a transient sinusoidal signal that starts at $t = 0$ interacts with such an ENG-MNG pair. Here we expect multiple reflections and transmissions at each interface to build up to the eventual steady state response of the pair, and in this process one can observe how the "growing exponential" phenomenon may occur inside this bilayer. We have simulated this problem using the Finite-Difference Time-Domain (FDTD) technique and the Drude model for frequency dependence of the permittivity and permeability of these slabs. This choice allowed the possibility of having the material properties of one or both of these regions to attain a negative real part around the frequency of the sinusoidal excitation. Our preliminary results thus far have confirmed our steady-state prediction regarding the "growing exponential" in the bilayer and the total transmission through it. However as expected, these responses are achieved only after a certain necessary number of time steps, which allow for the buildup of the interactions between the interfaces. The build-up time thus depends on the thickness of the slabs, among other parameters.

In this talk, we will review the basic concepts of the build-up of the resonant tunneling responses. We will review the FDTD simulations and present some of those results along with the corresponding physical justifications and explanations for our findings.

Experimental Studies on the Bulk Electromagnetic Properties of Frequency dependent Metamaterials

Vasundara V. Varadan[*] and Anilkumar Tellakula[+]
[*]Center for the Engineering of Electromagnetic and Acoustic Materials & Devices, The Pennsylvanaia State University, University Park, PA 16802
[+]HVS Technologies, Inc., 309 Science Park Road, State College, PA 16803

Electromagnetic metamaterials are structured composites formed either from periodic or random arrays of scattering elements. The interesting aspect of metamaterials is that they can exhibit a frequency region in which either the real part of permittivity is negative or the real part of permeability is negative or both. The index of refraction can be negative in these materials (V. G. Veselago, Sov. Phys. Usp. 10, 509, 1968.) Novel metamaterials are fabricated by using split-ring resonators (SRR), wires, and omegas as the scattering elements. Both periodic as well as random arrangement of SRRs is studied. Randomness is achieved on the periodic SRR sample by rotating each SRR about its axis by a random angle. Negative refractive index can be achieved by using a SRR and wire as the unit element.

These novel metamaterials are experimentally evaluated using a free space microwave measurement system, which is suitable for electromagnetic property measurements in the frequency range of 5.8 to 40 GHz (and extendible to 110 GHz). This method is based on illuminating the sample with plane waves by focusing the microwave beam to a measurement plane. Hence, a single sample can be characterized over the entire frequency range, unlike other techniques that are limited to a narrow frequency band. The TRL calibration technique is used for completely calibrating the free space system. The reflection and transmission coefficients (S-parameters) of the metamaterial are measured and inverted using closed form expressions to determine the complex permittivity and permeability. The results presented for these metamaterials will show that there is a frequency band where the real part of permittivity, real part of permeability, or both are negative. Such a quick and easy experimental method to determine the electromagnetic properties of metamaterials is invaluable for tailoring these materials for specific applications.

Several different types of samples will be characterized to understand the mechanisms that lead to negative material properties. Thus, we will study – (1) ordered and randomly positioned SRR samples with the split oriented parallel and perpendicular to the propagating electric field as well as randomly oriented splits; (2) combination of SRRs with wire elements and the effect of spacing; (3) discrete and connected omega particles and the effect of gap orientation. Conclusions drawn can be used to tailor material properties and frequency bands for specific applications

Smart Liquid Crystal Microstrip Phase Shifter

Liping Zheng[1], Thomas X. Wu[1], Haiying Wang[1], Wendell Brokaw[1,2] and Shin-Tson Wu[3]

[1]Department of ECE, University of Central Florida, Orlando, FL 32816
[2]Harris Corporation, Melbourne, FL 32902
[3]School of Optics, University of Central Florida, Orlando, FL 32816

Phase shifters are key components in phase-array antennas for automotive radar sensors and mobile communication systems. Phase-shift can be realized by using smart electromagnetic materials. One of the smart electromagnetic materials is liquid crystal (LC) that is well known for liquid crystal displays (LCD).

The permittivity of a nematic LC can be changed by orienting the director of LC molecules relative to the excited RF field polarization with an electro-static or magneto-static field. So the phase-shift of the LC microstrip can be controlled by adjusting the applied voltage (D. Dolfi, M. Labeyrie, P. Joffre and J. P. Huignard, Electronics Letters, 29, 926-928, 1993). The response time and insertion loss of the phase shifters can be improved by using the dual-frequency switching-mode liquid crystal, which is known to have a fast response time (T. Kuki, H. Fujikake and T. Nomoto, IEEE Tran. MTT, 50, 2604-2609, 2002).

In this paper, LC microstrip phase shifter is investigated. The simulation includes two steps: elastic simulation of LC director distribution and electromagnetic simulation of the guided wave in the microstrip.

Finite difference method (FDM) is used for the dynamic simulation of the LC director distribution between the two substrates. The simulation scheme is derived by minimizing the free energy in the LC layer where strong anchoring energy on the boundary surface is assumed.

The propagation of guided wave in the microstrip is simulated using vector finite element method (FEM). Triangular edge elements are used. The finite element scheme is derived from vector wave equations via a Galerkin procedure (L. Nuno, J. V. Balbastre and H. Castane, IEEE Trans. MTT, 45, 446-449, 1997). It can be used to simulate the general lossy inhomogeneous and anisotropic linear waveguides.

Since rectangular mesh is used for the director simulation in finite-difference method and triangular element is used for the electromagnetic simulation, interpolation is necessary to obtain triangular node values of the director distribution. Special treatments are considered when calculating the permittivity.

The phase-shift can be expressed as $\Delta\phi = l[\beta(V) - \beta(0)]$, where l is the length of the microstrip waveguide, and $\beta(V)$ and $\beta(0)$ are the phase constant at voltage V and at zero voltage. The simulated results are discussed and compared with experiments. The characteristic impedance of the LC microstrip is also calculated in a multiplayer dielectric environment.

20

An A Posteriori Error Estimator for the Multi-Level FE Solution of Time-Harmonic Fields

Volker HILL, Ortwin FARLE, and Romanus DYCZIJ-EDLINGER*
Theoretische Elektrotechnik, Saarland University, Saarbrucken, Germany
edlinger@lte.uni-saarland.de

In configurations of practical interest, the behavior of electromagnetic (EM) fields is usually characterized by the presence of singularities and regions of strong variation. To model such problems accurately and to avoid global performance deterioration due to pollution effects, highly non-uniform finite element (FE) discretizations are essential. To meet this requirement, auto-adaptive FE methods generate iteratively improved FE spaces by utilizing information from previous runs to control the density of every new mesh. For the robustness and efficiency of such methods, reliable a posteriori error estimators are of utmost importance. What types of error estimators are appropriate depends not only on the mathematical nature of the time-harmonic EM boundary value problem (BVP), but also on what output quantities are deemed important and, to considerable degree, on the specifics of the underlying FE implementation. In the present case, a nested hierarchy of tetrahedral elements supporting higher order $H(curl)$ and H^1 conforming basis functions is in use. The method is well-suited for fast multi-resolution solvers and, thanks to the incorporation of hanging variables, supports sub-domains of unequal refinement levels at any resolution stage.

The proposed error estimator is of implicit type, i.e., it does not deduce local error estimates from residuals directly, but by solving local field problems using enriched FE spaces. In this process, a residual projection technique is applied which accounts for the non-trivial null-space of the curl operator and enables us to distinguish between components in the space of irrotational fields and the space of weakly source-free fluxes, respectively. Suitable norms of the resulting local solutions are then taken as measures of error and passed on to an element marking scheme to adapt the global FE space accordingly. We have chosen a sub-domain method, i.e., the local field problems are solved on small element patches. While single-element approaches are computationally less expensive, they may result in Neumann BVP's that require extra care with regard to flux equilibration. On the other hand, sub-domain methods may use Dirichlet boundary conditions and hence bypass solvability issues. Since our FE framework provides us with all the infrastructure for nested element sub-division, the enlarged FE spaces for the local problems are taken to be the h-hierarchical FE bases obtained by regular refinement of the respective sub-domains. In our present error estimator, neither p-enrichment nor goal-oriented strategies have been considered.

In the presentation, we will detail the theory of the proposed error estimator and summarize the function of our multi-level solver and element marking strategy. To validate the efficiency and robustness of our approach, several numerical examples will be given.

A Study of Wideband Signal Propagation thru Cascaded Rectangular Cavities: Efficient Modeling using Matrix Interpolation Techniques

Vivek Ramani and Anthony Q. Martin*
Holcombe Department of Electrical and Computer Engineering
Clemson University, Clemson, SC 29634-0915
anthony.martin@ces.clemson.edu

A numerical study of signal propagation through a series of cascaded rectangular cavities connected by walls containing narrow slots and with thin-wire probes/posts inside the cavities is presented. Coupled integral equations are formulated in terms of the electric current on the probes and the equivalent magnetic current in the slots and a numerical solution technique based on the moment method is used to solve them.

The Ewald method is employed to accelerate the convergence of the free-space periodic Green's function appearing in the kernel of the integral equations. The Ewald splitting parameter is determined using a special method (D. Jackson, private communication) which allows for good accuracy in the summations over a wide band of frequencies, where the use of the usual optimum Ewald splitting parameter leads to erroneous results. The need to further speed up the computation led to the usage of matrix interpolation techniques (K. L. Virga and Y. Rahmat-Samii, "Efficient Wide-Band Evaluation of Mobile Communications Antennas Using [Z] or [Y] Matrix Interpolation with the Method of Moments," *IEEE Trans. Antennas Propagat.*, vol. 47, pp. 65-76, Jan. 1999) wherein matrix elements are computed by direct means at only a few frequencies and then interpolated at many interior frequencies. The interpolation technique effectively speeds up the calculation of coupling matrix elements which results in a massive improvement in overall CPU time to solution. A brief discussion of the performance of the Ewald method, how the interpolation technique is employed in this formulation, the overall CPU performance gains, and the numerical results obtained using this method will be presented in the talk.

The structures to be examined are cascaded rectangular cavities containing conducting probes/posts such that the cascaded cavities are coupled via narrow slots on common walls. The time-domain signal excitation may be applied in the region external to the cavities, in a slot, or at a feed point of a probe. The shielding effectiveness, a means of determining the influence of the transmission path (and environment) on the shape and magnitude of a transient exciting signal, is evaluated. Signals having various waveforms are used to excite the structure at various entry points. For example, a probe may be excited and the corresponding impedance data computed or the signal transmitted into another cavity (or into open space) may be recorded. The numerical analysis of the structures is handled in frequency domain, via the moment method and matrix interpolation techniques. It is hoped that the study will shed additional light on how the transmission path affects the characteristics of a signal which enters a complex electronic environment and reaches an interior point deep inside where a digital circuit may be located.

On the use of extrapolation methods to assess the effects of propagation path on signals penetrating electronic systems due to HPM sources

Chaitanya Sreerama and Anthony Q. Martin
Holcombe Department of Electrical & Computer Engineering
Clemson University, Clemson, SC 29634-0915
anthony.martin@ces.clemson.edu

The effects of the transmission path and environment on the characteristics of a transient signal due to a HPM source as it passes through an electronic system is of importance in discovering how the operation of digital circuits might be altered, since such signals are unexpected and contain spurious electromagnetic energy. If a signal of a specified form enters a system at a given point it is useful to know the salient features of the resulting signal that reaches a location within the system where a susceptible digital circuit is located. Moreover, it is useful to know if any of the features of the induced signal are primarily those peculiar to the entering signal or if they are more influenced by the properties of the transmission environment. Addressing these issues should help one gain an appreciation for the nature of a spurious signal arriving at the input of a digital circuit embedded deep within a complex system and perhaps that information can be used to eliminate deleterious effects on the operation of digital circuits.

With the powerful Maxwell equations solvers available today to perform electromagnetic simulation it is reasonable to assume they can be useful in characterization of such effects. However, given the complexity of real-world systems this still remains a daunting task, especially when wideband characterization is needed. For example, the use of the popular FDTD method for modeling electronics inside enclosures imposes serious memory, time, and accuracy constraints in generating the late-time response. Also, the use of MOM or FEM when generating the high-frequency response can be computationally overwhelming. Recently, researchers have reported on wideband extrapolation techniques which can potentially overcome some of these limitations by using only early-time and low-frequency data (Rao et al, "Simultaneous Extrapolation in time and frequency domains using hermite expansions" *IEEE Trans. Antennas Propagat.*, vol. 47, pp. 1108-1115, Aug 1999). By using only the early time and low frequency data, which contain mutually complementary information, one can simultaneously extrapolate the entire system response in both domains (Rao et al, "Simultaneous extrapolation in time and frequency domains using hermite expansions" *IEEE Trans. Microwave Theory Tech.*, vol. 47, pp. 1964-1969, Oct 1999).

The focus of this talk will be to examine how well these extrapolation techniques work for computing the signal that penetrates an enclosure due to an exterior transient source such as a HPM source. The FDTD method will be used to obtain the early-time response and a triangular surface patch code (or some other MOM-based code) will be used to obtain the low-frequency response. Hence, the numerical models will represent different discretizations of the enclosures. To further reduce complexity, only the features deemed electromagnetically essential and tractable will be included in the models. A variety of different waveshapes will be used to represent the exciting signals. The structures of interest will consist of metallic objects having cavities of different sizes and shapes, various types of slots/apertures for signal entry, and different arrangements and shapes of objects inside, including cables (wires) going from outside to inside. Attempts will be made to ascertain the accuracy of the approach as well as the CPU time savings measured against using either the FDTD or MOM tools separately.

Penetration Into Nested Cavities Through Apertures

D. Negri*, D. Erricolo, P.L.E. Uslenghi
Department of Electrical and Computer Engineering
University of Illinois at Chicago
851 South Morgan Street, Chicago, IL 60607-7053, USA
E-mails: dnegri1@uic.edu, derricol@ece.uic.edu, uslenghi@uic.edu

Under consideration in this research is the penetration of the electromagnetic field into nested cavities through apertures on the cavities. The investigated geometry consists of N perfect electric conducting nested cavities, each of which presents an aperture. The cavities divide the entire space in $N+1$ regions: the most external region, $N-1$ intermediate regions (regions between two cavities), and the most internal region. Since each cavity has an aperture, the electromagnetic field penetrates into the innermost cavity.

The solution of this problem is based on the equivalence theorem. By applying the theorem, the N apertures are closed by a PEC and N unknown equivalent surface magnetic currents are introduced on the apertures. In order to find the equivalent currents, the boundary conditions forcing the continuity of the tangential component of the magnetic field on the apertures are then imposed. The boundary conditions lead to N coupled integral equations, which can be solved by means of the method of moments. This procedure transforms the integral equations into N linear systems, or, equivalently, into one single comprehensive system of linear equations. Then, by inverting the system matrix the problem is formally solved, i.e. the equivalent currents become known. Once the equivalent currents are known, also the electromagnetic field in the $N+1$ regions and the induced surface electric currents on the N cavities are known, because they can be expressed as functions of the equivalent currents.

In order to provide an explicit form for all the terms that appear in the system, some "auxiliary problems" are introduced. This procedure follows the "generalized impedance matrix" approach, which was developed by R. F. Harrington, J. R. Mautz and T. Wang ("Electromagnetic scattering from and transmission through arbitrary apertures in conducting bodies"; IEEE Trans. Antennas Propagat., vol. 38, no. 11, pp. 1805-1814, Nov. 1990), and which was applied to the case of one cavity only.

The innovative element of the present research is the solution of the problem of the penetration into nested cavities through apertures. Furthermore, the problem is solved taking into account the contribution of the external scattering of each cavity.

Time Domain Adaptive Integral Method for EMI/EMC Applications

Ali E. Yılmaz*, Andreas C. Cangellaris, Jian-Ming Jin, and Eric Michielssen

Center for Computational Electromagnetics and Electromagnetics Laboratory
Department of Electrical and Computer Engineering
University of Illinois at Urbana-Champaign, Urbana, IL 61801, USA

Modern-day and real-world EMI/EMC problems continue to pose almost insurmountable challenges to even the most recent generation of fast solver technologies. Indeed, these problems often require the modeling of electromagnetically large platforms comprising of overmoded cavities loaded with small, geometrically complex, intricately interconnected, and possibly nonlinear systems that are subject to system-generated or externally produced interfering signals. The application of full-wave analysis tools to such problems – which we believe ultimately to be the only avenue for successfully tackling this class of problems – at present is hindered by the need to accurately account for disparate scales, modes, and frequencies of operation, which not only translates into a large number of unknowns but also gives rise to accuracy, convergence, and stability problems.

In this paper, we report on recent developments in the construction of an FFT-accelerated, time-domain integral equation-based, full-wave electromagnetic solver and its application to system-level EMI/EMC problems. Over the last few years, this solver has evolved from a time-marching FFT engine applicable to the analysis of scattering from free-standing uniformly discretized perfect electrically conducting (PEC) surfaces [A. E. Yılmaz et al., IEEE AWPL, vol. 1, pp. 14-17, 2002] to a tool permitting the analysis of non-uniformly meshed, combined dielectric volumes and PEC surfaces loaded with nonlinear circuitry that executes in a parallel environment [A. E. Yılmaz et al., in this conference]. This presentation focuses on extending the capabilities of this solver through its hybridization with a SPICE-like tool that permits the simultaneous analysis of the above-described structures *including* N-port components described by transfer functions in pole-residue form (Laplace elements). This extension is accomplished by loading N ports on the physical structure considered by the electromagnetic solver with delta-gap voltage sources whose amplitude depends on the past and present currents at these same ports. The current at all the ports are extracted from the full-wave solver at each time step and convolved with the appropriate transfer functions to obtain the port voltages at the next time step. This technique allows for the integration of a wide array of components following their characterization through measurements or simulation (as isolated sub-systems through model-order reduction techniques). In this work, the convolution is computed recursively in $O\left(N^2 N_t N_p\right)$ operations using $O\left(N^2 N_p\right)$ bytes of memory for N_p poles and N_t time steps of simulation. Because $N_p < N_t$ typically, recursive computation of the component response is often more efficient than direct convolution, which requires $O\left(N^2 N_t^2\right)$ operations and $O\left(N^2 N_t\right)$ storage space. Various scenarios that demonstrate the applicability of this component-loaded TD-AIM scheme to EMI/EMC problems, including the coupling of plane waves into airplane cockpits with computer-like enclosures and surface-mounted antennas, have been simulated and will be highlighted at the meeting.

Penetration through a Slot in a Conducting Plane Backed by a Channel, Part II: TM Excitation

Michael D. Lockard* , Chalmers M. Butler
Holcombe Department of Electrical and Computer Engineering
328 Fluor Daniel EIB
Clemson University, Clemson, SC   29634-0915 USA

Two types of integral equations are derived and solved for the unknowns associated with penetration of a field through a slot in a conducting plane backed by a channel. This is done for the purpose of verifying the validity and accuracy of the solutions of two types of integral equation by demonstrating the closeness of the solutions. In one case the solution of a single integral equation allows one to determine all quantities of interest, while in the other coupled integral equations are solved for two unknowns knowledge of which enable one to characterize all quantities of interest. Given the fundamentally different nature of the integral equations resulting from the two formulations, one acquires confidence in both methods when the data from one corroborates those from the other. In both methods, the slot electric field, or the equivalent magnetic current, is an integral equation unknown. Thus, the slot electric field, determined directly in both methods, can be compared to ascertain accuracy. No other direct comparisons can be made, but from the solutions obtained in both methods one can compute and compare the total field in the interior of the channel and outside the channel in the region above the conducting plane.

Derivations of the two types of integral equations are outlined and solution methods are mentioned. The coupled integral equation method is more general in that the configuration of the channel backing can be of arbitrary shape, but the other is more efficient since only one equation is involved. The boundary condition on the backing is enforced directly by one of the equations in the coupled equation method, while, in the single equation method, this condition is enforced by the inclusion of a backing-geometry-specific Green's function.

The total electric field in the slot, determined from the two methods, is compared for a number of cases of excitation, slot width, channel backing configuration, and material in the channel. In addition, for the same excitation and structural parameters, the field inside and outside the channel and the actual current on the conducting surfaces of the structure are computed by both methods. Data obtained from the two independent methods are shown to agree to a high degree. Solutions are found and comparisons are made for the cases of a hemicylinder-backed slot, a rectangle-backed slot, and a sector-backed slot.

Radiation from an antenna in a partially covered cavity near a 2D or 3D corner

D. Erricolo, P.L.E. Uslenghi
University of Illinois at Chicago, Dept. of ECE (MC 154)
851 South Morgan Street, Chicago, IL 60607-7053

Two three-dimensional boundary-value problems involving radiation of a magnetic dipole in the presence of partially covered cavities filled with isorefractive material and located at the corner of two or three mutually perpendicular metallic walls are solved exactly, in the frequency domain.

In the first problem, the cavity has the shape of one quarter of an oblate spheroid and is flush-mounted under a horizontal metal plane which contains the focal circle of the spheroid. The vertical wall of the cavity is part of a vertical metallic plane containing the symmetry axis of the spheroid. The cavity is coupled to the quarter-space above it by a semi-circular aperture whose edge belongs to the focal circle of the spheroidal cavity. The cavity is filled with a material that is isorefractive to the medium filling the quarter-space above the cavity. The primary source is a magnetic dipole located on the axis of symmetry, inside or outside the cavity, and oriented parallel to the axis. This problem, which features a cavity, a sharp curved edge and two different penetrable materials, is solved exactly by separation of variables, in terms of oblate spheroidal wave functions. Numerical results for surface currents inside and outside the cavity and for near and far fields are presented and discussed in terms of the source location, the cavity dimensions, and the ratio of intrinsic impedances of the isorefractive media.

The second problem has the same geometry of the first problem, but another metallic wall perpendicular to the other two walls and containing the axis of symmetry of the cavity is introduced. Thus, the cavity is now one-eighth of an oblate spheroid flush-mounted under the horizontal plane of a trihedral corner reflector, and is coupled to the octant of space above it via an aperture in the shape of a quarter circle. The source is a magnetic dipole located on the symmetry axis of the cavity, i.e. at the intersection of the two vertical walls of the trihedral reflector, and oriented parallel to the axis. The problem is solved similarly to the first problem.

The two problems solved herein are important because they represent new canonical solutions; additionally, they are useful for the validation of frequency-domain computer codes.

Incident Field Excitation of a Random Two-Wire Transmission Line

J.C. Pincenti*, P.L.E. Uslenghi
Department of Electrical and Computer Engineering
University of Illinois at Chicago
851 South Morgan Street, Chicago, Illinois 60607-7053, USA

The problem of finding the maximum power delivered to the load on a random two-wire transmission line excited by an external field is considered. Often in practice, the exact orientation of a transmission line is not known and therefore the electromagnetic field excitation of the line is probabilistic and has to be studied as such. This problem will be analyzed in the frequency domain using transmission line theory. In particular the line will be modeled as a non-uniform transmission line excited by an external field. The non-uniformity will be modeled by dividing the line into smaller discrete uniform sections and then cascading the segments together to approximate the overall line. Both the per-unit-length (PUL) parameters and orientation of each segment with respect to the incident field will be varied randomly thus creating an overall random cable. A number of such random cables will be generated producing a statistical solution.

The random nature will take two forms. First, the spacing between the wires is not maintained and will vary randomly along the length of the line. This will cause the PUL parameters of inductance and capacitance to vary accordingly. Second, the orientation of the wires with respect to the incident field will vary randomly along the length of the line. This is due to the various twists and bends of the wires and will affect the amount of coupling of the external field to the line. In addition, such variables as partial illumination of the line, resistive losses and the presence of a ground plane are considered.

From this model, it will be found that an exact optimal frequency for delivering maximum power to the load does not exist. This is due to the random nature of the line, and will cause the response to vary at a given frequency. Though an exact frequency cannot be determined, the results will show that an approximate frequency can be found.

Field Coupling Analysis of Multiconductor Transmission Lines in Presence of Complex Platforms via a Hybrid MoM-SPICE Technique

*Y. Bayram and J. L. Volakis

ElectroScience Laboratory, ECE Dept., The Ohio State University, Columbus, OH 43212, USA

bayram.2@osu.edu , volakis.1@osu.edu

This work proposes an efficient alternative approach for analysis of field-excited multiconductor transmission lines surrounded by arbitrary complex structures. The typical approach to such analysis is to modify telegrapher's classical equations by incorporating additional voltage and current sources to model the external excitation fields. This is also known as Multiconductor Transmission Line Theory (MTLT). However, this method is only valid for those cases where the transmission line is close to conducting surfaces -- in other words, where quasi-TEM conditions are valid. For reliable analysis, one must also consider the surrounding structure effects and their impact on the TL currents, implying the introduction of the common mode current.

To improve the MTLT approximation (by accounting for radiation generated by the transmission lines), a technique that modifies telegrapher's coupling equations with additional iterative source terms was proposed by Tkatchenko et.al. (IEEE Trans. Electromagnet. Compat., November 1995) for a finite conductor over a perfectly conducting infinite plane. Also, Haase et.al. (14th International Zurich Symposium on Electromag. Compat, Zurich, Feb. 2001) proposed an iterative transmission line method, employing the generalized form of telegrapher's equations in an iterative manner. A more general approach was also proposed by the authors (APS/URSI 2003 Conference, Columbus, OH) to extend the existing techniques to multiconductor transmission lines in presence of complex structures by introducing Telegrapher's Iterative Coupling Equations (TICE). However, convergence of the proposed method depends on quasi-static energy coupled to the transmission line bundle. In other words, the proposed technique is based on perturbation theory with the assumption that the current due to quasi-static field contributions is dominant.

In this work, we propose an alternative approach to Telegrapher's Iterative Coupling Equations. This approach relies on a different current decomposition approach within the transmission line bundle. Namely, the current on each transmission line is decomposed into push-push mode and push-pull mode currents. The similar convention is also followed by Friis and Schellknoff (Antenna Theory and Practice, Wiley, 1952) for analysis of two wire antennas in free space. The former accounts for the interactions between the surrounding structure and the transmission line bundle, and the latter is responsible for the current perturbation due to interactions among the transmission lines forming the bundle. Based on this model, we derive the Telegrapher's Generalized Coupling Equations (TGCE) for each mode. The push-push mode current is found by solving a test wire located at the center of the transmission line bundle in the presence of the surrounding structure. However, the push-pull mode current is computed iteratively (and rather rapidly) by taking the center transmission line as the return conductor/reference. SPICE models are then employed to analyze the equivalent circuits for the push-pull mode current. Concurrently, the nearby structures are treated with the Method of Moments (MoM). The convergence of our proposed technique depends on the strong coupling of the transmission lines forming the bundle. Results will be shown demonstrating the accuracy and generality of the new technique.

29

Scattering from Conducting/Dielectric Composite Objects Using Combined Field Integral Equation

Baek Ho Jung[1], Tapan K. Sarkar[2], Zhong Ji[2], and Magdalena Salazar-Palma[3]

[1] Department of Information and Communication Engineering, Hoseo University
Asan, Chungnam 336-795, Korea
e-mail: bhjung@office.hoseo.ac.kr

[2] Department of Electrical Engineering and Computer Science, Syracuse University
Syracuse, NY 13244-1240
e-mail: tksarkar@syr.edu, zji@syr.edu

[3] Departamento de Senales Sistemas y Radiocomunicaciones
Universidad Politecnica de Madrid, Madrid 28040, Spain
e-mail: Salazar@gmr.ssr.upm.es

In the analysis of conducting/dielectric composite bodies at frequencies, which correspond to an internal resonance of the structure, spurious solutions are obtained for the electric field integral equation (EFIE) or the magnetic field integral equation (MFIE). One possible way of obtaining a unique solution at an internal resonant frequency of the structure under analysis is to combine a weighted linear sum of the EFIE with MFIE and thereby eliminate the spurious solutions. This combination results in the combined field integral equation (CFIE). To analyze 3-D objects using a surface integral equation, the triangular patch modeling can be used. A suitable basis function for the triangle patch is the RWG (Rao, Wilton, Glisson) function. Although integral equation formulations have been used for 3-D composite bodies, the CFIE has not been applied for the analysis of scattering by arbitrarily shaped 3-D composite objects with triangular patch modeling. In this paper, we present a new formulation for the analysis of electromagnetic scattering from arbitrarily shaped three-dimensional (3-D) perfectly conducting and piecewise homogeneous dielectric composite body. The conducting/dielectric structure is approximated by planar triangular patches, which have the ability to conform to any geometrical surface. The surface covering the conducting body is replaced by an equivalent surface electric current and the surface of the dielectric by equivalent electric and magnetic currents. The surface currents are approximated in terms of RWG functions. The objective of this paper is to illustrate that the CFIE is a valid methodology in removing defects, which occur at a frequency corresponding to an internal resonance of the structure. Numerical results are presented and compared for composite scatterers with solutions obtained using other formulations.

Efficient Sensitivity Analysis using Coupled Circuit-Electromagnetic Simulation

Yong Wang*, Vikram Jandhyala and C.J. Richard Shi

Dept. of Electrical Engineering, University of Washington
Box 352500, Seattle WA 98195, Ph: 206-543-2186, Fax: 206-543-2186
Email: jandhyala@ee.washington.edu

With the rapidly increasing interest in applications such as radio frequency wireless communication and high-speed data processing, electronic systems are required to work at progressively higher frequencies. As the operating frequencies enter the high GHz range, phenomena such as cross talk, parasitic-induced delay, and substrate losses etc. can no longer be neglected. In order to design high-performance systems with short time-to-market, it is essential to perform EM simulation to include these layout related effects at design stages prior to fabrication. In particular, sensitivity of EM-related behavior, i.e. the analysis of variation of results with parametric changes in design, layout and material distribution is very important.

Traditional sensitivity computation employs a finite difference approach, for example, the sensitivity of a system performance P using the forward finite-difference approximation can be written as $\dfrac{\partial P(x_i)}{\partial x_i} \approx \dfrac{P(x_i + \Delta x_i) - P(x_i)}{\Delta x_i}$, where x_i is a design variable. In such methods, the system needs to be solved twice for each design variable thus making the method computationally expensive. Moreover, the accuracy of this method depends on the step size Δx_i; while a large value of Δx_i will lead to inaccurate sensitivity, a small value could also introduce numerical error due to solver precision. Recent approaches (Georgieva et. al., IEEE Trans. MTT, 50, 2751-2758, 2002) using the *adjoint variable method* greatly reduce the computation cost by employing the fact that the inverse of the system matrix can be derived with little cost once the problem is solved, and prove to be an effective way for calculating sensitivity.

The simulation approach used in this work is based on a coupled circuit-electromagnetic formulation. In this approach the system unknowns consist of both EM parts (typically surface currents related to the method of moments) and circuit parts (node voltages and branch currents). The system performance is itself typically related to a sub-set of the circuit unknowns, which are system unknowns in the coupled formulation. This leads to the sensitivity calculation being more convenient than with the adjoint method. Therefore there is no requirement to introduce additional adjoint variables, and the only extra computation needed for the proposed method is the calculation of the spatial derivative of the overall coupled system matrix versus design variable x_i, in addition to a few simple matrix-vector multiplications and additions. The spatial derivatives of the basis functions used in the system matrix are derived by analytical spatial differentiation of near- and far-field expressions of the method of moments matrix elements.

Efficient EM sensitivity computation as discussed above can help high frequency circuit design in two ways. First, it enables identification of EM structures that are extremely sensitive to small variations of geometric or material parameters; such structures could cause the system performances to be very different and unacceptable due to process and layout variation. Second, efficient and accurate sensitivity calculation enables gradient-based optimization of EM structures, which is useful to automate high-frequency circuit design.

On the Higher-Order MoM-PO Electromagnetic Modeling of Vehicles

Miroslav Djordjević and Branislav M. Notaroš[*]
University of Massachusetts Dartmouth, ECE Department
285 Old Westport Road, Dartmouth, MA 02747, bnotaros@umassd.edu

Modern radio, wireless, and satellite communication and radar systems often involve vehicles (cars, airplanes, helicopters, spacecraft, etc.). From the electromagnetic point of view, the vehicles are three-dimensional radiating and scattering structures of complex shapes. They are so complicated and general that classical electromagnetic analytical techniques cannot be used. On the other hand, they are too expensive and impractical to be used as physical models in measurements. Consequently, numerical tools have to be developed and used. In addition, given that today's communication and radar applications cover practically the entire radio spectrum, vehicles included in the communication and radar systems range from electrically very small to ultra large objects. Analysis of vehicles as electromagnetic structures is, by all means, one of the most challenging and practically important problems of applied computational electromagnetics.

This paper presents our work and recent contributions to the electromagnetic modeling and analysis of airplanes and automobiles. The vehicles are analyzed using an efficient and accurate higher-order, large-domain hybrid computational technique based on the method of moments (MoM) and physical optics (PO). The technique utilizes large generalized curvilinear quadrilaterals of arbitrary geometrical orders in both the MoM and PO regions. It employs higher order divergence-conforming hierarchical polynomial basis functions in the context of the Galerkin method in the MoM region and higher order divergence-conforming interpolatory Chebyshev-type polynomial basis functions in conjunction with a point-matching method in the PO region. The new technique exhibits an excellent accuracy and flexibility at modeling of both current variation and curvature of complex objects (vehicles). As an example of higher order geometrical modeling, shown in the figure are the geometrical models of a commercial aircraft constructed from 728 bilinear (first-order) quadrilateral elements and 182 biquadratic (second-order) quadrilateral elements, respectively, where using the second-order geometrical approximation provides a dramatic improvement in the precision of the geometrical model and the overall accuracy of the MoM-PO scattering simulation. Several examples of the MoM-PO analysis of aircraft and automobiles to be presented demonstrate the efficiency and accuracy of the hybrid higher-order computational technique and its advantages over conventional techniques and low-order (small-domain) models.

| (a) | (b) |
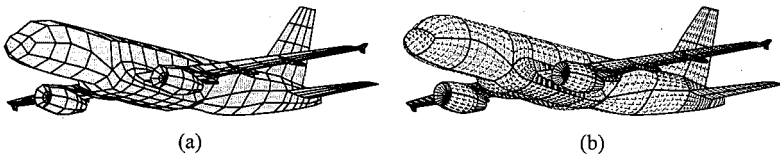
Higher-order large-domain MoM-PO simulation models of a commercial aircraft using (a) 728 bilinear quadrilateral elements and (b) 182 biquadratic quadrilateral elements.

Solution of Large Radiation and Scattering Problems Without Iteration Using the Fast Matrix Solver (FMS) and the Characteristic Basis Function Method (CBFM)

Raj Mittra, Tianxia Zhao, Junho Yeo and Sinan Koksoy
Electromagnetic Communication Laboratory, 319 EE East
The Pennsylvania State University
University Park, PA 16802
rajmittra@ieee.org

Abstract

Iterative methods are universally used to solve large problems that preclude direct solution owing to the limits of the available RAM size of the CPU. Despite the availability of fast solvers, the need to handle multiple right hand sides and range of frequencies can render the task of generating the solution to be quite time-consuming; hence, a search for alternate schemes for dealing with large problems still continues among researchers in computational electromagnetics.

One promising approach to direct solution is to employ the code FMS (Multipath Corporation), which can perform an LU decomposition of the MoM matrix using the hard disk, with little penalty in run time over the use of RAM. Obviously, solution of the problem with many RHS now becomes trivial and, since the hard disk is relatively cheap, the extra cost involved in the solution of large problems is minimal, and this is an important salutary feature of the FMS solver. However, the FMS is still expensive in terms of the CPU run time, because of the inherent nature of the LU decomposition algorithm, which is an $O(N^3)$ operation.

Recently, the Characteristic Basis Function Method (CBFM) has been introduced for solving large problems by using a "domain decomposition (DD)" type of approach. Unlike the conventional DD methods, however, which rely on iterative methods that do not always converge, the CBFM generates a reduced matrix as an intermediate step, by using the Galerkin's method, which preserves the numerical rigor of the technique. The generation of the CBFs entails the use of direct solution of moderate-size matrices in the range of 10,000 to 20,000, with multiple r.h.s., a task that can be handled at a moderate cost. The reduced matrix is again of moderate and manageable size--even when the original problem is large-- and direct method can be used once again, without the need to resort to iteration.

The paper will present illustrative problems involving canonical geometries, *e.g.*, RCS of a sphere (for validation), as well as EMI problem in objects such as antennas operating in topside environment of a ship (Fig.1). It is shown in the paper how the CBFs can be generated for multiple incident angles and frequencies. Unlike the iterative methods, the use of such CBFs obviates the need to start anew, and carry out the entire solution procedure from the beginning to the end, each time the incident angle or the frequency is changed.
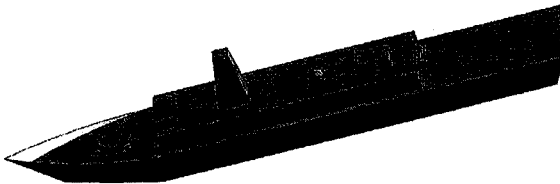
Fig.1. Topside environment for EMI modeling.

BOUNDARY INTEGRAL EQUATIONS FOR A MONOPOLE BACKED BY A GROUND PLANE

John S. Asvestas

NAVAIR, Radar and Antenna Systems Division 4.5.5, B2187, S2190
48110 Shaw Rd., Patuxent River, MD 20670

We have developed boundary-integral equations for the problem of radiation by a monopole of arbitrary geometry over an infinite ground plane. The monopole is fed by a semi-infinite coaxial line that comes from behind the ground plane and is perpendicular to it. The integral equations are an exact representation of the physics of the problem; moreover, they are restricted over the walls of the coax and the surface of the monopole only. The infinite ground plane is not involved in the integral equations. At the expense of introducing an extra unknown (the magnetic current density), the equations over the semi-infinite walls of the coax can be replaced by ones over a finite portion of the line. All surfaces are perfectly conducting and the coax is filled with air. Expressions for the far field in terms of computable quantities are also derived. The integral equations can be solved numerically for the unknown current densities using the method of moments. In the first case, one need use the natural modes of the line as basis/testing functions while in the second (finite portion of coax used) any traditional moment method will do. The second approach generates many more unknowns than the first.

The present approach is based on the method of Asvestas and Kleinman ("Electromagnetic Scattering by Indented Screens," *IEEE Trans. Antennas Propagat.*, Vol. 42, pp. 22-30, (1994)). The same approach can be used when the coax is replaced by a waveguide of arbitrary cross section and with a monopole present or absent. In case the modes of the waveguide are known, they can be used to reduce the dimension of the resulting linear system of equations.

Commission and Session: Commission B7 (Numerical methods: int. eq. based)
What new knowledge is contributed by this paper? This is the first time that boundary integral equations for a coaxial line radiating into a half-space are derived without introducing any physical approximations and without involving the infinite plane.
Relationship to previous work: Asvestas and Kleinman, "Electromagnetic Scattering by Indented Screens," *IEEE Trans. Antennas Propagat.*, Vol. 42, pp. 22-30, (1994).

COAXIAL LINE RADIATION INTO A HALF-SPACE

John S. Asvestas
NAVAIR, Radar and Antenna Systems Division 4.5.5, B2187, S2190
48110 Shaw Rd., Patuxent River, MD 20670

In a previous talk we derived boundary-integral equations for the problem of radiation of a monopole into a half-space. The geometry is the following. The outer conductor of a semi-infinite coaxial line opens into an infinite plane perpendicular to the axis of the coax. The center conductor extends to this plane or above it. Its extension can take an arbitrary shape or even become disjoint from the center conductor. All surfaces are perfectly conducting and the coax is filled with air.

As a special case, we consider here the case where the center conductor does not protrude into the half space to form a monopole but ends where the half-space begins, i.e., at the level of the ground plane. The TEM mode is used to excite the line and this, together with the circular symmetry of the geometry, is used to reduce the vector integral equations into three scalar equations. The unknown electric current densities on the walls of the line are expressed as infinite series in the natural modes of the line, the coefficients of the modes being the unknowns. Any of the three integral equations can be solved numerically using the method of moments. We choose the one over the annular ring where the coax opens to an infinite plane. We use the natural modes of the coax as testing functions and end up with an infinite system of equations in an infinite number of unknowns The unknowns are the coefficients of the modes and the impedance matrix comprises single, Sommerfeld-type integrals. This approach can also be used when the coax is replaced by a circular or rectangular waveguide.

The advantage of using the natural modes of the coax as basis and testing functions is that we can truncate the infinite system of equations to a small one and get very good results. It also allows us to observe how the reflected modes of the guide contribute to the magnetic-current density at the opening to the half-space and, in general, it yields analytic expressions for all quantities of interest. We conclude by showing results for an 11x11 system of equations, including graphs for far-field quantities, such as directivity and gain. In solving this system, we enhanced the convergence of the Sommerfeld-type integrals by extracting the static part from them and dealing with it separately.

Commission and Session: Commission B7 (Numerical methods: int. eq. based)
What new knowledge is contributed by this paper? This is the first time that the problem of a coaxial line radiating into a half-space is addressed in an exact way using the natural modes of the coax to express unknown current densities and all other quantities of interest.
Relationship to previous work: *Boundary Integral Equations for a Monopole Backed by a Ground Plane*, this conference by the same author in same Commission and Session.

Dielectric Loaded Slot in a Parallel-Plate Waveguide Coupled to a Conducting Cylinder

Cengiz Ozzaim
Department of Electrical Engineering
Dumlupinar University, 43100 Kutahya, TURKIYE

Study of the radiation characteristics of slotted parallel-plate waveguide (PPW) loaded by conductors, dielectrics, and their combination is required in many applications such as aperture coupled microstrip antennas, flush mounted waveguides, etc. Some investigators have analyzed slotted (and/or flanged) PPW, which contains in its half-space either a conducting cylinder or a strip, which is embedded in a circular dielectric cylinder or in an infinite slab. However, the results are available for some simple shapes of the dielectric load, which was either an infinite slab, or a circular dielectric cylinder.

In this work, the radiation characteristics of a PPW with a slot covered by a dielectric semi-cylinder of arbitrary cross-section, is studied. Disjoint from the dielectric semi-cylinder, the exterior half-space of the waveguide contains a perfectly electrically conducting (pec) cylinder as illustrated in Fig. 1. A similar configuration where no dielectric is present has been considered previously (P. D. Mannikko, C. C. Courtney, and C. M. Butler, Proc. Inst. Elect. Eng., pt. H, vol. 139, 193-201, 1992. The present work extends the technique by considering an arbitrarily shaped dielectric semi-cylinder covering the guide aperture on the side facing the half-space. This problem differs from previously studied problems because of the arbitrary cross-section assumption imposed on the dielectric load. The surface equivalence principle is used to obtain a set of coupled integral equations in terms of the slot electric field, the current induced on the pec cylinder and the equivalent surface electric currents on the dielectric cylinder. The method of moments is used to solve the integral equations numerically. The excitation is an incident TEM wave in the guide. From knowledge of the excitation, the slot electric field, and the equivalent currents on the cylinders one can determine all electromagnetic quantities. The analysis is applied to several practical cases of interest to determine the reflection, transmission and radiation for TEM excitation from within the PPW.
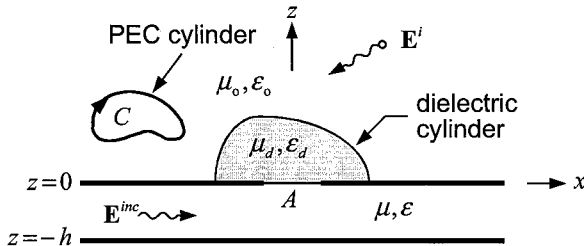
Fig. 1. A pec and a dielectric cylinder in the presence of a slotted PPW.

Flanged Parallel-Plate Waveguide Loaded by Conducting and Dielectric Cylinder

Cengiz Ozzaim
Department of Electrical Engineering
Dumlupinar University, 43100 Kutahya, TURKIYE

Study of the radiation characteristics of flanged parallel-plate waveguide (PPW) loaded by conductors, dielectrics, and their combination is required in many applications. Some investigators have analyzed flanged (and/or slotted) PPW, which contains in its half-space either a conducting cylinder or a strip, which is embedded in a circular dielectric cylinder or in an infinite slab. However, the results are available for some simple shapes of the dielectric load. In this work, the radiation characteristics of a flanged PPW covered by a dielectric semi-cylinder of arbitrary cross-section, is studied. Disjoint from the dielectric semi-cylinder, the exterior half-space of the waveguide contains a perfectly electrically conducting (PEC) cylinder as illustrated in Fig. 1. A similar configuration where no dielectric is present has been considered previously (C. M. Butler, C. C. Courtney, P. D. Mannikko, and J. W. Silvestro, Proc. Inst. Elect. Eng., pt. H, vol. 138, 549-559, 1991.) The present work extends the technique by considering an arbitrarily shaped dielectric semi-cylinder covering the guide aperture on the side facing the half-space. This problem differs from previously studied problems because of the presence of the dielectric cover, which has an arbitrary cross-section. The surface equivalence principle is used to obtain a set of coupled integral equations in terms of the slot electric field, the current induced on the pec cylinder and the equivalent surface electric currents on the dielectric cylinder. The method of moments is used to solve the integral equations numerically. The excitation is an incident TEM wave in the guide. From knowledge of the excitation, the slot electric field, and the equivalent currents on the cylinders one can determine all electromagnetic quantities. The analysis is applied to several practical cases of interest to determine the reflection, transmission and radiation for TEM excitation from within the flanged PPW.
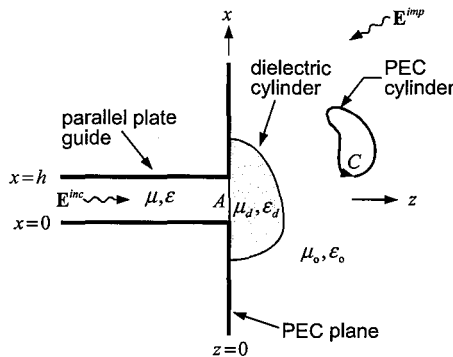
Fig. 1. A flanged PPW coupled to a conducting and dielectric cylinder

An Efficient Approach for the Evaluation of MoM Matrix Entries for Vertical Antennas in Planar Stratified Media

R. M. Shubair
Communication Engineering Department
Etisalat College of Engineering
P.O.Box 980, Sharjah, UAE
E-mail: rshubair@ece.ac.ae

Abstract

The boundary integral equation approach based on the use of Method of Moments (MoM) for the solution of a mixed-potential integral equation is one of the most commonly used numerical techniques for the rigorous analysis of arbitrary geometers in planar stratified media. In the MoM formulation, the matrix entries involve two-dimensional inner product integrals of the spatial domain Green's function with the correlation of basis and testing functions over finite domains. The spatial domain Green's function can be expressed in closed-form by using the Discrete Image Method (DIM) (R. M. Shubair, *Proc. IEEE AP-S*, pp. 827-830, 2003) and (R. M. Shubair, *Proc. URSI*, 2003), which approximates the spectral domain Green's function in terms of complex exponentials and uses the Sommerfeld identity for the transformation into the spatial domain. By using the Taylor series expansion of the closed-form Green's functions, the two-dimensional inner product integrals can be evaluated analytically. The analytical evaluation of the MoM matrix entries results in a substantial reduction in the matrix fill-in time and, hence, improves the computational efficiency of the method. A further improvement in efficiency of the method could be achieved if the MoM matrix entries are expressed in closed-form. This is done by extending the DIM so that the correlation of basis and testing functions is included (L. Alatan, *Proc. IEEE AP-S*, pp. 819 - 822, 2003).

In the proposed approach, once the spectral domain Green's function is approximated, the order of integrals for the spatial domain transformation and for the inner product are inter-changed. This allows the spectral domain representation of the correlation of basis and testing functions to be also approximated in terms of complex exponentials so that the MoM matrix entries are obtained in closed-form. In this paper, the formulation for the closed-form representation of the MoM matrix entries is presented for vertical antennas in planar stratified media. Numerical results will be given to demonstrate the accuracy and efficiency of the proposed approach.

INDOOR TRANSMITTER LOCALIZATION VIA DF/AOA TECHNIQUE

*Neslihan YILDIRIM GÜLER[1,2], İbrahim TEKİN[2]

[1]TÜBİTAK-National Research Institute Of Electronics And Cryptology, Gebze/KOCAELİ
[2]Sabancı University, Faculty Of Engineering and Natural Sciences, Orhanlı/İSTANBUL

The location of an indoor transmitter such as a mobile phone in a building can be determined by measuring power or relative timing of the transmitted signal from simultaneous receivers located in the vicinity of the transmitter. A Radio location finding system, consisting of two equivalent direction finders (DF), is placed outside of the building to pinpoint a transmitter located inside the building. Once the bearing angle is obtained from each DF system, the position of the transmitter is simply the intersection of two bearings from the direction finders. The performance of the location finder is directly proportional to the performance of direction finders. In our experiments, we mostly concentrated on the performance measurements of suggested direction finding system at various environments such as indoor and outdoor.

We implemented a one-coordinate direction finder to determine only the azimuthal angle of arrival (AOA) of the transmitted signal. The each DF system is composed of two dipole antenna array operating at the frequency of 155 MHz, receivers, and a laptop computer. A 4-channel sampling oscilloscope with a maximum sampling frequency of 4 Gs/s is used to receive and digitize the received signals. The digitized signals are then transferred to a laptop computer over a GPIB interface for further analysis to extract AOA information. Extraction of AOA information is based on time delay measurement technique. An electromagnetic wave impinging on two antennas separated by a distance of d experiences a time delay. This is due to the additional path that the wave should travel to reach antenna 1 shown in Figure 1. This time delay is a function of antenna separation d ($\leq\lambda/2$), speed of light c and the angle of arrival ϕ, given in Equation 1. One can estimate the angle of arrival ϕ using Equation 1, given the time difference of arrival measurement by the two antennas. The time difference of arrival between the received signals at the antenna terminals can easily be found by cross-correlating the signals. The delay is estimated as the time lag value where the peak of the cross correlation of two antenna signals occurs.

Many experiments in different environments such as anechoic chamber, an indoor RF laboratory and open air sites to measure the performance of direction finder. The initial experiments in full anechoic chamber showed that the system is %100 succesful in distinguishing the directions simply as left, right or front. For the aneoic chamber, both the transmitter and the DF system were located indoors. The results obtained in the RF laboratory were also satisfactory but there were errors arised from multipath effects of walls, windows or other equipments. The remaining of the experiments were done at open air sites where receivers were located outdoors, and the transmitter was indoor. From the data we have collected, the proposed simple DF system will work reasonably well for the location of a tranmitter inside a building.

$$\Delta t = (d/c)\sin\phi \qquad (1)$$
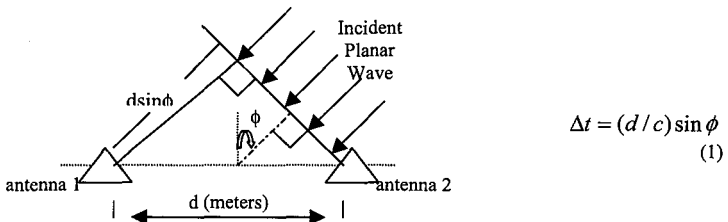
Figure 1: Time delay radio direction finding

Enhancing MIMO Channel Capacity through Co-located Loops and Dipoles

Anand Konanur*, Keyoor Gosalia, Sandeep Krishnamurthy, Brian Hughes and Gianluca Lazzi

Department of Electrical and Computer Engineering,
North Carolina State University, Raleigh, NC 27695-7914, USA

It has been proposed that the use of co-located loops and dipoles, both at the transmitter and receiver of a communication system in a richly scattering environment, can lead to significant increases in MIMO channel capacity. While being compact, these co-located systems compare favorably in terms of capacity with a spatial array with the same number of elements. Since there are three components of electric and three components of magnetic field at a point, a six-fold increase in capacity is theoretically possible. Previously, we had designed antennas with three elements (consisting of a co-polarized loop and two dipoles) and verified the predicted three fold increase in capacity (A. Konanur et al, IEEE AP-S , 2, 531-534, 2003).

As part of the current investigation we have designed an antenna system with four elements consisting of a loop (responding to a magnetic field component) and three orthogonally placed dipoles (responding to the three orthogonal electric field components) with slightly offset feeds. All the elements of the antenna system are well matched at the same frequency (2.2 GHz), with good isolation between themselves. Having designed two such antenna systems, we estimate the channel matrix through S parameter measurements between the various transmitting and receiving antennas. We estimate the ergodic and outage capacities from a set of measured channel matrices. Initial results show an increase in capacity by employing the four element system over and above that of a system employing three elements. Also, the capacity compares favorably with that of a spatial array with four elements. Thus an increase in capacity is observed despite some of the elements being co-polarized, in that an incident field of any polarization elicits a response in more than one antenna.

Such antennas find applications in wireless systems. The increase in capacity and robustness to fading need not be traded for compactness. In this talk, we will present designs of the antennas as well as the calculated channel capacity and compare it to those predicted by a model being developed to describe such MIMO channels.

Propagation Modelling of Composite Inhomogeneous Materials for In-Building Wireless Systems

Michael J. Neve*[†], Allan G. Williamson[†] and R. Paknys[‡]

[†]Department of Electrical & Computer Engineering   [‡]Electrical & Computer Engineering
The University of Auckland   Concordia University
Private Bag 92019, Auckland   Montreal, Quebec
NEW ZEALAND   CANADA

Recent advances in indoor wireless local area network technologies have realised the dream of untethered, low-cost, broadband access to internet services. However, the success (or otherwise) of these systems is very dependent on the decisions made at the time of their deployment — particularly with regard to the affect of the building environment on wireless transmissions. Techniques for modelling and predicting both coverage and levels of interference are needed, and these in turn require an understanding of the influence that composite inhomogeneous materials (which comprise typical building structures) have on the propagating fields. Experimental measurements have been performed and show that structures (such as reinforced concrete service ducts) can appreciably shadow the propagating fields, thereby causing coverage 'holes' or alternatively reducing levels of interference to cochannel users (K. S. Butterworth, K. W. Sowerby and A. G. Williamson, IEEE Trans., COM-48, 658–669, 2000). The majority of techniques/models developed to date are empirically-based, and accordingly do not give insight into the physical nature of the process and their general applicability is therefore questionable.

In this work we are attempting to develop practical planning tools for wireless systems in indoor environments based on analytical electromagnetic models for the propagating fields. To date this work has focussed on the steel wire reinforced concrete slab for which a near-field solution using a Green's function/Method of Moments formulation has been developed (R. Paknys, IEEE Trans., AP-51, 2852–2861, 2003). The initial analysis has shown that the presence of wires complicates the propagation such that the 'spreading loss' as modelled by geometrical optics (for an isolated homogeneous slab) is no longer representative. Techniques for experimentally validating this theory (using a vector network analyser for both a waveguide equivalent and open range measurements of a real slab) and for extracting a mechanistic characterisation from the observations (to form the basis of a useable planning tool) are also discussed.

Multi-Cavity PCB Mounted Enclosure Shielding Effectiveness Measurement and FEM/BE Analysis

Brian A. Lail[1*] and L. Scott Freeman[2]
[1]Department of Electrical and Computer Engineering
University of Central Florida
Orlando, FL 32816

[2] Government Communications Systems Division
Harris Corporation
Melbourne, FL 32902-0037

The coupling of electromagnetic fields between cavities within a single enclosure is considered. Single unit multi-cavity enclosures (SUME) are encountered in packaging as well as in shielded enclosures. Any enclosure that is electrically subdivided is a SUME. In particular, the application of SUME in PCB-mounted applications has become prevalent due to low cost and simple assembly. Previous studies have considered external coupling to single enclosures. In order to better understand the electrical containment and coupling in SUME, a study is carried out to measure and model the shielding effectiveness between cavities of a single enclosure.

A rectangular enclosure with dimensions $6'' \times 4'' \times 1''$ is studied. The enclosure is comprised of three components: the fencing, the lid, and the gasketing. The fencing is further divided into internal and external, however these are electrically bonded together. The external fencing forms the outer perimeter. The internal fencing divides the enclosure into six separate $2'' \times 2'' \times 1''$ sections. The gasketing is bonded to the top portion of the internal fencing. The fencing is designed such that when the lid is installed onto the external fencing it creates a low resistance electrical bond to the internal fencing, which is electrically bonded to the ground plane. Monopoles are mounted within each cavity as transmit and receive antennas. Shielding effectiveness between cavities is determined by sourcing a field within one cavity while measuring the received field in another cavity, with and without the enclosure present.

In order to model the fields within the SUME, a hybrid FEM/BE approach is utilized. The primary coupling is via equivalent apertures, which are modeled via the method of moments. The cavity interiors are modeled with finite elements. This hybrid approach is used to model the coupling between cavities for the same configurations as the measurements. Of primary interest is the peak coupling between cavities. With a single cavity illuminated, various coupled cavities are considered and peak coupling is determined. Additionally, the resonant interactions due to the cavity dimensions and aperture geometries are analyzed.

Applications of Shielding Techniques to Enhance the Antenna Performance and SAR Reduction in Mobile Communications

Shih-Chung Tuan*, Hsi-Tseng Chou and Jin-Song Wang

Dept. of Comm. Eng., Yuan-Ze University, Taiwan

From antenna point of view, current mobile communication systems have faced several difficulties on the performance optimization and SAR reduction.

On the base station side, the sectorization of base station coverage in order to increase the system capacities has resulted in coverage overlapping where handoff between sectors occurs. Due to a wide coverage range (typically 120 degree angular coverage per sector) the antennas usually radiate vertically narrow but horizontal wide patterns. The slowly varying of wide horizontal patterns usually cause large sector coverage overlapping, where the handsets will attach to two sectors simultaneously. It not only wastes the system capacities but also causes more interference to other cells. Similarly, the side- and back- lobes of the sector antenna radiations are also potential sources of interferences to other cells. On the handset side, the antenna radiation in the vicinity of humane head can result in over induction of SAR, and cause health concerns.

In stead of utilizing sophisticated antenna systems such as phased arrays, this paper presents antenna shielding techniques that potentially reduce the impact of the above mentioned problems. In the treatment of base station antenna, resistive plates based on the utilizations of resistive material are designed as shielding plates that are installed on the both sides of antenna horizontally to provide as reflecting surfaces. The fundamental concepts are to reflect the energy of the far end part of main lobe and side lobes from the overlapping regions to the angular regions that require more energy. The advantages of the resistive plates are that the edges are treated by resistive materials and edge diffractions as well as their associated multipath signals can be minimized. Experimental studies are performed in this paper.

In the handset aspects, we employ monopole antennas as demonstrating examples for the reason of omni-directional radiation, and propose magnetic material to design shielding structures. It is noted that near magnetic field has been shown to be the major cause of SAR, in which magnetic materials tend to be good choice in this case. The objectives are to integrate the shielding structures into the antenna and handset design, and therefore retain the integrity of the handset. Numerical studies based on finite difference time domain (FDTD) are performed and presented in this paper.

43

Eigenvalues of Sheath Waves in Uniaxially Anisotropic Plasma

Toshihiro Hashimoto

Yatsushiro National College of Technology, Yatsushiro 866-8501, JAPAN

When a conductor is immersed in a plasma, its surface is surrounded by a sheath. Taking the sheath into account, parameters of a linear antenna immersed in a plasma are deeply affected by the sheath waves. It is important to know the behavior of the sheath waves.

To solve the problem, we assume that (1) the plasma is cold, uniform and lossless, (2) a perfectly conducting cylinder is surrounded by a vacuum sheath with uniform thickness, (3) fields are axially symmetric, and (4) the external static magnetic field is uniform and parallel to the axis of the cylinder and has 0 or infinity in its magnitude. Under our assumptions the fields are separated to E-waves and H-waves. E-waves are discussed here, for those are affected by the external magnetic field more than the others.

From the boundary conditions at the surface of the cylinder and at the outer surface of the sheath, we obtain the secular equation. According to the signs of the square of the wave numbers in the sheath and in the plasma, we can discuss the equation separately. By the behavior of the cylindrical functions we can prove that there are no electromagnetic waves propagating to the radial direction in the plasma. Other main results are (1) the range of the eigenvalues are specified, (2) in isotropic case most eigenvalues are in finite range and one eigenvalue is in the semi-infinite range, (3) there are infinite number of eigenvalues when the plasma is uniaxially anisotropic, and (4) the propagation modes are confined to finite number. We also discuss the eigenvalues numerically. The numerical results agree well with the theoretical discussion. In the isotropic case, there exists the eigenvalue tending to infinity in its magnitude. The mode corresponding to it is a standing wave at the limitation to the cut-off frequency.

Interpretation of resonance at inclined multi-aperture rectangular iris with arbitrary locations in rectangular waveguide

J.A. Ruiz-Cruz and J.M. Rebollar*
Grupo de Electromagnetismo Aplicado y Microondas
ETSI de Telecomunicación, Ciudad Universitaria s/n, 28040, Madrid, SPAIN
E-mail: jmrm@etc.upm.es

Alternative interpretation of resonance of two-apertures iris in terms of the excitation of a TEM field of the structure was proposed by the authors of this contribution at (*2003 USNC/URSI Symp., 226*). This alternative interpretation proposed is very simple and useful to design bandpass filters with some improved stopband attenuation as it has been proposed at (*L. Mospan, VIII Int. Conf. MMET, 503-505, 2000*) and more recently at (*A.A. Kirilenko, MSMW'2001 Symposium, 690-692*). Moreover, this interpretation could be useful to prevent some spurious resonances that arise at some rectangular waveguide devices, therefore helping the designer to improve their electrical performances.

In this paper, with the main aim to confirm our alternative interpretation of the resonance in terms of a TEM field excitation, we consider a modification of the previous ones: a new iris structure composed by inclined multi-aperture rectangulars. The single inclined aperture was analytically analysed at (*R Yang and A.S. Omar, IEEE Trans. MTT- 41, 1461-1463*), and the inclined multi-aperture iris by means of the Generalised Scattering Matrix of generalised 2-port discontinuity concept (*J.M. Rebollar, IEE Proc., 1-7, 1988*). The analysis of the scattering parameters joint to a visualisation of the electromagnetic field vectors in the structure are employed to discuss and validate the interpretation of the resonance.

As a first example, an iris with only two rectangular apertures is considered. The excitation of the only one TEM-resonance is analysed vs. the inclination between the apertures and the waveguide walls.

A second example of an iris with three rectangular apertures is analysed too. The excitation of the two TEM-resonances of this iris it is also studied.

Quantitative results for the resonance frequency positions and field plots at these frequency points for the above mentioned examples will be presented.

The obtained results for the inclined two/three-apertures irises validate the interpretation of resonances in terms of the excited TEM fields.

Application of the 2.5-D Pseudospectral Time-Domain (PSTD) Algorithm to Eccentric Waveguide Analysis

Gang Zhao[*1], Scott A. Wartenberg[2], and Qing H. Liu[1]

[1]Department of Electrical and Computer Engineering, Duke University
Durham, North Carolina 27708
[2]RF Micro Devices, 7628 Thorndike Road
Greensboro, NC 27409

The multidomain pseudospectral time-domain (PSTD) algorithm has been developed as an accurate and flexible tool for the simulation of electromagnetic wave propagation and scattering in inhomogeneous lossy media. It has demonstrated remarkable improvement over the traditional FDTD method in terms of accuracy and efficiency. For a particular application of problems with 2-D inhomogeneities but 3-D field distributions, we have developed the 2.5-D multidomain PSTD algorithm, in which the evaluation of one of the spatial derivatives in Maxwell's equations is simplified by using Fourier transform (G. Zhao and Q. Liu, *IEEE Trans. Antennas Propagat.*, **51**, 619-627, 2003). As a result, the 3-D full wave problem is solved by the 2.5-D PSTD method for a series of 2-D problems, leading to huge savings in CPU time and memory requirement.

The 2.5-D PSTD method is ideal for waveguide analysis, which is essentially a 2.5-D problem since the medium is always invariant in the longitudinal direction. Previously, the 2.5-D PSTD algorithm has been used to calculate the dispersion curve for dielectric waveguide. In this work, we are particularly interested in one application of eccentric circular waveguide with an open side. This type of waveguide is part of a novel design of a multi-layer coaxial-to-microstrip transition system, in which the ground plane is incrementally removed from each metal layer and meanwhile the coaxial line is gradually shifted off-center. The new structure can reduce transmission losses by the minimized impedance discontinuity for the transition between the coaxial cable and the microstrip line (S. A. Wartenberg, and Q. H. Liu, "A coaxial-to-microstrip transition for multi-layer substrates," *IEEE Trans. Microwave Theory Tech.*, in press).

In this work, we apply the 2.5-D PSTD method to study dispersion of modes in the eccentric waveguide problems. The accuracy and efficiency of the PSTD algorithm will be further validated by analytical solutions and experimental data. This investigation is useful for the development of the novel coaxial-to-microstrip transition system.

Extension of Phase Shift by Installing Grooves or Steps in Slit Coupling on the Common Broad Wall between Two Shorted Rectangular Waveguides

Jiro Hirokawa[1], Minoru Furukawa[2], Keizo Cho[3] and Naohisa Goto[4]

[1]Tokyo Institute of Technology, [2]Nihon Dengyo Kosaku, [3]NTT DoCoMo and [4]Takushoku University

The authors proposed full double-layer configuration of a Butler matrix using rectangular waveguides, where the hybrids are used with broad-wall slit coupling and the layers are changed only at places for the phase shifters (J.Hirokawa et al., European Microwave Conf., M36-3, 2002). They also proposed the phase shifter using slit coupling as shown in Fig.1 (J.Hirokawa et al., IEEE AP-S URSI Intl. Symp., 38-9, 2003). A few slots are cut on the common broad-wall of two shorted waveguides. The structure is symmetrical with respect to the origin O in Fig.1. It could give 45-degree delay for a 4-way Butler matrix, but it could not give 22.5-degree and 67.5-degree delay for an 8-way matrix. This paper proposes extension of phase shift by adding grooves or steps above and below the places of the slits as shown in Fig.2 or Fig.3, respectively. The grooves make the phase delay smaller while the steps make it larger.

The phase shifters with two slits are analyzed by the mode matching method. They are designed to suppress the reflection below -40dB and to have a change less than 6 degrees in the transmission phase over a range of 3.9–4.1GHz by using the genetic algorithm and the modified Powell method together (M.Okamoto et. al, Math. Comp., 91, 63-72, 1998). The width a and the height b are 58.1mm and 14.5mm, respectively. The wall thickness t is 0.15mm. The parameters $s_0 = 1.20$mm, $s_1 = 1.52$mm, $l_1 = 0.81$mm and $d_1 = 5.71$mm in the phase shifter with grooves, for instance. Fig. 4 shows the frequency dependence of the transmission phase. The desired amount of phase delay is obtained in each phase shifter at 4.0GHz. The change of the phase delay over the 200MHz range becomes larger or the taper of the line becomes steeper in the figure, as the required amount of phase delay is large. The difference in this change between the 22.5-degree and 67.5-degree phase shifters is 6.4degrees, which is slightly larger than the requirement (6.0degrees). It is confirmed that the reflection is less than -30dB in the 67.5-degree phase shifter and it is below -40dB in the others over the frequency range.
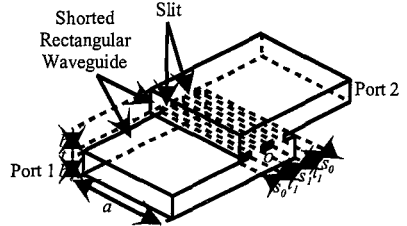
Fig.1 Conventional phase shifter
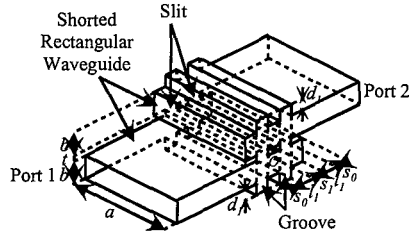
Fig.2 Phase shifter with grooves
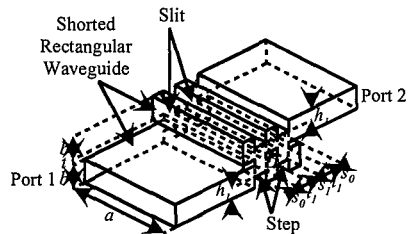
Fig.3 Phase shifter with steps
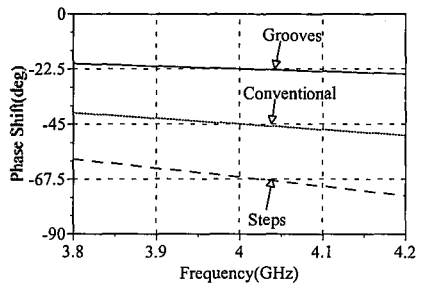
Fig.4 Transmission phase

Micromachining of High Frequency Integrated Waveguide Structures and Circuits

Wai Heng Chow, Anthony Champion and David Paul Steenson
Institute of Microwaves and Photonics, University of Leeds, LS2 9JT, United Kingdom

Commission B: Guided Waves and Wave Guiding Structures

A high precision and cost effective micromachining technique for the fabrication of various high frequency waveguide structures has been developed. The waveguide structures were fabricated using an ultra-thick negative photoresist called SU-8 with the properties of yielding exceptionally high aspect ratio featured with straight and smooth vertical sidewalls leading to its use for the fabrication of various precision waveguide components such as complex transitions, impedance steps, waveguide couplers, etc. Waveguide structures fabricated using SU-8 have high dimensional accuracy, are physically robust and have an excellent surface quality. This technique is sufficiently rapid, flexible and repeatable which permits the realization of complex 3-D waveguide structures with a fast photolithographic technique, basic cleanroom facilities and at low processing temperatures.

This approach also favours precise integration of waveguide structures and E-plane circuits such as finline transitions, metal insert filters, circuits incorporating active devices, and the precise alignment of these circuits is facilitated by the photolithography itself. This integration thus permits the formation of a compact hybrid subcomponent with accurately controlled features and predictable parasitics which are able to exploit the strengths of both the planer and 3-D circuits. The completed SU-8 waveguide structures are subsequently mounted in a conventionally machined metal block for measurement. The metal block was specifically designed so as to be reusable with any similar waveguide components with operating frequency from 75 GHz up to 600 GHz and beyond. The hybrid package incorporates locator pins and holes to enable the split blocks to be aligned and clamped together precisely and repeatability.

This technique is particularly beneficial at high frequencies especially at submillimeter wave and Terahertz frequency region where the dimensions of the waveguide components operating at these frequencies become very small and consequently are more difficult, expensive and time consuming to manufacture by conventional machining techniques especially for waveguide structures featuring complex inner structures. In addition, mounting and aligning active or passive devices inside these waveguides is often difficult. During the design, particular attention has been paid to the electrical performance, cost effectiveness and connectivity aspects with the aim of achieving an approach suited to mass production of various hybrid subcomponents with high commercial potential. A G-band 6-dB branch-guide coupler, an integrated rectangular waveguide with E-plane filter and membrane supported frequency tripler with operating frequencies up to 600 GHz have been fabricated and measured to verify the merit of this micromachining technique.
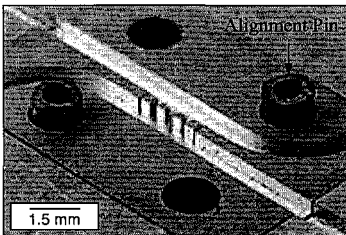
Fig. 1. Micromachined branch-guide coupler with high definition structures.
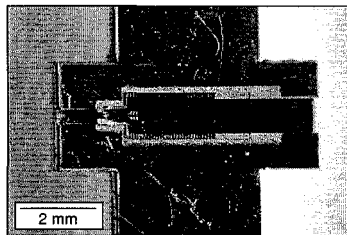
Fig. 2. Membrane supported frequency tripler integrated with stepped waveguide transition.

Dispersion Characteristics of Multilayer Open Microstrip Lines over Thin Metal Ground

L. Zhang[*] and J. M. Song

Department of Electrical and Computer Engineering
Iowa State University, 2215 Coover Hall, Ames, Iowa 50011

Nowadays continued advance of semiconductor techniques makes it possible to fabricate RF, microwave integrated circuit, analog and digital circuitry onto a multilayer-silicon-substrate. Furthermore, with the rising operating frequencies, the dispersion and loss characteristics of signal become essential and critical in the design of silicon based integrate circuits. As a result, the dispersive transmission characteristics of open microstrip over lossy silicon substrate have been studied extensively. And many accurate electromagnetic models are built to predict these frequency dependent properties.

Recently with the complexity of integrated circuitry increasing, most integrated devices are manufactured with deep-sub-micron technology on lossy silicon and metal with thickness in a fraction of a micron, while the working frequencies of most RF components are at GHz frequencies. In this frequency range, the skin depth of electromagnetic wave is in the order of microns, which is much thicker than the metal in interconnects and RF components. Therefore the electromagnetic wave could penetrate this kind of metal ground and reach further deeply into the layers under the mental ground. Considering this phenomenon, it is found the frequency dependent characteristics, such as RLCG (series resistance and inductance and shunt capacitance and conductance) per unit length, have changes remarkably (J.M. Song et. al., IEEE AP-S, 3, 973-976, 2003). However, the wide used classical model of microstrip line only deals with the ground as perfect conductor (PEC) or impedance boundary condition (IBC) which consequently ignores this penetrating effect. Furthermore, current electromagnetic methods do not adequately model the penetration of electromagnetic fields through thin metal layers.

We apply a full-wave analysis of this penetrating phenomenon using spectral domain approach (R. Mitrra and T. Itoh, IEEE Trans. MTT, 21, 496-499, 1973, and 28, 733-736, 1980). The corresponding 2-dimensional Green's function of open microstrip lines over multilayer lossy media is deduced. And method of moment is applied to solve the eigenvalue problem. We present that the electromagnetic field can penetrate a thin metal ground and interact with the layers under the ground. We also show the dispersion characteristics of the microstrip lines as functions of the thickness of the metal ground.

Analysis of Photonic-Crystal Fibers Using a Source-Model Technique

Amit Hochman* and Yehuda Leviatan
Department of Electrical Engineering
Technion - Israel Institute of Technology
Haifa 32000, Israel

A source-model technique (SMT) for the analysis of the modal fields of Photonic-Crystal Fibers (PCF) is described. The formulation is for a general cylindrical waveguide, made of a homogeneous dielectric bounded by an arbitrary smooth curve, which may be multiply-connected. Outside this boundary we assume the medium has the properties of free-space. This general geometry is adequate for the description of a variety of PCFs that have been suggested in the literature, and can take into account the finiteness of the PCF's cross-section.

In the SMT formulation, the field in the dielectric is simulated by the fields of an array of elementary sources located outside the region, near its boundaries. The array radiates in a homogeneous medium with the same parameters as the dielectric. Similarly, the fields in each free-space region outside the dielectric are simulated by an array of sources that surrounds the region, and radiates in free-space. The amplitudes of the sources are adjusted for the continuity conditions across the media boundaries, which are enforced at discrete set of points. This procedure leads to a homogeneous matrix equation for the amplitudes of the sources. Non-trivial solutions to this equation are found for specific pairs of angular frequency ω, and axial propagation constant β, for which the resultant matrix is singular. When these solutions are found, the modal fields can be readily obtained by evaluating the fields of the arrays.

As an example of the application of the method, we analyze a hollow-core PCF, which has a finite cross-section cladding, consisting of a triangular lattice of air veins that run parallel to the PCF axis. The symmetry properties of the structure are used both to classify the modes, and to reduce the computational burden. This is achieved by using arrays of sources which have the same periodicity as the analyzed mode. Strictly-bound modes, which have received little attention in the literature, as well as the more widely analyzed leaky modes, are considered. The strictly-bound modes may have fields confined to the vicinity of the PCF axis by the photonic crystal cladding, and will not be attenuated by radiation in the transverse direction. Modes of this type, which are close to being linearly polarized in the hollow-core of the PCF, will be shown. These modes transport a substantial amount of their power in the hollow-core region. For the leaky modes, calculation of the confinement losses is of interest. These modes can be analyzed by using sources with a complex propagation constant. The singularities of the matrix are then found in the complex β plane, and the losses (in dB/m) are proportional to the imaginary part of β. When β is close to the real line, the losses per wavelength are small, but in dB/m at optical frequencies, may be very large. The calculation of this small imaginary part of β may also be effected by perturbation methods while using sources with real β. The presented numerical results will include confinement losses and also dispersion curves and mode field patterns of a few modes.

Liquid Crystal All Optical Waveguide Switch

Md. Kaisar Khan[*], Thomas X. Wu[1], Yanging Lu[2] and Shin-Tson Wu[2]

[1]Department of ECE, University of Central Florida, Orlando, FL 32816, USA
[2]School of Optics/CREOL, University of Central Florida, Orlando, FL 32816, USA

In general, very high data rates require short duration optical pulses and it is anticipated that these systems will use return to zero (RZ) or soliton-like modulation (P. M. Ramos and C.R. Paiva, "Self-routing switching of solitonlike pulses in multiple-core nonlinear fiber arrays", J. OSA. B vol. 17, pp. 1125-1133, 2000). Therefore optical switches using RZ or soliton-like pulses are of interest, particularly in nonlinear directional couplers. The nonlinear directional coupler functions in the following manner; for low input power the light beam is transferred from one waveguide to the other, but for high input power the light beam remains in the same waveguide as shown in Fig 1.

Over the past years several types of optical switching devices have been used. Still people are investigating different material and technology to support high data rate at the optical network. Liquid crystals (LC) directional coupler is a potential device for this application. Dynamic switching behavior of LC has been determined by the external electric field. To date results have been presented for picoseconds (and ~100 femtosecond) duration pulses using optical fiber (K. Khan, M. Rahman, Xiang Li and M. Potasek, "Effects of pulse separation and bit-rate in multi-terabit/sec all-optical waveguide switches," OSA Conference on Laser and Optics, October 5-9, 2003, Tucson, Arizona). Nonlinear switching behavior of LC is governed by the nonlinear Schroedinger equation. We investigated the bit rate limitations for terabit/sec all optical nonlinear LC directional coupler switches. Our numerical results show that the bit spacing limitation in order to avoid interactions between adjacent pulses. Coupling length limitation due to soliton-soliton interaction has also been studied.
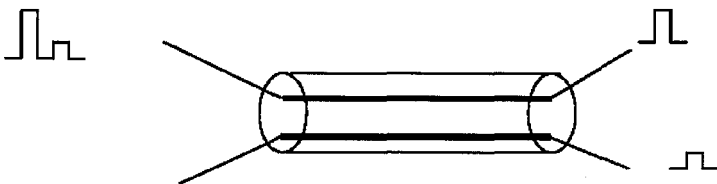
Fig. 1. Configuration of liquid crystal all optical waveguide switch

Non-Uniform Guided Waveguide Modeling of Printed Circuit Board Via Structures

Franz Gisin *
Director, Signal Integrity Design
Sanmina-SCI
2000 Ringwood Avenue
San Jose, CA 95131
franz.gisin@sanmina-sci.com

Dr. Zorica Pantic-Tanner
Dean, School of Engineering
University of Texas at San Antonio
6900 North Loop 1604 West
San Antonio, TX 78249
zptanner@utsa.edu

Abstract

High performance telecommunication and super computing systems routinely transmit digital information between semiconductor devices using serial point-to-point interconnects operating at data rates ranging from 2.5 GB/s to 12.5 Gb/s. A common practice is to interconnect these devices using a star, mesh, or switch-fabric architecture that necessitates routing one to two thousand of these high speed nets across backplanes and midplanes having more than 50 layers and thickness in excess of 0.350". The electrical connection to inner layers of the backplane/midplane is normally accomplished through plated-through hole (PTH) vias that are electrically long at these high data rates.

Historically, PTH via structures have been modeled as a simple lumped element capacitor or a inductance-capacitance-inductance Tee equivalent circuit, where the capacitance is derived from the region where the via passes through a conductive plane and the inductance is derived from the portion of the via barrel located above and below the conductive plane. For high layer count backplanes, however, the conductive layers are not uniformly distributed within the backplane (see Figure 1), nor is the current distribution uniform around the circumference of the via (see Figure 2), in which case equivalent circuit models based on lumped element extractions of quasi-static field solvers do not work very effectively.

To circumvent these problems, a series of via structures were simulated using the FDTD method. Pulse-shaped waveforms were then injected into the via, and its associated performance metrics were then directly obtained from the electric and magnetic fields created in the vicinity of the via as the pulse propagated through the via.
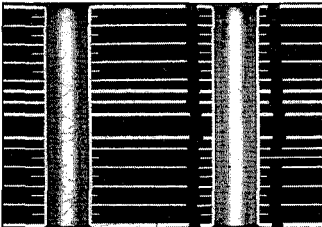
Figure 1
22 Layer Backplane Via Structure
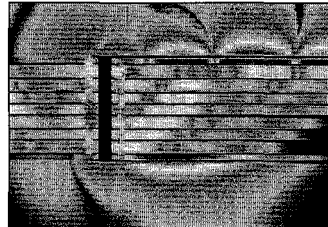
Figure 2
|E x H| Around a Via Structure

52

PROPERTIES OF GUIDED WAVES IN ARRAYS OF PERIODICALLY ARRANGED DIPOLES

Ari J. Viitanen

Electromagnetics Laboratory, Department of Electrical and Communications Engineering, Helsinki University of Technology, P.O.Box 3000, FIN-02015 HUT, Finland

Planar periodical arrangements of inclusions are of interest because they can be used as frequency selective surfaces and guided wave structures in microwave applications. In this study an array of periodical arrangements of dipole particles is considered. The dipoles, which may be small wire antennas or small thin longitudinal dielectric ellipsoids, are oriented in a same direction on a plane and are close to each other, forming a dense dipole array. The geometrical size of every separate inclusion is small compared to the wavelength and each dipole is characterized by the polarizability. To control their properties, the dipoles can be loaded by passive loads. The array forms a wave guiding structure and the properties of guided waves propagating along the dipole array are considered.

The interaction between the dipoles are calculated by full wave method which leads to the dynamic interaction constant of the dipole array. The lattice constant may be comparable to wavelength, then, strong spatial dispersion effects take place. The local field consists of interaction field and external field. The expression for the interaction field is evaluated in dynamic case which is important for obtaining electromagnetic characteristics in wide frequency regime. The interaction field arised from other inclusions in the plane is evaluated by using Fourier transformation such that it contains an infinite double summation expression of Hankel functions. This expression is simplified using recursive identities for Hankel functions and using Poisson summation techniques similarly as given in (P.A. Belov, S.A. Tretyakov, A.J. Viitanen, "Dispersion and reflection properties of artificial media formed by regular lattices of ideally conducting wires," Journal of Electrom. Waves and Applic., Vol. 16, No. 8, 1153-1170, 2002). As a result, an analytical solution for waves propagating along the array is obtained. Because the inclusions can be controlled with external loads, the dipole array can be used as a guided wave structure with controllable properties.

An Efficient Perturbation Analysis of Dielectric Periodic Structure

Xiaomin Yang* and Thomas X. Wu
Department of Electrical and Computer Engineering
University of Central Florida
Orlando, FL 32816

Dielectric grating has broad applications in microwave, millimeter wave, infrared, and optical systems. Although rigorous mode-matching method can give accurate results, it is rather complex and time-consuming.

In this paper, we propose an efficient perturbation analysis together with finite element method for guided wave propagation in dielectric periodic structure. The periodic structure in Fig. 1 can be divided into 3 regions: air region, dielectric layer, and grating layer in between. Using perturbation analysis, the electromagnetic fields in the grating layer are treated as superposition of both unperturbed and perturbed fields. For unperturbed case, the structure can be approximated as a 3-layer uniform planar dielectric waveguide. From its equivalent transmission line model (no source), the input power can be solved. For perturbed case, a periodic perturbation is added to the uniform dielectric waveguide. The space harmonics appear as the result of perturbation to the surface wave. To calculate the radiated space harmonics is to solve the equivalent transmission line (with source) problem. Once we get the transmission line solutions, we may find the expression of every space harmonic. Summing up the leakage power of all the harmonics, we then get the total leakage power. The leakage constant (as shown in Fig. 2) can be easily obtained from the surface wave power and the leaky wave power. At that point, the radiation characteristics of this structure are determined. In this work, we use finite element method (FEM) to solve the transmission line equations in the grating layer.
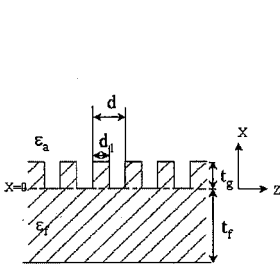
Fig. 1: Dielectric grating structure.
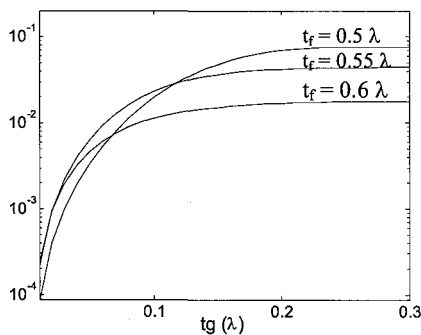
Fig. 2: Leakage constant versus thickness of grating.

An Application of the T Chart for Nonreciprocal Stub Tuners

D. Torrungrueng, C. Thimaporn*, T. Mekathikom and A. Darawankul
Asian University of Science and Technology
Department of Electrical and Electronic Engineering
89 Route 331, Banglamung, Chon Buri, Thailand, 20260
Email: dtg@asianust.ac.th

Nonreciprocal transmission lines have found various applications in microwave technology. Note that a nonreciprocal transmission line has different line parameters for waves propagating in opposite directions. Due to associated governing equations for nonreciprocal transmission lines are complicated, a *generalized* ZY Smith chart, called the T chart, has been developed to assist in analysis and design of nonreciprocal transmission lines. It is found that the T chart depends on the phase angle ϕ of associated characteristic impedances of nonreciprocal transmission lines, and it can be reduced to the *standard* ZY Smith chart when $\phi = 0^o$.

Nonreciprocal stub tuners can be designed using both analytic and T chart solutions. Although analytic solutions are more accurate and useful for computer analysis, they are complicated for *nonreciprocal* stub tuners. In contrast, the T chart solutions are fast, intuitive and accurate in practice. In this paper, the T chart is applied for both *nonreciprocal* single-stub and double-stub tuning circuits. In single-stub tuning, the design parameters are the distance from the load to the stub and the length of the stub. In double-stub tuning, the lengths of the two stubs are required, where the distance between them is fixed. It is interesting to point out that the *forbidden region* for double-stub tuning, where the load cannot be matched, *strongly* depends on the phase angle ϕ. In this study, both shunt and series stubs are considered. It is found that basic procedures for *nonreciprocal* stub tuners using the T chart are similar to those for *reciprocal* ones using the *standard* Smith chart. Due to the phase angle ϕ dependence of the T chart, a computerized T chart software has been developed and applied for studying stub tuners. It is found that results obtained from the software are accurate as compared to analytic solutions.

An Application of the T Chart for Solving Exponentially Tapered Lossless Nonuniform Transmission Line Problems

D. Torrungrueng, C. Thimaporn*, and T. Mekathikom
Asian University of Science and Technology
Department of Electrical and Electronic Engineering
89 Route 331, Banglamung, Chon Buri, Thailand, 20260
Email: dtg@asianust.ac.th

It is well known that *nonuniform* transmission lines (NUTL) have several advantages over uniform ones. One of the NUTL, the exponentially tapered lossless nonuniform transmission line (ETLNUTL), has found various applications in microwave technology as a resonator, an antenna and a matching device suitable for matching two unequal impedances over a *wide band* of frequencies. Due to complicated equations associated with the ETLNUTL, a graphical solution assisting in analysis and design of the ETLNUTL is needed. In the literature, a *generalized* Smith chart, which is one of the graphical solutions, is employed to study the ETLNUTL. It should be pointed out that a generalized Smith chart for the ETLNUTL is *not unique*. In this paper, a generalized ZY Smith chart developed for nonreciprocal lossless uniform transmission lines, called the T chart, is employed to solve ETLNUTL problems readily and intuitively. It should be pointed out that the T chart is totally different from the generalized Smith chart for the ETLNUTL existing in the literature.

In this paper, the voltage and current distributions along the ETLNUTL are determined exactly by solving associated differential equations. Once the voltage and current are known, the expressions of load and input impedances, which are the ratios of the voltage to the current at the load and at the input terminal of the ETLNUTL respectively, are arranged in terms of the voltage reflection coefficient at the load such that the T chart can be applied to solve problems of the ETLNUTL loaded by a *complex* load impedance. It is found that the T chart depends on the taper parameter of the ETLNUTL in a complicated fashion. Thus, a computerized T chart software is developed to study the ETLNUTL for different taper parameters efficiently. In addition, it also provides a useful way of visualizing phenomenon associated with the ETLNUTL. Numerical examples will be shown to illustrate the validity of the T chart for solving ETLNUTL problems.

A Diversity Antenna For 3G Wireless Communications

A.Khaleghi*   ali.khaleghi@lss.supelec.fr
A.Azoulay   alain.azoulay@supelec.fr
J.C.Bolomey   jean-charles.bolomey@supelec.fr

The need to increase the data communication speed in 3G wireless application leads to increase link quality, reduce fading and co-channel interference. Diversity antenna is a solution for 3G wireless communication.

In this paper, a stripped Y-shaped patch diversity antenna with two coaxial feed ports is presented. Operation in 1975-2115 GHz (7% bandwidth without any matching network) and 15dB isolation between the ports makes the stripped antenna structure as a first step for UMTS frequency band (1920-2170 MHz) application. Justification for the design is provided by considering the mutual coupling and Transmission Line Method (TLM) simulations. To evaluate the diversity performance 3D far field is measured and using the available propagation environment models, the Mean Effective Gain (MEG) and the cross correlation coefficient are estimated and lead to diversity gain calculation. The difference in MEG less than 1 dB and correlation coefficient ($\rho_e < 0.3$) for propagation environment (indoor, outdoor, outdoor-indoor) models (combination of Uniform, Gaussian, Laplacian, Elliptical distribution in azimuth and elevation planes) makes it appropriate for diversity application. Results including S-parameters, Radiation patterns, MEG's and correlation coefficients are also presented.

Keywords: Diversity antenna, Wireless, UMTS.

"Submitted for URSI 2004 Commission B (fields and waves); B1.2. Antennas for Wireless communication"

Extra explanation about the paper:

"This paper presents a novel striped printed patch antenna on a dielectric with two coaxial feeds, the structure is fixed on top of a ground plane by some distance between dielectric and ground plane. This structure introduces large band width 7% without any matching network and good performance for diversity application. Also 3D complex radiation pattern combined with some extracted models for propagating environments is used for diversity evaluation. The simulation method is based on Transmission Line Method analysis TLM. Improvement of the antenna with a matching network would make this antenna appropriate for UMTS application"
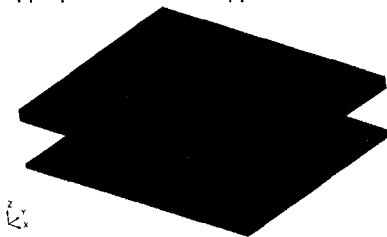
Printed patch diversity antenna, 3d view

Isolated Magnetic Dipole Antenna
for cell phone GPS and ISM applications

Sebastian Rowson, Gregory Poilasne, Laurent Desclos
Ethertronics, 9605 Scranton Road, suite 850, San Diego, CA, 92121

An electrically small, low-profile, antenna structure suitable for mobile devices such as cellular phones, PDAs and laptop computers is presented. One of the challenges in designing these products, continually shrinking, is the integration of internal antennas. Size reduction can be addressed in several ways but the most common are dielectric loading [W. L. Stutzman et al, Antenna Theory and Design, 2nd edition, , John Wiley and Sons, New york, 1981] or capacitive loading [*C.R. Rowell* et al, "A Compact PIFA suitable for dual frequency 900/1800MHz operation", *IEEE TAP,* Vol 46, No 4, April, 1998, pp596-598] of the antenna structure but usually leading to poor efficiencies and isolation. The basic antenna structure is shown in figure 1. The overall structure can be considered as a capacitively loaded inductive loop. The capacity is formed by the two top plates in area A of fig.1, the inductive loop B is formed by connecting the two top plates to the bottom layer. The resonant frequency of the antenna can be estimated using its physical dimensions in figure 1 to calculate L and C of the equivalent electrical circuit.

$$f = \frac{1}{2\pi\sqrt{LC}} \text{ with } L = \mu t\left(\frac{c}{a}\right) \text{ and } C = \varepsilon\frac{ab}{d} \quad f = \frac{1}{2\pi\sqrt{\varepsilon\mu\frac{cbt}{d}}}$$

The return loss of a 25x10x2.5 mm³ GPS antenna installed inside a cellular phone will give a typical 12 MHz bandwidth and around 70% free space efficiency. The various hand positions are also only affecting the magnitude of the matching but no significant detuning. This indicates that the mode created in the antenna mainly using the magnetic dipole behavior is suitable for this implementation. Further results demonstrating the high isolation and efficiency obtained with this antenna structure for GPS and ISM frequencies will also be presented. Multiple configurations based on the same structure will show its high integration flexibility. The radiation mechanism and isolation mechanisms will also be discussed as well as the choice of materials to realize this structure in the most effective way.
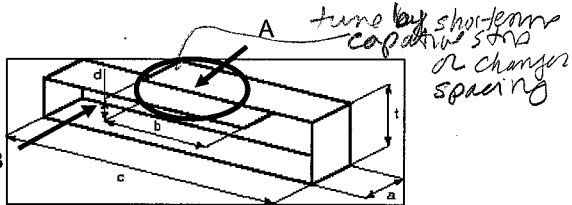
Figure 1: Antenna structure and dimensions used to estimate the resonant frequency of the antenna

58

Internal Antenna Placement on Folding-Type Phones

C. Rowell* and S. Zeilinger (Molex Inc.)

In this presentation, we analyze the different positions an internal antenna may be placed on a folding type phone (i.e. Motorola StarTac). This paper defines an internal antenna as an antenna that is completely within the phone's outer casing. This paper presents the measurement data--VSWR, SAR (specific absorption ratio), and the efficiency--for internal antennas placed on the following locations of a mobile phone: 1. Directly above the ground plane of one of halves of the phone, 2. Near the Mouthpiece of the phone, and 3. In between the two halves of the phone (where the external antenna is typically located). One problem in designing antennas for folding type phones is that the electrical length of the ground plane changes depending on whether the phone is open or closed. When an external antenna is used, the antenna has enough bandwidth (VSWR) to compensate for the change in the electrical length of the phone. Internal antennas, however, are usually narrow-banded and therefore more sensitive to a change in the length of the ground plane. There are several possible solutions, including the following: internal antennas utilizing a large surface area, internal antennas that are effectively external half-wave antennas covered by the phone's casing (these antennas typically have no ground plane directly beneath the antenna), and hybrid antenna combining the two solutions above. The solution of the internal antenna near the mouthpiece of the phone, while giving good VSWR performance, increases the SAR values in the region of the user's mouth. This paper will show that for when an antenna is placed in the mouthpiece of the phone, measuring the SAR values using standard methods gives SAR values within acceptable EU and FCC limits, but measuring the actual "hotspot" will give SAR values much higher than EU and FCC limits.

DESIGN OF A 26GHz UNIPLANAR MARCONI-FRANKLIN TYPE PRINTED ANTENNA ON A HIGH PERMITTIVITY SUBSTRATE

G. Mitropoulos[1], M. Gargalakos [2], R. Makri [2] and N.K. Uzunoglu[*]
[1]: National Technical University of Athens,
[2]: Institute of Communications and Computer Systems,
9, Iroon Polytechniou Str. 15773 Zografou, Athens, Greece
gmitr@esd.ece.ntua.gr

Abstract- A novel uniplanar Marconi-Franklin type printed antenna has been designed, simulated and measured to form part of an antenna phased array, for point-to-multipoint, PMP, radio links, at frequencies between 25.5 and 26.5GHz, following the work presented in paper "Design of a 26GHz Base Station Phased Array Antenna Element" (2003 IEEE AP-S). The current study involves the use of high permittivity dielectric substrate ($\varepsilon r=10$) and the substitution of the two in-plane balanced feed lines by an, in-plane, microstrip line. The choice of a high permittivity substrate is more suitable for the element to be integrated with microwave control devices as a compact antenna system, at frequencies around 26 GHz. The single feed is accomplished by means of an end launch SMA connector, locating on the z-axis. In fig. 1(a), detailed antenna geometry is illustrated, while in fig. 1(b) the manufactured (by the Microelectronics Laboratory of the University of Oulu) prototype is shown:

(a)   (b)
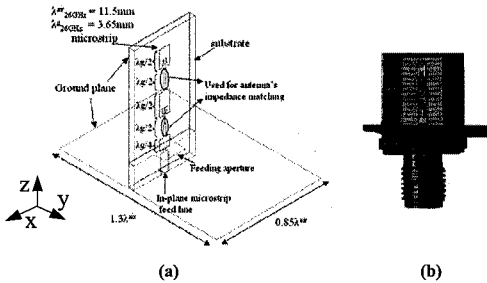
Figure 1: 3-D representation of the antenna geometry (a), manufactured prototype (b)

The proposed antenna has been tuned and simulated using Agilent High Frequency Structure Simulator (HFSS) software. In fig. 2(a)-(b), the simulated return loss (S11 in dB) and the corresponding input impedance loci, presented in a Smith Chart are shown, respectively:

(a)   (b)
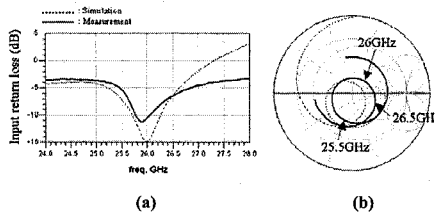
Figure 2: Input return loss (S11 in dB) (a), input impedance loci (b)

Measurements illustrate a clear agreement between theoretical, simulated and measured radiation diagram of the proposed antenna in x-y and y-z planes, having directivity of around 8dB and efficiency of approximately 60%.

60

Circular Scanning Array Antenna for Wireless Applications

C. F. du Toit*, J. E. Kvarnstrand, J. Patel, P. F. Acsadi, C. Sui, J. Norfolk
Paratek Microwave, Inc., 6935G Oakland Mills Road, Columbia, MD21045

In the last few years, wireless local area networks (WLAN), radio frequency identification (RFID) reader systems and Bluetooth® systems have emerged as very active areas of commercial applications and research. In the unlicensed spectrum of operation, the need for scanning antennas capable of suppressing unwanted interference with more gain and directivity is needed. As part of their Dynamically Reconfigurable Wireless Networks (DRWiN[TM]) line of products, Paratek has developed a range of antennas for these wireless applications.

The antenna system that will be described here, consists of a circular arrangement of antenna elements, each facing outward. The phase shifters, based on our Parascan[TM] voltage tunable material technology, together with a novel but simple switching arrangement allow a continuous beam scanning without any scalloping loss typical of a switched beam antenna. An integrated control system ensures seamless scanning of the beam over a full 360° angle. To take advantage of antenna diversity, which some systems support, the DRWiN[TM] antenna is also dual polarized, with the particular type of polarization tailored to the application.

Technical aspects of the DRWiN[TM] antenna will be described, measured antenna patterns will be shown (some are shown below in Fig. 1) and how the antenna integrates into the WLAN communication system, explaining the advantages over alternative approaches.
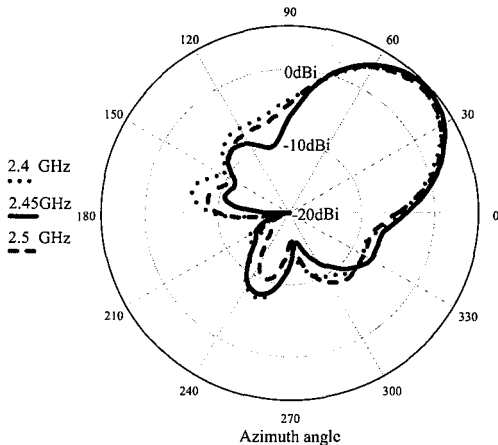
Fig. 1 Typical measured antenna gain patterns, scanned to 45° in the azimuth plane.

A 5-GHz Horizontally Polarized Printed Omnidirectional Antenna for 802.11a WLAN Applications

C.-C. Lin, S.-W. Kuo, and H.-R. Chuang
Department of Electrical Engineering,
National Cheng Kung University, Tainan, Taiwan, R.O.C
Tel: +886 6 2757575~62374   Fax: +886 6 2748690, E-mail: chuangh@ee.ncku.edu.tw
http://empc1.ee.ncku.edu.tw/

In the urban or indoor wireless environment, after complicated multiple reflection or scattering, the polarization of the propagating radio wave may change significantly. It has been reported that, using horizontally polarized antenna at both the transmitter and receiver will result in 10dB more power (in the median), as compared to the power received using vertically polarized antennas at both end of the link.   This paper presents the design simulation, implement, and measurement of a 5GHz omni-directional horizontally polarized planar printed antenna for 802.11a WLAN application. The HFSS 3-D EM simulator is used for design simulation. The antenna is fabricated on a double-sided FR-4 printed circuit board. The antenna pattern measurements are performed for the antenna is alone in free space, printed on a PCMCIA card, and that inserted inside a notebook PC.   In addition to be used alone for a horizontally polarized antenna, it can be also a part of a diversity antenna.

Dual Frequency Stacked-Patch Antenna for VHF-UHF

Vaughn P. Cable
California Institute of Technology
Jet Propulsion Laboratory
vcable@jpl.nasa.gov

Future Earth resource satellites will carry synthetic aperture radar (SAR) for mapping soil moisture over all land masses of the planet. Such systems are currently under study at JPL and elsewhere. Dual frequencies, e.g., one UHF and one VHF, and dual polarizations will be used to differentiate between vegetation canopies and the soil beneath. Relative changes in the observed backscatter for both frequencies and polarizations over time (e.g., season) will be calibrated to provide accurate mapping of soil moisture.

To achieve the desired 1 km resolution on the Earth's surface, the SAR antenna will require a directivity of ~ 30 dBi. This means that the proposed antenna will most likely be a large reflector (e.g., 30 m deployable). However, since the required pattern on the ground is a swath, the reflector does not have to be axially symmetric. Nevertheless, the proposed plan is to deploy a symmetric reflector with a feed that under illuminates in one axis. The candidate feed is a linear, two layer stacked-patch array consisting of 3 VHF elements behind 6 UHF elements (see Figure 1). The original design of this dual band dual polarized patch feed array was done at JPL by Dr. John Huang and presented by him at PIERS 2003. The design frequencies for this array are 137.5 MHz and 435 MHz and the overall dimensions of the full array will be on the order of 3 m x 1 m.

The subject of this presentation is the recent implementation and testing of one subarray of this feed; one VHF patch beneath 2 UHF patches. The prototype subarray is pictured in Figure 2. A pair of capacitively coupled probes and 2 conventional microstrip lines are used to feed the dual polarized (H and V) patches for VHF and UHF, respectively. Construction and testing of this unusually large patch antenna (1.1 m x 1.1 m) will be discussed, and return loss, radiation patterns and gain for will be compared to computer simulated results.
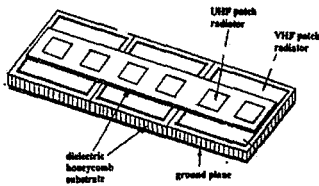
Figure 1. Full array feed (6 UHF patches over 3 VHF patches).
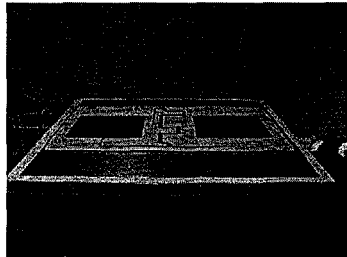
Figure 2. Feed prototype subarray (2 UHF patches over 1 VHF patch).

63

DUAL-BAND ELECTRICALLY SMALL MICROSTRIP ANTENNA

Choon Sae Lee* and Young Rock Cha
Electrical Engineering Department
Southern Methodist University
Dallas, Texas 75275

Microstrip antennas have been widely used in electronic devices for wireless communications because of their advantages over other types of antennas such as low cost and easy fabrication.   Since wireless components become increasingly smaller, the antenna size has to be also reduced.   Moreover the new wireless devices likely require multi-band antennas to receive/transmit signals in different frequency bands.   This presentation introduces a dual-band antenna that is much smaller that a wavelength.

The size of a microstrip antenna is determined by the effective electric length of the radiating patch. It has been proposed that the microstrip antenna size can be reduced substantially by introducing width discontinuities (C. S. Lee and K.-H. Tseng, Electronics Letters, 37, 1274-1275, 2001).   The size reduction scheme with width discontinuities produces a microstrip antenna that is completely planar without any vertical components. The planar structure provides convenience for easy fabrication. The proposed antenna for dual-band operation has double-layer structure, in which each layer contains such a planar microstrip patch with width discontinuities.

For the theoretical analysis, a cavity model is used, in which all the open edges are assumed enclosed by a perfect magnetic conductor (PMC). The cavity model has an advantage compared with other analytic methods in giving a physical intuition for dual-mode operation.   The antenna is designed such that two distinctive resonant modes are excited at desired frequencies.   One of the difficult design problems is to match the input impedances of those two modes simultaneously.   The double-layer structure provides sufficient number of variable geometrical parameters to give proper impedance matching at both frequencies.

The detailed theoretical results will be presented in comparison with experimental data.

Dual-Band BroadBand Microstrip Antenna
Inspired in the Sierpinski Fractal

Jaume Anguera[*][(1)], Enrique Martínez[(2)], Carles Puente[(2)], Carmen Borja[(2)], and Jordi Soler[(2)]

(1)   Technology Department, 358-2, Yatap-Dong, Bundang-Gu, Sungnam-Si, Kyunggi-Do, 463-828: Korea. jaume.anguera@fractus.com
(2)   Technology Department, Alcalde Barnils 64-68, Edificio Testa, Barcelona, Spain

Fractal geometry has been proved as an alternative methodology to design miniature monopole antennas like the Koch monopole, miniature microstrip antennas using the Sierpinski bowtie and Sierpinski gasket, multifrequency monopoles such as the Sierpinski monopole, multifrequency microstrip antennas using the Sierpinski gasket and high directivity patches [*C.Puente, "Fractal Antennas", Ph.D. Dissertation at the Dept. of Signal Theory and Communications, Universitat Politècnica de Catalunya (UPC), July 2001*], [*C.Borja, "Fractal microstrip patch antennas with fractal perimeter and self-affine properties", Ph.D. Dissertation at the Dept. of Signal Theory and Communications, UPC, July 2001*], [*J.Anguera, "Fractal and Broadband Techniques on Miniature, Multifrequency and High-Directivity Microstrip Patch Antennas", Ph.D. Dissertation at the Dept. of Signal Theory and Communications, UPC, July 2003*].

In the presentation, we present a dual-frequency microstrip patch antenna based on the Sierpinski gasket with broadband behavior achieved by using a multi-stacked structure as depicted in Fig.1. In the present case, the technique can be considered multi-mode, that is, we use a single patch radiator having two resonant modes with broadside radiation pattern; the parasitic patches are only for bandwidth enhancing purposes [*J.Anguera, E.Martínez, C.Puente, C.Borja, and J.Soler, "BroadBand Dual-Frequency Microstrip Patch Antenna with Modified Sierpinski Fractal Geometry", IEEE Trans. Antennas and Propagation, accepted paper, to appear in March 2004 issue*], [*"Multi-Triangular Antennas for cellular telephony GSM and DCS", patent app.WO9957784*], [*"Multilevel Antennas", patent app. WO0122528*].

A dual-frequency antenna based on the Sierpinski fractal with two parasitic patches to enhance the impedance bandwidth is presented. An electrical circuit model formed by RLC resonators is proposed to learn about the antenna physical behavior and to achieve the dual band operation minimizing a trial-and-error numerical/measurement proofs. The antenna has been designed using a MoM commercial code and has been experimentally tested, obtaining two bands with a bandwidth around 7%(SWR<2) and similar radiation pattern and gain.
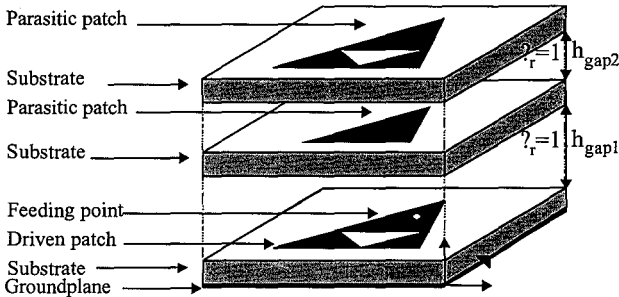
Fig.1 The multi-stacked microstrip patch antenna configuration based on the Sierpinski fractal gasket

Compact Multi-band Antennas for
Universal Mobile Applications

Sripathi Yarasi* and Ted Hebron
Centurion Wireless Technologies Inc., 3425 N 44th Street, Lincoln, NE 68504, USA
E-mail: sripathi.yarasi@centurion.com

Recently there has been a demand to include both American and European frequencies in world type phones with additional frequencies UMTS and GPS. It is known that as the phone gets smaller, the Q of the radiating element gets higher, meaning narrow band characteristics Hence to increase the bandwidth is very challenging. The primary purpose of this paper is the development of innovative and compact antennas for wideband operation. The paper will also show on achieving wide band operations even with a small clamshell type phones.

Meander line and coil antenna techniques were used in making stubby antenna for wide-band operation. Additional passive element matching network was also used to enhance the band-width and without degrading the efficiency of the antenna. These antennas are to be used in different flavors of phone that demonstrate features enable by OEM chipsets. Hand held devices, with this type of compact multi-band antennas, could also be used by service providers (SPs) to check out network functionality. Extending the scope of these antennas, dual/diversity antennas were made on same hand held devices. This type of hand-held devices, with dual antennas, can be used as demonstrators.

Figure 1 shows a typical VSWR plot of a multi band meander-line antenna covering both American, European, GPS and Universal bands. This paper also discusses its associated radiation patterns (both 2-d and 3-d) in all bands.
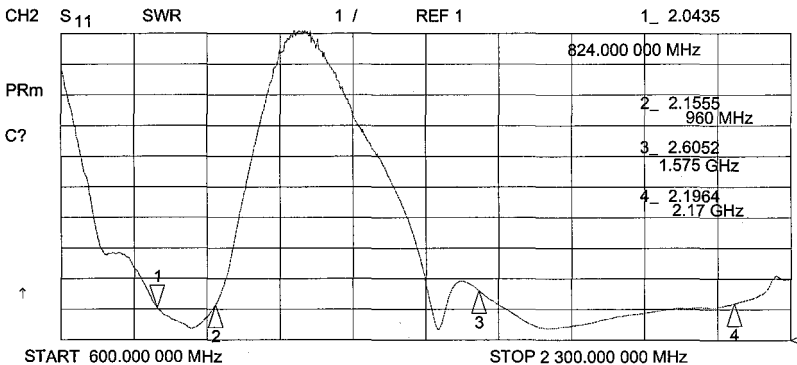
Multi-band capacitively loaded magnetic dipole

G. Poilasne[1], S. Rowson[2], L. Desclos[2]
(1) Now with KWC and Previously with Ethertronics
(2) Ethertronics Inc., San Diego, California, USA
9605, Scranton Rd, suite 850, San Diego, CA, 92121, USA.

Antennas for wireless communication systems have to be efficient and easy to integrate. In this paper, we present an antenna based on a capacitively loaded magnetic dipole –fig.1-. A set of antennas addressing single band and multi band applications will be presented [Patent US 6,456,243 *Poilasne*, Desclos, Rowson, September 24, 2002].

Capacitively loaded magnetic dipoles have the advantage of being very compact due to the capacitive loading, highly efficiency and with a very high out of band rejection (selectivity). During the presentation, we will show the different design and manufacturing trade-offs in order to obtain a high efficiency while keeping a good selectivity. We will also show multiple designs targeting different applications such as GPS, bluetooth or PCS. For GPS application, only one element is required as the targeted bandwidth is 0.4%. Typical dimensions are about 9 mm x 20 mm x 0.7 mm. 70 to 80% efficiency can easily be obtained.

In order to increase the working bandwidth, keeping a good isolation, efficiency and selectivity at the same time, it possible to add parasitic elements. Then, the main element excites the other elements through a magnetic coupling –fig.1-. The parasitic elements are tuned at slightly different frequencies in order to increase the band. Theoretically, an infinite number of elements can be placed, but their contributions to the bandwidth become smaller and smaller. Therefore, practically and by following several design rules, the use of three elements is sufficient. Figure 1 presents an antenna composed of three elements, and figure 2 shows the corresponding return loss. Three peaks appear on the return loss corresponding to the different resonant frequencies. During the presentation, we go over a case study covering the ISM 2.4GHz band showing the different trade-off between one, two or three elements. A typical rejection out of band is 25 dB in this case as the efficiency is 70% in the enclosure.

Fig.1 : 3 dipoles element capacitively loaded coupled magnetically	Fig.2 : Return loss of the antenna figure 1.
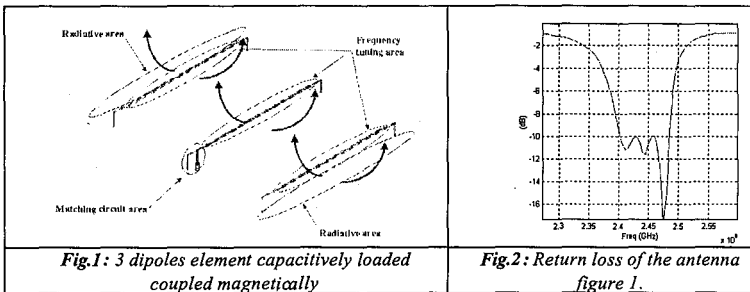
Wide and Tri-Band Microstrip LAN Antenna Design and GUI Tool Using a GA and FDTD

Lance Griffiths*, You Chung Chung, Cynthia Furse
University of Utah
Department of Electrical and Computer Engineering
50 S Central Campus Dr Rm. 3280
Salt Lake City UT 84112-9206
email: lgriffit@eng.utah.edu

Since the introduction of the genetic algorithm (GA) to the electromagnetics community, there has been much interest in using the GA to optimize electromagnetic problems. One such problem is the optimization of microstrip antennas. Microstrip antennas have been optimized with the GA for polarized, dual band operation. The method can be extended further to design multi-band microstrip antennas (H. Choo, H. Ling, "Design of Multiband Microstrip Antennas Using a Genetic Algorithm," IEEE Microwave and Wireless Components Letters, Vol. 12, No. 9, Sept. 2002). Other possible optimization parameters could include changing the dielectric substrate, its thickness, weight, cost, etc., to gain the best results.

This paper adds to this previous work through simultaneous optimization for radiation pattern (directivity and adaptive nulling), polarization, and impedance performance at multiple frequencies. The GA utilizes a combination of adaptable and fixed sections of a microstrip antenna and analyzes using the FDTD method. This makes the GA converge more quickly, thus allowing better optimization of complex designs.

Optimization for tri-band performance and radiation pattern are presented. Return loss is optimized to less that -10 dB for simple antenna feeds. Radiation patterns are optimized for gain in a desired direction. Different methods of generating antenna designs are compared for bandwidth enhancement including allowing the design to be fully or partially adaptable. Wideband designs and sensing applications are also explored.

A simple graphical interface is shown to be very useful in allowing changes to the GA parameters and antenna design goals. The population size, mutation rate, and the percentage of metal fill are available for adjustment. The user is given the choice of frequency bands to optimize for receiving or blocking along with weighting to determine the relative importance of each function. The user also enters the desired direction of radiation and polarizations with accompanying weights. The user can track the GA to see the optimization performed at each generation to check for convergence. This model can be used as a template for other GA interfaces, allowing the GA to better move into industry.

INVESTIGATION OF THE EFFECT OF FRACTAL SHAPES ON THE BROADBAND BEHAVIOR OF 1-DIMENSIONAL OPTIMIZED ANTENNAS

N. Vasiloglou, D. Staiculescu and M. M. Tentzeris
School of ECE, Georgia Tech, Atlanta, GA, 30332-0250, U.S.A.
(nvasil@ieee.org)

The irregularity has been very attractive to the antenna and packaging engineers. More specifically, the self-similarity has inspired many researchers to use them for broadband designs, due to the fact that a fractal antenna is a repeated shape in different scales, which can be interpreted as a multiscale ("multi-wavelength") radiator. In addition to this, the space filling property seems to be ideal for the antenna miniaturization. Although many experiments have verified the above properties, there are also counter examples that show the opposite. Comparison of fractal antennas with non-fractal ones that have some common characteristics, such as total wire length and same geometrical dimension, has shown that the last exhibit better behavior. Another drawback of the fractal antennas is that they are not fully realizable since they require infinite resolution. They can be manufactured up to a limited scale known also in the literature as prefractals. Despite the fact that there is no theorem to guarantee that a prefractal shape maintains the same properties with a fractal, it is empirically known that some properties such as fractal dimension is kept by a prefractal if the scale is small enough. For example internet traffic is a fractal curve although it is discrete.

In order to answer the question whether a fractal antenna is the optimal in bandwidth or miniaturization basis, it is suggested to optimize a generic-model 1-D wire antenna. Measurement of the fractal dimension of the optimal antenna can prove whether fractal properties are the main reason for the broadband behavior. A simple way to parameterize an antenna is to use a delta modulation algorithm. So if a piece of wire is divided into N segments, then it can be described as an N-size vector of $-\Delta$, $+\Delta$ values, leading to a staircase approximation. The cumulative sum of the vector gives the actual shape of the antenna within an error of Δ (quantization error). The authors believe that this is well suited parameterization since it fits to methods like simulated annealing and genetic algorithms. These stochastic optimization methods give a set of suboptimal solution as the uniqueness of the optimum cannot be proved mathematically. The fractal dimension of the suboptimal solutions will be measured with the Minkowski cover algorithm which gives very accurate estimations. The authors hope that the results will give an intuition about the effect of fractal geometry in design and show a direction for the design and optimization of more complex antenna geometries that will not require heavy computations in the future.

Ultra Wideband Array Elements

P S Hall*[1], T.W Hee[1], J Perruisseau[2]

[1]Department of Electronic Engineering, The University of Birmingham, UK
[2] Laboratoire d'Electromagnétisme et d'Acoustique, Ecole Polytechnique
Federale de Lausanne, Switzerland

In recent years, there has been increased interest in wideband and compact antennas. Existing elements of this kind are for instance the single-polarized tapered slot antenna and the dual-polarized spiral antenna. Here, we investigate novel antenna forms, which can be single-polarized but with a possible dual-polarized extension radiating two independent perpendicular single-polarized waves. The aim is to produce antennas that are broadband and low-profile.

It can be seen from Fig 1 that the antenna consists of a printed dipole suspended above an absorbing ground plane. Four connectors are shown in a dual polarized example. Fig 2 shows some of the dipole arms that have been examined. Dipole arms based on a square shape have been chosen to facilitate use in a closely packed array. It has been found that, both plain square (or diamond) dipole and arms based on the fractal Sierpinski carpet can give wideband action. The use of the fractal arrangement gives some reduction in the element size, which is useful to enhance the scan bandwidth in a scanning phased array. Both single layer and double layer elements have been examined. Impedance bandwidths greater than 4 to 1 have been achieved with well-behaved patterns over a smaller bandwidth. Whilst the square plain and Sierpinski carpet shapes have similar performance, the cut-away shape of Fig 2c was found to be necessary for low coupling between the polarizations in the dual polarized element.

Results will be given for various configurations. Measurements have been made with an planar ultra wideband balun based on smooth transitions between microstrip and twin strip line and this will also be described.

| (A) | (B) | (C) |

Fig 1 Ultra wideband element   Fig 2 Some of the dipole arms
                                    examined
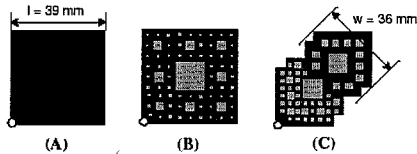
Ferro-Electric Materials for Miniaturizing Broad-Band Antennas

Kevin Buell*, Hossein Mosallaei, and Kamal Sarabandi

Radiation Laboratory
Department of Electrical Engineering and Computer Science
University of Michigan
Ann Arbor, MI 48109-2122, USA
E-mail: kbuell@umich.edu, hosseinm@umich.edu, saraband@umich.edu

Miniaturizing Broad-Band Antennas: Resonant antennas compose a major category of broad-band antennas and new developments in Ferro-Electric materials promise impressive potential benefits in broadband antenna miniaturization.

Resonant antenna bandwidth restrictions may be interpreted in terms of an antenna 'Q'-factor. Antenna Q-factor is both the ratio of energy stored to dissipated energy, and resonator bandwidth. This explains why antennas on lossy dielectrics exhibit high bandwidth while antennas aggressively miniaturized by dielectric scaling exhibit reduced bandwidth.

Dielectric miniaturization exploits the wavelength-scaling of the $\mu\epsilon$ product to achieve a large electromagnetic length from a physically short geometry ($\lambda_{medium} = \frac{Freq}{\sqrt{\mu_r\mu_0\epsilon_r\epsilon_0}}$). Increasing ϵ alone decreases the $\frac{\mu}{\epsilon}$ ratio and the intrinsic impedance of the medium ($\eta = \sqrt{\frac{\mu_r\mu_0}{\epsilon_r\epsilon_0}}$). This causes an impedance mismatch and reflections at the free space boundary. Waves internally reflected in antenna dielectrics do not radiate and these trapped waves increase the energy stored in the near-field, increasing the antenna Q-factor and reducing its bandwidth.

If relative permeability is matched to the dielectric constant these trapped waves are eliminated, significantly improving input matching. For example, a narrow-band patch antenna over a dielectric and ground-plane. Simulations show that for an aggressive miniaturization with $\epsilon_r = 25, tan_{\delta e} = 0.001$ surface waves trap energy, limiting bandwidth (0.64%) and efficiency (77%). With magnetic materials, $\epsilon_r = \mu_r = 5, tan_{\delta e} = tan_{\delta m} = 0.001$ the trapping of waves is eliminated and bandwidth improves better than by a factor of ten (7.94%) and efficiency is almost perfect (99%).

A resonant broad-band antenna has been developed named the FourPoint Antenna (Figure 1) offering 67% bandwidth with low dielectric substrates (Suh, Stutzman, and Davis, AP Symposium, 256-259, 2003).

Ferro-Electric Materials: Magnetic Ferrites are magnetic ceramics with a permeability greater than free-space. When properly processed certain garnet and hexagonal ferrites can provide useful, moderately low loss ($tan_\delta < 0.02$) permeabilities in the region of 50-500MHz by exploiting their uniaxial two-dimensional degeneracy. This VHF/UHF region is where miniaturization is most beneficial.

New ceramics exhibit the desired $\epsilon_r = \mu_r$ property in this useful frequency range. Alignment of the degenerate axis tangential to the substrate surface ($\mu_x = \mu_y$) produces a substrate appropriate

Figure 1: FourPoint Antenna

for broadband planar antennas and impedance matched to free space. These Ferro-Electric materials should enable us to miniaturize antenna design while maintaining broadband operation.

CHARACTERISTICS OF MICROSTRIP-FED PRINTED BOW-TIE ANTENNA FOR WIDEBAND PHASED ARRAY SYSTEMS

Abdelnasser A. Eldek, Atef Z. Elsherbeni and Charles E. Smith

Center of Applied Electromagnetic Systems Research (CAESR)
Department of Electrical Engineering, The University of Mississippi
University, MS 38677
atef@olemiss.edu

Printed microstrip antennas are widely used in phased array applications due to their advantages of being small, lightweight, high efficiency and ease of installation. Among the most widely used printed antennas used in phased array systems are printed dipoles and printed quasi Yagi antennas. The second type consists of printed dipole with a rectangular director element and fed by microstrip feed line through microstrip-to-coplanar strip transition. In this paper, the printed dipole and the director is replaced by a printed bow-tie, with expectation of bandwidth and gain improvements because printed bow-tie antennas are planar-type variations of the biconical antenna that has wideband characteristics. Moreover, the radiating area of the bow-tie is larger than that of the dipole, therefore gain improvement is expected. The simulation and analysis for this new antenna are performed using the commercial computer software package, Ansoft HFSS, which is based on the finite element method. Measurements of the return loss and radiation pattern are also conducted.

The proposed antenna is printed on Rogers RT/Duroid 6010/6010 LM substrate of thickness 25 mil. The antenna geometry and parameters are shown in Fig. 1 while the measured and simulated return loss for (W1, W2, W3, L1, L2, L3, L4, S) = (0.6, 0.3, 7, 9.9, 4.0, 1.7, 1.7, 2.1, 0.2 mm) are shown in Fig. 2. According to the measured return loss, this new antenna is operating from 6.7 to 12.5GHz with 60% bandwidth. The computed gain is 4.15dB while the gain of the corresponding quasi Yagi antenna is 3.11dB. The gain of two elements of this antenna is 7.5 dB while the corresponding gain of the quasi Yagi antenna is 5.4 dB. It is also worth mentioning that the coupling between elements for a linear array of these antenna elements is about 5 dB less than that of the corresponding configuration based on printed dipole and the radiator antennas.
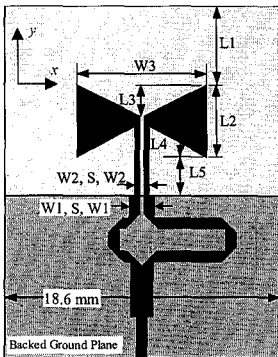
Fig. 1. Antenna geometry.
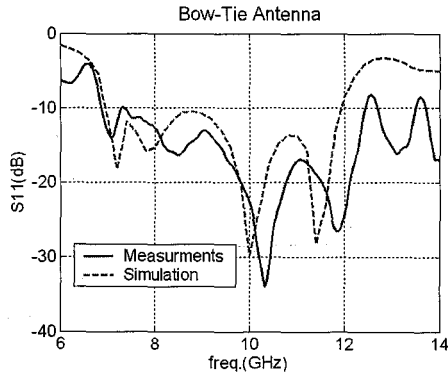
Fig. 2. Measured and simulated return loss.

72

Double-Sided Printed Bow-Tie Antenna for UWB Applications

K. Kiminami, A. Hirata*, and T. Shiozawa

Dept. of Communications Eng., Osaka Univ., 2-1 Yamada-oka, 565-0871 Osaka, Japan
Fax: +81-6-6879-7690, E-mail:hirata@comm.eng.osaka-u.ac.jp

Abstract: Much attention has been paid to commercial UWB systems, since the FCC adopted a "First Report and Order" that permits the marketing and operation of a new radio transmission technology in February 2002. Among others, it is of a particular interest to design a compact antenna with good impedance matching characteristics over the whole UWB frequency range (3.1- 10.6 GHz).

  Patch antennas are extensively used in wireless communications because of the following features: light weight, low cost, and ease to fabricate. However, it is well known that the bandwidth of patch antennas is narrow. Thus, many attempts have been made to widen the bandwidth of printed antennas. Bow-tie antennas are one of the promising candidates for UWB applications. However, the bandwidth of conventional printed bow-tie antennas is not yet sufficient to cover the ultrawide frequency band. In this paper, a double-sided printed bow-tie antenna is proposed (See Fig.1).

  The design of the double-sided printed bow-tie antenna was performed in an iterative manner. First, the widths of microstrip lines and twin-lead transmission line are determined so that their impedances reduce to coincident with 50 Ohm. Then, the rest parameters of a matching circuit (L_1, L_2, L_3, W_1, W_2, W_3) and the width of the bow-tie antenna (L) are optimized so that the return loss of the antenna becomes smaller than 10 dB over the specified frequency band. For this purpose, IE3D, which is a MoM / GA optimization code, is used. Figure 2 shows the return loss of the antenna with an optimal set of parameters. In order to verify the result obtained by IE3D, that by the FDTD method is also plotted. From this figure, the antenna proposed in this paper satisfies the requirement as a UWB antenna; return loss less than 10 dB over the frequency range of 3.1-10.6 GHz. More detailed discussion on this antenna will be presented at the conference.
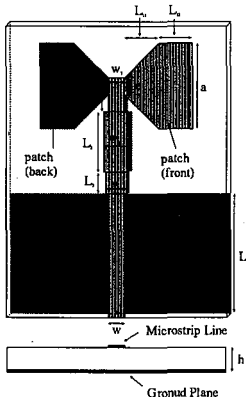
Fig.1 Geometry of the problem.
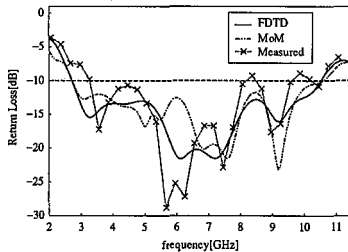
Fig.2 Return loss of the antenna.

ANOMALOUS BEHAVIOR OF THE TEM MODE WHEN RADIATING FROM AN OPEN-ENDED CIRCULAR WAVEGUIDE WITH IDEAL HARD WALL

Sergei P. Skobelev[1] and Per-Simon Kildal[2]

[1]JSC "Radiophyzika", 10, Geroev Panfilovtsev str., Moscow 125363, Russia
E-mail: jscapex@online.ru
[2]Antenna Group, Chalmers University of Technology
S-412 96 Gothenburg, Sweden
E-mail: simon@elmagn.chalmers.se

One of the important applications of the so-called hard surfaces is the TEM-mode horn antennas with high aperture efficiency and low cross-polarization. In this connection, the problem of electromagnetic radiation from the hard open-ended circular waveguide is of interest both in its own right and as a part of a more complex problem for the horn of finite length. The problem for the circular aperture corresponding to a longitudinally corrugated hard waveguide was solved first approximately (M. S. Aly and S. F. Mahmoud, *IEE Proc.* **132**(H), 7, 477-479, 1985) using the Kirchhoff-Huygens (KH) method. A rigorous approach, developed on the basis of the mode-matching method combined with the rigorous solution obtained by the Winer-Hopf-Weinstein method (S. P. Skobelev and P.-S. Kildal, *IEEE Trans.* **51**, 10, 2723-2731, 2003), has allowed considerable refining the results of the conventional approach.

In the present study, the problem of electromagnetic radiation from an open-ended circular waveguide exited in the dominant TEM mode is considered. The TEM mode is supported by the ideal zero thickness hard wall in the form of a pipe perfectly conducting the electric and magnetic currents in the longitudinal direction. By using the Weinstein method, the problem for the wall current spectral densities is reduced to the functional equations corresponding to the hard acoustic waveguide excited in the fundamental axially symmetrical mode. The rigorous solution obtained shows that the radiation pattern and aperture efficiency are the same as those for the acoustic case. However, the field of the reflected TEM mode, unlike that of the incident mode, shows the anomaly of being concentrated at the outer waveguide surface due to the wall anisotropy.

The results for the current-pipe model described above are compared to those obtained using the combined mode-matching/Weinstein method applied to a semi-infinite hard corrugated circular waveguide with the hard wall parameters corresponding to infinite permittivity of the material filling in the grooves of the longitudinally corrugated surface.

A Beam Steering Antenna Controlled with a EBG Material

P. Ratajczak*, P.Y. Garel, P. Brachat
France Telecom R&D, Antenna Department, 06320 La Turbie, France
philippe.ratajczak@francetelecom.com

In this communication, we purpose to present a omni-directional antenna associated to a Controllable Electromagnetic BandGap material in order to obtain a multi-band (GSM, DCS, UMTS) beam steering base station antenna.

The EBG material is a lattice of metallic wires where PIN diodes are inserted along each wire. So this EBG structure can be switched between two different states (reflector or transparent) in a large frequency band starting from zero GHz thanks to metallic periodic structure (*De Lustrac and all, proceeding AP2000, Davos, April 2000*). In order to control the radiation over 360° in the azimuth plane, the lattice has a multi-layers cylindrical distribution and it's placed around the omni-directional probe. The required coverage (single or multi-beam) is obtained by switching off the diodes for the desired azimuth directions and beamwidths.

The simulations with SR3D (*Ratajczak and al, JINA 2002, Nice, November 2002*) show the capabilities of this association (the experiments was realized with a simplified breadboard without diodes in the EBG material, we put or remove continuous metallic wires):

• the matching of the probe inside the EBG material although the behavior as cylindrical reflector of the EBG (fig. 1). We can see a good agreement between experiments and simulations. The input impedance could be optimized in order to eliminate parasitic resonance in the frequency bands.

fig. 1: S.W.R

• the control of the azimuth angle and the width of a single beam, or the management of multi-beam coverage (fig. 2) (the radiation pattern in E^θ polarization is plotted in a 2D polar representation where the axis agrees to $\theta = 0°$ and the exterior circle $\theta = 180°$).
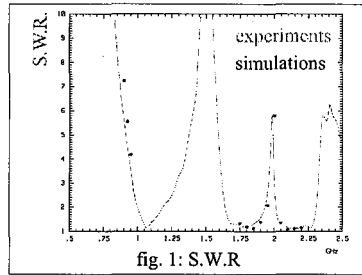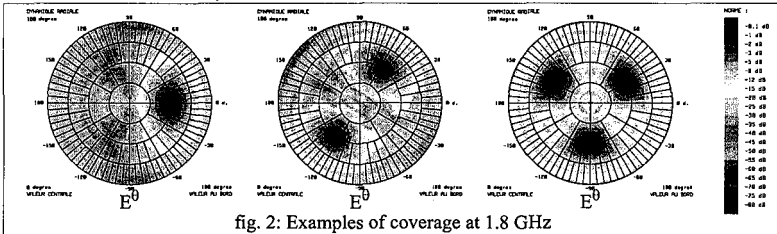
fig. 2: Examples of coverage at 1.8 GHz

The manufacturing of the complete structure with the diodes and the controlled system is actually in progress and would validate the concept of a beam steering base station antenna with a controllable EBG material.

Review of Empirical and Analysis Techniques to Derive Trends in EMI Effects Data

R. L. Gardner, Consultant
6152 Manchester Park Circle
Alexandria, VA 22310
Robert.L.Gardner@verizon.net

The prediction of electronic upset or burnout due to the illumination of a system by an electromagnetic wave begins with a description of the environment at the target and ends with a statement of the likely outcome. Traditionally, analytical techniques have been used to describe the coupling of the wave into the electronic system, predict currents near sensitive components and use threshold analysis to describe the end state of the target. In the end, the success of these predictions is judged by their agreement with experiments. Inference directly from the empirical results forms another way of building the tools for outcome prediction in electromagnetic interference (EMI) research.

The authors [Gardner, Stoudt and Latess, *Proceedings of the International Conference on Electromagnetics in Advanced Applications*, page 191, Turin, 2001] have previously described a multivariate statistical approach to deriving trends from empirical data taken from measured outcomes of hostile illuminations of electronic equipment. This technique is very powerful as long as there is sufficient data available. Not only can we develop a trend from this technique, but we can also easily get an idea of the quality of the fit as compared to the quality of the data itself.

Neural networks are much more powerful tools for finding complex patterns than traditional statistical methods but the neural net literature is far behind the statistical literature in finding goodness of fit data. We can find very complex patterns in the data using neural net techniques.

The paper uses computer failure data from the literature to demonstrate some simple feed forward networks and statistical methods. Unfortunately, there are few data sets available in the open literature. This paper uses most of the available ones to develop empirical as well as physical trends in the analysis.

Tradeoffs for Data Communication Protocols with Multiple Interfering Signals

I. Kohlberg*
Institute for Defense Analyses,
4850 Mark Center Drive, Alexandria, VA 22311, (703) 578-2744, ikohlber@ida.org

R. Boling
Institute for Defense Analyses
4850 Mark Center Drive, Alexandria, VA 22311, (703) 845-2105, rboling@ida.org

Intentional Electro-magnetic Interference (IEMI), directed at electronic and communication systems such as those used on aircraft, LANs, and computers, can cause serious disruption of a transmitted bit-stream, leading to a possible interruption in the flow of information and even loss of stability in controlled processes. Because the aforementioned systems normally operate in a secure environment, high signal-to-noise ratio (S/N), they frequently have minimal immunity to robust pulsed IEMI.

Boling and Kohlberg showed (ICEAA, Turin, Sept.2003) that bit errors due to pulsed interference in data communications could be completely eliminated for a wide class of waveforms by properly encoding signals. The price paid for error-free communications is a lower data rate and an increase in transceiver complexity. The greatest gain from message coding occurs for systems in which the interfering pulse repetition rate is significantly slower than the signaling bit rate, or where the pulse width of the interfering pulse is less than or comparable to the signaling bit pulse width.

In realistic environments (e.g., those that contain many scattering surfaces in a single room), an ideal single interfering pulse is rarely encountered. Multiple scattering of the incident pulse occurs. Each scattering event stretches and reshapes the previous incident pulse. In a recent paper (URSI, Boulder, 2004), the authors developed a generalized scattering model to show how multiple scattering could affect bit errors, and began the development for a rough bound on the effective data transmission rate as a function of bit pulse width using an average reflection coefficient. This paper extends the previous work to include actual reflection coefficients and associated pulse stretching from specific environments and equipment. Included within this context are contributions from diffraction effects at scattering surface edges.

Error-correcting coding schemes can mitigate the effects of unwanted modified incident waveforms. Choices in coding schemes and associated tradeoffs to determine the optimum communications capability include the following: incident waveform, basic EMC/EMI attenuation and multiple scattering. Examples of these tradeoffs are rendered.

77

Impact of Parameter Class Choices within the Framework of Multivariate Logistic Regression Applied to the Analysis of EMI Effects Data

Cynthia Ropiak[1]* and Paul Hayes[2]
[1]Envisioneering, Inc.
4485 Danube Drive, Suite 46
King George, VA 22485
CRopiak@earthlink.net
[2]CEMTACH Group
9964 Francis Folsom Dr.
King George, VA 22485
CEMTACH@earthlink.net

The analysis and subsequent application of results from electromagnetic interference (EMI) experiments is central to the success of any program aimed at generating susceptibility information for electronic equipment of interest. Devising a model that accurately captures the results of an EMI effects experiment in some functional form is generally a primary goal of the experiment. A secondary and arguably more important objective is for the model to be exportable, reasonably independent of the test house so that one may use the model to predict the outcome of new EMI experiments, or to simply draw general conclusions about the response of the test objects (electronic equipment) used in the experiment. Generalized models then permit cost savings and reasonable estimates (within confidence bounds of the model) of untestable scenarios.

The model itself should provide a functional connection between experimental parameters and the resulting EMI effects on the test objects. The more general the parameters, the better the chance of result exportability. For example, parameter classes that include things such as source location and orientation will be inherently tied to the source, whereas parameters classes that include things such as peak electric field on target or peak power on target are less dependent on that particular source and may be generalized to the point of association with a source type (or class of sources) making the results broader in applicability. Hence, the closer the parameter class choices are to electromagnetic (EM) environment descriptions and less contingent on source specifics the better.

Toward this end, a fabricated EMI data set is created and combined with a simulated EM environment. The statistical technique known as multivariate logistic regression (MLR) is used to provide a model for the data set. Different parameter class choices ranging from the most restrictive, source parameters, through electromagnetic environment parameters, and ending with induced current parameters are investigated. The strengths and weaknesses of each type of parameter class are investigated as they pertain to the accuracy of the fitted model as well as its exportability.

Effects of External EMI Pulses on Microprocessor Instruction Execution

P. Mazumder and B. Wang, Univ. of Michigan, Ann Arbor, MI 48109

To account for the performance degradation and circuit failures resulting from high-power invasive EM pulses that are coupled into power-line superimposing high-voltage pulses, we study here the EMI noise induced instruction failure mechanisms inside a generic RISC microprocessor chip. Fig. 1 shows the architecture of the studied baseline RISC microprocessor which is designed with 0.5 μm technology, includes 44 instructions. Our instruction failure simulation methodology is based on the timing analysis of synchronized digital circuits involving level-sensitive latches. Fig. 2 shows the instruction failure simulation flow. Firstly through critical path analysis with level-sensitive latches, we obtained the threshold power supply voltage for the normal execution of individual instructions in various catalogues. Secondly we generalized the timing analysis approach and applied it to the analysis of EMI noise impact on the execution of programs by considering the transient power-supply levels and correlation between adjacent instructions. The CPU cycle frequency degradation percentage, which measures the program failures possibilities due to EMI noise, can range from 7-26%, depending on whether the program is arithmetic intensive, logic intensive or memory I/O intensive.
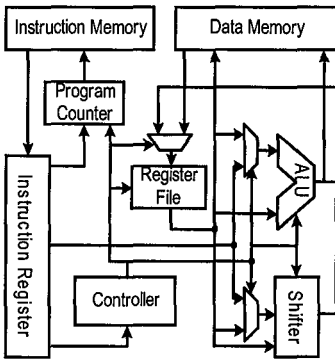
Fig. 1. The baseline RISC
microprocessor architecture
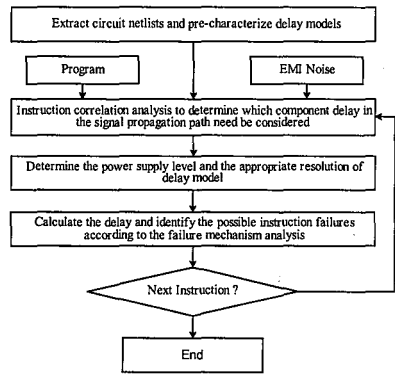
Fig. 2. EMI noise induced instruction
failure simulation procedure

In practical design of power/ground (p/g) network, the IR drop caused by the parasitic resistance has to be taken into account. The EMI noises on the voltage supply may deteriorate the voltage distribution on the chip (fig. 3). The EMI simulator performs the simulation to generate the voltage fluctuation on the p/g network. Based on the failure models described in Fig. 2 and the voltage distribution, the failure map is obtained to demonstrate at what condition of EMI the chip will fail.

The simulations in our study show that ALU is the part most sensitive to EMI noises. If the EMI noises have an amplitude of 25% of the supply voltage, the ALU will very likely fail.
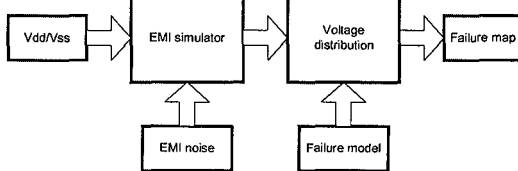
Fig. 3. EMI simulator and Failure map.

Diurnal and Synoptic Impacts on Coastal Ocean Radio Refractivity in the Lee of a Cold Front

Edward H. Burgess, III* and Robert E. Marshall, Naval Surface Warfare Center, Dahlgren Division, J Ross Rottier, The Johns Hopkins University Applied Physics Laboratory

Daytime heating of continental air flowing offshore in the lee of an east coast cold front passage creates a stable atmospheric boundary layer (ABL) over the colder downstream ocean. Increasingly drier air crosses the coastline and advects offshore hours after the cold front passes and effects of surface heating are evident. This will produce negative water vapor gradients in the stable layer. Atmospheric stability and negative water vapor gradients combine to produce superrefractive propagation.

This paper will present the results of a case study that demonstrates how diurnal heating in northwesterly flow during the Wallops Island 2000 Microwave Propagation Measurement Experiment (MPME) resulted in an extended radar horizon.

During the study day, northwesterly flow in the lee of a mid latitude cyclone pumped colder and drier air over the MPME area. As the day advanced, surface heating over the land increased the air temperature before it flowed over the marine surface layer producing a stronger stable layer. Lagging hours behind in the flow was drier Canadian air that eventually reached the coastline and dried the upper levels of the stable layer. This created a negative water vapor gradient. The combination of diurnal heating and synoptic drying produced a superrefractive propagation environment.

Land and sea based surface meteorological observations will show the diurnal heating and synoptic drying. A combination of range dependent marine atmospheric boundary layer (MABL) thermodynamic profiles, one-way propagation data, and S-band Space Range Radar (SPANDAR) clutter to noise ratio data from NASA/Wallops will demonstrate the spatio-temporal structure of the MABL and the resulting propagation environment.

The Relationship Between Modified Radio Refractivity and the Structure of the Atmospheric Boundary Layer-A Mathematical Bridge Between Radio and Atmospheric Scientists

Robert E. Marshall* and Edward H. Burgess, III, Naval Surface Warfare Center, Dahlgren Division, J Ross Rottier, The Johns Hopkins University Applied Physics Laboratory

Modified radio refractivity is employed by radio scientists to characterize propagation experienced by land and sea based communication and radar systems. The vertical structure of modified radio refractivity is a direct result of the vertical distribution of atmospheric temperature, pressure, and water vapor imposed by the structure of the atmospheric boundary layer (ABL).

Atmospheric scientists characterize the thermodynamic structure of the ABL in terms of the vertical gradients of potential temperature and water vapor mixing ratio. Potential temperature and water vapor mixing ratio are conserved in a well-mixed layer driven by mechanical and/or convective turbulence. Potential temperature is considered a measure of atmospheric stability in unsaturated ABLs.

A mathematical relationship between the vertical gradient of modified radio refractivity and the vertical gradients of potential temperature, water vapor mixing ratio, and atmospheric pressure is derived. This relationship indicates that in an idealized well-mixed layer in which potential temperature and water vapor mixing ratio are conserved, modified radio refractivity is weakly dependent on air temperature and pressure, is dependent to a lesser degree on water vapor, and remains in the normal range of clear air propagation one (1) to thirteen (13) M units above standard.

It is also demonstrated that ABL stability forces propagation towards superrefraction and that this tendency is enhanced as the water vapor mixing ratio decreases with height. In unstable layers in which water vapor mixing ratio is nearly conserved, it is demonstrated that propagation tends to remain in the normal range. It is shown that stable layers with positive water vapor mixing ratio gradients tend towards subrefraction with modified radio refractivity a strong function of temperature and humidity.

The validity of the derived relationship for various ABL structures is verified using measured marine atmospheric boundary layer profiles taken off Wallops Island, Virginia.

Rules of Thumb for Formation of Radar Surface Ducts

J Ross Rottier*, The Johns Hopkins University Applied Physics Laboratory
Robert E. Marshall and Edward H. Burgess, III, Naval Surface Warfare Center, Dahlgren Division

Radar surface ducts can have an important impact on radar performance. Surface ducts are caused by refractivity inversions that result from humidity and temperature inversions at altitudes of less than a km over the ocean or land surface. Some surface duct cases have been documented in the literature, which specify atmospheric conditions that produced the required inversions and resulting surface ducts. Prediction of these conditions requires careful observation of atmospheric parameters such as mean wind direction, atmospheric stratification, and vertical profiles of temperature and humidity.

Accurate meteorological observations are generally not available at sea to adequately characterize the local marine atmospheric for prediction of refractive features. Large-scale models may not resolve the physical parameters sufficiently to make accurate predictions and typically miss mesoscale features, such as the seabreeze that can lead to surface ducting. Mesoscale models are time consuming, not readily available, and require accurate observations that are generally not available.

Therefore we attempt to characterize conditions known to lead to the formation of radar surface ducts, to develop heuristic "rules of thumb" for the creation of surface ducts. It is anticipated that such rules would be useful at sea by alerting a ship to the likelihood of duct formation, when accurate predictions are not available. Rules are divided into 7 categories: 1) mean offshore flow, 2) mean onshore flow with topographic blocking, 3) mean onshore flow with shallow topography, 4) sea-breeze, 5) offshore mean wind shift, 6) subsidence compression of the marine boundary layer, and 7) thundercloud outflow. Examples taken from the literature, numerical studies, and unpublished observations are analyzed to provide an initial set of rules.

A Mesoscale Modeling Study of Wallops 2000 EM Refractivity Conditions

Stephen D. Burk[*] and Tracy Haack
Naval Research Laboratory
Monterey, CA

During the period (April-May 2000) of a field experiment at Wallops Island, VA, measurements were taken by groups from DOD laboratories, universities, and elsewhere including low-elevation radar frequency pathloss, meteorological conditions (e.g., from buoys, rocketsondes, helicopter profiles), and radar clutter returns (an extensive description of the field campaign appears in TR-01/132 of the Naval Surface Weapons Division, Dahlgren Division by Stapleton et al.). The "Delmarva" or Tidewater Peninsula along which Wallops Island lies (the Chesapeake Bay to the west and the Atlantic Ocean to the east) contains complex topographic and land surface characteristics, as well as pronounced spatial SST variability, all contributing to complex BL structures (e.g., internal BL's; sea/land breezes; coastal jets). This study uses the Naval Research Laboratory's Coupled Ocean/Atmosphere Mesoscale Prediction System (COAMPS) to investigate refractive structure during selected portions of Wallops-2000. To explore the COAMPS fidelity in forecasting subtle BL and refractivity variations in this region, we nest COAMPS down to an inner grid mesh having 3 km spacing and utilize high vertical resolution in the first several hundred meters above the surface. During the field experiment, measurements were collected along radials extending SE from the coast at Wallops I. a distance of ~65 km over the Atlantic. Similarity theory permits computation of evaporation duct height (EDH) based on the standard meteorological and oceanographic measurements. Model forecast EDH values may then be compared with those computed from observations. The nature of the refractivity profile above the surface layer (e.g., subrefractive, standard, superrefractive, trapping) was measured by the rocketsondes and helicopter profiles, including horizontal variations in refractive conditions along the measurement path. The ability of COAMPS to predict refractive structure and its variation along the measurement path will be assessed. Time periods dominated by synoptic forcing and frontal passages, as well as periods primarily forced on the mesoscale and diurnally will be addressed. Given the difficulty of this forecasting task, model shortcomings are anticipated and will be quantified; the data set will be used to explore and test methods of improving model parameterizations, boundary conditions, etc. Upon completion of such mesoscale model refinements, propagation forecasts using model refractivity fields will be compared with measured propagation factors.

COASTAL AND SEASONAL VARIABILITY OF MARINE LAYER ELECTROMAGNETIC TRAPPING CONDITIONS

Tracy Haack[*] & Stephen D. Burk
Naval Research Laboratory
Marine Meteorology Division
7 Grace Hopper Ave.
Monterey, CA 93943-5502
Phone: (831) 656-4727; Fax: (831) 656-4769
Email: haack@nrlmry.navy.mil

Abstract

The inhomogeneous nature of the marine atmospheric boundary layer (MABL) in coastal regions greatly affects vertical profiles of modified refractivity R_m. Layers defined by a negative gradient of R_m, responsible for trapping and ducting electromagnetic (EM) energy, are often found at the top of the MABL. As the MABL interacts with variations in the coastline and coastal topography, the depth of these layers may dramatically lower and thin or elevate and expand, and the intensity of trapping may strengthen or diminish. Recently numerical model forecasts of meteorological conditions have been employed to diagnose the topography of these EM ducting layers.

Utilizing output from a 9 km resolution COAMPS™[1] reanalysis over the U.S. West Coast, 3D hourly forecast fields of modified refractivity are computed for four months during 1999 each representing a different season. Statistical verification and time series comparison of buoy observations provide confidence in the model forecasts. From the fields of R_m, monthly averages of surface evaporative duct height, MABL duct occurrence, base height, strength, and thickness are obtained and examined to determine seasonal changes and coastal variability. The averages indicate that ducts are least likely to form in April when the percent occurrence is ~25% all along the coast, and are more frequent during October where they increase southward from 50% to 90%. Further, October trapping layers tend to be lower, thinner and stronger than the other months. Spatial distribution of EM ducting layers can provide valuable insight for locating optimal regions of extended signal ranges or potential radar holes along the U. S. West Coast.

---

[1] COAMPS is a trademark of the Naval Research Laboratory

PREDICTING LOW ALTITUDE RADAR DETECTION RANGES OVER THE OCEAN FROM METEOROLOGICAL DATA

Paul A. Frederickson* and Kenneth L. Davidson
Dept. of Meteorology, Naval Postgraduate School, Monterey, CA 93943-5114
Phone: (831) 656-2407; FAX: (831) 656-3061; pafreder@nps.navy.mil

Near-surface atmospheric physics and microwave propagation models have been developed to the point that high-fidelity radar detection range predictions are possible, given good quality meteorological data and target characterizations. In this study we will examine the use of the Naval Postgraduate School's Operational Bulk Evaporation Duct Model (NOBED) in conjunction with the Advanced Refractive Effects Prediction System (AREPS) to predict the radar detection of surface targets over the ocean.

The NOBED model is based upon Monin-Obukhov Similarity theory and uses the well-known and verified COARE surface layer model. Given time-averaged (or "bulk") values of wind speed, air and sea temperature and relative humidity, the NOBED model produces an estimate of the evaporation duct height and a vertical profile of the modified refractivity. This modified refractivity profile is then used by AREPS to determine the height versus range coverage of propagation loss, assuming a horizontally homogeneous atmosphere. Given a propagation loss detection threshold for a specific target, the radar detection range can then be estimated by finding the maximum range where the detection threshold propagation loss occurs at the target height.

In this study we will demonstrate how the predicted radar detection ranges vary as the atmospheric conditions, radar frequency and antenna heights change. A parametric examination will also be presented to show how measurement uncertainties in the NOBED model input parameters ultimately result in detection range prediction errors and how these errors vary with atmospheric conditions. Meteorological data obtained from the NPS buoy off the east and west U.S. coasts and Hawaii will be used to demonstrate how operationally significant detection range variations occur in littoral regions due to diurnal and synoptic phenomenon. Finally, we will compare detection range predictions derived from the Navy's Coupled Ocean-Atmosphere Mesoscale Prediction System (COAMPS) model and from in situ buoy measurements to examine whether radar performance can be accurately predicted in coastal regions up to a day in advance.

Commission F1 (Propagation Modeling and Measurements)

Uncertainty Analysis in the Refractivity from Clutter (RFC) Problem

Caglar Yardim*, Peter Gerstoft, and William S Hodgkiss

Marine Physical Laboratory, University of California San Diego
La Jolla, CA, 92037 - 0238 USA

Ducting, which usually is an important problem in seaborne radar applications, is caused by the refractivity inversion just above the sea surface. It can significantly affect low altitude propagation and hence there has been extensive research on estimating the ducting effects. This requires either measuring or estimating the refractivity profile above the surface. Traditionally, rocket or radio-sonde measurements are carried out for this purpose. Estimation of the refractivity profile using the radar clutter return has recently received attention.

Previously, refractivity profiles were estimated using radar sea clutter data in conjunction with Genetic Algorithms [P.Gerstoft et al, Radio Science, Vol.38, No.3, 8053, 2003]. Although these techniques provide us with estimates of the refractivity profiles, they do not give sufficient, unbiased information about the uncertainties in these estimated values. This is an important problem since the lack of knowledge of the uncertainties will strain the credibility of the overall inversion results.

To address the uncertainties in the estimated parameters, we need to determine basic quantities such as the mean, variance and marginal posterior probability distribution of each estimated parameter. These values also correspond to the moments of the multi-dimensional posterior probability density (PPD) and hence can be computed by taking multi-dimensional integrals of the PPD, which can be accomplished by utilization of a Monte Carlo sampling method.

This paper applies the Metropolis-Hastings sampling method to estimate the uncertainties in the RFC inversion problem. Metropolis Sampling is currently being used with success in areas with similar problems such as quantifying the uncertainties in geoacoustic inversion [S.E.Dosso, J. Acoust. Soc. Am., Vol. 111, No.1, Jan. 2002]. It specifically is selected because it estimates the aforementioned quantities by providing an unbiased sampling of the PPD, unlike genetic algorithms, which usually over-sample the peaks of the PPD and introduce a bias.

The Metropolis-Hastings sampling algorithm used in this work is first tested on synthetic data created by the Terrain Parabolic Equation program (TPEM) [A.E.Barrios, IEEE Trans. Antennas Propagat., Vol 42, pp. 90-98, Jan. 1994] and then applied to the data collected from the Wallops '98 measurement campaign conducted by Naval Surface Warfare Center, Dahlgren Division.

Effects of Rain on Millimeter-Wave (MMW) Line-of-Sight Communication: Time-Domain Analysis

Urachada Ketprom, Sermsak Jaruwatanadilok, Yasuo Kuga*, and Akira Ishimaru
Department of Electrical Engineering, Box 352500,
University of Washington, Seattle WA 98195-2500

Abstract

Millimeter-wave (MMW) and free space optics (FSO) communication systems are recently emerging as reliable and low-cost systems for line-of-sight communication in urban areas. Both MMW and FSO degrade under adverse weather conditions, but the MMW system is superior in performance compared to FSO in fog, clouds and smog where particle sizes are usually less than few micrometers. In the past, there have been extensive analytical and numerical studies of the attenuation characteristics of MMW through rain. If multiple scattering due to heavy rain cannot be ignored, the most accurate method to estimate the attenuation is the numerical solution of the radiative transfer theory. However, the previous research was usually limited to the CW case, and a study of the propagation characteristics of modulated MMW has not attracted much attention [R. Cheung and A. Ishimaru, "Multiple scattering effects on wave propagation due to rain," *Annales des Telecommunications*, 35, pp. 373-379, November-December 1980]. The effects of scattering and absorption degrade the quality of the communication link resulting in an increased bit-error-rate. Therefore, there exists a need for accurate channel characterization in the time-domain to understand and mitigate the problem. In this paper, radiative transfer theory is employed to study the behavior of an amplitude-modulated signal propagating through a random medium. We show the effects of the medium on a modulated signal and relate the outcome to the quality of the communication. Our approach is based on a new formulation of the CW radiative transfer equation, and it has also been applied to "photon density wave imaging" and FSO.

Modeling of Time Reversal Propagation
With Application to Communication and Imaging

*L. Li and L. Carin
Department of Electrical & Computer Engineering.
Duke University, Durham, NC USA

Time-reversal propagation was first demonstrated in nonlinear optics and was studied in detail in underwater acoustics. The property of reciprocity allows one to retransmit a time-reversed version of a multi-path dispersed probe pulse back to its origin, arriving time reversed, with the multi-path structure having been undone. To implement time reversal, a source-receiver array is typically used. It consists of an array of source-receivers that receive the probe signal coming from the transmitter, store it, and later reproduce it backwards in time. The generated waves propagate in a manner reciprocal to the original field, such that energy is automatically redirected towards the focus.

The environmentally self-adaptive mechanism in the time-reversal process makes it useful for various applications. It can be used to implement covert communications inside a multi-path environment, and high resolution imaging as well. In this paper, the propagation in the time-reversal process is simulated by a ray-tracing program. In electromagnetic communication, the role of the multi-path in communication quality is carefully examined. Results show that as the number of ray paths increases, the convergence of the reverse-transmitted signal gets better, however, at a price of losing much of the signal intensity, which is directly related to the signal-to-noise ratio. In other words, there is a trade-off between the 'covertness' of the signal and 'capacity' of the propagation channel.

The concept of time-reversal propagation is also applied to imaging in highly cluttered media. The forward scattering problem consists of transmitting signals from the source, which interacts with the random background media and the target, and receiving the highly distorted signal at the receiver-array. To separate the target-response from the 'background noise', which comes solely from the clutters, the received signal is subtracted from the clutter-response, leaving only the constituents that are involved with the target. In the TRM imaging, the Green's functions, which are responsible for propagation to and from the target, are matched only at points where the phase conjugation occurs, leading to a constructive adding of the image at the location of the target.

Application of PDE Methods for the Analysis of Scattering from Irregular Surfaces in Urban Areas

M. D. Casciato[1]* *Member, IEEE*, W. Thiel[1] *Member, IEEE*, and K. Sarabandi[2] *Fellow, IEEE*

[1]EMAG Technologies
1340 Eisenhower Place, Ann Arbor, MI 48108
phone: (734) 973-6600, email:casciato@eecs.umich.edu
[2]The University of Michigan
1301 Beal Avenue, Ann Arbor, MI 48109-2122
phone: (734) 936-1575, email: saraband@eecs.umich.edu

One of the most commonly used methods for the prediction of radio wave propagation is ray tracing. Current ray-tracing algorithms, when applied to urban propagation, model building faces as flat dielectric or impedance surfaces. While this is an acceptable approximation at low frequencies, at shorter wavelengths any surface irregularities can significantly effect the reflection and diffraction of radio waves, and must be accounted for. These irregularities can include surface grooves, indentations, recessed windows, etc. Also the impedance change across the surface, from concrete or steel to windows can also have a significant effect on the radio wave. The large size of the building structure precludes the brute force application of more exact numerical techniques, such as the Method of Moments (MoM), Finite Element Method (FEM), or the Finite Difference Time Domain (FDTD) method. In addition, high frequency techniques, such as ray-tracing, are inaccurate when these perturbations in the building surface are on the order of a wavelength. While ray-tracing methods are of acceptable accuracy as the electrical dimensions of the surface irregularities increase, the ray density necessary to capture the fineness of the structural details, makes the problem computationally intractable.

With these inherent limitations in current ray tracing techniques, a method is sought to model the reflection and diffraction from building surfaces in urban areas, in an accurate, and yet computationally tractable way. By studying the phenomenology of the scattering and diffraction of buildings it is proposed to develop a set of statistical algebraic models, or macromodels (MM), which when applied will accurately account for building reflection and diffraction, including fine features of the buildings. These MM will be developed in an heuristic fashion, based on analysis of the statistics of the reflected and diffracted fields from various building configurations, generated by applying locally an exact or numerical method on the building structure. For example, in order to study building reflections, an area of the building face will be simulated with the numerical method, and through a Monte Carlo simulation, the area statistically varied (essentially moved do a different area of the building face), and the statistics of the reflection coefficient generated for a given type of building. The developed MMs will be fully polarimetric, and the goal is to generate a library of these statistical reflection and diffraction coefficients, particular to certain types or classes of buildings, with the intent of providing an accurate and efficient method to account for the effect of building irregularities on wave propagation.

The application of partial differential techniques (PDEs), such as FEM, and FDTD, to the development of the MM, will inherently allow for the simulation of diverse structures, and also for the inclusion of fine details of building features. These methods are particularly useful for modeling objects which can have varied and layered dielectric properties, as well as an irregular or rough surface. The application of these methods is limited in the maximum size of the object to be simulated (say on the order of one to five wavelengths, depending on the method applied), and therefore the simulation will be restricted to sections of a building. In order to eliminate unwanted edge effects, inherent in the artificial limitation of the computational domain, a polarimetric, tapered beam approach will be applied.

Alleviation of Multipath Effects by Beacon Design

Ju-Lung Chu*, Chih-Feng Chou, and Jean-Fu Kiang
Department of Electrical Engineering and
Graduate Institute of Communication Engineering
National Taiwan University, Taipei, Taiwan, ROC
E-mail : jfkiang@cc.ee.ntu.edu.tw

The performance of wireless communication systems built for vehicular use is affected by factors like modulation, encryption, interleaving, bandwidth, vehicular speed, distribution of scatterers, base station distributions, weather, terrain, and so on. This work will focus on the effects of local environment. The signals scattered from a large number of nearby objects cause multipath effects on the receivers. The path loss, carrier frequency shifts and signal time delay in such a scenario can be described in terms of transmit signal strength, free-space path loss, reflection, Doppler shifts and time delays. In this work, we propose a concept of multipath-free zone in which these problems might be alleviated, hence the vehicular speed limit and communication performance can be increased at the same time.

In the multipath-free zone, directional antennas are used in the roadside base station to restrict the signal coverage in both uplink and downlink. The directional antenna restricts its coverage area to the line-of-sight (LOS) path to the receiver. In this configuration, it is reasonable to assume the LOS path exists in space above vehicles most of the time. However, the LOS path may be blocked behind a tall truck, for example, and degrade the expected performance. In such cases, antenna diversity techniques can be applied to alleviate the problems, and its effectiveness will be evaluated.

Since the coverage area is restricted, the base station will not receive signals scattered from out of the coverage. However, signals scattered from nearby vehicles in the same coverage area are also expected. In general, the smaller the coverage of each transceiver is, the less multipath effects will be incurred.

Other issues like high handoff rates, base station number, frequency allocation, and so on, may be raised due to the short communication link time. There are other parameters like suitable size of communication zone, transmitting power, and space diversity that need to be determined to optimize the system performances.

Dual Band Reconfigurable Slot Antennas Using Lumped Elements

Nader Behdad[*], and Kamal Sarabandi

Department of Electrical Engineering and Computer Science
University of Michigan, Ann Arbor, MI, 48109-2122
behdad@eecs.umich.edu, saraband@eecs.umich.edu

Dual band antennas are of interest in many wireless applications that use two different frequency bands for receiving and transmitting. Current advancements in printed antenna technology have resulted in a variety of different techniques for designing low profile, cost effective, and highly efficient dual band antennas. Most of these techniques use different methods to manipulate the current distribution of one of the higher order resonant modes of the structure and change its resonant frequency [Wong, K. L., *Compact and Broadband Microstrip Antennas*, Wiley, New York, 2002]. A class of antennas that is suitable for miniaturization and has great reconfigurability potentials without compromising efficiency is slot antennas. However, not much attention has been given to developing slot antenna topologies with dual band characteristics. In this paper, we propose a new technique to design reconfigurable dual band slot antennas.

This technique is based on loading a slot antenna with one or more fixed or variable capacitors to change the effective electrical length of the slot. If appropriately placed, the capacitors also lower both the first and second resonant frequencies or equivalently reduce the antenna's electrical size. The change in resonant frequency is a function of the number, value, and location of the capacitors. Therefore by replacing the capacitor with a varactor, it becomes possible to tune the resonant frequencies of both bands. Since both frequencies have similar electric field distributions, the antenna radiation patterns at both frequencies are similar which is essential for many dual band antennas. With this technique frequency ratios as low as 1.1:1 or as high as 1.8:1 can easily be obtained. Figure 1 shows a typical antenna response with f_u/f_l ratio of 1.8. It is shown that by changing the capacitor from 0.2pF to 2pF, f_u and f_l change over 1.38 GHz and 0.8 GHz respectively. Figure 2 shows the measured radiation patterns of the antenna at both frequency bands for a typical measurement. Details of the design procedure will be discussed and measurement results of a number of reconfigurable dual band antennas with different frequency ratios as low as 1.1 and as high as 1.8 will be presented.
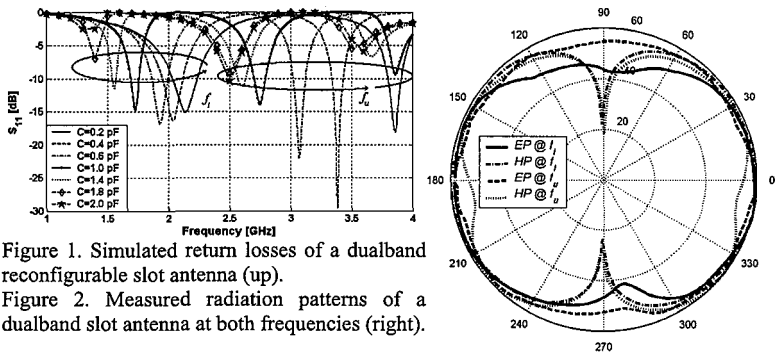
Figure 1. Simulated return losses of a dualband reconfigurable slot antenna (up).
Figure 2. Measured radiation patterns of a dualband slot antenna at both frequencies (right).

A Pattern Reconfigurable Microstrip Antenna Using Solid State Switches

S. Zhang* and J. T. Bernhard
Electromagnetics Laboratory
Department of Electrical and Computer Engineering
University of Illinois at Urbana-Champaign
Urbana, IL 61801
jbernhar@uiuc.edu; http://antennas.ece.uiuc.edu

Application of smart antennas on base stations has enabled systems to avoid noise sources and jammers and improve security. In recent years, pattern reconfigurable antennas in portable units have been proposed to further improve system performance and extend the battery life of wireless devices. There have been several reports on compact pattern reconfigurable antennas. Most of them use binary switches or varactors to control the current distribution on the antenna and hence control the radiation pattern (e.g., R. L. Li and V. F. Fusco, *Proc. IEEE Antennas Propagat. Soc. Int. Symp.*, 4, 788–791, 2001), and some of them use electrically controlled microactuators to achieve the desired reconfigurability (e.g., J. -C. Chiao, et al., *Int. J. RF Microw. CAE*, 11, 301-309, 2001).

This work reports on a diode-controlled pattern reconfigurable microstrip monoarray antenna. In comparison with some of the aforementioned antennas, this antenna has the advantages of being conformal, low cost, and easy to integrate. The antenna consists of a probe fed center monopole with parasitic monopoles on both sides, each with two switched connections. A proof-of-concept study using copper strips has shown that, by changing the lengths of parasitic monopoles to be longer or shorter than the driven monopole, the maximum radiation direction of the antenna in H-plane shifts between +35°, 0° and -35° with respect to broadside while maintaining a constant 2:1 VSWR bandwidth. PIN diodes are implemented as electrically controlled switches. The parasitic parameters of the diodes and the bias network affect the current distribution on the antenna. In particular, care must be taken to properly design the bias network so that the desired frequency response and beam tilt are achieved. Both simulations and measurements of diode-equipped monoarray antennas will be presented that illustrate the effects of diodes and bias network integration on this antenna.

Design and Analysis of Switching Circuits for Reconfigurable Antennas

S. Iyer* (iyer.28@osu.edu) and R. G. Rojas (rojas-teran.1@osu.edu)
The Ohio State University, Electrical Engineering, ElectroScience Laboratory
Columbus, OH 43212

Reconfigurable antennas can in principle modify in real time their radiation patterns, frequency of operation, polarization and other such characteristics. Switching circuits are used to modify the currents on the antenna and thus provide the reconfigurability. Therefore, the design of the switching circuit has a major impact on the achievable reconfigurability. Switching can be implemented using electronic means like PIN diodes or using electromechanical switches like MEMS.

The antenna under consideration proposes to implement pattern reconfigurability using electronic switching. For this purpose, the patch antenna is surrounded by a conductive switch-loaded ring. The reconfigurability is achieved through the use of switching strips located at specific positions around the ring. The switching is controlled through the use of appropriately biased PIN diodes. The switching action of the diodes leads to different ring geometries, and consequently different surface currents are set up for the on and off states of the diodes. This leads to the pattern reconfigurability. The biasing arrangement, in addition to switching the diodes between the on and off states, should also provide for isolation of the DC bias from the RF path, and prevent leakage of the RF signal into the DC bias path. Simulations on just an isolated switching section of the ring do not provide a proper insight into the working of the switch, and its effect on the overall pattern. The entire antenna structure including the switch-loaded ring needs to be simulated and the effect of biasing the diodes on and off on the pattern needs to be considered.

The patch with the switch-loaded ring was simulated using a Finite Element Method (FEM) simulator. The diodes were modeled using sheet impedance surfaces. Low and high impedance values simulated the forward and reverse bias conditions of the diodes, respectively. The capacitors and chokes were assigned appropriate values to discrete RLC elements. The simulations revealed the dependence of the far field pattern on a variety of factors. Shown in figure 1, the spacing between the two switching strips S in the switching gap affects the pattern, as do the lengths of the bias lines used for biasing the diodes. Further, the orientation of the bias lines with respect to the ring conductor also has a bearing on the pattern. The width of the switch-loaded ring W and the distance of the ring from the patch are also seen to have an effect on the pattern. All these factors were adjusted so as to achieve the maximum reconfigurability. Various results will be presented as well as design guidelines and physical interpretation of the effect of the switching circuits on the behavior of the reconfigurable antenna.
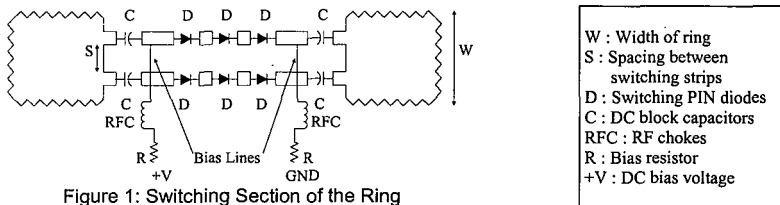
Figure 1: Switching Section of the Ring

W : Width of ring
S : Spacing between switching strips
D : Switching PIN diodes
C : DC block capacitors
RFC : RF chokes
R : Bias resistor
+V : DC bias voltage

93

Simplicity Study for a Self-Structuring Antenna in an Automobile Environment

B.T. Perry* and E.J. Rothwell

Department of Electrical and Computer Engineering, Michigan State University, East Lansing, MI 48824 e-mail:rothwell@egr.msu.edu

J. E. Ross

John Ross & Associates, 422 N. Chicago Street, Salt Lake City, Utah e-mail:johnross@johnross.com

L.L. Nagy

Delphi Research Labs, 51786 Shelby Pkwy, Shelby Township, MI

As in all design problems, the tradeoff between cost and functionality plays a major role in the design of the self-structuring antenna (SSA). To this end, a study was undertaken to determine the minimum number of switches required for proper functionality of the SSA in an automobile. We consider the simulation of a FM band self-structuring antenna placed in the upper part of the rear window of an automobile. Included in the simulations are the car body and the heater grid, which is located in the lower portion of the rear window, as well as the self-structuring antenna.

The simplification scheme used for this study involved decreasing the number of switches in the SSA template in several stages from 16 to 12, 8, and finally 4. This was done while maintaining the same overall size for the SSA template. Wire segment spacing inside the SSA template was increased with each simplification step in order to fill the template in a nearly uniform fashion.

Analysis was done using the Numerical Electromagnetics Code in the FM band (88-108 MHz), utilizing the standing wave ratio to determine the suitability of a given SSA configuration for use in the automobile. In the cases of 12 and 16 switches, a genetic algorithm was used to optimize the states of the self structuring antenna. This was done using GA-NEC, a software package developed by John Ross & Associates. For the cases of 4 and 8 switches, exhaustive searches were used to evaluate every possible self-structuring antenna configuration.

Design of Focal Plane Arrays for Lens-based Scanning Systems

Carsten Barth*, Abbas Abbaspour-Tamijani, Kamal Sarabandi

Department of Electrical Engineering and Computer Science, University of Michigan
Ann Arbor, MI 48109-2122, USA
E-mail: caba@umich.edu

ABSTRACT

Beam steering systems based on phase shifters are generally complex and expensive due to difficulties associated with fabrication, assembly and biasing of the phase shifters. Alternatively, focal plane scanning systems use a microwave lens and a feed matrix in the focal plane to reduce the complexity and the manufacturing costs.

In our work, we use focal plane scanning based on a novel planar high gain filter-lens array (FLA) to achieve beam steering. Assuming uniform illumination, the beam width at the output of the lens is about 7°, which enables a high scan resolution. A matrix of antenna arrays is placed in the focal plane of the planar FLA and fed by a microstrip corporate feed network with embedded low cost PIN diode switches. Thus, a simple and affordable PIN diode switch is used to activate each array of the matrix allowing excitation of the lens from different feed points on a grid in the focal plane.

Several constraints apply on the design of the focal plane antenna arrays. For a high efficiency, the lens aperture should be illuminated uniformly, which requires a maximally flat radiation pattern in the main lobe. Also, spill-over power is an important source of loss and should be minimized. Finally, the required scan resolution limits the distance between the feed arrays in the focal plane. These conditions are obviously conflicting and a compromise had to be sought. For example, a smaller beam width for low spill-over power can be achieved by a large array size at the cost of the scan resolution. On the other hand, the maximally flat antenna pattern inevitably increases the beam width of the main lobe and the spill-over power. However, the scan resolution can be increased without changing the antenna pattern by simply interleaving the feed arrays. A special resonant feed network must be used to overcome the unwanted mutual coupling effects between the elements resulting from interleaving. Several types of feed arrays were designed for application in the feed matrix and their performances were compared in terms of spill-over loss, scan resolution and efficiency. One array consists of 5 x 5 non-uniformly excited elements and provides an antenna pattern with a maximally flat main lobe to ensure uniform illumination of the lens. A second array with 4 x 4 non-uniformly excited elements was designed to minimize the spill-over power.

Analytical Modeling of Irregularly Shaped Power Planes for Mixed Signal Applications

Jeffrey McFiggins*, Jayanti Venkataraman, Rochester Institute of Technology, NY

The resonant modes of a power plane can be excited through a process known as ground/V_{dd} bounce. This occurs when a large current is drawn from the power supply planes. This event can in turn excite resonant modes in the cavity formed by the power and ground planes. These modes can couple as noise to circuits sharing the same power plane or to those on isolated neighboring power planes. Such coupled signals, although small, could still be comparable in magnitude to the RF signal resulting in reduced system performance. Irregular power planes have predominantly been analyzed using three methods; full wave solvers, the transmission line matrix method (TLM), and the distributed lumped element (RLC) method. These methods place restrictions on port placement and lead to large demands on computer resources as the frequency is increased.

This work presents an analytical method to model irregular shaped power planes using a segmentation technique in conjunction with a cavity model that allows for arbitrary port placement where the segments are combined with an interconnect matrix. The model also includes conductor and dielectric losses. To demonstrate the validity of this method the S-matrix obtained is compared with the full wave solver HFSS. An example of a rectangular ring shaped power plane as shown in fig. 1 is considered where the dielectric substrate is 5μm thick with ε_r as 4.0. Two 50Ω ports are placed at (0.15cm, 1cm) and (1.7cm, 1.25cm) and the number of segments is 8. The computation time and complexity is considerably reduced. Figure 2 shows excellent agreement between the S-parameters obtained using the present analytical method and HFSS.

Based on the technique described above a methodology has been developed to reshape a power plane such that cavity resonances do not occur in the frequency range of interest. In the two power plane system shown in fig. 3 the lowest resonant frequency in the system is dictated by the larger of the two sections (#1). A set of design graphs can be developed as shown in fig. 4 where W_1 is fixed and W_2 is varied and in each case the lowest resonant frequency is obtained (substrate thickness is 5μm and ε_r is 4.0). For a maximum operating frequency of 3GHz the designer can choose to place the first resonance at approximately 10-15% higher. Therefore at 3.4GHz several combinations of W_1 and W_2 are possible.
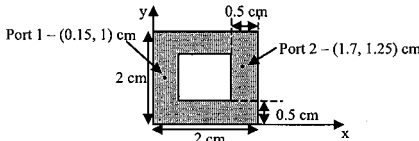
Fig. 1. Rectangular Ring Plane for Comparison with HFSS

Fig. 3. Definition of L-Shaped Plane Dimensions

Fig. 2. S-Parameter Comparison for the Rectangular Ring shaped power plane. (—— Present work, -⊙- HFSS)
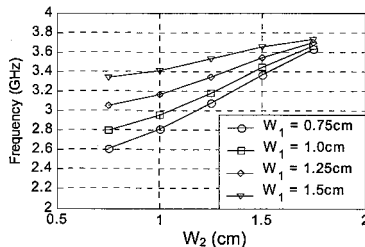
Fig. 4. Design graph for choosing dimensions of L-Shaped power plane

Application of Textured Ground Planes in Power Distribution System of High-Speed Digital Circuits

Ramesh Abhari

Dept. of Elect. & Comp. Eng., McGill University, Montreal, Quebec H3A 2A7, Canada

Simultaneous switching noise (SSN), also known as power/ground plane noise, has become one of the major considerations in the design of power distribution system of high-speed digital circuits. These circuits operate with low power, reduced noise budget and clock rates in microwave frequency range. Modern digital and mixed-signal circuits are pushing for even higher operating frequencies, where power/ground noise and package resonances become more prominent (R. Abhari, G. Eleftheriades, T.E. van Deventer, IEEE Trans. Microwave Theory and Techniques, vol. 49, no. 10, pp. 1697-1707, 2001). Different methods for mitigation of switching noise have been commonly exercised, which in many cases are rule of thumb engineering solutions such as placement of decoupling capacitors. Recently, an alternative approach to the design of reference voltage planes has been proposed that offers a global suppression of power/ground plane noise (R. Abhari and G.V. Eleftheriades, IEEE Trans. Microwave Theory and Techniques, vol. 51, no. 6, pp. 1629-1639, 2003).

In this method, a textured ground plane, which is designed based on electromagnetic bandgap (EBG) theory, replaces the conventional solid ground plane. The two-dimensional stopband filter provided by this structure blocks a wide spectrum of the switching noise current (with an insertion loss of more than 70 dB in a 2 GHz band). However, due to the complex physics of the modified ground planes, higher-order and spurious modes are potentially excited, which may compromise the quality of signal transmission. This paper investigates this concern through digital signal transmission experiments and observation of the respective eye diagrams. In this study, two groups of interconnect (striplines) test structures with similar geometries except for their power distribution system, i.e. one group contains EBG ground plane and the other has a solid ground plane, have been fabricated and their transmission characteristics have been compared. A pseudorandom binary sequence (PRBS) generator has been employed to inject the input signal to the interconnect under test. The transmitted signal is monitored by a high-speed digitizing oscilloscope, while the input clock rate is varied from 100 MHz upto10 GHz.

It has been observed that an acceptable quality of signal transmission can be achieved and can be further improved by interconnect design optimization. The transmitted signal experiences some degree of distortion imposed by the textured ground plane, but the presence of an alternative current path, i.e. the second conductor plane in the stripline structures, minimizes this filtering effect. Therefore, application of modified ground planes in high-speed digital circuits can be explored and considered as an option in the design of power distribution system.

New EMI Shielding Approaches using Electromagnetic Bandgap Structures

Baharak Mohajer-Iravani[1,3] and Omar M. Ramahi[1,2,3]
[1]Electrical and Computer Engineering Department, [2]Mechanical Engineering Department and [3]CALCE Electronic Products and Systems Center
2181 Glenn L. Martin Hall, A. James Clark School of Engineering,
University of Maryland, College Park, MD 20742, USA
www.enme.umd.edu/EMCPL/

Abstract

Electromagnetic Interference (EMI) in electronic devices is one of the major challenges in the design of high-speed electronic packages. These challenges are intensified by the increase in the level of system integration and the ever-increasing operating frequency of microprocessors. EMI takes place at different levels including the package, board, component and chip. The physical mechanism behind electromagnetic interference is the coupling of energy between different components within the package or chassis. This coupling can be either conducted or radiated. However, regardless of the coupling mechanism, surface currents are needed to support the field that eventually radiate, which constitute the electromagnetic interference in the first place. Minimizing these surface currents is considered a fundamental and critical step in minimizing EMI. In this work, we address novel strategies to confine surface currents. Unlike the traditional use of lossy materials and absorbers, which suffers from considerable disadvantages including mechanical and thermal reliability leading to limited life time, we consider the use of elctromagnetic Band Gap (EBG) structures which are inherently suited for surface current suppression. The effectiveness of the EBG as an EMI suppresser will be demonstrated using numerical simulations and experimental measurements.

98

ON THE ENHANCEMENT OF WIREBOND PACKAGE BANDWIDTH USING DOUBLE BONDING TECHNIQUE

Mostafa Abdulla

Intel Corporation
1900 Prairie City Road, FM3-123
Folsom, CA 95630, USA
mostafa.abdulla@intel.com

ABSTRACT

Nowadays, package-interconnect is a performance–limiting component in the RF and high-speed digital applications. The high frequency discontinuity introduced by the wirebond inductance could affect the high frequency circuit performance significantly. However, wirebond technology is still attractive due to its reliability and cost effectiveness.

Minimizing the wire length and maximizing its diameter is a well-known design rule to reduce wirebond inductance. Recently, double bonding became a manufacturing option which could reduce the total interconnect inductance while using same standard bondwire diameter. However, poor design of the double bonding cannot reduce the total inductance that much due to the mutual coupling. An optimized double bond configuration is needed to achieve the best bandwidth.

In this presentation, the impact of double bonding configurations on the package bandwidth will be presented. The trade-off between using bigger diameter and double bonding option will be discussed. Different bonding configurations such as in Fig.1 are evaluated using finite element method and de-embedding techniques. An optimized design and recommendations will be introduced. This study will help wirebond package designers to achieve wider bandwidth to accommodate high-speed applications.
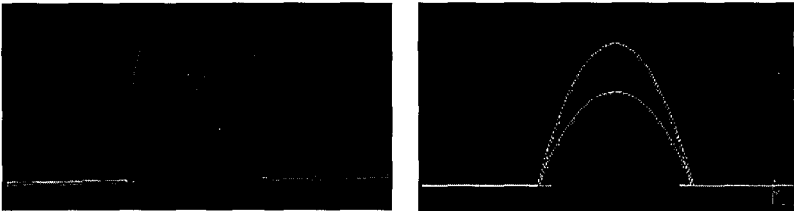
Fig.1 Different Double Wire Bond Configurations

Accurate Bonding Wire Modeling for SAW Cellular Duplexer

Hao Dong[*], Thomas X. Wu, University of Central Florida, Orlando, FL 32826
Benjamin P. Abbott, SAWTEK, Inc., Apopka, FL 32703

Bonding wires are extensively used in integrated circuit packaging and circuit design in RF applications. RF designers usually use approximate analytical formulae for straight wires to estimate bonding wire inductance and mutual inductance (T. H. Lee, The Design of CMOS Radio-Frequency Integrated Circuits, Cambridge Univ. Press, 1998). As the circuits become more complex, the package and bonding wires become more complex as well. For the high frequency, the parasitics of bonding wires, mainly inductance and capacitance, can no longer be ignored and require careful modeling. The inductance of the bonding wire is shape dependant. The general trend is that the larger curvature a wire has, the smaller its inductance. The reason that curved wires have smaller inductance is due to the mutual inductance cancellation of the different segments of a single wire (X. Qi, C. P. Yue, T. Arnborg, H. T. Soh, H. Sakai, Z. Yu and R. W. Dutton, IEEE Transactions on Advanced Packaging, 23, 3, 480-487, 2000).

In this paper, we discuss the modeling of bonding wires for SAW cellular duplexer using the full-wave analysis. At first, we use the full-wave analysis tool, Ansoft High Frequency Structure Simulator (HFSS) which is based on the finite element method (FEM), to model the single bonding wire. Then, we introduce the method to extract the inductor value from the S-parameters. After that, we separate the bonding wires into several groups according to their positions to investigate the mutual coupling. Finally, we model all the bonding wires together in the package to take into account of the mutual coupling among the bonding wires, package and die pattern as shown in Fig. 1. After combining the package, die and bonding wire models, we can get the total response of the cellular duplexer. Fig. 2 shows the comparison of simulation and measurement results for Tx channel and excellent agreement is found.
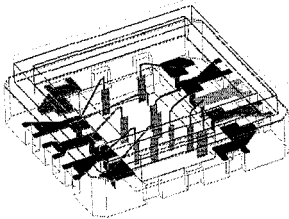
Fig. 1. Model the bonding wires together in the package to consider the mutual coupling among the bonding wires, package and die pattern.
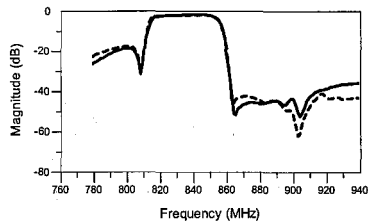
Fig. 2. Comparison of simulation and measurement results for Tx channel. The solid line shows the measurement result. The dashed line shows the simulation result.

100

Optimization and Fundamental Limits of Tunable Textured Surface Antennas

Dan Sievenpiper

HRL Laboratories LLC, Malibu, CA, USA

Using a periodic resonant texture, it is possible to create metallic surfaces with new electromagnetic properties. Such textures consist of capacitive and inductive regions, and by incorporating tunable elements such as varactor diodes, the surface can be electronically tuned to produce any desired boundary condition. For example, a textured surface can be tuned from an electric conductor to an artificial magnetic conductor, or to any surface impedance in between. These tunable surfaces can be programmed to provide any reflection phase as a function of position across the surface, and can serve as a distributed phase shifter. Tunable extured surfaces can be used to steer or focus reflected waves, so they can be used as a low-cost electronically scanned antenna (ESA). They can also control the propagation of surface waves or leaky waves, so completely planar low-cost ESAs are possible.

Antennas made from tunable textured surfaces can fill many roles for traditional steerable antennas but they can be much simpler and lower cost, since they replace a complex signal distribution network with surface wave guiding, and they replace conventional phase shifters with simple varactor diodes. One advantage of this architecture is that the antenna feeds can be located in a very sparse array, thus reducing the amount of RF circuitry, in exchange for structures requiring only DC control. Each RF feed, together with a sizeable ($>\square^2$) area of parasitically coupled textured surface material, can be considered as a single meta-element antenna. A sparse array of such meta-elements produces the same radiation pattern as a comparable conventional phased array because the steerable high-gain meta-element pattern eliminates the grating lobes that would otherwise arise from using such a sparse array.

These tunable textured surfaces have been studied in a variety of forms in the past, ranging from one-dimensional grid-array-like structures, to full two-dimensional lattices. For practical reasons, steering has been confined to one dimension. However, beam steering has been shown for both polarizations, thus demonstrating two-dimensional steering in principle.

Recently, a new tunable textured surface has been constructed to study completely arbitrary tuning in two dimensions. This presentation will include recent beam-steering results from this structure that provide evidence for the meta-element concept for low-cost ESAs. The presentation will also discuss the optimization of meta-element antennas, and their fundamental performance limits.

Artificial impedance surfaces as near-field screens

S. Maslovski, P. Ikonen, M. Kärkkäinen,
C. Simovski, S. Tretyakov*, V. Denchev

Radio Laboratory / SMARAD, Helsinki University of Technology, P.O. 3000
HUT, Finland. E-mail: sergei.tretyakov@hut.fi

In paper (S.A. Tretyakov, C.R. Simovski, Wire antennas near artificial impedance surfaces, *Microwave and Optical Technology Letters,* vol. 27, no. 1, pp. 46-50, 2000), a concept of using impedance surfaces to control near field distribution of planar antennas was proposed and theoretically demonstrated. In this paper, we present a prototype of a planar antenna utilizing artificial impedance surfaces to control the near field distribution. The antenna is a planar folded dipole placed above a finite-size artificial impedance surface (photo on Figure 1). We have found that the field screening is most effective if the surface is a metal conductor. However, to achieve a reasonable value of the radiation resistance the dipole should be located far off the screen. If the surface is a magnetic wall, the antenna design is more compact, but the field behind the screen is large. Here we realize a compromise solution using an inductive surface with a moderate surface impedance, which allows realization of an effective near-field screen with still a reasonably low-profile design.
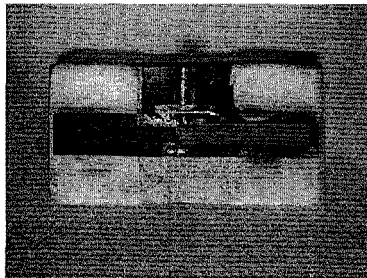
Figure 1: The prototype folded-dipole antenna with an integrated symmetrizing device. Behind the antenna a foam layer and the mushroom surface are seen.

A Two-Port Measurement Technique of Balanced Antenna Radiation Patterns

Koichiro Takamizawa* and William A. Davis
Virginia Tech Antenna Group
The Bradley Department of Electrical and Computer Engineering
Virginia Polytechnic Institute and State University

In this paper, we present a new technique for measuring antenna radiation patterns of balanced antennas. Traditionally, measurements of balanced antenna radiation patterns require a balun to feed the antenna. For a wide bandwidth antenna, the performance of the balun can degrade the radiation pattern and limit impedance bandwidth. This makes the feed an important part of the total RF system. It is often desirable to separate the performance of the antenna and the feed network during the pattern measurements.

The proposed technique uses two-port scattering parameters and two unbalanced radiation patterns of the balanced antenna. The technique is an extension of two-port input impedance measurement method (Davis, et. al, Proc. AMTA, 60-63, 1995). The two-port scattering parameters are determined by feeding each of the balanced input ports of the antenna as a port in a two-port network. Similarly, the complex valued (magnitude and phase) unbalanced radiation patterns are determined by feeding one port of the balanced antenna while terminating the other port with a reference impedance load used in the S-parameter measurements. Then, the balanced-fed antenna radiation patterns are computed from the S-parameters of the antenna element and the feed, and the measured unbalanced radiation patterns. The procedure presented is completely general, and it can be used to compute radiation patterns in directivity, gain or realized gain values from the same set of data.

For the feed scattering parameters, measured values of a balun circuit or computed values of an ideal balun can be used. The S-parameters of an ideal balun would provide the radiation patterns of the antenna independent of the feed design. The technique also allows computation and evaluation of balanced antenna radiation patterns under various feed conditions.

Both experimental and simulated results will be presented to validate the measurement procedure. Particularly, an example case of measuring radiation patterns of a balanced dipole will be presented to demonstrate the principles. Then, an application of the measurement technique in the evaluation of more sophisticated broadband balanced antenna involving Foursquare antenna will be presented.

An Automated Cylindrical Near-Field Measurement and Analysis System for Radome Characterization

Shantnu Mishra* and Matthew Giles
David Florida Laboratory (DFL), Canadian Space Agency (CSA)
Ottawa, ON

The performance of a radome degrades over time and it is therefore necessary to qualify a radome periodically to assure that it meets its original electrical performance specifications. This involves measuring the differential change in a number of antenna parameters in the presence of the radome. Some of the parameters that need to be evaluated include transmission efficiency, beam-width, side lobe levels, beam deflection, beam deflection rate, beam unbalance, null depth, and return loss. The variance in these parameters is then used as an indicator of the suitability of the radome for its designated application.

Traditionally, these measurements have been performed in a far-field range using conventional positioning and measurement systems and specialized instruments such as a null seeker. Recently the use of near field methods have been incorporated in radome measurement practices. This paper describes one such adaptation of a cylindrical near-field facility (CNF) for radome measurements.

In order to study the radome electrical performance using a near field technique one needs to perform volumetric near-field scans for multiple antenna configurations, for a number of antenna locations within the radome at different frequencies. Therefore, a typical measurement in a cylindrical near-field facility may involve measuring hundreds of cylindrical scans. This results in a large amount of collected near field data which in turn needs to be transformed to far-field and then analyzed for determination of the appropriate parameter. A high degree of automation, high speed of measurements and automated intelligent data analysis thus become necessary elements for a system to be practical for radome characterization.

Implementation of this automated process for unattended data acquisition and subsequent analysis to obtain the resulting radome performance characteristics will be described

The results of the study to assess the suitability of and to validate the CNF measurement approach for radome measurements will be presented along with sample data outputs.

Some of the issues that affect the overall duration of the measurement and have impact on the accuracy of resulting data will be discussed. These include the appropriate selection of measurement and analysis parameters such as cylinder size, sampling intervals, environmental conditions, alignment, gain calibration, and rf-subsystem stability. Measured results will be presented to elaborate measurement and analysis process optimization.

Comparisons of Antenna Radiation Measurement Techniques inside an
Anechoic Chamber with a Limited Space

Yu-Ting Hsiao*, Yu-Cheng Lu and Hsi-Tseng Chou
Dept. of Comm. Eng., Yuan-Ze University, Chung-Li 320, Taiwan

Anechoic chambers are popularly employed in the measurement of antenna radiation because of its utilizations of conducting shielding and absorbers to isolate external and internal interferences, respectively. The accuracy depends on factors of the absorber quality and internal structure arrangement, where improper arrangement can result in other multipath interferences. The validity is generally frequency dependent on the characteristics of absorbers and chamber sizes according to antenna characteristics.

Signal processing techniques are effective tools to improve the measurement accuracy and extend the valid frequency range of measurements at a minimum cost. This paper considers an existing chamber with limited space and applies various signal processing techniques to improve the accuracy. Three methods including time gating method (TGM), matrix pencil method (MPM) and Prony's method (PM) are examined and compared with respect to the measurement accuracy and influences caused by system components and parameters such as cable loss, antenna types and antenna bandwidths. In particular, conducting plates based on the utilizations of resistive materials (R-card) are designed to alter the multi-path effects so that characteristics of the chamber environment can be explored. Its impacts on the various processing methods can be evaluated. It is noted that TGM and MPM are time- and frequency-domain methods. The characteristics of the multi-path effects for this chamber in time- and frequency domains can be estimated. As for the impacts of system parameters and components, cable loss, antenna reflection coefficients, antenna bandwidth and R-card influence will be evaluated. Based on those studies, optimization of the environment characteristics and measurement accuracy can be performed. Evaluations based on measurement data and signal processing will be presented.

A Waveguide Frequency Doubler Using Patch Antennas on a Multi-Layered Substrate

H. J. Park, M. Kim, J. B. Hacker[†]

Electrical Engineering Dept., Korea University, Seoul, 136-701 Korea, roses7@nate.com
[†]Rockwell Scientific Company, 1049 Camino Dos Rios, Thousand Oaks, CA 91360

Components using solid state devices directly integrated with planar antennas have advantages of reduced loss in microwave and millimeter-wave frequencies due to their compact sizes. In this paper, we propose waveguide frequency doubler combined with specially-designed input and output patch antennas on a two-layered substrate inside standard rectangular waveguide. Because the two-layered substrate has a ground plane in the middle, the only signal path exists through the input and output antennas. Our doubler also uses two identical transistors to form a balanced circuit and eliminate the pump signal at the output antenna without using output filters (Fig 1a). The size and location of the input antenna pair along with the antenna feed positions were carefully chosen to achieve a decent matching at the pump frequency but prevent any second harmonic power radiations (Fig 2c). Currently, the doubler is being fabricated for operation with standard X and Ku-band waveguides. Compared with a conventional microstrip doubler, our circuit exhibits much narrower bandwidth imposed by the use of patch antennas, but it shows a similar maximum conversion gain. For the waveguide doubler using Fujitsu FHX35LG transistors, ADS simulations predict the maximum conversion gain of 0.5dB at 17GHz with the 3-dB output frequency bandwidth of 0.5GHz.
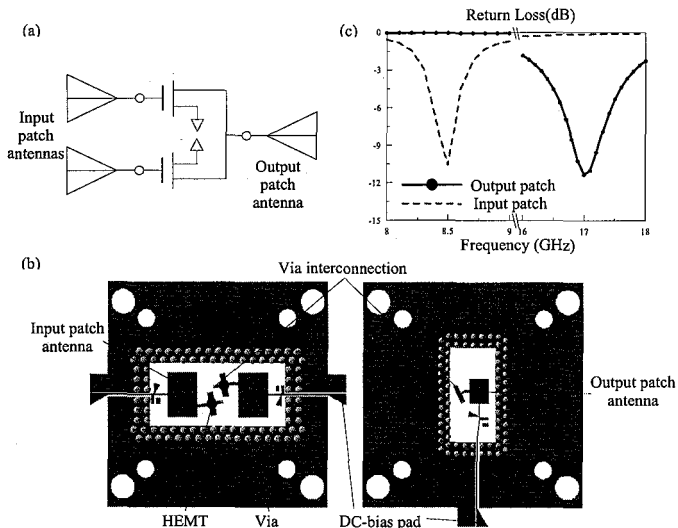
Figure 1. Circuit schematic (a), the layout of the waveguide doubler (b), and the input and output antenna simulation results from ADS (c).

Control of Coupling from a Micro Ring Laser Formed Coaxially on a Optical Fiber

Reyhan Baktur* and L. W. Pearson
Holcombe Department of Electrical and Computer Engineering
J. M. Ballato, School of Material Science
Clemson University
Clemson, SC 29634-0915
grehang@clemson.edu
pearson@ces.clemson.edu

Frolov, *et. al.* [*Appl. Phys. Lett.*, 72(22), pp. 2811-2813] have demonstrated lasing in a so-called microring created from an optically active polymer formed on a cylindrical mandrel. (Incidentally, an optical fiber was employed as the mandrel.) They provide an argument that the laser operates by virtue of a whispering gallery (WG) wave resonance. Slab waveguide modes, which also exhibit resonances, are a part of the complete field structure. Frolov, *et. al.* reason that conductor losses in the gold layer which they placed between the microring and the fiber would quench lasing in any stab waveguide mode.

Subsequent to the work discussed above, it has been observed that the laser light couples from the laser into the optical fiber, a potentially desirable effect in applications. This coupling is not easily explained, because in a circular laser on a circular fiber, the electromagnetic fields in both structures are harmonic in the angle around the circular structure, but the harmonic order is drastically different. The order of the laser resonance is order of magnitude 100, while the harmonic order of the dominant mode in the fiber is 1. This implies orthogonality of the two fields, and hence the absence of coupling.

We have recently conducted solutions for the related elliptic geometry. It is common today to employ elliptic-cross-section fiber in applications as a means of controlling polarization dispersion. Our solutions for coaxial elliptic geometries demonstrate that these cross sections exhibit coupling between the fields in the micro ring and the dominant mode in the fiber. The coupling occurs because the eigenvalues for the angular Mathieu functions in materials with different refractive index are different—a consequence of the presence of the refractive index as a parameter in the eigenvalue equation. The index in the active polymer in the micro ring is indeed different from the index of glasses used in fiber.

This opens the possibility of employing the ellipticity of the structures as a parameter for control of coupling. We present results for coupling coefficients between the laser mode in the microring and the dominant mode in the fiber as a function of the axial ratio of the ellipses involved.

*a.k.a. Rehanguli Gayiti

High-Sensitivity, Millimeter-Wave Detection via Optical Modulation and Carrier Suppression

C. A. Schuetz*,[1], S. K. Lohokare[1], S. Deliwala[2], and D. W. Prather[1,a]

[1]Department of Electrical and Computer Engineering, University of Delaware, Newark, DE
[2]Light Matters, Inc., Orefield, PA
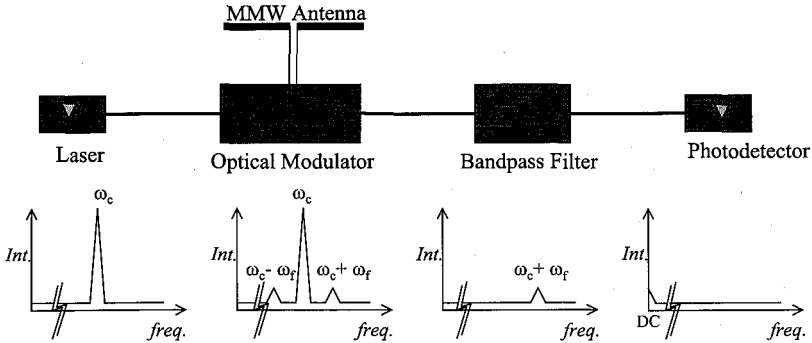
Millimeter-wave radiation has the unique ability to penetrate atmospheric obscurations such as smoke, fog, and light rain while maintaining the capability for high-resolution imaging. As such, high-sensitivity detectors operating in this frequency band are desirable for passive imaging and remote sensing applications. Current methods for detecting millimeter-wave radiation, such as microbolometer or MMIC based approaches either have insufficient sensitivities for many passive-imaging applications or are not amenable to fabrication in large pixel arrays desirable for high-resolution imaging. To this end, we present a millimeter-wave detector technology based on optical modulation with optical carrier suppression that promises both high sensitivity and scalability to large pixel arrays.

The proposed detector utilizes a high-speed optical modulator to transfer millimeter-wave radiation onto the sidebands of a near-infrared optical carrier frequency. The optical carrier frequency is subsequently suppressed via optical filtering techniques. The resultant signal is passed to a low-frequency photodetector, which converts the remaining sideband energy to a photocurrent proportional to the incident millimeter wave energy at the modulator input. Such a device offers high-sensitivity millimeter-wave detection without the use of RF amplifiers. Also, since each of the required components may be fabricated in III-V materials using planar semiconductor processing techniques, integration of multi-pixel arrays is feasible.

Herein, we present experimental results obtained using a baseline detector assembled from commercially available fiber optic components as well as efforts to integrate the desired functionality into a single GaAs substrate. An initial noise equivalent power (NEP) of the proposed detector has been demonstrated at sub-nanowatt levels, with improvements to sub-picowatt NEP's anticipated as the setup is optimized.

---

[a] E-mail: dprather@ee.udel.edu

Efficient Dynamic Analysis of Liquid Crystal Devices

Haiying Wang[1*], Thomas X. Wu[1], Liping Zheng[1] and Shin-Tson Wu[2]

[1]Department of ECE, University of Central Florida, Orlando, FL 32816, USA
[2]School of Optics/CREOL, University of Central Florida, Orlando, FL 32816, USA

Liquid crystals (LC) are now widely studied for their promising applications in display and optical, microwave and millimeter-wave devices. One of the technical challenges of LC devices is how to improve its response time. Therefore, dynamic analysis is important to design fast LC devices.

The response mechanism of the LC is related to the dynamic switching behavior determined by the external electric field. The dynamics of the LC director distribution is governed by the Erickson-Leslie equation (I. C. Khoo and S. T. Wu, *Optics and Nonlinear Optics of Liquid Crystals*, 1993). To efficiently analyze the dynamics of liquid crystal devices, mode expansion method is developed. The angle of the LC director distribution can be expressed as the superposition of spatial modes (S. T. Wu and C. S. Wu, Appl. Phys. Lett., 53, 1794-1796, 1988). Computer analysis also takes pretilt angle effects into consideration. The electric field calculation is optimized in our new program to speed up the simulation. Optimization of the program simplifies the calculation of the electric field. Good agreement between the mode expansion method and finite difference method is obtained as shown in Fig. 1. We find that the mode expansion method is faster than the finite difference method to get the same accurate results. The simulation results agree with experimental results.
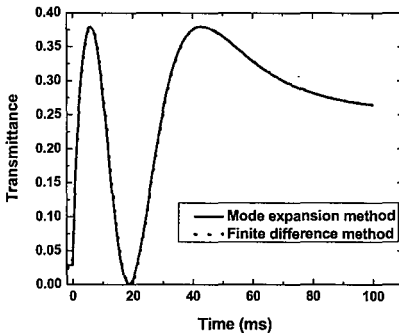
Fig. 1. Electro-optic curve of a PA E-7 cell at d = 4.04 um, λ=632.8nm, T= 22° after released from 10Vrms. The solid line is for mode expansion method, while the dot line is for finite difference method.

THE EFFECT OF SUBSTRATE MATERIAL AND ISOLATION TECHNIQUE ON THE NOISE COUPLING FOR RF AND MIXED-SIGNAL SYSTEM ON-A-CHIP (SOC)

Chao Iwen and Mostafa Abdulla
Intel Corporation,
1900 Prairie City Road
Folsom, CA 95630, USA
iwen.chao@intel.com, mostafa.abdulla@intel.com

ABSTRACT

With higher level of integrations in VLSI, the importance of limiting undesirable interactions between different circuits fabricated on a common silicon substrate is increasing. Such interaction, referred to as substrate coupling, is more significant in the mixed-signal integrated design, particularly in the high frequency applications.

One of the major issues in integrating system on a chip (SOC) is selecting the proper substrate conductivity and isolation techniques. This is because of the significant impact of the substrate coupling on the circuit integration and overall system performance. For example, for analog and RF circuit blocks, the high resistive material is preferred due to lower substrate coupling. In addition, the presence of a low resistivity layer under the epitaxial layer will cause monolithic inductors to have lower quality factor. However, the high resistive material will degrade the latchup performance, which is a major concern for digital circuit blocks.

In this presentation, the effect of substrate conductivity and isolation techniques on the substrate coupling will be presented using common substrate isolation techniques such as guard rings and deep N-wells. For instance, Fig. 1 shows the substrate coupling for three different substrate materials at fixed distance. The cross section along with the pros and cons of each structure will also be discussed. The effectiveness of isolation as a function of frequency, distance and substrate material will be presented. Design rules and recommendations for mixed-signal and RF designs will be concluded.
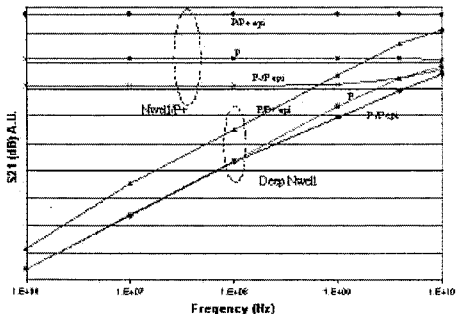
Fig. 1 substrate coupling with three different substrate materials

GREEN'S FUNCTION ANALYSIS OF AN
INHOMOGENEOUS MICROSTRIP CIRCULATOR

Jeffrey L. Young and Christopher M. Johnson*
Department of Electrical and Computer Engineering
University of Idaho, Moscow, ID 83844–1023

Traditional analyses of ferrite microstrip circulators have focused on circulator performance under the assumption that the ferrite is homogeneous. This assumption has some validity, especially for extremely thin ferrites. For thick ferrites, however, strong inhomogeneities exist due to the presence of the demagnetization field. A typical demagnetization factor N_{zz} can vary radially in a circular ferrite puck from 0.9 at the center to about 0.5 at the edge. This demagnetization factor impacts the value of the internal magnetic intensity H_o, which, in turn, impacts the value of the Larmor precession frequency ω_o. By definition, $H_o = H_a - 4\pi M_s N_{zz}$, where H_a is the applied magnetic intensity and $4\pi M_s$ is the magnetic saturation; $\omega_o = \mu_o \gamma H_o$, where γ is the gyromagnetic ratio. Given that ω_o is a key parameter in circulator design and analysis, it follows that an inaccurate account of its inhomogeneous property will impact that validity of that design and analysis.

In this talk we present a Green's function analysis of the circulator by modeling the radial inhomogeneities of the ferrite with concentric stratified sections; each section is homogeneous, per the model of Krowne and Neidert [*IEEE Trans. Microwave Theory and Tech.*, 44(3), 1996]. The circulator itself is modeled as a closed cavity consisting of PEC end plates and PMC walls. We show that a compact, recursive Green's function can be developed in terms of a summation of azimuthal Fourier modes that is rapid to compute and straightforward to represent mathematically. The singularity of the Green's function is also examined and is shown to be logarithmic in nature. The Green's function is used to compute the impedance and scattering parameters; these parameters are then used to deduce synthesis equations. Results are provided that show the validity of the Green's function data and the convergence property of the Green's function with and without singularity extraction. A circulator design is also presented and validated with data found in the literature and with data produced by a frequency domain finite element code.

Enhanced Transmission of Transient Pulses through Plates Perforated by Subwavelength Holes

Vitaliy Lomakin and Eric Michielssen

Center for Computational Electromagnetics
Department of Electrical and Computer Engineering
University of Illinois at Urbana-Champaign
vitaliy@emlab.uiuc.edu, emichiel@uiuc.edu

Recently, the phenomenon of enhanced transmission through metallic plates perforated by a single subwavelength hole or a periodic array thereof was observed in both the optical and microwave regimes (T.W. Ebbesen, *Nature*, (6668), 667-9, 1998; A.A. Oliner and D. R. Jackson, *IEEE AP-S*, 2003; Lomakin et al, *IEEE AP-S*, 2003, Columbus; Lomakin et al, *PIERS*, 2003,). The phenomenon was attributed to leaky waves that appear in response to the existence of surface waves scattered by a periodic grating on the plate surface; this periodic grating may be formed by the hole arrangement itself. In optics the SWs were associated with surface plasmon polaritons. In the microwave regime the SWs may exist on dielectric slabs, corrugated structures, or periodic hole arrays. It was shown that the LWs leading to the enhanced transmission appear when the wavenumber of one of the Floquet modes approaches that of the structure's SW.

Here the phenomenon of enhanced transmission is studied directly in the time domain using semi-analytical methods, leading to new insights into its origins and the identification of novel potential applications. Specific attention is paid to two-period perforated plates (Lomakin et al, *IEEE AP-S*, 2003, Columbus) and perforated plates residing in between dielectric slabs (Lomakin et al, *PIERS*, 2003, Honolulu). These structures are assumed to be excited by a TM_z field with temporal signature $f(t) = (e^{-\alpha t} - e^{-\beta t})\cos(\bar{\omega}t)$, where α and β define the field's bandwidth and $\bar{\omega}$ is its signal carrier frequency. This time dependence permits the structure's transmission properties to be studied using the singularity expansion method. That is, by expressing the transient field in terms of a Fourier integral, it is, upon closing the Fourier integration contour in the lower complex ω half plane, seen to include two distinct contributions. One is a sum over residues of poles of the transmission coefficient and is the time domain counterpart of the well-known resonant Wood anomalies (A. Hessel and A. A. Oliner, *Applied Optics*, (10), 1275-1297, 1965); this contribution is responsible for the enhanced transmission. Another contribution involves a sum over branch cut integrals corresponding to different Floquet modes and constitutes the time domain counterpart of the Rayleigh-Wood anomalies. The branch cut contributions can be evaluated asymptotically for late times (even though, under certain conditions complex poles may approach the branch point). This contribution is dominant for late times.

It is shown that, when the incident pulse is sufficiently short, two signals are observed. The first (early-time) transmitted signal is a weakly distorted and time delayed version of the incident pulse. The second signal, for intermediate and late times, is formed by the pole and branch cut contributions, respectively. In contrast, when the incident pulse is long, only one transmitted signal is observed. This signal is affected by the poles and branch points that under different conditions may lead to a positive or negative temporal shift of the transmission envelope.

Slot Based Electromagnetic Band-Gap Structures
for Surface Wave Suppression

N. Llombart[1], A. Neto[1], G. Gerini[1], P. J. I. Maagt[2]

[1]TNO-Physics and Electronics Laboratory,
P.O. Box 96864,2509 JG The Hague, The Netherlands.
llombart-juan, neto, gerini@fel.tno.nl
[2]ESA-ESTEC, 2200 AG Noordwijk, The Netherlands
Peter.de.Maagt@esa.int

Patch antennas have been objects of investigations for many decades. Among their advantages, they count low cost and weight and their intrinsic predisposition to be integrated with active components and circuitry. Nevertheless, one key disadvantage, when comparing the performances of these radiators with other type of radiators (i.e. wave-guide based) that are often used in array configuration, is their relatively small bandwidth. In practice the height of the substrate on which the patch antenna is printed dominates the bandwidth. If the height is small in terms of the wavelength the efficiency is usually high over a small frequency band, while for thick substrates larger bandwidths are achieved at the cost of a very low efficiency. Indeed, beyond a certain substrate height, the patch generates a dominant surface wave field. Surface waves do not radiate directly in free space, thus they constitute a power loss, and consequently also an efficiency loss. Furthermore, while compact circuit design can be achieved on high dielectric constant substrates, optimum performance patch antennas are built on low-permittivity substrates. Therefore, innovative technologies must be developed for an efficient integration and for improving the efficiency and bandwidth of printed radiators. EBG structures are now arising as the solution to these problems.

The objective of this work is to develop new analysis techniques and new technical solutions for the design Electromagnetic Band-Gap (EBG) structures used to enhance the bandwidth times efficiency product in printed antennas (R. Gonzalo et al. IEEE Trans. on MTT, Vol. 47, No.11 Nov. 1999). To achieve this goal, firstly the key propagation properties of the waves launched in an EBG loaded structure are investigated in two-dimensional and three-dimensional cases. Secondly slot based geometries are analyzed and proposed as alternative solutions to via-holes based solutions. These letter structures are widely proposed in literature to cancel the TM00. However it is also apparent that via-holes in the sub-strates are not always the preferred solutions from the manufacturing point of view. If the same performances could be achieved using slot based EBG geometries it would be extremely convenient. In this paper the possibility of using slot elements to kill the TM00 mode is investigated in detail.

The analysis is performed resorting to two different analysis tools. The first analysis tool is a particularly efficient element by element Method of Moments (MoM) by which a radiating element operating in a finite EBG environment is analyzed (A. Neto et al. IEEE Trans. A.P. Vol. 51, no. 7, July 2003). The second tool is also MoM based but considers an infinitely extended periodic structure excited by a single, non-periodic source. In this second analysis method, the field excited by the original source is expanded in terms of plane waves and then the interaction of each one of these plane waves with the EBG structure is analyzed in a full manner resorting to a MoM approach. The overall solution of the problem is then obtained as superposition of the plane wave responses. A similar approach for the 2D case was presented in (H.Y.D Yang, D.R. Jackson, IEEE Trans. on AP Vol. 48, No.4, April 2000). Cross validation of the two methods is first achieved by comparing the results obtained with the two modeling procedures. Significant improvements in the understanding of the physical phenomena involved have been achieved by using this second modeling procedure.

Micromilled Dielectric PBG Self-Collimation Devices in Millimeter-Wave Regime

Z. Lu*, C. A. Schuetz, C. Chen, S. Shi, D. W. Prather*

Department of Electrical and Computer Engineering, University of Delaware, Newark, DE

Recently, much interest has been shown in the area of photonic bandgap (PBG) devices for their high ability in wave routing and confinement. In this paper, we apply the principles of photonic crystal devices to the millimeter wave portion of the electromagnetic spectrum. To this end, we have developed custom Finite-Difference-Time-Domain (FDTD) electromagnetic calculation software for the analysis of both 2D and 3D PBG structures. Using this tool, we have designed and simulated millimeter wave photonic crystal devices, which in comparison to optical devices are much easier to fabricate since their feature sizes are much larger.

In our work, an accurate micro-milling system has been used to fabricate the millimeter wave photonic crystals. In order to characterize our structures, a millimeter wave imaging system was built based on an Agilent 85016D network analyzer, which encompasses a test and measurement capability from 45MHz through 110GHz. Using this system, we investigated the unique dispersion properties of millimeter wave photonic crystals, both in the amplitude and phase. In particular, we show for the first time self-collimation effects both in high and low dielectric constant PBG materials, as well as three-dimensional materials. A comparison between experimental and theoretical results is presented. In addition, we also demonstrate several novel devices and discuss their potential applications.
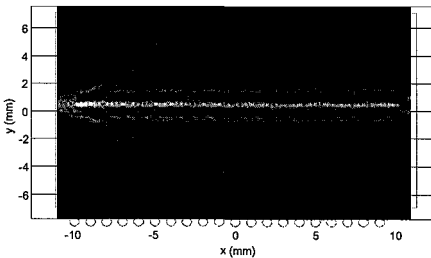
Figure 1. Self–collimation effect in low dielectric constant material (rexolite).
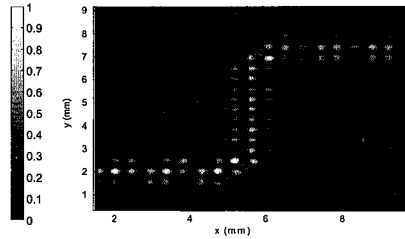
Figure 2. Self–collimation effect and 90° bending at mirrors.

* E-mail:dprather@ee.udel.edu   Webpage: http://www.ece.udel.edu/~dprather

Design and Simulation of a Cryogenic Electrical Motor

Liping Zheng[1*], Thomas X. Wu[1], Jay Vaidya[2], Dipjyoti Acharya[3], Krishna Murty[3], Limei Zhao[1], Chan H. Ham[3], Kalpathy B. Sundaram[1], Jay Kapat[3] and Louis Chow[3]

[1] Department of ECE, University of Central Florida, Orlando, FL 32816
[2] Electrodynamics Associates, Inc., Oviedo, FL 32765
[3] Department of MMAE, University of Central Florida, Orlando, FL 32816

Cryogenic devices are becoming increasingly important in space applications. Although semiconductor devices are more efficient at cryogenic temperatures than at room temperature, there are many challenging issues in designing cryogenic devices. In this paper, the design and simulation of a high-speed permanent magnet synchronous motor (PMSM) with the rating of 2000 W output power and 200 krpm shaft speed are described. The PMSM is designed for operation at the cryogenic temperature of 77 K.

The designed PMSM is a 2-pole, 3-phase and radial flux structure. The permanent magnet is centrally located inside the shaft. The slotless stator is made of laminated low-loss silicon steel. Multi-strand twisted Litz-wire is used to reduce eddy current loss in the winding. The Litz-wire is twisted with the same pitch as the stator length. High yield strength metal is used for the shaft material. Samarium Cobalt (SmCo) is chosen for the permanent magnet because it is very stable at low temperature and has very low temperature coefficient of coercive force (Hc) and residual induction (Br). The permanent magnet is inserted into the hollow shaft by cooling the permanent magnet and heating the shaft. In order to build the machine that can work at the cryogenic temperature (77 K), the materials are carefully selected to make sure that they can work at such low temperature.

Although the copper DC loss is greatly reduced at the cryogenic temperature due to the reduced resistivity, the eddy current loss of the windings due to the proximity effect that comes from the rotating magnetic field will increase greatly. The simulations of eddy current losses at both the cryogenic temperature and room temperature are provided in details. The optimization of winding size to balance the DC loss and the eddy current loss is discussed. The simulation of the eddy current loss in the shaft is also provided. The projected efficiency of the motor has been estimated to be about 95%. Overall size is about 50 mm in diameter and 100 mm in length.

Design of Multilayered Ring Filters

Chih-Feng Chou*, Ju-Lung Chu, and Jean-Fu Kiang

Department of Electrical Engineering and
Graduate Institute of Communication Engineering
National Taiwan University, Taipei, Taiwan, ROC
jfkiang@cc.ee.ntu.edu.tw

Recently, the increasing demands for wireless communications products like mobile phone and wireless LAN render them more compact and cheaper. In the RF front-end of these wireless communications products, passive devices like filters usually take the most area. Filters can be designed and implemented either in terms of lumped elements or resonators. In general, filters made of resonators have larger stop-band rejection rate than their lumped-element counterparts. Size of the resonator filters, like hairpin, coupled-line, and ring filter, is usually comparable to wavelength. Such filters usually occupy large area, especially for designs at low frequencies. Even larger area will be required if the performance is enhanced by cascading several resonators. Hence, lumped-element filter is more suitable at low frequencies. Both resonator and lumped-element types of filters can be designed and implemented using multilayered layout to reduce their size.

In this work, we design a band-pass filter using ring resonators. A ring filter can be viewed as a variation from the half-wavelength strip filter. Conventional ring filter has the circumference length of about one wavelength at the center frequency and has line-to-ring coupling structure.

An equivalent lumped-element circuit of multilayered ring filter will be used for analysis, from which design rules can be derived. Additional transmission zeros can be inserted from the mutual inductance between the coupled rings, which is expected to enhance the rejection rate at the band edges.

Next, a multilayered ring filter will be designed to implement the equivalent circuit. Sharper stop-band edges can be obtained if more resonators are cascaded. Results using a two-ring structure will be demonstrated by both simulation and prototypes.

The Enhancement of Electromagnetic Coupling between the Primary and Secondary Spirals of On-Chip Symmetrical Transformers

W. Y. Yin[1], L. W. Li[2], and S. J. Pan[2]

[1] : Temasek Laboratories; [2] : Department of Electrical and Computer Engineering;

National University of Singapore, 10 Kent Ridge Crescent, Singapore 119260,
E-mail: tslyinwy@nus.edu.sg

Abstract: In the radio frequency integrated circuits (RFICs), monolithic transformers can be used for impedance matching, balun implementation and low-noise amplifier feedback, *etc*. Based on different layouts, the electromagnetic characteristics of on-chip transformers fabricated using silicon IC technologies have been studied in the past few years (*C.P. Yue et al, Proc. IEEE Inter. EDM, 155 –158, 1996; J. Hogerheiden, IEEE Trans. MTT, 45, 543-545, 1997; A.M. Niknejad and R.G. Meyer, IEEE J. SSC, 33, 1470-1481, 1998; A. Zolfaghari et al., IEEE J. SSC, 36, 620-628, 2001; S. J. Pan, W. Y. Yin, and L. W. Li, Int. J. RF & Microwave CAE, 14, 2004*). However, as compared to the research on on-chip spiral inductors, and to the best of our knowledge, there remains much theoretical as well as experimental works to be done to effectively improve the performance of integrated transformers. Actually, the on-chip transformer models, including the primary and secondary spirals, are closely related to their layouts and applications. It is rather difficult to find a general way to achieve the maximum available gain of the transformer.

In this work, different distributed parameter effects of on-chip symmetrical interleaved center-tapped transformers (Fig.1), fabricated using silicon IC technology, on the electromagnetic coupling between the primary and secondary are examined for different turn numbers experimentally. Based on this work, certain ways are proposed to achieve the desired maximum available gain, which is useful to the practical transformer design used in RFICs.
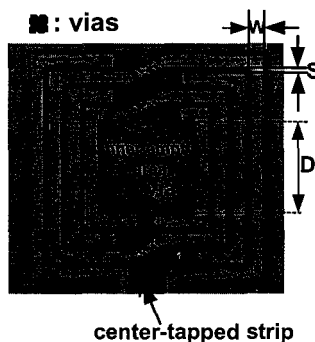
Figure1. Top view of a symmetrical on-chip transformer fabricated using silicon IC technology.

A Multi-Band Sub-Harmonic Self-Oscillating Mixer with Conversion Gain Enhancement

L. Chiu*, T. Y. Yum, Q. Xue, and C. H. Chan
Wireless Communications Research Center, City University of Hong Kong,
83 Tat Chee Ave., Kowloon, Hong Kong SAR China
E-mail: 50246038@student.cityu.edu.hk

A high-performance X-band sub-harmonic self-oscillating mixer is proposed. The core structure consists of a re-configurable transistor pair and an open and short circuit stub. This topology has a maximum conversion gain of 18.7 dB without using an IF amplifier or a low noise amplifier. The measured phase noise of oscillation for this self-oscillating mixer is –85.4dBc/Hz at an offset frequency of 100 kHz. This paper shows the potential of the sub-harmonic mixer with this transistor pair for high-performance compact down-converter at X-band.

Fig. 1 shows the schematic diagram of our sub-harmonic self-oscillating mixer. The base feedback circuit for the oscillator at Transistor T_1 consists of a coupled line band-pass filter and a section of microstrip line. The RF frequency (f_{RF}) falls within the passband of the filter with the LO frequency (f_{LO}) at the stop band. At the LO frequency, the band-pass filter has approximately the same characteristics as a resonator. The length of the transmission line between the base of T_1 and the band-pass filter is tuned such that the LO frequency is at 4 GHz. The oscillation occurs mostly at T_1 of the common-emitter configuration. Transistor T_2 serves as an auxiliary component contributing to the common-emitter oscillation and, hence, a highly stable oscillation is obtained. The series feedback of the common-emitter oscillation of T_1 consists of the base-emitter capacitor of T_2 and the open circuit stub. The short circuit stub at T_1 works as a return path for the RF. The LO signal is mainly generated by T_1 and its harmonics mix with the RF within T_1. The low-pass filter reflects the RF harmonics and other spurious signals while the IF can be extracted through the low-pass filter.

Because of the self-oscillating operation, the LO signal is constantly generated at 4 GHz. The RF mixes with the second and third harmonics of the LO signal to generate the IF signals. Therefore, four sets of down-conversion gain are obtained. For comparison of each frequency band in the multi-band operation, four different frequency bands of RF centered at 12.65, 11.35, 8.65 and 7.35 GHz are chosen so that the IF frequency (f_{IF}) is at around 0.65 GHz. The measured down-conversion gains for the RF frequency bands are shown in Fig. 2 with a maximum conversion gain of 18.7 dB.
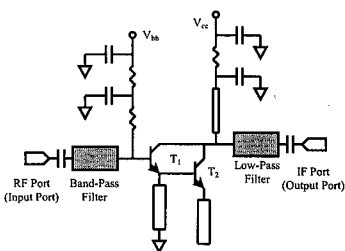
Fig. 1. Schematic diagram of the sub-harmonicself-oscillating mixer.
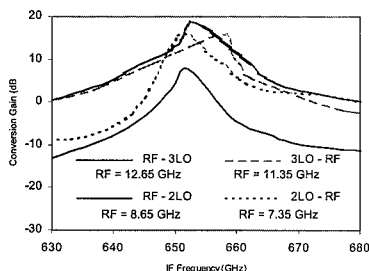
Fig. 2. Conversion gain versus IF frequency of RF frequency centered at 12.65, 11.35, 8.65 and 7.35 GHz

118

Implementation of the Thin-Strut FDTD Method for Dispersive Media in Biomedical Telemetry Applications

Stefan Schmidt* and Gianluca Lazzi

Department of Electrical and Computer Engineering,
North Carolina State University, Raleigh, NC 27695-7914, USA

In a wide range of biomedical applications, inductive coupling is used for the transfer of power. Further, inductive links can carry telemetry information to and from implanted biomedical devices without the need of wires piercing the skin, therefore reducing the risk of infection. Future developments in biomedical applications, such as a retinal prosthesis implant, will require the transfer of larger quantities of power and information than earlier applications. The stability and reliability of the inductive link and compliance with safety standards are of critical importance for these applications. Thus, in these biomedical telemetry applications, detailed numerical studies are necessary to assess the performance of the power coupling and the potential information transfer between implanted and external coils.

Electromagnetic problems involving inhomogeneous dispersive media are easily solved using the finite-difference time-domain (FDTD) method. The Thin-Strut formalism (R. Holland, L. Simpson, *IEEE Trans. Electromagn. Compat.*, **23**, 88-97, 1981) is a sub-cell model that allows embedding of linear wire elements with a specified wire radius into the FDTD grid. The Finite Difference Time Domain (FDTD) method extended by the Thin-Strut formalism was previously used to compute the coupling between coils in free space. The Thin-Strut FDTD formalism applied to the calculation of the coupling between different configurations of telemetry coils is in closer agreement to the analytical approximation than the standard FDTD code. Further, in contrast to the traditional FDTD method, results obtained with the Thin-Strut formulation are relatively insensitive to cell resolution for analyzing the coupling between coils in telemetry systems. However, the method, as previously proposed, does not allow the wire elements to be embedded in dispersive media.

In this study, the Thin-Strut formalism is extended to allow the modeling of lossy frequency dispersive media. The method is used to compute the coupling between an external coil and a coil implanted inside the eye of a human head model. Further, the specific absorption rate (SAR) resulting from a current in the external coil is computed while a secondary coil is present inside the head model. Results indicate that the extended Thin-Strut formalism is promising for computation of inductive power coupling and SAR in biomedical applications.

A Study of the Performance of the Data Telemetry Link for a Retinal Prosthesis using Extremely Compact Wire Antennas

Keyoor Gosalia* and Gianluca Lazzi

Department of Electrical and Computer Engineering,
North Carolina State University, Raleigh, NC 27695-7914, USA

In implantable prosthetic devices, wireless power and data communication is generally achieved via inductive coupling between external and embedded coils at low frequencies (2-10 MHz). To enhance bandwidth of the data link, in our previous work we suggested that the data link be established exclusively of the power link at microwave frequencies (1-3 GHz) using antennas. And specifically for a retinal prosthesis, the feasibility of data transfer at microwave frequencies (in two bands at 1.45 GHz and 2.45 GHz) using a pair of microstrip patch antennas was demonstrated. For this purpose, at both the frequency bands appropriately sized microstrip patch antennas (external antenna: 25×25 mm and implanted antenna: 6×7 mm on a 0.5 mm substrate with $\varepsilon_r = 9.2$) were designed and implemented and the performance of the data link characterized in the presence of an eye model. It was observed that the eye ball acted as a dielectric lens and improved the coupling between the antennas as compared to coupling in free space.

To design the extremely compact implantable (intraocular) patch antenna measuring 6×7 mm at 1.45 GHz, shorting posts were used and several fine slots were etched on the surface. Though in our previous work the intraocular antennas were realized by vertical milling machines, future antenna designs incorporating fine features on the surface (to increase electrical length) may have to be implemented using a solid state fabrication procedure. With such procedures, it is rather cumbersome to fabricate the ground plane (for patch antennas) because of the difficulty of bonding a metal layer like aluminum to silicon wafer. This necessitated the design of alternate antenna structures without a ground plane. Moreover, it was of interest to determine whether the coupling performance can be enhanced with different intraocular antenna structures.

Here, we used a simple space-filling curve to design an extremely compact intraocular dipole antenna. The size of the antenna and the dielectric constant of the supporting substrate was the same as for the patch ($\varepsilon_r = 9.2$) but the thickness of substrate was increased to 1.5 mm. The designed compact dipole antennas were probe fed and were matched both in free space and when embedded in the eye model using a simple method. For a similar external antenna, coupling was characterized at 1.45 GHz with both types of intraocular antennas (patch antenna and compact dipole antenna) in free space and in presence of the eye model. Detailed results of the coupling performance of the data links using both the types of antennas will be presented.

120

COMPARISON OF HELICAL and MICROSTRIP ANTENNAS IMBEDDED IN LOSSY DIELECTRIC USING GENETIC ALGORITHMS

By Pichitpong Soontornpipit, Ramadevi Bylapudi, Cynthia Furse, and You Chung Chung

Department of Electrical and Computer Engineering

University of Utah
Salt Lake City, Utah 84112
cfurse@ece.utah.edu
phone: (801) 585-7234
fax: (801) 581-5281
www.ece.utah.edu/~cfurse

Implantable medical devices such as cardiac pacemakers, hormone or medication pumps, and electrical simulation devices require communication with the outside world. The design of biocompatible antennas that can communicate with implantable devices is an interesting problem. These antennas must be designed for the Medical Implant Communication System (MICS) [2] band at 402-405 MHz. Although this relatively low frequency is good for transmitting energy through the lossy human body, traditional antenna designs would be disfunctionally large. Previous work has focused on microstrip antennas, and has shown that these antennas can be miniaturized to reasonable sizes. Another possible antenna type, the insulated helical antenna, operating in its normal mode, is also potentially attractive for this application because it has suitable radiation characteristics, wideband impedance characteristics and also it is mechanically simple.

In this paper, the parameters of the helical antenna are optimized using genetic algorithms to determine an appropriate design. The minimum and maximum limits of the helix parameters are:

Length	:	3 cm to 5 cm
Turn Spacing	:	0.5 cm to 2 cm
Wire Radius	:	0.02 cm to 0.05 cm
Radius of the helix	:	1 cm to 2 cm
Distance of the base above ground	:	0.5 cm to 1 cm

The cost function forces the resonant frequency to 402-405 MHz and also forces the real value of the impedance close to 45-55 Ohms. It then optimizes the imaginary value of the impedance close to Zero Ohms.

Suitable antennas were designed, prototyped, and measured, and it was found that the helical antennas could perform better than microstrip antennas, although it is not certain if they could be packaged for functional use.

Application of the Complex Source Point Method for Analyzing the Diffraction of an Electromagnetic Gaussian Beam by a Curved Wedge Using UTD Concepts

T. Lertwiriyaprapa, P. H. Pathak, K. Tap, and R. J. Burkholder

ElectroScience Lab, The Ohio State University
1320 Kinnear Road, Columbus, OH 43212, USA
E-mail: pathak.2@osu.edu

The complex source point technique (CSP) is combined with the ray based Uniform Geometrical Theory of Diffraction (UTD) to analyze the scattering by an arbitrary curved conducting wedge illuminated by a sequence of electromagnetic Gaussian beams (GBs) which can describe a relatively general antenna illumination (J. J. Marciel and L. B. Felsen, IEEE Trans. AP, vol. 37, pp.884-892, July 1989). UTD ray solutions have, over the years, been proved to be highly efficient in the analysis of radiation and scattering by electrically large structures. However, the UTD fails in the region of confluence of ray caustics and ray shadow boundaries. This failure can occur for instance in problems involving curved surfaces containing curved edges. Therefore, the UTD must be augmented by numerical Physical Optics (PO), or rigorous numerical methods, in such special regions; however the latter numerical approaches become highly inefficient and time consuming for large structures. On the other hand, the use of a GB approach via the CSP technique allows one to find the radiated/scattered fields analytically in closed form, even in the regions where the UTD fails.

A CSP based UTD approach has been studied and demonstrated in the recent past for treating the diffraction by straight wedges; however, that work was restricted mostly to scalar wedge diffraction in 2-D (H. D. Cheung and E. V. Jull, Proc. IEEE AP-S. Inter. Symp., vol. 2, pp.74 - 77, 2002). The GB method has also been recently employed within the PO approximation to rapidly analyze the pattern of large 3-D electromagnetic reflector antenna systems, but without the CSP technique (H. T. Chou, P. H. Pathak, and R. J. Burkholder, IEEE Trans. AP, vol. 49, pp. 880-893, June 2001). This paper presents the extension of the well established UTD ray analysis of the diffraction by a general curved wedge illuminated by a ray optical spherical wave generated by a point current (R. G. Kouyoumjian and P. H. Pathak, Proc. IEEE, vol. 62, pp.1448-1461, Nov. 1974) to treat the diffraction of an incident GB by the same structure via the CSP technique. In particular, in the CSP method, a point source in real space becomes a CSP by replacing its real position coordinates by appropriate complex values; in so doing, this CSP generates a GB field in its paraxial region. The diffraction of the GB incident on the conducting curved wedge is then found via the CSP technique by analytically continuing the corresponding UTD ray solution to include the complex point source coordinates. Since the point source is in complex space, the points of diffraction in general turn out to be in complex space as well. The CSP method thus allows one to directly obtain a closed form analytically continued UTD solution for the 3-D electromagnetic diffraction by general curved wedges illuminated by a GB. As mentioned earlier, a relatively general antenna illumination can be easily represented by a sequence of GBs. Therefore, by superposing the diffraction fields of each GB in the sequence, it is possible to find the total scattered field in an efficient manner from a large structure containing curved edges when the latter is illuminated by a complicated antenna pattern. The CSP-UTD analysis developed here for curved wedges will be demonstrated for efficiently analyzing the GB illumination of some curved edged structures.

A Numerical Approach Utilizing GBs for the Efffficient Analysis of EM Scattering by Large Multiple Plate Structures

K.Tap, P. H. Pathak, R. J. Burkholder and T. Lertwiriyaprapa

The Ohio State University, Electroscience Laboratory,
1320 Kinnear Road, Columbus, OH, 43212

In this study, the high frequency plane wave scattering from complex structures which can be built up a combination of multiple plate structures is analyzed via a Gaussian Beam (GB) based numerical physical optics (PO) approach. The conventional numerical PO integration technique rapidly becomes inefficient and even intractable when the electrical size of the plates increase. The IPO approach (P.H. Pathak and R.J. Burkholder, Topic 1.5.2 in *Scattering and Inverse Scattering in Pure and Applied Science*, edited by Pike and Sabatier, Academic Press) provides an alternative solution for multiple interaction problems, but may become intractable at these high frequencies as well. Thus, it is of interest here to investigate the use of GB basis functions to tractably and efficiently represent the field interactions between the plates. The utilization of GB basis functions can be justified by the fact that in contrast to the plane waves in a plane wave spectral (PWS) expansion for the field scattered from each plate, the GB in a GB expansion has a natural window that makes the field value on a GB decay rapidly away from its beam axis. As will be mentioned later, the latter property allows one to represent the field value at a particular observation point with the use of a small or selected set of GBs, rather than employing the full GB expansion. This makes it possible to efficiently analyze the multiple interactions between the plates. With the above view in mind, the GB based analysis of the plane wave scattering from a three-plate structure is investigated. For the sake of being specific, let the plates be numbered as 1, 2 and 3. Of particular interest in this three plate problem is the induced current on plate #3 due to fields doubly scattered from plates #1 and #2. First, plate #1, which is illuminated by the incident plane wave, is divided into identical subsections. The induced current on the plate is obtained by a PO approximation, which is reasonable for well illuminated large plates. Then, the fields scattered from each subsection is expanded in a set of GBs which are launched radially outwards from the center of each subsection (lattice points). The GBs launched from each lattice point are identical and almost equally spaced in angle. The coefficients of the GBs are found from the induced current on the plate. Next, the GBs launched from plate #1 propagate to plate #2 and induce a current on plate #2 which is approximated again by PO. The fields scattered from the second plate are represented in terms of a new set of GBs, as done for the first plate. Finally, the induced current on the third plate is obtained via PO from the GBs launched from the second plate. It is possible to apply this procedure successively to take into account subsequent interactions between the plates upto a finite number (based on appropriate convergence criteria) and compute the total scattered fields from the 3-plate structure in the far zone. Only those GBs which lie within e^{-1} of their on axis values at any observation point are retained. Therefore, only a few of the total GBs in each cluster are retained to produce a sufficiently accurate field value at that point, thus providing an efficient analysis of the multiple plate interactions and thus also the overall scattering from the 3-plate structure. This concept illustrated here for the three plate case can be generalized to more plates. Numerical results comparing the GB approach with the conventional numerical PO method in terms of accuracy and efficiency for scattering from a multiple plate structure will be presented.

A Novel GTD Ray Analysis for the Collective Radiation from Large Finite Cylindrical Conformal Antenna Arrays

P. Janpugdee* and P. H. Pathak

ElectroScience Lab, Department of Electrical Engineering, The Ohio State University
1320 Kinnear Road, Columbus, OH 43212, USA
E-mail: janpugdee.1@osu.edu, pathak.2@osu.edu

A novel high-frequency GTD solution is developed for describing the collective radiation from large finite conformal arrays of magnetic line sources on a large perfectly conducting cylinder in terms of just a few rays. Such a ray analysis provides useful physical insights into the array radiation mechanisms, which are generally not directly available from the other methods. An asymptotic GTD/UTD ray solution for a point source on a smooth convex surface has been previously developed via the method of canonical problems (P. H. Pathak, et al., IEEE Trans. AP., AP-29, 609-621, Jul. 1981). The solution for large antenna arrays on such a curved structure would, if based on the analysis for a single point source mentioned above, require an element-by-element summation of the fields radiated from each of the individual antenna elements of the array (V. Erturk and R. G. Rojas, IEEE Trans. AP., 48, 1507-1516, Oct. 2000). However, a collective or composite field produced by the entire array elements at once is not only be more efficient but, more importantly, it provides a physical picture for the radiation mechanisms for the array on a curved surface. The physical picture for the array radiation results from being able to, in this collective solution, describe the entire radiated field in terms of just a few rays, independent of the array size. A different asymptotic ray analysis of full ring and finite slit arrays on a conducting cylinder has been developed previously (J. Shapira, L. B. Felsen, and A. Hessel, IEEE Trans. AP., AP-22, 49-63, Jan. 1974). In that work, the edge effects of finite arrays had to be inferred heuristically from consideration of the numerical results. In this work, the asymptotic ray solution developed for finite planar arrays, in which edge effects are accounted for more rigorously (F. Capolino, S. Maci, and L. B. Felsen, Radio Science, 35, Mar.-Apr. 2000; P. Janpugdee, P. H. Pathak, et al., 2001 URSI Meeting, Boston MA, Jul. 2001), is extended to finite conformal arrays on a curved cylindrical surface, where in the latter case more complex wave effects are present. In addition to the Floquet waves and their edge and corner diffractions which are also present for the curved array as in the planar array case, there are now also surface rays which are launched from the array edges and corners, and propagate along the curved surface. Although the development in this work is illustrated on the two-dimensional geometry, the procedure can also be directly extended to the three-dimensional configurations, and also to the material coated surface. A uniform GTD, or a UTD solution for the present problem is in progress and will be reported later; this UTD solution is required to patch up the GTD analysis where the latter fails within the transition regions adjacent to the shadow boundaries of the rays excited on the curved surface.

An Asymptotic Green's Function Representation For Fields In The Vicinity Of An Arbitrary Convex Multilayer Coated Conducting Surface

Paul E. Hussar
Alion Science and Technology
185 Admiral Cochrane Dr.
Annapolis, MD 21401
phussar@alionscience.com; 410-573-7703; fax – 410-573-7634

Recently, new solutions have been introduced to provide a description of the propagation of creeping-wave fields over surfaces of general convex geometry and for boundary conditions other than perfect conductivity. These solutions have been obtained from solutions to corresponding circular-cylinder canonical problems via the application of a transformation/substitution process involving the Uniform Geometrical Theory of Diffraction (UTD) generalized torsion factor (P. H. Pathak and N. Wang, IEEE Trans. Antennas Propagat., 6, 911-922, 1981). First it was demonstrated (P. E. Hussar and E. M. Smith-Rowland, J. Electro. Waves Applic, 2, 185-208, 2002) that an order $k^{-2/3}$ approximate Maxwell solution for fields in a suitably-defined boundary layer neighborhood of an arbitrary convex impedance surface can be generated via application of the transformation/substitution process to the canonical circular-impedance-cylinder solution for the case of axial magnetic dipole excitation. Subsequently, a corresponding solution for fields radiated into the far zone of an arbitrary convex singly-coated surface was obtained by the same procedure (P. Hussar, E. Smith-Rowland and B. Campbell, USNC/URSI Natl Radio Sci Mtg 2002 Digest, 29, 2002). More recently, the method has been extended to provide dyadic Green's-function representations for fields exited by arbitrarily-oriented tangential magnetic sources (P. Hussar, 2003 IEEE Int. Symp. on EMC Symp. Rec.).

In this paper, the transformation/substitution process that was used to obtain the solutions listed above is employed in the construction of an asymptotic Green's-function solution for fields excited in the vicinity of an arbitrary convex multilayer coated conducting surface by an arbitrarily oriented surface tangential magnetic dipole source. The construction of the multilayer solution occurs in three stages. First, an approximate Maxwell solution for field components **(E,H)** within a boundary-layer neighborhood of an arbitrary convex multilayer coated conducting surface is obtained via the transformation/substitution technique as applied to Pearson's multilayer-circular-cylinder solution for the case of axial-dipole excitation (L. W. Pearson, Radio Sci., 4, 559-569, 1986). Next, an alternative approximate Maxwell solution is obtained as a generalization of the multilayer-circular-cylinder solution for the case of azimuthal-dipole excitation. Construction of the alternative solution relies on the source/excitation independence of the multilayer-coating reflection coefficient. Finally, the two new solutions for the case of arbitrary convex geometry are combined to construct a dyadic Green's-function representation for fields excited by an arbitrarily-oriented tangential magnetic source according to the prescription described in Hussar 2003 (op. cit.).

The dyadic solution is obtained in the form of creeping-ray modes attenuated by exponential factors that involve line integrals over the creeping-ray geodesic path as well as complex-plane pole loci that vary along the creeping-ray path according to the local surface geometry. At each point along a geodesic path, the relevant pole loci may be identified with the zeros of a function defined for circular-cylinder geometry, but abstracted to general convex geometry with the aid of the UTD torsion factor. Due to the creeping-ray modal format of the solution, it is suitable only for the far shadow zone.

Planar Phased Array Green's Function for an Angular Sector of Dipoles embedded in a Dielectric Multilayer: A Hybrid (Complex-Source)-Asymptotic Approach.

A. Polemi, F. Mariottini, M. Giannettoni, S. Maci

Dept. of Information Engineering, University of Siena, Via Roma 56, 53100 Siena Italy

e-mail: {polemale,fmariottini,macis}@dii.unisi.it, marcogina@libero.it

The array Green's function (AGF) represents the basic constituent for the full-wave Method of Moment (MoM) description of electromagnetic radiation from periodic patch arrays and scattering from periodic printed surfaces. One of the main objectives of an integral equation analysis is the reduction of the numerical effort that accompanies the AGF computation. In a recent work [A. Polemi, D. Nencini, S. Maci, A. Toccafondi, ICEAA 03, Torino, Italy, Sept. 8-12, 2003] the AGF of a rectangular array has been developed in high frequency regime, thus leading to a solution structured in terms of sectoral array diffraction contributions. The asymptotic nature of this solution confines the accuracy of the results in a region far in terms of a wavelength from array edges and corners. To extend this formulation to regions close to the truncations, a new hybrid approach is presented in this paper, where the complex source technique is introduced in the formulation. The MoM scheme we are referring to, imposes the evaluation of the field at the array plane, i.e. where the boundary conditions are applied. This case, which is the most critical, will be referred to in this formulation.

The formulation is structured as follows. The spatial summation over individual dipole contributions is first converted into a spectral domain integral using the technique presented in [S. Maci, F. Capolino, L. B. Felsen, Wave Motion, vol. 34, pp. 263-279, 2001]. The spectral domain integrand is next regularized in two subsequent steps. The first step consists on adding and subtracting the Floquet wave series representing the same field of the infinite array, but windowed at the angular sector. On one hand, this isolates the terms associated to the edge diffraction process; on the other hand allows the calculation of the regularizing contribution in an efficient form by the complex image process [R.M. Shubair and Y.L. Chow, IEEE Trans. Antennas Propagat., Vol. 41, N. 3, pp. 498-502, March 1993]. Next, a second regularization step is applied by using a canonical regularizing function which contains all the singularities of the actual integrand. The extracted part is reconverted in the space domain by using the canonical functions already introduced in the asymptotic analysis of the sectoral array problem in free space [F. Capolino, S. Maci, L. B. Felsen, Radio Sci., vol. 35, n. 2, pp. 579-593, 2000]. Far from vertex and edges, the residual contribution is evaluated in analytical form via two-dimensional saddle-point asymptotics. This leads to a high-frequency expression which contains the basic phenomenology of surface waves-Floquet wave interaction which is already described in our previous paper [A. Polemi, D. Nencini, S. Maci, A. Toccafondi, ICEAA 03, Torino, Italy, Sept. 8-12 2003]. When the asymptotic evaluation cannot be applied, i.e., close to the truncation, the residual regularized contribution is efficiently calculated by numerical integration. The overall process is general, accurate and physically appealing, and more efficient with respect to many alternative methods we have devised.

126

High Frequency Double Diffraction at the Edges of an Impedance Flat Plate

Alberto Toccafondi[1], Matteo Albani[2], Roberto Tiberio[1]

[1] *Dept. of Information Engineering, Univ. of Siena, Via Roma 56, 53100 Siena Italy,*
[2] *Dept. Matter Physics and Physical Advanced Tech., Univ. of Messina, Messina Italy*

High-frequency ray techniques provide effective tools for the prediction of electromagnetic fields in scattering and propagation problems involving electrically large objects within a complex scenario. In many cases, higher order diffraction contributions have to be added to Geometrical Optics and standard (singly diffracted) UTD rays, to augment the model accuracy and to achieve satisfactory continuous results. General uniform dyadic coefficients have been presented [F. Capolino et al., IEEE Trans. on AP, Vol. 45, no. 8, 1997] for the description of double diffracted rays at a pair of arbitrarily arranged perfectly conducting wedges. Recently, a revisited exact solution has been obtained for the electromagnetic problems of edges illuminated by a plane wave at skew incidence, for both a half-plane with surface impedance faces and a surface impedance discontinuity on a plane [O. M. Bucci et al., Radio Science, Vol.-11, 1976]-[R. Tiberio et al., Proc. of IEEE AP-S Symp., Columbus OH, Vol. 4., 2003]. This revisited exact solution explicitly exhibits reciprocity and is cast in a convenient matrix form, which provides a rigorous 2D-3D transformation machinery involving only trigonometric functions.

Here, this surface impedance diffraction solution is used to construct uniform dyadic diffraction coefficients to describe double diffraction at the edges in a flat plate with arbitrary impedance boundary conditions. This formulation can handle finite distance observation, skew illumination aspects, and skew (but coplanar) edges. This provides a significant extension of the applicability of previous works [R. Tiberio at al., IEEE Trans. AP, Vol. 31, No. 4, 1983], [M. I. Herman et al., IEEE Trans. AP, Vol. 36, No. 5, 1988] to electromagnetic 3D case which is useful for practical applications. The result is obtained via a spectral synthesis; the (singly) diffracted field from the first edge is represented as a spectral plane wave superposition. Each spectral plane wave is used to illuminate the second edge; its response in a spectral integral form is obtained by analytical continuation. The superposition of all the responses to each spectral plane wave provides a double spectral representation of the second order interaction of the two edges. Such two fold integral exhibits a double stationary phase point corresponding to a doubly diffracted field. Furthermore, the integrand contains optical and surface wave pole singularities in both variables, that may occur close to and at the stationary phase point determining field transitions. A uniform asymptotic closed-form evaluation of the doubly diffracted contribution is given, which involve suitable transition functions that typically occur in double diffraction problems. The transition functions allows to properly describe the various transitions that the doubly diffracted field may experience at different incidence/observation aspects; i.e. at singly diffracted field shadow boundaries. At a variance of the perfectly conducting case [F. Capolino et al., IEEE Trans. on AP, Vol. 45, no. 8, 1997], here, surface wave excited diffraction mechanisms need to be accounted for, when they are supported by the impedance plate. Numerical results will be shown during the presentation, to illustrate the edge interaction phenomenology as well as to verify the effectiveness and accuracy of the present formulation.

A Time Domain Incremental Theory of Diffraction (TD-ITD) and its reduction to TD-UTD

Filippo Capolino and Roberto Tiberio

Dip. Ingegneria dell'Informazione, Universitá di Siena, Via Roma 56, 53100 Siena, Italy.

The transient field scattered by metallic structures made of flat surfaces with curved edges can be approximately described by using the time domain-incremental theory of diffraction (TD-ITD). This technique is the TD version of its FD counterpart developed in [R. Tiberio et al., *IEEE Trans. Ant. Prop.*, **42**, 600-612,1994] and recently updated in [R. Tiberio et al., *in print for IEEE Trans. Ant. Prop.*, 2004]. There, the field is described as a continuous superposition of incremental ITD field contributions along the curved edges of the metallic structure. This method overcomes caustic singularities of ray techniques and extends the field prediction to observation aspects outside the diffraction cone. Analogously, also in TD the field evaluation presents the advantages shown in the FD, e.g., the transient field can be evaluated near and at caustics. The incremental TD or FD field contribution at any point l on a generally curved edge is defined by resorting to a convenient interpretation of the solution of the canonical problem of the locally tangent, infinite wedge at l.

In this paper, a time domain (TD) version of the ITD, preliminarily presented in [F. Capolino and R. Tiberio, *Int. Conf. Electromagn. Advanced Appl.*, Torino, 2002] is first shown, and formulated directly in the TD, which provides a self-consistent, early-time (high-frequency) description of a wide class of transient phenomena.

In this framework, the TD diffracted field $\hat{\psi}$ scattered by the whole curved edge is represented as superposition of impulses retarded by their travelling time needed by the incident field to reach the edge at any point l, plus the travelling time successively needed to reach the observer. The relevant expressions explicitly satisfy reciprocity. The impulsively excited wavefield $\hat{\psi}$ is valid only for *early times*, on and close to (behind) the wavefronts. However, convolution with an excitation waveform $\hat{G}(t)$ whose frequency spectrum $G(\omega)$ has no low-frequency components and is thus dominated by high frequencies may enlarge the range of validity of the resulting pulsed response to later observation times behind the wavefront.

Besides the advantages and the generality of applicability of the TD-ITD to a wide variety of scattering problems, we show here that away from caustics the TD-ITD recovers the TD-UTD (Uniform Theory of diffraction) for very early times [P. R. Rousseau and P. H. Pathak, *IEEE Trans. Ant. Prop.*, V.43, 1375-1382, 1995]. Then, the TD-ITD may extend the validity of the field description due to the more precise location of the incremental sources on the actual edge. This is a consequence of a neat physical interpretation of the UTD transition function in the FD and of its counterpart in TD.

The TD-ITD is then used in a UTD framework, where the geometrical optics (GO) field is shadowed by the scattering object, and the diffracted field is summed to the spatially discontinuous total GO. It is remarkable that the TD-ITD repairs these spatial discontinuities at the shadow boundaries of the GO by producing an opposite discontinuity.

A Discrete-Time Uniform Geometrical Theory of Diffraction for the Fast Transient Analysis of Scattering from Knife Wedges

Hsi-Tseng Chou[1]*, Hsien-Kwei Ho[2], Chung-Yi Chung[1] and Shyh-Kang Jeng[2]

1 Dept. of Comm. Eng.,Yuan Ze University, Taiwan

2 Grad. Inst. of Comm. Eng., National Taiwan University, Taiwan

Development of efficient time domain (TD) techniques to analyze transient EM wave phenomena attracted interest due to many applications including ultra-wide band radars and antennas for remote sensing and target identification. Frequency domain (FD) solutions utilizing Fourier transform to obtain TD solutions are time consuming if a wide frequency ranges are considered. Recently it tends to develop quasi-analytical TD solutions in closed form solutions that provide physical interpretations of wave behaviors. TD uniform geometrical theory of diffraction (TD-UTD) solutions are examples that were obtained by direct inverse Laplace transform or analytical time transform of the corresponding FD solutions.

The TD-UTD has the advantages of physical interpretation of the wave phenomena for general problems. However, earlier TD-UTD is inconvenient in use because a time convolution with the impulsive TD-UTD solutions needs to proceed for finite pulse width, which is cumbersome if the required number of basis functions is large for a complicated waveform. Also the interpretation of transition functions over shadow boundaries is not very straightforward as it is in FD.

This paper presents a discrete-time (DT) UTD to overcome the shortcoming of TD-UTD while in the mean time retaining the advantages of FD-UTD solutions. This DT-UTD is developed according to a time discretization and represents the time variation in terms of simple basis functions in the Maxwell's equations. This time discretization tends to transform the scalar time Maxwells' equations into a set of matrix-type equations, where each element of the matrix represents the field value at the discretized time steps and is in general functions of locations. The forms of the subsequent matrix equations are analog and dual to the Maxwell's equations of harmonic time dependence. As a result, the DT-UTD can be developed from the FD-UTD formulation via a simple notation transformation based on the duality relationship. The advantages of this DT-UTD are that it translates the time domain convolutions into a simple matrix multiplication and its solutions retain a form similar to FD solutions without going through complicate and difficult computation of special transition functions required in TD-UTD since the computation of FD solutions has been well-developed. Numerical examples will be presented to validate the DT-UTD solution.

129

A Multi-aspect Z-Buffer Algorithm for Ray Tracing in High-Frequency Electromagnetic Scattering Computations

Yong Zhou* and Hao Ling

Dept. of Electrical and Computer Engineering
The University of Texas at Austin
Austin, TX 78712-1084 USA

Ray tracing is a key step in high-frequency electromagnetic scattering computations. Numerical tracing of rays for a complex target model is often a very time-consuming operation. The multiplaten Z-buffer (MPZ) ray-tracing algorithm was proposed by J.-L. Hu et al (*Elec. Lett.*, **33**, 825-826, 1997) as an alternative to the traditional binary space partition (BSP) tree algorithm. Previously, we carried out a performance comparison of the MPZ ray tracer against that of the BSP tree-based algorithm (Zhou and Ling, URSI National Radio Science Meeting, 471, 2003). Our results showed that, in contrast to the BSP tree algorithm, the computational complexity of the MPZ is independent of the number of facets. Therefore, the MPZ algorithm can potentially outperform the BSP algorithm for targets described by a large number of facets. However, the complexity of the MPZ does depend linearly on the number of pixels a ray traverses.

In this paper, we propose a multi-aspect MPZ approach to further speed up the performance of MPZ algorithm. The approach is motivated by the fact that the number of pixels a ray traverses between bounces can be reduced dramatically by decreasing the angle between the ray direction and the Z-buffer direction. In the algorithm, multiple multi-layered Z-buffers are first generated from the scan conversion process along many aspect angles. The maximum number of multi-layered Z-buffers is limited only by the available memory resource. The more aspect angles that be stored, the less pixels a ray traverses in one bounce, and the better the time performance. During the ray trace, the multi-layered Z-buffer structure that has the closest aspect to the ray direction is selected to carry out the ray tracing. A ray is then tracked by moving along the ray direction inside this MPZ structure pixel-by-pixel to check for possible intersections. Once an intersection is found, the hit point and the reflection direction are calculated. Based on the new ray direction, a new MPZ is chosen, and the tracing process is iterated until the ray departs from the bounding box. The computation time performance of the multi-aspect MPZ ray tracer is evaluated against that of the single-aspect MPZ and the BSP tree algorithm. Results for various targets are tested to determine the computational complexity as functions of number of facets and memory size. Comparison shows a dramatic improvement of performance against that of the single-aspect MPZ.

Computing The Radiation Pattern Of An Antenna Mounted On A Complex Structure By Using Accelerated Physical Optics Method

Soner KARACA*
Naval Science & Eng. Inst.,
Turkish Naval Academy
Tuzla, Istanbul, Turkey.
skaraca@dho.edu.tr

Deniz BÖLÜKBAŞ
Gebze Inst. of Tech.,
Dept. of Electronics Eng
Gebze, Kocaeli, Turkey
dbolukbas@ttnet.net.tr

A. Arif ERGİN
Gebze Inst. of Tech.,
Dept. of Electronics Eng.
Gebze, Kocaeli, Turkey.
aergin@gyte.edu.tr

The locations of antennas on board complex platforms, such as ships and aircraft, are vital for proper operation of sensors and communication systems. Presence of the platform influences the coverage area of each antenna mainly through the mechanisms of shadowing and reflection. Therefore, while dealing with a complex structure, obtaining the location of an antenna, which gives the best radiation performance, is one of the main concerns. In this study, we try to compute the radiation patterns of antennas placed on complex platforms. By this way, it is possible to optimize the antenna performance with minimum cost.

In this study, the currents induced on the platforms are obtained by using the physical optics (PO) approximation. This has already been done in previous studies, e.g. (Taboada, *et.al*, Microwave and Optical Technology Letters, vol. 30, no. 5, 357-363, 2001). However, the present emphasis is on accelerating the evaluation of the radiation integrals that have the PO currents as the integrand. This acceleration is accomplished by using exact analytical formulas for the PO integrals instead of numerical or asymptotic integrations. Additional efficiency is gained in identification of shadowed regions by using either a z-buffer or a multilevel tree structure with ray tracing.

The analysis of the radiation pattern starts with a triangular mesh of the complex platform on which the antenna is placed. The platform can be composed of several structures that are not necessarily connected. There are two main steps while forming the radiation pattern. The first step is "identifying lit triangles," in which the triangles that model the platform are separated into two groups; the lit and shadowed triangles. This operation consists of two sub-steps: surface normal check and shadowing. The first sub-step eliminates each triangle for which the angle between the outward surface normal and the direction toward the antenna from the center of the triangle is obtuse. In the second sub-step, the remaining triangles that are shadowed by others are eliminated. This sub-step can be accelerated either by sorting the triangles according to their distance from the radiation source (z-buffer) or by using a multilevel tree (e.g., oct-tree). The second main step is "forming the radiation pattern", where the radiation from the induced currents on the lit triangles as well as that from the antenna are accounted for separately. While calculating the platform-induced radiation, integrals of surface currents are evaluated by using numerical quadrature near the antenna and an analytical formula for sufficiently remote triangles. The analytical formula is obtained using Radon transforms and is exact.
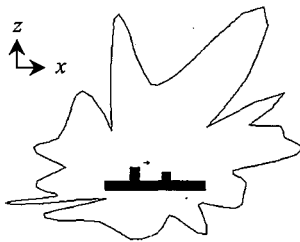
The computer implementation of this algorithm is realized in FORTRAN 90 and a graphical user interface (GUI) has been formed in MATLAB. The GUI accepts the inputs, such as the platform type, location, frequency, etc., and plots the radiation pattern. One of the structures, that has been examined and the radiation pattern of a dipole ($a_x + a_y$ oriented) mounted on this structure, is shown in the figure. Derivation of the PO integral formula and several examples demonstrating the accuracy and efficiency of the proposed scheme will be presented.

Software ANDERA : Analysis and Design of Reflector Antennas

José A. Martínez (*), Antonio G. Pino, Marcos Arias, Oscar Rubiños
Grupo de Antenas. Dpt. Teoría de la Señal y Comunicaciones. Universidad de Vigo
E.T.S. Ingenieros de Telecomunicación.   36200 VIGO-SPAIN

This paper presents ANDERA software, which has been developed for the analysis and design of reflector antennas. The program has been written under the Matlab programming language and a compiled version has been produced for the Windows platform. The kernel of the software is based on the Physical Optics algorithm described in (Arias, Rubiños and Pino, R.R.D. in Magnetics, vol.1 ,2000 pp.43-63. ISBN: 81-86846-89-1).

The geometry of the antenna can be defined in two different ways. The first one is by the use of the interactive design window included in the Software. In this window the user defines the main geometric parameters of the main reflector: Focal Length, Offset height, Dish Size etc. For the dual reflector case some additional parameters must be defined as Magnification Factor, Eccentricity, Interfocal Length etc. Once the geometry is defined, a set of triangular facets of the surfaces is automatically produced in order to perform the further electromagnetic simulation. The second way to define the surface is by importing the surface triangles from a file, allowing the analysis of shaped or measured surfaces.

The Software allows to carry out a tolerance analysis. In this module, the location and target point of the feed can be changed. Moreover, the feed pattern can be rotated about any of its axes. In the dual reflector case, the subreflector-feed system can be moved or tilted.

To illuminate the surface three kinds of feeds are implemented. The first one is a *cos-q* ideal model, defined by the polarization; taper and frequency. The second option is to introduce the feed numerically from a file containing the feed pattern. That allows the simulation with real measured feeds or simulated by an external program. The last way to feed the antenna is by an array of *cos-q* elements. Firstly, the program computes the fields produced by each element with unit excitation in presence of the reflector. Then, a array-design module is able to change the excitation vector of the array in order to synthesize the desired pattern.

Once the surface and feed have been established, an interactive window shows the Physical Optics currents (Figure 1-a). The field calculation window is then presented allowing the computation of near and far fields of the antenna. The fields can be depicted in 2D-cuts, contour plots or 3D-views (Figure 1-b). Moreover, a post-process module gives precise information of the pattern by interactive cursors.

Both the triangle description of the antenna and the computed fields can be saved into files to facilitate further analysis.
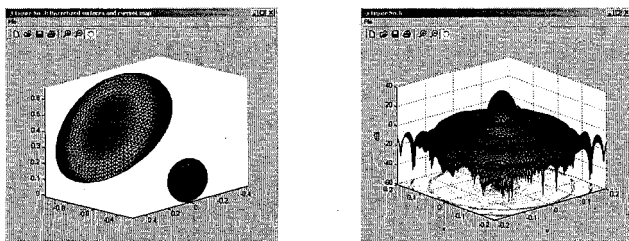
Figure 1-(a) Colour plots of the PO current across Discretized surfaces.
(b) 3D view of the far field across the U-V plane

Resonance Cone Phenomena in a Low-Profile Inhomogeneous Anisotropic Metamaterial Antenna

K.G. Balmain*, A.A.E. Lüttgen, and P.C. Kremer
The Edward S. Rogers Sr. Department of Electrical and Computer Engineering
University of Toronto
Toronto, Ontario, Canada M5S 3G4

The anisotropic metamaterial is based on a square-celled, planar wire grid having orthogonal capacitors and inductors embedded in it. The resonance cone is a high-field region that can be viewed most simply as the straight-line path of low impedance that extends outward across the grid, starting from the location of any concentrated signal source. The grid cells are of finite size and are simulated using full-electromagnetic, moment-method techniques validated with experiments. In previous publications, the grid has been positioned over a horizontal ground plane and has functioned either as a microwave interconnect or as an antenna, with the antenna function aided by the presence of inductors dropped to ground from the wire intersections in the grid.

Ongoing studies have uncovered phenomena more complex than originally foreseen, such as backward waves (negative refractive index), backward resonance cone refraction at an interface, and multiple-interface effects such as multiple cone refractions. The latter produce contracting square spirals that converge to vortices, expanding square spirals that can produce unwanted interactions when they encounter the grid edges, and completely contained cone patterns that never reach the grid edges. In the presentation, these phenomena will be updated with new data and interpretation.

Of particular interest are the modes that can exist, such as a quasi-parallel-plate mode between the grid and the ground plane, and a quasi-surface-wave mode that is tightly bound to the grid. The latter can be isolated by eliminating the ground plane and using an embedded dipole as the signal source, revealing a different subset of some of the phenomena already mentioned above. In particular, the grid surface wave mode apparently couples to the parallel-plate mode and steers cone-like fields between the grid and ground, thus influencing radiation effects.

In the simulations, a mode has been identified with approximately equal and opposite side-by-side currents, thus having some similarity to a two-wire transmission line. As well, over a finite propagation distance, mode conversion has been noted between the two-wire "balanced" mode and an unbalanced mode. These mode-coupling phenomena could have beneficial as well as detrimental effects, both of which will be addressed in the presentation.

VOLUMETRIC ARTIFICIAL MAGNETIC CONDUCTORS
FOR ANTENNA APPLICATIONS

Aycan Erentok* and Richard W. Ziolkowski

Department of Electrical and Computer Engineering
The University of Arizona
1230 E. Speedway
Tucson, AZ 85721-0104   USA

Tel: (520) 621-6173
Fax: (520) 621-8076
E-mail: erentoka@ece.arizona.edu, ziolkowski@ece.arizona.edu

Metamaterials are often generated by artificially fabricated, extrinsic, low dimensional inhomogeneities in some background substrate. Metamaterials that mimic known material responses or that qualitatively have new response functions that do not occur in nature have been realized. In particular, several artificial magnetic conductor (AMC) metamaterial designs have been introduced recently. These include the Sievenpiper class of mushroom surfaces, the Itoh-UCLA class of UC-PBG surfaces, and a variety of more standard FSS-based surfaces.

The design, fabrication and measurement of a metamaterial realization of a volumetric form of AMC will be presented. In contrast to the surface forms, the present design has no perfect electric conductor ground plane. Several AMC metamaterial designs based upon capacitively loaded loops (CLLs) have been conceived for X-Band operation at 10 GHz. Both ANSOFT's High Frequency Structure Simulation (HFSS) tools (FEM based) and Finite Difference Time Domain (FDTD) simulators have shown that the CLL metamaterial produces the desired in-phase reflection, $R = +1$, at the selected operational frequency. Moreover, these simulations have demonstrated the possibility of realizing the volumetric AMCs with subwavelength inclusions in Rogers 5880 DUROID ($\varepsilon_r = 2.2$) at X-Band frequencies.

These CLL designs will be reviewed. The CLL AMC metamaterial was fabricated and tested experimentally with a free space X-Band measurement setup. The measurement methods will also be described. The results of these AMC metamaterial experiments will be discussed. Very good agreement between the numerical and experimental results was achieved and these comparisons will be presented.

HFSS simulations of the use of the measured CLL AMC metamaterial block in antenna applications will also be presented. It will be shown that a dipole antenna placed optimally near the AMC block more than doubles the far field output and significantly improves the front to back ratio of the system. Moreover, near the antenna, it will be shown that the fields on the side of the CLL AMC block away from the dipole are significantly reduced.

Negative Index Lens Phenomena

David R. Smith* and David Schurig
Department of Physics, University of California, San Diego

There have been many applications and phenomena considered for materials with negative refractive index. Many of these—such as the "perfect lens," in which a negative index slab is used to refocus electromagnetic radiation with resolution beating the diffraction limit—rely on very strictly defined material parameters, perhaps at the edge of what is currently technologically feasible. While such exotic applications are within the realm of what is possible with these new artificially constructed negative index materials, there are existing applications that can more immediately benefit by the use of negative index materials. Here we consider the impact of negative index on the design of conventional (as opposed to "perfect") lenses.

The advantage of negative index in lens design stems from a fundamental asymmetry in nature: a material with a relative index of $n=+1$ has no refractive power, while a material with a relative index of $n=-1$ has considerable refractive power. The striking difference is manifest, for example, when one considers the focal length for a lens with radius of curvature R, $f = R/|n-1|$. An index of $n=-1$ has a focal length of $R/2$. The same focal length (for a given radius of curvature) would require a positive index of $n=+3$! Such a large index is not easily achieved in existing materials without utilizing fairly heavy ceramic materials. By contrast, the $n=-1$ condition is easily achievable in artificial materials, and can simultaneously occur with an impedance $z=+1$, implying minimized reflectance.

We will discuss the applicability of geometrical and Fourier optics to negative index lenses, and the use of those methods to optimize the design. The combined results of the analysis illustrate the remarkable potential that negative refraction may have on optical systems.

Space-Filling-Curve Elements as Possible Inclusions for Double-Negative Metamaterials

John McVay
Dept. of Electrical and Computer Engineering
Villanova University
Villanova, PA, 19085

Nader Engheta
Dept. of Electrical and Systems Engineering
University of Pennsylvania
Philadelphia, PA 19104

Ahmad Hoorfar
Dept. of Electrical and Computer Engineering
Villanova University
Villanova, PA, 19085

Abstract

The topic of complex materials in which both permittivity and permeability possess negative values at certain frequencies, known as left-handed (LH) or double-negative (DNG) media, has recently gained considerable attention. This idea was originally postulated by Veselago in 1967, who theoretically studied plane wave propagation in a material whose real ε and μ he assumed to be simultaneously negative [V. G. Veselago, "The electrodynamics of substances with simultaneously negative values of ε and μ," Soviet Physics Uspekhi, vol. 10, no. 4, pp. 509-514, 1968. (Usp. Fiz. Nauk, vol. 92, pp. 517-526, 1967.)]. Recently, Shelby, Smith and Schultz constructed such a composite medium for the microwave regime, using arrays of split ring resonators and metallic wires, and experimentally demonstrated the negative refraction in such a structure [R. A. Shelby, D. R. Smith, and S. Schultz, "Experimental verification of a negative index of refraction," Science, vol. 292, no. 5514, pp. 77-79, 2001].

With recent interests in the DNG metamaterials in mind, we explore numerically-analytically the possibility of forming such media by using metallic inclusions shaped in the form of space-filling curves. The inclusion geometries include the Peano and Hilbert space-filling curve elements, which in previous works have been shown to be resonant at wavelengths larger than the linear dimension of such elements [J. McVay, N. Engheta, A. Hoorfar, "High-Impedance Metamaterial Surfaces Using Hilbert-Curve Inclusions," to appear in *IEEE Microwave and Guided Wave Letters*]. These elements thus provide *compact* resonant inclusions with smaller footprints. In the present work, we first obtain numerically the electric and magnetic polarizability tensors for a single space-filling-curve inclusion via the method of moments. A bulk medium can then be conceptually considered by embedding many of these identical inclusions within a host medium, and the mixing rule such as the well-known Maxwell-Garnett formulation is used to evaluate the effective relative permittivity and permeability for this composite medium. We perform a parametric study with respect to the role of different factors such as iteration orders of space-filling curves, orientations of these elements, and frequency of operation, and we discuss under which conditions the effective permittivity and permeability may attain negative real values. In this talk, we will present some of our theoretical results, and will discuss physical interpretation for our findings.

A Study of Diversity Performance of Integrated Combinations of Fixed and Reconfigurable Antennas on Portable Devices

G. H. Huff, T. L. Roach, D. Chen, and J. T. Bernhard*
Electromagnetics Laboratory
Department of Electrical and Computer Engineering
University of Illinois at Urbana-Champaign
Urbana, IL 61801
jbernhar@uiuc.edu; http://antennas.ece.uiuc.edu

Simple, single antennas deployed on portable wireless data devices are usually minimally functional and limit noise immunity, battery life, and, ultimately, data throughput. This kind of limited antenna functionality could have a significant impact on performance of high-speed communication links in the future. One approach to expand system capability to meet new challenges is to develop reconfigurable antennas for portable devices. Ideally, new communication systems can then leverage this broad antenna functionality to take advantage of emerging techniques in wideband microwave circuits, signal processing, and protocols, resulting in more efficient, secure, and cost-effective high performance communication and sensing systems. While the possibility of integrating phased arrays (as proposed in S. Bellofiore et al., *Proc. IEEE Antennas and Propagation Int. Symp.*, 1, 2001, 26-29) may be remote, an alternative is to combine a small number of reconfigurable antennas to achieve diversity, direction-of-arrival capabilities, and limited beamforming (without phase shifters) depending on the operating environment and desired throughput.

The present study investigates this alternative approach by combining planar fixed and pattern-reconfigurable antennas (G. H. Huff et al., *IEEE Microw. Wireless Comp. Lett.,* 13, 57-59, Feb. 2003) on a portable device and exploring possible configurations that work to deliver diversity and/or beamforming in concert with the device chassis itself. Since the reconfigurable antennas implemented in this work are switched between a discrete set of states, antenna placement (relative to the chassis and to one another) determines the utility and uniqueness of operating states from each set of integration positions. Electromagnetic visibility studies and practical integration scenarios guide initial antenna placements, with changes implemented in light of integration effects, coupling effects, and desired operational goals (i.e., diversity, beamforming, etc.). Detailed results of measurements and calculations of diversity performance and beamforming will be presented in addition to directions for future work in this area.

Conformal Integration of Broadside to Endfire Radiation Reconfigurable Antennas onto Canonical Structures

G. H. Huff*, T. L. Roach, and J. T. Bernhard
Electromagnetics Laboratory
Department of Electrical and Computer Engineering
University of Illinois at Urbana-Champaign
Urbana, IL 61801
jbernhar@uiuc.edu; http://antennas.ece.uiuc.edu

Recent developments in the designs of reconfigurable antennas have demonstrated their ability to contribute additional degrees of freedom compared to conventional antennas with fixed radiation and frequency characteristics. However, to fully justify and utilize these antennas in a specific application, it is advantageous to gain a fundamental understanding of the antenna's local interaction with varying host geometries as well as other reconfigurable (and/or conventional) antenna elements. In turn, this information may be used directly when integrating the antenna onto specific geometries, or used in highly developed ray tracing tools to provide a better predictor of overall system performance in complex scattering environments. Once this knowledge is acquired, applications choosing to take advantage of these antennas can then exploit reconfigurable characteristics in the most innovative, practical, and successful manner possible.

This study reports on the performance of a pair of broadside to endfire radiation reconfigurable antennas (operating over a shared 2:1 VSWR bandwidth) mounted onto two canonical structures, specifically a cube and a cylinder. Structures are considered which are smaller than, equivalent to, and greater than an operational wavelength, with the reconfigurable antenna mounted in several integration positions. To further explore the effects of integration position for these antennas, an Electromagnetic Visibility Study (EVS) is performed and correlated to the analytical results for the two canonical structures. In addition, the spatial combination of the two radiation patterns will also be examined using array techniques. Using information extrapolated from these results, the two reconfigurable antennas are then conformally mounted to the host structures and an experimental investigation is performed. Measured performance of the antennas such as 2:1 VSWR bandwidth, impedance, coupling, and radiation characteristics, will be discussed. In addition, the obtainable diversity between the two antennas will also be considered for each of the structures.

Plane waves near directions of singularities of the wave vector surfaces

S. R. Seshadri
109 North Whitney Way, Madison, Wisconsin 53705-2718

For a biaxial crystal, in the principal coordinate system $\left(X_p, Y_p, Z_p\right)$, the real and different relative permittivities are $\varepsilon_X, \varepsilon_Y$, and ε_Z with $\varepsilon_X < \varepsilon_Y < \varepsilon_Z$. The wave vector surface constructed from the plane wave dispersion relation is a two-sheeted surface that intersects itself at four points lying on the $Z_p X_p$ plane. These intersection points lie along two diagonal lines (the binormals) which are on opposite sides of, and inclined at an angle β to, the Z_p axis. The direction of phase propagation is in the direction of the wave vector and the normal to the wave vector surface at the terminal points of the wave vector gives the direction of amplitude propagation. The intersection points are singular in that the stated normals are indeterminate requiring the treatment of amplitude propagation by the use of a limiting process of the wave normal near the directions of the binormals.

A rotated orthogonal coordinate system $\left(X, Y = Y_p, Z\right)$, where Z is along a binormal is used. The plane wave has the phase factor: $\exp\left[i\left(\mathbf{k}.\mathbf{R} - \omega t\right)\right]$ where $\mathbf{k}, \mathbf{R}$, and ω are the wave vector, the position vector, and the wave angular frequency, respectively. From the Maxwell's equations, the plane wave dispersion relation, $f\left(\mathbf{k}, \omega\right) = 0$, is deduced. Let $\mathbf{k} = \omega c^{-1} n$ ($\sin\theta\cos\phi$, $\sin\theta\sin\phi$, $\cos\theta$), where n is the effective refractive index, $\left(\theta, \phi\right)$ denote the direction of the plane wave and θ is the inclination angle of $\mathbf{k}$ with the binormal. Solving the dispersion relation, the first three terms in the expansion of n^2 in powers of θ are determined for the two existing modes. The time-averaged values of the energy density w and the Poynting vector $\mathbf{S}$ are expressed in terms of $f\left(\mathbf{k}, \omega\right)$. In the expansions of w and $\mathbf{S}$ in powers of θ, the leading terms, w_1 and $\mathbf{S}_1$, are proportional to θ. The leading term in the power series expansion of the ray vector $\mathbf{s} = \mathbf{S}/cw$ is independent of θ. Therefore, for $\mathbf{k}$ in the direction of the binormal, the direction of $\mathbf{S}$, namely, $\mathbf{s}_0$, exists and traces the surface of a cone as ϕ is varied from 0 to 2π. Since $w = |\mathbf{S}| = 0$ for $\theta = 0$, the amplitude along the cone of rays vanishes showing that the crystal does not support a plane wave with $\mathbf{k}$ in the direction of the binormal.

For $\theta \neq 0$ and small, $|\mathbf{S}|$ increases from 0 and the directions of $\mathbf{S}$ of the two modes move in opposite directions from their values for $\theta = 0$. A Gaussian amplitude term, $\exp\left[-\left(X^2 + Y^2\right)w_0^{-2}\right]$, where w_0 is the beam waist is included to take account of the small range in the direction of $\mathbf{k}$ about the binormal. Therefore, the amplitude of $\mathbf{S}$ near the binormal has the θ dependence of the form: $\theta\exp\left(-R^2\theta^2 w_0^{-2}\right)$ which vanishes for $\theta = 0$ and has a maximum for small θ. Hence, the light amplitude is maximum for small θ and is transported in the direction specified by $\mathbf{s}$, which is different for the two modes. Thus, the experimentally observed characteristic intensity distribution, namely, a dark circular strip $\left(\theta = 0\right)$ sandwiched by two nearly concentric $\left(\theta \text{ small}\right)$ bright rings is explained.

Electromagnetic Gaussian beam beyond the paraxial approximation

S. R. Seshadri

109 North Whitney Way, Madison, Wisconsin 53705-2718

The electromagnetic Gaussian beam that exists for $z > 0$ and propagates along the $z-$axis is constructed from an electric vector potential $F_y(\rho, z)$ in the $y-$direction. The potential is cylindrically symmetrical about the $z-$axis. The phase term $\exp(ikz)$ is factored out from $F_y(\rho, z)$ where k is the wave number. The remaining part, $f_y(\rho, z)$, is a slowly varying function of its arguments. If ω_0 is the beam width occurring at $z = 0$, it is usual for ω_0 to be large compared to the wavelength $2\pi / k$ so that $f_0^2 \left(= 1 / k^2 \omega_0^2 \right)$ is a small parameter, allowing $f_y(\rho, z)$ to be expanded into an infinite series in powers of f_0^2. The leading term is the paraxial beam and the $(m+1)$th term is the mth order nonparaxial beam. The paraxial beam is governed by the homogeneous paraxial wave equation and the nonparaxial beams are governed by inhomogeneous paraxial wave equations.

The governing equation for $f_y(\rho, z)$ is a second-order differential equation in z. There are two independent solutions. Therefore, two conditions are required at $z = 0$ and $z \to \infty$ to obtain unique solution. One condition is the radiation condition for $z \to \infty$ and the other is the specified value of the potential at $z = 0$. A singular situation occurs in that f_0^2 appears as a coefficient of the second derivative of z. Consequently, the governing equations degenerate into first-order differential equations in z requiring only one condition for obtaining a unique solution. The solution for the paraxial beam emerges satisfying naturally the radiation condition for $z \to \infty$. Therefore, the application of one condition, namely that at $z = 0$, leads to a correct unique solution. The governing equation for the $m = 1$ nonparaxial beam has a forcing term that is singular at $z = 0$ and therefore, is valid only for $0 < z \leq \infty$ and not at $z = 0$. The solution for the nonparaxial beam is expressed as a superposition of the particular integral corresponding to the specified forcing term and a complete set of cylindrically symmetric Laguerre-Gauss modes. The required behavior of the nonparaxial beam for $z \to \infty$ is deduced and applied to obtain all but one of the modal coefficients. The nonparaxial beam is excited by way of a resonant interaction with the paraxial beam causing the amplitude to grow with the distance in the propagation direction. This linear growth is nonphysical and is suppressed by appropriately choosing the one remaining modal coefficient. Thus, the nonparaxial beam has the required proper physical behavior near $z = 0$ and $z \to \infty$.

The electromagnetic fields are determined and the electrodynamics of the beam beyond the paraxial approximation is discussed. The present treatment is compared with a representative previous investigation.

Simulation of Quantum Computing Search Algorithms at Microwave Frequencies

Robert Nevels and Jaehoon Jeong

Department of Electrical Engineering
Texas A&M University
College Station, Tx 77845-3128
Email: nevels@ee.tamu.edu

One of the tasks in the successful creation of a quantum computer is the development of an effective quantum search algorithm, a concept originally introduced by L. K. Grover. Grover's algorithm effectively reduces the number of queries necessary to find a particular quantum bit, or qbit, of data in an N element array of data from ~N to ~$\sqrt{N}$. A number of search algorithms have been proposed since the publication of Grover's original paper. However, due to the expense and precision required to build measurement devices and perform tests on a quantum level, to date very little hardware has been developed to determine the validity of quantum search algorithms.

In this paper we present research that follows the line of reasoning put forward by Grover, but with the "query" performed with classical electromagnetic waves rather than by quantum mechanisms. The method we present takes advantage of the time reversal symmetry of Maxwell's equations to search a periodic structure containing an information bit. Time reversal is a method whereby an electromagnetic pulse is sent through a region concerning which the observer has considerable, but not all, information. The signal is reflected back from the region and received by a small number of probes. By processing the received signal using the knowledge available to the observer, information bits in the medium can be reconstructed.

In our case the quantum array is simulated at microwave frequencies by a 2-D array of microstrip ring resonators, with a 'target' bit represented by one ring having a slightly different resonant frequency. An electromagnetic wave is sent into the ring array in a sequence of rapidly repeating pulses. The sequence of pulses represent the queries directed at the quantum information array. It is shown that the number of queries necessary to locate the target ring with this approach is on the order of that predicted by the Grover algorithm.

141

Electromagnetic Properties of Aperiodic Tilings:
Background and Preliminary New Results

Giuseppe Castaldi[1], Rocco P. Croce[1], Vincenzo Fiumara[2], Vincenzo Galdi[1],
Vincenzo Pierro[1], Innocenzo M. Pinto[1], and Leopold B. Felsen[3]

(1) Waves Group, Dept. of Engineering, University of Sannio, Benevento, ITALY

(2) D.I.I.I.E., University of Salerno, Fisciano (SA), ITALY

*(3) Dept. of Aerospace & Mechanical Eng., Boston University, USA (part-time)
Also, University Professor Emeritus, Polytechnic University, Brooklyn, NY USA*

In a variety of applications in modern electromagnetics (EM) engineering, such as phased arrays, frequency selective surfaces and photonic band-gap (PBG) devices, reliance is placed on *periodic* geometries, i.e., truncated ordered repetitions of a given spatial pattern. Multiscale self-similar (fractal) configurations are sometimes used to achieve multi-band operation. In some applications (e.g., thinned arrays), *random* disordered geometries have been exploited to overcome specific limitations (e.g., grating lobes). While the typical wave phenomenologies characterizing *perfect periodicity* (e.g., bandgaps) and *absolute randomness* (e.g., diffuse scattering, strong localization) are relatively well understood, much less is known about the electromagnetic properties of geometries in the "gray zone" in between. This realm of "orderly disorder" encompasses a broad range of hierarchical order types, from "quasi-periodic" to "quasi-random".

Two-dimensional (2-D) "aperiodic tilings" are collections of polygons that cover a plane, without gaps and overlaps, and are devoid of any translational symmetry. Nevertheless, they can exhibit *local* (or *weak*) forms of *order* and *symmetry*, and can span a remarkable range of order types. Examples of such geometries, originating from computational logic problems, were known since the 1960s, but they have been regarded as no more than mathematical oddities until the discovery of "quasicrystals" (Shechtman *et al.*, *Phys Rev. Lett.*, **53**, p. 1951, 1984), i.e., materials whose X-ray diffraction patterns exhibit unusual symmetries (e.g., five-fold) that are not compatible with spatial periodicity. This discovery, which suggests that nonperiodicity rather than periodicity might be the generic attribute of solid state, raised new questions and furnished broader perspectives pertaining to the notions of "order" and "symmetry." Thus, use of certain aperiodic tilings (whose *weak* symmetries are capable of reproducing the above "forbidden" spectral symmetries) has been suggested to model the properties of real quasicrystals. The reader is referred to (Senechal, *Quasicrystals and Geometry*, Cambridge Univ. Press, 1995) for a nice introduction to and review on this subject area.

From the above discussion, aperiodic tilings and the associated discrete geometry seem to provide a rather general framework for systematic exploration pertaining to the electromagnetic properties of "orderly disorder." However, applications in EM engineering have so far been sparse, focused primarily on PBG quasicrystals (see, e.g., Chan *et al.*, *Phys. Rev. Lett.*, **80**, p. 956, 1998; Bayindir *et al.*, *Phys. Rev. B*, **63**, 161104(R), 2001). We have recently initiated a sequential study of the electromagnetic properties of 2-D aperiodic tilings, starting with the simplest problems in antenna array radiation and screen diffraction. In particular, we have selected a number of representative tiling classes for probing the range from quasi-periodic to quasi-random. Problems of interest may eventually include the synthesis of structures with unusual spectral signatures, as well as study of the effects of local order and symmetry in the dynamic EM response (bandwidth, grating lobes, polarization, etc.). The lecture will include a brief summary of relevant background theory as well as presentation of known and preliminary new results.

Discrete Helmholtz Decomposition, Euler's Formula, and the Degrees of Freedom of Lattice Electrodynamics

Bo He* and F. L. Teixeira

ElectroScience Laboratory and Department of Electrical Engineering,
The Ohio State University, 1320 Kinnear Road, Columbus, OH 43212, USA

Electromagnetic (EM) theory can be formulated on a irregular lattice (grid) from first principles using differential forms and tools from algebraic topology (Teixeira and Chew, *J. Math. Phys.*, **40**, 196-187, 1999). One key feature of lattice EM theory is the co-existence of both a primal and a dual lattice. We consider here the TE case on 2+1 dimensions and linear regime. The discrete EM fields are paired as follows: In the primal lattice, the electrostatic potential ϕ (discrete differential form of 0-th degree or 0-cochain) is paired with primal nodes, the electric field intensity E (1-cochain) with primal edges and the magnetic flux density B (2-cochain) with primal faces. In the dual lattice, the magnetic field intensity H (0-cochain) is paired with dual nodes and the electric flux density D (1-cochain) with dual edges.

Let $F^p(M)$ be the space of differential forms of degree p on the domain M. The Helmoltz (Hodge) decomposition can be written in general as

$$F^p(M) = dF^{p-1}(M) \oplus \delta F^{p+1}(M) \oplus H^p(M)$$

where $H^p(M)$ is the space of harmonic forms. Since $H^p(M)$ is already finite dimensional in the continuum theory, in the following we consider the $dF^{p-1}(M) \oplus \delta F^{p+1}(M)$ space only. For $p = 1$ on the primal lattice, dim $\left(dF^{p-1}(M)\right)$ represents the number of degrees of freedom $(nDOF)$ in the electrostatic field, while dim $\left(\delta F^{p+1}(M)\right)$ represents the $nDOF$ in the dynamic field.

Using the Helmholtz decomposition and the Euler's formula for a network of polygons, we can show that the number of dynamic DOF $(nDOF^d)$ of E equals the $nDOF^d$ of B in a lattice with (possibly mixed) *arbitrary* polygons, *if* the discrete fields are paired as above. Furthermore, due to the isomorphism (Hodge map) between E and D, and between H and B, we have in 2-D

$$nDOF^d(E) = nDOF^d(D) = nDOF^d(H) = nDOF^d(B) = N_p - 1 \qquad (1)$$

where N_p is the number of polygons used to discretize the domain.

This identity is helpful in removing static DOF before a time-domain update. This also provides a means to regularize otherwise singular problems. Moreover, there has been recent interest in applying numerical techniques developed for Hamiltonian systems to computational EM (Kole et al., *Phys. Rev. E*, **64**, 066705, 2001). It is not trivial to formulate Maxwell's equations as canonical equations of a Hamiltonian, because they behave as a *constrained* dynamic system (because of the div equations). In addition, a Hamiltonian requires the canonical pair to have the same $nDOF$. The above identity means that it is possible to formulate the Maxwell's equations as canonical equations if the discretization recipe described in the first paragraph is employed and the static DOF for both E and B (or H) are factored out a priori.

OBTAINING REACTIVE POWER DENSITY FROM COMPLEX POYNTING THEOREM

D. Marcano, A. Sharaiha*[1], K. Mahdjoubi[1], M. Díaz

Universidad Simón Bolívar.Dpto. Electrónica. Apdo.Postal 89000.Caracas 1080-A, Venezuela.
[1] Université de Rennes I- IETR. Campus de Beaulieu, 35042 Rennes Cedex, France

Poynting's Theorem was established using time dependent electromagnetic fields. However, generally the electromagnetic power calculations are based on the Complex Poynting Theorem (CPT), because it works very simply in the complex domain. The real part of the Complex Poynting Vector (CPV) is equal to the average of the Time Domain Poynting Vector (TDPV) and corresponds to the active power. Although the imaginary part of the CPV doesn't have physical meaning, there is a tendency to associate it with the reactive power density. In this paper we discuss on the applicability of the CPV and we show that its imaginary part is not equal to the reactive power density in general but only where the polarization is linear. We then propose a new formulation to obtain the reactive power density from the CPV applicable in general cases. Moreover, in the case of mode combinations, the polarization is not constant in the whole space and can change from point to point. One interesting case is the combination of two z oriented electric and magnetic dipoles excited in order to have the same electric far field magnitude, under these conditions the radial component of the CPV is purely real and its imaginary part is identically null for all frequencies and excitation phases. In this case, one can be tempted to conclude that the electric and magnetic stored energies compensate each other and the Q factor becomes zero and the bandwidth infinite for such a self oscillating structure. However, as we mentioned before the imaginary part of CPV does not represent the reactive power S_{re}. Fig. 1 shows S_{re} calculated by using the TDPV, versus phase shift between dipole excitations δ at the observation point $r=0.05\lambda$, $\theta=\pi/2$. S_{re} is null only when $\delta = \pi/2$. The reason is that at this point the natural phase shift between E_θ and E_φ is compensated totally by δ and the polarization becomes again linear. Fig. 1, also show the S_{re} obtained using new formulation proposed, and we can observe the perfect agreement with the results obtained from TDPV.
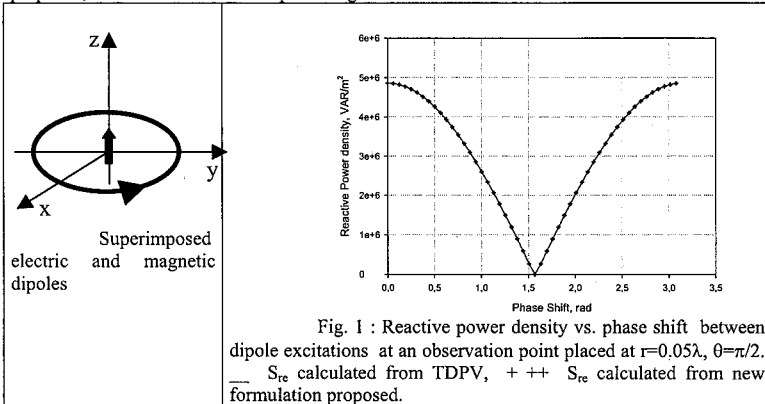
Fig. 1 : Reactive power density vs. phase shift between dipole excitations at an observation point placed at $r=0.05\lambda$, $\theta=\pi/2$. ___ S_{re} calculated from TDPV, + ++ S_{re} calculated from new formulation proposed.

Conclusions: In order to calculate correctly the reactive power density from the CPV, a new modified CPV formulation is proposed which is valid in the general case. The results obtained show a perfect agreement between the reactive power density obtained from the TDPV and the new formulation. The example analyzed here showed that the relative phase of excitation in the case of multiple modes has an important effect and has to be take in to account.

144

Windowed Radon Transform Frames and their Application in Short-Pulse Radiation

Ehud Heyman[1]* and Amir Shlivinski[2]

[1]School of Electrical Engineering, Tel Aviv University, Tel Aviv 69978, Israel
[2] Dept. of Electrical Engineering, University of Kassel, 34121 Kassel, Germany

We present a new class of windowed Radon transform (WRT) frames in $\mathbb{H}_2^\Omega$, the Hilbert space of band-limited, square-summable functions in $\mathbb{R}^3$. We also construct the dual frame set and determine the conditions for these frames to be snug.

The elements of the WRT frames are obtained by shifting and shearing a proper window function $\psi(x)$, $x = (x_1, x_2, x_3) \in \mathbb{R}^3$ in the form:

$$\psi_{m,n}(x) = \psi[x_1 - m_1\bar{x}_1,\ x_2 - m_2\bar{x}_2,\ x_3 - m_3\bar{x}_3 - n_1\bar{\xi}_1(x_1 - m_1\bar{x}_1) - n_2\bar{\xi}_2(x_2 - m_2\bar{x}_2)].$$

They are structured, therefore, upon a 5D phase space, comprising a discrete lattice of points $x_m = (m_1\bar{x}_1, m_2\bar{x}_2, m_3\bar{x}_3)$ tagged by the index $m = (m_1, m_2, m_3) \in \mathbb{Z}^3$ with $(\bar{x}_1, \bar{x}_2, \bar{x}_3)$ being lattice's unit cell; and a discrete lattice of directions $\xi_n = (n_1\bar{\xi}_1, n_2\bar{\xi}_2)$ tagged by the index $n = (n_1, n_2) \in \mathbb{Z}^2$ with $(\bar{\xi}_1, \bar{\xi}_2)$ being the unit cell of the shearing operation in a pseudopolar coordinate system structured about a preferred axis, which is taken here to be the x_3 axis. These cell dimensions are determined by the data bandwidth Ω. A given function $f(x) \in \mathbb{H}_2^\Omega$ is thereby described as a discrete phase space sum of shifted and tilted windows $\psi_{m,n}$ in the form:

$$f(x) = \sum_{m,n} a_{m,n}\psi_{m,n}(x), \qquad a_{m,n} = \langle f(x), \varphi_{m,n}(x)\rangle,$$

where the expansion coefficients $a_{m,n}$ are obtained by projecting $f(x)$ onto the dual frame $\varphi_{m,n}(x)$, obtained by shifting and shearing the dual window $\varphi(x)$. These operations are readily recognized as localized and discrete generalization of the conventional Radon transform and its inverse, hence the term WRT frames. Explicit expressions for $\psi_{m,n}$ and $\varphi_{m,n}$ are given for the class of isodiffracting windows, which can be matched to the (x_m, ξ_n) lattice to render both frames snug.

The WRT frame is applied next to the problem of radiation into the half space $z > 0$ due to a time-dependent aperture source distribution $u_0(x_1, x_2, t)$ in the $z = 0$ plane (Fig. 1). We use the WRT frame formulation to analyze the data u_0 in the 3D domain (x_1, x_2, ct), with c being the wavespeed, by projecting it on the dual frame $\varphi_{m,n}(x_1, x_2, ct)$ (Fig. 2). Each frame element gives rise to a pulsed beam (PB) propagator (Fig. 3), thus expressing the radiating field as a sum of PB propagators emerging from a discrete set of space-time points $(x_1, x_2, ct)\big|_m$ and directions ξ_n in the $z = 0$ plane as illustrated in Fig. 1.
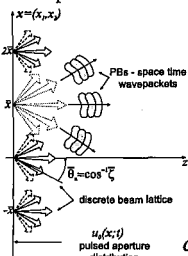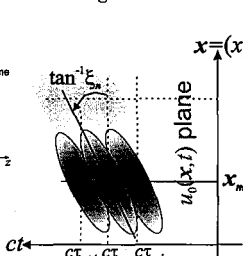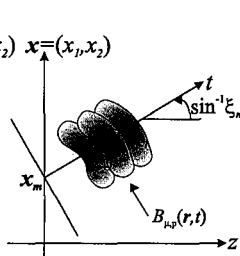
Figure 1   Figure 2   Figure 3

Dynamic Charge Density Model of
the Infinite Thin-Wire Dipole Antenna

Colin C. Bantin

Investigations into the time-domain behaviour of a perfectly conducting infinite thin-wire dipole have shown that the response to a short Gaussian voltage pulse applied across a (zero-width) gap is a spherical shell of electric field expanding at the speed of light. This field is highly concentrated at the surface of the wire and normal to the surface where it is supported by a surface charge density. The current flowing through the feed point initially follows the Gaussian shape of the applied voltage but then displays an overshoot as the voltage decays. This results in a negative current flow that persists long after the voltage has decayed to zero. These results have been explored using FDTD or MMFT (moment method with Fourier transform) techniques. The response can also be modelled by considering the dynamic behaviour of the surface charge density on the wire and using a simple electric circuit. This method also provides physical insight into the launching and radiation of energy by a thin wire dipole.

We construct a model based on observations made by other time-domain methods and some elementary physics. The two key observations are: the electric field is expanding at the speed of light, and the field is terminated in a surface charge density at the wire. Clearly the charge density cannot be made up of real moving particles such as electrons. If it were, the particles would need to move at the speed of light, which is impossible. The charge density is instead made up of apparent charge existing at the surface of a perfect conductor. It can be though of as an infinitely thin layer exposed by the local (infinitesimal) separation of (an infinite number) of charged particles by the electric field, just sufficient to terminate that field. The process requires no energy. All the energy resides in the fields. Nevertheless, the surface charge density can have some useful properties. For example it can travel at the speed of light.

If the applied voltage is an impulse it follows that the electric field is an impulse in the radial direction and the surface charge density is in the form of a ring. The physical process is that the application of the voltage impulse creates adjacent rings of oppositely charged surface charge density that immediately accelerate to the speed of light and move away from each other supporting the expanding fields, which carry away the energy. The feed point circuit model is therefore a resistance, to account for the energy carried away, in series with a capacitance created by the two coaxial charged rings. The capacitance is a function of time since the rings are moving.

The feed current from this model can be calculated by solving the differential equation for the series R, $C(t)$ circuit. The capacitance can be evaluated as a sum of Legendre polynomials, which are functions of the wire radius and the ring separation, $z = 2ct$. Here t is the time since the application of the voltage impulse and c is the speed of light. Also, in as much as the all the energy is in the electric and magnetic fields, and these fields form a TEM wave with the free space impedance of 377 Ohms, it seems appropriate to use this value for R. The feed point current found from this model agrees well with that found from the MMFT or other methods. The electric field for this model can be found by evaluating the relativistic expression for the field from moving (ring) charges. The result also agrees with those from other methods.

146

HOW ACCELERATED CHARGE CAUSES DISTRIBUTED RADIATION FROM SPECIFIED FILAMENTARY CURRENTS AND A PERFECTLY CONDUCTING STRAIGHT WIRE

Edmund K. Miller
Los Alamos National Laboratory (retired)
Lincoln, CA 95648
e.miller@ieee.org

It's been observed in both the frequency domain and the time domain that radiation occurs along the length of a PEC straight wire [E. K. Miller and G. J. Burke, *ACES Journal*, **16**, 3, pp. 190-201, 2001] as demonstrated using a technique called FARS (Farfield Analysis of Radiation Sources). Length-wise distributed radiation is also observed for a sinusoidal current filament [*ibid*] and a Gaussian-pulse current filament (GPCF) [G. S. Smith and T. W. Hertel, *IEEE AP-S Magazine*, **43**, 3, pp. 49-62, 2001], sources that satisfy no boundary condition on the tangential electric field. Why the radiation is distributed along a straight PEC wire or a current filament rather than at only the ends, and possibly the feedpoint, is the subject of this paper.

The key to this question can be deduced from the fact that the impedance a constant-radius PEC wire presents to a propagating current/charge wave varies with distance. This impedance variation in turn causes a partial reflection of the propagating charge, a small, but never-the-less significant, effect. This is because the reflected charge is accelerated, a phenomenon shown by the Lienard-Wiechert potentials to produce a 1/R, or radiation, field. It's straightforward to demonstrate that this is why peaks in the distributed radiation coincide with peaks in the standing current wave along the wire in the frequency domain. A similar phenomenon occurs in the time domain, but because there is no standing wave, the radiation varies smoothly along the wire.

For a specified current such as the SCF or GPCF, the radiation is similar to that found for the PEC wire. While there is a different explanation for the physics of the radiation process for such currents, the root cause is still charge acceleration, of course. For the SCF, there is no time-average power flow along the filament as is the case for the PEC wire, but its distributed radiation is surprisingly similar to that of the latter. An IEMF analysis of the SCF, which matches its FARS results within a per cent or so, reveals that the local radiation is due to the tangential electric field produced by the current, and is correlated with the current magnitude along the wire. This result is also compatible with the concept of a distributed radiation resistance for a SCF [S. A. Schelkunoff and C. B. Feldman, *Proc. IRE*, **30**, pp. 511-516, 1942]. A similar conclusion can be proposed for the GPCF. These observations will be illustrated with results computed using the NEC (Numerical Electromagnetic Code) and TWTD (Thin-Wire Time Domain) computer models.

The Effective Point of Radiation for a Microstrip Patch Antenna

Lorena I. Basilio[*], Jeffery T. Williams[1] and David R. Jackson[1]
[*]Sandia National Laboratories, P.O. Box 5800, Albuquerque NM, 87185-1152
[1]Dept. of ECE, University of Houston, Houston, TX 77204-4005

In this presentation the issue of defining an effective point of radiation (EPR) for a single frequency, linearly-polarized rectangular microstrip patch antenna is addressed. For some applications, such as high-precision GPS, an accurate knowledge of the antenna EPR as a function of the observation angle is important. Knowledge of the EPR allows for the positional offsets introduced by the radiation characteristics of the antenna to be compensated for, and, hence, a more accurate geometric satellite-to-user range measurement to result. Although circularly-polarized antennas are usually used for GPS applications, a linearly-polarized rectangular patch is used here to demonstrate the general characteristics of the EPR for a microstrip antenna. The general conclusions are directly applicable to other shapes of microstrip patches and polarizations.

Two different methods for defining an EPR are compared in this presentation. The first method uses the concept of an antenna phase center, and is based on the curvature of the radiated equiphase surface. Although this is a common method used to account for the EPR of an antenna, it is shown that only under certain very specific conditions does a unique phase center exist for a microstrip patch. The second method is based on the time delay of the signal, using either the time delay of the signal content (group delay) or the carrier (phase delay). This method is directly relevant to GPS, since a GPS measurement is based upon the apparent transit time of the transmitted signal. Unlike the phase-center method, the time-delay method is shown to always provide an unambiguous result, although the EPR that is obtained will in general be dependent on the polarization of the received signal as well as the observation angle.

In the time-delay method, the EPR that is calculated from the time delay of the carrier is independent of the input impedance of the patch, assuming only the dominant mode. However, the variation of the input impedance with frequency (due to the cavity nature of the patch antenna) has a significant effect on the EPR calculated using the group delay. The EPR calculated using the group delay is examined when the patch is fed by a practical probe feed in order to substantiate this, and it is shown that the overall group delay of the signal is dominated by the phase behavior introduced by the input impedance variation with frequency.

Focusing Properties of a Three-Parameter Class of Oblate, Luneburg-like Inhomogeneous Lenses

J. A. Grzesik

Northrop Grumman Space Technology
Antenna RF Engineering Department
One Space Park, MS R11/2856AA
Redondo Beach, CA 90278

The celebrated focusing properties of spherical, inhomogeneous Luneburg lenses are part of the common microwave/optical folklore, and need little by way of introduction [R. K. Luneburg, *Mathematical Theory of Optics*, University of California Press, Berkeley and Los Angeles, 1964, pp. 181-188; Samuel P. Morgan, "General Solution of the Luneburg Lens Problem," Journal of Applied Physics, Vol. 29, No. 9, Sept. 1958, pp. 1358-1368]. Nevertheless, as these lenses are burdened by the practical defects of both bulk and weight, scant use has heretofore been made of them in a satellite setting. In particular, the question arises whether these defects can be simultaneously mitigated through compression into a genuine lenticular, oblate spheroidal shape, while retaining some measure of the desired focusing attributes.

With this objective in mind, we have considered a three-parameter family of refractive index distributions involving arbitrary center and edge values, and a geometric profile measure gotten as the ratio of major to minor external ellipsoid axes. Such distributions are a natural generalization of those which underlie classical, spherical Luneburg lenses, and share with them the property of having all constant-index surfaces strictly similar to that of the lens exterior. We have found ray trajectories in closed form on the basis of Fermat's equation which, in the present circumstances, is easily brought to quadrature.

Ray transcription into computer code followed by numerical experimentation reveals the possibility of virtually perfect collimated focusing to infinity (the paramount lens objective) and, with an additional bending boost due to surface (Snell's law) refraction, also a focusing between conjugate foci each at finite distance. We have further placed collimated focusing (with a unit surface refractive index matched to that of free space) on a somewhat stronger analytic footing by demanding, for a fixed focal distance, that individual rays aim perfectly toward infinity, and then averaging over the spectrum of center indices thus determined. Graphical examples are given of the focused ray pencils so obtained.

While stigmatic focusing is the premier lens objective, ray pencil behavior acquires an additional allure of both a scientific and aesthetic sort by having physics and code each stressed with large, presumably nonrealizable indices. A subset of rays is then denied the option of a complete lens traversal, being destined instead to undergo alternate fates of internal reflection and, still more drastically, of full interior reversal. Adroit coding routes are required to channel these possibilities via suitable splicing of individually closed-form analytic ray fragments. We give examples of some typical ray families encountered along these lines.

Mutual Impedance of Vertical Antennas above a Semi-Infinite Ground in Closed-Form

R. M. Shubair
Communication Engineering Department
Etisalat College of Engineering
P.O.Box 980, Sharjah, UAE
E-mail: rshubair@ece.ac.ae

Submit to *URSI* Commission B: Topic **B1** or **B11**

Abstract

Using the induced EMF method and the simulated image method, the input impedance of a vertical antenna above a dielectric half-space has been obtained in closed-form in terms of Sine and Cosine integrals (R. M. Shubair, *Proc. IEEE AP-S*, pp. 827-830, 2003) and (R. M. Shubair, *Proc. URSI*, 2003). In doing this, the induced EMF method assumes a sinusoidal current distribution along the vertical dipole and uses the closed-form potential Green's functions.

This paper extends the use of the induced EMF method for the calculation of the mutual impedance of two opposite vertical antennas above a dielectric half-space. To do this, we use a Green's function approach to obtain a spherical-wave representation of the half-space scalar and vector potentials associated with an infinitesimal vertical electrical dipole (VED) above a dielectric half-space. The simulated image technique is then used to derive closed-form expressions for the potential Green's functions. Using this technique allows us to model the effect of the lower dielectric half-space by introducing a finite set of simulated image antennas. The result is an equivalent problem in which the lower dielectric half-space has been replaced with free-space so that the simulated image antennas form a simulated image array located in homogeneous free-space. The derivation of this simulated image array allows for the use of induced EMF method to calculate the mutual impedance in a manner similar to free space. In this approach, once a simulated image array is found for a given height above the dielectric half-space, then for different antenna heights, say upwards, the image array remains unchanged except that it is bodily translated downwards by the same distance. This means that as the induced EMF method is applied *only once*, then at other heights the convergence is even faster since the simulated image antennas need not to be recalculated.

To verify the accuracy and convergence of method, numerical results are obtained showing the complex coefficients of the simulated image antennas, as well as, the mutual impedance as a function of height above the dielectric half-space, with or without loss.

The Effect of Common Test Environments on LF Magnetic Field Measurements

Joseph D. Brunett* and Valdis V. Liepa
Radiation Laboratory, Electrical Engineering and Computer Science Department,
The University of Michigan, Ann Arbor

Direct measurement of near-field, low frequency mutual coupling between two electrically small loop antennas is performed in a number of common test environments. The test environments considered include loops above a finitely conducting ground plane, in a semi-anechoic chamber, and in an unloaded shielded room or cavity. This data is then compared with exact analytical formulations for the mutual coupling in each scenario, proving accurate simple models which provide good correlation between the differing measurement environments. From the measurement and the theory of a loop above a non-ideal ground plane, a set of mutual impedance values and Normalized Site Attenuation (NSA) values are provided for correlating Open Area Test Site (OATS) measurements with those in semi-anechoic chambers and unloaded shielded rooms, including considerations for chamber size, source and receive loop size, and proximity to chamber walls. (The figure below demonstrating the field strength variation for measurements made in an unloaded shielded room verses those made on an OATS.) At the present time, measurement of magnetic field strength using a loop probe is frequently performed without giving attention to the errors induced by differing test environments or loop probe/source dimensions. Since the field attenuation rates are so dramatic, typically 60dB/dec, measurements are made very close to the source and are then extrapolated to greater distances. However, the general consideration of loop dimension and the effects of loop proximity to ground and walls, as well as other obstacles, must be considered for an accurate extrapolation of the magnetic field.

151
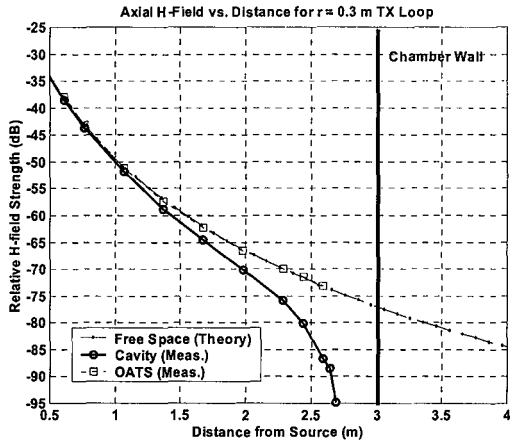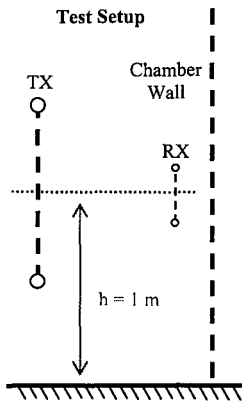
Near-Earth Wave Propagation Simulation for an Irregular Terrain

Il-Suek Koh [*], and Kamal Sarabandi

Radiation Laboratory

Department of Electrical Engineering and Computer Science

The University of Michigan, Ann Arbor, Michigan 48109–2122.

Abstract

Due to proximity of source and observation point to ground, near-earth wave propagation problem is rather complex. The complexity arises from complex image contribution, effect of small and large scale terrain irregularities, existence of vegetation and other surface covers such as snow. This problem has recently attained significant prominence for civilian and military applications. The military applications include performance assessment of unattended ground sensors. For civilian applications wireless ground sensors are proposed for environmental monitoring. Therefore the goal of this paper is to develop a comprehensible wave propagation simulation tool that can accurately predict the path-loss, field fluctuations, and other important channel parameters.

Electromagnetic (EM) wave propagation over earth surface has been studied intensively over a century. As early as 1909 the first important analysis was published by Sommerfeld where he formulated radiation of a short dipole over a flat lossy dielectric half-space. Much has been done since then to make the Sommerfeld solution computationally efficient, and to include propagation over curved earth, etc. With advent of computational tools, it is possible to solve relatively large EM problems. However since the domain of propagation problem is very large, the "brute force" computational methods still are not possible. However, to maintain the high fidelity of numerical technique and at the same time to keep the computation time tractable, hybrid (analytical/numerical) methods can be considered. In these methods the fine near-field of the environment near the transmitter and the receiver can be handled by a numerical method and analytical methods can be used to propagate the wave between two distant points. To consider wave propagation between two distant points, different scenarios must be considered. One scenario is when a transmitter is located at a flat top of a hill and a receiver is at the bottom of the hill. A general terrain profile for this example can be modeled as s-shaped surface. A uniform solution of scattering by a s-shaped PEC surface can be formulated in terms of Airy functions using Physical Optics (PO) approximation. However, such solution does not provide accurate results for an observation point in shadow regions.

Based on UTD a model can be developed for the propagation problem when the surface is smooth. In this approach the surface can be modeled with many straight line segments, and diffraction at each corner can be computed using direct diffraction coefficients. Also the multiple scattering among the corners can be considered using uniform diffraction coefficients. Exact diffraction coefficients are known only for PEC and impedance wedges. Hence an impedance surface can be used for the model of the ground plane. This approximation is very accurate for a lossy ground up to 3GHz. To verify the accuracy of the approach, a numerical method such as Method of Moment (MoM) is used and results are compared for several situations.

152

Measurement of UWB Propagation through Wall Structures

Junfei Li[1*], Heinrich Foltz[1], and James McLean[2]
[1]Department of Electrical Engineering
University of Texas-Pan American
Edinburg, TX 78541

[2]TDK R&D Corp.
Cedar Park, TX 78613

Abstract

Ultra-wide-band (UWB) radar detection and imaging of targets behind walls is gaining interests for physical security and rescue applications. It is believed that both the occluding wall structures and the UWB frequency range give rise to problems not considered in a conventional free-space, narrow band radar system. In this paper, we characterize UWB propagation through building structures by collecting and analyzing measurement data in the 2-13.5GHz frequency range.

The measurement system consists of a 50MHz-13.5GHz vector network analyzer, two 1-18GHz double-ridged horn antennas, and two 2-18 GHz high-gain power and low noise amplifiers. The system is first calibrated with a through-connection for the cables, connectors and amplifiers and free-space propagation condition for the antennas. Different sample wall structures are measured for their propagation loss and detestability of occluded targets. In more realistic settings, we measure the UWB propagation characteristics of buildings with and without human beings and/or man-made targets.

In the data modeling and analysis part, we focus on identifying the wall interferences and mitigating their effects on the UWB radar performance. Adaptive joint time-frequency representation is used to separate the dominant propagation and scattering mechanisms from clutter returns. The basis functions are chosen based as a trade-off between model simplicity and matching capabilities. The algorithm is tested with simulated data and then applied to the measurement data.

Finally, we compare three radar measurement results from 1) targets in free-space propagation and traditional processing; 2) wall occluded targets and traditional processing; and 3) wall occluded processed using the proposed physics-based processing to account for wall propagation. This work is believed to provide insightful interpretation and processing of existing UWB radar data for through-wall radar detection and imaging applications.

VALIDATION OF THE ADVANCED PROPAGATION MODEL (APM) FOR VHF SIGNALS ON LOW ALTITUDE MOBILE RECEIVER PATHS

Amalia Barrios*, Kenneth Anderson
SPAWARSYSCEN SAN DIEGO, 2858
Atmospheric Propagation Branch
49170 Propagation Path
San Diego, CA 92152-7385
amalia.barrios@navy.mil

VHF signal strength data from NOAA weather radio transmitters in the southern California and Arizona deserts were collected over a wide range of topography ranging from relatively flat to mountainous terrain. Signal strength data were collected using a mobile receiver traveling over distances from 10 to 100 miles, with the receiving antenna at a constant height of 2.2 meters above the ground. This data is used as the basis for a validation study of the Advanced Propagation Model (APM) specifically for mobile radio communications applications. Available meteorological information was obtained from local radiosonde measurement stations at Miramar (NKX), Yuma International Airport (YUM), and Yuma Proving Ground (1Y7).

This presentation will focus on the results obtained, both measured and modeled, along with error analysis performed between predictions and observations. Possible sources of error will be discussed relating to differences in terrain resolution from different terrain database sources (USGS vs. DTED) as well as errors arising from the propagation model itself due to inadequate range sampling of the terrain elevation.

Characterisation of On-Body Communication Channels

P S Hall*[1], Y I Nechayev[1], A S Owadally[2], Y Hao[2],
C C Constantinou[1] and C Parini[2].

[1]Department of Electronic Engineering, The University of Birmingham, UK
[2]Department of Electrical Engineering, Queen Mary University of London, UK

Modern communication systems are now driven by the concept of being connected anywhere and anytime. Wearable computing technology has a role to play in achieving this ambitious goal. More specifically, wearable computing aims to merge the user's information space with its workspace. Currently wearable computing devices use wired technology. However the above seamless integration can provide an enhanced user experience if wireless technology is used. Thus we are investigating the use of the human body as a communication channel between wearable wireless devices.

Preliminary experimental results inside and outside an anechoic chamber have been obtained using patch antennas at the frequency of 2.4GHz. A pair of patch antennas were attached to the body, Fig 1. In the case in Fig 2 below, one was placed on the belt (left) and the other one on the left wrist. Various body postures were investigated such as standing, sitting, reaching forward, bending and changed every 20 seconds. Also various transmitter (Tx)/receiver (Rx) orientations were investigated. It is concluded that, in this case, for trunk movements, the channel loss is steady, but when the arms and hands are moved changes of more than 30dB can be experienced.

To complement the measurement campaign a simulation approach is used. The human body will be modelled and the field distribution over it will be evaluated using a conformal FDTD technique. Since the body is essentially acting as a surface wave guiding structure, a simplified homogeneous model is used to characterise the radio propagation over the body. The human body can be modelled according to the various positions tried out during the measurement campaign. Simulation results will be presented at the conference.
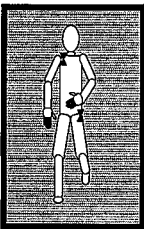
Fig 1 Body with attached antennas
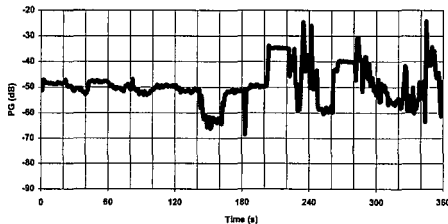
Fig 2 Path Loss for Belt to Hand Path (body posture changes every 20seconds)

Ground Wave Propagation Measurement in the HF to VHF Frequency Ranges over Non-Line-of-Sight Terrains

R. L. Rogers[1], W. Vogel[1], S. Lacker[1], H. Ling[2]

[1]Applied Research Laboratories, The University of Texas, Austin, TX
[2]Department of Electrical and Computer Engineering, The University of Texas, Austin, TX

The use of ground waves in the high HF to low VHF frequencies to provide extended-range, non-line-of-sight (NLOS) links is of interest for a variety of communications. In this paper, we present results of a propagation measurement campaign collected over NLOS terrains in the 30 to 100 MHz frequency range. The transmitting antenna used in the measurement was powered by a frequency synthesizer and power amplifier, and the receiving antenna was connected to a RF spectrum analyzer. The antennas used in the test include commercial whips, copper-tubing monopoles, folded conical helix dipoles (J. A. Dobbins and R. L. Rogers, IEEE Trans. Antennas Propagat., 49, 1777-1781, 2001), and wire antennas designed by genetic algorithms (H. Choo and H. Ling, *Elect. Lett.*, 39, 2003). Propagation loss data were collected over distances ranging from a few hundred meters up to several kilometers. The terrains profiles between the transmitter and the receiver were obtained using GPS information and topographical maps. In addition, soil parameters were measured based on the self impedance of a short monopole probe connected to a vector network analyzer. The collected propagation loss data were analyzed as a function of distance, terrain profiles, frequencies, soil parameters and antenna types. The results were also compared against NEC simulation of line-of-sight paths. From the measured data, link margin calculations were performed for different scenarios to aid in the design of NLOS communication links in this frequency range.

1. **New knowledge contributed by the paper:**
   Propagation of ground waves in the HF and VHF spectrum is generally either treated for flat surfaces or as special cases of non-line-of-sight paths. This work attempts to parameterize the behavior of the paths into a few geometrically relevant parameters and provide a heuristic means based on measured data to quickly estimate the path loss.

2. **Relation to previous work:**
   This work a similar effort on previous work on low elevation propagation paths at millimeter wave frequencies. The previous work focus on paths where the majority of the path between the transmitter and the receiver contained scatterers or terrain in the first fresnel zone.

A Printed Reflectarray with Annular Patches

Mario Orefice, Paola Pirinoli, Claudio Zuin

Dipartimento di Elettronica, Politecnico di Torino, I-10129 Torino, Italy,

Fax: +39-011-5644099, Email: mario.orefice@polito.it, Phone: +39-011-5644057

Printed reflectarrays are nowadays one of the most challenging themes of research in the antenna field, because of their promising characteristics in many telecommunication systems both for space and terrestrial applications. Among the possible advantages that can be obtained from the use of this types of structures, just to name a couple, are the possibility of having high directivity antennas with deployable lighweight flat structure, and the reduction of the losses of the feed system, combining favourable properties of reflectors and arrays.

The most popular printed reflectarrays configurations have square (or rectangular) patches, where the phasing characteristics are obtained either with different length open circuited transmission lines connected to the patch, or with different dimensions of the patch, or, for circular polarization, with different angular rotation of the patch in its plane.

Less investigation (although with some interesting results) has been carried out on printed reflectarrays consisting of non-square/rectangular shapes, as circular, annular, etc. In particular, the use of annular patches may be interesting because in the fundamental mode TM11 the resonant size is significantly lower than for the circular or rectangular patch, and also because of the additional degree of freedom coming from the aspect ratio (outer/inner radius).

In this communication printed reflectarrays with annular patches have been studied, where the different phase of the reflection coefficient has been obtained by varying the size of the patch and in particular the inner ring radius. In this way, the outer overall dimensions of the patch may remain always the same, and this allows a more regular layout of the patches; in a rectangular grid, the distance between the edges of adjacent elements is also constant, allowing an easier treatment of the mutual coupling effects.

The analysis of the structure and the computation of the phase curves needed for the design of the patches have been done with full wave tools, taking into account the interaction among the elements. Parametric analyses for different values of aspect ratio, thickness, dielectric constants have been carried out, to obtain suitable phase curves for the reflected field, with wide range and relatively low sensitivity to the tolerances, that will be presented. The results, that include a frequency analysis, have shown a good pattern behaviour, with relatively low sidelobes and pattern symmetry. It was also seen, however, that a wide element spacing, as the maximum possible to avoid grating lobes and often used to minimize the number of elements, may generate a sidelobe increase or even a spurious lobe due to the specular reflection of the dielectric loaded ground plane among the elements. Consequently, the spacing among the patches must be lower than that used in conventional arrays. The element number is therefore higher but this is not a problem, thanks to the absence of the BFN in reflectarrays.

In conclusion, the use of annular patches in reflectarrays opens interesting possibilities and options that are absent in rectangular patch shapes.

Microstrip Reflectarrays Consisting of Multi-layer Stacked Patches

Sembiam R. Rengarajan
Department of Electrical and Computer Engineering
California State University
Northridge, CA 91330-8346

Microstrip reflectarrays are becoming popular nowadays because of their low profile and ease of manufacture and they are deployable in spacecraft applications. The design and analysis of many large microstrip reflectarrays are based on the solution of the canonical problem; the determination of the reflection coefficient and the element pattern of an infinite array of microstrip elements illuminated by a plane wave. Many reflectarrays designed using the results of the canonical problem are found to yield good performance. Reflectarrays employing rectangular patches or dipoles exhibit two limitations. The phase of the reflection coefficient is sensitive to the patch length when the elements are near resonance. In addition the range of values of phase compensation available by changing the size of the patch is limited to about 330°. It was shown that both of these limitations may be overcome by employing two or three layers of stacked microstrip patch elements in reflectarrays (Encinar, IEEE Trans. Antennas Propagat., 49, 1403-1410, 2001).

We investigated microstrip reflectarrays employing multiple layers of substrate and superstrate materials and multiple layers of stacked conducting patches. The infinite array problem was formulated in terms of integral equations for the induced currents in a unit cell of stacked patches. The integral equations were solved by the method of moments employing global sinusoidal basis functions with the necessary edge conditions. The required Floquet series Green's functions in spectral domain were obtained from the TE and TM mode transmission lines. Numerical results were validated by comparison with the commercial program HFSS employing the finite element technique. Numerical results over a range of physical parameters such as the patch sizes, dielectric substrate, and superstrate parameters will be presented. These results will find applications in the design of reflectarrays with increased bandwidths and etching tolerances.

Scanning Properties of Large Reflectarray Antennas

Richard E. Hodges*, Mark Zawadzki
Jet Propulsion Laboratory, California Institute of Technology
Pasadena, CA 91109

It is well known that one can scan the beam of a reflector antenna over a limited angular region by repositioning the feed near the focal point. This mechanism can similarly be used to scan the beam of a reflectarray antenna. This paper examines the scanning properties of reflectarrays compared with traditional reflector antennas. We examine the effect of F/D for both prime focus and offset configurations.

An important finding in the work is that offset-fed reflectarrays can provide dramatically better scan performance than an equivalent reflector for some configurations. Figure 1 illustrates a reflectarray antenna with a projected aperture of 93.0 x 15.5 λ and a focal length of 119.6λ. The three feed positions correspond to elevation scan of 0 and ±3.3°. Figure 2 shows that corresponding elevation patterns do not degrade significantly. Directivity increased +0.41dB for the upper feed position, and decreased by -0.32dB for the lower feed position. Azimuth patterns also hold up over scan.

In contrast, scan loss for an equivalent parabolic reflector was −2.86dB and −3.75dB for the upper and lower feed positions. Elevation patterns for the parabolic reflector are commensurate with those of the reflectarray, but the azimuth patterns have extreme beam broadening (roughly double the beamwidth) and high sidelobes near boresight.
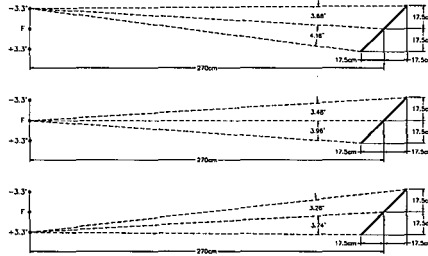
Figure 1 Side view of a reflectarray showing feed locations needed to achieve a scan of ±3.3°
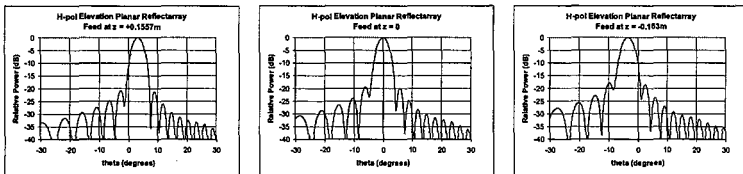
Figure 2 Elevation patterns corresponding to the reflectarray feed positions shown in Figure 1.

159

Surface Reflection of Waveguide Lens Antennas

T. K. Wu
Northrop Grumman Space Technology
Antenna RF Engineering Department
One Space Park, MS: R11/2856AA
Redondo Beach, CA 90278

ue to the low sidelobes and blockage-free advantages, waveguide lens has been applied
a variable Earth coverage X-band satellite antenna system (A.R. Dion and L.J. Ricardi,
roceedings IEEE, 59, 252-262, 1971). J. Wolcott, et al., also showed a light weight and
eployable waveguide lens antenna for satellite communication applications (US patent #
,818,395, 1998). Different from the reflector antenna, dielectric or waveguide lens
itenna has a unique surface reflection loss due to the mismatch in the propagation
iedium as the signal or wave passes through the lens. To accurately determine the
aveguide lens antenna gain performance, it is very important to account for and
timate this lens surface reflection loss.

ion (in A. Rudge, et al., The Handbook of Antenna Design, p. 315, 1986) suggested that
r lenses made of square waveguide elements, the reflection coefficient (or R) is
proximately $(1-\eta) / (1+\eta)$, where η is the refractive index of the lens. The reflection
ss (dB) is next calculated as $10 \log (1- R^2)$. He also stated that the reflection loss is
out 0.5 dB for a waveguide lens with $\eta = 0.6$. However, a 0.28 dB (not 0.5 dB)
flection loss is obtained, if one uses the above mentioned formula. So which loss value
ould one use for the case of $\eta = 0.6$?

answer that question, two different approaches are implemented in this paper to
timate the reflection loss of waveguide lenses. First, the waveguide array is assumed to
: semi-infinite and is locally a planar periodic array. Thus the reflection loss can be
aluated by the mode matching technique (V. Galindo and C. P. Wu, IEEE Trans., AP-
;, 149, 1966). Note that the lens thickness is always finite and most waveguide lenses
quire zoning to reduce its thickness hence its weight. Therefore, the second approach
sumes the waveguide array with a finite length instead. Numerical results obtained for
: waveguide lens reflection loss by the two approaches will be discussed and compared
Dion's results in the presentation.

Design and Anaylsis of a Tri-Band Center-Fed SATCOM Reflector Antenna

Griffin Gothard* and Jay Kralovec
Harris Corporation
PO Box 37 • Melbourne, FL 32902-0037

A five foot tri-band (C-, X-, Ka-band) SATCOM terminal has been designed for shipboard applications. The terminal has two independent replaceable feeds; C-band and simultaneous X/Ka-band. The following lists the three bands realized with the two independent feeds:

- C-Band: 3.625-4.225 GHz Rx, 5.825-6.425 GHz Tx

- X-Band: 7.250-7.750 GHz Rx, 7.900-8.400 GHz Tx

- Ka-Band: 20.20-21.20 GHz Rx, 30.00-31.00 GHz Tx

Offset prime-focus and dual-reflector designs are optimum from a performance standpoint for a reflector of this size, however the scarcity of real estate on shipboard drives the design to a center-fed type. Of the available center-fed reflector types, a shaped ring-focus configuration was chosen since the ring-focus reflector has several advantages over Cassegrain/Gregorian types for reflectors in this electrical size range (see G.K. Gothard et. al., "Design of Quad-band ring-focus reflector antenna" *APS*, Columbus, Ohio. June 2003.)

The two basic types of ring-focus reflector antennas are the classic dual-reflector configuration and the coupled-feed configuration. Classic ring-focus reflector antennas (also called delta-gap or displaced axis) are dual-reflector optical systems; i.e. the feed aperture is multiple wavelengths from the subreflector vertex. The coupled-feed ring-focus antenna approach involves a backfire type prime ring-focus feed, where for example an open-ended waveguide with choke rings is reactively coupled (typically less than 1λ) to a splash plate. Usually a dielectric support is used to physically couple the two parts of the feed together. This composite structure forms a single feed network that results in a highly-efficient and low-sidelobe reflector antenna design.

In the current design implementation, the C-band and X/Ka-band feeds are quite different from each other, both in physical form and operating principles. The C-band feed is realized using the backfire type feed. Unlike optical dual-reflector approaches, the backfire type feed works quite well for feed/splash plate diameters as small as 2λ, thus minimizing the required size of the blockage region. The simultaneous X/Ka-band feed utilizes a coaxial configuration and combines the backfire type approach with the classic dual-reflector approach to realize X-band and Ka-band, repectively. Matching features and a shaped and tuned delectric support are used to meet axial ratio and return loss specs. The shape of the sub and main reflectors is derived numerically using GO shaping techniques, while the feed and feed support designs were developed using the BOR MoM, FEM, PMM, and PO/PTD. The antenna has been constructed and tested and to date measurements match predictions.

Terrestrial Based Deployable Dish Antennas

*Dr. Larry T. Lowe (ltlowe@phaseiv.com)
Phase IV Systems, Inc.

Paul A. Gierow, PE (pgierow@stg.srs.com)
Ronald D. Hackett, PE (rhackett@stg.srs.com)
SRS Technologies, Inc.

Al Danis (Al.danis.osd.mil)
Office of Secretary of Defense

Abstract:
    A 4.8-meter diameter inflatable dish antenna has been developed by the authors that demonstrates a significant reduction in weight, volume, and cost when compared to conventional ground-based dish antennas. The dish is constructed using high strength, lightweight, thin film polymers used in space-based deployable structures. The deployable dish consists of two inflating structures: the lenticular and the radome. The lenticular is formed by seaming two parabolic dish films together. One film is coated with a silver flake conductive paint, the other is RF transparent. The lenticular is inflated to hold the parabolic shape of the dish and is attached to the inside of an inflatable spherical radome. Once inflated, the radome provides environmental protection to the thin film lenticular. The lenticular and radome are designed such that the focal point is located on the surface of the radome. An RF feed is attached to the radome at the focal point. A solar calibration routine was used to measure the gain of the dish. The deployable dish was deployed with a SATCOM system at Pearl Harbor, HI in April 2003, and was successfully used as the receive antenna for multiple data link transmissions. Currently, efforts are underway to construct a 2.5 meter dish and a 5 meter or larger dish antenna. This paper will present the measured RF performance of the two deployable antennas and discuss the current integration and test activities underway. The drastic reduction in weight and stowed volume offered by this technology makes it attractive for many applications including: backpack deployed antenna for Special Operations Forces, transportable ultra-large aperture antennas for high bandwidth data links, back up antennas for contingency scenarios, and a perhaps even a lunar based deployment.

a.

b.
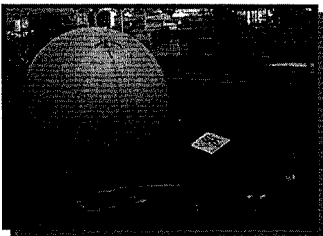
Figure 1. a. Lightweight deployable terrestrial based antenna integrated with SATCOM system. b. Next generation inflatable dish concept.
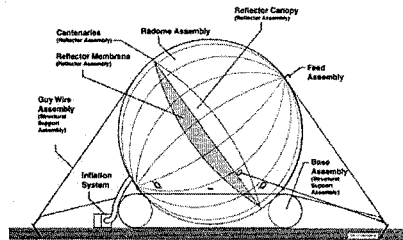
A Variably Reflective Surface Using FSS With Application To Reflector Antennas

Jay Kralovec, Tim Durham, and Verlin Hibner
Harris Corporation
PO Box 37 • Melbourne, FL 32902-0037

Many reflector antenna applications require low sidelobes (i.e. to meet beam-to-beam isolation requirements for Multi-Beam Antennas (MBA)). Improvements in sidelobe performance may be achieved by optimizing the reflector illumination, however constraints on feed size in the array environment limits the feed horn pattern. In (David Jenn et. al., "Low-Sidelobe Reflector Synthesis and Design Using Resistive Surfaces," *IEEE Trans. Antennas Propag.* 39(9), Sept. 1991), resistive surfaces on the reflector surface were used to adjust the reflector illumination. However, in space-based reflector systems, the effects of heating on reflector surfaces can be detrimental to pattern performance due to surface distortions. Therefore, something other than a resistive surface was required.

An inovative FSS design (Timothy Durham et. al., *Reflector Antenna Having Varying Reflectivity Surface That Provides Selective Sidelobe Reduction*, U.S Patent #6,563,472) was developed to implement a variably reflective surface with minimal RF loss within the surface and thus minimizing thermal distortion effects. By designing the material sandwich to be comprised of two separated FSS layers of different resonance, the resultant response is found to be relatively flat at some value of reflectivity other than perfect (i.e. $\Gamma < 1$).

A hybrid reflector antenna architecture for improving beam-to-beam isolation in a multi-beam reflector antenna will be presented. The design employs a solid central dish surrounded by multiple annular rings. The annular rings are made up of intellegently controlled frequency selective reflectivities which provide the desired aperture taper. The specific application is for operation at Ka-Band (i.e. transmit at 20GHz and receive at 30GHz) similar to (Yves Patenaude et. al., *Dual Band Hybrid Solid/Dichroic Antenna Reflector*, US Patents #6,140,978 and #6,421,022). The previous references detail a hybrid reflector with a central solid dish and a surrounding dichroic ring. The dichroic ring was tuned to maintain the electrical size of the reflector aperture over Ka-band Tx and Rx. This presentation discusses using the new FSS design to not only control the electrical size, but also the aperture taper.

CAPACITIVE KA-BAND FREQUENCY SELECTIVE SURFACE FOR DEEP SPACE ANTENNAS

Piermario Besso[1], Maurizio Bozzi[2], Luca Perregrini[2], Luca Salghetti Drioli[3]

[1] European Space Agency, ESOC, Darmstadt (Germany)
[2] University of Pavia, Department of Electronics, Pavia (Italy)
[3] European Space Agency, ESTEC, Noordwijk (The Netherlands)

This paper presents the design and testing of a capacitive frequency selective surface, operating in the Ka-band. The structure consists of an array of annular rings, patterned on a thin dielectric substrate of Mylar with thickness 75 μm (Fig. 1a). The dimensions are chosen in order to provide minimum insertion loss in the X band (7.145-7.235 GHz, 8.4-8.5 GHz), and complete reflection in the Ka band (31.8-32.3 GHz). The angle of incidence of the impinging plane wave is $\theta=35°$, $\phi=0°$.

The analysis of the scattering performance of the frequency selective surface was performed by using the MoM/BI-RME method (M. Bozzi and L. Perregrini, *IEEE Trans. on Antennas & Propagation*, Vol. AP-51, No. 10, pp. 2830-2836, Oct. 2003).

The structure was fabricated by photo-etching technique, and was glued on a aluminium frame, to guarantee mechanical stiffness. The measurements were performed in an anechoic chamber, under TE and TM linearly-polarized illumination.

The comparison between theoretical and experimental results is reported in Fig. 1b, showing a good agreement over the whole operation band, and proving that the structure meets the design specification in the Ka band. The small discrepancy between measured and simulated results is supposed to be due to the tolerance on the substrate thickness and dielectric constant and to the finite thickness of the metallization (35 μm), not taken into account in the simulation. The performance in the X band is less critical and the design specs are fully satisfied.

(a)   (b)
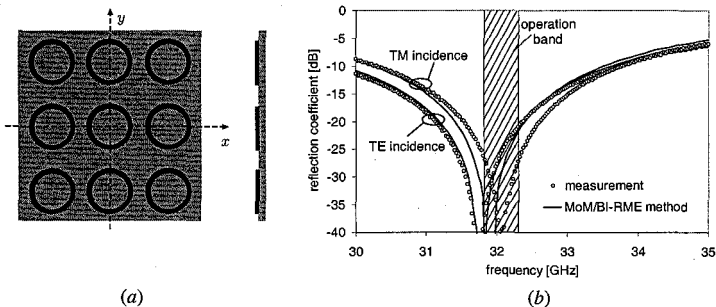
Fig. 1: Capacitive frequency selective surface operating in the Ka band: (a) top and side view of the structure; (b) comparison between simulated and measured reflection coefficients in the Ka band.

MODELING FINITE AND CURVED FREQUENCY SELECTIVE SURFACES WITH APPROXIMATE IMPEDANCE BOUNDARY CONDITIONS

Bruno Stupfel, Yannick Pion
CEA/CESTA, Commissariat à l'Énergie Atomique
B.P. 2, 33114 Le Barp, France

Frequency selective surfaces (FSS) have wide applications in many electromagnetic devices, such as reflectors or sub-reflectors in antenna systems, or else radomes. When these devices are electrically large and not planar, a full-wave and accurate calculation of the scattered field using an integral equation (IE) and/or finite element method becomes overbearing, if not impossible, on account of the very large number of unknowns, let alone the difficulties associated with the mesh generation. The numerical complexity of the problem is still more formidable when the devices are made up of multiple FSS sandwiched between thin dielectric layers.

A physical optics (PO) approach, such as the one proposed in [Y. Rahmat-Samii et al.,*IEEE Trans. Antennas Propagat.*, 1993], renders the problem tractable. However, the alteration of the electric and magnetic PO currents due to the curvature, the multiple interactions that may exist between the FSS and the surrounding objects, as well as the scattering from these objects, are difficult to account for in a systematic way when a PO technique is employed. An IE based formulation, used in conjunction with adequate approximations for the currents on the FSS [see, e.g., T. Cwik et al.,*IEEE Trans. Antennas Propagat.*, 1988], seems to be a promising candidate to circumvent the above mentioned difficulties.

Within this IE framework, we consider in this paper the simplified problem of scattering from a single, finite, FSS approximated by an impedance boundary condition (IBC). When the FSS is planar and infinite, this IBC yields the exact reflexion and transmission coefficients for the fundamental Floquet's mode when illuminated by a plane-wave at a given incidence. When the FSS is curved, and/or the direction of the incident wave is unknown, an enhanced high-order formulation is proposed for this IBC that is valid in a large angular range. It can be implemented in a MoM formulation for fully 3-D problems using the standard RWG test and basis functions. Its numerical efficiency is evaluated for a curved strip grating invariant in one dimension, and compared with the one of PO. Also, we show that, if a simple procedure is employed for the representation of the currents on the sheet modeling the FSS, it is possible to reproduce the radiating Floquet's modes in the scattered field even though those are not accounted for in the IBC.

The Synthesis of Planar Left-Handed Metamaterials from Frequency Selective Surfaces Using Genetic Algorithms

M. A. Gingrich* and D. H. Werner
The Pennsylvania State University
Applied Research Laboratory
PO Box 30
State College, PA 16804-0030, USA

A. Monorchio
The University of Pisa
Department of Information Engineering
Via Diotisalvi, I-56126 Pisa, Italy

This paper describes the design of a thin, planar frequency selective surface (FSS), which exhibits a negative index of refraction (NIR) for plane waves of normal incidence. The surface consists of a periodic conductive pattern on a dielectric substrate, optimized by means of a genetic algorithm. As such, it represents a thinner, lighter and less complicated means of obtaining a negative index of refraction than current methods that employ, for example, a periodic array of electric dipoles and split-ring resonators (R.A. Shelby et al., *Science*, **292**, 77-79, 2001) or backward-wave transmission lines (A. Grbic and G.V. Eleftheriades, *J. Appl. Phys.*, **92**, 5930-5935, 2002). A surface such as the one described here is simple to realize at microwave frequencies on a printed-circuit board and would have a wide range of potential applications including radomes, filters, focusing lenses, and as metamaterial surfaces for small antennas. This type of planar surface is also easily scalable to higher frequencies, such as the infrared (IR) and optical frequencies. The surface shown in Figure 1 was synthesized via a genetic algorithm to exhibit an index of refraction of $n = -1.50$ at 10 GHz. The recovered index of refraction, $n = -1.496 - j0.036$, was obtained via inversion of simulation data from a full-wave periodic moment-method analysis. Moreover, the real parts of the recovered permittivity ε and permeability μ are simultaneously negative, as expected. Several examples will be presented that demonstrate how the genetic algorithm technique can be used to synthesize planar NIR or left-handed metamaterials from FSS that have desirable characteristics such as broad bandwidth or low loss for relatively distortion-free transmission.
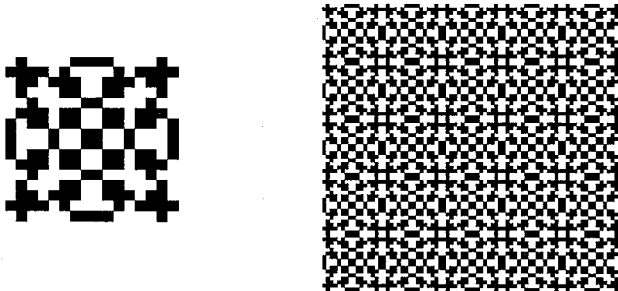
Figure 1. FSS unit cell (left) and a 5 x 5 tiling (right) for a planar NIR or left-handed metamaterial synthesized via a genetic algorithm.

Nano-Scale Frequency Selective Surfaces
For Thermophotovoltaic Energy Conversion

Richard L. Chen, Ji Chen, Keping Han, Ariel Ruiz,
Paul Ruchhoeft and Mark Morgan*

Department of Electrical and Computer Engineering
University of Houston, Houston, TX 77204

* EDTEK, Inc, Kent, WA 98032

Photovoltaic energy conversion typically has poor efficiency with thermal (i.e., non-solar) sources because the energy of most photons lies outside the narrow energy band near the bandgap of the semiconductor where the conversion process is most efficient. One solution to the problem of low conversion efficiency is to place a frequency selective surface (FSS) between the photocells and the thermal source to pass only those photons that can be efficiently converted to the photocells while reflecting out-of-band energy back into the source where it is reabsorbed. Using a blackbody radiator at 1650 °K, GaSb photocells (peak absoprtion at a wavelength of 1.4μm), and cross-shaped FSS structures in a gold film, the overall thermophotovoltaic (TPV) efficiency can be increased from ~1% to as high as 20%.

The efficiency of the TPV system is determined by the ability to reflect long wavelength radiation while maintaining high band-pass transmission. In addition, the cost to manufacture the filters is tied to the sharpness of the corners of the FSS elements as it affects the cost of the lithography step that defines FSS pattern. In an effort to optimize both FSS performance and cost, the effect of non-idealities (i.e., rounding of the corners of the cross structures, variations in material thickness, small changes in dielectric constants, etc.) must be fully understood. Although lower-cost lithographic techniques, ideal for prototyping, have been developed, strong modeling capabilities will be essential to the optimization process.

Accurate modeling, including skin depth effect, polarization effects, etc., can be achieved using computational electromagnetic methods. The finite element method (FEM) and finite difference time domain (FDTD) method are both good candidates for multi-layer unaligned FSS structures. In this paper, these techniques will be used to study band-pass characteristics of IR FSSs with various element shapes (cross dipoles and rings) at different pitches. Our objective is to design optimal IR filter to improve the performance (increased slope of the cut-off and reduced sensitivity to incident angle variations) while minimizing the amount of spatial information in the FSS pattern itself (to reduce manufacturing complexity). The results from numerical analyses and experimental results will be compared in the presentation.

A Near Infrared Optical Thermo-photovoltaic Filter Design Using Frequency Selective Volumes

E. Topsakal, Zach Hood
Department of Electrical and Computer Engineering
Mississippi State University, MS, 39762
topsakal@ece.msstate.edu, azh1@msstate.edu

Frequency selective surfaces/volumes are screens with frequency selective properties. There are many applications of FSS/Vs such as band pass band stop filters, radoms, reflectors etc. One of the applications where FSS/Vs are of interest is the design of infrared filters for thermo photovoltaic devices. Traditional solid state photovoltaic (PV) cells (Fig. 1a) convert electromagnetic radiation from the sun directly into electricity without any moving parts; this solar energy is approximately 6000 K at 150 million km. Fig. 1b illustrates the analogous operation of thermo-photovoltaic (TPV) converters. Though similar, the design of TPVs allows direct conversion of secondary thermal radiation from a heat source of 1500 to 2300 K at approximately a few cm into electricity using a semiconductor device. These converters achieve maximum efficiency at the wavelength of the secondary radiation.
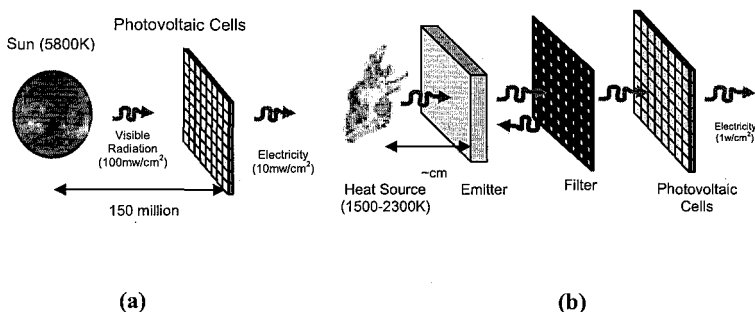
Fig. 1. Energy generation using (a) Photovoltaics and (b) Thermophotovoltaics.

The performance of the spectral filter between the emitter and the PV cells plays a vital role in the overall efficiency of the system. Only those frequencies with the wavelength of the secondary radiation should pass through the filter. The filter should reflect all other frequencies to conserve energy, thereby, substantially boosting overall system efficiency.

In this paper, we consider the design of a spectral-control filter, which is highly reflective for an incident wavelength greater than 2.4 microns and is highly transmissive from 1 micron to 2.4 microns. The performance requirements of the filter are: High reflection (>90 %) for $\lambda > 2.4$ μm, high transmission (>90 %) for $1 < \lambda < 2.4$ μm, incident angle θ = 45 °, insensitivity to large $\Delta\theta$, insensitivity to polarization, broadband operation (1-10 μm), high efficiency.

A Broad–Band Millimeter-wave IMPATT Oscillator Using Coaxial -Waveguide Cavity

Subal Kar
Institute of Radio Physics and Electronics, University of Calcutta
92, A.P.C. Road, Calcutta; 700009, India

Theoretical studies on coaxial-waveguide cavity was done earlier (A.G.Williamson, Proc. IEE, vol.129, 262-270, 1982) for possible applications in the design of millimeter-wave oscillators. However, design methodology and experimental performance characterization of such oscillators are not readily available in published literature. In the present report the broad-band characteristics of such oscillator has been studied using computer-aided analysis of the circuit for optimum performance. Also an experimental verification of the computer-aided characterization result has been done by using five sets of coaxial spacers having different hole diameter and spacer thickness. An operational bandwidth of more than 8.0 GHz has been realized with over 1.0 Watt millimeter-wave power at 34.25 GHz. The schematic of the coaxial-waveguide oscillator, optimum design dimensions and the photograph of the designed oscillator is given below.
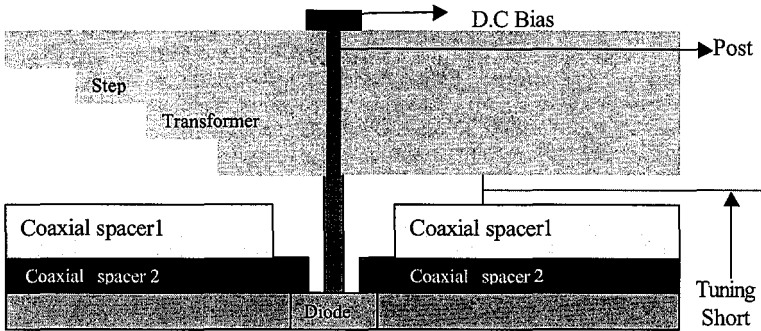
Optimum
Design Dimensions

Diameter of the post :   = 0.14 cm
Diameter of coax. 1 : = 0.497 cm
Diameter of coax. 2 :   = 0.153 cm
Length of coax. 1 :   = 0.2 cm
Length of coax. 2 :   = 0.165 cm

VSWR Variation allowed :
⟹ 1.075---1---1.075
Center frequency of op. = 34.25 GHz
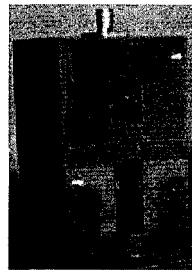
The mm-wave Oscillator

A Comparison of Different Enhanced FDTD Schemes on Generalized Grids

Fredrik Edelvik*, Marco Cinalli, Rolf Schuhmann and Thomas Weiland

Technische Universität Darmstadt,
Institut für Theorie Elektromagnetischer Felder (TEMF)
Schlossgartenstr. 8, D-64289 Darmstadt, Germany,
email: edelvik/schuhmann/weiland@temf.de

The finite-difference time-domain method is one of the most popular methods for time-domain solution of the Maxwell equations. In its standard formulation it is used on a staggered Cartesian grid. The main drawback with this method is its inability to accurately model curved objects. This is due to the Cartesian grid, which leads to a staircased approximation of the geometry. Several methods have been suggested to overcome this difficulty for example conformal FDTD (I. A. Zagorodnov, R. Schuhmann and T. Weiland, Int. J. of Numerical Modelling, 16, 127–141, 2003), hybrid FDTD-FEM (T. Rylander and A. Bondeson, Comput. Phys. Comm., 125, 75–82, 2000), and finite volume type methods, to name a few.

In the conformal FDTD method the cells at the boundary are modified such that they give a better approximation of the geometry. Since only the cells at the boundary are affected this method has a very small additional overhead compared to the standard FDTD method. Unlike previous approaches the method proposed by Zagorodnov et al. does not require a reduction of the time step compared to the standard staircased FDTD. Hybrid FDTD-FEM methods use an unstructured grid close to complex objects and by using as few unstructured cells as possible this method provides efficient and accurate results for very complex problems (F. Edelvik and G. Ledfelt, Int. J. of Numerical Modelling, 15, 475–482, 2002). By using an unconditionally stable FEM method the time step for the hybrid solver is dictated by the FDTD method. Generalization of FDTD to general non-orthogonal unstructured grids has traditionally suffered from instability problems. Recent publications suggest different techniques to symmetrize the constitutive matrices to overcome this problem (M. Marrone, Compumag 2003). However, symmetric constitutive matrices are not sufficient to guarantee stability, the matrices also have to be positive definite. We propose a different technique that produces symmetric and in addition also positive definite constitutive matrices.

In this paper we compare the accuracy, efficiency and stability of the above mentioned methods for cavities of different shape. The results show that we can save a substantial amount of memory requirements and execution time for complex geometries by using more sophisticated methods than FDTD on highly resolved grids.

Unconditionally Stable, Nonstaggered FDTD Scheme for Hybrid FDTD/FETD

Shumin Wang* and Fernando L. Teixeira+

*General Electric Company, Magnetic Resonance Center
3200 N. Grandview Blvd. W-832, Waukesha, WI 53188, U.S.A
e-mail: James.Wang@ieee.org
+ElectroScience Lab, The Ohio State University
1320 Kinnear Rd, Columbus, OH 43212, U.S.A
e-mail: flt@ieee.org

Vector (edge) -based finite-element time-domain (FETD) is known to be more flexible and accurate method to handle complex geometries than Yee's finite-difference time-domain (FDTD). Moreover, unconditional stability in FETD can be easily achieved by using the Generalized-Θ (time update) method. A drawback of the FETD, however, is the increased computational cost compared to FDTD for same discretization size.

The increased modeling flexibility of the FETD is largely due to the use of unstructured grids based on tetrahedrons, which are more suitable for characterizing fine structures and large field gradients than Cartesian grids. However, in many applications, these capabilities need to exist only over a small portion of the domain. In regions where rectangular cells (bricks) are sufficient, tetrahedrons can increase the number of unknowns by at least 50%.

The direct hybridization of FETD with Yee's FDTD poses obstacles because of basic differences in the nature of their discretization, among them the fact that FETD is based upon a non-staggered grid, while Yee's FDTD uses a staggered grid. Here, we propose a new Implicit Non-Staggered Finite-Difference Time-Domain (INS-FDTD) which is better suited for hybridization with the implicit FETD. Moreover, when compared against low-order brick elements of traditional FETD schemes, the bandwith of the global matrices in the new INS-FDTD is reduced from 33 to 13. The INS-FDTD exhibits larger dispersion error than the Yee's FDTD and FETD for same discretization size. However, they exhibit basically same dispersion anisotropy. Therefore, simpler dispersion compensation schemes can be used to make the INS-FDTD dispersion error equal to FDTD.
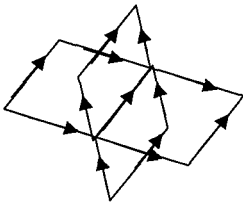
Fig. 1. Stencil of the proposed non-staggered scheme.
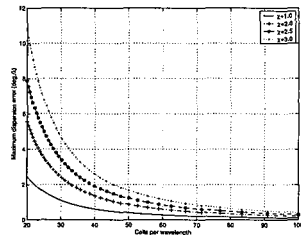
Fig. 2. Numerical dispersion error of INS-FDTD for different Courant factors.

171

Non-Standard Finite Difference in Electromagnetics

Bo Yang* and Constantine A. Balanis
Department of Electrical Engineering
Arizona State University
Tempe, AZ 85287-5706

ABSTRACT

Yee's FDTD algorithm has been applied to almost every aspect of computational electromagnetics. However, in electrically large problems, whose electrical sizes are very large compared to the wavelength, Yee's algorithm suffers from accumulative dispersion and anisotropic error due to the second-order approximation to the derivative. To maintain the dispersion and computational cost within an acceptable level, one promising solutions is to use higher-order schemes.

One of the higher-order schemes is the NSFD (Non-Standard Finite Difference), proposed by R. E. Mickens and applied to electromagnetics by J. B. Cole. The method incorporates additional terms derived from the monochromatic solution of wave equation to improve the accuracy. At the same time, it superposes several anisotropic Laplacians to construct a nearly isotropic Laplacian. As the result, NSFD allows very coarse mesh resolution and minimizes the anisotropic errors. However, like most other higher-order schemes, NSFD uses an expanded stencil which causes a challenge in modeling material discontinuities. As a frequency optimized method, it obtains low dispersion only within a narrow band near a single frequency. In addition, due to the asymmetrical split of the Laplacian, only one of the field components, E or H field, achieves great isotropic performance. Apart from these disadvantages, NSFD is a very suitable method to solve electrically large problems.

In the oral presentation of this paper, NSFD algorithm will first be reviewed. After that, implementation issues, such as Absorbing Boundary Condition, will be discussed. Finally, simulations will be presented for 1D, 2D and 3D cases to show the attributes of NSFD. The results will be compared with measurements and/or other available data.

The Accuracy of ADI-FDTD:
Recent Insights about Truncation Errors and Source Conditions

Salvador Gonzalez Garcia[1], Amelia Rubio Bretones[1], and Susan C. Hagness[2]
1) Depto. Electromagnetismo y Fisica de la Materia
Facultad de Ciencias, University of Granada, 18071 Granada, Spain.
2) Department of Electrical and Computer Engineering
University of Wisconsin-Madison, Madison, WI 53706
(email: salva@ugr.es, hagness@engr.wisc.edu)

Recently, alternating-direction implicit (ADI) methods have been successfully adapted for finite-difference time-domain (FDTD) solutions of Maxwell's curl equations (Namiki, *IEEE T-MTT*, 47:2003-2007, 1999; Zheng et al, *IEEE MGWL*, 9:441-443, 1999). We have shown that the ADI-FDTD scheme can be expressed as a second-order-in-time perturbation of the implicit Crank-Nicolson (CN) scheme and is therefore unconditionally stable (Gonzalez-Garcia et al, *IEEE AWPL*, 1:31-34, 2002). The higher-order perturbation permits factorization into a two-step procedure. The individual factored operators are each implicit in one direction only, so that the solution proceeds by solving for a specific field component implicitly along one direction in the grid during the first sub-iteration and then solving for that same field component implicitly along another direction during the second sub-iteration. The unconditionally stable ADI-FDTD scheme has been shown to be a computationally efficient approach for several classes of problems where very fine meshes with respect to the wavelength are required for at least part of the computational domain.

Casting the ADI-FDTD scheme in the framework of the CN-FDTD scheme has led to two important accuracy-related insights about the ADI-FDTD scheme. These issues are highlighted in this talk. First, we review potential accuracy limitations imposed by the truncation error on the time step. We have shown that although ADI-FDTD is unconditionally consistent with Maxwell's curl equations, some terms of the truncation error grow with the square of the time increment multiplied by the spatial derivatives of the fields. These terms give rise to potentially large numerical errors as the time step is increased above the Courant limit even though key temporal features of the modeled electromagnetic field waveform may be highly resolved. The CN-FDTD scheme does not present these problematic truncation error terms. Second, we propose a new method of implementing current sources in the ADI-FDTD scheme. It had been previously pointed out (Lee and Hagness, *IEEE Int. Symp. Ant. Propagat. Digest*, pp. 142-145, 2001) that any desired electric (magnetic) current source must be embedded within the affected tridiagonal matrix system associated with the implicitly updated electric (magnetic) fields. The source condition proposed therein involved evaluating the current source waveform at $(n+1/4)$ in the first sub-iteration and at $(n+3/4)$ in the second sub-iteration of the ADI-FDTD scheme to ensure consistency with Maxwell's equations within each sub-iteration. We have recently discovered a more accurate approach where the current source waveform is evaluated at $(n+1/2)$ in both sub-iterations. Supporting numerical examples for all of these insights will be provided in this talk.

A hybrid method combining ADI-FDTD and MoMTD: applications

A. Rubio Bretones, S. González García, R. Godoy Rubio,
and R. Gómez Martín

Dept. of Electromagnetism. Univ. of Granada 18071 Granada (Spain). arubio@ugr.es

The simulation of the transient excitation of permeable bodies is a problem of current interest in areas such as: Ground Penetrating Radar (GPR), breast tumor detection, etc. The problem includes the modeling of radiating elements in the presence of inhomogeneous bodies, which are close to the antennas, and therefore strongly influence their radiation characteristics. Appropriate numerical methods able to accurately analyze this complex problem should be used. However, it is not always possible to find a single numerical technique appropriate to deal with the whole configuration, and then it is necessary to resort to hybrid methods. This is, for example, the case when thin--wire are antennas are chosen as radiating elements, which is relatively frequent due to their simplicity and flexibility.

The hybrid FDTD-MoMTD (A. Rubio Bretones, *et al.*, *IEEE Microw. Guided Wave Lett.*, **8**, 281–283, 1998) has been successfully employed to address the above mentioned problems. Its formulation is quite general but since it employs the traditional explicit FDTD algorithm, the time increment cannot exceed the Courant stability limit. Furthermore, in some cases, the hybrid FDTD-MoMTD technique leads to unstable results.

The Alternating Direction Implicit Finite Difference Time Domain (ADI--FDTD) method (T. Namiki, *IEEE Trans. on Microw. Theory and Techn.*, **47**, 2003–2007, 1999) (F. Zheng, *et al.*, *IEEE Microw. Guided Wave Lett.*, **9**, 441–443, 1999) is a powerful alternative to the traditional FDTD method. Its unconditional stability permits to choose the time increment independently of the space increment, which may lead to significant CPU time reductions for a number of practical cases.

In this paper we show how the hybridization of the ADI-FDTD with the Method of Moments in time domain (MoMTD) permits to build a robust simulation tool that can be applied to solve complex problems. A main advantage of the ADI--FDTD--MoMTD is that it has exhibited a stable behavior in the problems where the FDTD-MoMTD becomes unstable. Examples of application to Ground Penetrating Radar, breast tumor detection, SAR prediction, etc., simulated with this new tool will be shown.

Full wave Analysis of Horn antennas in the presence of a Radome by using the Conformal Finite Difference Time Domain (CFDTD) Algorithm

Agostino Monorchio

Microwave and Radiation Laboratory, Department of Information Engineering,
University of Pisa, Via G. Caruso, I-56122 Pisa, Italy.
a.monorchio@iet.unipi.it

Antenna problems in the presence of a curved radome are usually too complex to be analyzed rigorously, especially if the antenna is highly directive. In open literature, different techniques have been presented that make use of some simplified assumptions to render the problem manageable. One common assumption is that the radius of curvature of the radome is large with respect to the wavelength so that the transmission and reflection can be seen as local phenomenona. Ray tracing techniques are therefore used in order to obtain the overall response of the radome. However, when the antenna is highly directive, the radome resides very easily in the near field region of the antenna, so that particular care must be used. A numerical approach (MoM procedure) can also be used, relying on the determination of the induced unknown current distribution on the radome. This latter technique requires a high computational cost in terms of memory and CPU time since a matrix inversion is required which is dense and very large when the dimensions of the radome increase. This, in turn, limits the application of this technique to two-dimensional problems, implying that, from a practical point of view, only rotationally symmetric configurations can be analyzed.

In this paper, we propose the use of the Conformal Finite Difference Time Domain algorithm in order to analyze this kind of problems, which revealed very suited to handle arbitrary geometries (W. H. Yu, R. Mittra, R., 'A conformal finite difference time domain technique for modeling curved dielectric surfaces', *IEEE Microwave and Wireless Comp. Lett.*, Vol. 11, nr. 1, Jan 2001, 25:27). The conformal approach enables us to use a relatively coarse mesh compared to the conventional FDTD without compromising the simulation accuracy, and thus allows us to model larger problems than would be possible with the regular FDTD. The method has been applied to analyze the performances of a horn antenna in the presence of a parabolic radome. Since a full wave three-dimensional approach is employed, the radome can also be tilted in the computational domain, not being restricted to rotationally symmetric geometries. Moreover, the interaction between the antenna and the radome is rigorously taken into account allowing us to estimate the SWR of the antenna affected by the presence of the radome. In Fig. 1, we show a sample of the cases under investigation: a horn antenna with a directivity of approximately 20 dB is operating in the presence of a radome (which can be tilted) whose height is about 15 λ. A preliminary analysis of the stand-alone antenna has been performed in order to check the accuracy of the algorithm against the theory of horn antennas (continuous line in Fig.2), and the results were found to be excellent. In the same Fig. 2, we show the results relevant to the directivity pattern in the H-plane of the antenna in the presence of the radome for two different arrangements of the radome. In this case, the CFDTD is able to predict the distortion of the directivity pattern due to the tilting of radome.
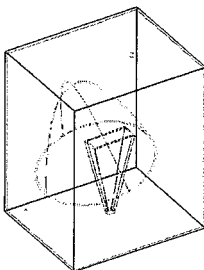
Fig.1
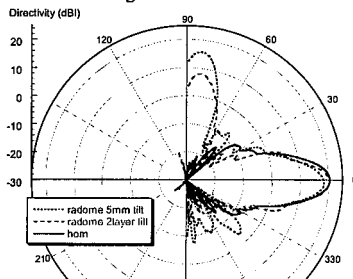
Fig.2

The Dielectric Supported Electrically Small Circular Patch Antenna

Ted Simpson*, University of South Carolina, Columbia, SC
Yinchao Chen, University of South Carolina, Columbia, SC
Jose Chavez, SPAWAR Systems Center, San Diego, CA

Dielectric support above an electrically small circular patch antenna, shown in Fig. 1, is found to enhance electrical performance to the extent that the polarization in the dielectric above the metallic patch aids radiation. This is shown in contrast to the detrimental effect that dielectric polarization has on both antenna bandwidth and efficiency when the dielectric is placed below the patch where the induced polarization detracts from the radiation associated with conduction current in the feed post.
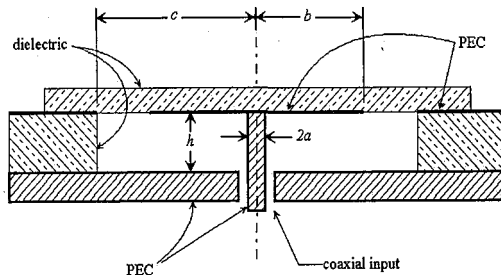
Fig. 1. Cross section of a dielectric supported circular patch antenna driven by a coaxial input over a PEC ground plane.

While the detrimental effects of interior dielectric loading on top loaded antennas was recognized very early by Schelkunoff and Friis (*Antennas: Theory and Practice*, Wiley, 1952), contemporary applications involving metallic patch antennas on microwave substrate have largely neglected this problem, seeking relief from the inherent bandwidth reduction by enlarging the size and shape of the patch. Thus it seems that the theoretical complications attendant to the dielectric substrate on the one hand, offset by the routine availability of powerful cut-and-try methods supported by FDTD analysis on the other, have stymied the systematic development of general design criteria for patch antennas similar to those achieved by Wheeler ("Fundamental Limitations of Electrically Small Antennas," *Proc. IRE*, 1947) in regard to such antennas devoid of dielectric loading.

In this study we have attempted to show that by extracting the elements of a physically plausible and electrically faithful equivalent circuit, and by relating the performance of this circuit to the frequency bandwidth and radiation efficiency, we can formulate simple rules for optimizing patch antenna designs. To accomplish this we have used the input impedance spectrum obtained from FDTD analysis verified by comparison to measurements where possible.

Results are limited to the electrically small case in order to relate dielectrically loaded patch antennas to the body of material (Simpson, "The Disk Loaded Monopole Antenna," IEEE AP/S, to be published in 2004) available for such antennas in air. In addition, the electrically small case leads to an intuitively appealing clarity in the relation between the elements of the equivalent circuit and the physical structure.

176

Compact Dual-polarized 4-port Microstrip Antenna with Decoupling Network

Yi-Hao Lu[1] , *H.J. Chaloupka[2] , and J.C. Coetzee[1]

1. Dept. of ECE, National University of Singapore, Singapore 117576
2. Dept. of EIE , University of Wuppertal, D-42119 Wuppertal, Germany

It is well known that wireless communication systems using multi-port antennas at both ends, denoted as MIMO (Multiple Input Multiple Output) systems, can greatly enhance channel capacity. However, demands for low correlation between the signals from different antenna ports and for the prevention of gain reduction by cross-talk are difficult to meet at small mobile devices, such as handsets and laptops. An approach which combines a novel array concept with the use of dual polarization serves as a promising alternative to circumvent this problem. In this talk, a compact dual polarized 2.45 GHz microstrip array is described, which consists of four patch antennas and a decoupling network (DN). These four patches are aperture coupled and provide different polarization, each with two elements. Furthermore, a new point of view to consider the mutual coupling in highly packed arrays is put forward. That is, with the use of DN, while all four elements are excited, the four ports of the array are still decoupled from each other. In this way, mutual orthogonality between the complex-valued vector radiation patterns of the 4 ports is achieved. Figure 1 below shows the numerical results for the scattering parameters of the decoupled ports from IE3D. Due to the symmetry, S41 coincides with S21, and thus, is not shown. To verify the theory, one antenna was manufactured, as shown in Figure 2. The top substrate used here is the Duroid 5870 (ε_r= 2.33, t=3.18mm), while the bottom with DN is the RT 4003 (ε_r= 3.38, t =0.51mm). Measured data confirm the simulation. The diameter of the whole array is 65.1 mm and can be further reduced with substrates of a higher dielectric constant, which enables its use on mobile devices.
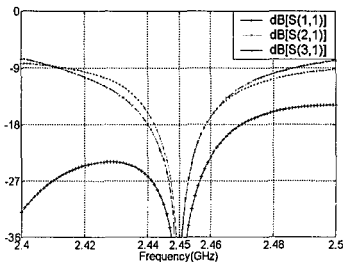
Figure 1. Simulated S Parameters
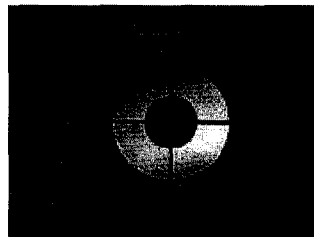
Figure 2. Photograph of the Antenna

177

Structural Integrated Airborne Antenna Array

Wolfgang von Storp, EADS Deutschland GmbH, Ulm, Germany*
Robert Sekora, EADS Deutschland GmbH, Munich, Germany
Markus Boeck, EADS Deutschland GmbH, Ulm, Germany

Airborne platforms are equipped with many antenna systems for different applications and frequency ranges. Especially data link antennas are often mechanically steered and require large radomes decreasing the aerodynamic performance of the air vehicle. The growing need for broadband data links requires a new antenna technology: the structural integrated antenna, where the functionality is completely integrated within the aircraft structure without decreasing its capability to take up mechanical stress. The configuration of the antenna elements is adapted to the curved surface of an aircraft. The presentation will show the electrical design of a structural integrated antenna array. Measured and simulated results will be included. The main challenge of the electrical design was the development of a single radiating element within the X-band antenna array using a given multilayer structure. Materials and layer dimensions are defined according to aircraft requirements and cannot be adapted for the RF structure. The antenna gain of a single radiating element is more than 3.5dBi in boresight direction with a circular polarised radiation pattern. An impedance bandwidth of more than 10% was obtained to cover various requirements for current and future applications.
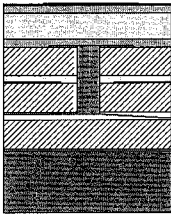
Fig 1: Layer Structure

Principal of the RF design

The single element is realised as a circular stacked patch antenna (parasitic and driven patch). The circular polarised radiation pattern is based on the excitation of two orthogonal patch modes having the same resonant frequency and a 90 degree phase shift. The lower patch is directly coupled to the stripline distribution network using two probe connections. Equal power with a 90 degree phase shift between both feed points is obtained by a common 3dB power splitter and a transmission line with quarter wave length. Reflections related to a mismatch of the probes are partially compensated by this design technique and a good impedance bandwidth behaviour is achieved.

The feeding technique also supports good axial ratio performance, which is 2dB in boresight direction. Parasitic modes within the stripline network structure are suppressed by via holes connecting the ground layers. Fig. 2 shows a subgroup of the antenna array. The four single elements in one subgroup are combined by a distribution network containing three power dividers. An electrical beam steering in one dimension is performed by using external phase shifters for each subgroup.
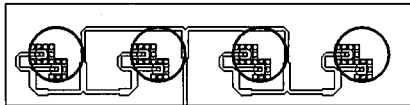
Fig. 2: Subgroup of 4 single elements

Fig. 3: Farfield Pattern of a Single Subgroup
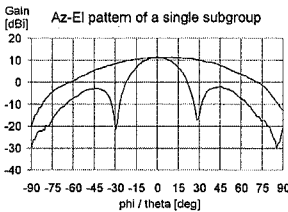
Measurement results

The measurement results of a subgroup are close to the simulated data. Fig.3 shows exemplarily the antenna gain function for the azimuth and elevation plane at midband. The radiation pattern is quite symmetric and a maximum of 11dBi is achieved in boresight direction.

References

[1]   Sekora R.; "Structure Integrated Patch Element for X-Band Application"; Antenna Application Symposium, Monticello / Illinois, 2002

Broadband Dual-Mode Performance of a Two-Arm Slot Spiral

Dejan Filipović[*], Milan Lukić, Quinton Mathews, and Thomas Cencich[(1)]
University of Colorado; Dept. ECEN; Boulder, CO 80309-0425
[(1)]Lockheed Martin; P.O. Box 179; Denver, CO 80201
E-mail: dejan@colorado.edu

From the time spiral antenna was invented in 1954 until 1960, a significant research was conducted to obtain a broadband dual-mode operation with a two-arm spiral. Although two modes were demonstrated, they were not simultaneously broadband over wider bandwidths. Radiation from the central region of the antenna due to the unbalanced feed when spiral is fed for the difference mode of operation causes pattern degradation. Then, in 1960, Shelton suggested that at least three-arms are necessary for the simultaneous broadband dual-mode operation. It was determined that from the N arm spiral a total of N-1 broadband, balanced, modes of operation are possible [see for example B. Corzine, J. Mosko, Artech House, 1990].

In this work we utilize a two-arm slot line based spiral geometry. Although two arm slot spirals have been thoroughly investigated in the past, they all have had continuous slot line in the center, and were fed by a Dyson type horizontal balun. The continuous nature of the slot line at the center does not allow a broadband 2nd mode operation since the magnetic current can not be simultaneously excited in opposite directions from the two points forming the feed to slot line transition [D. Filipovic, J. Volakis, IEEE TAP, 51, 430-440, 2003]. To obtain over an octave wide dual-mode bandwidth, we propose a discontinuous two-arm slot spiral with the open-end like apertures in the center. Use of two modes of operation of a coplanar waveguide can then provide proper phasing. As shown in the figure, two modes of operation are demonstrated with excellent axial ratio/cross-polarization performance at the peak gain elevation angles. Plotted are 36 overlaid elevation cuts of co-and cross polarized patterns for the two modes of operation. It is important to note that in the 1960s, major efforts were undertaken for the printed and wire antennas, while slot line based structures were neglected. At that time, very little information was available on the slot lines, and the coplanar waveguide was introduced much later. Finally, with obtained design a realization of a very simple and inexpensive mode-forming network (beam-former) is straightforward.
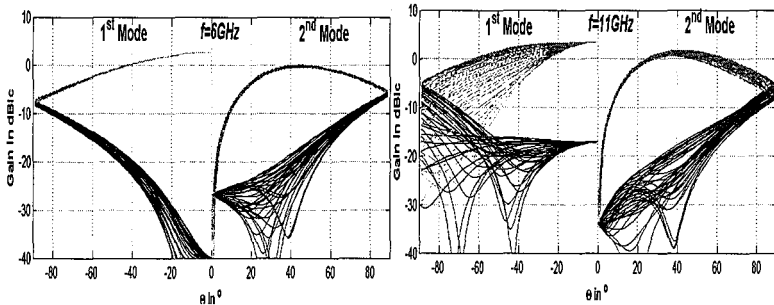
Figure. Dual-mode radiation patterns at 6GHz and 11GHz.

179

Low-Profile, Wide-Band, Archimedean Spiral Antenna

Bell, Jodie*, Iskander, M.F.
Hawaii Center for Advanced Communications
University of Hawaii at Manoa
Honolulu, HI, USA

Spiral antennas have the characteristics vital for communications in many applications. Their wideband characteristics accompanied with their low profile as well as their low cost to manufacture make them prime candidates for vehicle use. Traditional implementation of Archimedean spiral antennas entailed using a ground plane placed at a distance lambda/4 below the antenna to produce a unidirectional beam. This implementation alters the inherent frequency independent behavior of the spiral antenna and in some cases suggested the use of slot spiral arrangement to help with maintaining acceptable radiation characteristics while maintaining the much desired low profile design. In this paper we present a new implementation of an Archimedean spiral antenna. This approach uses PBG technologies to allow the antenna to maintain its frequency independent behavior as well as giving the antenna a reduced profile. This paper first shows the traditional implementation of an Archimedean spiral antenna. We show the effects of reducing the ground plane distance on the radiation of the antenna. We then show the implementation of an Archimedean spiral antenna placed over a PBG structure. Showing that with the PBG structure the Archimedean spiral antenna can keep its inherent wide band characteristics, as well as reduce the profile of the antenna, and reduce back radiation. Additionally, we compare the traditional centrally fed mode of excitation with a new mode of excitation by feeding the outer ends of the spiral arms. This method of excitation has been shown to produce directional radiation, desirable for vehicle applications. This paper introduces a PBG backed Archimedean spiral antenna that has a low profile, wide band characteristics, and low back radiation. Obtained radiation and impedance characteristics will be compared with those of the traditional spiral and slot-spiral designs.

Self-Complementarity and miniaturization in antenna design

Reza Azadegan*, Kamal Sarabandi

The University of Michigan, Radiation Lab
Ann Arbor, MI 48109-2122 USA
FAX: +1-734-747-2106
email: azadegan@eecs.umich.edu

1. ABSTRACT

The concept of self-complementarity has been introduced by Mushiake. This principle asserts that the input impedance of a self-complementary antenna is equal of its complementary structure equal to $\eta/2$. The frequency independent characteristics of these structures makes them unique insofar as wide bandwidth is concerned. However, there are some ramifications of self-complementary structures including: the infinite size of the structure, the impedance matching of $Z_{sc} = 60\pi$ to the standard $50\,\Omega$ lines, and the symmetry requirements of the medium which prohibits the use of substrate. The frequency independence might be drastically deteriorated when any of the necessary conditions for self-complementarity are not met. For miniaturized planar antenna structures, all of the above requirements should be relaxed, or otherwise, the miniaturization will be superseded. For example, the self-complementary structure cannot be extended all the way to the infinity, and thus the truncation is inevitable. On the other hand, introducing matching network and dielectric substrate in the structure are among additional factors which are relaxing the self-complementarity conditions. It is thus required to further investigate how to minimize the effect of the above mentioned imperfections in the frequency independent performance.

The authors have already introduced a novel miniaturized slot antenna with dimensions of $0.05\lambda_0 \times 0.05\lambda_0$ with the bandwidth of 0.3% [1]. In general, resonant slot antennas are rather narrow-band, and when miniaturized, their bandwidth reduces even further. In order to increase the bandwidth of this miniaturized slot antenna, two approached are discussed. One is to use folded structure [2], and another is to use the idea of self-complementary structures. In the presentation, the miniaturized slot antenna of [1] is extended to its complementary and self-complementary realizations. The effect of miniaturization on the self-complementary performance, as well as the effects of self-complementarity on the bandwidth of miniaturized antennas are investigated and presented.

REFERENCES

[1] R. Azadegan, K. Sarabandi, "A novel approach for miniaturization of slot antennas," *IEEE Trans. Antennas Propagat.*, vol. 51, pp. 421-429, Mar. 2003.

[2] R. Azadegan, K. Sarabandi, "Miniaturized folded-slot: an approach to increase the bandwidth and efficiency of miniaturized slot antennas," *in Proc. IEEE Antennas Propagat. Symp.*, San Antonio, TX., June 2002, pp. 14-17.

A Leaky Slot Printed Between Two Infinite Dielectrics: a Non Dispersive Design with Constant Input Impedance.

S. Bruni[1], A. Neto[1], G. Gerini[1], F. Marliani[2]

(1) Integrated Front End Solution, TNO-FEL
Oude Waalsdorperweg 63, 2597 AK, Den Haag, The Netherlands
bruni, neto, gerini@fel.tno.nl

(2) European Space Research and Technology Center (ESTEC),
2200 AG Noordwijk, The Netherlands
Filippo.Marliani@esa.int

In this contribution, we investigate the design of a leaky slot antenna printed between two infinite dielectrics. The Green's function of the canonical structure, characterized by constant width has been presented in (A. Neto, S. Maci, "Green's Function of... Part I: Magnetic Currents" *IEEE Trans. on A.P.* Vol. 51 no. 7 July 2003, and "... Part II: Uniform Asymptotic Solution" to be published). Also the calculation of the input impedance of the canonical antenna has been investigated in (A. Neto, S. Maci, "Input Impedance of ....", submitted to *IEEE A.W.P.L.*). As a result of this investigations, it turns out that a slot printed between two infinite dielectrics present ultrawide band properties. This is due to the fact that the mode excited on the slot is a leaky wave mode. So all the power launched in the slot is radiated before arriving to the end point, if the slot is sufficiently long. However, when one wants to design an antenna derived from such a slot printed between air and one dielectric material, it turns out that the propagation mode is non dispersive only when the material presents low dielectric constant. On the contrary, the input impedance of such slots are almost constant with frequency only when the dielectric constant is relatively high. In practice, in order to achieve an antenna that present simultaneously low disperisivity and constant impedance a varying width of the slot must be assumed. The design of such slots can be rendered simpler if one has an estimate of the characteristic impedance of the canonical (constant width) slot. From this characteristic impedance one can evaluate the input impedance of a varying slot resorting to simplified methods by cascading transmission lines with varying impedance. This is a well known procedure (Ramo Whinnery, Van Duzer "Field and Waves in Communication Electronics", *John Whiley and Sons*) that in the present case we adapt to the present design. However, before doing so the characteristic impedance of the leaky slot, while has not been previously presented, has to be evaluated.

Moreover once the characteristic impedance is available it is also possible to derive an equivalent circuit that consents to describe the input impedance and propagation features of the slot antenna in analytical form at least for low dielectric constants.

Unconventional Traveling Wave Antenna for Telemetry Purposes

Michael Hamid*, University of South Alabama, Mobile, Alabama 36688 and
N. Gholson and L. Curvin, Science Applications International Corporation,
Gulfport, Mississippi 39507

The paper deals with a z-oriented vertical mast antenna, in the form of an aluminum tube of 182.5 cm length (L) and 1.11 cm radius (a), supported by an ocean buoy and arranged to transmit telemetry data to an approaching aircraft. While the azimuthal pattern is circular, a basic requirement for this application is that the elevation pattern must not have lobes along the ocean surface (i.e. at $\theta = \pm 90°$) to avoid interference. While this requirement can be met in principle by operating the antenna as a monopole over a ground plane (MGP) and at a sufficiently high frequency, the resulting break up of the pattern from 2 to 4 to 6 lobes is also undesirable. Also, the antenna must have high gain over a wide frequency range and low reflection coefficient (S_{11}) to avoid matching networks.

The above requirements can be partially met by converting the MGP to a vertical traveling wave antenna (TWA) of several wavelengths ($L/\lambda >> 1$) by terminating the antenna with its average characteristic impedance (Z_c) which converts the standing wave current to a traveling wave current. The resulting radiation pattern is derived using the standard approach of evaluating the magnetic vector potential from the current distribution. Although Z_c can only be approximated ($\cong 575\Omega$) using classical theory of the antenna as an opened-out transmission line (see Jordan's text on Electromagnetic Waves and Radiating Systems, Prentice Hall, 1950, chapter 13), a resistor R was used in our outdoor experiment. The values of R and frequency f were varied to meet the specifications resulting in f=407 MHz, R=499Ω, antenna input impedance Z_{in} with a 50 Ω coaxial feed=50 – jl, $S_{11} \cong$ -40 dB (see Fig. 1). The measured direction of the main lobe was at $\theta \approx 29°$ with a 3-dB beamwidth of $\approx$ 23.5° as compared to predicted values of approximately 31° and 24°, respectively (see Fig. 2), where the lobe shift is due to positioner drift error at θ =90° The radiation resistance was also evaluated from the integral of the pattern function squared and the results will be presented and compared to the MGP. The measured bandwidth, which is a critical function of R, will also be presented and is presently under investigation particularly since the measured bandwidth was much larger for other values of R and f which were not pursued experimentally due to inadequacies in the test site at those frequencies.
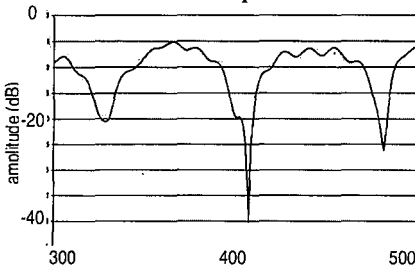
Fig 1 Reflection Coeff of TWA vs. f (Mhz) for R = 499
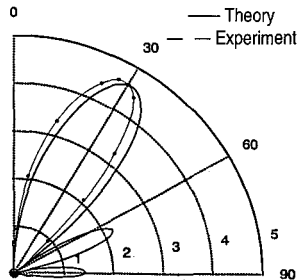
Fig 2 Elevation Pattern of TWA

183

Spheroidal Dielectric Resonator Antenna

A. Tadjalli*, A. Sebak, T. Denidni[1], and A. Kishk[(2)]
ECE Dept, Concordia University, Montreal, QC, Canada H3G 1M8
(1) INRS-EMT, 800 de la Gauchetiere, Montreal, QC, Canada H5A 1K6
(2) EE Dept, University of Mississipi, University, USA

The dielectric resonator antenna (DRA) is a ceramic-type material shaped in a particular manner, mounted on a ground plane, and fed in some fashion. The most common shapes are rectangular, hemispherical and cylindrical. The reason that these shapes are used is the simplicity of these shapes to analyze, simulate and fabricate. A dielectric resonator antenna with spheroidal shape will introduce another degree of design parameters and may lead to a simple feeding mechanism for generating circularly polarized waves. Canonical structures, including spheroidal geometries, require no magnetic wall assumption in the problem formulation and hence an accurate solution can be obtained, especially for DRA with lower permittivity.

One kind of the most useful DRAs is the Hemispherical DRAs that mounted on a ground plane fed with a single probe (A. Kishk, et al., IEEE Antennas and Propagation Magazine, 36, # 2, pp. 20-31, 1994). This kind of antenna has 3 design parameters: permittivity of dielectric, radius of sphere and position of probe along the radial direction on the base with the permittivity and radius directly related to each other. These parameters control the excitation of different modes. Hemispheroidal DRAs are potentially attractive and add more design parameters in terms of different semi-axes dimensions. Another parameter that may lead to better results is the more diversity of mode excitation compared to hemispherical DRA. For analyzing hemispheroidal DRAs we use a classical hybrid method that combines specialized dyadic spheroidal Green's functions with Method of Moments. Details of the analytical development of the solution and numerical modeling together with varieties of numerical results will be presented and discussed.
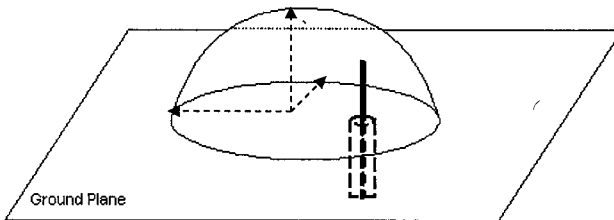
Figure 1. Hemispheroidal DRA mounted on ground plane

The Butterfly-loop Antenna – A New Structure with Better Performance

Sivanand Krishnan*[1,2], Le-Wei Li[1], Mook Seng Leong[1] and Pang Shyan Kooi[1]
[1]ECE Dept., National University of Singapore, 10 Kent Ridge Crescent, Singapore 119260
[2]Institute for Infocomm Research, 20 Science Park Road, #02-21/25, Singapore 117674
E-mail: sivanand@i2r.a-star.edu.sg

Abstract

Circular loop antennas of more than a wavelength in circumference are known to have good directivities. However, the antennas cannot be directly fed by a coaxial line as they are balanced structures, like dipoles, and so require the use of a balun. One way to avoid the use of baluns and to also have a more compact antenna is to use a half-loop structure that is probe-fed through a ground plane. In this configuration, for most practical purposes, the elevation pattern with respect to the ground plane is considered to be most significant. While the conventional half-loop provides a somewhat directive pattern in this plane, the beam is still rather broad. Thus, to further improve on the performance of the conventional half-loop, we present a new loop structure in this paper. The new structure, the Butterfly-loop, provides much better directivity and cross-polarization characteristics. Also presented is an accurate method for analyzing it.

The Butterfly-loop basically consists of 2 identical half-loops which are connected at an angle (φ) to each other as shown in Fig. 1. At the feed point, the loops are jointly connected to a coaxial probe and at the point opposite the feed, they are connected to the ground plane. The antenna is analyzed using entire-domain sinusoidal basis functions. The analysis yields the solution of the current on the loops in the form of a Fourier-series expansion. The input admittance of the structure is then obtained simply by a summation of the Fourier coefficients. The complete formulation for the analysis will be presented and shown to be accurate through comparison with measured results. From the Fourier coefficients of the loop currents, the radiation fields from each loop is directly obtained using the closed-form expressions by Li *et al.* (IEEE Trans. Ants. Prog., v12, pp. 1741-1748, 1997). The total radiation pattern is obtained by summing the contribution from each loop after coordinate transformation. Fig. 2 provides a comparison between the elevation pattern in the x-z plane of a Butterfly-loop constructed from one-wavelength long half-loops with angle φ equal to 120° and that of a corresponding conventional half-loop. The new structure is seen to have a 3 dB beamwidth of 55° compared to 155° in the conventional case. The gain is also seen to be higher by 4 dBi for the Butterfly-loop. These results clearly illustrate the superior performance of the new structure.
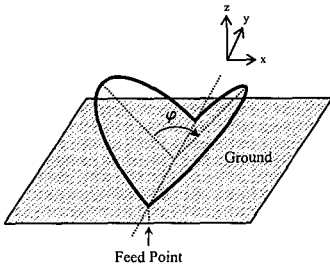
Fig. 1: Geometry of the Butterfly-loop
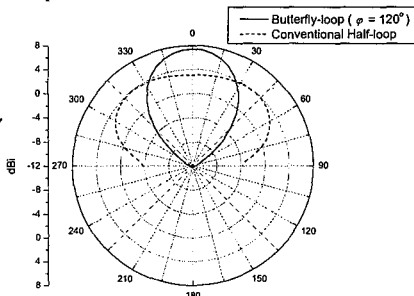
Fig. 2: Radiation Pattern in x-z plane

Design of Broadband Impedance Matching Anisotropic Quarter-Wave Polarizers

Hsin-Lung Su* and Ken-Huang Lin

Department of Electrical Engineering, National Sun Yat-Sen University,

Kaohsiung 80424, Taiwan

hlsu@pcs.ee.nsysu.edu.tw, khlin@mail.nsysu.edu.tw

Anisotropic media are widely used in microwave and optics because of their unique properties. There are two different propagating velocities in the anisotropic medium so this kind of medium can be used as a polarizer. Similarly, this polarizer has two different intrinsic impedances. The method to match both intrinsic impedances simultaneously for a quarter-wave polarizer was proposed by Su and Lin (H. L. Su and K. H. Lin, APMC2002 conference, 3, 1549-1552,2002). However, the impedance matching method is narrow band in nature. It is known that the maximum axial ratio bandwidth of the quarter-wave polarizer is about 42% (Y. C. Huang and K. H. Lin, Radio Sci., 38, no. 1, 1012, doi:10.1029/2002RS002611,2003). If the impedance matching can be further extended, the quarter-wave polarizer becomes more useful.

In this paper, we present a design to extend the quarter-wave polarizer impedance bandwidth while the axial ratio bandwidth remains unchanged. We consider that a uniaxial anisotropic quarter-wave polarizer with the optical axial lying on the yz-plane. When a pane wave is normally incident into the polarizer along the z direction, the plane wave can be separated into two parts, x-polarized and y-polarized wave or transverse electric and transverse magnetic wave. For the x-polarized wave, the impedance matching is imposed; therefore, the x-polarized wave has no reflection for any frequency. For the y-polarized wave, the Binomial impedance transformer of the microwave circuit theory is used; thus, the impedance matching bandwidth of the y-polarized wave becomes wider. It is easy to keep the reflection to be smaller than 0.05 over a 50% frequency band. It can be shown that the axial ratio band is still maintained at a 42% frequency band. In our design, the same medium can be used for the design of the Binomial impedance transformer by rotating the optical axis of the medium. There is thus no need to find extra anisotropic media.

Design of Dual-Band Dual-Polarized Antenna with Frequency Selective Surface Cover and Artificial Impedance Surface

Heeduck Chae*, Yonghoon Kim, Hyojun Kim, and Sangwook Nam

Applied Electromagnetics Laboratory, School of Electrical Engineering and
Computer Science, Seoul National University, Seoul, Korea

Recently, much interest has been drawn to the periodic structures that have useful characteristics. Such periodic structures include Photonic bandgap (PBG), frequency selective surface (FSS), artificial impedance surface (AIS), and artificial magnetic conductor (AMC). PBG structures have been used to improve the antenna performances by preventing surface wave or using as a reflector that acts like magnetic conductor. Nowadays PBG materials are used as the cover of patch antenna or dipole antenna and those structures which operate like Fabry-Perot resonator enhance antenna directivity dramatically.

To use PBG materials as Bragg mirror in Fabry-Perot cavity, two or more layers are required and those layers are bulky for antenna applications. Thus we use one FSS layer instead of PBG layers in order to reduce total antenna height. FSS is composed of slot arrays and it has less than 10% of transmission ratio. Patches or dipoles are periodically loaded on substrate and they can be considered as artificial impedance surface. The proposed antenna is fed by microstrip patch antenna which is placed on the center of AIS. Figure 1 shows the basic structure of proposed antenna (feeding antenna is not shown).

The distance d between two surfaces (FSS and AIS) determines resonant frequency which satisfy the following equation:

$$2\beta_0 d - \varphi_{FSS}(f) - \varphi_{AIS}(f) = 2\pi n$$

here, $\varphi_{FSS}(f)$ and $\varphi_{AIS}(f)$ are reflection phase on FSS and AIS, β_0 is phase constant in free space and n is integer.

Because the element patch or dipole of AIS is not square, reflection phases are subject to the polarization of the incident wave. Therefore, proposed structure can support two orthogonal polarizations and they have different resonant frequencies. Thus, the proposed antenna has dual operating frequencies with dual polarizations in one antenna structure. Moreover, resonant frequency is controllable by changing not only the distance d but also the element size of AIS.
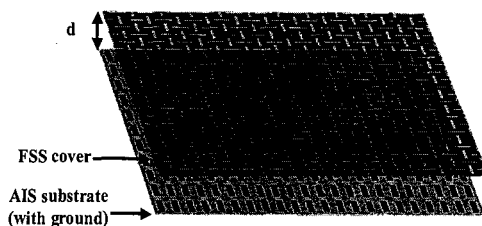
Figure 1. Basic structure of proposed antenna with FSS cover and AIS

An Open-ended Waveguide System for SAR Measurement System Validation and Effect of Dielectric Properties on the Peak 1- and 10-g SAR for 802.11a Frequencies 5.15 to 5.85 GHz

Gang Kang*, Qingxiang Li and Om P. Gandhi
Department of Electrical and Computer Engineering
University of Utah
Salt Lake City, Utah 84112, U.S.A.

Compliance with safety guidelines prescribed in terms of maximum electro-magnetic power absorption (specific absorption rate or SAR) for any 1- or 10-g of tissue is required for all newly-introduced personal wireless devices such as wireless PCs. The prescribed SAR measuring system is a planar phantom with a relatively thin base of thickness 2.0 mm filled with a lossy fluid to simulate dielectric properties of the tissues. A well-characterized, broadband irradiator is required for SAR system validation for the new 802.11a frequencies in the 5-6 GHz band. This paper describes an open-ended waveguide system that may be used for this purpose. Using a fourth-order polynomial least-square fit to the experimental data gives SAR variations close to the bottom surface of the phantom that are in excellent agreement with those obtained using the FDTD numerical method. The experimentally-determined peak 1- and 10-g SARs are within 1 to 2 percent of those obtained using the FDTD both at 5.25 and 5.8 GHz.

Even though the dielectric properties of the human tissues are known to be nonuniform and highly variable, relatively rigid adherence to prescribed dielectric properties (ε_r, σ) is required by U.S. Federal Communications Commission (FCC, Supplement C (Edition 01-01) to OET Bulletin 65 (Edition 97-01)) and International Electrotechnical Commission(IEC TC 106/PT62209) for compliance testing of such devices. Using three typical near-field irradiators (i.e., dipole antenna, wave-guide irradiator, and patch antenna), we have examined the effect of dielectric properties for SAR measurement fluids with conductivities varying by 2:1 to show that both 1- and 10-g SARs vary by less than $\pm$ 2-4% for the 802.11a band 5.15 to 5.825 GHz. This is due to higher surface SAR but shallower depth of penetration of EM fields for the higher conductivity media resulting in nearly identical SARs for cubical volumes associated with 1- or 10-g of tissue, respectively. Also studied is the effect of lower ε_r fluids recommended in some standards which results in slightly higher and thus a conservative assessment of SAR.

FDTD Computation of SAR Reduction in the Human Head for Mobile Communication Handsets at 1800MHz

*Chih-Ming Kuo and Chih-Wen Kuo

Department of Electrical Engineering, National Sun Yat-Sen University, Taiwan
E-mail : cwkuo@mail.nsysu.edu.tw

Abstract

In recent years, mobile communications gradually becomes popular and public concerns of potential hazards incurred by the EM waves of handsets have been increasingly growing. This is no surprise since the transmitting antenna of the handset is pretty close to the user's head when it's in use. Henceforth, consideration of the possible health hazards due to this type of EM exposure is very important. The power absorption inside a human head is measured by the specific absorption rate (SAR) averaged over either 1g or 10g of tissue. The SAR distribution inside the head is affected by the current distribution on the antenna, the handset metal box and obstacles in the vicinity of the antenna. One effective approach of reducing the SAR values is to use materials such as a ferrite sheet on the handset cover to absorb radiation toward the direction of the user's head.

In this paper, we use the FDTD method to calculate the effects of SAR reduction of ferrite sheets. The handset is modeled as a quarter-wavelength monopole antenna mounted on a rectangular conducting box and operated at 1800MHz. The dimensions of the handset are L cm × 4 cm ×2 cm. The dimensions of the ferrite sheet attached on the front side of the handset are h cm × 4cm × 2.5mm. The lengths of h and L increase along the $-z$ direction from the top surface of the handset. We calculate the 1-g-averaged spatial peak SAR and the total absorbed power P_h in the human head by varying the lengths of the metal box and the lengths of the ferrite sheet. In order to compare the effects of SAR reduction in all cases, the antenna output powers is set to 1W. The numerical results are shown in Table 1. For four different lengths of the metal box, 1-g-averaged spatial peak SAR and total absorbed power in the human head decrease as the length of the ferrite sheet increases. It can be found that the numerical results are similar when the length of the ferrite is 5cm. the effects of SAR reduction depend on the surface current of the metal box when we use the same ferrite sheet on the handsets with the different lengths of the metal box.

		L=5cm	L=7cm	L=9cm	L=11cm
h=0	SAR_{1g}(W/kg)	10.92	6.69	7.08	7.83
	P_h (%)	43.45	44.19	40.05	41.47
h=1cm	SAR_{1g}(W/kg)	8.87	5.50	5.72	6.30
	P_h (%)	38.21	39.71	35.79	36.77
h=3cm	SAR_{1g}(W/kg)	5.98	5.40	5.44	5.65
	P_h (%)	30.58	33.30	31.64	31.28
h=5cm	SAR_{1g}(W/kg)	5.43	5.27	5.35	5.44
	P_h (%)	29.46	30.38	29.51	29.62

Table 1. 1-g-averaged spatial peak SAR and total absorbed power in the head
Antenna output power is 1W at 1800MHz

1.) Commission and Session : Commission K2 (Biomedical applications)
2.) The peak values of SAR_{1g} decrease to the similar values when the maximum SAR reduction is achieved for the four different lengths of the handset.
3.) See reference above.

Unconditionally Stable ADI-FDTD Method with Resistive Source Implementation for Specific Absorption Rate (SAR) Computations

Stefan Schmidt* and Gianluca Lazzi

Department of Electrical and Computer Engineering,
North Carolina State University, Raleigh, NC 27695-7914, USA

As more applications of wireless devices in the personal space are emerging, the interaction between electromagnetic energy and biological objects has become increasingly important to researchers and the public. Due to the fear and awareness that health damage may be caused by the use of wireless equipment, it is important to minimize the electromagnetic interaction between wireless designs and the human body. Repetitive prototyping and measurements for specific absorption rate (SAR) minimization can often be too expensive and time consuming; hence, efficient and fast numerical methods are a very attractive alternative.

Electromagnetic problems involving inhomogeneous dispersive media are easily solved using the finite-difference time-domain (FDTD) method. For explicit FDTD methods, the fine geometric detail given in anatomical models, which is often far smaller than the wavelength under investigation, would dictate rather small time steps due to the Courant-Friedrichs-Levy (CFL) stability bound. An unconditionally stable D-H alternating-direction-implicit (ADI) FDTD with a material-independent formulation of the perfectly matched layer (PML) absorbing boundary condition was previously proposed for the simulation of bioelectromagnetic problems and the computation of SAR. For spherical geometries, the method showed good agreement with experimental results and the explicit FDTD method. However, the ADI FDTD method, as previously proposed, does not converge as quickly as the explicit FDTD methods with resistive source implementation.

We developed a new resistive source condition for the unconditionally stable ADI method to achieve convergence rates that are similar to those of the explicit FDTD method. The method was used for the computation of SAR in spherical geometries and models of the human head. The results, obtained using the resistive source condition, were compared to the explicit FDTD method as well as previously published experimental results.

Modeling of Bone Marrow Cells in Low-Frequency Electric Field

Roanna Chiu and Maria A. Stuchly
Department of Electrical & Computer Engineering, University of Victoria, BC, Canada

Electric fields in tissues of human body models have previously been computed for low frequency (50 or 60 Hz) electric and magnetic fields, and for contact currents. Only bulk properties of each tissue have been considered. Bone marrow is the tissue of a particular interest in considering role of the fields in leukemia development. The objective of the research reported is to examine whether a non-uniform structure of bone marrow results in enhanced electric fields in some sub-structures. Computational methods are employed to simulate the distributions and enhancements of fields. Electrostatic condition of a uniform applied electric field was considered based on the sizes of the components of the bone marrow. As an initial model, a two-compartment structure consisting of cancellous bone and bulk solute were modeled. The model was obtained from a CT scan (courtesy of Dr. B. van Riethergen of the Eindhoven University of technology) and consisted of 282×282×282 voxels of 14μm resolution as shown in Figure 1; for the purpose of our experiments, we selected a subset of 50×50×50 voxels. A reconstruction of the model using the iso-surface feature of MATLAB is shown in Fig. 2.
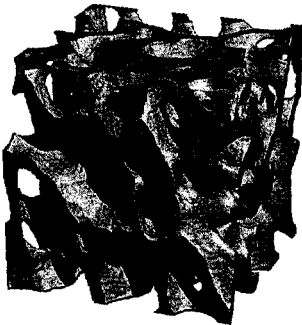
Figure 1: CT Image of the Cancellous Bone
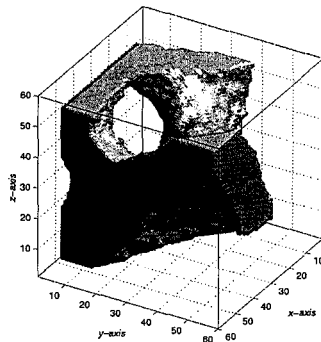
Figure 2: Iso-surface Plot of the 50×50×50 Model

The two domains of the structure were assigned dielectric properties of bone and bone marrow, respectively. The problem was solved using two methods, namely the scalar potential finite difference (SPFD) method and finite element method (FEM). The SPFD solver was developed in-house, while a commercial FEM package, FEMLAB (COMSOL Inc.), was selected. The SPFD method used a structured grid therefore the voxel representation of the bone model could be introduced to the solver directly. However, in order to take advantage of the irregular grid in FEM which allowed better conformity to the geometry, the model needed to be imported into FEMLAB first. Alternatively, we employed a different approach to avoid memory issues: the problem was meshed without the geometry, while the dielectric properties were returned using interpolation which was incorporated into the FEMLAB solving algorithm.

Initial results of the two methods were in good agreement, thus validating the model as well as the setup of both numerical methods. We then analyzed the field distributions in each of the domains when different dielectric properties were assigned. We also identified areas where electric fields were more enhanced and their correlations to the geometry.

191

Numerical Assessment of Induced Low Frequency Currents in the Human Head due to Mobile Phone Battery Currents

Sami Ilvonen, Ari-Pekka Sihvonen[†], Kimmo Kärkkäinen[*],
Seppo Järvenpää and Jukka Sarvas
Electromagnetics Laboratory
Helsinki University of Technology, Finland
[†]Radiation and Nuclear Safety Authority of Finland

A mobile phone user is exposed, in addition to the widely studied intensive high frequency antenna fields, also to the low frequency fields due to battery currents. The resulting magnetic field induces low frequency currents in the head of the user. The purpose of the research is to assess the strength of these currents and compare the results with the allowed limits stated in the ICNIRP (International Commission on Non-Ionizing Radiation Protection) Guidelines.

In this talk we present the numerical assessment of the induced currents computed from experimentally measured magnetic field of the battery currents. The field measurements were carried out by the Radiation and Nuclear Safety Authority of Finland. The mobile phone model used in the measurements was Nokia 6210. The spatial distribution of the magnetic field was measured in a regular lattice in front of the mobile phone by using a wire loop sensor. The measured field cannot be used in numerical analyses as such because of the noise and other measuring uncertainties. Therefore, the measured field distribution was used to derive the equivalent source model of the battery currents. This model was used in the numerical analysis of induced currents in the head.

The numerical algorithm for computing the induced currents in the head was based on a quasi-static field formulation and the finite element method (FEM). The solved equation system was of the form

$$\begin{cases} \nabla \cdot [\sigma(\mathbf{r})\nabla u(\mathbf{r})] = -\nabla \cdot [\sigma(\mathbf{r})\mathbf{A}_0(\mathbf{r})], & \mathbf{r} \in V \\ \frac{\partial u}{\partial n}(\mathbf{r}) = -\mathbf{n}(\mathbf{r}) \cdot \mathbf{A}_0(\mathbf{r}), & \mathbf{r} \in \partial V, \end{cases}$$

in which $\mathbf{A}_0$ is the vector potential of the source model and $\sigma(\mathbf{r})$ is the conductivity distribution in the head. The FEM algorithm was tested by analyzing a layered sphere and comparing the results with the accurate results calculated using the spherical vector wave functions (the Mie-series expansion). In the assessment of the induced currents a realistic head model with about 500 000 division cubes and anatomic conductivity data was used. In the presentation we will also show the calculated current distribution in the head and compare it to the guidelines of ICNIRP.

Radiofrequencies Related Headache and Facial Pain

Suraiya Al-Dousary and Suhail Maqbool Mir
ENT Department
King Abdul Aziz University Hospital
Riyadh, Saudi Arabia

Abstract

Mobile phone use has become widespread and is now a common part of the lifestyle of people of all ethnic backgrounds. Unfortunately this rapid introduction and acceptance of new technology has not seen a corresponding increase of efforts by the scientific community to study and measure the effects of interfering radiofrequencies on the health of its users.

In keeping with this, the ORL department of King Abdul Aziz University Hospital, Riyadh, Saudi Arabia undertook a hospital based survey by setting up a mobile phone clinic in which mobile phone users were encouraged to attend. This report presents the user's experience, our examination findings and the conclusions thereof.

A standard questionnaire was filled about the users demographic data, type and model of the mobile telephone, the duration of calls and the side used most frequently. Attention was paid to the auditory, vestibular and Head and Neck symptoms. Noise-exposure and smoking habits as well as past medical histories were considered. Clinical assessment of the auditory and vestibular apparatus and of the head and neck was performed.

Pure-tone air and bone conduction audiometry was carried out. These users were requested to comeback every three months for re evaluation.

Headaches and facial pain was complained by a substantial number of the mobile users. These symptoms increased with increased exposure, significant when used for more than 60 min / Day.

Theoretical Principles of Ultrawideband Microwave Space-Time Beamforming for Hyperthermia Breast Cancer Treatment

M. C. Converse, E. J. Bond, H. Tandradinata, S. C. Hagness, B. D. Van Veen
Department of Electrical and Computer Engineering
University of Wisconsin
Madison, WI 53706 USA

A persisting challenge in the use of microwave hyperthermia for breast tumors is non-invasively heating cancerous tissue without harming superficial and surrounding healthy breast tissue. Consequently, a great deal of research has been conducted to develop more effective techniques. Most investigations in microwave hyperthermia have employed narrowband (NB) phased array techniques. For example, Fenn et al (*Int. J. Hyperthermia*, 15:45-61, 1999) have developed an adaptive NB technique that uses minimally invasive electric-field probes placed inside the breast to provide feedback. Investigations of an alternative NB annular phased-array approach using three frequencies (Jacobsen, *Electronic Lett.*, 34:1901-1902, 1998) suggest that distributing the transmitted power over a frequency band produces fewer auxiliary foci than single-frequency hyperthermia.

We are currently investigating a new non-invasive ultrawideband (UWB) microwave space-time beamforming approach for focusing microwave energy at a lesion site. The focus is achieved by passing an UWB pulse train through a bank of finite-impulse response filters, one in each antenna channel, that compensate for dispersive propagation effects. The signals are also time delayed and simultaneously transmitted into the breast. Thus, analogous to NB methods, this UWB approach exploits constructive/destructive interference in space. However, UWB hyperthermia may also exploit incoherent combining of power across frequency and space. Furthermore, this approach is a natural companion to UWB space-time microwave imaging method for breast cancer detection (Bond, *et. al., IEEE T-AP*, 51(8):1690-1705, 2003).

In this talk, we explore theoretical principles of this novel approach. Finite-difference time-domain (FDTD) electromagnetic and thermal models of MRI-derived breast phantoms are used to examine its efficacy. The models include a breast phantom containing a small (< 0.5 cm) tumor, surrounding deionized water bolus, and an array of antennas, each transmitting a tailored UWB differentiated Gaussian pulse. Results show excellent microwave focusing and promising thermal gradients for tumors located at various positions within the breast phantom. To date, we have assumed knowledge of the exact dielectric properties of the specific breast being treated as well as a precise positioning of the antennas. In this study we present a numerical investigation of the effects of non-ideal conditions and imprecise a priori knowledge of the dielectric properties. The evaluation is done in two steps. First, a transmit focusing procedure is simulated and the deposited electromagnetic energy (SAR) distributions within the breast are calculated using an FDTD solution to Maxwell's equations. This model includes the dispersive properties of biological tissue, as well as the heterogeneity of the breast derived from MRI data. Second, the SAR distributions are used in an FDTD solution of the bio-heat equation to calculate temperature distributions in the breast. Focusing efficacy is measured using both SAR and temperature distributions. Finally, an examination of the UWB signal used in the focusing procedure is made to determine what effect frequency content and impulse shape has on focusing.

Treatment System of Interstitial Microwave Hyperthermia: Clinical Trials for Neck Tumor and Improvement of Antenna Elements

Kazuyuki Saito[1]*, Keiko Miyata[2], Hiroyuki Yoshimura[2], Koichi Ito[1],
Yutaka Aoyagi[3], and Hirotoshi Horita[3]
[1]Research Center for Frontier Medical Engineering, Chiba University
[2]Faculty of Engineering, Chiba University
1-33 Yayoi-cho, Inage-ku, Chiba 263-8522, Japan
[3]Department of Radiology, Ichikawa General Hospital, Tokyo Dental College
5-11-3 Sugano, Ichikawa 272-8513, Japan

In recent years, various types of medical applications of microwaves have widely been investigated and reported. In particular, minimally invasive microwave thermal therapies using thin applicators are of a great interest. They are interstitial microwave hyperthermia and microwave coagulation therapy (MCT) for medical treatment of cancer, cardiac catheter ablation for ventricular arrhythmia treatment, thermal treatment of BPH (Benign Prostatic Hypertrophy), etc. The authors have been studying thin coaxial antennas for the interstitial microwave hyperthermia.

Hyperthermia is one of the modalities for cancer treatment, utilizing the difference of thermal sensitivity between tumor and normal tissue. In this treatment, the tumor is heated up to the therapeutic temperature between 42 and 45 °C without overheating the surrounding normal tissues. Moreover, we can enhance the effect of other cancer treatments such as radiotherapy and chemotherapy by using them together with the hyperthermia.

The interstitial microwave hyperthermia is applied to localized tumor by inserting thin antennas into the targeted tumor. We have investigated the coaxial-slot antenna to apply to the interstitial microwave hyperthermia and have experienced some clinical trials using the coaxial-slot antennas. Figure 1 shows an example of the treatment. In the treatment, the array applicator composed of four coaxial-slot antennas were employed for heating. In addition, we observed the temperature in and around the tumor using three thermo sensors. At that time, the targeted tumor was completely covered by therapeutic temperature.

Moreover, we have studied the improvement of the input impedance of the coaxial-slot antenna. We used a matching circuit of simple structure at a position close to the feeding point (see Fig. 2). As a result of optimization on structure of the matching circuit, we could obtained an $S_{11} < -10$ dB at the operating frequency (2.45 GHz). It is useful to realize an effective power feeding for treatments.
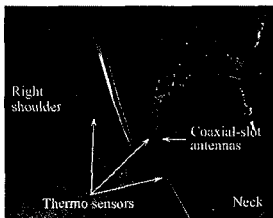
Fig. 1   Photograph of the patient during the treatment.
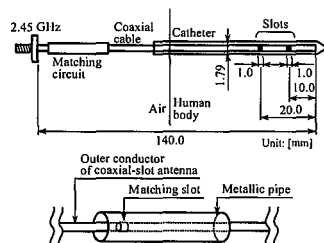
Fig. 2   Coaxial-slot antenna and structure of the matching circuit.

Directional Aggregation Approach for Fast Field Evaluation

Khona Garb[1], Achi Brandt[2], and Amir Boag[1]*

[1]   Department of Physical Electronics, Tel Aviv University, Tel Aviv 69978, Israel

[2]   Department of Applied Mathematics, The Weizmann Institute of Science, Rehovot 76100, Israel

Rigorous analysis of scattering by arbitrary shaped inhomogeneous bodies is often effected via a numerical solution of the pertinent integral equations. For simplicity, we analyze two-dimensional scattering by an inhomogeneous dielectric cylinder via the Electric Field Integral Equation (EFIE). The number of field and current sampling points on the cross section of the cylinder is proportional to its area (normalized to wavelength squared), i.e., of $O(N)$, where $N = (kR)^2$. Here, R is the radius of the smallest circle circumscribing the scatterer and k is the wavenumber. The $O(N^3)$ computational complexity of conventional direct solvers necessitates an iterative approach when analyzing electrically large problems. When solving the EFIE, each iteration requires the evaluation of the electric field due to a given polarization current. Straightforward evaluation of the field at $O(N)$ points by integration involving summation of $O(N)$ terms amounts to $O(N^2)$ operations. This high computational burden underscores the need for using fast field evaluation techniques such as the fast multipole method (FMM).

In this paper, we develop a novel multilevel directional aggregation (DA) technique that facilitates the numerically efficient evaluation of the field produced by a given current distribution. The proposed algorithm improves the one proposed by the second author (A. Brandt, *Comp. Phys. Comm.* 65, 24-38, 1991) This work extends our previous study of planar (O. Livne, A. Brandt, A. Boag, *Microwave Optical Technology Lett.,* 32, 454-458, 2002) and quasi-planar scatterers (O. Livne, A. Brandt, A. Boag, *URSI Radio Science Meeting*, San Antonio, TX, June 2002.). In the DA scheme, at each level one distinguishes several "propagation directions", and performs a separate aggregation (anterpolation) process per each such direction. The field produced by each aggregated domain of that process is intended to be calculated only on a specific *sector* of the radial grid emanating from that domain, namely, only in directions around the specific propagation direction. The number of propagation directions increases with the level, typically doubled upon each coarsening step in 2D problems. The aggregation is *anisotropic*: typically the mesh size of the source grid is *quadrupled* in the propagation direction while only being *doubled* in the perpendicular direction(s). This exploits the fact that the bandwidths of the field produced in that specific sector are not affected by this more aggressive coarsening in the propagation direction. As a result, upon each coarsening step the total number of domains decreases faster than the increase in the number of points in the grid sector associated with each of them. Hence, the asymptotic complexity attained by the DA scheme is $O(N)$ for volumetric scatterers and $O(N\log N)$ for surface ones, both similar to the FMM.

A Fast Integral Equation Method with Fast Fourier Transform for Solving PEC Scattering Problems

Seung Mo Seo[*] and Jin-Fa Lee
ElectroScience Lab., Dept. of Electrical Engineering
The Ohio State University
sms@esl.eng.ohio-state.edu

Method of moment has been very popular in solving electromagnetic wave scattering from three-dimensional conducting objects. Recent advancements of FMM (J. M. Song and W. C. Chew, *Mico. Opt. Tech. Lett.*, pp 14-19, 1995) have made significant inroads toward solving realistic large-size problems. However, the strength and can be also argued as the weakness of FMM is its strong dependence on the fundamental solution, or the Green's function.

In recent years, there are a few developments focused on fast integral methods that are less integral kernel dependent. Among them, we mention IE^3 (S. Kapur and J. Zhao, *MTT-39*, pp. 141-146, 1997), IE-QR (Seung Mo Seo and Jin-Fa Lee, *IEEE Trans. Antennas Propagat.*, to be published), ACA (M. Bebendorf, *Numer. Math.*, pp. 565-589, 2000), and H^2 matrix (Wolfgang Hackbusch, steffen Borm, *Applied Numerical mathetatics*, pp. 129-143, 2002) algorithms. However, all these methods, when combined with multi-level implementations can achieve $O(N\log N)$ complexity for static or low frequency electromagnetic problems. Once these methods are applied to solve electrically large EM scatterings, the complexity achieved only approximately $O(N^{1.5})$.

This paper presents an algorithm, IE-FFT that is some what a compromise between FMM and kernel independent. The multi-level IE-FFT algorithm proposed here works for any Green's function, which exhibits Toeplitz property. Thus, the same algorithm or codes can be easily used for both low (Laplace) and high (Helmholtz) frequency applications. The memory requirement of the algorithm is shown to be of order $O(N)$, though, in the worst case scenario it could be $O(N\log N)$. Whereas, the CPU time complexity is roughly $O(N\log N)$, and at worst can be $O(N(\log N)^2)$.

Singularity Subtraction Technique For High Order Vectorial Basis Functions On Planar Triangles

Seppo Järvenpää* and Matti Taskinen

Electromagnetics Laboratory, Helsinki University of Technology
P.O. Box 3000, FIN–02015 HUT, Finland

Solving boundary integral equations numerically with the method of moments requires computation of integrals that may have singular integrands. One possibility is to use singularity cancellation methods such as Duffy's method or polar transformation, but unfortunately they can produce inaccurate results. Also computation of the so called near-singular integrals suffer from numerical cancellation.

Another method that can be applied in the case of flat triangular elements and linear basis functions such as RWG functions is the singularity subtraction technique. The idea is to remove suitable terms from the integrand. These terms are chosen so that they exhibit the same asymptotic behavior at the singularity point as the integrand, thus leading to a sufficiently smooth new integrand that can be evaluated with standard numerical quadratures. The removed terms are then integrated analytically and added to the result.

This method allows accurate computation of the near-singular integrals and cases where the kernel is the derivative of the Green's function can be easily taken care of. The method has been recently extended to polynomial basis functions of arbitrary order [S. Järvenpää, M. Taskinen, P. Ylä-Oijala, Int. J. Numer. Meth. Engng, **58**, 1149–1165, 2003].

In this talk we present a new set of formulas that lead to much simplified implementation. These new formulas are derived by presenting arbitrary order nodal basis function as a polynomial function of linear shape functions. We address the problem of how to compute the system matrix elements when high order RWG basis functions are used. We demonstrate the effectiveness of the presented formulas in terms of computation time versus the accuracy of the obtained matrix elements with different kernels.

Including Linear Phase Propagation Terms in the RWG Basis Functions for the Analysis of Large Structures with the Method of Moments

*J. M. Taboada[1], F. Obelleiro[2], J. L. Rodríguez[2] and I. García-Tuñón[2]

[1]Universidad de Extremadura, Departamento de Informática, Escuela Politécnica de Cáceres, 10071 Cáceres, Spain, e-mail: tabo@unex.es
[2]Universidad de Vigo, Departamento de Teoría de la Señal y Comunicaciones, ETSI Telecomunicación, 36200 Vigo, Spain

The Method of Moments (MoM) is the most widely used technique for solving electromagnetic scattering and radiation problems. In the case of arbitrary three-dimensional (3D) configurations, most MoM approaches are based on the electric field integral equation (EFIE), using the triangular-type "rooftop" vector basis functions introduced by Rao, Wilton and Glisson (RWG) for modeling the surface current density. The use of the EFIE allows to deal with both open and closed surfaces, while the RWG functions ensures the surface current density continuity over adjacent triangles, which is specially important for the accuracy of the solution when dealing with the EFIE.

The main drawback of the conventional MoM formulation is the exorbitant dependence on computer storage and solution time for electrically large electromagnetic scattering problems. To overcome this limitation, in this work, we have incorporated a linear phase (LP) propagation term into the RWG basis functions. Special procedures have been developed in order to include these LP-RWG (linearly phased RWG) basis functions in an EFIE-MoM formulation, including a new analytical treatment of the singularities due to the presence of the free-space Green function in the integrals.

The phasefront characteristics of the surface currents can be numerically extracted from approximated solutions. In this work, as a first approach, it has been directly obtained from the high-frequency physical optics (PO) currents, although more rigorous solutions could be used. So, in (K. Do-Hoon, R. J. Burkholder and P. H. Pathak, IEEE TAP, 49, 583-591, 2001), the Fourier spectrum of a lower-frequency MoM solution (obtained for the same problem) is used to provide the phasefront parameters.

The new MoM with LP-RWG basis functions has shown to greatly relieve the storage and solution time of the conventional MoM (with RWG basis) while accurately reproducing the induced surface currents and scattered fields of some chosen targets.

199

A High-Order Integral Equation Method for Non-Smooth Objects

Jianguo Liu* and Qing H. Liu
Electrical and Computer Engineering, Duke University
Durham, North Carolina 27708
Email: jliu@ee.duke.edu, qhliu@ee.duke.edu

Surface integral equations are widely used in computational electromagnetics. Traditional method of solution is based on the method of moments (MoM), and more recently, the fast multipole method for the acceleration of the iterative solution. Most published results use zeroth and first order basis functions, although more recently some higher order (up to third order) accurate results have been shown.

Recently, the integral equations for electromagnetic scattering from objects with smooth boundaries have been solved efficiently with a spectral integral method (J. Liu and Q. H. Liu, "A Spectral Integral Method for Periodic and Nonperiodic Structures," *IEEE Microwave and Wireless Components Letters*, in press). It has been shown that for smooth objects, we can obtain exponentially accurate results by solving the integral equation with fast Fourier transform (FFT). However, such a method assumes that the objects are smooth. For objects with corner singularities , it is still a challenge to obtain high-order results in computational electromagnetics.

In this work, we propose to develop an integral equation method in 2D to achieve higher-order accuracy in the calculation of the current and scattered fields from non-smooth objects with corner singularities. First, similar to the method used for smooth objects, the "singularity subtraction" method is used to deal with the singularities in the integral equation. Then, Nyström method is used to convert the integral equation into a matrix equation, which is then solved iteratively. Appropriate Gaussian quadrature schemes are chosen according to the different corner singularities. To obtain high accuracy in evaluating the matrix, especially for the values on the main diagonal, a high-order "quadrature" for the evaluation of hypersingular and logarithmically singular integrals , known as the "local correction", is applied. We show that the "local correction" is easy to extend to 3D integral equations. Examples will be shown to illustrate the high-order accuracy of the scattering solution from non-smooth objects.

Analysis of scattering from dielectric bodies using the single integral equation and the Nyström method

*C. Lu, J. Yuan and B. Shanker

2120 Engineering Building, Dept. ECE, Michigan State University,
East Lansing, MI 48824, USA, {luchuan,yuanjun,bshanker}@egr.msu.edu

Methods for analyzing scattering from dielectric bodies have largely relied on either the PMCHWT or the Müller formulations. These formulations involve both electric and magnetic equivalent currents. Alternatively, it has been shown that scattering from a dielectric body can be computed using a single unknown; combined source formulations that guarantee uniqueness of solutions have also been derived. This formulation has seen a resurgence in the recent past in terms of implementation (M. S. Yeung, *IEEE Transactions on Antennas and Propagation*, **47**, 1615-1622, 1999; M. Y. Xia, C. H. Chan, S. Q. Li, B. Zhang, and L. Tsang, *IEEE Transactions on Antennas and Propagation*, **51**, 1142-1149, 2003).

The method presented to reduce the integral equation to a matrix equation in the papers cited earlier proceeds as follows: (i) currents are expressed using RWG basis function, and (ii) line testing is used to reduce the resulting set to a matrix equation. Both authors use a single equivalent source, and do get unique solutions as the geometries that they analyze do not support resonant modes. Likewise, both report that the condition number of the impedance matrix is excellent. However, line testing leads to large errors. To overcome this deficiency, we have implemented the Nyström method together with local correction. This will guarantee higher order accuracy as well as better geometric representation of the scatterer. Also, to avoid problems with internal resonances, we have implemented the formulation proposed by Mautz (J. R. Mautz, *IEEE Transactions on Antennas and Propagation*, **37**, 1070-1071, 1989). Finally, to aid in the solution to scattering from electrically large problems, this scheme will be augmented with the Fast Multipole Method. As is evident, incorporation of the latter calls for two tree's with different sets of interaction lists (as the wavenumber in the two media are different). Details of the method and numerical results that demonstrate its efficiency will be presented.

Surface Integral Equation Formulation for the Electromagnetic Analysis of Composite Metallic and Dielectric Structures

Pasi Ylä-Oijala, Matti Taskinen and Jukka Sarvas*
Electromagnetics Laboratory, Helsinki University of Technology
P.O. Box 3000, FIN–02015 HUT, Finland

The composite objects made of conducting and piecewise homogeneous dielectric material have important applications e.g. in radar, antenna and microwave technology. The method of moments is a popular numerical methods for the analysis of such composite structures. By using the surface equivalence principle the fields inside each homogeneous subdomain can be expressed in terms of an incident field and the equivalent electric and magnetic surface currents. Different types of surface integral equations can be obtained by enforcing the boundary conditions on the interfaces and by combining the integral equations so that the interior resonance problem can be avoided. A popular formulation is the EFIE-PMCHWT formulation, i.e., the electric field integral equation (EFIE) on the metallic surfaces and the PMCHWT formulation on the dielectric surfaces. The system of surface integral equations is converted into a matrix equation via Galerkin's method. This traditional approach is well documented for problems with single and isolated objects with no junctions. In the composite multi-material case with junctions the treatment becomes more complicated. This is the so called junction problem how the basis functions for the surface currents should be chosen and how the testing of the combined equations should be performed. Kolundzija (IEEE Trans. Antennas and Propagation, vol. 47, no. 7, pp. 1021-1032) has treated this problem by introducing special junction basis functions, called multiplets. Chew et al ('Fast and Efficient Algorithms in Comp. Electromag.', Artech House, Boston, 2001) treat the problem with the number of unknowns reduction (NOUR) scheme. In these and other traditional approaches the testing procedure at the junctions remains problematic.

In this talk a novel approach based on the surface integral equation method with the Rao-Wilton-Glisson (RWG) basis functions and Galerkin testing is presented for the electromagnetic analysis of composite metallic and dielectric structures. The developed method simplifies the formulation of complex composite problems, the treatment of the surface currents and the testing procedure at the junctions. Our main idea is to separate the testing from the enforcing of the boundary conditions and the integral equation formulation. The usual Galerkin discretization and testing is first carried out individually in each domain and, thereafter, the boundary conditions and the integral equation formulation (EFIE-PMCHWT) are enforced to the discretized equations. These two steps can be condensed into a few simple bookkeeping rules by which the final impedance matrix of a composite problem can be directly assembled. A great benefit of our method is that it avoids the aforementioned problems at the junctions because no special junction basis functions or testing procedure at junctions are needed. Our formulation is general and can be extended to other basis functions and integral equation formulations. The developed method is verified by numerical examples.

Mixed Mesh Approach for the Discretization of Hybrid Surface and Volume Integral Equations of EM Scattering

Z.Y. Zeng[*1], C. C. Lu[2] and C. Yu[3]

Department of Electrical and Computer Engineering
University of Kentucky
453 Anderson Hall
[1]zzeng2@uky.edu, [2]cclu@engr.uky.edu, [3]cyu@engr.uky.edu

The hybrid surface and volume integral equation approach is an attractive method to solve electromagnetic scattering and radiation problems involving conducting and/or dielectric objects. However, one of the difficulties in this approach is how to effectively model a complex structure. It is generally accepted that triangle shaped meshes are more flexible than quadrangle shaped meshes. If triangle meshes are used to model a surface, then tetrahedron should be used to model the volume part (for coating material) that is in contact with the surface, leading to very low mesh efficiency compared to quadrangle/hexahedron meshes. To overcome this efficiency/flexibility conflicting problem, mixed mesh elements are used to discretize the objects. Triangular or quadrangular patches are used to model three-dimensional complex surfaces. Tetrahedral, triangle-based prismatic or hexahedral cells are used to model complex dielectric volumes. It is true that quadrangle/hexahedron mesh pair maintains the minimal number of unknowns to discretize the objects in the above mesh types. But for sharp shapes, the object can be modeled more accurately and more efficiently by triangular-based meshes, such as triangle/tetrahedron, or triangle/prism meshes, compared to quadrangle/ hexahedron meshes. Thus, applying the mixed mesh elements to discretize a complex scatterer, we can model the object more accurately and flexibly and still maintain the minimal number of unknowns. Quadrangle-based pyramidal elements must be used for the transition between different volume cells such as tetrahedron to prism, and tetrahedron to hexahedron. As a result, we developed a discretization scheme to employ these different types of elements to model complex surface and volume scatters.

On the other hand, for thin, long conducting objects, such as thin wire antennas, thin wire model is more efficient to model the objects rather than triangular or quadrangular meshes. Special basis function is developed to treat the junction of thin wire model objects and conducting surfaces meshed with triangular patches.

Numerical results will be shown in the presentation to demonstrate the validity and the application of the mixed elements discretization scheme for solving the hybrid integral equations.

An Integral Equation Formulation for Electromagnetic Scattering from 3D Bodies with Anisotropic Surface Impedance Boundary Conditions

A. Pujols *, M. Sesques
CEA/CESTA, France

Electromagnetic scattering from arbitrary shaped bodies composed of both perfectly electric conducting structures and dielectric materials can be solved efficiently by boundary integral formulation provided that dielectric objects are homogeneous (or piecewise homogeneous) and isotropic. When the dielectric coatings are anisotropic materials, Green's functions can not be determined in general. However, under restrictions on material properties or coating thickness, the effect of a material coating can be taking into account by an impedance boundary condition. For anisotropic medium, an impedance tensor must be employed.

A crucial point to solve the Maxwell's problem with the impedance boundary condition is the choice of the variational formulation. The one we used is obtained by a combination of the Electric Field Integral Equation and the Magnetic Field Integral Equation using the Rumsey's reaction, leaving implicit the impedance relationship. Therefore the unknowns are both the electric and magnetic currents. Then the final linear system is twice bigger than the one for the perfect conductor case. Nevertheless, this formulation has very attractive features: it is shown to be well-posed at all frequencies and very accurate. In particular, for axisymmetric scatterer, the well-known Weston's theorem is verified with very great accuracy (for example, near -100 dB for a cone). Moreover the impedance tensor only appears in single integral terms. Thus there is no difficulty to consider variable anisotropic surface impedance. The main point is to compute impedance tensor and its inverse with respect to the axes of the chosen finite element basis.

A computer code, named Arlene, including this impedance formulation has been developed at the French Atomic Energy Agency. Arlene is based on a classical finite element approximation of surface integral equations such as EFIE and CFIE. All the interfaces between materials are meshed by planar triangles and unknown electric and magnetic currents are expanded using first order basis functions given in (Rao-Wilton-Glisson, IEEE TAP, 27, 1979). This code can compute electromagnetic scattering for three-dimensional complex structures which are composed of combinations of perfectly conducting bodies (thin wires, thin metallic plates, thick bodies) and dielectric media. All connections between wires, patches and thick conducting bodies are possible. A wire object can even penetrate an interface between two dielectric layers. Discrete symmetries of the geometry can also be used to reduce the computation time and memory. The Arlene code has been running on a parallel Terascale machine composed of 2640 processors.

The impedance formulation of Arlene code has been validated on many test cases for isotropic tensor impedance. For anisotropic tensor, we present comparisons with other formulations (integral one or hybrid Partial Differential Equations with Integral Equations).

A Hybrid Muller and VIE formulation for the Calculation of EM Scattering from Objects with Electric and Magnetic Material

Chong Luo, Caicheng Lu and Chun Yu

Department of Electrical and Computer Engineering
University of Kentucky
453 Anderson Hall
Lexington, KY 40506
cluo0@engr.uky.edu

Hybrid Volume Surface Integral Equation (VSIE) is a formulation that possesses the advantage of both Volume Integral Equation (VIE) and Surface Integral Equation (SIE).. In this presentation, we will present the implementation of the hybrid Muller's formulation and VIE formulation. The advantage of this hybridization is that large homogeneous material region is more efficiently modeled by the Muller's formulation. Small and inhomogeneous material regions are more effectively modeled by VIE formulation.

When Surface Integral Equation (SIE) is used to solve the problem of scattering by dielectric material, integral equations should be constructed for the exterior equivalent problem as well as for the interior equivalent problem. For the exterior problem we have

$$ik_1\eta_1\overline{L}_1 \cdot \vec{J} - \overline{K}_1 \cdot \vec{M} + \vec{E}^{inc} = -\vec{M} \tag{1}$$

In the above, L and K are integral operators. For the Interior problem the integral equation is given as

$$-ik_2\eta_2\overline{L}_2 \cdot \vec{J} + \overline{K}_2 \cdot \vec{M} = \vec{M} \tag{2}$$

These two equations are non-independent of each other, they must be combined to find unique solution. There're many ways to combine these two equations. Consequently, there are different formulations based on the different ways in which these equations are combined. By adding (1) to (2), we have the PMCHWT formulation, which is a first kind integral equation. By subtracting (2) from (1), we have the Muller's formulation. The Muller's formulation is a second kind integral equation. Based on this fact, the Muller's formulation is expected to have smoother operator than PMCHWT formulation. As a result, hybrid Muller and VIE formulation is expected to have smoother operator than the combination of PMCHWT and VIE. In this work, we combined the Muller's formulation and the VIE formulation to solve the problem of scattering by three-dimensional material scatterer. In our formulation, the large, homogeneous material scatterer will be modeled using Muller's formulation; VIE formulation will be used for the small inhomogeneous part. Our formulation uses quadrilateral mesh for the surface modeling and hexahedron mesh for the volume modeling. Validation numerical results will be presented in presentation.

Applications of Complex Coordinates to the MLFMA

F. Olyslager*, J. De Zaeytijd, K. Cools, I. Bogaert, L. Meert, D. van de Ginste and
D. Pissoort
Department of Information Technology (INTEC), Ghent University
St.-Pietersnieuwstraat 41, B-9000 Gent, Belgium
E-mail: frank.olyslager@intec.Ugent.be

Perfectly matched layers, as invented by Bérenger, have shown their extreme valuableness during the past decennium for FDTD and FEM problems. It was shown by Chew, Jin and Michielssen that in frequency domain a PML can be regarded as an isotropic medium with complex thickness. This fact has been exploited by us to introduce the complex-coordinate formalism in semi-analytical and integral equation problems in frequency domain. It has yielded new series expansions for Green functions of layered media (F. Olyslager, Discretisation of Continuous Spectra Based on PMLs, Accepted for SIAP) or has been used to study waveguide discontinuities.

The new series expansion of the Green functions have been shown to be very useful as a combination with the MLFMA technique (D. Vande Ginste, et. al., "A Fast Multipole Multilevel Technique for Layered Media Based on the Application of PMLs – the 2D Case," Accepted for IEEE Trans. on Ant. Propagat.) leading to an $O(N)$ algorithm in 2D. For each of the terms in the series a separate translation matrix is defined. The use of complex coordinates has also shown to be a valuable tool to terminate infinite electromagnetic crystals by continuing a few periods of the crystal in the complex plane (D. Pissoort and F. Olyslager, "Termination of Periodic Waveguides by PMLs in Time-Harmonic Integral Equation Like Techniques," Accepted for IEEE AWPL).

In the present contribution we consider two other problems where we combined MLFMA with complex coordinates. First we consider a 2D TM or TE structure that consists of a number of isotropic regions embedded in an homogeneous isotropic background. The structure typically is a passive optical structure that is excited by one or more waveguides (slabwaveguides in the 2D case). We model the excitation of this structure by an eigenmode in one of the waveguides by using a boundary integral equation combined with MLFMA. To represent the infinite waveguides we terminate them abruptly after continuing them smoothly in complex space. This means that in the MLFMA some of the regions are located along lines in complex space.

Second we consider a typical homogenisation problem consisting of a large number of metal wires embedded in a host medium. This could constitute a metamaterial. The scattering problem is solved with a 3D MPIE combined with a low-frequency MLFMA (W.C. Chew et. al., Fast and Efficient Algorithms in Computational Electromagnetics, Artech House, 2001). From the results of the scattering problem the effective material parameters are estimated. To mimic the infinite extend of the medium we propose again to continue the medium at a certain distance in complex space before terminating it abrubtly. Hence, again the MLFMA algorithm is extended to complex space.

Subject: B7

Mixed Volume and Surface PEEC Modeling

Albert Ruehli[1], Dipanjan Gope[*1,2], and Vikram Jandhyala[2]

1 IBM Research, T.J. Watson Research Center, Yorktown Heights, NY 10598
2 Department of Electrical Engineering, University of Washington, Seattle WA 98195.
Email: ruehli@us.ibm.com, {dip,jandhyala}@ee.washington.edu

The Partial Element Equivalent Circuit (PEEC) formulation is an integral equation based approach for the solution of combined circuit and electromagnetic (EM) problems. With the increase in operating frequencies, the combined circuit-EM solution is necessary to accurately predict the electrical performance of a wide range of electronic equipment from mobile products to computer systems. Owing to the complexity and the variable nature of the test structures, the modeling scheme for these problems require extreme flexibility. In the same solution process, volumetric formulations are suitable for certain structures while surface based schemes are more efficient for others. In the presented approach, the solution of the electromagnetic part is transformed as much as possible into the circuit domain so that general well known circuit solver techniques can be applied. We are interested in both time and frequency domain analyses similar to a Spice type circuit solver.

The modeling of the skin effect and current re-distribution, is an example of one of the problems which requires a flexible solution approach. This is the case especially for solutions in the time domain where the current is re-distributed from a *DC* solution for the steady state to a high frequency surface type solution for rapidly changing transients. The existing PEEC formulation (Ruehli *et. al*. IEEE Trans. Elec. Comp. 45(2): 167-176, May 2003) includes an inherent Volume FIlament(VFI) skin effect model where the conductors are subdivided into cells. This volume model has proven to be very efficient for on chip problems where the skin depth is not extremely small in comparison to the conductor dimensions. This is in contrast to some high frequency problems, where the skin depth is very small in comparison to the conductor thickness. Surface approaches (Yang *et. al*. IEEE EPEP 12: 371-373 Oct. 2003) are more efficient for the solution of these problems in terms of the number of unknowns generated.

Recently, the PEEC method has been implemented as a surface formulation (Rong *et. al*. IEEE EPEP 12 367-370 Oct. 2003). In this paper a volume-surface integral equation solution scheme is presented. The surface formulation is based on the combined field integral equations (CFIE) which are transformed into a PEEC circuit representation using two sub-circuits which are connected by mutual coupling. The first sub-circuit represents the electric field with electric surface current density $\mathbf{J}^s$ and potential ϕ^e unknowns. The second circuit represents the the magnetic field where the corresponding unknowns are magnetic current density $\mathbf{M}^s$ and magnetic scalar potential ϕ^m. The surface formulation is coupled with the usual PEEC volume scheme which also has ϕ^e and the volume current densities $\mathbf{J}^v$ as unknowns. The proper couplings between the surface and the volume unknowns are included. Mathematical derivations for individual circuit elements will be given in the presentation. Validation examples and the time and memory efficiency results for the combined volume-surface formulation will also be presented.

Nanotechnology and Electromagnetics Research at NSF
Vasundara V. Varadan
Division Director – Electrical & Communications Systems Division
National Science Foundation, Arlington, VA 22230

Research in nanoscience and nanotechnology has proliferated in the last decade thanks to the large infusion of funding from the government and the industrial sector. All developed and developing nations have invested vast amounts to assure themselves a prominent place in the 'nano economy' of the 21st century. One of the greatest impacts of nanotechnology has been the crumbling of the disciplinary walls between physics, chemistry and biology. Indeed, biology has now become the fourth pillar that defines engineering, the others being physics, chemistry and mathematics. Until recently, research was largely curiosity driven, with every researcher describing different parts of the 'nano elephant'. This has resulted in a number of papers to design, fabricate and characterize nanotransistors, nanoparticles, nanotubes and nanowires. In the coming decade, the research must evolve from empirical research to one involving modeling, numerical simulation and integration of nanocomponents into functional engineering systems. Even as CMOS technology was speeding up electronic circuits to GHZ frequencies and correspondingly small wavelengths, nanoelectronics will further shrink size and wavelength. Lumped parameter models used to describe electronic circuits will no longer be applicable. New models and algorithms must be developed to model electromagnetics of engineered nanosystems and multiscale nano, micro, macro systems not only for research purposes but very soon industry will be demanding design tools such as PSPICE and that work in the nano regime. This is a challenge and an opportunity.

The purpose of this talk is to discuss the above issues and to outline the investments that the National Science Foundation has made in the Nano Science and Engineering Initiative (NSE) and specific programs within the Electrical and Communications Systems Division related to design, modeling and characterization of nano devices and components integrated into NEMS, nanoelectronic chips, nano-bio systems. The behavior of electric and magnetic fields in such devices and systems is integral to this research.

208

Plasmonic Nanophotonics

Vladimir M. Shalaev
School of Electrical and Computer Engineering, Purdue University
West Lafayette, IN 47907

Metal nanostructured materials can open new avenues for manipulating light on the nanoscale and sensing molecules. We study specially designed plasmonic structures that act as "smart" optical nano-antennas focusing light on nanometer scale areas, with high spatial and spectral control of the energy concentration. These nano-antennas are capable of strong enhancing a number of optical phenomena, such as the extraordinary optical transmittance, Raman scattering, nonlinear photoluminescence, Kerr optical nonlinearity, and many other important optical effects. We show that plasmonic nanoantennas open up the feasibility to detect molecules with unsurpassed sensitivity and perform lithography with nanometer spatial resolution. Plasmonic nanostructures can be employed for developing photonic nano-circuits where photons are controlled in a similar manner as electrons in conventional electronic circuits. They can also be employed for developing novel left-handed materials with negative refraction index in the optical spectral range that can revolutionize the current photonics.

Strong Quadrupole Scattering from
Ultra Small Metamaterial Spherical Nano-Shells

Andrea Alù[1], and Nader Engheta[2,*]

[1]*Università di Roma Tre*
Department of Applied Electronics, Rome, Italy
alu@uniroma3.it, http://www.dea.uniroma3.it/lema/people/andrea_alù.htm

[2]*University of Pennsylvania*
Department of Electrical and Systems Engineering
Philadelphia, Pennsylvania 19104, U.S.A.
engheta@ee.upenn.edu, http://www.ee.upenn.edu/~engheta/

Properties of metamaterials with negative effective real permittivity and/or permeability has recently attracted the attention of many research groups worldwide, and various interesting potential applications for such materials in the microwave regime (for the left-handed media) and in the optical regime (for the plasmonic nanophotonic materials) have been speculated. One of these features is the resonant high scattering amplitudes for subwavelength tiny spheres and cylinders and nano-wires and nano-wires containing metamaterials with negative constitutive parameters, as already studied theoretically in some of our earlier works (A. Alù, and N. Engheta, Proceedings of the ICEAA'03 Meeting, Torino, Italy, Sept. 8-12, pp. 435-438). We showed that in a concentric two-shell scatterer with epsilon-negative (ENG) and mu-negative (MNG) or double-negative (DNG) and double-positive (DPS) combinations, total scattering amplitudes may be enhanced for a specific *ratio* of the shell radii, regardless of the total size of the particle. This effect, which is similar to the plasmonic resonance for nanoparticles made of noble metals, was explained by the presence of an intrinsic resonance at the interface between the two "conjugate" shells.

The high scattering amplitude from the spherical nano-shells described above was for the dipolar term, and as is well known, as the size of the sphere increases, higher order multipoles begin to contribute more. However, in our analytical study of scattering from these nano-shells we have found that for the two-shell spheres with a combination of ENG, MNG, DPS, and or DNG materials, with a different ratio of radii for these shells one can obtain strong resonant scattering amplitude for a higher-order multipole (e.g., quadrupole or octopole) while the lower-order and the rest of the higher-order multipoles remain weak and the electrical size of the object can still be kept very small. Therefore, in principle, an ultra small nano-shell made of a combination of ENG, MNG, DNG, and/or DPS materials can scatter a quadrupolar or octopolar fields, if the ratio of the radii is chosen judiciously. It is interesting to notice that electrically small scatterers conventionally re-radiate like small dipoles, since the phase retardation within them is negligible. However, our ultra tiny two-shell spheres may scatter like a quadrupole. This may offer interesting potential applications for possibility of optical nano-transmission lines made of arrays of these nano-shells for transport of optical energy below diffraction limits and as nano-antennas with quadrupole and higher-order multipoles radiation patterns.

Experimental Subtleties of Negative Refraction in Metamaterials

David R. Smith*[1], Anthony F. Starr[2], Jack J. Mock[1] and Patrick Rye[2]
[1]Department of Physics, University of California, San Diego
[2]Department of Mechanical and Aerospace Engineering, University of California, San Diego

The material property of negative refractive index is readily probed by performing a Snell's law refraction experiment on a wedge composed of material whose refractive index is negative. In a typical experiment, a microwave beam is incident normally onto the first interface of the wedge sample, propagates through the sample, and is refracted into air at the second interface. A measurement of the angle of deflection of the beam at some radius from the sample allows the determination of the sample's refractive index.

In principle, the Snell's law experiment is straightforward to perform. However, as there are no naturally occurring negative index materials, the samples that have been measured to date have been artificially structured *metamaterials*, based on periodically arranged conducting scattering elements. For these recently demonstrated samples, designed to operate at or near X-band frequencies (8-15 GHz), the repeated cell dimension has been approximately one-sixth to one-tenth that of the free space wavelength (R. Shelby, D. R. Smith and S. Schultz, *Science* **292**, 77, 2001; A. A. Houck, J. B. Brock and I. L. Chuang, *Phys. Rev. Lett.* **90**, 137401, 2003). Moreover, in some cases the materials have been anisotropic (C. G. Parazzoli, R. B. Greegor, K. Li, B. E. C. Koltenbah and M. Tanielian, *Phys. Rev. Lett.* **90**, 107401, 2003).

The material—or metamaterial—aspects of negative index media make the conceptually simple Snell's law experiment more complicated. The finite unit cell size, for example, can lead to conditions where both refracted and diffracted transmitted beams are observed. Anisotropic samples that are not isotropically negative index must be implemented carefully; such samples can exhibit excess internal reflection and also produce multiple beams. We will discuss the subtleties of negative refraction experiments on metamaterial samples, providing numerical and experimental examples of different scenarios. Through this analysis, some of the apparently inconsistent data that has been presented in the literature can be explained.

FDTD MODELING OF GAUSSIAN BEAM INTERACTIONS WITH NANO-STRUCTURES FOR OPTICAL APPLICATIONS

Richard W. Ziolkowski*

Department of Electrical and Computer Engineering, University of Arizona, Tucson, Arizona, USA, ziolkows@ece.arizona.edu

With the current excitement associated with nanotechnology, the need for accurate modeling of the interactions of electromagnetic waves with nano-structures has increased dramatically. The nanotechnology area holds much promise for the realization of ultra-small and ultra-fast devices with a variety of interesting applications. The optical sector is an immediate beneficiary of nanotechnologies because of the wavelengths associated with optical devices. For instance, a wavelength of 1.5 μm represents a well-known optical communications value. If one wants to structure a material or an environment to modify the behavior of the propagation of light, for instance with a photonic bandgap (PBG) structure, one needs to arrange features with spacings between them that are less than half that wavelength in size, or 750 nm, and to create the features themselves, which are even smaller yet. Visible wavelengths require yet smaller sizes. Realization of PBG structures for these wavelengths clearly requires nanotechnology fabrication processes.

We have been studying analytically and with the finite difference time domain (FDTD) approach, the scattering of Gaussian beams from sets of nano-cylinders and spheres. We selected the FDTD approach because of its versatility in the choices and configurations of materials and structures that can modeled. This versatility makes it an excellent candidate for studying the behavior of these ultra-small systems. However, it is noted that for even for 500 nm wavelength light, a 50 nm radius scatterer is $\lambda/5$ in size. Thus, the FDTD problem sizes can be quite large even for simple problems with a small number of scatterers if high resolution results, e.g., $\lambda/100$, are desired.

The use of the nano-structures in our studies has been targeted mainly to optical memory storage applications. It has been found that by properly taking into account the actual material characteristics at optical frequencies and by properly designing the nano-structures to take advantage of plasmon effects, one can achieve enhanced scattering and, hence, distinguishability between scattering states. These results have also stimulated the potential use of these nano-scatterers as inclusions for metamaterial applications. Furthermore, relying on back-door coupling phenomenology investigations of canonical aperture coupling problems that have shown resonant coupling even for extremely small apertures, several corresponding nano-structure configurations have been examined and have led to additional enhancements for the data storage and metamaterial applications. Typical sizes of the scatterers under consideration have been in the 30-50 nm range.

We will review several of the basic nanotechnology scattering problems that we have been modeling. Samples of these FDTD simulation results will be presented. Their potential data storage and metamaterial applications will also be discussed.

Investigation of Effective Medium Theories for Micro- and Nano-scale Electromagnetic Metamaterials

N. Wongkasem* and A. Akyurtlu
Department of Electrical and Computer Engineering, University of Massachusetts
Lowell, MA 01854

Recently, there is an increasing effort to understand and model the effects of double negative (DNG) materials which simultaneously have negative permittivity and permeability within the same frequency region, and possess unique properties, such as reversal of the Doppler Effect and Snell's Law (R. W. Ziolkowski, *IEEE Transactions on Antennas and Propagat*ion, vol. 51, pp. 1516-1529, 2003). These materials have promising applications in nanoantennas, polarizers, filters, phase shifters, selective lenses, waveguides, to name a few. Modeling efforts of these metamaterials have been effective yet many questions still remain to be answered, including the accurate representation of the bulk material parameters of such materials and extraction methods of these parameters from measurements. Consequently, it is important to study electromagnetic wave interactions with metamaterials, composed of micro- and nano-scale inclusions and develop effective medium theories (EMTs) which not only provide essential insight into the physics but also help to establish more efficient computational techniques and validation for extracted material parameters.

In this paper, three-dimensional finite-difference time-domain (FDTD) analysis of the electromagnetic wave interactions with metamaterials is conducted to establish accurate effective medium models for composite materials with inclusions of varying sizes, down to the nano-scale. The FDTD model is composed of an infinite periodic array of inclusions (which can include wires, omega structures, split-ring resonators, etc.) embedded within a dielectric slab located inside a waveguide. Perfect electric conductor (PEC) walls and perfect magnetic conductor (PMC) walls located in the transverse direction and in the direction of periodicity, respectively, form the boundary conditions of the model. A Gaussian beam, normally propagating through the slab is used as the source of excitation, at the two input ports. Furthermore, an FDTD/Prony method is applied to analyze the periodic structure to reduce the computational time required to produce accurate results (J.A. Pereda, L.A. Vielva, and A. Prieto, *IEEE Microwave and Guided Wave Letters*, vol. 2, pp. 431-433, 1992). The results will be validated via the analytical solutions for reflection and transmission coefficients for plane wave scattering at normal incidence.

The FDTD results for the transmission/reflection coefficients will be used to determine the magnetodielectric properties of the composite material, which will then be compared with results of the effective medium theories. A range of FDTD simulations with various randomly positioned micro- and then nano-scale inclusions will be conducted to obtain a comprehensive understanding of the average characteristics of the composite materials. Comparative analysis of the effective permittivity and permeability for different metamaterial geometries of micro- and nano- composites from reflection and transmission coefficients will be presented. The effects of decreasing the scale of the modeled structures on the accuracy of EMTs will be studied and EMTs which more accurately represent the material properties of the composites, at these scales, will be investigated.

COMPARISON BETWEEN A FOURIER-HARMONIC AND A MODAL EXPANSION OF THE ELECTROMAGNETIC FIELDS IN COMPLEX MEDIA WITH IRREGULAR BOUNDARIES

Ezekiel Bahar* and Paul Crittenden
University of Nebraska-Lincoln

Starting with a Fourier-Harmonic expansion of electromagnetic fields in stratified chiral media, a modal expansion associated with branch cut integrals and residues at pole singularities are derived. These modal expansion permit the imposition of exact boundary conditions at irregular interfaces. Thus those complete modal field expansions can be used to determine the electromagnetic fields scattered at rough interfaces between two chiral materials with laterally varying electromagnetic properties. The complete field expansions together with exact boundary conditions are substituted into Maxwell's equations to obtain the generalized telegraphists' equations for irregular chiral media. The telegraphists' equation are a set of coupled ordinary differential equations for the forward and backward wave amplitudes of the transverse components of the magnetic field and the electric field. The solution to these equations can be used to find the electromagnetic fields above and below the interface. This has direct applications to the detection and characterization of chiral materials, the discrimination between different chiral media and the optimization of desired electromagnetic characteristic of artificial materials with significantly enhanced chirality.

Similar sets of equations were derived by Schelkunoff using a rigorous full wave method of mode matching in irregular archiral waveguides. Unlike the discrete waveguide mode spectra, the spatial wave spectra in this work are both continuous and discrete. The discrete part of the spectra is associated with surface waves and the four pairs of branch cuts (continuous spectra) are associated with lateral waves that creep just above or below the interface. The physical interpretation of the results, based on the modal expansions, is critical in determining the location and type of probes needed to optimally characterize the complex media. To derive the generalized telegraphists' equations, no assumptions are made about the characteristics of the rough interface, the frequency of the source, or the locations of the source and observation points. Therefore, they provide advantageous starting points for deriving near and far field solutions to a broad variety of physical problems. In electrical engineering, waveguides with organic chiral cores are being investigated for possible applications to integrated optics devices, including polarization transforms, modulators and directional couplers. In all these application, sub-wavelength fluctuations in the interfaces between the media can significantly affect the physical characteristics of the chiral structures. Since biological materials possess chiral properties, this work has applications in biosecurity.

An Improved Finite Difference Eigenvalue Algorithm for the Analysis of Photonic Crystal Band Structures

Chin-ping Yu* and Hung-chun Chang[†]

Graduate Institute of Communication Engineering
National Taiwan University, Taipei, Taiwan 106-17
[†]also with Department of Electrical Engineering, and Graduate Institute of
Electro-Optical Engineering, National Taiwan University

Since the idea of photonic crystal concept was first proposed in 1987, there has been a growing interest in the development of electromagnetic and photonic crystal materials. Photonic crystals (PCs) are characterized by their photonic band gaps (PBGs) resulting from periodic material structures and are widely employed in many applications such as new means of waveguides, resonators, antennas, and microwave components. As we know, these PBGs are very sensitive to the geometry of the periodic structure, and a variety of numerical methods have been utilized to calculate their band structures. Among these the most used are the plane-wave expansion (PWE) method and the finite-difference time-domain (FDTD) method.

In this paper, based on the Yee's differential cell which has been widely utilized in the FDTD method, we derive the finite-difference frequency-domain (FDFD) equations for the analysis of the band structures of 2-D PCs. Two algorithms are proposed to improve the accuracy of the computation of PBGs. One is to use an implicit scheme for approximating the differential operators in Maxwell's equations and an index average scheme for improving numerical convergence and accuracy. The other is to use the central difference scheme in the formulation and fulfill the boundary conditions at the dielectric interfaces in the Yee's cell with the normal and tangential field components which are approximated by interpolation and extrapolation. Both algorithms, when combined with the Bloch's theorem, result in a matrix eigenvalue equation in terms of the field components. The band structures can then be determined by solving the eigenvalue equation with the eigenvalues being the existing bands in the PCs.

Using the proposed algorithms with 40 divisions in a lattice distance, it takes only a few minutes to obtain the band diagrams of TE and TM modes on a Pentium IV 2.0 GHz personal computer for a typical PC composed of dielectric rods in the air or of air holes in a dielectric substrate. By solving the bands with variant numbers of division points, both algorithms show very fast convergent properties. Very good agreement with the calculation using the MIT Photonic-Bands (MPB) package, which is based on the PWE method, has been achieved.

SIMULATION OF THE FINITE PHOTONIC CRYSTALS AND HF CIRCUITS BASED ON COMPLEX MATERIALS

R. Zaridze*, D. Karkashadze, A. Bijamov, V. Tabatadze, I. Paroshina
Tbilisi State University, 3 Chavchavadze Ave, 380028 Tbilisi, Georgia.
Tel.: +995 32 290821, fax: +995 32 290845, e-mail: lae@access.sanet.ge

In the paper "The Method of Auxiliary Sources for complex medium objects" (Zaridze, Bogdanov, Karkashadze, at the IEEE AP/URSI Symposium, Boston, USA, 2001) the ability of the method to deal with the complex – chiral or biisotropic medias efficiently was presented. The investigation of the Finite Photonic Crystals implementation as the base for various devices using complex materials is of high interest. In this paper MAS application to the computer simulation of the Finite Photonic Crystal made of complex materials based devices, as well as IC is discussed.

The periodic structures with defects attracted much interest and are widely used in High-Density Integrated Optics. The main feature of these structures is that for some frequencies within the band gap introducing defects to the lattice in special way one can form resonant channels serving as the waveguides, which can direct wave in the desired way without losses. Special distribution of defects in some area can form even more complicated structures, revealing some complex functionality – such as frequency filtering, signal splitting, etc. Usage of complex materials as the base of the crystal opens up wider possibilities of wave propagation controlling due to the presence of two additional degrees of freedom, connected with the biisotropic parameters of the media. The same idea can be transferred to SHF frequency band for the efficient directed and beem steering capable antenna structures creation.

A special attention is paid to the influence of the finite manufacturing precision on the operation of the device. A software package with the user friendly GUI has been developed for the development and simulation of such devices made of complex materials. MAS analyses of particular FPC – based devices, antennas and ICs will be presented and the effectiveness of this approach will be discussed..

In fig. 1 the flow block and appropriate FPC circuit for remote exploration of some surfaces is presented, consisting of divider, circulator and mixer.
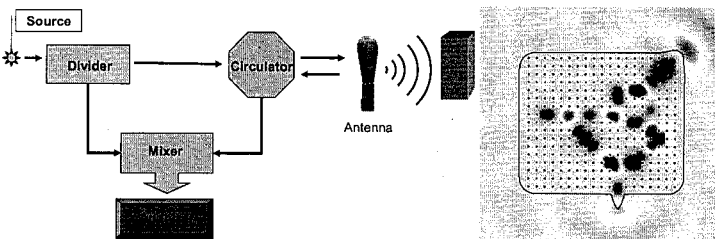
Fig.1 Remote Exploration of Dielectric Body

216

Introductory Remarks
Andreas C. Cangellaris
University of Illinois at Urbana-Champaign
Urbana, IL   61801

COMPUTATION OF IMPULSE ARRAY FIELDS
USING HALLEN'S TIME-DOMAIN INTEGRAL EQUATION

Michael A. Morgan
Electrical and Computer Engineering Department, Code EC/Mw
Naval Postgraduate School, Monterey, CA 93943-5121
mmorgan@nps.navy.mil

Transient currents and radiated fields from a wire impulse array antenna is computed using a time-domain Hallén integral equation (T. K. Liu and K. K. Mei, Radio Sci., 8, 797-804, 1973).   The impulse antenna being considered is composed of a center-fed radiating dipole with parallel wire reflectors arranged in a parabolic cylinder (Fig. 1).
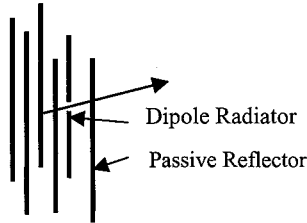
Figure 1 Impulse Array Structure

Focal length of the parabolic cylinder is adjusted to constructively add delayed reflected fields from the reflectors with the direct field from the radiator.   Driven element and reflector lengths are set to those of an optimized 2-element Yagi with center frequency equal to that of the excitation spectrum. Computed peak field gain patterns are compared in Figure 2 for a damped sine voltage applied to the driven dipole element both without and with the reflectors. Forward peak gain is increased from 2.01dB for the dipole alone to 7.50 dB with the 5 added reflectors. Further, the reflector structure provides a strong reduction in backward radiation with a forward-to-back ratio in peak gain of 8.95 dB

Dipole $G_{max} = 2.01$dB   Array $G_{max} = 7.50$dB; *FBR* $= 8.95$dB
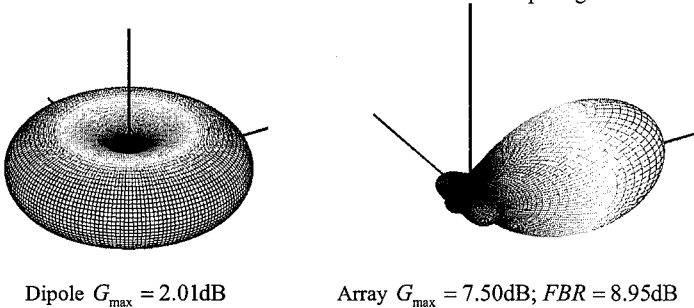
Figure 2 Peak Field Gain Patterns for Dipole Feed and Reflector Array

Further refinement of focal length and lengths of the driven element and reflectors for specific input waveshapes will be performed using a genetic algorithm.

218

Insight Of Removing Numerical Errors In Field Computation
-- Generation of Super-Absorbing Boundary Condition

Jiayuan Fang

Sigrity, Inc.

Among numerous things that I learned from Prof. Kenneth K. Mei during my graduate study at the University of California at Berkeley, the most valuable of all is Prof. Mei's approach to technical challenges – think outside the box to find solutions. The finding and the development of the super-absorbing boundary condition (Superabsorption – A Method of Improve Absorbing Boundary Conditions, K. K. Mei and J. Fang, IEEE Trans. Antenna Propagation, vol. 40, No. 9, Sept. 1992, 1001-1010) is one of such examples.

In 1980s, the research group under Prof. Mei was among the first in applying the finite-difference time-domain (FDTD) method for the modeling of microwave and millimeter wave passive components. For such applications, FDTD method appeared to have many advantages; but a big challenge encountered and first realized by Prof. Mei's group was the unsatisfactory absorbing boundary conditions that were available to be used in FDTD.

It was found that reflections from outer computation boundaries were often the primary reason that prevented us from getting reliable results in modeling microwave passive components. The absorbing boundary conditions commonly used at that time, mainly the Mur's first and second order boundary conditions, were not good enough to model even the simplest structures such as a single microstrip line. A relative small error in the time domain due to reflection noise from the outer computation domain could lead to significant error in frequency domain results. Extensive search was thereby carried out on absorbing boundary conditions used in computational electromagnetics, acoustics and other computational physics communities; and intensive tests and investigation of absorbing boundary conditions were also carried out.

Instead of following the routes of other investigators, Prof. Mei discovered an entirely unique approach. He led to the finding that the numerical reflection from an outer computation boundary terminated by tangential electric nodes was of the opposite polarity to the numerical reflection from the outer boundary terminated by tangential magnetic nodes. He also suggested that, without doing two or more separate computations in the entire computation domain, the two types of errors could be cancelled near outer boundaries through certain mathematical operations in a single run of FDTD computation. Prof. Mei's insight led to the successful development of a totally new approach in the handling of absorbing boundary conditions. The super-absorbing boundary condition thus developed was a process that led to significant improvement of the original absorbing boundary condition, and it was found applicable to all the existing absorbing boundary conditions at that time. Such a progress, in turn, greatly facilitated the advance of modeling of various microwave passive components over broadband frequencies using FDTD.

219

The Measured Equation of Invariance: Thinking Out of the Box in EM Computational Methods

Prof. Rafael Pous, Ph.D., Department of Signal Theory and Communications, Technical University of Catalonia, Barcelona, Spain.

Among the many methods to solve EM propagation, scattering and radiation problems through numerical techniques, the Measured Equation of Invariance (MEI), stood out from its very genesis. Rather than looking for a solution to the equations, the MEI is a method to find an equation derived from the solutions.

The exciting thing about working in the team that derived the MEI method, was that it meant thinking out of the box with respect to the common wisdom of the time. Traditionally, EM computational methods are derived in a step-by-step manner, starting at the unquestionable foundation of Maxwell's equations. The derivation of the MEI method was based on stating a postulate, that is, an unproven, although reasonable, assumption. The postulate of invariance is the assumption that if a linear relationship among the field values (the MEI equation), is numerically accurate for a set of solutions to the boundary value problem, it will also be numerically accurate for any other solution to the same boundary-value problem. As long as a set of solutions can be found to the boundary-value problem, even if the excitation related to each solution is unknown, the MEI can be derived, and later used to find the solution to the problem at hand, that is, the solution to the same boundary-value problem for a given excitation.

Investigating the MEI method really was like doing experimental research, in which one tries different hypotheses, and designs experiments to prove them right or wrong. In fact all numerical methods have initially used assumptions in their derivations, such as assuming that enforcing the boundary conditions at a discrete set of sample points will yield a numerically accurate solution. As it often happens in science, proof of the numerical accuracy of the invariance postulate has been later derived. But the key to the MEI method was the bold, "out of the box" approach of using a postulate as the starting point to derive a numerical method.

Microwave-Based Breast Cancer Detection: A Detection-Theoretic Approach

S. K. Davis*, H. Tandradinata, M. Lazebnik, S. C. Hagness, B. D. Van Veen
Department of Electrical and Computer Engineering, University of Wisconsin--Madison
1415 Engineering Drive, Madison, WI 53706-1691 USA
skdavis@cae.wisc.edu

Microwave-based methods for breast cancer detection have received substantial attention in recent years, motivated in part by the significant dielectric contrast observed between malignant and normal breast tissue. Previous investigations have primarily focused on deterministic imaging techniques. In this paper, we present a preliminary investigation of detection-theoretic techniques for determining the presence and location of scatterers (such as tumors) in the breast. We assume the data is ultrawideband microwave backscatter obtained from an antenna array near the breast surface and that dominant artifacts such as the reflection at the skin-breast interface have been removed (e.g. using the approach proposed in Bond, *et. al., IEEE T-AP*, 51(8):1690-1705, 2003).

In order to apply detection theory to this problem, we first make assumptions about the distribution of the microwave backscatter data. The data is assumed to consist of three additive components: signal, clutter, and noise. The signal is backscatter due to tumors, clutter is backscatter due to normal breast tissue which is a heterogeneous mixture of fatty, fibroglandular and connective tissues, and any remaining component is noise. We obtain a sample covariance matrix for the clutter and assume the noise is white Gaussian. The signal is modeled as a deterministic linear combination of waveforms with unknown coefficients, where the waveforms are based on the analytical backscatter solutions for a cylindrical or spherical scatterer. The backscatter is therefore assumed to be Gaussian distributed with known covariance. For design purposes we assume the data is white since we can theoretically pre-whiten the data.

Our investigation covers two detection-theoretic techniques for constructing images of detected scatterers: a generalized likelihood ratio test (GLRT), and a penalized expectation-maximization (EM) algorithm. Given the observed backscatter data and a candidate scatterer location, the GLRT is a binary test comparing the likelihood that the backscatter resulted from a single scatterer at the candidate location versus the likelihood of the alternative. The F-distributed GLRT test statistic is thresholded at a level that restricts the probability of false detections, and we say that a tumor is detected when the test statistic exceeds the threshold. The second technique, the penalized EM algorithm, is an iterative algorithm well-suited for solving an ill-conditioned maximum-likelihood problem such as finding the maximum-likelihood estimate of the unknown signal coefficients. We formulate the problem such that each signal coefficient corresponds to backscatter from a candidate scatterer location. Then the estimated coefficients are plotted as an image of detected scatterers in the breast. This estimation problem is often ill-conditioned, so a penalty term is introduced to regularize the problem and enforce a sparse solution.

In this paper we present both computational and experimental investigations for the decision-theoretic techniques described. Computational investigations are based on simulated backscatter from MRI-derived FDTD breast phantoms including a sample covariance matrix for the clutter. Experimental investigations involve multi-layer physical breast phantoms with a homogeneous normal breast tissue simulant. These physical phantoms lack clutter, so no sample covariance matrix is required for the experimental investigation. Both sets of phantoms introduce small (less than 0.5 cm) synthetic tumors into the modeled breast which exhibit dielectric contrasts that realistically represent the contrast predicted for malignant and normal breast tissue. Our investigations suggest that a Gaussian distribution provides a reasonable description of the backscatter statistics. Furthermore we verify that these two techniques are capable of detecting small scatterers at various locations and even multiple scatterers. The algorithms have convenient forms that enable us to include additional candidate scatterer properties such as tumor size and breast density. We provide examples that illustrate the capability of correctly detecting the presence, location and diameter of scatterers as well as the density of normal breast tissue.

A Three Dimensional Multiresolution Impedance Method for Low-Frequency Bioelectromagnetic Interaction

Patrick Brown* and Gianluca Lazzi

Department of Electrical and Computer Engineering,
North Carolina State University, Raleigh, NC 27695-7914, USA

A 3D multi-resolution Impedance Method (IM) is presented for the analysis of low-frequency, quasi-static bioelectromagnetic problems. While our implementation of the Impedance Method uses the same underlying principles as the conventional Impedance Method, a multi-resolution meshing algorithm has been introduced to reduce memory consumption and computational requirements. Our preliminary simulations show that substantial reductions in simulation size can be achieved while still maintaining a level of accuracy comparable to conventional Impedance Method simulations. The method was developed to aid in the design of an intraocular retinal prosthesis and is currently being used to analyze current densities induced in the human retina by epi-retinal electrodes.

The Impedance Method was introduced by Gandhi in 1984 as a simulation method suitable for the solution of low-frequency electromagnetic problems. Conceptually, this technique is relatively simple and particularly well suited to bioelectromagnetic applications because the method remains simple even when used to analyze complex simulation spaces such as the human body. The Impedance Method requires discrete models of the simulation space, meaning that larger, higher resolution models would provide more accurate results than smaller, coarser resolution models. However, like many numerical simulation techniques, memory requirements and the computational load are directly related to the number of computational units. Because a high resolution model has many discrete units, this can necessitate the use of less realistic, lower resolution models.

To permit the use of larger models, a multi-resolution meshing scheme was introduced to reduce the number of total computational units. In the Impedance Method, fine detail is most important in regions where different materials meet, while large homogenous sections of material do not require high resolution for accurate modeling. Our multi-resolution meshing scheme takes advantage of this by combining the many small cells in large homogenous sections of the model into fewer, larger cells, while leaving cells near boundaries between material types at the maximum resolution.

Preliminary simulations show that cell reductions between 30-50% are achievable in retinal models. Further refinement of the meshing algorithm could lead to even more substantial reductions in cell count. Also, some multi-resolution Impedance Method simulations have been linked with highly developed circuit simulators such as SPICE. Linking the method with circuit simulators allows the inclusion of non-linear passive and active circuit elements in simulations, creating new opportunities for modeling bio-electric phenomena.

A 2-D Electrical Impedance Tomography System and Image Reconstruction

G. Shi*, K. H. Lim, J. Di Sarro, J. Hu

R. T. George, G. Ybarra, W. T. Joines, and Q. H. Liu

Electrical and Computer Engineering

Duke University

Durham, North Carolina 27708

Email: qhliu@ee.duke.edu

We have developed a prototype electrical impedance tomography system for biomedical imaging, and are in the process of studying its feasibility for breast cancer imaging. The impetus for this research is the reported large contrast in electrical conductivity between the normal breast tissue and malignant breast tumors.

In our 2-D electrical impedance tomography system, the data acquisition apparatus consists of a 32-electrode applicator, a multimeter, a signal generator, a DC power source and a personal computer working as the control center. The applicator is a plastic container with 32 brass electrodes attached to its inner boundary. One of the 32 electrodes is fixed as the ground, while all other electrodes work both as the voltage source and the measuring point. We built an electronic multiplexer to control the source and receiver electrodes in order to make a complete sweep of 31×31 voltage measurements. The applied voltage is an AC source with frequency ranging from 100 Hz to 10 kHz. The computer sends out digital control signals to the multiplexing system through the I/O card and reads the voltage signal back from the multimeter through a GPIB interface.

The image reconstruction from the measured EIT data is a nonlinear inverse problem. We formulate this inverse problem using the distorted Born iteration method. From the measured 31×31 voltage results, we reconstruct the spatial distribution of conductivity $\sigma(r)$ inside the applicator. The algorithm starts with an initial guess of the conductivity $\sigma(r)$ and computes the corresponding potential by a forward solver based on the finite-element method. The difference between the acquired voltages and the computed potentials on the electrodes is taken. With this potential misfit functional, the difference in conductivity σ is inverted by the distorted Born approximation to update the conductivity $\sigma(\mathbf{r})$. This updated conductivity is then fed back into the forward solver to obtain the next potential misfit functional. The iterative process is repeated until the data misfit is sufficiently small. We will demonstrate the EIT image reconstruction with real data obtained in the laboratory.

Modeling the Resonance Phenomenon of Electromagnetic Waves Scattered from Malignant Breast Cancer Tumors

Magda El-Shenawee
University of Arkansas
Department of Electrical Engineering
Fayetteville, AR 72701
479-575-6582
magda@uark.edu

As investigated by other researchers, several promising advantages can be achieved using electromagnetic waves in detecting breast cancer such as: (i) the electromagnetic modality is non-ionizing and non-invasive. It is safer than X-ray methods, which have side effects of potentially causing other types of cancer. Also, the electromagnetic modality does not require surgery for diagnosis compared with other medical procedures (e.g., fine needle biopsy). (ii) The electromagnetic modality succeeds, by definition, for large contrasts in electrical properties, which is normally the case in breast cancer. At certain microwave frequencies, e.g., 1GHz–10GHz, reported experimental measurements show that the electrical properties of malignant tumors are significantly different from those of normal breast tissue. This contrast allows electromagnetic methods to detect smaller tumors when compared with ultrasound, for example, which is successful for detecting larger tumors. (iii) Radar technology has become very advanced and economical in recent years.

The purpose of this work is to model and analyze the signature behavior of malignant tumors over the frequency range 1-10 GHz. An intensive numerical study of resonance scattering of malignant breast cancer tumors is presented here. The fast forward three-dimensional electromagnetic solver, the steepest descent fast multipole method (SDFMM), previously implemented to model the scattering from targets buried beneath the random rough ground surface, will be used in this work.

The results show that non-spherical malignant tumors can be characterized, based on its spectra, regardless of orientation, incident polarization, or incident or scattered directions. The spectra of the tumor depend solely upon its physical characteristics (i.e., shape and electrical properties); however, their locations are not functions of the depth of the tumor beneath the breast surface. Although the scattered fields exhibit an obvious resonant radiation when a tumor is present in the breast, however, the magnitude of these waves is considerably reduced due to the absorption of transmitted waves by breast tissue. This study can be a guide in the selection of the frequency range at which the tumor resonates to produce the maximum signature at the receiver.

Quasistatic Reconstruction of Layered Biological Tissues

M. Dolgin* and P. D. Einziger,

Department of Electrical Engineering, Technion-Israel Institute of Technology

Abstract

Direct wave problem associated with layered medium as well as an inverse proce-
dure, dealing with its reconstruction, are well known and intensively discussed in the
scientific literature. In particular, the estimation of electrical and geometrical parame-
ters of biological tissues has recently become of increased scientific and public interest.
Wave-type problem features an outstanding characteristic, namely, electromagnetic
energy localization in either space-time or space-frequency domains, enabling high
resolution profile reconstruction, however, at the cost of massive numerical and an-
alytical efforts. Unfortunately, in the quasistatic limit, which leads to significant
simplification of both the mathematical derivation and the practical implementation,
this feature is, generally, not applicable. Herein, we focus on a novel quasistatic re-
construction method aiming to extend the locality feature into the quasistatic domain
via the recently proposed image series expansion scheme (P. D. Einziger et al., IEEE
Trans. Antennas Propagat., 50(12), 1813-1823, 2002).

The quasistatic potential for plane stratified media excited by a point source is
given by Green's function $G(\mathbf{r}, \mathbf{r}')$ via Fourier Bessel integral representation

$$G(\mathbf{r}, \mathbf{r}') = \frac{1}{2\pi} \int_0^\infty \xi g(z, z') J_0(\xi\rho) d\xi, \qquad (1)$$

where $\mathbf{r} = \rho\hat{\rho} + z\hat{z}$ and $\mathbf{r}' = \rho'\hat{\rho} + z'\hat{z}$ denote the observation and the source points,
respectively. The characteristic Green's function $g(z, z')$, representing the spectral
content of $G(\mathbf{r}, \mathbf{r}')$, is specified by the electrical and the geometrical parameters of the
tissues (to be reconstructed). Expanding $g(z, z')$ as

$$g(z, z') = \sum_{m_1} \sum_{m_2} \cdots \sum_{m_n} g_{m_1, m_2, \ldots, m_n}(z, z'_{m_1, m_2, \ldots, m_n}), \qquad (2)$$

for $n + 1$ layers, and taking the integral in (1) term by term, results in the desired
image series (L. Livshitz et al., ACES J., 16(2), 145-154, 2001)

$$G(\mathbf{r}, \mathbf{r}') = \sum_{m_1} \sum_{m_2} \cdots \sum_{m_n} G_{m_1, m_2, \ldots, m_n}(\mathbf{r}, \mathbf{r}'_{m_1, m_2, \ldots, m_n}). \qquad (3)$$

The terms $g_{m_1, m_2, \ldots, m_n}(z, z'_{m_1, m_2, \ldots, m_n})$ and $G_{m_1, m_2, \ldots, m_n}(\mathbf{r}, \mathbf{r}'_{m_1, m_2, \ldots, m_n})$ as well as
$z'_{m_1, m_2, \ldots, m_n}$ and $\mathbf{r}'_{m_1, m_2, \ldots, m_n}$ correspond to the image contributions and their loca-
tions, respectively. It should be noted that the locality feature is readily maintained,
since each term represents interaction of a unique layer and its neighbourhood, result-
ing in a one to one mapping between each layer and the corresponding image term.
Furthermore, the limit for which the contribution from each layer's neighbourhood can
be neglected leads to the WKB approximation.

Computations based on our novel quasistatic procedure for discrete and contin-
uous profiles, in both ρ and ξ domains, provides accurate, efficient and stable re-
construction, particularly, when relatively small data base and, consequently, shallow
penetration are required.

Investigation of Wideband Spiral Antennas on Flexible Substrates for Use in Biomedical Applications

Michael D. Seymour[*], Jayanti Venkataraman, Rochester Institute of Technology, NY

The frequency-independent nature of planar spirals makes them ideal for the ultra-wideband requirements of microwave imaging, where higher bandwidths facilitate the propagation of very narrow pulses necessary for high-resolution imaging. The benefits of using a spiral antenna in lieu of other wideband antennas, such as a resistively-loaded bowtie or Maltese cross, is its ease of fabrication since the conductive material is homogeneous. Also it allows for methods of excitation which conform well to integrated circuit design and could also perhaps serve as an inductive component in the associated circuitry. Such a coil may also be fabricated on flexible dielectric films without changing its characteristics significantly. Flexible substrates are desirable because they conform more easily to the curvature of human subjects and could therefore provide more accurate imaging.

In the present work, the characteristics of the classic dual-fed Archimedean spiral have been investigated for a specified bandwidth and center frequency. This can be achieved by feeding two ports at 180° out of phase and determining the necessary inner and outer radii of the antenna to propagate the desired range of frequencies. The phase difference between the currents at adjacent points P and P' is then: $\angle[\hat{I}(P)] - \angle[\hat{I}(P')] = \pi(1 + 2\pi\rho/\lambda)$ (1), where ρ is the radius and λ is the desired wavelength. With the currents being in-phase when the ρ is equal to odd multiples of β^{-1}, maximum radiation will occur.

Using this current band theory, an antenna designed for a 2:1 pattern bandwidth centered at 6GHz has been compared to other ultrawideband antennas used for microwave imaging (S. C. Hagness et al., *2003 IEEE MTT-S Int. Microwave Sym. Dig.*, 1, 379-382, 2003). The substrate of the antenna can be any simple dielectric sheet, since no ground plane is required. The input and radiation characteristics will be assessed as the dielectric substrate takes difference shapes. Fig. 1a gives the layout of the Archimedean spiral and the corresponding radiation pattern at 6GHz is obtained using Ansoft Designer, fig. 1b. Using the Finite Difference Time Domain technique, a Gaussian pulse is allowed to propagate through multiple layers of diseased and healthy human tissues, which have vastly different electrical parameters such as dielectric constant and conductivity. Fig. 2a and 2b show the reflections from healthy and diffused-diseased tissues, respectively, which could be used as a disease-monitoring tool when assessing treatments over time.

(a)   (b)
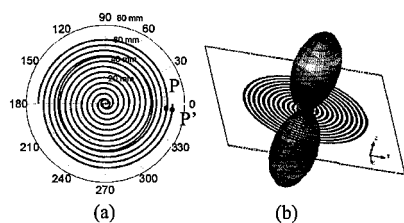
Fig. 1. (a) Antenna Layout with Current Bands and (b) Radiation Pattern for Archimedean Spiral

(a)

(b)   Time [ns]
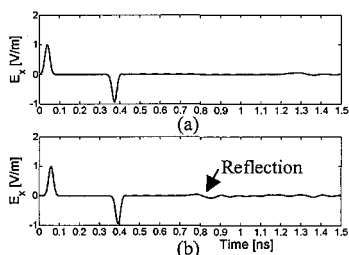
Fig. 2. Antenna Response for Tissue Samples: (a) Healthy (b) Diseased, via 1D FDTD

Guided Wave Propagation in H-guides using Double Negative Materials

António L. Topa, Carlos R. Paiva, and Afonso M. Barbosa

Instituto de Telecomunicações and *Instituto Superior Técnico*
Technical University of Lisbon
Av. Rovisco Pais 1, 1049-001 Lisboa, Portugal.
E-mail: antonio.topa@lx.it.pt

Metamaterials, where permittivity and permeability both have negative values, usually termed double-negative (DNG) materials, can be used in the design of compact microwave devices, such as subwavelength cavity resonators (N. Engheta, *IEEE Antennas Wireless Propagat. Lett.*, **1**, 10-13, 2002) and miniaturized printed antennas.

The H-guide was originally introduced by Tischer (F. J. Tischer, *Proc. IEE*, **106B**, suppl. 13, 47-53, 1959). Usually, a distance smaller than half a wavelength separates the parallel metal plates, in order to overcome the radiation losses at curved sections and discontinuities (T. Yoneyama and S. Nishida, *IEEE Trans. Microwave Theory Tech.*, **MTT-29**, 1188-1192, 1981). The analysis of waveguides using this technology has been developed for isotropic, anisotropic, ferrite (A. César and R. Souza, *IEEE Trans. Microwave Theory Tech.*, **41**, 647-651, 1993) or omega media (A. L. Topa, C. R. Paiva, and A. M. Barbosa, *IEEE Trans. on Microwave Theory and Tech.*, **46**, 1263-1269, 1998), so far.

This paper addresses the problem of electromagnetic wave propagation in an H-guide where the common double-positive (DPS) slab is replaced by a DNG slab. A full-wave analysis of the LSE and LSM modes propagating in this structure is developed. As an example, the operational and dispersion diagrams for the first LSM modes are depicted in Fig. 1 and Fig. 2, for $\varepsilon = \mu = -2$, where b represents the parallel plate separation and l slab thickness. New propagation characteristics, such as anomalous dispersion and super-slow waves, are observed. Numerical results using an adequate model for the material dispersion were obtained. Waveguide miniaturization and anomalous mode coupling were also investigated through the use of paired DPS and DNG slabs.
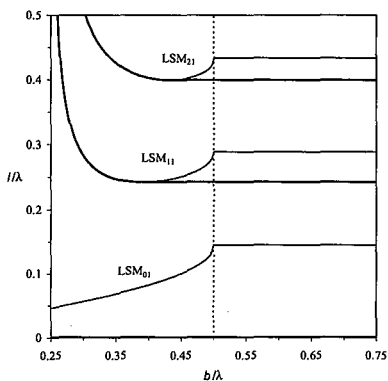
Fig. 1 Operational diagram
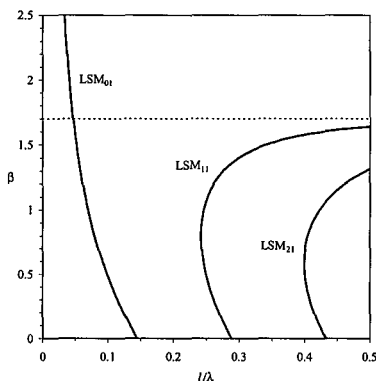
Fig. 2 Dispersion diagram

Design of Single and Double Negative Metamaterials by Using Genetically Optimized Frequency Selective Surfaces

Agostino Monorchio*, Sebastiano Barbagallo, Giuliano Manara

Microwave and Radiation Laboratory, Department of Information Engineering, University of Pisa, Via Diotisalvi 2, I-56126 Pisa, Italy. (a.monorchio@iet.unipi.it)

In this communication, the behavior of planar Frequency Selective Surface as Single and Double Negative Metamaterials (SNG-DNG) is investigated. The proposed design procedure is based on a proper inversion of the equation relating the reflection and transmission coefficients (Γ and τ, respectively) of the screen to the value of the effective permittivity and permeability of the structure, considered as a homogenous medium. In particular, we start by considering a slab of metamaterial with a given thickness d and a fixed value of the effective permittivity ε and permeability μ, which can be either positive and negative or both negative. Then, the corresponding values of the complex coefficients Γ and τ are determined through the equations $\Gamma = f_1(d,\varepsilon,\mu)$ and $\tau = f_2(d,\varepsilon,\mu)$. The values of Γ and τ are therefore used in the fitness function of the Genetic Algorithm used to design the corresponding FSS, as for instance in (A. Monorchio et al., *IEEE Antennas and Wireless Propag. Lett.*, p. 196:199, 2002). It is important to observe that particular care must be used in the inversion formulas employed to evaluate the effective permittivity and permeability of the slab, since the functions f_1 and f_2 are not injective, *i.e.*, the same reflection and transmission coefficient, in some cases, can be presented also by a double infinity (both positive and negative) of values of ε and μ. In order to avoid this problem, a procedure based on the continuity of the dispersion relations in the frequency domain is employed. In this way, some structures are designed that behave like a metamaterial for a certain range of frequency from a macroscopic point of view. Since one of the required characteristics of a metamaterial is the homogeneity along the direction of propagation, further analysis has been performed on the resulting structures to investigate this aspect. It will be shown that the proposed structure behaves as a DNG or SNG at different bands by changing the thickness of the dielectric layer without modifying the shape of the FSS. This, in turn, can be used as a parameter to tune the frequency behavior. As an example of the structure derived by this procedure, we show the results relevant to a DNG slab realized by using a planar FSS embedded in a lossless dielectric layer with a thickness of 1 cm and $\varepsilon_r = 2$. The shape of the resulting screen is shown in the inset of Fig. 1 (the dimensions of the elementary periodicity cell are 1 cm×1 cm). In Fig. 2, we show a test performed to recover the correct behavior of the metamaterial; in particular, the DNG previously described is cascaded with a slab of the same thickness presenting the complementary values of permittivity and permeability for the frequency of 11.5 GHz ($\varepsilon_r = -0.49$, $\mu_r = -2.03$). As apparent, at the frequency where the values of ε and μ of the two slabs are exactly complementary, the transmission coefficient is equal to 1 with a null phase. Finally, we point out that a research activity is in progress to obtain structures with very small periodicity along the two main directions of the FSS in order to get the homogeneity of the metamaterial also for oblique incidence angles.
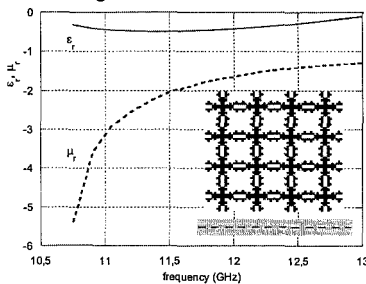
Fig. 1
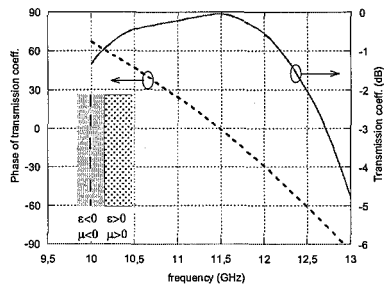
Fig.2

Embedded-Circuit Band-Gap Metamaterials for The Design of High Performance Antenna Arrays

Kamal Sarabandi and Hossein Mosallaei
Electrical Engineering and Computer Science
University of Michigan, Ann Arbor, MI 48109-2122
saraband@umich.edu

Since their invention back in 1960's, microstrip patch antennas have found numerous applications for their simplicity in fabrication, compatibility with planar circuitry, low profile and planar structures, and unidirectional radiation capability. Despite many nice electrical and mechanical features of microstrip antennas, their use for a number of applications have been limited due to their limited bandwidth and/or size. As an element for antenna array application it is desired to minimize the size of a microstrip element to reduce the mutual coupling among. Considering the fact that the size of a microstrip element is of the order of a half a wavelength in the substrate dielectric material, usually substrates with relatively high permittivity ($\varepsilon_r \geq 4$) is used for dense arrays. The bandwidth of each element, however, depends on the thickness and permittivity of the substrate. That is, microstrip antennas with thicker substrate and lower permittivity present a higher bandwidth. On the other hand there is a limitation on the thickness of the substrate. This limitation is enforced by the requirement on the suppression of the surface waves, which can drastically increase the mutual coupling among the array elements which in turn perturb the array performance considerably. Hence in practice patch array antennas demonstrate a rather low bandwidth.

To improve the bandwidth of patch array antennas without increasing the element size or array spacing an approach must be developed that should allow substrate thickness increase at the same time suppress the mode transition to surface waves. In the literature use of periodic dielectric and metallo-dielectric Electromagnetic Band-Gap (EBG) structures is proposed as a means of suppressing surfaces waves [1], [2]. However, the periodicity of such structures are comparable to the wavelength and at least a few periods are required to achieve high isolation. Although this approach is appropriate for making resonators and filters, it is not suitable for suppression of surface waves in a large array structure due to a maximum element spacing 0.7λ. To circumvent this difficulty a novel approach based on the application of embedded-circuit band-gap metamaterials is proposed. An Embedded-Circuit Metamaterial (ECM) is made up of periodic tank circuits with a frequency dependent effective permeability that can assume negative values over a certain frequency band (band-gap) [3]. Unlike traditional EBGs the periodicity of ECM can be a very small fraction of a wavelength (<0.05λ). Fig. 1(a) depicts the geometry of a 1-layer ECM. The transmission coefficient for a plane wave illuminating a very thin layer of ECM is shown in Fig. 1(b). The stop-band behavior is clearly demonstrated. Such thin layers are inserted between tiles of patch antenna elements with thick substrates to suppress mutual coupling as shown in Fig.2.

(a)   (b)
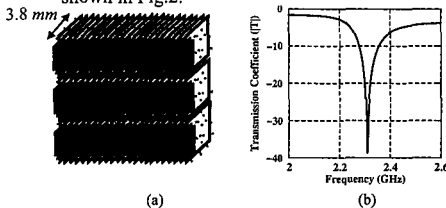
Fig. 1. (a) Embedded-Circuit Metamaterial (ECM) and (b) its performance.
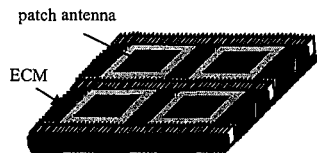
Fig. 2. Patch array antennas with ECM inserted between them.

References
[1] Y. Rahmat-Samii and H. Mosallaei, "Electromagnetic band-gap structures: Classification, characterization, and applications," *IEE International Conference on Antennas and Propagation*, UMIST, Manchester, UK, 2001.
[2] F. Yang and Y. Rahmat-Samii, *IEEE Trans. Antennas Propagat.*, vol. 51, no. 10, pp. 2936-2946, Oct.. 2003.
[3] K. Sarabandi and H. Mosallaei, "Novel artificial embedded circuit meta-material for design of tunable electro-ferromagnetic permeability medium," *IEEE International Microwave Symposium*, Philadelphia, Pennsylvania, 2003.

229

RECIPROCAL PROPERTIES OF SCATTERING FROM SPHERES WITH DOUBLE NEGATIVE COATINGS AND SOURCES WITHIN DOUBLE NEGATIVE SPHERICAL SHELLS

Allison D. Kipple* and Richard W. Ziolkowski

Department of Electrical and Computer Engineering
The University of Arizona
1230 E. Speedway Blvd.
Tucson, AZ 85721-0104

Tel: (520) 621-6173
Fax: (520) 621-8076
E-mails: kipplea@ece.arizona.edu, ziolkowski@ece.arizona.edu

The effect of surrounding an electrically small dipole antenna with a shell of double negative (DNG) material ($\varepsilon_r < 0$ and $\mu_r < 0$) has been investigated both analytically and numerically. The results of these investigations have been reported by us in [R. W. Ziolkowski and A. D. Kipple, IEEE Trans. Antennas Propagat., vol. 51, pp. 2626-2640, October 2003]. Analysis of the reactive power within this dipole-DNG shell system indicated that the DNG shell acts as a natural matching network for the dipole and free space. Matching occurs at particular shell sizes and results in significant enhancements of the radiated power with corresponding decreases in the radiation Q.

The scattering of plane waves from cylindrical and spherical metamaterial objects has been considered by A. Alu and N. Engheta, for instance, in [A. Alu and N. Engheta, Proceedings of the ICEAA'03 Meeting, Session 14, Torino, Italy, Sept. 2003]. Particular emphasis was given to epsilon-negative (ENG) and mu-negative (MNG) and to DNG and double positive (DPS) combinations. They found that resonant scattering occurs at particular relative electrical sizes of the scatterers and coatings.

The natural question arose as to the relationship between the enhanced source and scattering results. If reciprocity holds for the DNG scatterers, then the correspondence between the particular DNG dipole-shell systems and the scatterers that produce the enhancements should be one-to-one. To verify that reciprocity holds for these DNG and ENG-MNG systems, a very general sphere scattering problem was considered analytically and numerically. In particular, plane wave scattering from a sphere that was coated with two concentric spherical shells, which could be DPS, DNG, ENG or MNG materials, was analyzed. The coated spheres were considered to be located in a DPS medium, i.e., free space. This allowed a direct comparison with the concentric ENG-MNG and DPS-DNG sphere results presented by Alu and Engheta, a direct comparison of the free-space sphere embedded in a DNG shell with the reciprocal DNG dipole-shell system, and other interesting combinations of DPS, DNG, ENG, and MNG shells. The results of these investigations will be presented. It was verified that reciprocity holds for the DNG configurations studied.

230

Reducing Scattering from Cylinders and Spheres Using Metamaterials

Andrea Alù[1], and Nader Engheta[2,*]

*[1]Università di Roma Tre
Department of Applied Electronics, Rome, Italy
alu@uniroma3.it, http://www.dea.uniroma3.it/lema/people/andrea_alù.htm*

*[2]University of Pennsylvania
Department of Electrical and Systems Engineering
Philadelphia, Pennsylvania 19104, U.S.A.
engheta@ee.upenn.edu, http://www.ee.upenn.edu/~engheta*

Metamaterials with negative real effective permittivity and/or permeability, which are being extensively studied by various groups, exhibit interesting features in guidance, radiation and scattering of electromagnetic waves. In some of our previous works, we have shown how a resonance phenomenon may be induced by properly covering a homogeneous dielectric cylinder or sphere with a concentric shell of metamaterials with negative effective constitutive parameters, leading to highly strong scattered fields for such electrically thin scatterers. This increase in scattering cross section, which occurs for a particular ratio of shell radii and is similar to the plasmonic effect in nano-particles with noble metals, was shown to be due to the induced resonance at the interface of the "conjugate" shells (A. Alù, N. Engheta, Proceedings of the ICEAA'03 Meeting, Torino, Italy, Sept. 8-12, pp. 435-438).

In the present work, we show how an opposite effect may also be achieved for similar scatterers. For a different ratio of radii of shell and core, a "transparency" condition may essentially be achieved, resulting in drastic reduction of total scattering cross section of the object. In the case of thin cylindrical and spherical scatterers, for which their total cross section is generally dominated by the dipole term in the multipole expansion, this dipolar scattering may be vanished with a proper choice of two-shell radii, and the total scattering cross section can thus be reduced. When larger scatterers are considered, this overall reduction is less effective, since the multiple contributions from different multipole orders contribute more to the overall scattering cross section, and thus not all of them can be reduced simultaneously. However, a noticeable effect is still present in this scenario for certain proposed geometries.

In this talk, some physical insights into this phenomenon along with some of our results will be presented, and potential applications will be mentioned.

Efficient Interface between Numerical Antenna Modeling and Environmental Simulation Codes

Jeanne T. Rockway*, Edward H. Newman and Ronald J. Marhefka
The Ohio State University, ElectroScience Laboratory
1320 Kinnear Road
Columbus, OH 43212-1191
rockway.1@osu.edu, newman@ee.eng.ohio-state.edu, and marhefka.1@osu.edu

Modern antenna systems, such as those buried in multi-dielectric layers or electrically large ones, in the presence of complex obstacles are vital for many applications. These multi-structural systems increase the computational difficulties for the electromagnetic field calculations. For instance, calculating the fields of the antenna and the coupling between the structures with the antenna using a whole wave method is prohibitive. To decrease the computational time for design purposes, the spherical harmonic representation technique provides an efficient means of transferring an antenna's current representation between the antenna code and scalable environmental code.

First, the spherical harmonic representation technique allows for the calculation of the antenna currents independently of the environment. The antenna currents can be found from any number of numerical techniques such as Boundary Element Method (BEM), Finite Element Method (FEM), or Method of Moments (MoM). Specifically, the MoM code, Electromagnetic Surface Patch Code (ESP), was used to calculate the antenna currents for validation purposes. Second, the antenna's currents are represented by even and odd spherical harmonics. These harmonics provide an efficient representation of the antenna fields. In the past the vector spherical wave analysis by Chen and Simpson was used to compactly represent this field patterns for dipoles. For the final step of the technique, the spherical coefficients of the spherical harmonics will be used as an input into an environmental simulation code. The environmental simulation code determines the effects of the surrounding structural environment on the antenna's radiating fields. Specifically, the Uniform Theory of Diffraction (UTD) code of Numerical Electromagnetic Code – Basic Scattering Code (Nec-Bsc) will be used to calculate the effects of the different structures on an antenna radiating fields.

It will be shown that the spherical harmonics representation technique decreases the design time needed to calculate the radiated fields of a complex antenna system. The accuracy of the representation of the antenna is dependent upon the number of spherical harmonics. As the electrical length of the antenna or the distance from the origin to the antenna increases, the number of spherical harmonics needed for a given accuracy must also increase. To decrease the number of spherical harmonics, more radiating centers (i.e. phase centers) should be used for the antenna. On the other hand, the more radiating centers that an antenna has, the more computations are needed by the environmental simulation code. This increase in radiating centers will increase the design run times. A method was developed, based upon the current weights and phases, to determine an accurate representation for the fewest spherical harmonics and radiating centers.

A Lanczos Spectral Element Method for High-Speed Electronic Circuit Simulation

Yaxing Liu* and Qing H. Liu
Department of Electrical and Computer Engineering
Duke University
Box 90291
Durham, North Carolina 27708
Email: yliu@ee.duke.edu, qhliu@ee.duke.edu

The desire for faster transition speed in electronic packaging results in many challenging design issues, such as signal integrity, electromagnetic compatibility (EMC) and electromagnetic interference (EMI). Accurate and efficient signal integrity analysis is indispensable in these high-speed circuit design. Most signal integrity analysis tools are based on circuit simulators like SPICE which are suitable for low-frequency signals. For the high-speed circuits, time delay is no longer negligible. Therefore, full-wave electromagnetic field simulators are necessary.

The finite-difference time-domain (FDTD) method has been widely used to analyze transient electromagnetic fields. But for electrically large structures, the Courant-Friedrich-Levy stability condition of the FDTD method limits the time step and consequently, huge computational cost is involved. To circumvent this difficulty, an efficient numerical method for computing the electromagnetic fields in time domain and frequency domain is presented. The proposed method utilizes the spectral element method to discretize Maxwell's equations together with unsplit PML boundary conditions. Then a so-called reduced model is established by a modified Lanczos/Arnoldi scheme, which is based on the Krylov subspace approximation of the solution. Several examples illustrate the advantages of the proposed approach: (a) higher accuracy even with fewer nodes; (2) higher efficiency due to its exponential convergence with the polynomial order; (c) more flexibility in modeling various geometries and media. Moreover, the inherent parallelism of the spectral element method make it easier to parallelize simulations.

A Fast Multipole Method For Green's Functions Of The Form $r^{-\lambda}$

Indranil Chowdhury(*) and Vikram Jandhyala,
EE Department, Univ . of Washington, 98195

Email: burunc@u.washington.edu, jandhyala@ee.washington.edu

It is shown here that the well-known multipole expansions (Greengard, MIT Press, Cambridge, MA, 1988) for the electrostatic Green's function r^{-1} can be extended to functions of the form $r^{-\lambda}$ where λ is any real number. These expansions have made it possible to derive truncated multipole, local and translation operators necessary for the implementation of an error-controllable generalized Fast Multipole Method (FMM) for these functions.

In molecular dynamics apart from electrostatic (r^{-1}) interactions there are other molecular interactions including the Van der Waals and H bond forces which have the form r^{-6}, r^{-10} and r^{-12}. Present methods for fast computation of these forces use Ewald summations and uniform grid based Fast Fourier Transforms. A Multilevel FMM (MLFMM) is well suited for accelerating computations of such N-particle interactions. As a first step, a single level FMM code has been developed based on the new operators that can compute the N-particle interactions in roughly $O(N^{1.5})$ time for all values of λ. Sample results are shown in Figs. 1 and 2. Fig. 1 shows the total setup and matrix-vector product costs versus number of particles (N). Fig. 2 shows the error behavior as the number of multipoles (p) are increased.

A full MLFMM for the new functions will also be presented. The related memory, computational requirements and error behavior of the multilevel code will be discussed. Prospects of extending this research into molecular dynamics and micro-fluidics applications will also be presented.
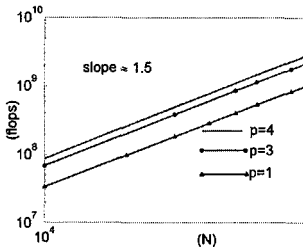
Figure 1: Total cost vs. N
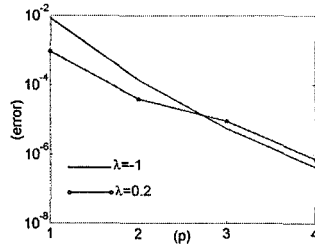
Figure 2: Error vs. no. of multipoles (p)

A Symmetric FEM-IE Formulation with a Multi-Level IE-FFT Algorithm for Solving Electromagnetic Radiation and Scattering Problems

Seung Mo Seo, Seung-Choel Lee, Kezhong Zhao*, and Jin-Fa Lee
ElectroScience Lab., EE Dept., The Ohio State University, OH 43212, USA
(Commission B-B8. Numerical methods: hybrid/other tech.)

The hybrid Finite Element Method-Integral Equation Method (FEM-IE) is one of the most appealing methods for the analysis of unbounded electromagnetic problems. Despite its accuracy advantages over other methods, it has two major drawbacks. The matrix resulting from the coupling of the two methods, usually leads to a non-symmetric system of equation. This naturally doubles the memory requirements. Moreover, due to the lack of effective and efficient preconditioners, the resulting FEM-IE matrix equations are usually solved using direct solution techniques. For some special problems, direct solution techniques, such as multifrontal methods, can outperform iterative matrix solution methods. However, in general when an effective and efficient preconditioner is found, iterative matrix solution approach is the choice for large size problems both in terms of memory and CPU time. The second major limitation of FEM-IE has to do with the memory and computational effort required to assemble the dense IE matrix block. In a problem with N_s IE unknowns, both the storage and the CPU time for a single matrix vector product are of $O(N_s^2)$ requirements, assuming iterative matrix solution is employed.

In this paper both drawbacks of the "conventional" FEM-IE are tacked. The approach is based on a novel *symmetric* coupling between finite element and integral equation methods, inspiration of which is originated from the previously understated work of Hoppe (D. J. Hoppe, L. W. Epp, and J. F. Lee, *IEEE Trans. Antennas Propagat.*, 42, 798-805, 1994) and the recent work by Hiptmair (R. Hiptmair, *SIAM J. Numer. Anal.*, 40, 41-65). The major building blocks of the current approach are: 1) A symmetric hybrid FEM-IE formulation is proposed which is based on the employment of the *Calderon-projector*. 2) A new multi-level IE-FFT algorithm is developed to achieve $O(N_s \log N_s)$ complexity for integral equation. 3) A p-type MUltiplicative Schwarz (pMUS) preconditioner, which has been developed previously for solving the FEM matrix equations arisen from Maxwell equations using hierarchical curl-conforming basis functions, is extended and modified to solve the resulting symmetric complex matrix equation of the hybrid FEM-IE formulation.

ASYMPTOTICALLY DRIVEN LOCAL BASIS FUNCTIONS WITH APPLICATION TO THE FAST MULTIPOLE METHOD

L. Carin and *Z. Liu

Department of Electrical & Computer Engineering.
Duke University, Durham, NC USA

Along the smooth and electrically large portions of a target the induced current has a relatively simple for, characterized by fast (traveling-wave) phase variation and an associated frequency- and geometry-dependent diffraction coefficient. There has been previous research in the context of the method of moments (MoM) in which such high-frequency basis functions are utilized on appropriate localized regions of a given target, with the remainder of the target characterized by traditional piecewise bases. While such approaches have been demonstrated to work, they typically yield poorly conditioned matrices. When performing a direct (LU-decomposition) inversion of the associated matrix, the poor conditioning is not a significant problem. However, recently there has been much interest in iterative (conjugate-gradient) solvers, for which poor matrix conditioning may be a serious problem. The fast multipole method (FMM), for example, is a fast numerical solver that employs an iterative matrix solver.

Rather than utilizing a traveling-wave asymptotic basis function directly, we use asymptotic techniques to design basis functions that yield well-conditioned matrices. Assume that the asymptotic current over a given region may be expressed as

$$J(r,\omega) = \sum_{m=1}^{M} j_m(r,\omega)\exp[-j\,\beta_m \cdot r] \tag{1}$$

where j_m is the mth diffraction coefficient and β_m represents the associated vector wavenumber. Note that the current amplitude j_m is in general a function of position r, allowing consideration of curved surfaces. Rather than utilizing the currents in (1) directly as basis functions, we expand the slowly-varying (with r) amplitude j_m in a traditional piecewise basis set, for example the RWG basis functions. Since the fast-varying phase $\exp[-j\,\beta_m \cdot r]$ has been explicitly extracted, the relatively slowly varying $j_m(r,\omega)$ may be expressed using a coarse basis representation (much coarser than the traditional ten-points per wavelength).

The overall procedure is as follows. Scattering from a given electrically-large target is first analyzed efficiently via an asymptotic ray-based technique. The main objective is to acquire the fast-varying current terms $\exp[-j\,\beta_m \cdot r]$ on smooth portions of the target. The asymptotic representation for $j_m(r,\omega)$ need not be accurate, since it will be characterized by a piecewise basis with coarse sampling (i.e. the numerical algorithm will accurately solve for $j_m(r,\omega)$). Over the complicated regions of a target, for which the asymptotic solution is less accurate, traditional fine-scale piecewise basis functions are employed. Over the smooth electrically large regions coarse-scale piecewise basis functions are used for representation of $j_m(r,\omega)$, and the fast phase variation is explicitly extracted (as in (1)).

It is important to note that throughout piecewise basis functions (*e.g.*, RWG) are being employed, and therefore the resulting matrices are relatively well conditioned. The computational gain is manifested in the fact that over the smooth electrically large regions relatively coarse spatial sampling is used, since the fast phase variation is extracted, and therefore the total number of unknowns is reduced significantly. The resulting matrix equation is solved using a multi-level fast multipole algorithm (MLFMA) analysis.

CURRENT MODES IDENTIFICATION FOR THE ANALYSIS OF RADIATION AND SCATTERING FROM LARGE STRUCTURES

*Carlos Delgado, Miguel Fernández, M. Felipe Cátedra
Escuela Politécnica, Universidad de Alcalá
28806 Alcalá de Henares. Madrid. Spain
Fax: +34 91 885 6699 e-mail: felipe.catedra@uah.es

Several approaches are available to analyze rigorously radiation and scattering from large complex problems using high performance computers, like for instance the FMM (Fast Multipole Method) that avoids the extremely large matrices that appear solving these problems using the Moment Method. However, FMM needs to sample the fields or currents considering a spatial rate of several subdomain functions per wavelength. This means a large disadvantage because the scattered field and the induced current should be computed at a very large amount of sampling points. That requires a large number of calculations and a huge need of computer memory. In this communication an approach that minimizes the spatial sample rate is presented to reduce this large need of computer memory and CPU-time. The approach is based on the representation of the currents or fields in terms of a series of exponential functions, called "current modes", whose amplitude and exponent are functions that vary slowly along the smooth part of the surfaces of the scatters.

The couple of functions, (amplitude and exponent), that define a current mode can be easily interpolated from their values in a reduced number of sampling points, as they are slow varying functions along the smooth surfaces of the scatters. The procedure for the interpolation of the phase term requires that the function to be sampled has not any jump of 2π radians. This problem can be avoided considering for interpolation the components of the spatial frequency vector (the spatial phase derivatives along the tangent vectors to the scatter surface). The phase function $\Phi(u,v)$ is obtained integrating the components of its gradient that are the spatial frequencies of the current mode.

In order to identify the set of existing modes over a surface, space-frequency localization algorithms such as the STFT (Short-Time Fourier Transform) can be used. The use of a sliding window provides information about variations in the amplitude function of each mode over the patch. It is not necessary to obtain the spatial frequencies very accurately, due to the capacity of the amplitude function to "absorb" small frequency shifts in reduced regions.

Analysis of Localized Defects in Photonic Crystals Using a Source-Model Technique

A. Ludwig* and Y. Leviatan
Department of Electrical Engineering
Technion — Israel Institute of Technology
Haifa 32000, Israel
E–mail: ludwig@techunix.technion.ac.il

The design of novel photonic crystal devices rely on the development of new analytical and numerical techniques for efficient modeling of electromagnetic scattering by photonic band-gap crystals with a localized defect. Towards this end, a novel solution method based on the source-model technique is presented to solve the problem of scattering of an electromagnetic plane wave by a two-dimensional photonic crystal slab that contains an arbitrary localized defect (perturbation). In this method, the electromagnetic fields in the perturbed problem are expressed in terms of the fields due to the fictitious periodic currents obtained from a solution of the corresponding unperturbed problem plus the field due to a yet to be determined fictitious correction current sources placed in the vicinity of the perturbation. The number of yet to be determined localized fictitious correction current sources naturally depends on the perturbation range of influence, defined as the range in which the scattered fields due to the perturbed slab differ substantially from the scattered fields of the unperturbed slab. The perturbation range of influence is frequency dependent and is expected to be limited in extent for frequencies within the bandgap of the unperturbed photonic crystal. This is because at those frequencies the fields decay rapidly as they propagate inside the photonic crystal. This property is expected to enable a numerically efficient analysis of devices operating at frequencies within the bandgap of the photonic crystal. Two error measures, assessing the extent to which the required continuity conditions and the power conservation low are satified, are defined and used to validate the numerical results. To demonstrate the versatility of the proposed method, a few representative structures are analyzed. The power transmission properties of a waveguide perturbation and the characteristics of the resonant frequency in the case of a cavity perturbation are discussed in some detail.

Improved Full-Vectorial Finite Difference Frequency Domain Method for Dielectric Waveguides by Matching Boundary Conditions at Dielectric Interfaces

Chin-ping Yu* and Hung-chun Chang[†]
Graduate Institute of Communication Engineering
National Taiwan University, Taipei, Taiwan 106-17
[†]also with Department of Electrical Engineering and Graduate Institute of
Electro-Optical Engineering, National Taiwan University

The finite difference method (FDM) is a well-known numerical method featured by its simple implementation and the resultant sparse matrix, which make it popular in analyzing the propagation characteristics of the dielectric or optical waveguides, especially for those complicated ones without analytical solutions. In most FDMs, each mesh point is surrounded by four subregions whose permittivities are allowed to be different (K. Bierwirth, N. Schulz, and F. Arndt, J. Lightwave Technol., 34, 1104-1113, 1986). The sparse matrix is formed by discretizing the Helmholtz equations and matching the boundary conditions at the interfaces of all the subregions. Another way is to discretize the wave equations derived from Maxwell's equations (C. L. Xu, W. P. Huang, M. S. Stern, and S. K. Chaudhuri, Inst. Elec. Eng. Proc.-J., 141, 281-286, 1994), which has usually been used in the beam propagation method (BPM). In the conventional FDM, the staircase approximation is widely applied to deal with the dielectric interface in a mesh and the derivatives crossing different media are one main source of the numerical errors. Besides, to well capture the geometry of the dielectric boundary, much finer meshes are needed and large computer storage is consumed.

In this paper, a finite difference frequency domain (FDFD) mode solver based on the uniform Yee's 2-D mesh is derived by directly discretizing Maxwell's equations using the central difference scheme to form two sets of matrix equations involving the six components of the electric and magnetic fields. After some algebra, we can obtain an eigenvalue equation in terms of either transverse electric fields or transverse magnetic fields. The propagation constants and field distributions of guided modes can be obtained by solving the eigenvalue equation using the shift inverse power method. Instead of the staircase approximation for the curved dielectric interface in the Yee's mesh, the boundary conditions are fulfilled at the dielectric interface with the normal and tangential field components which are approximated by interpolation and extrapolation.

As a numerical example, consider a circular step-index optical fiber with core diameter of 6 μm and the refractive indices of core and cladding being 1.45 and 1,respectively. The analytical solution of the mode index for the fundamental mode at wavelength λ=1.5 μm is n_{eff}=1.438604. Using the proposed FDFD mode solver, rapidly convergent and accurate results can be achieved even with very sparse grids. For example, with the grid size of 0.2 μm, we obtain n_{eff}=1.438610 which corresponds to an error of 6×10^{-6}.

Eigenvalues of Arbitrarily-Shaped Waveguides
Using a Mixed-Element Formulation

Gregory M. Wilkins*
Morgan State University
Department of Electrical
and Computer Eng.
Baltimore, MD 21251
(443) 885-3915
gwilkins@ieee.org

Manohar D. Deshpande
NASA Langley Research Center
Electromagnetics Research Branch
Hampton, VA 23681
(757) 864-1774
m.d.deshpande@larc.nasa.gov

John M. Hall
Lockheed Martin Space Operations
c/o NASA Langley Research Center
Hampton, VA 23681
(757) 864-8132
j.m.hall@larc.nasa.gov

A convergence study is performed to assess the effect of a mixed element formulation. Electric field components are represented using a hybrid edge element approach and the corresponding cutoff wavenumbers (eigenvalues) for propagating modes in waveguides with irregular cross sections are determined. Origins of spurious modes commonly encountered in finite element analysis of waveguides are discussed, as well as the specific requirements necessary to overcome this type of nonphysical behavior. The means of solution involves using finite element methods solved on grids that require multi-scale meshes over regions of the waveguide. An algorithm is developed and implemented to account for the field behavior in these regions by considerations of the variation in both location (inhomogeneity) and direction (anisotropy) of the materials within the waveguide. Additional considerations include the modification of the mesh element type for regions where extremely thin layers are used, as well as modifications in the vicinity of a perfect electric conductor. This requires changing from the standard triangular mesh element to the rectangular mesh element for configurations with rectangular boundaries, or changing to quadrilateral elements for boundaries of arbitrary shape (Figures 1 and 2). This allows for a smoother transition in thin multilayer regions and ensures that the natural boundary conditions for electric fields are satisfied at the conductor interface.
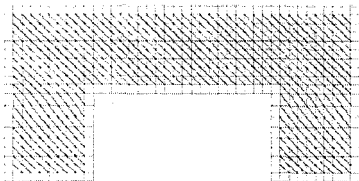
Fig.1: Ridge Waveguide
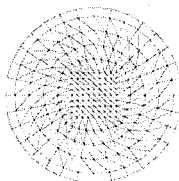
Fig. 2: Circular Waveguide

A BMIA/AIM Formulation for the Analysis of Thin Stratified Large Patch Antennas

Francesca De Vita*, Alessandro Mori, Paolo De Vita, Angelo Freni

Department of Electronics and Telecommunications
University of Florence
Via di Santa Marta n. 3, 50139 Florence (Italy)
Tel. +39.055.4796381, fax: +39.055.4796441

The analysis of large-scale complex patch antennas using the method of moments (MoM) usually requires large computational resources in terms both of dynamic memory and computation time. An efficient numerical method is desiderable in the case of an optimization process in which several slightly different structures must be analyzed. Several techniques have been developed for the fast computation of this problem. These techniques, based on a modification of the classical method of moments (MoM), allow a fast evaluation of the reaction integral and, when an iterative solver is used, a fast matrix-vector multiplication. Examples include the adaptive integral method (AIM), the steepest descent-fast multipole method (SDFMM) , the matrix decomposition algorithm (MDA), and the banded matrix iterative approach/canonical grid method (BMIA/CAG). The BMIA/CAG method, conveniently modified, can be profitably employed for the analysis of large-scale stacked patch antennas. However, the original formulation has to be modified in order to describe patches of arbitrary shape and size in a regular grid and a BMIA/AIM method [A. Freni et al., MMET*02, 1, 48–53, 2002] has been introduced by considering a set of auxiliary basis functions based on a multipole expansion as in the AIM. This approach seems to be convenient when compared to the Conjugate Gradient-FFT in the case of stacked patches on a ground plane consisting of more than two levels; moreover it can consider the presence of elements not necessarily parallel to the ground plane. The key feature of the BMIA/AIM is the use of a factorized approximation of the Green's function in the form $\underline{G}(\vec{\rho} - \vec{\rho}', z, z') = \sum_{n=1}^{N} (\vec{\rho} - \vec{\rho}') U_n(z) V_n(z')$, where primed and unprimed coordinates refer to source and test position respectively. Here, we present a formulation that allows us to extend the applicability of the BMIA/AIM method to multilayered structures, maintaining its accuracy without increasing its complexity. In particular, we use a closed form expression for the spatial domain Green's functions performed applying the discrete image method [K. A. Michalski et al., IEE Proc.- Microw. Antennas Propag., 142, 3, 1995]. This method approximates the spectral domain Green's function through a series of complex exponentials, using the generalized pencil of function method (GPOF) [Y. Hua et al., IEEE Trans. Antennas Propagat., AP-37, 2,229–234,1989], thus avoiding the numerical evaluation of the Sommerfeld Integral. Applying the well-known Sommerfeld identity we then obtain an expression for the spatial domain Green's function similar to that obtained in the free space case. Therefore, considering the source and test point in the same layer, we can still apply a Taylor's series expansion, thus obtaining the spatial domain Green's function in a form suitable for the BMIA/AIM method. Following this procedure only a few modifications to the available codes are required and efficiency remains unchanged.

Domain Decomposition Method in Conjunction with DP-FETI for Modeling RCS Computation of Large Finite Arrays

Kezhong Zhao*, Marinos Vouvakis, Seung-Choel Lee, and Jin-Fa Lee
ElectroScience Lab., EE Dept., The Ohio State University, OH 43212, USA
(Commission B-B6.1 Frequency domain methods)

The domain decomposition method (DDM) is very popular and very effective in solving Lapace\Possion equations. However, when solving the Helmholtz equation, the classical DDM is not effective because the convergence mechanism has encountered problems. The widely used Dirichlet-to-Dirichlet, Neumann-to-Neumann, and Dirichlet-to-Neumann transmission conditions do not converge well. Even with Robin's condition, only the propagating mode damps, but not the evanescent mode. In this paper, we extend the optimum Robin transmission condition suggested by Gander, Magoules, and Nataf (M. J. Gander, F. Magoules, and F. Nataf, *SIAM J. Sci. Compt.*, 24, 38-60) to the vector wave equation so that the convergence of DDM is greatly improved.

Another very important technique for modeling large antenna arrays is the Mortar technique (C. Bernardi, Y. Maday, and A. T. Patera, *Nonlinear partial differential equations and their applications*, 13-51, 1994). With Mortar technique, the meshes in the interface between any two domains do not need to be conforming. This significantly relaxes the constraint imposed on mesh generation. The Mortar method is most valuable in optimal design studies. For example, if some parameters in a certain region need to be changed, using "brute-force" FEM, the computation needs to be re-done on entire geometry, while with Mortar method, the additional computation is only performed on the perturbed region. However the classical Mortar method was implemented through the use of the Lagrange multiplier technique. It results in undesirable zero diagonal terms in the final matrix. Following the insight from reference (R. Dyczij-Edlinger, G. Peng, and J. F. Lee, *CMAME*, 169, 297-309, 1999), which suggests that Lagrange multiplier is a special case of gauge condition, this paper formulates a new Mortar technique that avoids the undesirable zero diagonal block, and introduces unknowns which are more physically meaningful than the Lagrange multiplier unknowns.

Finally, a dual-primal Finite Element tearing and interconnecting (DP-FETI) like algorithm is introduced to further speed up the DDM process and more importantly to significantly reduce the memory requirement. The proposed approach has been applied to a 300 by 300 Vivaldi antenna arrays, which would require close to 1 billion unknowns if "brute-force" FEM is attempted, using only 1.4 GB memory and obtain the solution exactly the same as the "brute-force" FEM solution in 12 hours.

New Numerical Methods for the Prediction
of EM Scattering by Electrically Deep Cavities

Nolwenn Balin[*] [1,2,3] and Abderrahmane Bendali [2,3]

[1] MBDA-France, 2 rue Béranger, 92323 Châtillon, France
[2] CERFACS, 42 av. G. Coriolis, 31077 Toulouse, France
[3] MIP, UMR5640 (CNRS-UPS-INSA), INSA, 135 av. de Rangueil, 31077 Toulouse, France

It is well known to specialists in stealth technology that an inlet significantly contributes to the Radar Cross Section (RCS) of the surrounding aircraft. Today, the RCS computation of air-breathing aircraft is a major challenge because this case cannot be efficiently handled by standard methods. Indeed, inlet shapes result in lower accuracy for the asymptotic methods and difficulties to converge for the fast iterative full wave solvers. Likewise, Finite Element (FE) or Boundary Integral (BI) methods cannot be used directly, because of the huge size of the full problem.

Recently several approaches based on domain decomposition or hybrid techniques have been proposed: FE-BI formulations coupled with Shooting and Bouncing Ray (SBR) methods, or multi-methods based on generalized matrices, ... But none of them has been successfully applied in the general cases. In this paper, we present a new method based on a BI formulation coupled with an asymptotic method for analyzing the scattering of deep open-ended cavities, residing in a big and relatively smooth (aircraft-like) structure.

At first, the cavity contribution is determined through an efficient BI formulation. The principle is to define a domain decomposition consisting of p successive pieces, the interfaces of which are sectional surfaces of the cavity. Next, the pieces are successively eliminated one by one, so that the cavity's behavior is reduced to the determination of the currents on the aperture. Thus, instead of solving one problem of size N, p problems of size N/p are solved, hence significantly reducing the computational costs. Even though the principle is the same as the usual procedure in FE calculation, the use of BI here also yields a very low numerical dispersion.

Once this method has been applied, the cavities can be considered closed for the external coupling part of the process, which is then better suited for asymptotic or multipole methods and consequently for the coupling step. Then, we define an overlapping boundary decomposition, where each subsurface corresponds to a solution procedure (exact, asymptotic or multipole). Finally, the coupling process between the subsurfaces is derived from an additive overlapping Schwarz method.

Good results have been obtained for predicting the scattering behavior of the COBRA cavity with cap, a test geometry inspired by a benchmark case proposed by MBDA-F at the JINA workshop 2002. Numerical results will be presented.

Teaching the FDTD Method in the Junior Undergraduate Electromagnetics Course

John R. Natzke
Department of Math, Computer Science, and Engineering
George Fox University
Newberg, OR 97132-2697

The primary objective of this initiative was to increase the exposure of numerical methods to the electrical engineering undergraduate students. With a numerical methods requirement becoming less prevalent in engineering curricula, a need was seen to introduce the students to some of these methods wherever possible. A separate numerical methods course is now mostly offered as an elective, in part because software applications with advanced, built-in functions are readily available. However, it would greatly benefit the students to develop some of these advanced techniques themselves. This approach also provides the advantage of experiencing it within the context of particular engineering courses.

One of those opportunities presented itself in our Electromagnetic Fields and Waves course taught in the junior year. With the introduction of transmission lines in Chapter 2 of the text (F. T. Ulaby, *Fundamentals of Applied Electromagnetics*, Prentice-Hall, 2004), the finite difference form of the telegrapher's equations were readily derived and coded on the computer by the students themselves. Granted, some electromagnetics texts include various numerical techniques, but these are relegated to the later chapters of the book. The approach here was to infuse the course with the FDTD method when applicable, as opposed to a full-fledged presentation on the technique, especially since our three-hour course is already limited on time.

By the introduction of the FDTD method, the electromagnetics students were able to gain greater insight on propagation and reflection of waves on transmission lines. Also considered were lossy lines, discontinuities, and simple radiators. The coding was done in MATLAB, which enabled immediate animation of the transient solution through its graphics tools. In the steady state, the students compared the results to their analytical solutions of the wave equation, and both the advantages and limitations of numerical methods became readily apparent. A pedagogical analysis and critique of the effort will be presented, along with a sampling of student work.

Although various numerical techniques could be utilized, a time-domain method capitalizes on the visualization appeal, an undeniable trend in academics in these times. Furthermore, the students are then given the opportunity to program FDTD solutions in other courses, such as our microwave engineering senior elective. Application to the transient analysis in the sophomore circuits course is also being considered.

A Fourth-Order FDTD Scheme with Long-Time Stability

Kyu-Pyung Hwang
Intel Corporation
Components Research
CH5-166
5000 W. Chandler Blvd.
Chandler, AZ 85226-3699
Tel:(480)552-0394 Fax:(480)554-7214
E-mail:kphwang@ieee.org

As an alternative to standard second-order Yee's finite-difference time-domain (FDTD) method, various forms of high-order FDTD methods have been explored for their superior numerical accuracy. For time-domain electromagnetic simulations involving electrically large structures, the advantage of these high-order FDTD methods in terms of numerical efficiency become more pronounced over second-order FDTD method. A large scale time-domain electromagnetic simulation typically requires stable time integration for a very long time and thus a stable and accurate time integrator is an essential part of a high-order FDTD algorithm to produce reliable high-order time-domain solutions. It is also desirable for a high-order scheme to maintain the same order of accuracy both in space and time.

In this paper, a new high-order FDTD scheme is proposed with fourth-order accuracy in space and time. The fourth-order backwards differentiation method is used for time integration while spatial derivatives are discretized by fourth-order finite difference approximation. This new combination of time and space discretizations is employed to derive FDTD equations for two-dimensional (2-D) TE case. Special modifications (K.-P. Hwang and A. Cangellaris, *Proc. 2001 IEEE AP-S Int. Symp. USNC/URSI National Radio Science Meeting,* URSI Digest, 251, Boston, MA, July 2001) are made near metallic and dielectric boundaries to preserve the fourth-order accuracy and long-time stability of the time-domain solution. Unlike in Fang's (4,4) scheme (J. Fang, *Time Domain Finite Difference Computation for Maxwell's Equations, Ph.D. Dissertation.* Berkeley, CA: Univ. California at Berkeley, 1989) where coupled time and space operators cause troubles in treating electric and magnetic losses, the anisotropic PML absorbing boundary condition (S. D. Gedeney, *IEEE Trans. Antennas Propat.,* 129, 1630-1639, 1996) is easily implemented in this fourth-order FDTD scheme. The fourth-order convergence rate of the proposed FDTD solutions in space and time is verified using 2-D rectangular cavities in terms of L_2 norm errors. Based on the cavity simulation results, comparison is made between the proposed fourth-order FDTD scheme and Yee's second-order FDTD scheme in terms of computational efficiency. A large scale 2-D electromagnetic scattering problem is considered to prove the numerical advantage of the new (4,4) scheme.

Time-Domain Split-Field Formulation for Both Periodic Boundary Condition and PML

Davi Correia* and Jian-Ming Jin
Center for Computational Electromagnetics
Department of Electrical and Computer Engineering
University of Illinois at Urbana-Champaign
1406 Green St., Urbana, IL 61801. E-mail: dcorreia@uiuc.edu

Periodic structures as frequency selective surfaces and double negative metamaterials have gained increasing attention in the last decade or so. Analysis of such structures in the frequency domain has successfully been done. In the time domain a split-field technique has recently been proposed to solve the problem of delay in the grid (J. A. Roden, S. D. Gedney, M. P. Kesler, J. G. Maloney and P. H. Harms, *IEEE Trans. Microwave Theory Tech.*, vol. 46, no. 4, pp. 420-427, 1998) where the authors used uniaxial perfectly matched layers (PML). In this talk we will present an equivalent formulation based on split-field PML as well as split-field for periodicity. When working with the split-field PML one separates the field due to x-derivative from the one due to y-derivative (J. P. Berenger, *J. Comput. Phys.*, vol. 114, no. 2, pp. 185-200, 1994). This is the same idea behind the split-field formulation for periodic boundary conditions where the derivative in the periodicity direction adds an extra term to the update equations. Working with a formulation that involves split-field for both cases, the effect of the PML is detached from the effect of the periodicity. The final equations involve auxiliary variables $P_z = E_z e^{jk_y y}/\eta_0 = P_{zx} + P_{zy}$, $Q_x = H_x e^{jk_y y}$ and $Q_y = H_y e^{jk_y y}$ in the two-dimensional case. The variable P_{zx} will be attenuated in the PML region while P_{zy} will take into account the time delay in the grid in the periodicity direction. After splitting the P_{zy} term into "a" and "b" components and manipulating the terms we have

$$\frac{j\omega\epsilon_r}{c_0} P_{zy}^a = -\frac{\partial}{\partial y} Q_x$$
$$\frac{j\omega\epsilon_r}{c_0} P_{zx} = \frac{1}{s_x}\frac{\partial}{\partial x} Q_y$$
$$(\epsilon_r - \sin^2\theta) P_{zy}^b = [\sin\theta Q_x^a + \sin^2\theta (P_{zx} + P_{zy}^a)]$$

where θ denotes the incident angle and s_x is the standard lossy term for the PML. A similar procedure is done to Q_x and Q_y. Note that the PML works only on P_{zx} (and Q_y, not shown) while the periodicity is taken care by P_{zy} (and Q_x, not shown).

The technique is equivalent to the uniaxial PML implementation but the effects of periodicity and attenuation are seen more clearly with our approach. The comparison of the two split-field approaches and their similarities will be considered in this study. The extension to the three-dimensional problems is straightforward and will also be addressed.

Multiresolution Time-Domain Using Spatially Varying Basis Functions

*N. Kovvali, W. Lin and L. Carin
Department of Electrical and Computer Engineering
Duke University
Durham, NC 27708-2091

The multiresolution time-domain (MRTD) algorithm has recently emerged as a powerful tool for numerical solution of the time-domain Maxwell's equations. It has been shown that the MRTD technique exhibits good dispersion properties as compared to the finite-difference (FDTD) technique, even at very low sampling rates. This approach is based on a multiresolution analysis, utilizing orthonormal (or biorthogonal) scaling function and wavelet expansions. Importantly, for a given spatial sampling rate, it is the choice of basis which determines the properties of the space spanned. This ultimately dictates the numeric accuracy of the final solution. It is desirable to be able to control the accuracy of the solution as a function of spatial position. All these approaches, however, are based on a multiresolution analysis, utilizing the same basis over the whole domain, and hence the accuracy of the solution is the same at any spatial position.

In this work we present an MRTD framework wherein it is possible to control the accuracy of the solution as a function of spatial position. Our approach is based on a multiresolution analysis, utilizing spatially varying basis functions. The computational domain is divided into several intervals and a *different* orthonormal basis expansion is used on each interval. Specifically, we use the orthonormal basis expansion on an interval in Y. Meyer's construction. This construction uses a Gram-Schmidt orthogonalization procedure to obtain the basis functions which span an interval. The bases themselves are from the compactly supported Daubechies least-asymmetric family, with different orders (vanishing moments) used in different intervals. Therefore the accuracy of the solution is different in each interval. In the regions where the fields are expected to vary smoothly we use basis functions with larger support, and in the regions where the fields are expected to be fast-varying we use basis functions with smaller support. This is justified, because (at the same scale) the basis functions with larger support span a much smaller function space than those with smaller support. Although the memory and CPU requirement of this approach is very similar to the conventional MRTD scheme, it provides us with a framework to use a different scale in each interval. The scale dictates the number of expansion coefficients, and this in turn determines not only the accuracy of the solution but also the memory and CPU requirements. In the regions where the fields are expected to vary smoothly we use basis functions at a lower scale, and in the regions where the fields are expected to be fast-varying we use basis functions at a higher scale. This is justified, because the basis functions at a lower scale span a much smaller function space than those at a higher scale. This is analogous to a multi-grid scheme where the grid-size can be varied as a function of spatial position.

The spectral properties of the 'edge' basis functions from Meyer's construction of orthonormal wavelet bases on the interval are not completely satisfactory. In fact, due to the nature of the construction, the 'edge' basis functions have smaller support. This leads to 'edge' basis functions which are typically higher bandwidth than the 'interior' functions. Numerical accuracy issues arise in the computation of the stencil coefficients. We therefore consider another construction of orthonormal wavelet bases on the interval, due to Cohen, Daubechies and Vial. The basis functions obtained from this construction have better spectral properties than those obtained from Meyer's construction.

These ideas are demonstrated with several numerical examples.

Multiresolution Time-Domain Using Ridgelet Basis Functions

*W. Lin, N. Kovvali and L. Carin
Department of Electrical and Computer Engineering
Duke University
Durham, NC 27708-2091

The multiresolution time-domain (MRTD) algorithm has recently emerged as a powerful technique for numerical solution of Maxwell's equations. The MRTD scheme utilizes a field expansion in terms of orthonormal (or biorthogonal) basis of scaling and wavelet functions. In many applications of interest, certain properties of functions manifest themselves in higher dimensions only. The aforementioned procedure of choosing a basis (with some properties) in one dimension and extending the basis to the higher dimension may then prove to be too limiting. Therefore, it is preferable to start with an orthonormal (or biorthogonal) basis, directly in the higher dimension. One can now aspire to capture the desired properties of a higher dimensional function by proper choice of this basis.

From a mathematical point-of-view, in higher dimensions, wavelets are not very effective in describing linelike, hyperplane and other non-pointlike structures. This has motivated the development of ridgelets which constitute a complete and orthonormal basis in $\mathbf{L}^2(\mathbf{R}^2)$ for example. Problems of this nature exist, for example in image analysis. In electromagnetics, the phenomenon of wave propagation often manifests itself as a hyperplane in two or three dimensions. Ridgelets are therefore the natural mathematical tool to analyze this phenomenon.

The orthonormal ridgelet is composed of the superposition of ridge functions, and in two dimensions it is given by,

$$\rho_{k,l}(x,y) = \tfrac{1}{4\pi} \int_0^{2\pi} \psi_k^+(x\cos\theta + y\sin\theta) w_l^\varepsilon(\theta) d\theta$$

where, $\psi_k^+(x)$ denotes the result of the Riesz order-1/2 fractional differentiation operation on the k-integer translate of the wavelet $\psi_k(x)$ and $w_l^\varepsilon(\theta)$ denotes the l-integer translated periodized scaling (for $\varepsilon = 0$) or wavelet (for $\varepsilon = 1$) functions. By appropriate choice of the wavelet $\psi(x)$, we can construct biorthogonal ridgelets, which we apply as basis functions for the field expansion in this work.

The advantage of the ridgelet framework as compared to the conventional MRTD is that it usually requires less expansion coefficients (unknowns) to describe the fields. In a large problem, the memory and CPU-time savings can be large, especially for sparsely distributed inhomogeneous systems (this is due to the infinite-support property of the ridgelet).

Another important advantage of the ridgelet framework is that we can apply Radiation Boundary Conditions (RBC) naturally, as opposed to using the more complex and computationally intensive Perfectly Matched Layer (PML) absorbing boundary condition to truncate the computational domain. The analysis in two or three dimensions is therefore greatly simplified.

These ideas are demonstrated with several numerical examples.

Metamaterial Modeling Using Composite Cell MRTD Techniques

Nathan Bushyager* and Manos Tentzeris
School of ECE, Georgia Institute of Technology, Atlanta, GA 30332
nbushyager@ece.gatech.edu

Recently a new method has been presented that allows the modeling of complex PEC/dielectric structures within a single multiresolution time-domain (MRTD) cell (Bushyager and Tentzeris, Proc. 2003 EuMC, Munich, Germany, Oct. 2003). This technique uses wavelet decomposition to apply pointwise effects at the equivalent grid points in the MRTD grid. The equivalent grid points in an MRTD cell are the points inside the grid where distinct field values can be reconstructed (Sarris and Katehi, IEEE Trans. MTT, 50.7, 1752-1760, July 2002). Initially, this technique was presented as a method of modeling perfect electrical conductors (PECs) with an MRTD cell, but the technique has been further expanded to allow other localized effects to be modeled such as lumped elements. Using this technique it is possible to use the time and space adaptive grid that is inherent in the MRTD method for complex microwave structures. By using this grid coarse cells can be used in the majority of the grid and high resolution cells can be used only when needed. Furthermore, the resolution can be changed with time to account for the propagation of high frequency signals through the circuit. This decreases the simulation time and makes it possible to simulate larger and more complicated problems.

One class of structures that is particularly well suited for simulation with this technique is metamaterials. Metamaterials are characterized by a repeating array of finely detailed structures. Using the subcell MRTD technique, it is possible to place part or even an entire metamaterial unit cell within an MRTD cell. The space surrounding this complex structure can be treated with more coarse cells, leading to a very efficient simulation. In addition, like other time-domain full-wave simulators, the complete physics of Maxwell's equations are simulated, allowing these structure's complex electromagnetic interactions over a broad band to be fully modeled. Both electric and magnetic conductors can be modeled at the subcell level, as well as lumped elements. This allows the technique to be applied to printed elements in layered materials (Ziolkowski, IEEE Trans. Ant. Prop., 51.7, 1516-1529, July 2003) and to metamaterials that consist of periodically loaded lines (Siddiqui, Mojahedi, and Eleftheriades, IEEE Trans Ant. Prop., 51.10, 2619-1215, Oct. 2003).

Using this simulator a number of properties of metamaterials can be simulated. In addition to S-parameters of the devices, the fields inside the devices can be determined to examine their operation. Comparisons between the theory of operation of the device and the simulation of the fields inside the device can be made. The focusing properties of the device can be measured as well as near and far field radiation parameters. Finally, it should be noted that this technique is perfectly compatible with periodic structure simulation techniques that have been developed for the FDTD method.

249

High order and highly stable MRTD techniques: Formulation and Applications

Costas D. Sarris

The Edward S. Rogers Sr. Department of Electrical and Computer Engineering,
University of Toronto, Toronto, ON, Canada
E-mail: cds@waves.toronto.edu

Several Multiresolution Time Domain (MRTD) schemes have been formulated and presented in the literature, following the Method-of-Moment (MoM) based procedure outlined in [Krumpholz and Katehi, IEEE Trans. Microwave Theory Tech., 1995]. According to the latter, electromagnetic field components are expanded in basis functions of choice in space and pulses in time. As a result, the MRTD time integrator is the well-known leap-frog scheme, also employed in FDTD. An obvious shortcoming that this formulation results in, is the significant decrease in the stability limit of MRTD, that turns out to be a fraction of the FDTD stability limit (typically less than one-half of it in two and three dimensions).

This paper offers a new perspective for this problem. It is explicitly shown that the origin of the decrease in the stability limit is the low-order temporal expansion of field components, that previous MRTD formulations had adopted. On the other hand, if the MoM procedure that Krumpholz and Katehi applied in the space domain is extended to the time domain as well, the stability properties of the scheme are completely recovered. In addition, MRTD becomes a high-order of convergence scheme, in the sense that its truncation error decreases with the cell size in a faster than quadratic rate. Moreover, this development addresses the questions that [Shlager and Schneider, IEEE AP-S Symp. Antennas Prop., 1997] raised, indicating through a Battle-Lemarie MRTD dispersion analysis that this scheme did not demonstrate the dispersion performance of a high-order scheme. This also is a consequence of relying on leap-frog for the time integration. It is noted that the use of scaling functions, such as Coifman or Daubechies in the time domain is completely free of the well-known boundary condition and material modeling issues that accompany any MRTD scheme. Hence, this paper presents a systematic way of formulating time-stepping methods, that present an excellent alternative to established high-order techniques, such as the Adams-Bashforth and Runge-Kutta methods.

In order to facilitate the practical application of the proposed MRTD schemes, several hybridizations of those are studied and demonstrated. Including wavelets in the formulation, multi-resolution schemes are derived and hybridized with single-level (scaling function based) techniques. It is noted that an S-MRTD scheme is easily interfaced to a W-MRTD scheme (of the same wavelet family), by just choosing the cell size of the former to be equal to 2^l times the cell size of the latter, l being the number of wavelet levels of W-MRTD.

Applications of interest involve the modeling of wireless channels. Wavelet-based adaptive gridding provides a rigorous way to implement an "effective" moving window [Luebbers et al., IEEE AP-S Symp. Antennas Prop., 1997] that follows the signals accross a large scale wireless link. The high order of convergence, along with the high stability and adaptivity of the proposed MRTD, underlines the capability of this technique to become a reliable and efficient numerical tool for this type of problems.

Efficient Indoor Wireless Channel Modeling with a High-Order MRTD Technique

Abbas Alighanbari and Costas D. Sarris
The Edward S. Rogers Sr. Department of Electrical and Computer Engineering,
University of Toronto, Toronto, ON, Canada
E-mail: cds@waves.toronto.edu

The application of the conventional Finite Difference Time Domain (FDTD) technique to electrically large problems is severely limited by the phase errors accumulated by numerical waves propagating in an FDTD grid. In order to limit these phase errors, a dense discretization is typically employed. However, this obviously results in a significant increase in the computational resources needed to simulate practically important cases, such as the wave propagation in indoor wireless channels. For the efficient solution of such problems, several high-order methods have been proposed, such as the modified FDTD (2,4) scheme of [Hadi and Piket-May, IEEE Trans. Antennas Prop., 1997].

A family of methods that has yet to be applied to wireless propagation problems is the Multiresolution Time Domain Scheme of [Krumpholz and Katehi, IEEE Trans. Microwave Theory Tech., 1995]. A dispersion analysis of the latter shows that it does not exhibit the convergence properties of a high-order scheme, due to the fact that it employs pulse functions for the temporal expansion of field components. As a result, its temporal integrator is the well-known FDTD leap-frog scheme, that is second-order only.

This paper proposes MRTD schemes with high-order spatial and temporal finite difference operators, stemming from the expansion of electromagnetic field components in Daubechies and Coifman functions [I. Daubechies, Ten Lectures on Wavelets, SIAM, 1992] in both space and time. These schemes present excellent convergence properties and constitute an efficient class of methods for the simulation of electrically large structures. In addition, the use of wavelet bases provides for the straightforward implementation of adaptive mesh refinement, via the thresholding of wavelet coefficients, in the sense of the wavelet based image compression, applied in signal processing.

The proposed techniques are applied to two-dimensional indoor wireless channel modeling. Source modeling is rigorously studied and a total-field-scattered field approach, appropriately formulated for the basis functions employed in this work, is suggested. The application of boundary conditions is extensively studied. In addition to the simple perfect electric conducting conditions that have been discussed in the literature before [Krumpholz and Katehi], impedance boundary condition and knife edge modeling (both metal and dielectric) is presented.

A New Domain Decomposition Approach For Solving Large Problems using the FDTD

Hany E. Abd El-Raouf and Raj Mittra
Electromagnetic Communication Laboratory, 319 EE East
The Pennsylvania State University
University Park, PA 16802
rajmittra@ieee.org

Abstract

Solution of large problems using a numerically rigorous approach is always challenging because of the heavy burden they impose on the CPU. Domain decompositions is one approach to solving such problems by breaking them into smaller and manageable sizes. However, typically the iteration approach that is using to construct the solution in the domain decomposition approach applied in the frequency domain techniques lead to convergence problems; hence, such an approach has not found widespread use in the literature.

The situation is very different in the time domain where the physics of the wave propagation enables us to set up a scheme that synthesizes the solution in a systematic, step-by-step manner. We use the scattered field formulation in the context of the FDTD algorithm and solve the field problem in the first domain, using PML layers to terminate the end of the domain. We store the tangential electric field in the time-domain at an interface located in the overlap region, which penetrates the PML layers. This field is then used to generate the solution in adjacent domain, and the process is continued until all the domains have been analyzed, including (if necessary) along the reverse direction.

For the sake of illustration, consider the case of a rectangular box whose dimensions are $3\lambda \times 10\lambda \times 1\lambda$. (Note: The problem size can be orders of magnitude larger and can still be handled by the domain decomposition method, though not by a direct approach.) Let the incident wave be θ−polarized with the direction of propagation $\theta = 45°$, $\phi = 180°$. We divide the box along the y-direction and, for this case, it is sufficient to send the field information only once from the two edges toward the center of the box, as shown in Fig.1. Figure 1b compare the direct (no decompositions) FDTD result to those derived by using the present technique. The agreement is seen to be excellent between the two results in the E-plane, and only some minor differences are seen to be present in the H-plane results.

(a)

(b)
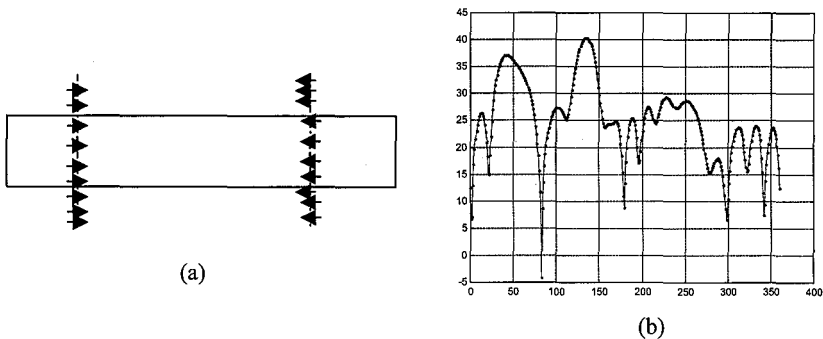
Fig. 1. Scattering from a rectangular box. (a) configuration for sending the information between the domains, (b) RCS / λ^2 (solid : direct , dots: domain decomposition).

252

An FDTD-based Domain Decomposition Approach to the Solution of Coupling Problem between two Arrays.

Hany E. Abd El-Raouf and Raj Mittra
Electromagnetic Communication Laboratory, 319 EE East
The Pennsylvania State University
University Park, PA 16802

Abstract

Modeling and Simulation of large Arrays is a challenging problem, and it becomes even more formidable as one deals with the coupling problem between two arrays, especially when the separation distance between them is not small, and the structure between the array is inhomogeneous, coated with RAM material, for instance. In this paper we present an FDTD-based domain decomposition approach to the solution of the above coupling problem. Since the original problem is very large, it is difficult to handle the entire geometry in one step. To render the problem manageable, we divide the computational domain into two sub-domains. The first one of these includes the transmitting antenna with a part of the absorber (or the buffer in this example). The two domains overlap and the first one is terminated by PML layers. The tangential electric field at the planar interface between the two sub-domains is stored in the time domain, and is later used as a boundary condition when analyzing the next sub-domain, which contains the second array. Figure 1 shows the geometry of coupling problem between the two arrays, each one of which is 10 x 10 patch elements excited by a coaxial probe. The two arrays are above a substrate covering an infinite ground plane. The PEC buffer has the same height as that of the substrate. The current in the first element of the receiving array is shown in Fig.1(b), and the coupling between the two arrays is computed to by processing the FDTD results. The coupling level was found to be –28 dB for this problem.
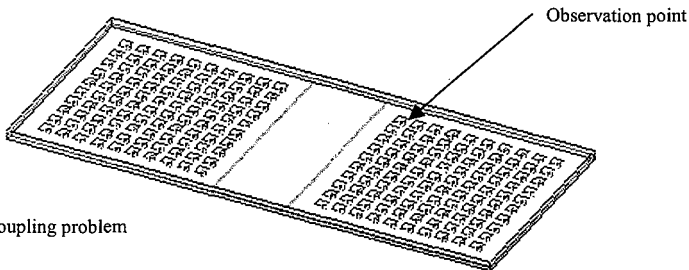
(a) Array coupling problem

Observation point
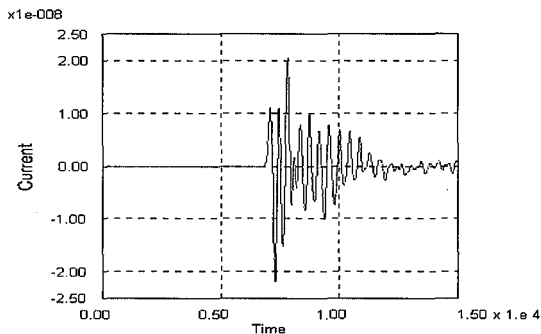
(b) Time-Domain signature in the receiving array

253

Accurate Representation of Complex 3-D Geometries for Conformal FDTD Simulations Including Solids and Thin Sheets

S. Benkler*, N. Chavannes, J. Fröhlich, H. Songoro and N. Kuster
Foundation for Research on Information Technologies in Society (IT'IS); ETH Zurich
Schmid & Partner Engineering AG (SPEAG), 8004 Zürich, Switzerland
Phone: +41-1-245 9684, Fax: +41-1-245 9779, e.mail: benkler@iis.ee.ethz.ch

Introduction

The Finite-Difference Time-Domain (FDTD) method originally presented by Yee has become the most widely used technique in electromagnetic computations. However, the classical staircasing approach may lead to significant uncertainties for grid non-conformally aligned structures. An effective way to reduce staircasing errors is the incorporation of locally conformal meshes, e.g., sub-cells as presented in (S. Dey et al., IEEE-MW GWL, 7, 273-275, 1997) in which modifications in the original Yee scheme need only be applied to cells in the immediate vicinity of the structure's material interfaces.

This study presents novel methods enabling an automated, rigorous analysis and processing of arbitrary complex 3-D CAD geometries and their application for enhancement of FDTD modeling through the incorporation of sub-cell techniques.

Objectives

The objectives of this study were (1) the development and implementation of novel and robust 3-D CAD analysis algorithms for the fully automated generation of locally conformal FDTD meshes from arbitrarily complex geometries and (2) their application to different sub-cell schemes enabling improved FDTD material transitions.

Methods

All implementations and simulations were conducted by application of the FDTD based platform SEMCAD (SPEAG, Zurich, Switzerland, www.semcad.com) which provides a 3-D ACIS based solid modeling environment: (1) To determine all intersections with the surface triangles mesh of the CAD object, computer graphics methods are used, e.g., the scan converting algorithm in 2-D and 1-D. In addition, ideas from the ray-tracing algorithm have been applied, but were modified to a computationally less intensive method. (2) By distinguishing topologies and distances between entry and exit points along FDTD grid lines, thin-sheets and solids can be separately treated in the same framework. (3) The problem of a continuous representation of tilted thin PEC sheets in FDTD was solved with an innovative new approach. Instead of first selecting the nearest grid node, the exact intersection position is kept. With the cut-pattern of a voxel, a topologically correct 'rounding' algorithm was derived, guaranteeing continuity and connectivity.

Results and Discussion

The developed and implemented techniques were applied and validated to different largely inhomogeneous, complex 3-D configurations, e.g., CAD models of cars, mobile phones and anatomical human models, each consisting of several hundred distinguished sub-parts. The techniques have proven to be suitable for the generation of locally conformal 3-D FDTD grids for real-world geometries without any limitations to complexity.

Aside from collecting and processing staircase and conformal information about the geometry, two additional problems have been solved: (1) Objects with solid and thin sheet character can be discretized in a fully automated manner. (2) A new and fully automatic algorithm addresses the problem of continuous discretization without determining threshold numbers and monitoring the assigned edges.

In addition, the suitability and limitations of the new methods were validated on the basis of different sub-cell schemes for improved modeling of PEC and dielectric structures.

254

Efficient Analysis of On-Chip Interconnects by Compact

Crank–Nicolson (CN) FDTD Method

Dagang Wu* and Ji Chen
Department of Electrical and Computer Engineering
University of Houston
Houston, TX 77204

With the increasing clock rates and chip area, the performance of high-speed mixed-signal circuits become more dependent on the designs of on-chip interconnects. Accurate characterization of the on-chip interconnects frequency-dependent behavior is essential to optimal circuit system designs. Various full-wave numerical methods have been proposed to efficiently extract the frequency-dependent parameters of interconnects. The compact finite difference time domain (FDTD) has been successfully applied to perform such extractions for general on-chip interconnects. However, due to the Courant-Friedrichs-Lewy stability condition, the number of iterations in the simulation is on the order of millions and it becomes computationally expensive to model such electrically small integrated circuits (IC) and on-chip interconnects.

To remove the limitation of such small time step sizes, some unconditionally stable FDTD methods have been proposed. Compact alternating direction implicit (ADI) FDTD algorithm has been applied to analyze on-chip interconnect structures. However, recent research has shown that the truncation error of this algorithm is case dependent and its accuracy degrades as the time step size increases.

The compact Crank–Nicolson (CN) FDTD, an unconditionally stable FDTD method with low truncation error, is employed here to make efficient modeling of interconnects. Although the dispersion error of this algorithm is larger than that of the FDTD method, it can be controlled for the electrically small interconnects. In this work, several interconnect structures will be simulated using this new approach. The accuracy and efficiency of this algorithm are demonstrated through the comparison with the those of the traditional FDTD method.

255

Integrated Passive Circuit Design for RF Switch-Filter Module

Xiaomin Yang[1], Thomas X. Wu[1], Riad Mahbub[1,2], David Whiteman[2], Berry Leonard[2], and Albert Gu[2]

[1]University of Central Florida, Orlando, FL 32816
[2]Sawtek, Inc., Apopka, FL 32703

Wireless communication has become increasingly important in the past several years. The size and cost have become the most critical factors to be considered for the design of wireless components. Current trends in the architecture and design of wireless handsets are based on multi-band and multi-mode operation. This requires multi-port switch solutions, which involve antenna switching, mode selection switching, and band selection switching. As a result, the component count in handsets also increases. However, continued reductions in the size of individual, discrete components, particularly in the field of passive components, are having diminishing returns. There is a new trend based on the multi-chip module (MCM) technology in the design. The basic idea of MCM technology is to interconnect chips inside a single package. There are several basic components needed to build switch-filter modules, including switches, control logic ICs, and passive circuits and filters. The integration of a number of passive components into one single chip results in a part of smaller dimensions and a reduced number of surface mount placements as compared with a discrete implementation on a PCB. This, in turn, reduces the overall number of parts needed for manufacturing and leads to more efficient wireless products with reduced size and weight.

In this paper, we focus on the integration of passive circuits. We present the development of our modeling and simulation methodologies. For different EM simulators, the tradeoffs between accuracy and simulation time are discussed. The right design tool and the accurate model lead to the success of integrated passive device (IPD) design, so that we can well predict the performance of an IPD with simulation, and shorten design cycle. Low-pass filter and diplexer are two important components to be integrated in the switch-filter module. We have designed and optimized low-pass filters and diplexers on the GaAs substrate. The reduced die size is able to lower the cost, which is surely preferable.

Analysis of Critical Manufacturing Tolerances on Millimeter-Waves Transitions

T. Cavanna[1], E. Franzese[2], E. Limiti[3], G. Pelosi[2], S. Selleri[2], A. Suriani[1]

[1]Alenia Spazio	[2]DET	[3]DIE - University of
Via Saccomuro 24	*University of Florence*	*Rome 'Tor Vergata'*
00131 Rome, Italy	*Via C. Lombroso 6/17*	*Viale Politecnico 1,*
	50134 – Florence, Italy	*00133 Rome - Italy*

Millimeter wave satellite communications devices often presents Rectangular (RW) to Coplanar (CPW) waveguide transitions to connect RW antenna feeding networks to CPW transmitting and receiving circuits. These transitions need to be as broadband and low insertion loss as possible for performance issue but are sometime also requested to be airtight, so a 90° mounting system can be exploited (E. Limiti, E. Martini, G. Pelosi, M. Pierozzi, S. Selleri, *J. Electromag. Waves Appl.*, 15, 1027-1035, 2001).

The very small sizes characterizing these devices make them strongly influenced by the effects of manufacturing tolerances. In this contribution Finite Element (FEM) based electromagnetic simulations are conducted over a parametric model of the device. Linear dimensions are randomly changed in an uncorrelated way within the manufacturing tolerance limits to produce models on which the numeric simulation takes place.

Simulation results are then used to create statistics of the behavior of the scattering matrix of the junction via a Monte Carlo approach. The statistic is validated by performing it on an incremental number of uncorrelated simulations, up to convergence of the statistical parameters of the computed scattering matrices.

Analysis of the results allows not only to get the statistical parameters of the scattering matrix but also to recognize the influence of single parameters, or the mutual influence of two parameters on the scattering matrix. By selecting set-ups where only one or two parameters are allowed to vary in their full tolerance range, while the other have a smaller, yet still random, variation, a new set of statistical parameter is obtained, from which the most tolerance-critical design parameters can be recognized.

Numerical results are validated with measures on prototypes.

FDTD Modeling of Transmission through Sub-Wavelength Apertures

K. Caputa and M. A. Stuchly

Dept. of Elec. & Comp. Eng., University of Victoria, Victoria, BC, Canada

Recently, there has been considerable interest in understanding physical phenomena, numerical modeling, experiments and applications of sub-wavelength apertures with periodic structures operating at optical wavelengths. Since the report by Ebbesen, et al (*Nature,* 391:667, 1998) of the enhanced transmission of light in an array of holes in a metal film, numerous papers have been published on light transmission through slots with periodic surfaces and arrays of holes. Qualitatively identical phenomena are exhibited by perfect conductors ($\sigma = \infty$), and actual metals having negative ε at optical frequencies. However, as expected, differences in the resonance wavelengths are observed. Published numerical analyses of periodic structures have only addressed structures made of perfect conductors using mode matching and the method of moments. However, in practice thin metallic films are characterized by the plasma equation, and even more importantly are deposited on an electrically thick substrate (on the exit face). Rigorous modeling and optimization of such structures by the mode matching/method of moments presents a serious computational challenge.

In this contribution, we explore the FDTD technique for modeling of sub-wavelength apertures with periodic impedance surfaces. A 2D code with PML absorbing boundary and the plasma equation representing metals at optical frequencies are used to model slots and slots with grooves on both surfaces. To verify our program, our computational results are compared for perfect electric conductor with the published data (Y. Takakura, *Physical Review Letters,* 86 (24): 5601-5603, 2001, F. J. Garcia-Vidal, H. J. Lezec, T. W. Ebbesen and L. Martin-Moreno, *Phys. Review Letters,* 90(21):21 3901 - 1-213901-4, 2003). Excellent agreement has been obtained for a single slot and a slot with periodic groves on one or both sides. Computations for silver and gold have indicated that the wavelengths of enhanced transmission due to the leaky waves produced by corrugations are shift with respect to those for a perfect conductor. Effects of glass substrate on either side of the metal have also been investigated. For slots with periodic surfaces 2D FDTD facilitates fast evaluation and optimization of periodic structures.

To simulate performance of holes of sub-wavelenght dimensions, 3D FDTD has been used. Modeling of perfect conductors and silver with periodic arrays of holes of various shapes has also been performed and results compared with published experimental data.

Genetic Optimization of Monopole Antenna Loaded with Shielded Loads

Michael D. Lockard* , Chalmers M. Butler, and Jeremy P. Rudbeck
Holcombe Department of Electrical and Computer Engineering
328 Fluor Daniel EIB
Clemson University, Clemson, SC   29634-0915 USA

The effects of loading a cylindrical monopole antenna mounted on a ground plane are investigated. The monopole is loaded by means of an impedance element in a small cavity, similar to that of Pisano and Butler (*IEEE Trans. Antennas Propagat.*, vol. 50, no. 4, pp.457-468, April 2002).   The cavity, which is integrated into the body of the monopole, is essentially a section of coaxial guide, shorted at both ends, with a circumferential slit in its outer conductor through which coupling to the exterior takes place.   The exterior radius of the outer conducting wall of the cavity is the same as that of the monopole proper, causing the monopole to be of uniform radius except at the slit, and the outer radius of the cavity is equal to the monopole radius minus the thickness of the outer conducting tube.   The monopole is loaded either by coaxial cavities filled with a material of high permeability or by coaxial cavities containing ferrite-cored coils in place of a portion of the coax center conductor. The dimensions of the antenna, the load and features of the cavity, and the position of the slit can be adjusted to control the properties of the monopole antenna.

The current on the cavity-loaded monopole is determined from the solutions of coupled integral equations, whose unknowns are the electric field in the slit and the electric current on the exterior surface of the monopole. The field in the loaded cavity is represented by an eigenfunction expansion containing a parameter which can be determined from a measurement performed on the impedance-loaded cavity. This measured parameter appears also in one of the integral equations and accounts for the interaction of the impedance-loaded cavity and the exterior antenna current   Because the parameter is measured and appears in one of the integral equations, the solution procedure can be looked upon as a hybridization of experimental and integral equation methods. The input impedance of the loaded monopole is calculated over a broad range of frequencies from the solutions of the coupled integral equations, and the effects of the filled cavity on antenna performance are examined. A genetic algorithm is utilized to optimize the performance of the antenna relative to specified performance criteria. The input impedance of a number of loads is measured to form a library from which the genetic algorithm selects the optimum loads for the monopole to achieve a prescribed antenna performance. The genetic algorithm determines the monopole dimensions and its load configuration (load type, load position, slit width, etc.) that is optimum relative to the performance criteria. Antennas that perform well in the optimization simulations are constructed and data obtained from the computations are compared with those from measurements.

Optimization of Performance of Top-Hat Monopole Antennas by Adding Material Loading

Mohammad R. Zunoubi[*], Hassan A. Kalhor
Department of Electrical and Computer Engineering
State University of New York
New Paltz, NY 12561

Small vertical monopole antennas have been used in the low frequency range for many years to provide azimuthally isotropic radiation patterns. These simple antennas, however, have low radiation resistance, low radiation efficiency, and a large reactive input impedance and require matching networks at their inputs. The idea of loading the antenna to improve its characteristics has been proposed many years ago [Gangi *et al.*, *IEEE Trans. Antennas Propagat.*, vol. 13, pp. 864-871, Nov. 1965]. More recently, a monopole antenna loaded with radial layered lossless and lossy dielectric was analyzed by a mode matching procedure [Francavilla *et al.*, *IEEE Trans. Antennas Propagat.*, vol. 47, pp. 179-185, Jan. 1999]. In their approach, an artificial upper ground plane was introduced that made it possible to use cylindrical wave expansions in various structure regions. The fields were then matched at the boundaries to calculate unknown mode amplitudes. Some improvements in antenna characteristics were reported.

In this study, a finite-difference time-domain (FDTD) method is used for analysis of the top hat loaded monopole antenna. This method is general and can deal with any loading profile including inhomogeneous loading. We will expand on our previous results [Zunoubi and Kalhor, 2002 *IEEE AP-S/URSI Int. Symposium*] to include the effects of the size of the metallic hat and loading of the lossless and lossy material to optimize antenna characteristics. Although our method is not limited to a cylindrical symmetric geometry bounded by an artificial upper ground plane, we will initially use this geometry as shown so that we can compare results with available results.

artificial ground plane
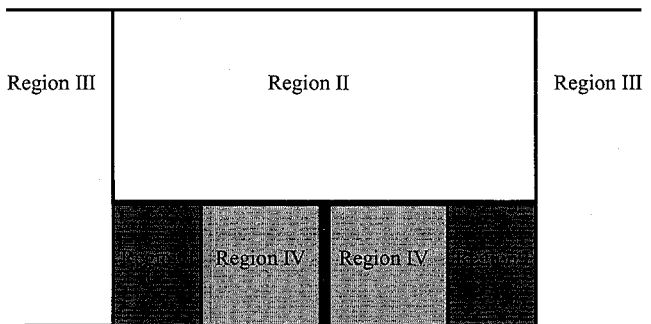
ground plane

A Bandwidth-Enhanced PIFA for Space Application

Patrick W. Fink*, Gregory Y. Lin, Justin A. Dobbins,
Andrew W. Chu, Larry W. Abbott, Steven E. Fredrickson
NASA Johnson Space Center
Houston, TX 77058

The PIFA (Planar Inverted-F Antenna) has received much attention in the past decade due to its miniaturized size and application in commercial wireless markets. There have been several publications with respect to enhanced bandwidth operation of PIFAs on small, handheld devices and on the effects of the ground plane on the bandwidth of the PIFA. There has also been interest in this type of antenna with respect to non-commercial, "high-reliability" applications (V. Jamnejad, J. Huang, H. Endler, and F. Manshadi; *Aerospace Conference, 2001, IEEE Proceedings*, v2, 843-851, March 2001). Our application for a PIFA antenna is in support of a Wireless Ethernet 802.11b (3.3% bandwidth) link for Mini-AERCam, a 7 ½ inch diameter, essentially spherical, free-flying nano-satellite. Mini-AERCam is intended to provide remote viewing and external inspection capabilities for future human spaceflight missions, including potential Shuttle and International Space Station applications.

We start with a capacitively fed, capacitively loaded PIFA (C. R. Rowell and R. D. Murch, *IEEE Trans. Antennas Propagat.*, vol. 45, no. 5, 837-842, May 1997). To permit further size reduction of the PIFA while maintaining a 2:1 VSWR impedance bandwidth over the 802.11b band, we apply the so-called "antenna-filter" technique (D. A. Paschen, *Proc. 1986 Antenna Appl. Symp.*, Sept. 1986). In this technique, the impedance bandwidth of the microstrip antenna is enhanced using an integral Tchebyscheff filter. We use a quarter-wave transformer on a high dielectric to affect a series RLC circuit from the parallel RLC tank presented by the PIFA. We find this parallel-to-series transformation is necessary in order to obtain realizable values for the filter components. Both the quarter-wave transformer and filter are printed on a high-dielectric layer, while a Teflon/glass/ceramic composite is employed for the PIFA construction. The resulting initial prototypes are approximately 1.6 cm in diameter (0.13 λ_0) and 0.35 cm thick. A means of securing the resulting antenna for high reliability applications, while maintaining a compact size, is discussed. The measured radiation characteristics of this antenna are examined for the case of the antenna mounted on a 7 ½ inch diameter sphere. These measured results are then compared with those obtained using a hybrid FEM/BEM numerical analysis.

Increasing Polarization Bandwidth for Single-Layer, Circularly-Polarized
Microstrip Patch Antennas Incorporating Size Reduction Techniques

Ryan M. Christopher* [+], Brecken H. Uhl[+], Russell P. Jedlicka[+]
[+] Klipsch School of Electrical and Computer Engineering, New Mexico State
University, Las Cruces NM 88003 {ryachris, buhl, rjedlick} @nmsu.edu

Microstrip patch antennas have many useful characteristics, these being a broadbeam radiation pattern, relative ease of design and fabrication, as well as being inexpensive. Circular polarization (CP) can be achieved through a nearly-square implementation, trimmed-corners, or a forced excitation using a network such as a 90° hybrid.   Each of these techniques, however, have drawbacks associated with them. The trimmed-corners and nearly-square implementations have a limited CP bandwidth, on the order of 0.3% at 1.5GHz for an axial ratio of less than 3dB and 0.5% for an axial ratio of less than 6dB (60 mil substrate with ε_r = 3.2 and $\tan\delta$ = 0.003). The dual-feed or forced implementations have a much larger polarization bandwidth, but suffer from a significant increase in required area (on a single layer), making them difficult to implement in an array.

The goal of this research is to implement a combination of a hybrid feeding network and microstrip patch using size reduction techniques to increase the CP bandwidth over that of a trimmed-corners or nearly-square microstrip patch in an area that is nominally (or slightly larger than) the same size as a nearly-square patch at the same frequency. The basic approach is illustrated below: progressing through nearly-square patch, square patch with 90° hybrid, square patch inside a 270° hybrid, and loaded patch inside a meandered 270° hybrid.
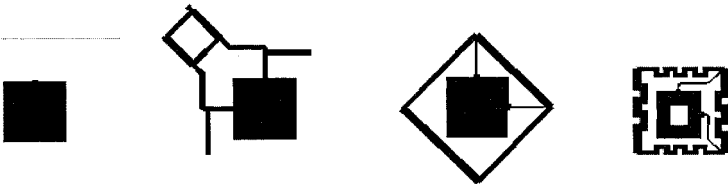
Preliminary results have shown the ability to fit a square microstrip patch inside a 270° hybrid; this configuration resulted in nominally the same directivity, gain, and impedance bandwidth while increasing the CP bandwidth to 1.3% at an axial ratio of less than 3dB and that of 3.0% at an axial ratio of less than 6dB on the same substrate cited above. Although this represents a significant CP bandwidth increase of the unloaded patch antenna, the area is 2.25 times that of the nearly-square patch.   By meandering the hybrid and using patch size reduction techniques this configuration will be reduced to the nominal size of the unloaded patch while retaining the increased CP bandwidth and an acceptable efficiency. Comparison between simulation and measurement for this new technique will be presented.

Ultra-Low-Profile Dipole Antenna in a Quadruple Mode

Tadashi Takano* and Arpa Thumvichit[†]

*The Japan Aerospace Exploration Agency

† The University of Tokyo

3-1-1 Yoshino-dai, Sagamihara, 229-8510 Japan

A dipole antenna with a reflector at a quarter wavelength distance has been widely used as a low profile antenna with wide radiation patterns. Furthermore, an ultra-low profile dipole (ULPD) with a distance of a several-tensth wavelength is desired for several purposes. From the viewpoint of electro-magnetic field analysis, the radiation characteristics of ULPD gather much interest due to the lack of its knowledge.

Conventionally, ULPD's have been studied on the basis of the image method and the far-field patterns of a dipole. The radiation characteristics were expressed using the equations for the far-field [1]. As the current phase of the image is 180deg. different from that of the dipole due to the boundary condition on a perfect electric conductor (PEC), the radiated fields from the dipole and its image cancel each other in this model. Some book predicted no radiation in the boresight of PEC. On the other hand, the analysis on the basis of the method of moment (MOM) shows maximum radiation in the boresight [1],[2]. But they seem to have failed in its physical explanation.

This paper analyzes a dipole antenna in the proximity of PEC plate. It is shown that the maximum radiation occurs in the normal direction to the plate with the gain about 9dBi. The electric field distribution at each instance shows that the field lines run between the opposite tips of the dipole and its image in addition to the field lines between the tips of the dipole itself, and that the electromagnetic energy flows along the PEC plate in addition to the main flow in the boresight. This status could be named a quadruple mode instead of a dipole mode of a single dipole in a free space.

Another concern of this type of antennas is the impedance matching because of the existence of a metallic structure in its proximity. The analysis shows that the antenna can be matched with a feed line by the offset feeding and by shortening the length of the dipole. The current at the both ends of the dipole is not zero, as implies that the energy is stored around the both tips.

References

[1] C. A. Balanis, *Antenna Theory - Analysis and Design*, John Wiley & Sons, 1997.

[2] J. D. Kraus, *Antennas*, McGraw-Hill, 1988.

BROADBAND PRINTED QUADRIFILAR HELIX ANTENNA

Y. LETESTU, A. SHARAIHA, S. COLLARDEY

IETR – Université de Rennes1, campus de beaulieu 35042 Rennes Cedex – France
yoann.letestu@univ-rennes1.fr

In recent years, the printed quadrifilar helical antenna (PQHA) has widely been used in satellite mobile communication systems in the L or S band frequencies such as GPS, INMARSAT. It is a good candidate for these applications due to its features of circular polarization, good axial ratio and low cost. Currently the conventional PQHA that were investigated offers either operation over a single band (7%) or dual band that is narrow (less than 4%) and could be insufficient for such applications. In this paper, we propose a PQHA with a second parasitic PQHA leading to improve the matching efficiency and the bandwidth. Therefore, we use the mutual coupling effect between the conductor arms and the parasitic strips to obtain the Broadband PQHA (BPQHA) (Sharaiha A., Letestu Y., Louvigne J.C., "*Antenne hélicoïdale à large bande*", FR patent 0211696, septembre 2002). This antenna is able to produce a wider bandwidth up to 30%.

The configuration of the proposed BPQHA is obtained by printing four parallel conductor arms and four parasitic strips on a flexible dielectric substrate wrapped around a cylindrical support. The BPQHA is analysed by using a finite element method (ansoft HFSS v8.5) and gives good theoretical results in comparison with the experimental one.

A prototype of the BPQHA is realized operating in L-band. It can provide 30% of bandwidth covering all the frequency bands of positioning systems (GPS, Galileo...), as shown in figure 1. It can also receive or transmit circular polarized signals over a large angular region with a gain greater than 1.5dB in all the bandwidth, as shown in figure 2. We can note that the radiation patterns remain the same as for a conventional PQHA.
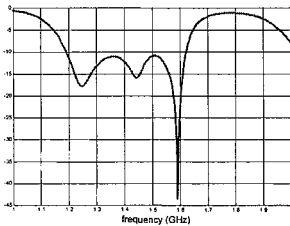
Figure 1: Measured Return Loss (dB)   Figure 2: Measured Gain (dB)
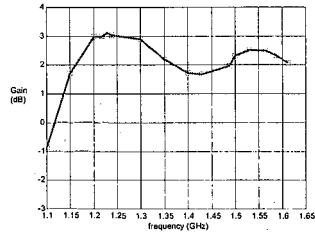
A novel PQHA is proposed and studied. It has allowed a bandwidth increase of >3.5:1, compared to a conventional PQHA. More details and results will be shown during the presentation.

Design of Tag Antennas for RFID Using a Pareto Genetic Algorithm

Hosung Choo*, Chihyun Cho and Hao Ling[+]
School of Electronic and Electrical Engineering
Hongik University, Seoul, Korea

[+]Department of Electrical and Computer Engineering
The University of Texas at Austin
Austin, TX 78712 U.S.A

The emerging technology of Radio Frequency Identification (RFID) requires an electrically small tag antenna with a planar profile that can easily be attached to a variety of surfaces. One of the challenges of tag antenna design is that as the antenna size is reduced and its profile restricted to be planar, both the achievable antenna efficiency and bandwidth decrease. Although bandwidth is not so important a consideration due to the low data transmission rate of RFID, high efficiency is very important for increasing the readable range between the tag antenna and the reader. The other challenge is to ensure that the tag antenna will operate efficiently on surfaces of different materials. The dielectric materials near the tag antenna may degrade the antenna performance as well as shift its resonant frequency.

In this paper, we explore planar antenna structures that permit high efficiency, small size and reliable performance on a variety of dielectric materials. To achieve these multiple design goals, we employ a Pareto genetic algorithm (GA) to find optimal structures that satisfy these multiple objectives. In our application, the antenna should fit within the physical size of 3cm×3cm. The structure considered in this paper is an inductively coupled antenna, which consists of a feed loop and a radiating antenna body. We previously found that this inductively coupled structure performs well for antenna sizes kr in the 0.2 to 0.6 range (Choo and Ling, *Elect. Lett.*, **39**, 1563-1564, Oct. 2003).

We present several optimized structures that results in small, high-efficiency antennas whose performance are relatively unaffected by nearby dielectric materials. The operating physics of these antennas is explained using a simple circuit model. The performances of the optimized antenna structures are measured both with and without proximity dielectric materials, and they are compared to various small antennas as well as to the theoretical performance limits. The radiation pattern, antenna efficiency and bandwidth of the optimized design are presented. Finally we study how these candidate tag antennas affect the readable range in an RFID system.

Genetic Algorithms for the Optimization of Dual Frequency Profiled Corrugated Circular Horns

L. Lucci[1], R. Nesti[2], G. Pelosi[1], S. Selleri[1], M. Tornielli[1]

[1] Department of Electronics and
Telecommunications
University of Florence
Via C. Lombroso 6/17
50134 – Florence, Italy

[2] Arcetri Astrophysical Observatory
National Institute for Astrophysics
Largo Enrico Fermi, 5
50125 - Florence, Italy

In many applications systems working at two different frequencies are requested. Using a single horn for both frequencies, instead of two different structures, is more convenient because one can simplify the design of the cluster of feeds illuminating the reflector. This does not only reduce costs but also defocusing as a lower number of feeds can be more tightly packed. Genetic Algorithms (GAs) have been successfully used for the optimization of Profiled Corrugated Circular Horns (PCCHs) at a single band (L. Lucci, R. Nesti, G. Pelosi, S. Selleri, *IEEE AP-S International Symposium*, 2, 338 - 341, 2002; L. Lucci, R. Nesti, G. Pelosi, S. Selleri, PIER (*Progress in Electromagnetics Research*), 46, 127-142, 2004).

In this contribution GAs are employed for the otpimization of dual frequency PCCHs. Contributions related to the problem of the synthesis of a multi-band horn have been given in the past (L. Cooper, H. Aintablian, *IEEE AP-S International Symposium*, 23, 307-310, 1985), where different feeding ports are used for different operative frequencies. Whereas the geometry used here allows one to realize a dual frequency horn, which can be fed using a single feeding waveguide. This is a very desirable feature because it results in a simplification of the overall structure.

To work at two different frequencies the horn presents a more complex profile with respect to that of a standard horn: two independent sets of corrugations are separately optimized for the two bands. In particular in place of each single corrugation a double corrugation is defined, that consists of a corrugation for the upper frequency, followed by a second corrugation for the lower band.

Software simulations have been demonstrated that dual frequency horns can be successfully optimized, with stable phase center and small dimensions.

Integrated Antenna/Solar Array Cell (IA/SAC) System for Flexible Access Communications

Richard Q. Lee*, Eric B. Clark, Anna Maria T. Pal and David M. Wilt
NASA Glenn Research Center
21000 Brookpark Road
Cleveland, OH 44135, U.S.A.

Carl H. Mueller
Analex Corporation, Cleveland, OH 44135, U.S.A.

Present satellite communications systems normally use separate solar cells and antennas. Since solar cells generally account for the largest surface area of the spacecraft, co-locating the antenna and solar cells on the same substrate opens the possibility for a number of data-rate-enhancing communications link architecture that would have minimal impact on spacecraft weight and size. The idea of integrating printed planar antenna and solar array cells on the same surface has been reported in the literature. The early work merely attempted to demonstrate the feasibility by placing commercial solar cells besides a patch antenna. Recently, Integrating multiple antenna elements and solar cell arrays on the same surface was reported for both space and terrestrial applications. The application of photovoltaic solar cell in a planar antenna structure where the radiating patch antenna is replaced by a Si solar cell has been demonstrated in wireless communication systems (C. Bendel, J. Kirchhof and N. Henze, 3rd Would Photovotaic Congress, Osaka, Japan, May 2003). Based on a hybrid approach, a 6x1 slot array with circularly polarized cross-dipole elements co-located on the same surface of the solar cells array has been demonstrated (S. Vaccaro, J. R. Mosig and P. de Maagt, IEEE Trans. Ant. and Propag., Vol. 51, No. 8, Aug. 2003). Amorphous silicon solar cells with about 5-10% efficiency were used in these demonstrations.

This paper describes recent effort to integrate advanced solar cells with printed planar antennas. Compared to prior art, the proposed IA/SAC concept is unique in the following ways:

• Active antenna element will be used to achieve dynamic beam steering
• High efficiency (30%) GaAs multi-junction solar cells will be used instead of Si, which has an efficiency of about 15%.
• Antenna and solar cells are integrated on a common GaAs substrate.
• Higher data rate capability. The IA/SAC is designed to operate at X-band (8 – 12 GH) and higher frequencies. Higher operating frequencies enable greater bandwidth and thus higher data transfer rates.

The first phase of the effort involves the development of GaAs solar cell MIMs (Monolithically Integrated Module) with a single patch antenna on the opposite side of the substrate. Subsequent work will involve the integration of MIMs and antennas on the same side of the substrate. Results from the phase one efforts will be presented.

An optimum method for designing the quadrifilar helix antenna

Pejman Rezaei

p_rezaei@itrc.ac.ir

Iran Telecommunication Research Center (ITRC)
Tarbiat Modarres University, Department of Electrical Engineering

In this paper regarding to an optimum algorithm idea for template matching in image processing, present a simple and fast method, and a quadrifilar helical antenna (QHA) was designed with this systematic method in some stages for a Small satellite. Template matching can be finding by complete searching in the sub images that needs lots of time. One of the modified algorithms is Coarse-to-Fine method, which in this method, first an image with low resolution is used to the searching for the template in the sub images, with suitable correlation degree. By reducing the resolution, number of samples and time of calculation is reduced. In next steps, this searching with higher resolution will be done near the found place or places out of last step (M. Gharavi-Alkhansari, IEEE Trans. Image Processing, 4, 526-533, 2001). Now, this method is being used for designing QHA antenna. First, according to desired pattern, a useful region for designing parameters has been defined (C. C. Kilgus, IEEE Trans. Antennas & Propag., 5, 392-397, 1975). Then with simulating few points that has been selected throw the collection uniformly, the pattern generator region near the desired pattern will be discovered. By getting smaller region and repeating the search with a higher resolution in it, finally the desired pattern is accessible.
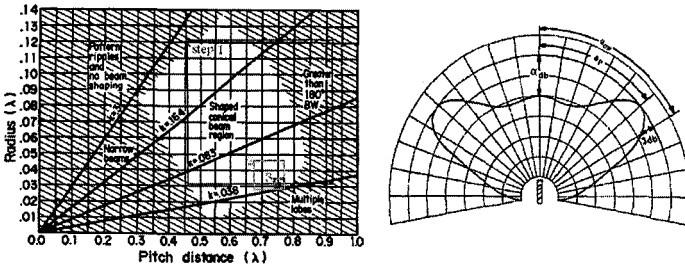
Fig1. Region of saddle-shape pattern and typical radiation pattern

This method is used for achieving the saddle-shaped pattern with 1.5dB gain depth between the angles zero and 65degree, that 0.75turn antenna recognized proper. Capability of this method is the recognition of existence the proper result in defined region at first step, and cease of process in undesired region. Simulations have been done using the NEC-Pro software. The results, consist of place of main lobe and the gain depth of pattern, are shown in tables1, 2. The region with little dimensions (r,p) create end fire pattern and in large size create a central grating lobe, thus the suitable saddle-shaped pattern is limited between two above domains. This method is proposed for designing antennas such as QHA, whit out the exact relations between physical parameters and radiation pattern.

Table1. Simulation results in first step

p(cm) r(cm)	30	40	50	60
8	θ_p	46	59	Center lobe
	α	1.63	5.34	↓
6		47	59	
		1.14	3.37	
4		50	61	68
		.88	2.41	4.28
2	↑	56	66	71
	End fire	.34	1.77	3.78

Table2. Simulation results in second step

p(cm) r(cm)	44	46	48	50
3	58	60	62	63
	1.19	1.47	1.77	2.07
2.6	59	61	63	64
	1.05	1.34	1.63	1.95
2.2	60	62	64	65
	.94	1.22	1.52	1.83
1.8	62	63	65	67
	.79	1.09	1.39	1.71

Ultrawideband Radar Methods and Techniques of Through Barrier Imaging

John T. Chang*, Stephen G Azevedo, Dave Chambers, Peter Haugen,
Richard R Leach, Christine Paulson, Carlos E Romero, Alex Spiridon,
Mark Vigars, James Zumstein

The LLNL impulse radar sensor program has been involved with the investigation into the science and technology necessary to enable real-time multi sensor imaging to detect and monitor objects through barriers. This presentation will describe some of the methodologies and recent findings. The typical existing approaches have severe limitations in capabilities. In general, there are extreme tradeoffs between range of detection (especially through obscurants at distance), specificity, data processing time, and portability. As an example, techniques that detect and screen for *objects* often do not have the capability to monitor in real time targets in motion. LLNL efforts take into account this multi-parametric space and developed potential solutions that can be readily adapted to specific application needs.

The use of field programmable gated arrays integrated with high resolution ultra wide band (UWB) electromagnetic sensors for imaging through barriers will be described. In addition the real-time imaging issues of detecting and tracking of small objects will be described.

Techniques of UWB beam forming and steering will be described. Among other attributes, UWB system developed at LLNL has been shown to penetrate many materials (wood, some concretes, non-metallic building materials, some soils, etc.) with high range resolution. Further, monostatic and multi static systems will be presented.

Results of system characterization based upon current prototype systems will be presented. The figure below shows an image frame of a circular plate target from the laboratory system.
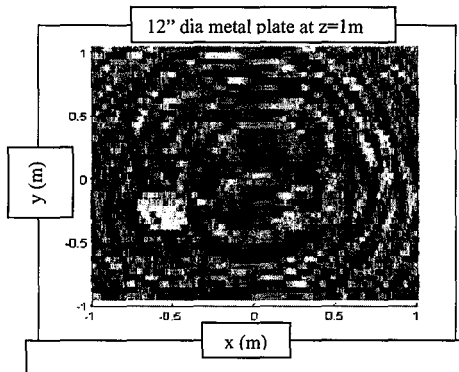
Figure. Laboratory acquired radar image frame of circular plate target taken by 7 transmitter, 1 receiver array. Target is located at the edge of the detection field of view. Target is 12 inches in diameter and 1 meter in range.

Echo Cancellation using The Homomorphic Deconvolution

Wonsuk Choi, Tapan K. Sarkar

Department of Electrical Engineering and Computer Science
Syracuse University, 121 Link Hall, Syracuse, NY 13244
Email: wchoi01@syr.edu; tksarkar@mailbox.syr.edu

Deconvolution is an important preprocessing procedure often needed in the spectral analysis of transient exponentially decaying signals. Homomorphic deconvolution techniques is studied and applied to the problem of canceling the echo in the signal. Signal processing applications use the collection of nonlinear techniques known as cepstral analysis. These are based around the core concept of the complex cepstrum. One of the more important properties of the cepstrum is that it is a homomorphic transformation. Under a cepstral transformation, the convolution of two signals becomes equivalent to the sum of the cepstra of the signals. Multiplication and convolution are also common means of mixing signals together. If signals are combined in a nonlinear way (i.e., anything other than addition), they cannot be separated by linear filtering. Homomorphic techniques attempt to separate signals combined in a nonlinear way by making the problem become linear. That is, the problem is converted to the same structure as a linear system. The logarithm of the power spectrum of a signal containing an echo has an additive periodic component due to the echo, and thus the Fourier transform of the logarithm of the power spectrum should exhibit a peak at the echo delay. In the time domain, the signal, which contains echo component, is combined by convolution of original signal and impulse train. In the cepstrum domain we can distinguish the echo component and also eliminate the echo component.

In this paper we simulated electromagnetic waves scattered from a conducting sphere, along with its echo components to demonstrate the applicability of this procedure.

Image Formation Through Walls Using A Distributed Radar Sensor Network

Allan R. Hunt

AKELA, Inc., 5276 Hollister Avenue, Suite 263, Santa Barbara, CA 93111
ahunt@akelainc.com

Interest in methods for obtaining surveillance information through walls has been increasing for both domestic and military security applications. While detecting the presence of individuals inside a building structure is useful, being able to know where they are, and how the interior of the structure is laid out provides an additional important tactical advantage. Sensors that can form images through walls take away the ability of individuals to hide, reduce the risk to security personnel, and increase the probability that security operations will conclude without casualties.

The electromagnetic propagation properties of building materials, access to building surroundings, and operational requirements all play a role in defining imaging system operating parameters. Frequencies between 250 MHz and 3 GHz provide acceptable penetration for nearly all building materials, including concrete. Low frequency antennas with good resolution tend to be too large for practical application. Improving resolution through aperture synthesis from a moving platform can't always be achieved because of limited access to a building's surrounding area. System size and weight is always an issue because of the need for portability.

While we have demonstrated acceptable imaging performance by synthesizing a large antenna aperture from a portable, collapsible antenna array, these operational constraints have driven AKELA to a concept of operation where images are created by a distributed array of individual sensors. Each sensor is a high range resolution radar that can be either fixed in place or carried by an individual. The sensors are connected with a wireless communication network that distributes timing and control information, receives data, determines sensor location, and fuses the data from each sensor to generate imaging and motion detection information. The variable aperture achieved by allowing sensor movement reduces ghost images and improves resolution where needed. Coherent detection preserves phase information that is useful for determining the presence of metal and the breathing response of a stationary individual.

We have developed a frequency agile radar operating between 500 MHz and 2 GHz that has a maximum range of 250 meters and allows image formation at 10 frames per second. This radar is the sensor element in our networked concept. Recent experiments show that this new radar has the capability to detect the breathing response of a stationary individual through a wall at a distance of 5.5 meters.

271

Effects of Wall Parameters and Standing Waves between Walls in Through-Wall-Imaging Applications

Natalia Bliznyuk[*]
University of Pennsylvania, Dept. of Electrical and Systems Engineering
200 S 33 St, Philadelphia, PA 19104-6390
215-898-8548
natali@ee.upenn.edu

Nader Engheta
University of Pennsylvania, Dept. of Electrical and Systems Engineering
200 S 33 St, Philadelphia, PA 19104-6390
215-898-9777
engheta@ee.upenn.edu

Ahmad Hoorfar
Villanova University, Department of Electrical and Computer Engineering
800 Lancaster Avenue, Villanova, PA 19085
610-519-7223
hoorfar@ece.villanova.edu

Problems of "seeing" through walls involve modeling of wave scattering from objects embedded in multilayered media, and they are computationally challenging due to electrical dimensions of the domain of interest. An efficient hybrid technique based on the Love equivalence principle and the Green's functions for layered media has been developed in order to estimate the scattered fields from 3-D conducting or dielectric objects located within parallel layered media [N. Bliznyuk, N. Engheta and A. Hoorfar, "An Efficient Hybrid Computational Technique for Certain Radiation and Scattering Problems in Layered Media" *2004 IEEE Aerospace Conference, Big Sky, MT*, March 6-13, 2004]. This is an approximate technique, which does not take into account standing waves between the scatterer and the walls, but does take into account multiple reflections between the walls (in the absence of the scatterer) and the propagation of the first response from the scatterer through the walls. This approximation essentially works well, especially in the TWI applications because the first signal from the scatterer after going through the wall is stronger compared with the subsequent echoes. Furthermore, in some cases, the radar only receives and processes the first reflection from the target and the rear wall. The validity of this approach and its range of applicability have been checked by applying it to certain canonical cases and then comparing the results with the exact known solutions or with the solutions obtained by other numerical techniques such as FDTD.

In this talk, we will discuss the role of wall thickness and the effects of the standing waves between the parallel walls on the received signals at the detector. We will show how the wall separation, wall materials, and the related parameters can play a role on this signal. The effect of the rear wall in producing images of the target will also be mentioned. As sample targets, we will consider perfectly conducting and dielectric spheres of different radii. We will first present a brief overview of the computational technique we use in this problem, and we will then present our numerical results along with physical justification and explanation of our numerical findings.

272

Backward-wave materials: How to realize and how to use them

S. Maslovski, C. Simovski, S. Tretyakov*

Radio Laboratory / SMARAD, Helsinki University of Technology, P.O. 3000
HUT, Finland. E-mail: sergei.tretyakov@hut.fi

In this review presentation we will discuss artificial materials that can support backward waves. The main subject will be the media that can be considered as effectively continuous materials with physically meaningful material parameters like permittivity and permeability (it is well known that backward waves can exist in various periodical structures, which is a different class of media with different potential applications).

Basically, two conceptually different materials capable to support traveling backward waves are known: materials with negative real parts of the permittivity and permeability and bianisotropic materials (e.g. chiral composites). We will discuss backward-wave properties of both of these materials.

The presentation will start with a historical overview. Next, we will consider possible physical realizations of materials with negative parameters (combinations of wire arrays and split-ring resonators and composites with resonant inclusions). The emphasis will be on an overview of the result obtained in our research group. For example, analytical models of wire media and their properties, the role of field interactions between wires and magnetic resonators, alternative realizations of negative magnetic permeability. In the following, we will discuss the limitations of material description in terms of effective parameters for composites supporting backward waves and consider the role of periodicity of the microstructure in the electromagnetic response of these composites.

In the following part of the presentation we will overview backward wave propagation, reflection and refraction in another class of effective media supporting backward waves: chiral composites. We will explain under what conditions such solutions are possible and discuss electromagnetic phenomena on material interfaces.

We will conclude with a discussion of potential applications of backward-wave materials.

273

DESIGN OF A MINIATURE BROADBAND SATCOM ANTENNA USING TEXTURED DIELECTRIC LOADING VIA TOPOLOGY OPTIMIZATION

G. Kiziltas [1,*], J. L. Volakis[1], N. Kikuchi[2] and J. Halloran[2]

[1]ElectroScience Lab., ECE Dept
The Ohio State University
Columbus, OH 43212
gkiziltas@esl.eng.ohio-state.edu
volakis.1@osu.edu

[2]The University of Michigan
Ann Arbor, MI, 48109-2121, USA
{kikuchi,peterjon}umich.edu

Many military and commercial applications require smaller, light-weight antennas with broad-band and high gain performance. One such application is the UHF SATCOM antenna, which presents a significant advance in providing portable satellite communications technology for uses in the field. Although existing SATCOM antennas provide broad pattern coverage, they are still too large (15"-30"), heavy and bulky and therefore not quite portable. The goal of this paper is to propose a design which is much smaller in aperture (6") by modifying the dielectric loading applied to a slot spiral antenna. The bandwidth of interest is 240-318 MHz and the required gain is greater than 3dB. Also, circular polarization is expected for this SATCOM application.

The challenge is to miniaturize the spiral and still retain its bandwidth with a satisfactory gain performance. Instead of the more traditional approaches to optimizing the shape or geometry of the antenna via reactive loading, parasitic coupling and etching, here we focus on the material substrate/superstrate of the slot spiral using high-contrast LTCC material. Recent efforts on metamaterials indicate that properly designed dielectrics or a combination of different materials can lead to designs which have greater bandwidth and small size (G. Kiziltas et al, IEEE T-AP, pp. 2732-2743, 2003). Nevertheless, the focus so far has been on narrowband antennas. Here, we present how to deliver the optimal SATCOM performance in terms of size, gain and impedance matching by optimizing the metamaterial profile of the broadband slot spiral antenna. The employed design method is the Solid Isotropic Material with Penalization (SIMP) technique (M. P. Bendsoe, Structural Optimization, 1, 193-202, 1989). Unlike conventional design methods, SIMP is a topology design method that draws from a broader class of design solutions. Through a simple continuous material model, geometrical and material configurations are effectively designed from 'scratch'. The continuous model allows for a design problem formulation in a non-linear optimization framework using the Finite Element–Boundary Integral method as the computational engine. Sequential Linear Programming (SLP) is then used to solve the optimization problem with sensitivity analysis based on the adjoint variable method for complex variables (G. Kiziltas et al, TAP, 51, 10, 2732-2743, 2003). The proposed design method allows for inhomogeneous material modeling and design to increase the bandwidth of a fixed size square slot spiral antenna using a high-contrast LTCC superstrate.

274

Enhanced Transmission through Coaxial Apertures Perforated in Thick Metallic Films

Vitaliy Lomakin, Shuqing Li, and Eric Michielssen

Center for Computational Electromagnetics
Department of Electrical and Computer Engineering
University of Illinois at Urbana-Champaign
vitaliy@emlab.uiuc.edu, sqli@emlab.uiuc.edu, emichiel@uiuc.edu

Recently, the phenomenon of enhanced transmission through metal films perforated by subwavelength holes has attracted much attention. The phenomenon was observed in both the optical and microwave regimes (T.W. Ebbesen, *Nature*, (6668), 667-9, 1998; Lomakin et al, *IEEE AP-S*, 2003; A.A. Oliner and D. R. Jackson, *IEEE AP-S*, 2003) and associated with Leaky Waves (LWs) generated by Surface Waves (SWs) scattered by different types of gratings. These SWs can originate from different physical phenomena, e.g. surface plasmon polaritons, or surface waves supported by periodic hole arrangements, surface corrugations, or dielectric slabs. Enhanced transmission was observed through holes of simple connected cross section, e.g. circles and squares, as well as through apertures comprising multiple connected cross sections, e.g. infinite slits and coaxial apertures. It was shown recently by Baida and Labeke (F.I. Baida, F.I. and Van Labeke, D., *Physical Review B*, v 67, n 15, 15 April 2003, p 155314-1-7) that a periodic array of coaxial apertures provides an efficient channel for field transmission. However, the same authors stated "we are not yet able to explain the shape of this spectrum" and "the interpretation of these original results is not entirely clear".

Here, such an interpretation and investigation are carried out, their ultimate goal being the articulation and interpretation of all mechanisms leading to enhanced transmission through periodic arrays of coaxial apertures. Specifically, we consider an array of subwavelength coaxial apertures that perforate a thick metallic plate and that is excited by a TM_z time-harmonic plane wave. The transmission coefficient as a function of the incident angle and frequency for different structure parameters, i.e. film thickness and period, is required. We first show that enhanced transmission can be observed only for sufficiently oblique incident angles. This is because normally incident fields cannot couple to the TEM coaxial mode due to the symmetry of the aperture. Then, we show that for oblique incident angles, there are two phenomena that lead to enhanced transmission. One is a Fabry-Perrot type coaxial waveguide resonance between the upper and lower coaxial apertures. The enhanced transmission associated with this phenomenon occurs when the film thickness is close to a integer number of half-wavelengths and the corresponding frequency does almost not depend on the incident angle and the periodicity. Another phenomenon is due to the existence of surface waves of two types. One is the known surface plasmon polariton. Another one is the surface wave that arises due to effective impedance of the perforated surface, and exists even if the film is perfect electrically conducting. A simple model explains the origin of such impedance by modeling the coaxial waveguide by an open (or loaded) transmission line (TL). The corresponding surface impedance can be either capacitive or inductive depending on the film thickness (the length of the TL of the model) and the frequency. When the impedance is inductive it can support a TM surface wave. The surface wave, through the periodic aperture arrangement, generates leaky waves, which lead to enhanced transmission. The enhancement generated through this mechanism strongly depends not only on the frequency and the thickness of the film but also on the structure's periodicity. A full wave analysis and numerical study are performed to verify the above theoretical observations.

Interaction between Plasmonic and Non-Plasmonic Nanospheres and Their Equivalent Nano-Circuit Elements

Nader Engheta[1], Natalia Bliznyuk[1], and Andrea Alù[2]

[1]University of Pennsylvania
Department of Electrical and Systems Engineering
Philadelphia, Pennsylvania 19104, U.S.A.
engheta@ee.upenn.edu, http://www.ee.upenn.edu/~engheta/

[2]Università di Roma Tre
Department of Applied Electronics, Rome, Italy

Optical wave interaction with metallic nanoparticles is one of the important problems in nanotechnology and nano-photonics nowadays. It is well known that in certain noble metals such as Ag, Au, the plasma frequency is in the visible or ultraviolet (UV) wavelengths, and thus these metals behave as plasmonic materials in the optical frequencies, i.e., their permittivity has a negative real part. As a result, interaction of optical signals with plasmonic nanoparticles involves surface plasmon resonances [J. P. Kottmann, O. J. F. Martin, D. R. Smith, and S. Schultz, "Spectral response of plasmon resonant nanoparticles with a non-regular shape," *Optics Express,* Vol. 6, p. 213, (2000)]. These particles can be much smaller than the optical wavelength; however their dimensions can be comparable with the skin depth of these metals in the optical frequencies.

When the permittivity of a material has a negative real part, one can argue that phase difference between the electric field and the displacement current at each point in such a medium is 180° different from the corresponding phase difference in a material with positive permittivity. This may lead to the interpretation that if in a conventional material, the equivalent circuit element is capacitive, in an analogous epsilon-negative material, the corresponding circuit element will be inductive [G. V. Eleftheriades, A. K. Iyer, and P. C. Kremer, *IEEE Trans. Microwave Theory Tech,* vol. 50, no. 12, pp. 2702-2712, December 2002; A. K. Sarychev, D. A. Genov, A. Wei, and V. M. Shalaev, *Proceedings of SPIE, Complex Mediums IV: Beyond Linear Isotropic Dielectrics,* August 4-5, 2003, pp. 81-92]. So if we consider two nanospheres, one made of metal (e.g., Ag, Au) and the other made of a dielectric material, the interaction between these two spheres in the optical regimes can be modeled as an equivalent L-C circuit. In this work, we find equivalent values for such "nano-inductors" and "nano-capacitors" in terms of the relevant parameters such as material parameters in each sphere, sphere dimensions, and interparticle distance. This analysis can provide us with the possibility of forming a resonant L-C "nano-circuit", small compared with the optical wavelength of operation, as we put a plasmonic (i.e., metal) and a non-plasmonic (i.e., dielectric) nanosphere next to each other. By choosing the size of the spheres and their separation, we can modify the values of these nano-elements of circuit. This idea may be extended to more complex circuits with more than two such nanospheres, providing various nano-inductors and nano-capacitors arranged in many different ways. This will lead to various applications for nano-photonic and nanoelectronic circuits involving such tiny spheres as nano-inductors and nano-capacitors. We will describe the results of our analysis, and will forecast some of these ideas.

Generalized Surface Plasmon Resonance Sensor Using Metamaterials and Negative Index Medium
(Speacial session in Metamaterials)

Akira Ishimaru
Sermsak Jaruwatanadilok
Yasuo Kuga

Box 352500, Department of Electrical Engineering
University of Washington, Seattle, Washington, 98195
Tel: 206-543-2169, Fax: 206-543-6185, E-mail: ishimaru@ee.washington.edu

Surface plasmon resonance has been known for a long time and has been used for chemical sensors and in remote sensing systems. It makes use of a prism and a thin metal layer deposited upon the prism. The p-polarized (TM) reflected light exhibits a sharp dip at the angle corresponding to the surface plasmon between the metal and the bulk material. This resonance occurs due to the negative dielectric constant of the metal, such as gold or silver, at optical frequencies.

In this paper, we explore the use of the NIM (negative index medium), and more generally metamaterials, to produce the surface plasmon resonance at microwave frequencies. First, we discuss the surface wave (surface plasmon) modes between NIM and the dielectric. This requires the study of all wave types which may exist between the medium with arbitrary e and m and the ordinary medium. We discuss the classification of wave types. In particular, we discuss the regimes in an m-e diagram where the forward and backward surface waves exist. These regimes give rise to the surface waves, and the reflection coefficient exhibits a sharp dip at this particular angle, similar to the conventional optical surface plasmon resonance sensor.

We clarify the relationships between the p (TM) and s (TE) polarizations. The fields inside NIM are examined, as well as the interesting behaviors of the Poynting vectors, pointing to the opposite direction in the inside and outside of NIM. We discuss the angular and frequency sensitivities of this phenomenon and difficulties in implementing this for practical applications.

A New Very High Resolution Interference Rejection Method for Arrays

John Minkoff , ITT Aerospace and Electronic Systems, Clifton, NJ 07014

A scheme for interference rejection at an array is presented, in which the interference, represented as vectors, is removed by an operation in which none of the physical array characteristics such as beam width and resolution come into play. As a result, observation of signals of interest from weak sources, intact, unaffected by the presence of interfering signals from stronger sources arbitrarily close in angle --- e.g. fractions of an array beamwidth --- to the weaker sources, is possible. The essential limit on this capability is determined solely by receiver noise. Rejection of up to M-1 interfering sources with an array of M elements is accomplished by a single operation.

In this approach the rejection is accomplished by projecting the interference, represented as vectors, into the null-space of a matrix: a null-space transformation(NST). The interference is transformed into the zero vector. The scheme differs fundamentally from conventional beamforming/nulling schemes in that the projection operation is applied directly to the observables, the array outputs, rather than to beam steering vectors. The geometrical relationship between the signal and interference subspaces is irrelevant; the issue of subspace orthogonality does not arise. Beamforming plays no part. None of the limitations associated with physical array characteristics such as beamwidth and resolution come into play, which yields an intrinsic high-resolution interference rejection capability not present in conventional schemes employing beamforming/nulling operations. There is no fundamental limitation on the minimum angular separation between an interfering source that can be rejected and a signal of interest that can be recovered intact, undesturbed by the process. Excluding possible implemental hardware issues, which we do not consider here, the practical limit on the extent to which this property of the scheme can be realized is determined solely by receiver noise. Other desirable properties of the scheme are (2) for N interfering sources an array of only M = N+1 elements are necessary; M>>N is unnecessary. (3) interference rejection is accomplished by a single matrix multiplication independently of the number of interferers. (4)The interfering signals are removed selectively at each array element with signals of interest completely recoverable. As evidence of this, beam patterns after interference rejection, if desired, are identical to what they would be with no interference, and coherent summation over the array of the recovered signals yields the usual 10logM dB improvement in signal-to-noise ratio. Results of computer experimnts are presented validating all aforementioned assertions.

A Numerical Investigation into the Accuracy of FE-BI and MoM for Canonical Structures

Matthys M. Botha*, Thomas Rylander and Jian-Ming Jin

Center for Computational Electromagnetics, Department of Electrical and Computer Engineering, University of Illinois at Urbana-Champaign, 1406 West Green Street, Urbana, Illinois 61801. E-mail: mmbotha@uiuc.edu

In any discrete representation of an infinite dimensional function space, an error is introduced. In the cases of the finite element method (FEM), the finite element-boundary integral (FE-BI) method and the method of moments (MoM), this is exactly what happens. This paper will explore this error numerically within the setting of time-harmonic, electromagnetic analysis in three dimensions, comparing results obtained with various numerical formulations. The specific test problems considered are dielectric and/or PEC spheres and coated spheres — all of which can be treated analytically as well. The quality of a solution is measured as the L^2-norm of the error in the bistatic radar cross section (RCS), i.e.

$$\varepsilon_\sigma = \|\sigma(\theta, \phi) - \tilde{\sigma}(\theta, \phi)\|_{L^2(\Lambda)}$$

where $\sigma(\theta, \phi)$ and $\tilde{\sigma}(\theta, \phi)$ represent the exact and calculated bistatic RCS, respectively; and Λ represents the surface of the unit sphere. By examining the convergence of this quantity with respect to the cell size (h) in the mesh (on a set of regular, hierarchically nested grids), the relative accuracies of the various formulations can be observed in a clear way. The accuracy of a formulation has two components to it: rate of convergence and relative scaling. The rate of convergence relates to a formulation's asymptotic behaviour as $h \to 0$. The relative scaling relates to the proportionality constant in the error behaviour, which could make one formulation preferable to another, even though both have the same asymptotic rates of convergence.

A selection of the following formulations will be considered in the study:

- *FE-BI:* FEM hybridized with the EFIE/MFIE/CFIE/1st order ABC (including dual field formulations) [J.-M. Jin, *The Finite Element Method in Electromagnetics.* New York: John Wiley and Sons, 2nd ed., 2002]; Stationary FE-BI (volume-trace and volume-volume, including dual field formulations) [M. M. Botha and J.-M. Jin, "On the variational formulation of hybrid finite element-boundary integral techniques for time-harmonic electromagnetic analysis in 3D," *IEEE Trans. Antennas Propagat.*, submitted for publication, 2003];

- *MoM:* EFIE, MFIE and CFIE [J.-M. Jin, *The Finite Element Method in Electromagnetics.* New York: John Wiley and Sons, 2nd ed., 2002]

The relative accuracies in the various formulations will be discussed with respect to the effects of discretization error, dispersion error and the influence of the boundary conditions.

Error Analysis of Moment Method Solutions for 3D Scattering Problems

Clayton P. Davis* and Karl F. Warnick
Department of Electrical and Computer Engineering
Brigham Young University
459 Clyde Building, Provo, UT 84602

There are two common approaches to validating numerical results in computational electromagnetics—validation by test case and numerical analysis. Engineers often compare moment method solutions to measured data or to known solutions for simple geometries such as the sphere. Though this approach has provided sufficient confidence for succesful application of CEM methods in many areas, empirical validation alone cannot guarantee solution accuracy for arbitrary problems. An alternate approach is to study the moment method using functional analysis, giving abstract error estimates that prove solution convergence. These important results establish that numerical solutions converge to exact solutions in the limit of infinite mesh refinement. The difficulty with these types of error estimates is that they contain unknown constants and are given in terms of norms that can be difficult or impossible to compute. In previous work [K. F. Warnick and W. C. Chew, "Error analysis of surface integral equation methods," in *Fast and Efficient Methods in Computational Electromagnetics*," W. C. Chew, et al., eds., Artech House, Boston, MA, 2001] attempts have been made to bridge the gap between test case validation and general convergence theory by developing error estimates in terms of standard norms with known constants for a number of 2D scattering geometries. We are now seeking to extend these results to 3D problems.

We have conducted numerical error studies of moment method solutions for several benchmark scatterers. Highly refined reference solutions are compared against low-order solutions to estimate RCS error. Many factors contribute to the error in the numerical solution, including quadrature error in the integration of moment matrix elements, flat-facet modeling of a curved geometry, and discretization error. We specifically address the effects of irregular discretization on final solution accuracy, compare the accuracies of flat-facet models to curved-facet models, and compare the accuracy of different quadrature rules. Using insights obtained from previous theoretical studies of 2D problems, we attempt to isolate these error sources and quantify their relative impact on solution error. Based on two-dimensional studies, we expect flat-facet modeling and low-order quadrature to be the most significant error sources.

Singular Higher Order Models
of Surface Integral Problems

Roberto D. Graglia*, Guido Lombardi, Politecnico di Torino, Torino, Italy.
Donald R. Wilton, University of Houston, Houston, TX, USA.

This paper considers the problem of electromagnetic scattering by arbitrarily shaped objects with sharp edges. To effectively solve surface integral equations via the Method of Moments (MoM) one must use higher order models for both the geometry and the equivalent surface currents. Since higher order regular vector bases generally perform poorly near the edge of a wedge, in the edge regions we employ higher-order singular divergence-conforming bases directly defined in the parent space of curved triangular and quadrilateral elements. The figure illustrates the improved modeling of the longitudinal current distribution near the edges of a square metal cylinder with sides of electrical length $ka = 1$ for TM plane wave illumination. The method used to construct such bases is simple and general, and can be used for any order (R.D. Graglia and G. Lombardi, IEEE **TAP**–52, 2004, to appear). These bases incorporate the edge condition and are able to approximate the unknown surface current in the neighborhood of the edge of a wedge for any order of the singularity coefficient ν that is supposed given and known *a priori*. For metal wedges of aperture angle α, one has $\nu = (2\pi - \alpha)$. Our divergence conforming singular functions are compatible with standard p-th order vector functions in adjacent elements (R.D. Graglia *et al.*, IEEE **TAP**–45, 329–342, 1997), and guarantee normal continuity along the edges of the elements allowing for the discontinuity of tangential components, adequate modeling of the divergence, and removal of spurious solutions. Evaluation of the MoM matrix elements when both the Green's function and the basis function are singular is effectively performed by using a new integration technique (D.R. Wilton and M. A. Khayat, URSI EM Theory Int. Symp., Pisa, Italy, 2004). Several results for the scattering by circular and square plates will be presented and discussed.
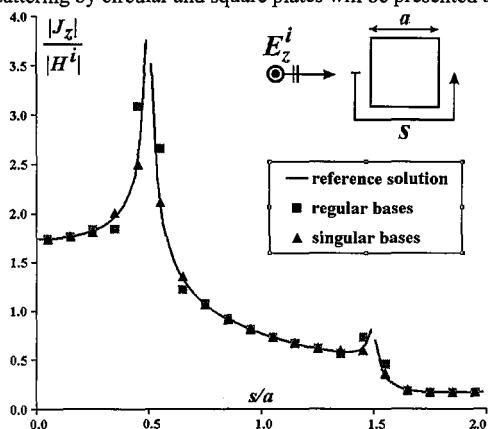
On the Degrees of Freedom in the Synthetic Functions Analysis of Large Antenna and Scatterers

Ladislau Matekovits, Valeriu Adrian Laza, Giuseppe Vecchi

LACE, CERCOM, Dipartimento di Elettronica, Politecnico di Torino
C.so Duca degli Abruzzi 24, I-10129 Torino, Italy.
Phone: +39 011 564 4119, Fax:+39 011 564 4015
ladislau.matekovits@polito.it, adrian.laza@eln.polito.it,
giuseppe.vecchi@polito.it

The Synthetic Function eXpansion (SFX) method consists in the employing a few, "global" unknowns (SFs) defined on different portions of the structure, into which in the first step the entire geometry was broken down (called blocks), reducing the complexity of the MoM analysis of antenna and scattering problems. The generation of these aggregate functions is effected via the original electromagnetic problem and based on its properties, rather than on matrix manipulations.

The SFX technique always resorts to a set of basis functions (more or less) larger than that of the "natural" solutions of the single sub-structures in isolation (one per port). It is to be noted that the method proposed here is *not* iterative or recursive in nature: the necessary aggregate basis functions are generated once, and used afterwards as basis functions in the MoM. The method includes mutual coupling in the formulation in a rigorous manner.

Following the Equivalence theorem, if sources are placed around the block, and the response (solution) is found for each source configuration, this set of responses will make up the space of all (rigorous) solutions, restricted to that block. Sources have first of all to be placed at the feeding ports: the associated responses will be called "natural" synthetic functions. On the other hand, one also needs SF that efficiently describe the effect of embedding it in the actual structure: these are called "coupling" SF, and require excitation outside the block. A typical choice places sources on a circular/square box around the considered block (analyzed in isolation).

It can be observed that the underlying question behind SFX and all the aggregate-function quest is "what is the number of *degrees of freedom* of the solution we are looking for on each block", and the implicit assumption that this number should be much smaller than the number of basis functions involved in discretizing the problem in the conventional way. In the SFX method, the question can be turned into the following: how many sources generate independent responses; this leads to the determination of the "minimum" or "optimum" number of such sources and responses. The natural mathematical tool to address these questions is the Singular Value decomposition (SVD) applied to the space represented by the independent solutions.

The method was applied to different examples confirming its validity.

A Comparison of Two Partial Differential Equation Techniques for Determining the Electromagnetic Scattering by Bodies of Revolution

Richard K. Gordon(*) and W. Elliott Hutchcraft
Department of Electrical Engineering(*)
University of Mississippi
Anderson Hall Box 41
University, MS 38677
Phone: (601) 234-5388
Fax: (601) 232-7231
Email: eegordon@olemiss.edu

Both integral equation and partial differential equation techniques have been used in the analysis of the electromagnetic scattering by a body of revolution. For situations in which the scatterer is a perfect electric conductor coated with homogeneous dielectric layers, the use of integral equation techniques is generally the best choice in terms of both efficiency and accuracy. But in cases in which the material properties are continuously varying rather than piecewise constant, the use of a technique based on an integral equation generally requires a rather time-consuming volume formulation. In this case, the use of a partial differential equation technique becomes an attractive alternative. One option would be to use a traditional approach such as the finite element method. Another would be to employ a meshless technique such as collocation. If the finite element method is used, an efficient approach for mesh truncation must be used. If collocation is used, there is no mesh; but there still must be some method for discriminating between incoming and outgoing fields.

This research employs a body of revolution formulation based on the coupled azimuthal potentials (CAPs) (M. A. Morgan, S. K. Chang, and K. K. Mei, *IEEE Trans. Antennas Propagat.*, 25, 413–417, 1977). The CAPs are scaled versions of the azimuthal components of the electric and magnetic field intensities. An attractive feature of the CAPs is that in problems with azimuthal symmetry these potentials represent tangential components of the fields and are therefore continuous across dielectric and magnetic interfaces. This makes them well suited for use in determining the scattering by bodies of revolution.

Two techniques, one employing finite elements in conjunction with the CAPs and the other using collocation together with the CAPs, will be discussed. Methods for truncating the mesh, in the case of finite elements, or discriminating between incoming and outgoing fields, in the case of collocation, will be presented. Results obtained from both techniques will be shown, and the advantages and disadvantages of each will be discussed.

Higher-Order Expansions for Iterative
Current-Based Hybrid Methods

Erik Jørgensen[1], Peter Meincke[2], and Olav Breinbjerg[2]

[1]TICRA

Læderstræde 34, DK-1201 Copenhagen K, Denmark

ej@ticra.com

[2]Technical University of Denmark, Ørsted·DTU

Ørsteds Plads, Bldg. 348, DK-2800 Kgs. Lyngby, Denmark

Electrically large scattering and radiation problems can be solved with hybrid methods based on the method of moments (MoM). The most well-known method is the hybrid PO/MoM (Jakobus and Landstorfer, Trans. Ant. Propagat., 2, 162-169, 1995) in which the electric field integral equation (EFIE) is used in a small domain and physical optics (PO) is used in the remaining large domain. This method includes all interactions between the two domains and is solved through an efficient iterative procedure. The hybrid EFIE/MFIE iterative method (HEMI) (Hodges and Rahmat-Samii, Trans. Ant. Propagat., 2, 265-276, 1997) improves the accuracy of the PO/MoM method for closed objects by using Neumann iterations to solve the magnetic field integral equation (MFIE) in the large domain. However, this method does not appear sufficiently robust for general problems.

The current-based hybrid methods cited above, as well as other similar methods, require that a known quantity is projected onto a set of basis functions or that a projection matrix involving the inner products of testing and basis functions is inverted. This is relatively easy when picewise linear basis functions, flat patches, and point matching are employed as in the above-mentioned works. On the other hand, if the more efficient higher-order basis functions are used on curved patches and/or Galerkin testing is used, the inverse projection matrix is generally hard to obtain. The commonly used divergence-conforming basis functions impose continuity between patches which means that the functions on each patch are non-orthogonal and that the projection matrix is a large banded matrix involving all patches. These problems have caused some authors to solve auxiliary equation systems (Edlund, Lötstedt, and Strand, Int. Jour. Num. Meth. Eng., 56, 1755-1770, 2003) or to use point matching and complicated interpolatory functions (Djordjovic and Notaros, PIERS, Honolulu, Hawaii, p.140, 2003).

This presentetation reviews a set of recently introduced higher-order hierarchical basis functions that allow current continuity to be enforced. These functions are aimed at enhancing the convergence rate of iterative solvers by maintaining low matrix condition numbers for high expansion orders. In addition, we show here that a known quantity is easily projected onto these basis functions and that the inverse of the projection matrix needed in the HEMI approach is known analytically. These properties hold even when the current continuity is enforced and Galerkin testing is used. Consequently, the hybrid PO/MoM, the HEMI method, and other hybrid techniques can be implemented without resorting to point matching, without formulating special interpolatory basis functions, and without solving auxiliary systems of equations. Numerical results for high expansion orders will be presented for the PO/MoM and HEMI methods. The latter appears to be the first higher-order implementation of the HEMI method.

Experimental Study of the Transient Field Reflected from a Layered Material

B.T. Perry* and E.J. Rothwell
Department of Electrical and Computer Engineering, Michigan State University,
East Lansing, MI 48824 e-mail:rothwell@egr.msu.edu

G.J. Stenholm
Air Force Research Laboratory, Wright-Patterson AFB, OH 45433
e-mail: garrett.stenholm@wpafb.af.mil

It has been shown theoretically (J. Oh, et. al., Journal of Electromagnetic Waves and Applications, vol. 17, no. 5, pp. 673-694, 2003) that the transient field reflected by a single layer of conductor-backed lossy material may be written as a natural mode series. We predict that the reflection from a stack of materials can also be written as a resonance series. To demonstrate this we consider the measured field reflected from multiple-layer materials.

Measurements of material stacks are made both in the time and frequency domains using the MSU reflectivity arch range. This free-field range, designed and built by the Georgia Tech Research Institute, is a circular metallic structure 6.096 m in diameter and 1.219 m high. Antennas may be arranged along the metal rails to provide a variety of bistatic configurations. The time domain system uses an HP54750A 50 GHz sampling oscilloscope along with a PPL 4015B pulse generator to produce 20 picosecond Gaussian pulses of amplitude 3V. The pulses reflected by the material stack are measured in the time domain using a 20 GHz vertical channel of the oscilloscope. The frequency domain system consists of an HP8510C vector network analyzer connected directly to the transmit and receive antennas. The bandwidth of both systems is determined by the 2-20 GHz bandwidth of the antennas. Calibration of both measurement systems is done in the frequency domain, using a metallic sphere or a metal plate as a known calibration target.

The measured transient responses are compared to the theoretical reflected field found from a frequency domain analysis, and to that found using a natural-mode representation.

E-pulse Discrimination of R-Cards in a Layered Environment

E.J. Rothwell* and L.C. Kempel
Department of Electrical and Computer Engineering, Michigan State University,
East Lansing, MI 48824 e-mail:rothwell@egr.msu.edu

Resistance cards (R-cards) are often included among stacks of materials applied to aircraft to reduce their radar cross-section. Misapplication or degradation of these materials results in a decrease in performance, and thus a technique to determine the value of the R-card while within the stack is useful for diagnosis and repair.

Consider a stack of materials containing an embedded R-card. Previous work (J. Oh, et. al., Journal of Electromagnetic Waves and Applications, vol. 17, no. 5, pp. 673-694, 2003) has shown that the transient field reflected by a single layer of conductor-backed lossy material may be written as a natural mode series. Thus the E-pulse technique may be used to differentiate between layer parameters such as thickness and permittivity We hypothesize that the field reflected by a stack of materials may also be written as a modal series. In particular, we study the response of an R-card sandwiched between a lossy dielectric layer and a nylon layer.

E-pulses are constructed from the measured transient responses of stacks with five R-card values: $0\Omega/?$ (no R-card present), $54\Omega/?$, $105\Omega/?$, $202\Omega/?$, and 1389 $\Omega/?$. Convolution of an E pulse with the response it was constructed for ideally yields a null result, while convolution with a different response yields a non-zero result. This allows the identification of the R-card by association with the smallest convolution value. To automate the discrimination among R-cards the E-pulse discrimination number (EDNa) and the E-pulse discrimination ratio (EDRa) are computed from the normalized late-time energy in the convolution outputs (G. Stenholm , et. al., "E-pulse Diagnostics of Simple Layered materials," IEEE Transactions on Antennas and Propagation, to appear). It is shown that each of the R-cards may be discriminated from the others based on the EDNa and the EDRa.

Prediction of Package and Chip Substrate Loss Effects in Microelectronic Circuits Using Time-Domain Surface-Integral Equations

Chuanyi Yang* and Vikram Jandhyala

Dept. of Electrical Engineering, University of Washington

Box 352500, Seattle WA 98195, Ph: 206-543-2186, Fax: 206-543-2186

Email : {cyang1,jandhyala}@ee.washington.edu

With the modern microelectronic industry entering a new era featured by progressively higher speed and higher integration mixed-signal systems on chip, accurate modeling of distributed electromagnetic behavior of sections which may includes signal traces, power planes, substrates etc, is crucial during the design flow. Driven by broadband and non-linear circuit design, time domain coupled electromagnetic and circuit simulation has been gaining popularity. In particular, integral equation methods have proven to be useful since radiation conditions are built in and only surface meshing and modeling is needed. In this work, the time-domain integral equation (TDIE) method is enhanced to model realistic loss behavior in substrates, which is a crucial component for quality factor prediction of integrated passives, as well as for thermal pattern prediction.

The EM simulation environment in present and future 3D integrated circuits is characterized by multiple piecewise homogeneous regions. Each region is comprised of lossy materials, which may or not have a strong impact on the overall performance. In general, for higher speed and higher sensitivity systems such as RF and analog methods, the loss is a crucial factor in determining system specifications and performance. The TDIE approach has been shown to work with lossy material (M. J. Blunk and S. P. Walker, Antennas and Propa, 49, 875-879, 2001) wherein the Green's functions, besides possessing delta functions in time, also include a broadly exponentially decaying "wake". This leads to the implementation issue that the spatial integrals at retarded times have to be replaced by temporal convolutions. This convolution brings not only coding complexity but also increases the computational cost dramatically.

In the presented work, the multi-region substrate geometry is addressed with a TDIE solver. An equivalent surface approach for each region is used along with the following method to tackle the lossy medium Green's function. To circumvent the difficulty caused by the convolution in time, the decaying "wake" in the Green function is approximated by a sum of decaying exponentials via Prony's method. It is shown that for circuit dimensions and realistic losses, the decaying "wake" changes slowly with the variation of the distance between the source and observation point. This allows the building of an exponential fitting table for discrete distances. The use of the exponential models permit the convolutions in time to be computed recursively. This then achieves the purpose of reducing computational complexity, with an added constant, to be the same as that of a TDIE solver for lossless media.

Transmission and Reception by UWB Antennas in Time Domain

Debalina Ghosh, Tapan K. Sarkar
121 Link Hall, Syracuse University
SYRACUSE, NY, 13210, USA
Phone: 315-443-3775 Fax: 315-443-4441
Email: deghosh@syr.edu, tksarkar@mailbox.syr.edu

The transmission and reception properties of several UWB antennas, including the biconical antenna and the TEM horn antenna, are presented. In the time-domain, the transmitting transient property for a UWB antenna is proportional to the derivative of the receiving transient property (Dr. Motohisa Kanda, Time-Domain Measurement in Electromagnetics, 1986). The radiated wave from a biconical transmitting antenna is exactly identical to the driving point voltage waveform. Following the general property of UWB antennas as stated before the current induced in a biconical receiving antenna is the integral of the input waveform. On the other hand, in the case of a receiving TEM horn antenna, the induced current is a replica of the incident field. If the TEM antenna is used for transmission then the radiated E-field is the first derivative of the input pulse.

All of these properties have been verified by simulating the antennas by using the WIPL-D software (B. M. Kolundzija, J. S. Ognjanovic, T. K. Sarkar, R. F. Harrington, WIPL Software for Electromagnetic Modeling of Composite Wire and Plate Structures, 1995) which can simulate the antenna response for a wide band of frequencies. The time-domain response is obtained by inverse Fourier transform of this data. The input is the derivative of a very short duration Gaussian pulse. It is seen that several reflections occur due to the finite length of the antennas. So during simulation these reflections can be reduced by rounding off of the edges by placing additional structures at the edges or by decreasing the discontinuities of the structures. It is seen that during transmission from a biconical antenna to a TEM horn antenna, the wave-shape of the input pulse is identical to the output pulse. So by this process we can obtain direct measurement of the input by observing the output.

Further analysis using a dipole antenna has shown that in the wide band the dipole behaves in a manner similar to a biconical antenna when the duration of the transient input pulse is very small compared to the electrical length of the dipole. But in the case of a dipole it is hardly possible to avoid the reflections from the edges of the dipole.

Transient Responses of Short-Pulse Signals in Scattering Problems

Mengtao Yuan, Mary C. Taylor and Tapan K. Sarkar

Department of Electrical Engineering & Computer Science

121 Link Hall Syracuse University

Syracuse, New York 13244-1240

Phone : 315-443-3775

Fax : 315-443-4441

Email : myuan@mailbox.syr.edu, cannella@mailbox.syr.edu, tksarkar@mailbox.syr.edu

The transient responses of short-pulse (ultra-wideband) signals are analyzed in electromagnetic scattering problems. An efficient way to simulate the short-pulse measurements is introduced. In short-pulse measurement, we usually generate some incident wave by a transmitting antenna and radiate the wave toward the target. The scattered wave will be reflected back by the target and observed by a receiving antenna. For narrow band or single frequency scattering problems, we don't need to care about the properties of the transmitting and the receiving antennas. We take the incident wave as the replica of the exciting voltage in transmitting antenna and the induced voltage in the receiving antenna as the far scattered field. However, it's not true for ultra-wide band or time domain analysis. Each antenna in practice will illustrate some non-linear properties through the broad band, and these properties will distort the input signals (T. K. Sarkar, M. C. Wicks, M. Salazar-Palma, and R. J. Bonneau, Smart Antennas, 2003). If we ignore the properties of antennas, the information we get or observe will be different from the real data.

Each electromagnetic component can be seen as a linear time invariant (LTI) system. The system of measurement can be divided into cascaded subsystems. We take the transmitting antenna as the first system and the input of the subsystem is the exciting voltage and the output is the radiated wave. The target is the second system with the input of the incident wave (wave radiated from the transmitting antenna) and output of the scattered wave. The receiving antenna is the third system. If we replace the second system with the wireless channel, the whole system can be looked as a system of ultra-wideband wireless communications. We can analyze each subsystem by sequence, and get the final output (the induced voltage of the receiving antenna).

Examples of both metallic and dielectric targets are simulated and the short-pulse responses are analyzed. The exciting voltage of the transmitting antenna is a short Gaussian pulse. If we put a short wire-like receiving dipole at the observing point, it does the temporal derivative of the scattered wave. This nonlinear property will filter out the low frequency component of the scattered wave and some late-time pulses will be shown in the induced voltage. These late-time pulses are caused by the resonance of the structure and can be used to analyze the target.

Using the Laguerre Polynomials as Temporal Basis Function to Solve the Time Domain Magnetic Field Integral Equation

*Zhong Ji[1], Tapan K. Sarkar[1], Baek Ho Jung[2], and Magdalena Salazar-Palma[3]
[1] Department of Electrical Engineering and Computer Science, Syracuse University
Syracuse, NY 13244-1240
zji@.syr.edu, tksarkar@syr.edu
[2] Department of Information and Communication Engineering, Hoseo University
Asan, Chungnam 336-795, Korea
bhjung@office.hoseo.ac.kr
[3]Dpto. SSR, E.T.S.I. Telecomunicacion, Universidad Politecnica de Madrid
Ciudad Universitaria s/n, 28040 Madrid, Spain
m.salazar-palma@ieee.org

ABSTRACT- Numerically rigorous transient analysis is based either on the differential or integral equation approach. A time-domain integral equation (TDIE) method that requires only a surface discretization is sometimes preferred over the differential one using a volumetric discretization and do not call for absorbing boundary conditions. Furthermore TDIE implicitly impose the radiation condition and there exists no grid dispersion. In this paper, we present a numerical method to solve the time domain magnetic field integral equation (TD-MFIE) for arbitrary shaped conducting objects. The TD-MFIE technique has been employed to analyze many electromagnetic scattering and radiation problems. However, the most popular method to solve the TD-MFIE is a marching-on-in-time (MOT) method, which may suffer from its late-time instability. One explanation for the cause of instability is that if the temporal basis function has a rich high-frequency content, the spatial discretization may not be sufficient for these high frequencies. In this paper, a simple, stable and accurate method is presented to solve the integral equation in time domain for arbitrarily shaped perfectly conducting structures using weighted Laguerre polynomials as temporal basis and testing. The characteristic properties of the weighted Laguerre polynomials such as causality , orthogonality and convergence have been used in our formulations. Furthermore, these orthogonal polynomials can be calculated recursively. We also perform a more accurate evaluation for the integrals for the matrix elements. By using these orthogonal basis functions for the temporal variation, the time derivatives can be handled analytically and stable results can be obtained even for late-time. Several examples are simulated both for radiation and scattering problem. The results are compared with the inverse discrete Fourier transform (IDFT) of frequency domain data and they agree well.

EFFICIENT RAY-TRACING TECHNIQUES FOR OUTDOORS AND INDOORS PROPAGATION ANALYSIS

Felipe Cátedra, Oscar Gutiérrez, Iván González, Carlos Delgado, Francisco Sáez de Adana

Escuela Politécnica, Universidad de Alcalá
28806 Alcalá de Henares. Madrid. Spain
Fax: +34 91 885 6960 e-mail: felipe.catedra@uah.es

ABSTRACT.

The analysis of outdoor and indoor propagation scenarios using ray tracing in wireless communications represents a challenging problem because the large number of facets that should be includes in realistic models of these scenarios. Efficient algorithms are absolutely needed to accelerate the ray tracing in the computer analyses in order to obtain results with affordable computational cost in a reasonable time. A review of some efficient algorithms to accelerate the ray tracing for wireless applications will be presented. Different outdoor scenarios such that micro cells and pico cells, indoors pico cells, tunnels and corridors will be considered. The facets could be made of any building material and can support specular or diffuse reflection. Several ray tracing acceleration techniques like the SVP algorithm (Space Volumetric Partitioning), the BSP (Binary Space Partitioning), the AZB (Angular Z-Buffer), radiosity and other ones will be outlined and compared. Analyses examples for different scenarios will be presented.

Multi-layer Bistatic MIMICS

Pan Liang, Mahta Moghaddam, Leland Pierce

The University of Michigan, Radiation Lab, Ann Arbor, MI 48109, USA

In this paper, we propose a bistatic microwave forest canopy scattering simulator using a multi-layer canopy model. In the remote sensing field, the forest canopy is usually modeled as two cascading independent vegetation layers over a dielectric ground surface. The Michigan Microwave Canopy Scattering model (MIMICS) is such a model that has been developed to simulate microwave backscattering from tree canopies. The crown layer includes leaves, needles and branches and the trunk layer includes vertical tree trunks. All the tree components are modeled as basic microwave scatterers like flat rectangular disks and cylinders. However, this division is too restrictive for the canopy coverage. For many forest structures we are dealing with a mixtures of different tree types having different densities, sizes and heights: The very tallest trees that stand over the rest of the plants make up the overstory; The understory is made up of sapling or immature trees and tall bushes that are completely submerged under the canopy. In many cases the young trees and bushes can be further divided into two distinct layers. In such cases, we can't simply categorize the canopy as the crown layer and trunk layer.

We propose a multi-layer MIMICS model to remove the two-layer canopy restriction. The model can handle arbitrary layers of canopy as necessary. Rather than characterize the layers with definite names, we treat all the layers as part of the vertical profile. Every layer can be composed of branches, leaves, needles and trunks. While the composition differences among layers are distinct, the type and distribution of scatterers inside each layer are relatively homogeneous. To simulate the bistatic scattering from this multi-layer canopy configuration, we can solve an array of radiative transfer equations. The first order solution indicates that each layer contributes to the total scattering in four ways. They are (1) Direct scattering from the scatterers in the layer; (2)Scatterers scattering — Ground reflection; (3) Ground reflection — Scatterers scattering; and (4) Ground reflection — Scatterers scattering — Ground reflection. The total canopy scattering is the sum of all layer contributions and direct bistatic scattering from the rough ground. In the specular direction, we also have an additional term to represent the coherent specular ground reflection.

Furthermore, we are more interested in the interactions between adjacent layers. Thus the layers are allowed to overlap to account for the situations such as the mixtures of tall tree trunks and short tree crowns and extending trunks into the crown layer. Therefore, the scattering from each layer is no longer independent of the other layers, the solution will include the layer interactions. This model is a versatile tool for studies on forest canopy studies. It is an efficient realization of the real forest structure and can be shaped for specific interest of forest parameters. We will build a realistic 3-D forest using a fractal tree generator as the input canopy for model application.

The main contributions of this paper are (1)The multi-layer canopy configuration to better represent the forest structure. (2)The canopy layers are related and the interactions between layers are included. (3) Using a fractal tree generator to build a realistic forest model.

Near-Earth Wave Propagation Simulation in Presence of Vegetation Layer

DaHan Liao* and Kamal Sarabandi
Radiation Laboratory, The University of Michigan—Ann Arbor, MI
Email: liaod@umich.edu

Abstract

A network of unattended ground sensors can be used to gather information in a variety of environments. These sensors can be electric, magnetic, photonic, acoustic, or other types of detectors. Each effectively serving as a communication node in the network, a sensor is usually low-profiled and miniaturized in nature employing a low-power electronic module that contains a microprocessor, transmitter, and receiver. If the host environment is a vegetation-covered terrain, complicated node-to-node signal-propagation issues can arise and would have to be characterized to facilitate optimal network performance.

In this study, radiation from an arbitrarily oriented dipole at high frequency in the presence of a vegetated terrain is examined using a two-layer half-space model. In order to estimate the mean path-loss, the vegetation layer is represented by a homogeneous dielectric slab with a permittivity equal to the effective dielectric constant of the vegetation layer. This approximation is valid from low frequencies through the UHF band. In the case when both the source and receiver are embedded in the vegetation, it is shown that the mean field at the receiver is composed of the direct field, the reflected fields, and lateral waves. The reflected fields—which come from the saddle point contribution in the integral of the spectral representation of the dipole field in the two-layer half-space dielectric—can be further separated into a wave that is reflected from the vegetation/air interface and one that is reflected from the ground/vegetation interface. The former is the first-order term in the saddle point expansion; the latter—also known as the Norton surface wave—is a result of the higher-order terms. Similarly, in the same mathematical terminology, the lateral waves are the branch cut contributions in the forementioned integral. Higher-order lateral waves can also exist and are included in the model.

The study indicates that the direct and reflected fields decay exponentially with the separation distance (ρ) between the source and receiver, while the lateral waves attenuate in the form of $\sim 1/\rho^2$. Therefore, at large distances, the mean field is dominated solely by lateral waves. In order to generalize to the more realistic case when the vegetation/air interface is rough rather than uniformly flat, the existence of a hypothetical induced polarization current at the interface is assimilated into the formulations through the use of distorted Born approximation. These formulations are asymptotically evaluated and the results are compared to those obtained from numerical methods. The study also investigates the case when the source, or the receiver, or both reside above the vegetation layer by properly taking into account the modification needed in the calculation of the different major field components.

A VHF/UHF Simulator for Soil Moisture Beneath Forest Canopies

Leland Pierce, Mahta Moghaddam*
The University of Michigan, Radiation Lab
Ann Arbor, MI 48109-2122 USA
FAX: +1-313-747-2106   email: lep@eecs.umich.edu

Ernesto Rodriguez, Paul Siqueira
JPL, Radar Sciences Group
Pasadena, CA, USA

ABSTRACT

A simulator for UHF/VHF propagations and scattering has been developed for use in the context of forest canopies. The goal is to be able to be able to accurately simulate the performance of a space-borne UHF/VHF radar platform (MOSS) that is intended to map soil moisture world-wide.

The simulator is a modification of our microwave forest simulator: MIMICS. Interaction with leaves, branches, trunks, and rough wet soil has been suitably modified to use low-frequency approximations so that the simulator accurately models the backscatter of UHF/VHF signals. We also modified the dielectric constant models for both moist soil and moist wood to allow them to produce accurate results for this new frequency range.

MIMICS is a radiative-transfer-based code that breaks the canopy into 3 layers: (1) branches and leaves, (2) trunks, and (3) soil surface. The scattering characteristics of each of these constituents is then simulated separately. This is then combined using up to second-order scattering mechanisms: (1) direct-crown, (2) direct-trunk, (3) direct-ground, (4) crown-trunk, (5) crown-ground, and (6) trunk-ground. Using this approach we have shown that we can accurately simulate the microwave backscatter from a tree canopy while simultaneously obtaining insight into the important scattering mechanisms in each case.

A tower-based system has been deployed to validate the MOSS concept. We present comparisons of that dataset with our simulations over a variety of canopy and soil moisture conditions. The ability to vary tree canopy and radar platform parameters will allow this simulator to be invaluable in the design phase of MOSS.

PARABOLIC EQUATION MODELLING OF VHF GROUND RADAR WAVE INSIDE FOREST

Marc LE PALUD
CREC St-CYR / French Ministry of Defense
marc.lepalud@st-cyr.terre.defense.gouv.fr

Since several years, strong interest has been shown for the detection of targets located inside forested areas. Several RADAR systems are under development that operate in the VHF band for better penetration with airborne or mast-elevated antennas. As these systems work with grazing incidence beams, propagation effects have a significant influence on the signal-to-clutter ratio.

In previous work we have shown that the Parabolic Equation (PE) algorithm (A.E. Barrios, IEEE Trans. on Ant. Prop., Vol. 42, No. 1, 90-98, 1994) was well suited to describe propagation characteristics in such environment. In our PE algorithm the vegetation bulk was treated like an absorbing atmospheric layer characterized by a complex refractive index. We have found strong asymmetry in the treatment of the upward and the downward links: for instance, computation of the transmitting antenna beam is relatively straightforward while the scattered field (used as "starter field") transmitted by the illuminated target inside the vegetation layer is far more difficult to determine as we will discuss.

We have obtained results for operation both in continuous wave mode and in pulse mode. Depolarization effects are not taken into account at this point ; we are currently working to improve this issue.

The following results are 2D plots of path loss in CW mode using a pseudocolor dB scale:
- left : downward link (from transmitter to target)
- right : upward link (from target to receiver)

The transmitting antenna (frequency 100MHz, vertical polarization, omnidirectional beam, and height 10m) is located at range 0km outside the forest. The forest area (height 25m) starts at range 5km and is characterized by equivalent permittivity $\varepsilon=1.04$ and conductivity $\sigma=1.310^{-4}$ S/m while the electromagnetic parameters of ground are $\varepsilon=15$ $\sigma=10^{-3}$ S/m. The target (omnidirectional scattering pattern, height 10m) is located inside the vegetation at range 20km.

2D pseudocolor dB scale
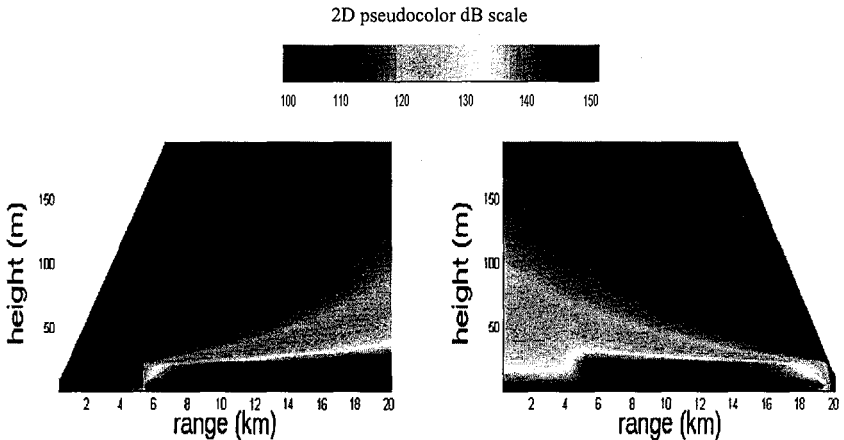
95 GHz Polarimetric Radar Signatures of Pristine Crystals Mixed with Aggregates and Rimed Crystals

K. Aydin* and J. Singh
Penn State University
Department of Electrical Engineering
University Park, PA 16802
Phone: (814)865-2355,Fax: (814)863-8457
E-mail: k-aydin@psu.edu

Millimeter wave radars operating at 95 GHz are now being used for the remote sensing of ice clouds from ground-based and airborne platforms for cloud microphysical studies and for understanding the effects of clouds on the Earth's radiation budget. Two important goals are to identify ice crystal types and to estimate bulk parameters such as the ice water content. Polarimetric radars at 95 GHz have the potential for doing both. Two-dimensional particle probe (2D-C cloud and 2D-P precipitation probe) measurements in clouds show that ice crystal aggregates are observed more often than "pristine" or single type of ice crystals (e. g., hexagonal columns, hexagonal plates, stellar crystal, etc.). This paper focuses on polarimetric radar signatures of ice crystal aggregates, rimed crystals, and their mixtures with pristine crystals. A detailed computational study of the radar signatures of these ice crystals is conducted and compared with airborne 95 GHz radar measurements and in situ particle probe images. The measurement data is from field experiments conducted in 1997 (February through April) in Wyoming. During these experiments as the aircraft penetrated through the clouds, the onboard radar and particle probes collected data simultaneously. Polarimetric radar signatures of ice crystal aggregates were obtained with the assumption that the closest two range gates (at 120 and 150 m, with 30 m gate spacing) from the radar were highly correlated with the images obtained by the probes on the aircraft wings. Results from computational simulations and experimental data for the reflectivity factor (Z_h), differential reflectivity (Z_{DR}), and linear depolarization ratio (LDR) agreed very well. The various ice crystal mixtures showed different clustering characteristics on the $Z_h - Z_{DR}$, $Z_h -$ LDR, and $Z_{DR} -$ LDR planes. (Although the correlation coefficient for copolarized signals (ρ_{hv}) was not among the measured parameters, computational results showed that the signatures on the $Z_{DR} - \rho_{hv}$ plane could provide additional information for distinguishing crystal types.) These results are expected to be very useful in ice crystal classification algorithms based on 95 GHz polarimetric radar observables.

1. Commission F : F5 Remote sensing of oceans and atmosphere
2. 95 GHz polarimetric radar signatures of mixtures of pristine crystals (e.g., hexagonal plates and stellar crystals), their aggregates and rimed forms are developed based on computational and experimental results. These signatures are essential for ice crystal classification algorithms using radar.
3. Earlier computational studies focused on pristine crystals. This work is an extension to mixtures of ice crystals (including aggregates), which are encountered more often in clouds.

Three-Dimensional FDTD Modeling of
the Response of the Global Earth-Ionosphere Waveguide
to Seismically-Induced Sources

Jamesina J. Simpson* and Allen Taflove
ECE Department, McCormick School of Engineering
Northwestern University, Evanston, IL 60208

In a recent publication (Simpson and Taflove, IEEE Trans. Ant. Prop., in press), we reported a novel, finite-difference time-domain (FDTD) algorithm suitable for highly detailed three-dimensional (3-D) modeling of extremely low-frequency (ELF) propagation within the entire Earth-ionosphere waveguide. The algorithm incorporates a latitude-longitude FDTD space lattice which wraps around the complete Earth-sphere. Adaptive combination of adjacent grid cells in the east-west direction minimizes cell eccentricity upon approaching the poles and hence maintains Courant stability for relatively large time steps. Employing a 40 × 40 × 5 km baseline grid-cell size, we obtained agreement to within ± 1.5 dB for ELF propagation attenuation per megameter relative to that reported in the literature over the frequency range 50 – 500 Hz. Our technique permits an efficient, direct time-domain calculation of impulsive, round-the-world ELF propagation accounting for arbitrary horizontal as well as vertical geometrical and electrical inhomogeneities / anisotropies of the excitation, ionosphere, lithosphere, and oceans.

In this paper, we apply the algorithm summarized above to study the response of the inhomogeneous global Earth-ionosphere waveguide to potential seismically-induced sources in the lithosphere. Specifically, we calculate what amounts to be the Green's function of the global Earth-ionosphere waveguide for impulsive current sources located at various depths below the Earth's surface in the vicinity of the epicenter of the 1989 Loma Prieta earthquake near San Francisco. More generally, we are exploring the possibility of the global ELF electromagnetic environment being perturbed by localized transient currents within the lithosphere generated by several mechanisms resulting from accumulating stress. Our ultimate goal is to provide as rigorous as possible a physics basis for proposed earthquake prediction schemes employing either land-based or satellite-based detectors of ELF anomalies.

Investigation on fading of High-Frequency signals propagating in the Ionosphere: From both the theoretical and experimental perspective

Kin Shing Bobby Yau - The University of Adelaide, Australia

This paper describes a project to investigate the fading of HF signals propagating in the ionosphere. The investigation involves the development of a theoretical model for fading of HF signals based on perturbation techniques, and a set of experiments using an advanced channel probe based on software radio for the monitoring of signal fading in the ionospheric channel.

There are two main contributors to the fading of HF signal propagating in the ionosphere: polarization and amplitude. Polarization fading occurs because of the rotation of the polarization plane of the wave in a process known as Faraday rotation. The current project models the effects of polarization fading using perturbation techniques based on Fermat's principle. The model has been shown to produce fast and accurate algorithm for the prediction of fading compared to a full ray-tracing algorithm (K. S. B. Yau, HF 2003, IEE Conf. Pub. 493, 131-135, 2003). This paper presents the extension of the model to incorporate the effects of amplitude fading. Amplitude fading is caused by the focusing and defocusing of the wave as it propagates through a layer of ionospheric irregularity. The effects of amplitude fading can be modelled by using a parabolic approximation to Maxwell's equations (J. F. Wagen and K. C. Yeh, Radio Sci., 4, 583-640, 1986), and involves a complexified version of diffusion equation. This approximation can be used to describe the fluctuation of the signal amplitude as the wave propagates through the irregular ionosphere.

The major advancement in the theoretical model is an analytical expression for the fading effects and it results in an efficient algorithm for the prediction of signal fading in a given ionosphere. Efficient algorithms are important for systems which rely on the forecast of channel conditions to maintain the minimum operational signal levels. Based on the theoretical signal fading model, it is possible to develop an efficient computational algorithm that can predict signal fading in real-time according to current ionospheric condition.

The practical aspect of the project involves a set of experiments to observe the behavior of a real ionospheric channel. Current experiment have used signals of opportunity such as the WWV and WWVH stations. Simultaneous observations are carried out in multiple frequencies (5, 10, 15 and 20 MHz in the case of WWV). The main constituents of the channel probe include a workstation equipped with a wide-band digital receiver and the active crossed-dipole antennas. The compact crossed-dipole active antenna provides the capability to simultaneously monitor both horizontal and vertical polarization. The experimental data is used to verify the theoretical model for signal fading in the HF band.

The outcome of this project is a HF ionospheric channel simulator that can incorporate both amplitude and polarization fading effects. Eventually, it is hoped that the channel simulator will form a test-bed for mitigation techniques to combat signal fading. A model that can accurately predict the signal fading mechanisms will provide the potential for model-based signal processing that can help overcome the effects of fading.

Near Real-time Ionospheric HF Propagation Modeling and Prediction

Liang Hong, Brian A. Lail* and Linwood Jones
Central Florida Remote Sensing Laboratory
Department of Electrical and Computer Engineering
University of Central Florida
Orlando, FL 32816

In order to utilize ionospheric channels for high frequency (HF) communications, a suitable frequency must be selected in order to ensure propagation. The highest frequency which will be refracted by the ionosphere is preferred. The propagation characteristics of the ionosphere are dynamic, with major influence being variations in solar flux and subsequent changes in ion density and height of the F2 layer. In some cases these effects are rapidly varying, and attempts to predict propagation frequencies may be outdated at the time of transmission. If HF communications are to be reliable, it is imperative to have timely knowledge of ionospheric properties. In this paper, near real-time ionospheric propagation prediction is presented based on empirical findings from an extensive HF communications network.

Traditional prediction models incorporate both theory and measurements, but struggle to be timely in their predictions. The diurnal cycle produces daily variations that may adversely affect HF communications if the transitions are not accurately accommodated in predictions. Additionally, periods of high solar activity give rise to short term variations that will impact HF propagation. A prediction scheme based on real-time HF propagation data provides improvement in the timeliness of predictions, resulting in better reliability for HF communications.

The HF network operated by Global2Way, Inc. of Melbourne Florida extends over the entire United States, consisting of 44 transmitters and 9 receivers. The transmitters and receivers are roughly uniformly distributed, providing a test network with extensive coverage. The transmitters continuously scan the HF spectrum, with a full scan approximately every 35 minutes. Logfiles record the transmitter identifier, frequency of propagation, and whether the signal was received at each of the 9 receivers. A predictive algorithm is presented, based on the test data from the HF network described. Improvements in the timing and the geographic range of the test data produce near real-time prediction capabilities for HF communications over the entire United States.

Long-term observations of the 3-D wind field by using CLOVAR VHF wind-profiler radar.

Radian G. Belu
College of Engineering
Wayne Sate University,
Detroit, Michigan, USA

and

Wayne K. Hocking
Department of Physics and Astronomy,
The University of Western Ontario,
London, Ontario, Canada

In the past three decades, VHF/UHF radars were used extensively for studying the structure and dynamics of lower and middle atmosphere. Wind-profiler radars offer the capability for measuring atmospheric wind motions with excellent temporal resolution and moderate height resolution. The CLOVAR VHF radar is located at 43°04.44' N, 81°20.20'W, operates at a frequency of 40.08 MHz, peak power of 10 kW (average power of 800 W) and is owned and operated by the University of Western Ontario, London, Ontario, Canada. The VHF MST radars have provided a new tool for continuously monitoring of all three components of the air velocity vector over a single location, and they are relatively unique in their ability to measure and monitor the vertical and horizontal wind velocity components.

The important influence of dissipating and interactions of gravity waves on the circulation of many regions of lower and middle atmosphere is now widely acknowledged. Gravity waves generated by various sources, throughout the atmosphere play an important role to the shaping and structure of atmospheric circulation. The can transport significant momentum and energy from the regions, where they are generated to the other parts of the atmosphere. Analyzing the generation, propagation, and climatology of these waves is important to the understanding of middle and upper atmosphere dynamics. Long-term radar measurements of the tropospheric wind velocities provide considerable insight into gravity wave processes, making it possible to study temporal and spatial variability of these waves. MST radars have proven to be a key tool in providing high-resolution measurements of the wave-induced velocity fields, which in turn have led to advances in our theoretical description of these processes. The seasonal variation of wind velocity and momentum fluxes induced by gravity waves in the troposphere have been studied using wind observations by the CLOVAR VHF radar at London, Ontario, Canada from January 1996 to December 1998. Our wind velocity variance and momentum flux estimates were correlated with information about weather systems taken from daily weather maps. The CLOVAR wind-profiler is located in a flat region of Eastern Canada, so that the gravity wave generation is not affected by orography.

A Simple Practical Model of Fields and Currents in Lightning Discharges

By

Radian G. Belu[1], and Alexandru Belu[2]
1) College Of Engineering,
Wayne State University,
Detroit, MI 48202, USA
2) Department of Computer and Electrical Engineering,
The University of Western Ontario,
London, Ontario, Canada

Lightning discharge constitutes one of the most severe sources of electromagnetic interference (EMI) to many systems such as: aircraft, vehicles, communication and power networks. Electric and magnetic fields from lightning return strokes can be uniquely calculated from Maxwell's equations if the spatial and temporal distribution of either the current or the charge along the channel is known. Several return stroke current models have been proposed, during the last century which predict the spatial temporal variation of the current in terms of the current at the base of the of the channel since lightning current properties have been measured at ground level. We proposed a simple theoretical/numerical model to evaluate electric fields, radiated both by the leader and return stroke phases of the lightning discharges based on a transmission-line representation. In this model, we employ an equivalent electrical network to represent the lightning discharge, the parameters of which are determined from electromagnetic field and gas discharge theories. The model also incorporates resistance non-linearities and corona, and also takes in account the presence of the thunderstorm cloud. It uses the fact that the discharge channel may be likened to a long conductor and employs a typical RCL representation for a single conductor line. For all phases of the discharge, the same circuit is used in modeling the change of the stage with variable resistances and inductances. It allows us to determine the currents of the leader and return stroke, the corresponding charge, the potential drop along the leader channel, the power and the energy injected into the discharge gap and the leader propagation velocities. As we already mentioned a particular feature of this model is that it incorporates resistance non-linearities, the effect of corona and the cloud. The inclusion of these features is an important factor in obtained correct predictions.

The model that we developed is based on a self-consistent analysis. Generally, the results obtained results are found to be in accordance with experimental and measurement date found in the literature. We also compared it with other models found in the literature. Our work is now in progress to improve this model and to develop an application to estimate the interaction of EM fields, radiated by lightning with power and communication networks.

Effects of a Non-Standard Design of a Dielectric in a Blumlein-configuration Parallel-plate Pulse-forming Line

Miroslav Joler*, Christos G. Christodoulou, Edl Schamiloglu, and John Gaudet
The University of New Mexico, Electrical and Computer Engineering Department
Albuquerque, New Mexico, USA

In an ongoing collaborative effort to develop portable yet high-power microwave systems (www.ece.unm.edu/cp3), we are studying the pulse-forming section of the system. In particular, we have chosen a Blumlein configuration-based parallel-plate transmission line. At this point, to compromise the goals of high-power capability and small-scale dimensions, the line undergoes a non-standard design, as the one shown in Fig. 1. By "non-standard" we refer to a dielectric being wider than the conductor plates, and the structure having bends. The width of the dielectric is to enable a gradual decay of the electric field near the edges of the plates and thus a reduction of high concentration of the electric field that may cause breakdown. The bends are used to satisfy the requirement of the pulse length, yet occupy a smaller volume than a straight pulse-forming line would.

For a proper operation of the line, it is necessary to provide a good match between the load impedance and the line (characteristic) impedance. Whereas the expression for a parallel-plate-transmission-line impedance with a standard design (i.e. the dielectric as wide as the plates) can be found in the literature (e.g. D. M. Pozar, *Microwave Engineering*, 2nd ed., Wiley, 1998), the effects of this non-standard-design dielectric (M. Joler, C. G. Christodoulou, E. Schamiloglu, and J. Gaudet, 14th Int'l Pulsed Power Conf., pp. 253-257, 2003) have not been addressed in great detail.

In this work, we investigate the impact of such a design on the characteristic impedance, phase velocity, electric field distribution, and energy density of the pulse-forming line. These parameters are important for a desired performance of the structure, and they may be affected by either the extraordinary width of the dielectric or the curvature in the geometry. We will report on the characteristics of this design in comparison with the standard design, while paying particular interest to the parameters described above.
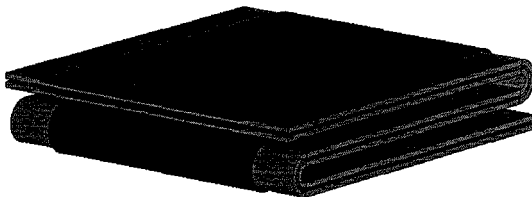
Fig. 1   A non-standard design of a Blumlein-configuration pulse-forming line

Coupling to a Loaded Thin Wire in a Cylindrical/Coaxial Cavity

*Charles L. Bopp, III, Chalmers M. Butler, and Fred M. Tesche
Holcombe Department of Electrical and Computer Engineering
336 Fluor Daniel EIB
Clemson University, Clemson, SC 29634-0915

The electromagnetic field coupling to a loaded thin wire in a cylindrical/coaxial cavity is investigated. There is an interest in understanding how electromagnetic fields couple to wires and tubes that may be present in an enclosed structure and how to efficiently analyze this coupling as part of an overall system. The cavity may consist of multiple cascaded coaxial and circular cylindrical sections with sections coupled through apertures and conducting elements common to more than one section. The sections may have different axial and radial dimensions and may be filled with material having different magnetic and electric properties. The technique for analyzing the field in these cavities with the wire absent was presented at the 2003 APS-URSI Symposium in Columbus, OH. A loaded thin wire protrudes into a cavity section and is placed in close enough proximity to the outer wall of the section that transmission line approximations are valid. The coupling of the cavity field to the wire is accounted for via a distributed voltage source model similar to that outlined by Agrawal, Price, and Gurbaxani (*IEEE Trans. on Elect. Comp*, May 1980) for a transmission line in open space or a wire parallel and close to a conducting surface, The characteristic impedance of the wire in the presence of the cavity wall is developed. A Green's function for the current and voltage along a loaded transmission line due to a set of distributed voltage sources is developed and used to calculate the voltage and current at points along the wire. For the purpose of demonstrating the accuracy of the procedure and numerical solutions obtained from this analysis, a cavity model is constructed and measurements made on the laboratory model are compared with computed results. The measured voltage and current at a port on the wire is compared with values obtained computationally at the port.

The Impact of Increasing Thickness on the Shielding Effectiveness of a Doubly-Periodic Conducting Screen Evaluated Using a Mode-Matching Technique

D.C. Love and E.J. Rothwell*
Department of Electrical and Computer Engineering
Michigan State University
East Lansing, MI 48824
lovederi@msu.edu, rothwell@egr.msu.edu

Prior efforts have investigated the use of mode-matching techniques to evaluate the transmission of electromagnetic waves through screens perforated with apertures. Typically, the focus has been on screens that are thin compared to the aperture dimension, and their behavior within a narrow frequency range. The technique is now being extended to determine the shielding characteristics of very thick screens (many times the aperture dimension) perforated with apertures that exhibit two-dimensional periodicity. This paper investigates the impact of considering thicker screens with rectangular apertures over a broader range of frequencies and the differences when compared to thin cases. Some aspects that are considered include number of modes used, contribution of non-propagating modes, and change in incidence angle. As a comparison, the results using the mode-matching technique are compared to results using the "waveguide below cut-off formula."

The screen apertures are modeled as an array of cylindrical waveguides, where the cross-section of the waveguides is rectangular. The reflected field above the panel and the transmitted field below the panel are represented with Floquet modes. The fields within the panel are modeled using rectangular waveguide modes. After enforcing boundary conditions and building a system of linear equations, the system is then truncated to produce a matrix equation which is solved using standard techniques. The shielding effectiveness of the screen is then determined by comparing the transmitted power to the incident power. It is clear that as the thickness of the screen increases, the transmitted power is greatly reduced at frequencies below the waveguide cut-off frequency. However, increasing the thickness also attenuates the higher-order waveguide modes at a greater rate, leading to non-convergent solutions to the matrix equation. By selectively eliminating higher-order modes from consideration, meaningful solutions can be found.

In comparing the mode-matching results to the "waveguide below cut-off formula", it is apparent that the two approaches are very closely related when the thickness is about five times the width of the waveguide or greater. When that ratio is less than five, the results still agree, but only within a smaller frequency range.

Broadband over Power Line - Radiation and Propagation

Alakananda Paul*, Jonathan Williams, Cou-Way Wang, James Richards, Thomas Sullivan and Gerald Hurt
National Telecommunications and Information Administration, U.S. Department of Commerce, Washington, D.C.

In 2003, The Federal Communications Commission (FCC) issued a Notice of Inquiry (NOI) regarding Broadband over Power Line (BPL) technology. Earlier, FCC issued experimental licenses to several power and telecommunication companies for trials of BPL technology in the 1.7 – 80 MHz frequency range. Among the important issues to be addressed are radiated emission limits and measurements methods to be applied to determine compliance. In order to address the issues mentioned above, National Telecommunications and Information Administration (NTIA) has started an investigation consisting of research, analysis, measurements and modeling.

RF signals are conducted along power lines in BPL systems, but signals may be unintentionally radiated, resulting in interference to other radio services, depending on the radiated power, distance from the line and physical arrangement and dimensions of the line. The amount of radiation also depends on the symmetry of the network. Any discontinuity in the transmission line (which may be a coupling device) or a change in the direction of the line may produce radiation. Even if the RF energy is injected into one wire, the remaining wires generally will act as parasitic radiators and, therefore, the lines will act as an array of antennas. Radiation may come from one or more point radiators corresponding to the coupling devices as well as one or more lines. Numerical Electromagnetics Code (NEC) used with realistic physical arrangements and impedances of the power lines, can be applied to simulate the current distribution on the power lines and the radiated fields. Propagation mechanisms for emissions toward or below the power line horizon will be by ground waves. The ground wave signal can be a composite of a direct wave, a ground reflected wave and/or a surface wave. For emissions in directions above the power line horizon, the propagation may be either by ground waves for shorter distances or by sky waves for larger distances. In a dense deployment of BPL systems, there may be cumulative, co-frequency unintentional radiation. In order to correctly estimate the effects of aggregation, the key parameters to be considered are the density of co-frequency BPL installations within the deployment area and the co-directed EIRP of each radiating element. In this paper, radiation and propagation issues related to BPL will be discussed. Typical power line configurations have been studied with NEC models. The results of the investigation will be presented

A Study on the Design of STL/TTL System Simulator for M/W Band Digital Broadcasting Relay System

Sungjin Kim, Y. S. Choi

Radio Resources Team, Digital Broadcasting Division, ETRI, Korea

ABSTRACT

In this paper, we analyzed standard and characteristic of microwave digital STL/TTL transmission system in multipath fading channel environment as basis step of research about share way of M/W broadcasting relay frequency. And, we analyzed system performance through simulator design. Domestic case, digitize progress about broadcasting relay is propelled. Therefore, we wish to execute channel Performance and interference evaluation for M/W important duty broadcasting relay frequency reassignment and utilize to basis data about domestic broadcasting relay standardization using simulator of digital STL/TTL system designed by this research.
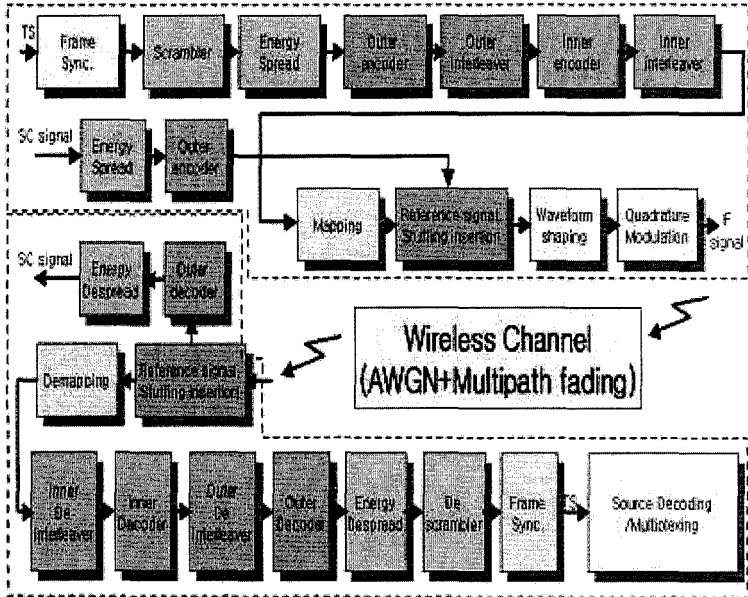
Figure 1: Block diagram of Simulation

* (1) E; Electromagnetic Noise and Interference, E3; Spectrum management and Utilization
  (2) Interference Modelling, Analysis of Performance in Spectrum Management

The Analysis of Capacity Decrease by Calculating Statistically the Amount of Interference from IMT-2000 TDD to FDD System

S. J. Kim, Y. S. Choi

Radio Resources Team, Digital Broadcasting Division, ETRI, Korea

ABSTRACT

There are two systems for IMT-2000 Service. One is FDD (Frequency Division Duplex), the other is TDD (Time Division Duplex) system. At the 1920MHz, they have common boundary in IMT-2000 frequency allocation of Korea. In this paper, The amount of Interference From TDD MS (Mobile Station) and BS(Base Station) to FDD BS is Analyzed for Investigation on capacity variation of FDD service by frequency separation. The result and methodology in this paper will be used basically for calculating the guard-band between FDD and TDD service in the future.

Figure 1: Frequency of IMT2000 in Korea

Figure 2: Interference Model from TDD to FDD

Figure 3: Amount of Interference by Freq.

Figure4: Capacity Decrease by interference
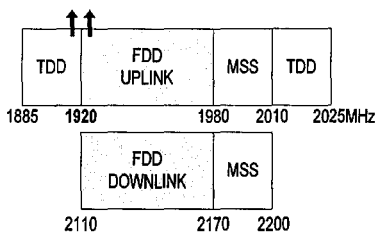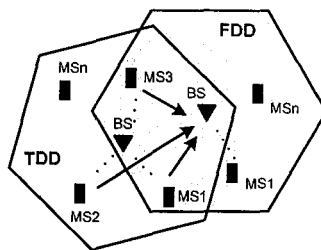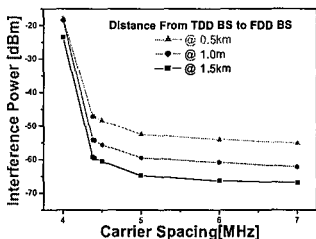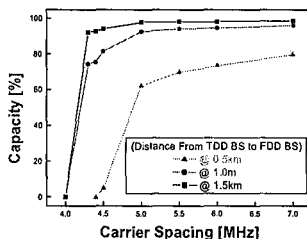
* (1) E; Electromagnetic Noise and Interference, E3; Spectrum management and Utilization
   (2) Interference Modelling, Analysis in Spectrum Management

Maximum Users per Unit Area of CDMA System for Evaluation of Spectrum Usage Efficiency

Jong Ho Kim
Radio Technology Group, Electronics and Telecommunications Research Institute

Abstract

The mobile service operators require an additional spectrum allotments for deficiency of spectrum by the rapid growth of mobile radio service and the advance in multimedia. But the government or the organization of spectrum management wants to solve the problem by more than efficiently use the allocated frequency. The acceptance of the requirements are decided by actual spectrum usage efficiency.

In order to assess the spectrum usage efficiency in mobile radio services, it is imperative to agree upon a measure of spectral efficiency which accounts for all pertinent system variables within such services. Considering an ever increasing demand for cellular services, system limits in terms of maximum offered capacity are of great concern from the service operator viewpoint. Hence, a key criterion for selecting the air-interface for the future mobile system should be the maximum achievable capacity/km^2, i.e. the capacity obtained when cell-size is reduced down to the lowest acceptable value. This paper proposes a method to evaluate the "densification limit" of a CDMA system. The maximum achievable capacity per km^2, is viewed as a meaningful figure of merit for a cellular system and a method is proposed here to estimate the minimum achievable distance between adjacent base stations in the case of CDMA. The probability for entering in soft handover state is used as a limit for densification in a CDMA system. From this criterion, conditions on the minimum possible cell radius are derived.

In Korea, there are 3 of mobile communication service providers, one is operated at 900 MHz, and the others are 1.9 GHz. Using the proposed method and an old method, the spectrum usage efficiency about CDMA2000 1X service types of them expressed as table 1 and 2.

Table 1. SUE of CDMA2000 1X

Provider	A	B	C
Max. Erlang	615	180	250
BW(MHz)	9.84	3.69	4.92
Min. Cell Area(km^2)	0.0333	0.0346	0.0346
	0.0115	0.00366	0.00366
Users/MHz/ km^2	37,537	28,197	29,372
	118,062	299,140	317,660
SUE	31.8 %	9.4 %	9.2 %

Table 2. SUE by not consider the cell area

Provider	A	B	C
Capacity	85/Cell/FA	72/Cell/FA	75/Cell/FA
Max. Capacity	680/Cell	216/Cell	300/Cell
Designed Traffic	668 Erlang	202 Erlang	286 Erlang
SUE	92.1 %	89.1 %	87.4 %

The old method of table 2 shows that all service providers have similar spectrum usage efficiency because they have evasion of facility investment and using of full capacity in the current situation. But the proposed method of table 1 shows that spectrum usage efficiency of provider A is decreased to 1/3 of old method, and the others are decreased to 1/9. As a result of new method, we can distinguish the spectrum usage efficiency of all providers.

Reference
(Viterbi, A.J., CDMA-Principles of spread spectrum communications, Addison-Wesley, 1995)
(Husni Hammuda, Cellular mobile radio systems: Designing systems for capacity optimization, John Wiley & Sons Ltd., 1997)

Exploiting Noisy Transient Response
Using the Fractional Fourier Transform

Seongman Jang[1], Tapan K. Sarkar[1] and Carl Baum[2]

[1]Department of Electrical Engineering and Computer Science
Syracuse University, 121 Link Hall, Syracuse, NY 13244
Email: sejang@mailbox.syr.edu; tksarkar@mailbox.syr.edu
[2] AFRL, Kirtland AirForce Base, Albuquerque, NM

The goal of this paper is to obtain the electrical properties of the target from the received transient noisy time domain waveforms. Because of their aspect independence, complex resonant frequencies of a conducting object are used as a signature of the object to discriminate it from others for the purpose of target identification. The singularity expansion method (SEM) proposed by Baum has been applied to express electromagnetic response in an expansion of complex resonances of the system. It has been shown that the dominant complex natural resonances of a system are a minimal set of parameters that define the overall physical properties of the system. So, a transient scattering response is analyzed in terms of the damped oscillations corresponding to the complex resonant frequency of the scatterer or target. Since the resonances describe global wave fields that encompass the scattering object as a whole, the SEM series representation encounters convergence difficulties at early times when portions of the objects are not yet excited. Early time response is strongly dependent on the nature of the source, the location of the source, and the location of the observer. Usually the early time response shows impulse-like characteristics. Because of this difficulty, most previous techniques such as Matrix pencil method (MPM) used just late time signals only. It is necessary to include 'entire function' to represent early time impulse-like components. The 'entire function' is subset of the analytic function but it doesn't have any singularities.

In this paper, the transient noisy electromagnetic response is considered in the time domain and in the fractional Fourier transform (FrFT) domain. The whole time domain data set is used to test. Fractional Fourier transform (FrFT) is a generalized Fourier transform. Using the FrFT it is possible to discriminate an impulse-like component from the other components of the signals. Because of this property, impulse-like early time components can be separated from the damped exponentials. To describe the early time response a Gaussian pulse is selected. Gaussian pulse is an entire function and is quite adequate to describe pulse-like components in early time. Complex exponentials are used to describe the late time signals. The concept of a 'Turn-on time' is utilized to consider a time when the fully excited resonance can be used, formally. The results for wire scattering element and finite closed cylinder with various SNR show that if SNR is greater than 30dB it is possible to get meaningful parameters using proposed techniques.

Statistics of Chaotic Impedance and Scattering Matrices

Thomas M. Antonsen, Xing Zheng, Edward Ott
Institute for Research in Electronics and Applied Physics,
Sameer Hammedy, Steven Anlage
Center for Superconductivity Research,
University of Maryland College, Park MD, 20742, USA

Abstract

We propose a model to study the statistical properties of the impedance (Z) and scattering (S) matrices of open electromagnetic cavities with several transmission lines or waveguides connected to the cavity. The model is based on assumed properties of chaotic eigenfunctions for the closed system. Statistical properties of the cavity impedance Z are obtained in terms of the radiation impedance (i.e., the impedance seen at a port with the cavity walls moved to infinity). Effects of wall absorption and nonreciprocal media (e.g., magnetized ferrite) are discussed. Theoretical predictions are tested by direct comparison with numerical solutions for a specific system.

Efficient Well-Log Data Inversion with Chaotic Optimization Algorithm

Jaideva C. Goswami[1]*, Zhao Lu[2], and Denis Heliot[1]

1. Schlumberger Tech. Corporation
   Sugar Land Technology Center
   110 Schlumberger Dr.
   Sugar Land, TX 77478
   jcgoswami@ieee.org   heliot@slb.com

2. Dept. of Elect. and Computer Engg.
   University of Houston
   Houston, TX 77025

   zlu@mail.uh.edu

In a typical oilfield exploration environment, a wellbore (about 15 to 30 cms in diameter) is drilled through earth formation to a depth that may extend to a few kilometers. Estimation of formation properties such as conductivities, from data (referred to as a "log") measured by sensors placed inside a wellbore, is a challenging inverse problem. The conventional gradient-type optimization method often proves ineffective because of multimodal nature of objective functional associated with many geophysical inverse problems. In a previous paper (Goswami, *et al, IEEE Trans. AP*, May 2004), we have discussed application of differential evolution (DE) algorithm, a member of class of evolutionary algorithms that are based on multiple initial points and probabilistic transition rule from one set of points to the other in a multi-dimensional parameter space. The major conclusion of the aforementioned paper is that while DE provides robust answers, it is numerically less efficient compared with conventional method. Furthermore, premature and sub-optimal convergence of genetic algorithm – DE, to somewhat lesser extent is also affected by this – continues to be an important issue with application of such methods.

In this paper Chaotic Optimization Algorithm (COA) is applied to invert for earth formation parameters. Chaos, apparently disordered behavior that is nonetheless deterministic, is a universal phenomenon that occurs in many nonlinear systems in all areas of science. Due to the instability, the long-term behavior of chaotic systems shows typical stochastic properties. However, chaos is not equivalent to randomness; it inherently possesses exquisite structure. A chaotic movement can traverse every state in a certain domain by its own regularity, and every state is obtained only once. It is this property that is used to obtain next solution vector from the current one. The COA starts with single point in the parameter space and uses a logistic map function to generate new points. Initial numerical results indicate that the method requires fewer runs of forward model than DE.

FREQUENCY BISTATIC ANALYSIS – A NEW TOOL FOR RADAR CROSS SECTION POST-TREATMENT

Sébastien Vermersch

CEA/CESTA, Commissariat à l'Énergie Atomique, B.P. 2, 33114 Le Barp, France

Design of low Radar Cross Section targets depends, to a very large extent, on the adequate treatment and interpretation of individual signal contributors such as geometrical singularities, antennas,... The method usually employed to deal with problems of that kind is based on what is known as *'bright point analysis'*. Fourier Transforms of frequency-dependent responses are thereby needed, implicitly assuming that all electromagnetic contributors possess a stationary behaviour. The above method has two main drawbacks :

➢ it relies on the computation of RCS data in a rather large frequency band; for calculations performed in the frequency domain, such an approach can be very costly,

➢ the stationary assumption is seldom verified, especially when the frequency band has to be broadened to provide higher resolution.

In order to circumvent the second drawback, narrower frequency bands are often used in post-treatments based on the so-called 'hyper resolution methods'. However, a correct interpretation of the results is not as straightforward as one might think, and the need for RCS computations at discrete frequencies still prevails.

In the present paper, we propose a new post-treatment method which requires the calculation of the RCS for only one frequency, and which relies on no particular hypothesis with regard to the target response :

♦ first, the electric and magnetic currents are computed for frequency f_0,

♦ then, the scattered field is computed from these currents in the frequency range of interest.

As a consequence, a *'frequency bistatic RCS'* is obtained. It allows a rather good interpretation of electromagnetic contributors for frequency f_0 on the basis of only one calculation, thus eliminating the non stationary effects.

We illustrate and justify this *'frequency bistatic RCS'* approach by means of a few numerical examples. Also, as a potential application of this technique, frequency interpolation of RCS is discussed.

The Optical Theorem for Electromagnetic Scattering by a Three-Dimensional Scatterer in the Presence of a Lossless Halfspace

D. Torrungrueng[1*], B. Ungan[2] and J. T. Johnson[2]

[1] Asian University of Science and Technology
Department of Electrical and Electronic Engineering
89 Route 331, Banglamung, Chon Buri, Thailand, 20260
Email: dtg@asianust.ac.th

[2] The Ohio State University
Department of Electrical Engineering
ElectroScience Laboratory
1320 Kinnear Road, Columbus, Ohio 43212

The optical theorem has been known for more than a century, and has been frequently applied in many areas of physics. In electromagnetics (EM), the classical optical theorem is applicable to scattering of a plane wave by objects in homogeneous media. The theorem is useful for computing the total extinction cross section when the scattering amplitude in the forward scattering direction is known. This relation facilitates the calculation of the total extinction cross section, since it otherwise must be obtained by integration of the power flux density over a closed surface bounding the scatterer. In addition, the theorem also serves as an energy conservation condition in the verification of analytical and numerical methods in EM scattering theory.

In this paper, the classical optical theorem is extended to the case of a scatterer in the presence of a lossless halfspace. This case is of practical value due to interest in problems involving scattering from an object in the presence of the ground surface. The extended optical theorem is derived based on energy conservation concepts, and the method of stationary phase is employed to obtain the final form. Note that previous works have considered similar problems for acoustic scattering in waveguides, or for EM scattering from two-dimensional scatterers in the presence of layered media. However the case of EM scattering from a three-dimensional scatterer in the presence of an isotropic halfspace apparently has not been previously presented. For the case of a scatterer in the presence of a lossless halfspace, it is found that the total extinction cross section is related to the scattering amplitudes in the specular directions for reflected and transmitted fields. Numerical results are presented to illustrate use of the theorem for evaluating the energy conservation properties of an EM simulation.

Comparison of Approximation Models and a Full-wave Method for Microwave Scattering from Lossy Dielectric Elliptical Disks

Yisok Oh

School of Electronic and Electrical Engineering, Hongik University, Mapo-Gu, Seoul, Korea, 121-791.

E-mail: yisokoh@hongik.ac.kr

The generalized Rayleigh-Gans (GRG) approximation had been commonly used to compute the scattering amplitudes of lossy dielectric disks smaller or comparable to a wavelength, while the physical optics (PO) approach with the resistive sheet approximation had been usually used for disks larger or comparable to the wavelength. In this study, the scattering amplitudes of various lossy dielectric elliptical disks are computed using those theoretical scattering models (GRG and PO) at different frequencies. Then, the accuracies of the approximation models for microwave scattering from lossy dielectric disks are re-investigated by comparing with a full-wave solution, *i.e*, the method of moment (MoM). An integral equation was formulated to compute the volumetric polarization current inside the scatterer using the MoM. Volumetric integral equation as opposed to surface integral equation is preferred because the scatterer is very thin compared to the wavelength. The accuracy of the numerical code has been verified using other existing numerical results and experimental observations.

It was found in this study that both the GRG and the PO approximation models could be applicable to compute the scattering amplitudes of lossy dielectric elliptical disks over the range of length $0.1\lambda \leq 2a \leq 10\lambda$ (or 0.25 GHz $\leq f \leq 25$ GHz for a disk with a length of 12 *cm*). Therefore, it can be recommended that both the PO and the GRG models be alternatively used for the purpose of computing the scattering matrices (or the phase matrices) of natural deciduous leaves in a vegetation canopy at microwave frequencies.

Testing the Validity of Impedance Boundary Conditions Applied to Periodic Structures

Hassan A. Kalhor[*] and Mohammad R. Zunoubi
Department of Electrical and Computer Engineering
State University of New York
New Paltz, NY 12561

Periodic structures find many applications in optics, microwaves, and electromagnetics because of their strong frequency dependent behavior. Many ingenious numerical methods have been applied to the analysis of scattering of electromagnetic waves by such structures. Most of these methods assume that the material used is perfectly conducting. In practice however, most materials are lossy and can not be treated by these methods. The effects of finite conductivity in gratings with triangular grooves have been calculated by a surface impedance method [Kalhor and Neureuther, *J. Opt. Soc. Am.,* Nov. 1973]. Recently, surface impedance models have been employed to treat structures made up of lossy conductors as well as dielectrics. The validity of surface impedance models, however, has to be established.

The purpose of this paper is to solve a number of periodic structures of finite conductors as well as dielectrics by rigorous analysis technique based on the finite-difference time-domain and compare results with those obtained by simple methods based on surface impedance. A uniform E or H-polarized wave is considered incident on a planar periodic structure as shown. The structure period is d, element spacing is a, and thickness of elements is t.
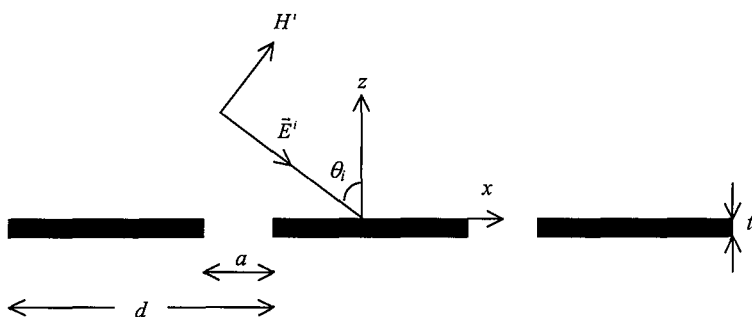
A Study of Vehicle Influences on the Performance of Automobile Antennas

*Meng-Yi Lin[1], Ken-Huang Lin[2]
Department of Electrical Engineering, National Sun Yat-sen University,
Kaohsiung, 80424, Taiwan
[1]ace@pcs.ee.nsysu.edu.tw; [2]khlin@mail.nsysu.edu.tw

Many antenna designs need infinite size metallic ground plane as a basic part of their structure ideally. However, it is impossible to implement in practice due to their infinite size. When finite size ground planes are used instead, the diffractions and reflections occur on the edge will significantly influence the antenna radiation patterns and input impedances (D. W. Griffin, AP-S, 1, 223–226, 1982). The current distributions on the metallic ground plane show a periodic standing wave behavior (R. W. Wang, and V. V. Liepa, AP-S, 2, 769–771, 1985). These current distributions are another source of radiation also. They primarily cause periodic ripples in a wide angle range on the elevation antenna patterns. This phenomenon makes it difficult to satisfy some specific antenna requirements like SDARS (M. Daginnus, R. Kronberger, A. Stephan, SAE 2002 World Congress, Society of Automotive Engineers, Detroit, March 4–7, 2002). Several edge treatment techniques can be used to diminish the edge interactions, such as serrating the edges, rolling or bending the edges, application of absorbing material near the edges, and resistive edge loading.

The number of modern antenna systems for automobile applications is now increasing very quickly due to the trend of intelligent transportation systems. In this study, we investigate the finite size ground plane effects of some vehicle antennas. These antennas suffer from the finite ground plane effects, too. For antenna systems mounted on the roof, their grounding situations are not as simple as mentioned above. The roof should not to be simplified to a flat square ground plane, yet the whole three-dimensional car body should be taken into account. Therefore, those edge treatment techniques can not to be applied directly. An edge treatment technique suitable for automobile applications will also be proposed.

# EFFECT OF FLIGHT CINEMATIC ON HELICOPTER ROTOR RADAR SIGNATURES

P. POULIGUEN, J.F. DAMIENS
Centre d'ELectronique de l'ARmement (CELAR), Division DIRAC,
35170 Bruz, FRANCE

A high frequency model, using Physical Optics (PO) and the Method of Equivalent Currents (MEC), has been proposed to calculate helicopter main and tail rotor Radar Cross Section (RCS) *(P. Pouliguen et al., IEEE TAPS, Vol. 50, No. 10, 2002)*. Rotors are made of N rotating blades positioned symmetrically with equal spacing angles. The problem is treated by using the quasi-stationary approach which is allowed since rotor rotating velocities are much less than light velocity and because their angular frequencies of rotation are very small compared to the angular frequency of radar waves *(J. Van Bladel, Proc. IEEE, Vol. 64, No. 3, 1976)*.

Recently, *realistic motions* of rotor blades (pitch, flap and drag motions) have been integrated into the electromagnetic calculations thanks to a flight cinematic calculation software. That allows furnishing the exact coordinates of each node of rotor components at each instant of the RCS simulations.

In this paper results are given where temporal and spectral characteristics of generic rotor radar signatures are studied versus several configurations of helicopter stabilized flight. Some of them show important effects of flight cinematic. For example the two following RCS diagrams, calculated without (on the top) and with (on the bottom) flight cinematic, exhibit the broken of periodicity and the attenuation of some flash blades when a stationary flight configuration is taken into account.
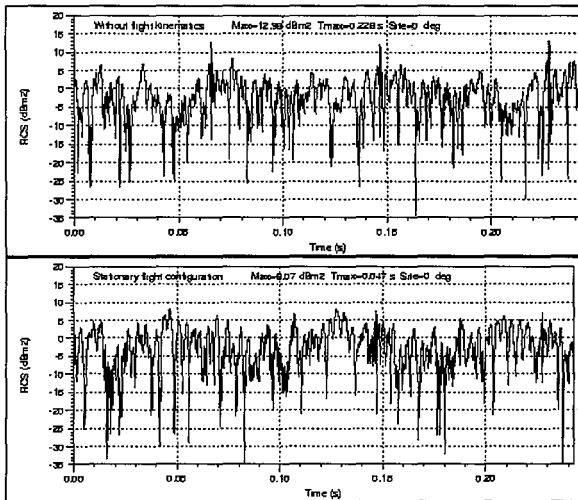
EM Scattering of many plane waves by a conducting sphere

A. Helaly
Department of Engineering Physics,
Faculty of Engineering, Cairo University, Giza 12211, Egypt

. Dr. Helaly is currently with Phys. Dept., Sohar College of Education,
P.O. Box : 135, Postal Code : 311, Sultanate of Oman

Abstract

The multiple scattering of a uniform plane wave incident on an arbitrary configuration of objects is an important problem in scattering theory. Here, the reverse problem is considered, i.e., an object is excited by many electromagnetic sources from different directions. Plane waves are chosen for this study for several reasons. The far-field radiation from any transmitting antenna has the characteristics of a plane wave sufficiently far from the antenna. The incoming wave impinging on a receiving antenna can therefore usually be approximated as plane wave. Also, the exact field radiated by any source in a region of space can be constructed in terms of a continuous spectrum of plane waves via Fourier transform.

The purpose of this paper is to introduce a systematic computational tool to handle the problem of electromagnetic scattering of many plane waves by a conducting sphere. The solution procedure starts with the basic Mie series solution for the scattering by a single plane wave, propagating in the axial direction, which is referred to as primary plane wave. Then applying the superposition principle to compute the contribution by other incident plane waves, which are referred to as secondary waves, via a transformation matrix. The solution is rearranged so that the contribution of each secondary wave is related to the primary wave through an amplitude and phase-shift modifiers. This results in reducing the computation time over the straightforward approach of expressing the total scattered field as the sum of Mie series for each incident wave. Details of the solution procedure and a sample of the corresponding numerical results will be presented.

Diffraction of a plane wave by a screen occupying a plane angular sector

Bair V. Budaev and David B. Bogy

Department of Mechanical Engineering, University of California, Berkeley, CA 94720

A challenging problem of electromagnetic wave scattering consists of computing the field $\Phi(r, \theta, \phi)$ which satisfies the Helmholtz equation $\nabla^2 \Phi + k^2 \Phi = 0$, which vanishes at the surface $\Gamma = \{\theta = \pi/2, \alpha < \phi < \beta\}$ and satisfies certain conditions at infinity.

To find explicit solution of this problem we employ a novel random walk method (B.V.Budaev and D.B.Bogy, JASA, v.114, pp.1733-1741, 2003). Thus we represent the solution as $\Phi = \Phi_g + \Phi_d$, where Φ_g is the pre-defined piece-wise continuous field wave including incident and geometrically reflected waves, and Φ_d is a wave diffracted by the tip of the screen. The diffracted field is sought in the product form $\Phi_d = \phi\, e^{ikr}$ with the amplitude ϕ which satisfies the complete transport equation

$$\frac{i}{2k} \nabla^2 \phi - \frac{\partial \phi}{\partial r} - \frac{1}{2r} \phi = 0,$$

vanishes at infinity and satisfies certain 'jump condition'

$$\left[\phi\right]_s = f, \qquad \left[\partial \phi / \partial \vec{n}\right]_s = 0,$$

where s is a conical surface completely determined by the reflecting screen and by the incident wave, and $f(r, \theta, \phi)$ is an explicitly known function on s.

Problems of this type are well suited for the analysis by the random walk method which makes it possible to represent ϕ explicitly as the mathematical expectation

$$\phi(r, \theta, \phi) = \frac{1}{r}\, \mathbf{E} \left\{ \sum_{\tau_\nu < \tau} \delta_\nu\, \xi_{\tau_\nu}^1\, f(\vec{\xi}_{\tau_\nu})\, e^{-w_{\tau_\nu}^1 - \frac{1}{2}\tau_\nu} \right\},$$

computed over the trajectories of the three-component random motion $\vec{\xi}_t = (\xi_t^1, \xi_t^2, \xi_t^3)$ governed by the stochastic differential equations

$$d\xi_t^1 = \xi_t^1 dw_t^1 + \xi_t^1 \left(1 + ik\xi_t^1\right) dt, \qquad \xi_0^1 = r, \qquad (1)$$

$$d\xi_t^2 = dw_t^2 - \tfrac{1}{2} \tan(\xi_t^2) dt, \qquad \xi_0^2 = \theta, \qquad (2)$$

$$d\xi_t^3 = dw_t^3 / \cos(\xi_t^2), \qquad \xi_0^3 = \phi, \qquad (3)$$

driven by the independent one-dimensional Brownian motions w_t^1, w_t^2, and w_t^3. This motion is launched at the time $t = 0$ from the observation point $\vec{\xi}_0 = (r, \theta, \phi)$; it crosses the conical surface s at times $t = \tau_\nu$; and it stops at the exit time $t = \tau$ when the screen Γ is reached. As for the factors δ_ν, they are defined by the position of the random motion $\vec{\xi}_t$ at the moments $t = \tau_\nu$.

Probabilistic formulas admit many modifications and generalizations which make it possible to solve various problems of wave propagation including but not limited to problems of scattering in canonical wedge-shaped or conical domains, as well as problems of scattering by surface breaking cracks and cavities of arbitrary shape. Numerical simulations of the presented solution may be based on simple perfectly scalable algorithms with unlimited capability for parallel processing. The obtained results agree with the known qualitative and numerical data.

Electromagnetic Field Scattering on a Transparent Transient 2D Cylinder.

Nataliya Sakhnenko, Alexander Nerukh

Kharkov National University of Radio Electronics
14 Lenin Ave., Kharkov, 61166, Ukraine
E-mail: n_sakhnenko@yahoo.com

This paper is devoted to the mathematical investigation of electromagnetic field propagation in transient medium. In modern nonstationary electromagnetics the methods that allow to study phenomenon directly in time domain attract the great interest. Using of the traditional Fourier transform for such problems leads to great computational difficulty.

It is solved the problem of normal incidence of the plane monochromatic wave on the transient 2D cylinder dielectric permittivity of which changes from background value ε to value ε_1. Influence of such a phenomenon on the initial wave is studied. Search is based on the Volterra integral equations approach that equivalent to the Maxwell's equation with initial and boundary conditions [Nerukh A. G., Scherbatko I. V., Marciniak M. Electromagnetics of modulated media with applications to photonics. – Warsaw 2001, –265 p.]. The solution of this problem is constructed analytically in the case of instantaneous permittivity change.

Abrupt changing of dielectric permittivity in unbounded space gives splitting of the initial wave into forward and backward propagating waves that have new frequency $\omega_1 = \sqrt{\dfrac{\varepsilon}{\varepsilon_1}}\omega_0$, where ω_0 is the frequency of the initial wave [Felsen L.B., Whitman G. M. Wave propagation in time-varying media // IEEE Trans. on Antennas and Propag. –1970. –V. AP–18, ¹ 2. –P.242– 253].

Electromagnetic field interaction with nonstationary dielectric cylinder leads to the qualitatively new results. In the case of medium changing inside a cylindrical domain, besides the waves of the new frequency, wave with original frequency survives. The spectrum has sharp maximum on shifted frequency that corresponds to the cylindrical waves propagating in opposite directions. Besides of these maxima there are ones that correspond to oscillations on all possible eigenfrequencies of dielectric cylinder. In external space cylindrical transient layer appears and expands with the phase velocity that corresponds to the initial permittivity.

This method opens the way to study the effect of transient bounded region on initial electromagnetic field. The motivation for studying such phenomena includes wavelength shifting and wave generation by the time modulation of medium parameters.

FIELDS IN THE PRESENCE OF AN UNCLOSED IRREGULAR STRUCTURE.

Elena K. Semenova*, Vladimir A. Doroshenko
Kharkov National University of Radio Electronics
14, Lenin av., Kharkov, 61166, Ukraine
Email: *h_semenova@yahoo.com*

This paper is devoted to investigation the model excitation problem with conical geometry. Conical structures have some special features. They are omnidirectional and super-wide-band in radiation pattern and matching. The structure under consideration is a semi-infinite perfectly conducting circular cone with longitudinal slots. The field behavior studying near the structure singularities, such as the cone tip or edges, is important for an efficient computation of the scattered fields from conical structure.
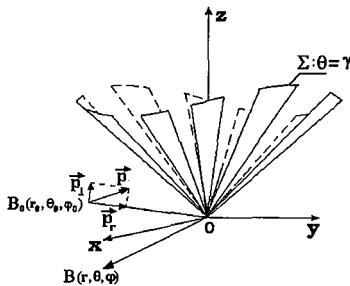
The source of an incident field is a harmonic dipole (electric or magnetic) or a plane wave. The method for solving the correspondent electromagnetic problem is a combination of the Kontorovich-Lebedev integral transforms and the semi-inversion method. In previous works we have obtained the numerical results for the case, when the source is placed to the cone axis *(E.K.Semenova, V.A.Doroshenko, "Source field scattering on a cone with longitudinal slots", IEEE AP-S Symposium, Columbus, OH, USA June 2003).*

The main task of this work is to obtain the numerical solution for arbitrary structure parameters, provided that the source is at any point of the space. The problem parameters effects are analyzed by virtue of given scattered field patterns. The field behavior near the tip of a conical structure is studied. In the present paper we focus our attention on the singularity of the electric and magnetic excitation types at the tip of a perfectly conducting cone with longitudinal slots.

It's common knowledge that the singularity of the electric field proportional to $r^{-1+\mu}$, where μ depends on structure parameters. There are many interesting particular cases of this conical unclosed structure, such as a cone with a slot, plane angular sector (the opening angle is equal to $\pi/2$, one arbitrary width slot). The obtained results for the plane sector coincide with the values published in the work *("Electric Field Behavior Near Metallic Wedges" S.Marchetti, T.Rozzi, IEEE Trans. Ant. Propagat., vol.38, No.9, 1990 pp.1333-1340),* that demonstrate the accuracy of the given results.

321

Causality, Minimum Phase and Inverse Scattering

Michael A. Fiddy

Center for Optoelectronics and Optical Communications
University of North Carolina, Charlotte, NC 28223

The inverse scattering problem can be formulated in terms of a Fourier relation between scattered field data and a secondary source, the product of the scattering function and the total field $\Psi(r)$ in the domain of the scatterer $V(r)$. Only in the weakly scattering case, e.g. the first Born approximation, can one assume that the total field is well approximated by the incident field, allowing one to recover an estimate of the scattering distribution. While extended or iterative Born approximation methods have been developed, imaging of strongly scattering objects remains a difficult problem to solve in practice. Our previous work has adopted a different approach to attack this problem based on a nonlinear filtering method designed to numerically separate the scattering function from the unwanted total field $\Psi(r)$. It might be necessary to illuminate with several different incident fields, leading to different fields, Ψ in order to extract information about V in an unambiguous way. This kind of filtering is known as cepstral or homomorphic filtering and involves taking the logarithm of the inverted scattered field data, followed by Fourier transformation and linear filtering. It rarely succeeds because $\log V\Psi$ is not usually a continuous function and hence its Fourier transform is noisy. Preprocessing $\log V\Psi$ to ensure it is a continuous function requires that $V\Psi$ has no zeros which is unlikely since V by definition is the fluctuation of, say, the permittivity about the background mean permittivity and Ψ is an oscillating field. A condition which remedies this problem is when $V\Psi$ is a minimum phase function; i.e. if the phase of $V\Psi$ is continuous and lies between $\pm\pi$. Then the real and imaginary parts of $\log V\Psi$ are related by a Hilbert transform and it follows that the Fourier transform of $\log V\Psi$ must be causal from Titchmarsh's theorem. The Fourier transform of $\log V\Psi$ is also known as the cepstrum of $V\Psi$. We discuss some methods which allow one to enforce the minimum phase condition on an arbitrary $V\Psi$, by including the addition of dinear phase factor. There is therefore an equivalence between enforcing the minimum phase condition in this way, and adding a reference wave to a scattered field in order to form a hologram. In either case, we have imposed a condition for which the amplitude of $V\Psi$ encodes the phase. The significance of this relationship and the ability to then calculate an estimate of the strongly scattering function $V(r)$ by nonlinear filtering is explored.

A New Method for Landmine Detection Using Norton Surface Waves

Traian Dogaru*
US Army Research Laboratory
2800 Powder Mill Rd, AMSRL-SE-RU
Adelphi, MD 20783-1197

Gary Brown
ElectroMagnetic Interactions Laboratory
Virginia Polytechnic Institute & State University
Blacksburg, VA 24060-0111

Buried mines and unexploded ordnance (UXO) comprise a major problem in areas of the world where land warfare has taken place in the last fifty years. The problem has recently been exacerbated through the use of plastic casings for mines, thus rendering them essentially undetectable by conventional magnetic anomaly methods.

Several acoustic, magnetic, electromagnetic, and chemical techniques have been tried in the past, with varying degrees of success. In the radar community, the efforts have mainly focused on airborne systems, operating from UHF to the X frequency bands. One major problem encountered by these systems is discriminating the targets in a clutter environment, especially when a rough air-ground interface is present. In this paper we propose an alternative approach to the airborne ground penetrating radar (GPR), by using a Norton surface wave pulsed radar in order to achieve a standoff detection and location of the mines in the field. The antenna for this system will be located on the ground but a distance away from the minefield so that no entrance into the minefield area prior to detection and location of the mines is necessary. Using the distance measuring capability of the pulsed radar to locate the mines in the range coordinate along with an antenna array that is both phased, to achieve beam scanning, and focused in the near field, to achieve high angular resolution, it will be possible to locate the mines in the field.

There are some important questions that need to be answered in order to demonstrate the feasibility of such a system. At a basic level, they relate to the efficient launching of the Norton surface waves, their propagation in a complex media environment and their scattering by mine-like objects. In this first study, we address the propagation and scattering of Norton waves by performing numeric simulations. We use a two-dimensional version of the finite-difference time-domain (FDTD) algorithm and discuss some issues related to propagating surface waves via this numeric technique. Since the rough air-ground interface is likely to represent the main source of clutter, we model the propagation of the Norton surface waves along a random rough interface, and obtain clutter levels via Monte Carlo averaging over many realizations. We compare these levels with the returns from mine-like objects, considering different scenarios with respect to rough surface parameters and target materials. Our preliminary results (in terms of signal-to-clutter ratio) indicate that detection is possible for certain reasonable sets of parameters.

323

Joint Electromagnetic/Acoustic Reconstruction of Underground Structures

Qing H. Liu*, Fenghua Li, and Lin-Ping Song
Electrical and Computer Engineering, Duke University
Durham, North Carolina 27708
Email: qhliu@ee.duke.edu

Image reconstruction of inhomogeneous objects of arbitrary shape buried in the earth is an important research area in subsurface sensing. In particular, such applications are common to geophysical exploration, environmental characterization, and subsurface sensing of landmines, unexploded ordnance and underground structures.

Traditionally, both electromagnetic and seismic waves have been widely used to detect and characterize underground structures. However, little has been done to jointly utilize electromagnetic and acoustic waves for a better characterization. In this work, we explore the joint electromagnetic/acoustic characterization in order to improve the reconstruction of underground structures.

The joint reconstruction problem is cast as an inverse scattering problem in a multilayered medium. A two-dimensional joint inversion technique, based on a least-squares criterion of the data misfit, has been developed using electromagnetic (EM) and acoustic scattering data to assess the feasibility of reconstruction for underground structures. The joint nonlinear inverse problem is solved iteratively via the conjugate-gradient approach; within each iteration, the problem is linearized by Born and Distorted Born approximations. The forward solution for both electromagnetic and acoustic waves in layered media is provided by the stabilized biconjugate-gradient fast Fourier transform (BCGS-FFT) method. The numerical results show that the joint EM/Acoustic inversion method can provide more information for the underground structures that the stand-alone electromagnetic or acoustic imaging modalities. This improved imaging results using the multi-modality measurements are due to the complementary nature of electromagnetic and acoustic waves in underground structures. Examples will be shown to demonstrate the improve resolution of the joint inversion in realistic environments.

2D Nonuniform Fast Fourier Transform (NUFFT) Method for Synthetic Aperture Radar and Ground Penetrating Radar Signal Processing

Jiayu Song* and Qing H. Liu
Electrical and Computer Engineering
Duke University
Durham, North Carolina 27708
Email: js1@ee.duke.edu, qhliu@ee.duke.edu

Synthetic Aperture Radar (SAR) and Ground Penetrating Radar (GPR) systems are widely used for object detection. SAR technology provides broad-area imaging at high resolutions for environmental monitoring, earth-resource mapping, and military systems, while GPR provides critical information concerning structural integrity and the exact location of subsurface utilities. Both technologies take advantages of the SAR processing algorithm where 2-D Inverse Fourier Transform (IFT) is a critical step. The performance of the 2-D IFT significantly influences the final resolution of the image as well as the processing speed. In the SAR imaging system, due to the interdependence of wavenumbers in different directions and the wave frequency in the spectral data, the spectral samples are nonuniformly spaced, in which case regular 2-D Inverse Fourier Transform cannot be applied directly.

Instead of using the conventional solution with simple interpolations, a new algorithm is proposed for 2-D Fast Fourier Transform of nonuniform (unequally spaced) data. The algorithm efficiently interpolates every nonuniform spaced point to a high order uniform grid and calculates the weights matrix (called the regular Fourier matrix). New Fourier coefficients are then computed based on the regular Fourier matrices, with which 2-D FFT can be evaluated using the uniform algorithm. 2-D Gaussian accurate factors matrix are used in the algorithm for a higher accuracy purpose. As a remarkable advantage over simple interpolation, the regular Fourier matrices are only dependent on the sampling point locations, but not the data values, which avoid recalculation for the identically sampled data. In this work, we applied NUFFT to SAR and GPR data processing. Numerical and computer simulation results show that NUFFT approach yields better accuracy and faster speed in the processing algorithm when compared to the previous results with simple interpolation method.

Hybrid Extended Born Approximation and Contrast Source Inversion for 3-D Inversion in Layered Media

Lin-Ping Song*, Qing H. Liu, and Fenghua Li

Electrical and Computer Engineering, Duke University

Durham, North Carolina 27708

Email: {lpsong,qhliu,fhli}@ee.duke.edu

Three-dimensional electromagnetic inverse scattering problem in multilayered media, which involves a complicated dyadic Green's function and complex interaction of vectorial waves with layers and objects, is considerably more difficult and challenging than that for a homogeneous background. In this work, we develop a hybrid fast inverse scattering technique in layered media based on the extended Born approximation (EBA) and the contrast source inversion (CSI) method.

First, we develop the 3D EBA for a layered medium by approximating the electric field inside an object through a depolarization tensor. This approximation is based on the singular nature of the dyadic Green's function. The depolarization tensor is source independent and partially accounts for the multiple scattering within the scatter. We show that the EBA has much better accuracy than the conventional Born approximation but is equally rapid in computation. Based on this approximation, we then develop a robust 3D EBA inversion procedure to reconstruct the electric parameters of the objects in a layered medium. The procedure is to iteratively construct the scattering tensor at the current model and then solve the linear inverse problem with respect to the model parameters until the prescribed error level is reached.

Since the EBA is an approximate method, the inverse procedure based on the EBA to reconstruct the complex permittivity profile may not always be adequate, especially for very high contrasts often encountered in practice. Thus, the 3D CSI method we developed previously for layered media can be used to further improve the reconstruction. However, it is known that the straightforward CSI method converges slowly. To overcome the slow convergence, we use the EBA inversion result as the preconditioner for the CSI method. This novel combination of the EBA and CSI method is advantageous in two aspects: First, it provides a seamless procedure that is valid for both low and high contrast; secondly, it converges faster that the CSI method for high contrasts because of the effective EBA preconditioner. Through numerical examples, we illustrate that our combined inverse technique is able to achieve better results than the EBA inversion or the CSI alone in terms of accuracy and speed.

Inversion of Scattering Properties of a
Multilayer Subsurface with Rough Interfaces

Mahta Moghaddam*, Chih-Hao Kuo, and Leland Pierce
Electrical Engineering and Computer Science Department
The University of Michigan, Ann Arbor, MI 48109
mmoghadd@umich.edu, Tel: 734-647-0244

URSI Commission B
B.5 (Inverse Scattering), B.9 (Rough Surfaces and Random Media)

Layered rough surfaces commonly exist in natural and human-made settings, and quantitative characterization of their properties has significant implications for geosciences (ice properties, soil moisture), surveillance (underground structures), archeology (ancient buried sites), among other disciplines. Each homogenous rough layer can be defined by its average thickness, permittivity, and rms interface roughness assuming a known surface spectral distribution. As the number of layers increases, the number of measurements needed to invert for the layer unknowns also increases. To nondestructively calculate the characteristics of the rough layers, a multifrequency polarimetric radar backscattering approach can be used. One such system is that developed for the Microwave Observatory of Subcanopy and Subsurface (MOSS) mission concept, where a tower-mounted radar makes backscattering measurements at VHF, UHF, and L-band frequencies. To solve the inverse scattering problem, we use an iterative technique based on a forward numerical solution of the layered rough surface problem. The layers are each defined in terms of a small number of unknown distributions as given above. An a priori estimate of the solution is first assumed, based on which the forward problem is solved for the backscattered measurements. This is compared with the measured data and using modified conjugate gradient techniques an update to the solution for the unknowns is calculated. The process continues until convergence is achieved. The numerical forward solution is a finite-difference time-domain (FDTD) solver, which for each iteration needs to be solved multiple times to simulate a random rough surface. Two techniques are considered for reducing computational time: (1) to build a prior database of the forward solution as a function of all the unknowns, which is used to construct a closed-form multidimensional function to be used in inversion, and (2) to develop an approximate analytical solution. The latter is discussed in a separate paper in this conference, and the former will be discussed here. Numerical results will be shown using actual radar data acquired with the MOSS tower radar system in Arizona in Fall 2003, and compared with in-situ measurements. Although the inversion of the scattering properties of a single rough surface has been addressed in some previous works using approximate forward solutions, the inversion of the properties of a multilayer rough subsurface has not been solved before, and as such presents a unique contribution from this work. Furthermore, application of this technique to actual data at proper (low) radio frequencies is new.

Numerical Modeling and Inverse Scattering in Nondestructive Testing: Recent Applications and Advances

René Marklein, Jinghong Miao, Karl J. Langenberg, Volker Schmitz*
University of Kassel, Electrical Engineering and Computer Science, Electromagnetic Theory,
Wilhelmshöher Allee 71, D-34121 Kassel, Germany; *Fraunhofer-Institute for Nondestructive
Testing, University of the Saarland, D-66123 Saarbrücken, Germany; E–mail:
marklein@uni-kassel.de, miaojong@uni-kassel.de, langenberg@uni-kassel.de,
volker.schmitz@izfp.fraunhofer.de

Abstract— This paper presents recent advances and future challenges of the application of different linear and nonlinear inversion algorithms in acoustics, electromagnetics, and elastodynamics. The presented material can be understood as an extension of our previous research on this topic (R. Marklein, *et al.*, *Inverse Problems*, 17, 6, 1597-1610, 2001; R. Marklein, *et al.*, *Inverse Problems*, 18, 6, 1733-1759, 2002; R. Marklein, *et al.*, *Proc. XXVIIth General Assembly of URSI*, CD-ROM, 2002). The inversion methods considered in this presentation vary from linear schemes, like the Synthetic Aperture Radar (SAR) applied electromagnetics and the Synthetic Aperture Focussing Technique (SAFT) as its counterpart in ultrasonics, and the linearized Diffraction Tomography (DT) to nonlinear schemes, like the Contrast Source Inversion (CSI) combined with different regularization approaches. Inversion results of the above mentioned inversion schemes are presented and compared for instance for time-domain ultrasonic data from the Fraunhofer-Institute for Nondestructive Testing (IZFP, Saarbrücken, Germany). Convenient tools for nondestructive evaluation of solids can be electromagnetic and/or elastodynamic waves; since their governing equations, including acoustics, exhibit strong structural similarities, the same inversion concepts apply. In particular, the heuristic SAFT algorithm can be and has been utilized for all kinds of waves, once a scalar approximation can be justified. Relating SAFT to inverse scattering in terms of diffraction tomography, it turns out that linearization is the most stringent inherent approximation. A comparison of the inversion results using the linear time-domain inversion scheme SAFT and well tested nonlinear frequency-domain inversion schemes demonstrates the considerable potential to extend and improve the ultrasonic imaging technique SAFT while consulting the mathematics of wavefield inversion, yet, in particular if the underlying effort is considered, the relatively simple and effective SAFT algorithm works surprisingly well. Since SAFT is a widely accepted imaging tool in ultrasonic NDE it seems worthwhile to check its formal restrictions and assumptions whether they could be overcome and whether they would outperform the standard and original SAFT algorithm. Fig. 1 shows an aluminum test sample with six air-filled circular cylinders which is in the experimental setup embedded in a water environment. Fig. 2 displays a nonlinear inversion result applying the CSI. Final conclusion: Not very much remains to be done regarding the theoretical formulation of linear wavefield inversion, yet improvements with nonlinear inversion can certainly be made. Ockham's razor is simple: Will it work in practice?
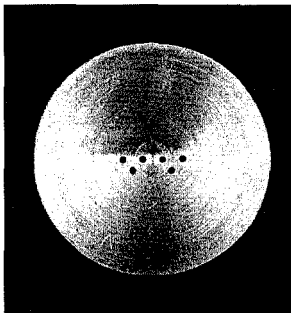
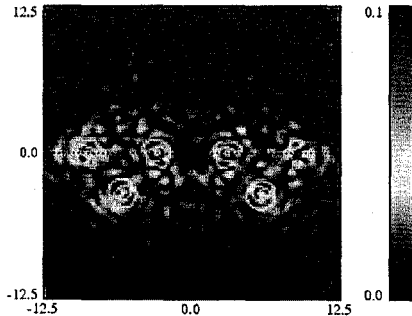Fig. 1.   Aluminum test sample embedded in a water environment with six air–filled holes

Fig. 2.   CSI reconstruction using experimental ultrasonic multi-bistatic (multi-pitch-catch) data

328

Non-Destructive Evaluation of Steel Fiber Reinforced Concrete Slabs

A. Franchois*, S. Van Damme, D. De Zutter, F. Olyslager and L. Taerwe[†]
Department of Information Technology (INTEC-IMEC), Ghent University
St.-Pietersnieuwstraat 41, B-9000 Gent, Belgium
E-mail: Ann.Franchois@intec.UGent.be
[†]Department of Structural Engineering, Ghent University
Technologiepark-Zwijnaarde 904, 9052 Gent, Belgium

Steel fiber reinforced concrete exhibits excellent isotropic mechanical properties and is typically being used for slabs on grade, such as pavements, industrial floors and airport runways. When mixing the fibers with the fresh concrete in a truck mixer, care needs to be taken to obtain a uniform distribution and a random orientation of the fibers. At present the concentration and uniformity of the fibers in the hardened slab only can be checked in a destructive manner. In this paper we present a non-destructive microwave measurement technique to measure the steel fiber volume fraction of a dry hardened slab. Experimental results for slabs with various fiber concentrations are discussed.

The microwave technique is based on an open-ended coaxial probe reflectometry method to measure the reflection coefficient of the concrete slab. A large (OD = 4 cm) and a very large (OD = 20 cm) 50 Ω open-ended coaxial probe have been constructed. The effective permittivity of the slab is derived from the measured reflection coefficient by means of an accurate model for the probe-aperture admittance. In this paper, we apply two such models: a full wave model developed by (P. De Langhe et al., IEEE Trans. Instrum. Meas., 42, 879–886, 1993) and a rational function model developed by (S.S. Stuchly et al., IEEE Trans. Microwave Theory Tech., 42, 192–198, 1994). With the rational function model it is possible to perform an exact inversion of the reflection coefficient for the unknown permittivity in real time. We discuss the optimum operating conditions for each probe. From a practical point of view the proposed technique is well suited for the characterization of reinforced concrete slabs since it is easy to position the probe on the surface of the slab, since spatial variations of the effective permittivity can be measured with satisfactory resolution and since the method is sufficiently sensitive to variations in the fiber concentration.

Typically, the length l of the fibers is in the range 10 mm $< l <$ 80 mm, the thickness d is in the range 0.1 mm $< d <$ 1 mm and the aspect ratio $A = l/d$ is in the range 30 $< A <$ 100. The amount of steel fibers added to the concrete depends on the required strength and is in the range 20 kg/m^3 to 80 kg/m^3, which corresponds to sparse mixtures with volume fractions f_v between 0.002 and 0.01. Consequently it is possible to apply a mixing rule from the classical homogenization approach. In this paper we apply a Maxwell-Garnett formula for randomly oriented conducting prolate spheroids. When assuming the relative permittivity of concrete to be $\varepsilon_{rh} = 6.5$ and for volume fractions and aspect ratios in the ranges mentioned before, the Maxwell-Garnett formula then predicts an effective permittivity $\varepsilon_{r,eff}$ in the range 6.5 $< \varepsilon_{r,eff} <$ 55. From a measurement of the effective permittivity of the reinforced slab and given the permittivity of the concrete, the fiber volume fraction then is obtained by inversion of the Maxwell-Garnett formula. We also present a full-wave Method of Moments technique with which the field scattered by a collection of PEC wires contained in a canonical shape is simulated and to which the effective permittivity of a homogeneous volume within the same canonical shape is fitted.

Technical Topic: B9

329

An Inversion Technique using the Genetic Algorithm for Retrieval of Soil Moisture and Surface Roughness from Multi-polarized Radar Observations of Bare Soil Surfaces

Yisok Oh

School of Electronic and Electrical Engineering, Hongik University, Seoul, Korea

E-mail: yisokoh@hongik.ac.kr

The genetic algorithm (GA) is applied to a semi-empirical polarimetric backscattering model for retrieval of both the volumetric soil moisture contents and the rms surface heights from multi-polarized radar observations of bare soil surfaces. This inversion technique uses the semi-empirical polarimetric scattering model which had been developed based on an extensive database comprising the multi-polarized measurements of ground-based scatterometers as well as an airborne SAR system. The output parameters of the scattering model are the Mueller matrix elements, which can be computed with the vv-, hh-, hv-backscattering coefficients and two parameters of the co-polarized phase-difference statistics, $i.e.$, the degree of correlation and the co-polarized phase-difference.

The genetic algorithm is an optimization process using genetic recombination as follows; (1) each input parameter of the scattering model, $i.e.$, the soil moisture, the rms height and the correlation length, is encoded using N-bit binary digits (N=6). (2) M random chromosomes (M=180) are generated using the binary input parameters. (3) The cost function for each chromosome is evaluated using the scattering model. (4) The chromosomes are ranked according to the corresponding cost function. (5) The inferior chromosomes are discarded and the superior chromosomes mate each other. (6) About 1% of the chromosomes are mutated for avoiding local minima. (7) The cost functions are computed again, and iterate this process for convergence.

Good agreement was found between the values of the rms height and the soil moisture content estimated by the inversion technique and those measured in $situ$. It was also shown that the correlation coefficient between the estimated and measured parameters increased after averaging the multi-frequency multi-angle data.

Multistatic Microwave Imaging of Perfectly Conducting Objects

Chao-Hsiung Tseng* and Tah-Hsiung Chu
Graduate Institute of Communication Engineering
National Taiwan University, Taipei, Taiwan, R.O.C.
Tel: 886-2-23635251 ext. 541, Fax: 886-2-23683824
E-mail: chtseng@ew.ee.ntu.edu.tw, thc@ew.ee.ntu.edu.tw

The frequency-swept quasi-monostatic microwave imaging arrangement using multi-source illumination (C. H. Tseng and T. H. Chu, AP-S Symposium, 179-182, 2003) is shown in Fig. 1 (a) and its acquired Fourier-domain data is illustrated in Fig.1 (b). In this arrangement, the number of lines of Fourier-domain data is determined by the number of sources. In this paper, further extension of this arrangement to multistatic case as shown in Fig. 2 (a) is studied. Namely, the perfectly conducting object is illuminated by multiple incident plane waves and the scattered far fields are received by multiple receivers. With the use of frequency-swept technique, each pair of source and receiver is shown to yield a line of Fourier-domain data. As shown in Fig. 2 (a), a two-source and two-receiver multistatic arrangement can give a total of four lines of Fourier-domain data as shown in Fig. 2 (b). Whereas a two-source and one-receiver quasi-monostatic arrangement shown in Fig. 1 (a) gives two lines of Fourier-domain data as in Fig. 1 (b). Therefore, one can effectively increase the number of lines of Fourier-domain data by using the multistatic arrangement. In addition, the multistatic arrangement is shown to give a wider object aspect angle. The image reconstruction formulas to extract the Fourier-domain data from the received scattered field under multi-source illumination for the multistatic microwave imaging of perfectly conducting objects will be reported in the presentation with measurement arrangement and results.
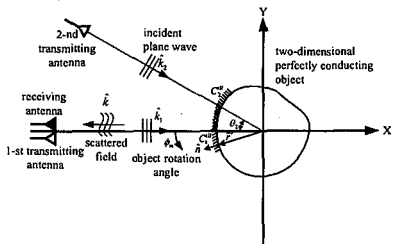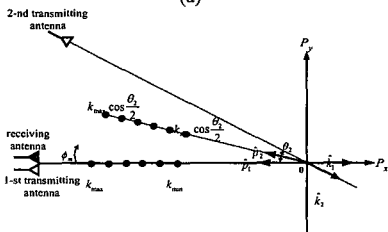
Fig. 1(a) Quasi-monostatic backscattering geometry using two-source illumination and (b) its frequency-swept Fourier-domain.
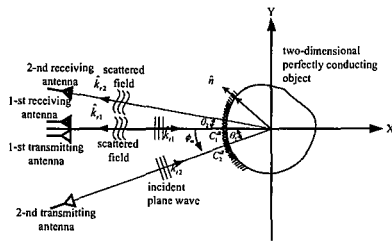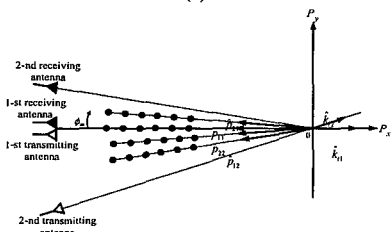
Fig. 2 (a) Multistatic backscattering geometry and (b) its frequency-swept Fourier-domain.

A Novel Time-Domain Ultra-Wideband Microwave Imaging Radar System Design

Fu-Chiarng Chen
Department of Communication Engineering
National Chiao Tung University
1001 Ta-Hsueh RoadHsinchu, Taiwan 300
fchen@mail.nctu.edu.tw

This paper presents a novel time-domain (TD) ultra-wideband (UWB) microwave imaging radar system design based on a recently developed multiplexing nonlinear inverse scattering methodology. The new TD-UWB microwave imaging radar system design is an improvement of a previous work on TD-UWB microwave imaging radar system developed at the University of Illinois at Urbana-Champaign (UIUC). The UIUC system has a switched Vivaldi antenna array which consists of five transmitting antennas and six receiving antennas. There are two single-pole, six-throw (SP6T) mechanical switches to control the transmitting and receiving antennas. The two switches are controlled by a multi-channel relay actuator card in the PC control. One switch controls five transmitters while the other switch controls six receivers. Each switch chooses one antenna at a given time slot. Therefore, the UIUC system will collect 30 sets of measurement data in a given 30 time slots. At each time slot, only one transmitter and one receiver are functioning. Therefore, it is very time consuming for the UIUC system to take measurement data. To improve the previous UIUC system, we propose a new system design based on a multiplexing architecture which is similar to the multiple access schemes in the wireless communications. Recently the multiplexing schemes have been successfully incorporated into the nonlinear inverse scattering algorithm such as distorted Born iterative method (DBIM) and local shape function (LSF) method to reduce their computational complexities. Similarly, incorporating the multiplexing schemes into our TD-UWB imaging radar system design can reduce the measurement time significantly. In this talk, we will present and discuss the new TD-UWB imaging radar system hardware based on the multiplexing architecture.

Shape Reconstruction of Three-Dimensional Conducting Patches Using Physical Optics Approximation, NURBS Geometric Modeling and The Genetic Algorithm

A. Saeedfar, K. Barkeshli
Computational Electromagnetics Laboratory
Electrical Engineering Department
Sharif University of Technology
Azadi Avenue, P.O. Box 11365-9363, Tehran, IRAN
Email: barkeshli@sharif.edu

In this paper, we reconstruct the three-dimensional patches using the physical optics approximation, NURBS geometric modeling, and the genetic algorithm. It is assumed that the patch dimensions are much larger than the operating wavelength. We use NURBS geometric modeling and a simple genetic algorithm to reconstruct the three-dimensional patches.

Figure 1 shows the physical optics scattering from a circular cylinder of radius and height of one meter. Using the above procedure, we have reconstructed the circular cylinder.
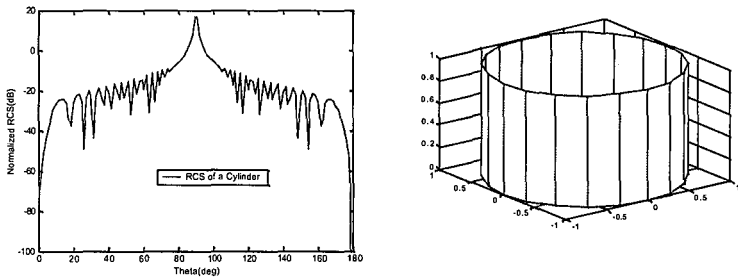
Figure 1- Reconstruction of a circular cylinder of R=1 m and h=1 m based on physical optics approximation, NURBS geometric modeling and the genetic algorithm.

Finite Element Modeling of Embedded Passives for System-On-Chip and System-In-Package Integrated Electronics

Hong Wu[*] and Andreas C. Cangellaris

Center for Computational Electromagnetics,
Department of Electrical and Computer Engineering,
University of Illinois at Urbana-Champaign, Urbana, IL 61801

This paper considers the unique modeling issues associated with the computer-aided electromagnetic characterization of the integrated passive components (e.g., interconnects, power dividers, filters, impedance transformers, couplers, etc.) encountered in state-of-the-art and future System-on-Chip (SoC) and System-In-Package (SiP) integrated electronics. Contrary to traditional, planar single-layer implementations of such passives, recent trends in system miniaturization and multiple functionality have prompted multi-layered, truly three dimensional, and even hybrid designs (that is, designs that combine distributed with lumped components). The choice of the finite element method for their electromagnetic characterization is motivated by the geometric and material complexity that is encountered in the SoC and SiP environment.

Among the numerous challenges confronting the designer, the following three are most representative of the added complexity that the increased circuitry density, the three-dimensional layout of the distributed component and the aforementioned hybridization with lumped elements. a) The distributed and lumped components must be modeled concurrently; b) The lack of (quasi-TEM) "modal" ports for the definition of network parameters (e.g. scattering parameters) necessitates the application of new excitation and termination schemes for the extraction of such parameters, in a manner such that all effects that impact these parameters during the actual operation of the component (e.g., surface waves, higher-order modes, radiated emissions) are accounted for in the model; c) Component design optimization cannot be done without taking into account the circuitry (e.g., other components and/or any shielding structure introducing intentionally for component isolation and interference suppression).

The proposed computational finite element framework for addressing the aforementioned challenges is based on the enhancement of the so-called *E-B* finite element approximation of Maxwell's curl equations (Y Zhu and A. Cangellaris, *IEEE Microwave and Wireless Components Letters*, Vol. 11, May 2001, pp 211-213) with the capability to include lumped elements such as resistors, capacitors and inductors, as well as lumped sources. In this manner, in addition to enabling the electromagnetic modeling of hybrid passives, "non-modal" ports can be introduced anywhere in the structure at which, provided that a pair of terminals can be defined, port voltage and current quantities can be defined immediately in terms of appropriate line integrals of the electric and magnetic field intensities. Subsequently, frequency-dependent network admittance or impedance matrices can be extracted readily. Representative examples of three-dimensional designs of integrated passives are to illustrate the way the resulting modeling methodology addresses the aforementioned modeling challenges and the differences between the extracted network parameters and those obtained if "modal ports" are employed instead.

An Evaluation of Error Estimators for P-Refinement with the Vector Finite Element Method

Gi-Ho Park* and Andrew F. Peterson
School of Electrical and Computer Engineering
Georgia Institute of Technology
Atlanta, GA 30332-0250
peterson@ee.gatech.edu

The vector finite element method (FEM) has been successful for analyzing electromagnetic field problems with arbitrary boundary shapes and materials. Most implementations have been non-adaptive, where a mesh of the domain is generated entirely in advance and used with a constant-degree polynomial basis to assign the degrees of freedom. Adaptive procedures can reduce the computational cost by distributing the degrees of freedom to where they are most needed within the computational domain. Of the adaptive procedures proposed to date, most utilize *h-refinement*, where the cell dimensions are selectively modified as the process is carried out. Recent research considers *p-refinement*, where the polynomial degree of the expansion functions in each cell is independently adjusted. In connection with this research, several families of curl-conforming hierarchical vector bases have been proposed.

Adaptive methods rely on a local error estimator, a measure of the solution error in each finite element that is used to decide which elements need more degrees of freedom. Such an error estimator can sometimes also be used to predict the global error of the FEM result, information not traditionally obtained with vector FEM methods. To date, there has been little research on the assessment of error estimators for vector FEM applications.

In this presentation, a vector FEM formulation for a heterogeneously-filled waveguide is used as a platform for studying local error estimators. Several error estimators, including one based on the normal-field discontinuity between cells, one based on the residual error, and one based on the relative magnitudes of coefficients of higher-order bases within the hierarchical set, will be evaluated in terms of implementation complexity and accuracy. Preliminary numerical results for an adaptive p-refinement algorithm incorporating the best estimator, and hierarchical bases, will be presented.

Assessing the Accuracy of Finite Element Formulations for Fine Details

Pedro Barba*, Rensheng Sun, Leo Kempel, and B. Shanker

The Wireless Integrated Microsystems (WIMS) Center
Department of Electrical and Computer Engineering
Michigan State University
East Lansing, MI 48824-1226

Considerable effort over the past several decades, performed by research groups around the world, has been expended to develop high fidelity models for complex electromagnetic problems. Of the various methods available to the computational electromagnet engineer, the finite element method is arguably the most popular, and powerful, for modeling time-harmonic fields in an inhomogeneous volume. Annually, advancements in finite element formulations and new applications for the method are presented in international technical conferences. Indeed, in some sense, finite element analysis for vector electromagnetic problems is a tool nearing maturity based on the several very powerful commercial finite element analysis programs being offered.

One area of research, with the promise of making a revolutionary rather than evolutionary contribution, is in the area of expansion (also known as shape) functions that have some superior capability compared to conventional shape functions. Several strong research groups have been investigating higher-order interpolatory functions, hierarchical functions, and combinations that have the potential for a higher unknown field representation with a reduction in the number of unknowns. Other efforts have been expended in developing functionals and expansion functions that yield an improved conditioning of the resulting system thereby improving the accuracy of the method.

In this work, the focus of effort is on improving accuracy of the formulation for discretizations of the computational volume with very fine elements relative to a wavelength. The premise is that conventional CT/LN basis functions will fail to accurately represent the unknown fields for cases where the linear dimensions of the elements are much smaller than a wavelength. The cause of this failure lies in the fact that in using such an expansion, solenoidal fields are explicitly excluded from the expansion. The accuracy, as measured by deviation from an exact solution of a canonical problem, for both the traditional divergence-free expansion as well as one including solenoidal fields will be examined.

On the Higher-Order Hexahedral Meshing for FEM in Electromagnetics

Anđelija Ž. Ilić, Milan M. Ilić, and Branislav M. Notaroš[*]

University of Massachusetts Dartmouth, Electrical/Computer Engineering Dept.
285 Old Westport Road, Dartmouth, MA 02747-2300, bnotaros@umassd.edu

The finite element method (FEM) for discretizing partial differential equations in electromagnetics is an extremely powerful and versatile general numerical methodology for full-wave three-dimensional (3-D) electromagnetic simulations. Traditionally used FEM tools are low-order small-domain techniques – the finite elements are on the order of $\lambda/10$ in each dimension, λ being the wavelength in the medium, and the fields within the elements are approximated by low-order (zeroth-order and first-order) basis functions. Only recently FEM techniques based on curved elements for geometrical modeling and/or higher order basis functions for field modeling have been employed, with an objective to significantly reduce the number of unknowns and computational resources for a given (high) accuracy when compared to low-order solutions. However, because these new and emerging elements are much more complex and flexible in shapes and sizes, generation of optimal meshes for practical 3-D electromagnetic problems based on any particular class of higher order finite elements is an enormously difficult and challenging research task, with a great interest to the electromagnetic community.

This paper presents our development of higher-order large-domain FEM meshing techniques based on recently proposed Lagrange-type curved hexahedral finite elements of arbitrary geometrical orders with hierarchical curl-conforming polynomial vector basis functions of arbitrarily high field-approximation orders (M. M. Ilić and B. M. Notaroš, IEEE Transactions on Microwave Theory and Techniques, Vol.51, No.3, 2003, pp.1026-1033). These elements can be electrically quite large (large domains), on the order of λ in each dimension, thus fully exploiting the accuracy, efficiency, and convergence properties of the higher order FEM. We propose a semi-automatic algorithm for the higher-order large-domain hexahedral mesh generation that represents a combination of the domain decomposition and mapped meshing techniques. It utilizes the "top-down" approach to mesh generation, where the first step is a creation of a parametric mesh of topologically equivalent elements with correct connections (adjacencies), based on the problem topology and adopted orders of elements. Interpolation nodes are then assigned to the elements, where the number of nodes and their proper ordering depend on the geometrical orders of elements. Next, parts of the structure are mapped from the parametric space to the curved hexahedral elements in real three-dimensional space (geometrical embedding). Finally, these forms (sub-meshes) are connected together appropriately into an optimal large-domain mesh. The trade-off between the shape/quality of the elements and their sizes will be discussed. The importance of adopting the optimal combination of the field approximation orders will also be explained and possible refinement strategies addressed. Several examples illustrating the effectiveness and flexibility of the proposed mesh generation technique will be presented. The results of the electromagnetic analysis of complex 3-D waveguiding structures demonstrate an excellent accuracy while reducing the number of unknowns by approximately 80% when compared with the existing techniques in the literature.

Analysis of Chiral Grating Using Finite Element Method

Satish Vellakkinar*, Thomas X. Wu and Xiaomin Yang
Department of Electrical and Computer Engineering
University of Central Florida
Orlando, FL 32816

In this paper, we investigate the scattering of chiral grating as shown in Fig. 1 using finite element method. A combination of finite element method and eigenfunction expansion technique is employed to treat unbounded electromagnetic field problem (J. M. Jin, *The Finite Element Method in Electromagnetics*, second edition, Chapter 11, John Wiley and Sons, 2002). In this approach, using variational principle a functional equivalent to the boundary value problem for the chiral grating is formulated. Then the unbounded region is truncated to finite region with the introduction of fictitious boundaries placed at each side and the truncated finite region is divided into an interior and exterior region. Finite element method is used to formulate the fields in the interior region and fields in the exterior region are represented by an expansion of Floquet eigenfunctions. Interior region of the domain is discretized into a number of two dimensional elements, linear triangular elements, and the unknown function is approximated using appropriate two dimensional interpolation function. In the exterior region (boundaries) of the domain, one dimensional linear element discretization is done and linear interpolation function is used. With the functional, elemental equations for the interior and exterior regions of the problem domain are formulated and evaluated at each element. Then the system of equation is formed by summing the elemental equations over all elements. From the system of equations the required unknown quantity in the problem domain is determined.

Based on the analysis, numerical results are obtained and explained by underlying physical insights. We investigate the influence of chirality parameter, periodicity, incidence angle, polarization and frequency on the scattering properties.
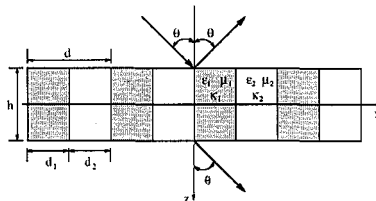
Fig. 1. Configuration of a chiral grating.

Analysis of 3D Eigenvalue Problems Based on a Spectral Element Method

Joon-Ho Lee* and Qing H. Liu
Department of Electrical and Computer Engineering
Duke University
Box 90291
Durham, North Carolina 27708
Email: jhlee@ee.duke.edu, qhliu@ee.duke.edu

The finite element method based on edge elements is free of nonphysical, spurious modes. It has become the popular numerical method for 3D Eigenvalue problems because of its superior geometry and material modeling versatility. However, this method is usually only second-order accurate, and thus requires large amount of computation time if high accuracy is required or if the problem geometry is electrically large.

We proposed an efficient algorithm based on a spectral element method (SEM), which is known for its high degree of accuracy with minimal number of unknowns, to analyze 3D eigenvalue problems. The most important feature of the SEM is that the mass matrix is diagonal due to the use of Legendre polynomials, thus resulting in a very efficient solver. This is a significant advantage over the classical finite element methods. In the SEM, the edge element is also employed to suppress spurious solutions and it is a natural choice for treating 3D geometries. In order to apply a Legendre spectral element to the eigenvalue problems, the physical domain is divided in terms of a set of non-overlapping elements as in a classical FEM. Each of the elements is individually mapped to a reference domain based upon an invertible local mapping. Within each element a spectral representation based on the N-th order interpolation is used. SEM is similar to the p-type FEM, but differ in that it uses interpolation as trial functions.

In order to validate the proposed method, we applied the algorithm to 3D cavities for homogeneous medium and inhomogeneous medium including partly filled with conductive material. The accuracy and computation time of the method are compared with those for analytic solution and for the finite element method using first-order tetrahedron edge elements. From the results we can infer that the proposed method is an efficient tool for analysis of 3D eigenvalue problems.

On the Use of Cubic Wavelet-Like Functions in a Finite Element Time-Domain Algorithm

W. Elliott Hutchcraft(*), Richard K. Gordon
Department of Electrical Engineering(*)
University of Mississippi
Anderson Hall Box 7
University, MS 38677
Phone: (662) 915-6934
Fax: (662) 232-7231
Email: eeweh@olemiss.edu

Wavelet analysis has recently received significant attention in the scientific community. Wavelets and wavelet analysis has been used in many different algorithms including compression techniques as well as the numerical solution of partial differential equations and integral equations. For example, wavelet methods for differential equations have been developed by Jaffard and Laurencot (S. Jaffard and Ph. Laurencot, <u>Wavelets: A Tutorial in Theory and Applications</u>, pp. 543-601, 1992). In the past several years, wavelet analysis has become increasingly used in the field of computational electromagnetics. For example, Yilmaz, Jin, and Michielssen have employed the wavelet transform in a compression technique to reduce the large storage requirements of the time-domain adaptive integral method (TD-AIM) (Ali E. Yilmaz, Jianming Jin, Eric Michielssen, *2003 URSI Digest*, pg. 712, Columbus, OH, June, 2003). Battle LeMarie wavelets have been used for the expansion of the electric and magnetic fields in the multiresolution time domain (MRTD) method (M. Krumpholdz and L. P. B. Katehi, *IEEE Trans. on Microwave Theory and Techniques*, vol. 44, no. 4, pp. 555-571, April 1996).

In this research, cubic wavelet-like basis functions will be incorporated in a finite element time domain algorithm. Previous results for linear wavelet-like basis functions in a time domain approach have been shown (Hutchcraft and Gordon, *Microwave and Optical Technology Letters*, vol. 39, no. 3, pp 221-226). A brief discussion of the generation of the basis will be presented. The traditional FETD method typically requires the solution of a large matrix equation for each time step; however, in the time domain approach presented here, the solution of a matrix equation for each time step is not required. A time-stepping procedure is possible with the FETD algorithm incorporating wavelet-like basis functions. This makes the method similar to the traditional FDTD technique originally developed by Yee (Yee, *IEEE Trans. Antennas Prop.*, vol. AP-14, pp. 302-207, 1966). In the discussion, the FETD algorithm using wavelet-like basis functions will be used for the solution of several problems and the results will be compared to analytic solutions and solutions obtained using the FDTD method. Advantages and disadvantages of the technique will be discussed.

Application of Preconditioned Iterative Solvers to the Time-Domain Finite Element Method

Thomas Rylander[*], Matthys M. Botha, and Jian-Ming Jin
Center for Computational Electromagnetics
Department of Electrical and Computer Engineering
University of Illinois at Urbana-Champaign
Urbana, Illinois, 61801-2991

Many realistic electromagnetic problems involve, in comparison to the wavelength, small geometrical features or rapid field variations around singularities. Such situations require local grid refinement in a small part of the computational domain and, consequently, the finite element mesh can have a wide range of cell sizes. On the other hand, it can be advantageous to use larger finite elements of higher polynomial order in regions where the solution is regular. Both local grid refinement and higher order basis functions are known to make the use of iterative solvers more demanding. In this talk, we consider various aspects of preconditioned iterative solvers applied to time-domain finite element computations with higher order basis functions and large variations in cell sizes. The time-domain finite element method for the vector wave equation representation of Maxwell's equations computes a time sequence of the electric field solution vector $\mathbf{E}^n$ by solving a system of linear equations for each time step. For unstructured grids of tetrahedrons, the Newmark method $(\mathbf{M} + \Delta t^2\theta\mathbf{S})\mathbf{E}^{n+1} = (2\mathbf{M} + \Delta t^2(2\theta - 1)\mathbf{S})\mathbf{E}^n - (\mathbf{M} + \Delta t^2\theta\mathbf{S})\mathbf{E}^{n-1}$ is a popular choice since it allows for unconditional time stepping when the implicitness parameter θ is chosen equal to or larger than $1/4$. Here, we express the electric field in terms of higher order hierarchical vector elements for tetrahedrons, which offers the possibility of combining different polynomial orders within a finite element grid.

The talk will contain a comparative study of the error in the electric field solution as a function of cell size and polynomial order, given a model problem with a regular solution. In this context, the computational cost for a field solution with some a priori specified error will be examined, where computational cost refers to both the memory requirements and the number of floating point operations for the preconditioned iterative solver applied to the matrix $\mathbf{M} + \Delta t^2\theta\mathbf{S}$. The computational cost will also be investigated for tetrahedral grids with varying cell size and polynomial order. A number of different preconditioners will be compared, in terms of efficiency and memory consumption, for some of the above mentioned cases and we will also investigate the effect of a simple preconditioning procedure applied on the elemental level. The presentation will conclude with a summary of our experiences concerning the application of preconditioned iterative solvers to the time-domain finite element method.

A Time-Domain Finite Element Formulation for Periodic Structures

L. E. Rickard Petersson* and Jian-Ming Jin
Center for Computational Electromagnetics
Department of Electrical and Computer Engineering
University of Illinois at Urbana-Champaign
Urbana, IL 61801

In this talk, we will present a formulation of the time-domain finite element method (TDFEM) that incorporates periodic boundaries. This method solves for a transformed field variable (instead of solving directly for the electric field) in order to easily enable periodic boundary conditions in the time domain. The idea for the transformed field variable has already been introduced in association with finite-difference time-domain analysis (FDTD) (M. E. Veysoglu, R. T. Shin, and J. A. Kong, *J. Electromagnetic Waves and Applications*, 7, 1595-1607, 1993), and there are successful implementations reported in the literature using this technique in the aforementioned setting. However, to our knowledge there exist no formulations for TDFEM using this transformed field variable, or any other technique for that matter, that includes periodic boundaries. The perhaps obvious advantage of using TDFEM for periodic analysis compared to FDTD is that the former method allows for unstructured grids that can model complex structures with large variation in length scale as well as elements that can better conform to curved boundaries. To be able to analyze complex structures and curved boundaries can be important for various problems, but one that comes to mind is composite structures that contain unit cells with "ring like" elements such as some of the proposed implementations of double negative materials. The advantage of a time-domain method compared to a frequency method is that the former allows for a broadband frequency response in one single execution.

We now briefly outline the derivation of the method for a two-dimensional problem where all quantities are invariant in the z direction and the periodicity is in the y direction with the periodic boundaries at $y = 0$ and $y = y_p$, and the electric field can be described by a scalar variable, E_z. The starting point is the scalar Helmholtz equation for E_z in the frequency domain with the following periodic boundary condition: $E_z(x, y = 0) = E_z(x, y = y_p) \exp(jk_y y_p)$ where k_y is the wavenumber in the y direction. The next step is to make a substitution of $E_z = P_z \exp(-jk_y y)$ into the Helmholtz equation, which alters the periodic boundary condition to become $P_z(x, y = 0) = P_z(x, y = y_p)$. Now, this modified Helmholtz equation is transformed into the time domain, and note that the periodic boundary condition stays the same. This last equation is then solved by using a Galerkian method in space and finite difference in time. Initial results demonstrate the validity of this method.

NON-UNIFORM GRID (NG) ALGORITHM
FOR FAST POTENTIAL EVALUATION

A.Boag* and B. Livshitz
Department of Physical Electronics, Tel Aviv University, Tel Aviv 69978, Israel

The capacitance extraction problem in complicated interconnect geometries is often effected by a numerical solution of the integral equation, which is based on a representation of the electrostatic potential in terms of unknown surface charge densities. Discretization of the integral equation using the conventional Method of Moments (MoM), also referred as the boundary element method, leads to generation of a system of linear equations. Due to the geometrical complexity of the structures of practical interest, the number of unknowns N is typically quite large. To this end, the $O(N^3)$ computational complexity of direct MoM solvers necessitates the use of iterative schemes. When solving the integral equations iteratively, each iteration requires an evaluation of the electric potential due to a given surface charge. The classical evaluation of this potential at $O(N)$ points by surface integration using $O(N)$ quadrature points (an equivalent of direct MoM matrix-vector product) requires $O(N^2)$ operations. This high computational burden underscores the need for fast field evaluation techniques, such as the Fast Multipole Method (FMM), the multiscale (MultiGrid) methods and the Singular Value Decomposition (SVD) compression approach, all of which evaluate the potential in $O(N)$ operations as opposed to $O(N^2)$ cost of the direct computation. However, the large constant multipliers hidden in the $O(N)$ complexity and memory requirements of the above methods remain to be improved.

In this paper, we present a novel static version of the recently proposed Non-uniform Grid (NG) approach (Boag et al., *IEEE Antennas Wireless Propagat. Lett.*, 1, pp. 142-145, 2002), which facilitates a numerically efficient evaluation of potentials produced by given charge distributions. The approach is based on the observation that the potential at a sufficient distance away from a finite size source can be interpolated from its samples on a spherical NG. Furthermore the number of points in the NG depends only on the distance of the observation domain from the source domain normalized to the size of latter. With this in mind, the NG algorithm relies on a multilevel domain decomposition of the sources, whereas the potential is computed directly for the NGs surrounding the smallest subdomains at the finest level of decomposition. Also, the near-field potentials are computed directly. Subsequently, the potentials of progressively larger subdomains on the corresponding NGs are computed by interpolation and aggregation. Finally, the potential at the observation points is computed by multilevel interpolation employing a hierarchy of local grids.

The resulting hierarchical algorithm attains an asymptotic complexity of $O(N)$ similar to that of the FMM. The NG approach can be considered a spatial counterpart of the FMM, which is relying on spectral (multipole) representation. Also note that the computational structure of the NG approach is related not only to that of other fast MoM analysis schemes, but also to that of algorithms introduced recently in the context of high frequency scattering, image processing, and radar imaging. The time-domain version of the NG technique has also been presented.

Initial studies have shown that the NG algorithm behaves favorably in comparison with the FMM. The former also appears to be easier to adapt to specific geometric configurations and to implement, especially as an enhancement to existing MoM codes.

Hybrid PO-PWTD scheme for analyzing scattering from deep cavities

* G. Kobidze[†], B. Shanker[†], and E. Michielssen[‡]

[†]2120 Engineering Building, Dept. ECE, Michigan State University,
East Lansing, MI 48824, USA, {kobidze, bshanker}@egr.msu.edu
[‡]Center for Computational Electromagnetics, 1406 W.Green St., Dept. ECE,
University of Illinois, IL, 16801, USA, emichiel@uiuc.edu

Transient analysis of scattering from deep cavities is a computationally challenging problem. In the frequency domain, this problem has been most efficiently tackled by separating the the problem into two domains, viz., regions interior and exterior to the cavity. Suitable solvers (either finite element based or integral equation based) have been used in the interior region, and these are coupled to the exterior fields using integral equation based methods (C. C. Lu and W. C. Chew, *IEEE Transactions on Antennas and Propagation*, **45**, 1857-1862, 1997; J. M. Jin, J. Liu, Z. Lou and C. S. T. Liang, *IEEE Transactions on Antennas and Propagation*, **51**, 2420-2429, 2003). However, in the time domain, such analysis is virtually non-existent.

To this end, we propose a novel algorithm to solve for scattering from such cavities. We shall leverage off our earlier work on hybrid PO-PWTD algorithm (G. Kobidze, B. Shanker and E. Michielssen, *Proceedings of the IEEE International Symposium on Antennas and Propagation*, **3**, 547-550, 2003). Our computational scheme proceeds as follows: the computational domain is partitioned into an exterior and an interior region by closing the aperture using a perfectly electrically conducting sheet and placing both electric and magnetic currents on either side. Such a partitioning now permits the analysis of both the interior and the exterior regions using the combined field integral equation, and the coupling between the fields in the two regions is accomplished via currents imposed on the aperture. To reduce these equations to a discrete set, the currents are expressed using the well known RWG basis functions, and their temporal signatures are represented using a set of shifted Lagrange polynomials. Galerkin testing in space and point matching in time yields a set of equations that can be solved using the marching-on-in-time method. To accelerate the solution procedure, the equations in the interior domain are augmented with the plane wave time domain method, whereas those on the outside are solved using our hybrid PO-PWTD algorithm. Details of this scheme as well as several numerical results that demonstrate the accuracy of this scheme will be presented at the conference.

Analysis of Transient Scattering from Multiregion Bodies Using a closed form evaluation of time domain fields and the PWTD algorithm

* J. Yuan [†], M. Lu[‡], B. Shanker[†], and E. Michielssen[‡]

[†]2120 Engineering Building, Dept. ECE, Michigan State University,
East Lansing, MI 48824, USA, {yanjun, bshanker}@egr.msu.edu
[‡]Center for Computational Electromagnetics, 1406 W.Green St., Dept. ECE,
University of Illinois, IL, 16801, USA, {mlu,emichiel}@uiuc.edu

Integral equation based methods for time domain scattering analysis has faced two stumbling blocks; they are (i) computationally intensive, and (ii) these methods were largely perceived to be unstable. The former has, to a large extent, been alleviated by the introduction of the plane-wave time domain algorithm. Indeed, algorithms whose complexity scale as $\mathcal{O}(N_t N_s \log^2 N_s)$ for scattering from surfaces exist. Here, N_t denotes the number of time steps used in the analysis and N_s is the number of surface unknowns required for modeling the surface current. This algorithm has now been applied to the abalysis scattering from electrically large perfectly electrically conducting bodies (B. Shanker, A. A. Ergin, M. Lu and E. Michielssen, *IEEE Transactions on Antennas and Propagation*, **51**,628-641, 2003) and penetrable bodies (B. Shanker, A. A. Ergin, and E. Michielssen, *J. Opt. Soc. Am. A*, **19**, 716-726, 2002).

Our interest lies in analyzing transient scattering from arbitrarily shaped bodies that are best described as a union of regions with different electrical properties. Our method of analysis will be to derive Stratton-Chu equations in each region to relate the fields to the surface equivalent currents. Boundary conditions beetwen regions is enforced using the scheme proposed by Medgyesi-Mitschang *et. al.* (L. N. Medgyesi-Mitschang, J. M. Putnam, and M. B. Gedera, *J. Opt. Soc. Am. A*, **11**, 1383-1398, 1994). To obtain a set of matrix equations, we expand the currents using the well known RWG basis functions. The temporal dependance of these function is represented using a set of simple polynomials, and their convolution with the Green's fucntion will be performed anlaytically. Our earlier work in developing a similar analysis tool focused on using both polynomials and approximate prolate spheroidal functions to represent the temporal signature of each basis function, and their convolution with the Green's function was computed numerically. This approach suffered from a principal deficiency, viz., inaccuracies due to increased time step size necessary to make the marching procedure sufficiently stable. It has been observed (M. Lu and E. Michielssen, *Proceeding of International Symposium on Antennas and Propagation*, **1**, 74 - 77, 2002; T. Abboud and T. Sayah, *Centre de Mathematiques Appliquees, Ecole Polytechnique, Technical Report R. I 390*, 1998) that using analytical methods to convolve the temporal signature with the Green's function results in considerably more accurate results. In this paper, an marching-on-in-time (MOT) will be developed using this procedure, and will be augmented with the PWTD scheme. To implement the latter, multiple trees and interaction lists are necessary (one for each region) as the wave speed is different in each domain. Details of the method and numerical results that demonstrate its efficiency will be presented.

Fast Evaluation of Near-Field Contributions
in a PWTD-Enhanced MOT Scheme for Lossy Media

P. L. Jiang*, and E. Michielssen

Center for Computational Electromagnetics
Department Electrical and Computer Engineering
University of Illinois at Urbana-Champaign, Urbana, IL61801

The recently developed plane wave time domain (PWTD) method (A. A. Ergin et al, IEEE AP Mag. 41(4), 39-61, 1999) has been shown to drastically accelerate the solution of time domain integral equations (TDIEs) pertinent to the analysis of numerous electromagnetic scattering problems involving objects immersed in lossless backgrounds by permitting the rapid space-time convolution of temporary bandlimited sources with "free-space" time-domain Green functions. A PWTD scheme for evaluating fields generated by sources residing in lossy media was proposed too (P. L. Jiang, et al, IEEE APS Int. Sym., 3, 22-27, 2003), but to date remains unapplied in the analysis of real-world problems. Indeed, while the scheme effectively reduces the computational cost of evaluating so-called far-field interactions from $O(N_s^2 N_t^2)$ to $O(N_s N_t \log N_s \log N_t)$ (N_t and N_s are the number of temporal and spatial degrees of freedom of the scatterer current), it fails to effectively handle Green function tails in the near-field. As a result, our present PWTD-enhanced lossy medium TDIE solver still evaluates near-field interactions using classical convolution schemes at a cost of $O(N_s N_t^2)$. The near-field evaluation cost thus dominates that of computing far-fields and renders the overall scheme computationally inefficient.

The present work aims to accelerate the evaluation of near-field interactions in TDIE solvers that use lossy medium Green functions. To this end, the convolution of the Green function and the temporal basis function, here denoted by $s(R,t)$, is approximated by a sum of complex exponentials as $s(R,t) \approx \sum_{i=1,m} a_i(R)e^{\lambda_i(R)t}$ where R is the distance between spatially impulsive sources and observers. The pole residues a_i and associated exponentials λ_i are estimated via the generalized pencil-of-function method (Y. Hua, et al, IEEE Trans. AP, 37, 229-234, 1989). Since near-field interactions are to be evaluated for only a small range of $0 < R < R_{max}$—the PWTD kernel evaluates all interactions for $R_{max} \leq R$ — a table of residues and poles representing $s(R,t)$ for a discrete set of R's can be pre-computed and $s(R,t)$ for arbitrary $R < R_{max}$ can be obtained by spatial interpolation from its values at the samples that define the table. Needless to say, the above exponential approximation to $s(R,t)$ permits near-field interactions to be evaluated by recursive convolution. This, in turn, leads to a reduction in computational cost provided that the number of exponentials in the above representation, m, is small. Unfortunately, generally speaking, m grows with N_t. To keep the number of exponentials in the approximation to $s(R,t)$ in check, the time span of the analysis is subdivided into $O(\log N_t)$ subintervals of durations that scale inversely with the maximum temporal variation of $s(R,t)$ and a separate table is constructed for each interval. In can be shown that the computational cost of the resulting near-field evaluation scheme scales as $O(N_s N_t \log N_t)$, viz. subdominantly to that of computing far-field interactions using PWTD.

Towards an Implicit-Implicit ADI-FDTD Method

*Mohamed A. Mohamed**
Melinda Piket-May
Edward F. Kuester
Department of Electrical and Computer Engineering
University of Colorado
425 UCB, Boulder, CO 80309-0425
email: Mohamed.mohamed@colorado.edu
mjp@colorado.edu

Christopher L. Holloway
National Institute of Standards and Technology
Electromagnetics Division
U.S. Department of Commerce, Boulder Laboratories
325 Broadway, Boulder, CO 80305

Although the ADI-FDTD method, in which we solve implicitly for the electric field and explicitly for the magnetic field (an implicit-explicit method), is stable unconditionally, the errors increase with increasing time step. In this work we solve Maxwell's equations implicitly for both the electric and magnetic fields. This gives us the advantage of handling problems that have a magnetic wall as well as ones that contain an electric wall or even ones that have heterogeneous boundary conditions. This opens up the capability to work for a wide range of different electromagnetic problems. Furthermore, the matrix that we deal with in this algorithm is a two-by-two block tri-diagonal matrix which is easy to handle. In this paper, we will investigate the stability, error, and the performance for this implicit-implicit ADI-FDTD method.

The implicit-implicit ADI-FDTD method is to be applied to solve the problem of the transmission and reflection of electromagnetic waves at a metafilm, a two dimensional version of a metamaterial, placed in a rectangular waveguide. A metafilm can be designed from magnetic, dielectric or magnetodielectric materials.

On the other hand, a perfectly-matched layer (PML) algorithm for the implicit-implicit ADI-FDTD has been analytically calculated. The algorithm has to be tested to obtain the memory required to solve a problem with PML. A comparison of the memory required and the time consumed between FDTD, implicit-explicit ADI-FDTD and implicit-implicit ADI-FDTD will be made for a particular boundary problem. Optimization of the code and other considerations still remain to be done.

Analysis of Transient Electromagnetic Coupling into Platform-Mounted Cables Using the Time-Domain Adaptive Integral Method

Hakan Bağcı*, Ali E. Yılmaz, Andreas C. Cangellaris, and Eric Michielssen
Center for Computational Electromagnetics,
Department of Electrical and Computer Engineering,
University of Illinois at Urbana-Champaign, Urbana, IL 61801

Modern vehicles come replete with sophisticated electronic communication and navigation systems. As these systems' clock rate and line density rises, their proper functioning is threatened by electromagnetic interference from onboard or external, direct- or (multi-conductor) cable-coupled signals. Accurate and efficient broadband modeling of platform-cable interactions therefore is essential to gauge the immunity of such systems to interference.

Here, a new full-wave time-domain methodology for analyzing transient electromagnetic coupling into platform-mounted cables is proposed. To enable the analysis of large-scale and geometrically intricate systems, a parallel implementation of the time-domain adaptive integral method (TD-AIM) (A. E. Yılmaz et al., *IEEE AP-S Digest*, 3, 543-546 2003), viz. the time-domain counterpart of the frequency-domain AIM procedure, is used. The algorithm requires $O\!\left(N_t N_c \!\left(\log N_c + \log^2 N_t\right)\!/P\right)$ CPU resources per processor for analyzing electromagnetic phenomena spanning N_t time steps on P processors using N_c auxiliary Cartesian point sources. This accelerated parallel solver is far more efficient than classical time-domain integral-equation solvers, the CPU requirements of which scale as $O\!\left(N_t N_s^2/P\right)$, where $N_s \sim N_c^{2/3}$ is the total number of surface and cable unknowns. The solver approximates all conductor surfaces by triangular patches and uses Rao-Wilton-Glisson basis functions to approximate their current distribution. Here, we extend the previously developed TD-AIM solver with a view to performing accurate analysis of platform-cable interactions. While cylindrical surfaces can be used to model wires without introducing new solver capabilities, doing so invariably leads to fine spatial discretizations and elevated unknown counts; this avenue for analyzing cables therefore should be avoided at all costs except where dictated by the local geometry being analyzed, e.g., near complex junctions. Thus, a thin-wire-like approximation is used, instead, to model the electromagnetic interactions with cables of subwavelength radius. To accurately model time-domain common-mode current variations, surface-wire junctions are modeled in a manner that ensures current continuity while avoiding fictitious charge accumulation at the junctions (J. S. Zhao et al., *Microwave Opt. Tech. Lett.*, 28(3), 155-160, 2001). A decomposition of the wire currents into differential-mode (transmission-line) and common-mode components is used to facilitate the modeling of electromagnetic coupling to and emissions from the wires as well as the effect of the coupled radiation on the functionality of the driver and receiver electronic circuits attached at the ends of the cables.

An Embedded Boundary Method to Eliminate the ADI-FDTD Staircasing Error

Mei Chai* and Qing H. Liu
Department of Electrical and Computer Engineering
Duke University
Box 90291
Durham, North Carolina 27708
Email: mchai@ee.duke.edu, qhliu@ee.duke.edu

The alternating-direction implicit finite-difference time-domain (ADI-FDTD) method is an unconditionally stable time-domain method. It allows the time step to be increased beyond the Courant-Friedrichs-Levy limit within the regular FDTD method. The successful implementation of this scheme has the potential to impact the application of the ADI-FDTD method to problems where a very fine mesh (compared to the wavelength) is required because of the geometric details. Such applications are widespread in electronic circuit packaging and interconnects.

However, we have found that the numerical errors of the regular ADI-FDTD method are unacceptably high, greatly limiting its application. These large numerical errors are mainly due to the numerical dispersion error associated with the spatial discretization in the FDTD method. As is now well known, this spatial discretization error is only first-order accurate for discontinuous media. This large spatial discretization error is coupled to the temporal discretization, making the error of the ADI-FDTD much larger for inhomogeneous media than for homogeneous media.

We report a novel embedded boundary method to improve the ADI-FDTD method. This method can be considered as an extension of the staggered upwind embedded boundary (SUEB) method that was developed for the explicit FDTD method (T. Xiao and Q. H. Liu, IEEE Trans. Antennas Propagat., in press). This embedded boundary method uses a uniform Cartesian grid so that the conventional central difference scheme is used for the regular grid points away from the material boundaries (embedded boundaries). The attention will focus on developing difference schemes for irregular grid points near the embedded boundary. We will show that with small additional cost, the derivatives near the embedded boundary can be obtained more accurately than the regular ADI-FDTD method. The embedded boundary ADI-FDTD method correctly represents the location and problems caused by the staircasing approximation. Examples will be shown to demonstrate the application of this method to interconnects.

A New Pseudospectral Time-Domain (PSTD) Algorithm Based on Discontinuous Galerkin Method (DGM) and Hexahedral Elements

Gang Zhao* and Qing H. Liu
Department of Electrical and Computer Engineering
Duke University
Durham, North Carolina 27708

The pseudospectral time-domain (PSTD) algorithm has been demonstrated remarkable improvement over the FDTD method in both accuracy and efficiency (G. Zhao and Q. Liu, *IEEE Trans. Antennas Propagat.*, **51**, 619-627, 2003). The multidomain PSTD method features a non-overlapping subdomain decomposition conformal to the material interfaces, thus no staircasing errors are present. Nevertheless, accurate and effective treatment of subdomain interfaces remains a key subject under investigation. Inappropriate treatment of boundary conditions could also result in a late-time instability. Simply speaking, this can be attributed to the singularity phenomenon of the multidomain scheme for partial differential equations, in which the field at the boundary such as edges or corners may have inconsistent values for different subdomains.

To enforce the boundary conditions, the multidomain scheme requires an extra computational step, namely subdomain patching, to reconcile the field values at the interface of nonoverlapping subdomains. Previously, we have developed the characteristic patching condition and the physical patching condition to deal with the subdomain interfaces. These schemes modify the field values to satisfy the correct boundary conditions after the field is updated by the differential equations. However, all these techniques require the use of numerical filters in order to guarantee long-time stability; unfortunately, the numerical filters may cause a degradation in accuracy in high frequency bands.

A recent progress in domain patching techniques for spectral methods is the penalty method (J. Hesthaven and T. Warbutron, *J. Comput. Phy.*, **181**, 186-221, 2002) introduced to a spectral element framework. It is an equivalent extension of the well-known Discontinuous Galerkin method (DGM) to linear hyperbolic systems. In this work, we shall apply the Discontinuous Galerkin method to our 3-D multidomain PSTD algorithm based on hexahedral elements, since this approach has been demonstrated superior stability in finite element families. The high efficiency of the previous PSTD scheme will be maintained by the use of Legendre nodes and Gauss Quadrature such that the mass matrix will be fully diagonal. The introduction of the DGM method will increase the robustness of the PSTD algorithm, and make it an efficient EM solver for large-scale applications.

A 3D Spectral Discontinuous Galerkin Method with Hybrid Elements

Tian Xiao* and Qing H. Liu
Department of Electrical and Computer Engineering
Duke University
Box 90291
Durham, North Carolina 27708

Recently, high-order and spectral time-domain methods have received considerable attention because of their potential to solve large-scale problems with increased computational efficiency than the lower-order methods. Of particular interest to us is the Discontinuous Galerkin Method (DGM). It provides a high-order spatial approximation, curved geometry flexibility, and ease for parallel computation. When the problem contains some curved objects, an unstructured mesh is usually exploited to capture their curved surfaces. However, in the most common scenario, the unstructured mesh may reduce significantly the efficiency of DGM if most portion of the problem domain does not include curved surfaces.

Here we introduce structured elements instead of unstructured ones in the problem region where no curved surfaces are present. This allows the Kronecker-product based computation for the structured elements, which is much more efficient than that for unstructured elements. Therefore, for a 3D problem, the elements available include tetrahedrons, prisms and hexahedrons. The spectral DGM is applied in each element by choosing a set of discrete points. Those points are distributed denser near the element boundary to ensure a spectral approximation property. The field representations in each element are only based on these points. Then the fields within each element are updated separately. In order to ensure the correct boundary conditions between adjacent elements, the fields discontinuities between elements are penalized by a face-based flux communication between adjacent elements. In addition, to simulate unbounded problem, a well-posed PML is used to truncate the computational domain. Numerical experiments show that the hybrid-element DGM is stable and much more efficient than the regular DGM.

An Efficient and Flexible Pseudospectral Time-Domain (PSTD) Method for Maxwell's Equations

Tian Xiao* and Qing H. Liu
Department of Electrical and Computer Engineering
Duke University
Box 90291
Durham, North Carolina 27708

Recent interests in modeling large-scale broadband electromagnetic problems have made the use of high-order and spectral time-domain methods more attractive because of their high efficiency and accuracy. However, there are two major problems which challenge their practical applications.

First, disparate spatial scales in different regions will degrade the efficiency of a high-order method if a uniform grid density is used everywhere. This issue arises because for regions with small electrical scales it is wasteful if a high-order grid is used; obviously, for these small-scale regions, a lower-order approximation is sufficient for the accuracy.

Secondly, the mesh generation for a problem with complex geometry is challenging in a high-order method. Unlike the traditional finite-difference time-domain methods, the spatial discretization is much more complex for high-order or spectral methods because they need to accurately model the interfaces and boundaries. Mesh generators are normally good for a problem with regions having roughly the same scale, and are not ideal for mixed-scale problems.

To overcome these two problems, we present an efficient and flexible pseudospectral time-domain method. With the aid of interpolation, the inter-element communication can be implemented in a flexible way. The collocation points across the interface between adjacent elements are no longer required to overlap. Therefore, it allows the accuracy order and the grid density to vary from element to element, in an optimal way according to the overall accuracy requirement. Different regions can be meshed separately. Numerical tests on the stability, accuracy and efficiency of the novel PSTD method by 2D problems show that it has tremendous potential in solving complex practical problems.

Nyström Discretization of Time-Domain Integral Equations Using a Filtered Green's Function and Predictor/Corrector

Raymond A. Wildman[*] and Daniel S. Weile

Dept. of Electrical and Computer Engineering, Univ. of Delaware, Newark, DE

While the discretization of the time-domain integral equations of electromagnetic scattering has traditionally been achieved with a Galerkin approach, the locally-corrected Nyström method represents a possible alternative. The Nyström method is inherently simpler as it solves for samples of the current density at points on the scatterer and has several advantages over a Galerkin method: It requires only the evaluation of the Green's function to compute most matrix elements and complex, mutipatch parametric basis functions are completely avoided (L. F. Canino, J. J. Ottusch, M. A. Stalzer, J. L. Visher, and S. M. Wandzura, *Journal of Computational Physics*, vol. 146, pp. 627-663, 1998). This paper outlines a method for the numerical solution of two-dimensional transverse magnetic time-domain integral equations using the locally-corrected Nyström method with a predictor/corrector solution approach.

In the spatial or temporal discretization of any equation, aliasing must be considered. For the spatial discretization, the use of a bandlimited incident field and a sufficient number of samples (in the Nyström method) or basis functions (in a Galerkin method) per wavelength at the highest frequency ensures that minimal spatial aliasing occurs. Unfortunately, any Green's function with a temporal singularity is not bandlimited in time and so any temporal sampling will result in significant aliasing. Moreover, a temporal or spatial singularity in the Green's function is itself problematic in the computation of the impedance matrix elements. The locally-corrected Nyström method accounts for the spatial singularity via local corrections to the impedance matrix at and near the singularity but it does not consider the temporal singularity. To address both of these problems, the Green's function can be filtered temporally. The filter function used in this work is based on the bandlimited interpolation function (BLIF) of Knab (J. J. Knab, *IEEE Transactions on Information Theory*, vol. IT-25, pp. 717-20, 1979). With a bandlimited and nonsingular Green's function, a simple linear approximation is then used in the temporal discretization of the current.

Though the filtered Green's function is nonsingular and bandlimited, it is also, unfortunately, noncausal. To solve the system via time-marching, a predictor/corrector approach is used. While other methods, such as bandlimited extrapolation, are available to overcome this difficulty, the predictor/corrector method is the simplest approach that yields stable and accurate results. Another advantage of the predictor/corrector approach is that since extrapolation is avoided, much larger time steps result in stable simulations. In the predictor/corrector method, the current at the present time step is "predicted" by solving for the current without regard to the noncausal portion of the Green's function. The past values of the current are then "corrected" by solving again based on the predicted or future values of the current. The number of past time steps that are corrected is chosen to be equal to or slightly exceed the number of noncausal time steps in the filtered Green's function. Numerical results that verify the stability and accuracy of the proposed method will be presented at the conference.

Comparison of the SBTD with the FDTD and Other Finite-Difference Time-Domain Methods

Stanislav Ogurtsov* and George Pan

Department of Electrical Engineering

Arizona State University, Tempe, AZ 85287, USA

george.pan@asu.edu

Abstract

We present the Sampling Biorthogonal Time-Domain Method (**SBTD**), a time-domain wavelet based full-wave numerical method for electromagnetic simulations. The properties of the method are analyzed and compared to those of Yee's FDTD, MRTD and other finite-difference time-domain methods in terms of approximation order, stability and numerical dispersion. Using computational results from a number of 2D and 3D EM problems, the performance of the SBTD is compared with that of Yee's FDTD. It is shown that the SBTD method can reduce computational burden significantly.
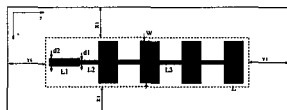
Geometry of Microstrip Antenna Array

Figure 1: Geometry of antenna array
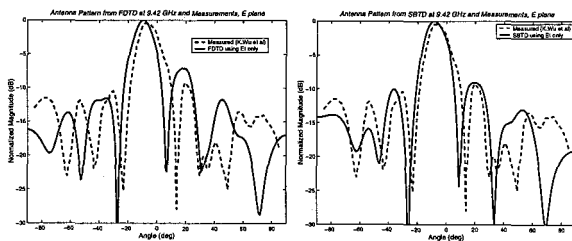
Figure 2: E-palane pattern: (a) with FDTD (b) with SBTD

The Method of Auxiliary Sources (MAS) for Three Dimensional Time Domain Scattering Analysis

Jungwon Lee* and Sangwook Nam
Applied Electromagnetics Laboratory, School of Electrical Engineering and
Computer Science,
Seoul National University, Seoul, Korea

In recent years, Time Domain Integral Equation (TDIE) method for scattering analysis has received much attention and is believed to be in a mature stage, although a few problems concerning stability and accuracy still remain. The most widely used scheme is to discretize the scatterer with triangular patches and perform Marching-On-in-Time (MOT) with RWG basis function in space and linear interpolation in time. In this scheme, basis functions for space and time are decoupled to avoid time-consuming space-time integrations and the retarded time is accounted for only approximately. There are papers dealing with aforementioned problems but their approaches sacrifice computational complexities.

The Method of Auxiliary Sources (MAS) (D. I. Kaklamani and H. T. Anastassiu, "Aspects of the Method of Auxiliary Sources (MAS) in Computational Electromagnetics," *IEEE Antennas and Propagation Magazine*, vol. 44, no. 3, pp. 48-64, Jun. 2002) is a variation of the standard Surface Integral Equation (SIE) technique and has been used successfully for frequency domain analysis. Unlike the SIE technique, where equivalent distributed sources are situated at the scatterer surface, discrete impulsive sources (auxiliary sources) located inside the scatterer are adopted for MAS in PEC scattering analysis. These discrete impulsive sources simulate the fields outside the scatterer accurately once the solution is obtained. Because of these sources, all the source integrals in SIE can be replaced by summations in MAS. Therefore MAS is computationally very efficient and simple to implement. But, there has been little effort to apply MAS in time domain. As far as we know, only two dimensional problem has been investigated (G. G. Bit-Babik et. al., "The Method of Auxiliary Sources for Investigation of Pulse Scattering in Time Domain", *DIPED-98 Proceedings*, pp. 11-14, 2-5 Nov. 1998).

In this paper, MAS for three dimensional time domain scattering analysis is presented for the first time. MAS in time domain inherits all the advantages of MAS in frequency domain. Moreover, due to the use of spatially impulsive sources, decoupling of the basis functions for space and time is already done and the retarded time is accounted for exactly. Because various kinds of numerical error affect the stability and accuracy of the time domain solution, this feature is very important which means removal of one source of numerical error. In other words, solutions from MAS in time domain can be more accurate and stable than those from the standard SIE technique in time domain.

We used implicit scheme for time marching and linear interpolation in time. And to handle the interior resonance problem, we adopted combined field source solution, since combined field integral equation technique is not directly applicable to MAS formulation.

Details of the method and the results will be discussed.

Multiple Scattering Effects on Radar Cross Section (RCS) of Objects in Random Media Including Backscattering Enhancement and Shower Curtain Effects

Akira Ishimaru
Sermsak Jaruwatanadilok
Yasuo Kuga

Box 352500, Department of Electrical Engineering
University of Washington, Seattle, Washington, 98195
Tel: 206-543-2169, Fax: 206-543-6185, E-mail: ishimaru@ee.washington.edu

When an object is in a random medium, the conventional theory gives the apparent radar crosssection (RCS) of the object, which is reduced from the RCS in free space due to the scattering and absorption effects of the random medium. This reduction is represented by the optical depth of the medium. However, this does not include multiple scattering effects.

In this paper, we present a multiple scattering theory of RCS in a random medium using scalar fields. We consider Dirichlet objects. We assume that the size and the surface radius of curvature of the object are greater than a wavelength; therefore, the Kirchhoff approximation is applicable. Also, we make use of the parabolic equation approximation for propagation, which should be applicable to many practical problems in microwave and optical scattering in the atmosphere and the ocean, as well as optical scattering in biological media. The medium is characterized by the Gaussian and Henyey-Greenstein phase functions.

The formulation is based on the use of the circular complex Gaussian assumption. Making use of the stochastic Green's functions, RCS is expressed as the surface integral over the object. It consists of three terms. The first is the coherent component, the second represents the correlation between the coherent and incoherent components, and the third is the diffuse component. It includes the fourth-order moments, which are decomposed to the second-order moments by circular complex Gaussian assumption. It includes two effects: backscattering enhancement and shower curtain effects. Both phenomena have been discussed recently, but have not been included in most RCS studies.

As an example, we consider a square conducting plate for the object. The shower curtain effect shows that RCS is greater when the random medium is close to the transmitter. The backscattering enhancement effect shows that RCS is increased if the correlation between the incident and scattering waves is included. The angular dependence of the RCS shows that RCS becomes insensitive to the angular variation of the object as the optical depth increases.

ON THE STOCHASTIC RADIATIVE TRANSFER IN A DISCRETE RANDOM MEDIUM

Mostafa A. Karam
Northrop Grumman Cooperation
Navigation Systems Division, Litton Industries, Inc.,
21240 Burbank Blvd
Woodland Hills, CA 91367, USA
E-mail" Mostafa.Karam@ngc.com"

A radiation treatment of a random medium having discrete particles and a transparent background is presented based on the stochastic radiative transfer equations. The radiative transfer equations treat the medium as a binary stochastic mixture and they account for both vertical and lateral variations in the medium characteristics (F. Malvagi, et al., J. Atmos. Sci., 50, 2146-2158, 1993). The equations also permit the particles and the background to have different thermal temperatures.

The stochastic radiative transfer equations are reformed based on the transparent characteristics of the medium background and then solved in a discrete random layer over a rough interface. The particles within the layer are distributed within ellipsoidal spatial cells of various sizes with an average height and a horizontal extent. In solving the equations a semi-analytic technique that accounts for multiply scattered radiation is applied (M. A. Karam, J. of Electromagnetic Waves and Applications, 17, 829 – 848, 2003). Numerical simulations based on the solution of the stochastic radiative transfer equations are performed to evaluate the performance of the linear spectrum-mixing model LSMM. The LSMM is widely used in hyperspectral data analysis, and it assumes that the observed spectrum within a sensor footprint or within a pixel is generated by a linear combination of small number of unique constituent spectral signature known as endmembers.

The numerical simulations showed that the LSMM is valid if either of the following conditions is satisfied.

- Both the average height and the horizontal extent of the spatial cells are very large
- The discrete random layer is either sparsely or densely populated.

The simulations also showed that the LSMM is valid only near nadir incidence if the height of the spatial cells is very large, and it is valid only near grazing incidence if the horizontal extent of the cells is very large. The discrete random layer is considered in this study because it could be used to model varieties of natural media such as broken clouds, discontinuous vegetation, foams over sea surface, precipitation, atmospheric aerosols, etc.

The Enhanced SSA for Rough Surface Scattering

Shira L. Broschat

School of Electrical Engineering and Computer Science
Washington State University
PO Box 642752
Pullman, WA 99164-2752

To be practical, a rough surface scattering model must be easy to implement and easily incorporated into existing models. At the same time, it must be accurate enough to give useful results. Here "practical" is defined to mean (1) no more than N-D integration away from low grazing angles, where N represents the dimension of the surface, (2) no more than 2N-D integration at low grazing angles, and (3) accuracy to within a few dB.

The lowest-order small slope approximation (SSA) satisfies all three criteria away from grazing angles, but does not satisfy the third criterion for large-scale roughness at low grazing angles. The nonlocal small slope approximation (NLSSA) is accurate at low grazing angles, but in its original form, 1-D surfaces require 5-D integration and, thus, the NLSSA does not meet the second criterion. Earlier, we introduced an approximation that reduces the integration by two dimensions while retaining the accuracy at low grazing angles. We refer to this as the approximate NLSSA (ANLSSA). However, the ANLSSA still does not satisfy the second criterion since it involves triple integration. In past work, we showed that the NLSSA cross section can be written as the sum of the lowest-order SSA cross section and an additional term, the latter of which can be considered a correction term for the lowest-order SSA. The approximation in the ANLSSA is made only to this correction term, and the ANLSSA can still be written as the sum of two terms—that is, the lowest-order SSA and a correction term (which has been approximated). To meet the second criterion for practicality given above, an additional approximation must be made to the correction term. To avoid confusion with the SSA, NLSSA, and ANLSSA, we call the resulting approximation the enhanced SSA (ESSA). The ESSA cross section is written as the sum of the lowest-order SSA cross section and the new correction term. Previously we proposed a scheme for a practical rough surface scattering model based on the ESSA. In this scheme, the SSA result is used away from low grazing angles where it is accurate and where the correction term makes no contribution. The correction term is added only at low grazing angles where it makes a contribution.

To reduce the integration complexity of the correction term, the correlation functions $C(x)$ in the innermost integrals have been approximated by the first three terms of the Taylor series expansions about $x = 0$. Initial numerical results using a Gaussian roughness spectrum based on this approximation will be presented and discussed.

Frame-Based Gaussian Beams Modeling of Rough Surface Scattering in Complicated Media

Goren Gordon[1], Ehud Heyman[1]*, and Reuven Mazar[2]

[1]School of Electrical Engineering, Tel Aviv University, Tel Aviv 69978, Israel

[2] Department of Electrical and Computer Engineering, Ben-Gurion University of the Negev, Beer-Sheva 84105, Israel

The frame-base beam-summation method is a rigorous technique that decomposes any field in an aperture of a real or virtual (i.e., induced) source to a phase space set of beam propagators that emerge from a discrete set of points and orientations in the source domain. Using Windowed Fourier Transform (WFT) frames with Gaussian windows enables the complete and accurate decomposition of any source in the aperture to a set of simple Gaussian beams (GBs) that, unlike plane wave basis functions, can be easily and efficiently propagated in inhomogeneous media.

The implementation of the GB procedure in rough surface scattering applications is managed by decomposing the incident and scattered fields into sets of GBs that are connected via GB-to-GB scattering matrices for the coherent and non-coherent fields. The rows of each matrix represent the scattered GB fields (coherent or non-coherent) due to a single incident GB. These scattering matrices are the GB equivalent of the scattering cross section of plane waves in the conventional spectral analysis of rough surface scattering. They provide the phase space representation of the local rough surface scattering mechanism, which can be extended thereby to non-plannar/non-stationary boundaries. One can now use the GB-to-GB scattering matrices in the overall problem of an inhomogeneous medium with rough surface boundaries, by propagating the GBs easily within the medium and using the scattering matrices to acquire the relevant GBs scattered from the rough surfaces.

Explicit results for the scattering matrices are calculated for weakly perturbed rough surface with Gaussian spectrum, and for a plane-parallel rough-surface waveguide.

Scattering of Electromagnetic Waves from Three-layer Rough Surfaces Using the Small Perturbation Method

Alireza Tabatabaeenejad*, and Mahta Moghaddam

Radiation Laboratory
Department of Electrical Engineering and Computer Science
The University of Michigan, Ann Arbor, MI, 48109-2122
Phone: (734) 936-4393, Fax: (734) 647-2106
[alirezat, mmoghadd]@eecs.umich.edu

Scattering of electromagnetic waves from multilayer rough surfaces has numerous applications including estimation of multiyear sea-ice depth, detection of subsurface characteristics for planetary applications, detection of oil spills on oceans, and estimation of multilayer soil moisture to varying depths. So far analytical methods have focused on a single rough surface, while multilayer rough surfaces have been treated by numerical techniques like the Steepest Descent Fast Multipole Method (SDFMM) or the FDTD. While the numerical techniques are capable of producing accurate results for these complex problems, their utility can often be undermined by the very high computational demand and long run times. As a result, their ultimate use in inverse scattering, the main goal of the applications above, is hindered. An analytical solution for the multilayer rough surface scattering problem could greatly benefit the efficiency and speed of the geophysical product calculations, and essentially lead to real-time geophysical product generation from remote sensing instruments. In this paper an analytical method to calculate the bistatic scattering coefficients of a three-layer rough surface is introduced. The problem deals with a three-region dielectric structure of which the top and bottom ones are half-spaces. The two boundaries are considered zero-mean stationary random processes. All layers are considered lossless and homogeneous. While most analytical methods on rough surfaces use dyadic Green function and the Extended Boundary Condition Method, in this paper we simply represent all fields in spectral domain with unknown coefficients. Small Perturbation Method is used to represent these unknowns in the form of convergent series. Boundary conditions are then applied to find a system of linear equations to solve for the zeroth and first order coefficients. The Method of Stationary Phase is used to calculate the fields, which leads to finding a closed form solution for bistatic scattering coefficients. The results are first compared against canonical cases of smooth surfaces. Results are then validated using those from numerical techniques for the general case of two rough interfaces. The solution derived here is planned to be extended to the general case of an N-layer rough surface problem.

NUMERICAL METHODS FOR ANALYSIS OF EM SCATTERING FROM AN ELECTRICALLY LARGE OCEAN SURFACE

Z. Zhao, L. Li and L. Carin
Department of Electrical & Computer Engineering.
Duke University, Durham, NC USA

Numerical methods have been widely used to analyze microwave scattering from rough surfaces. Finite computational resources dictate that the surface must be artificially truncated. If the artificial surface edge is not treated properly, they may induce non-physical diffraction that could mask scattering from the actual rough-surface features of interest. Several methods have been proposed previously to solve this problem. In this paper a half-space Green's function formulation is proposed, to simulate rough-surface scattering with plane-wave incidence. In this formulation there is a smooth transition from the finite rough surface to an infinite half-space background. As discussed in this talk, such an approach has demonstrated good performance in minimizing edge effects. Compared with the traditional resistive-taper rough-surface termination, this method has the advantage of no extra artificial extended area (and hence a reduced number of basis functions). Moreover, since a combined-field integral equation (CFIE) may be used with this method, the half-space formulation has a significant advantage *vis-à-vis* the electric-field integral equation (EFIE) required by the resistive taper. Both the EFIE resistive-taper and CFIE half-space formulations are considered here, each solved via the multilevel fast multipole algorithm (MLFMA). The CFIE is generally better conditioned than the EFIE, yielding faster convergence of the iterative matrix solver used in the MLFMA model. We compare the numerical results of the half-space and resistive-taper MLFMA formulations, with good agreement observed. However, for the reasons indicated above, the CFIE-based half-space formulation is computationally more efficient, in both CPU and RAM.

To consider rough surfaces of size beyond the capabilities of a rigorous MLFMA formulation, we also consider a high-frequency analysis. In particular, a ray tracing method is investigated, and validated where appropriate via the MLFMA. The ray tracing used in this paper is a combination of traditional ray tracing and PO (physical optics).

In these studies large-scaled rough surfaces are generated by using a Bretscheider wave spectrum. The Bretscheider wave spectrum is well matched to the water-tank surfaces for which scattering measurements were also performed. The numerical and measured scattering data are compared in the talk. For the surfaces consider, and for these forward-scattering studies, the numerical results show that the ray-tracing method performs well even when the incidence angle tends to grazing. The two MLFMA formulations and the ray-tracing model are compared to wideband high-frequency measurements performed in the large water-tank scattering measurements.

Scattering from a Target on a Rough Sea Surface using a Decoupled Approach

*K. Jamil and R. J. Burkholder**
[1]Dept. of Electrical Engineering, The Ohio State University,
ElectroScience Lab, 1320 Kinnear Rd., Columbus, OH 43212
Phone 614-292-4597 E-mail rjb@esl.eng.ohio-state.edu

The prediction of the radar scattering from a realistically large and complex target such as a ship on a rough sea surface is very challenging. Numerical methods such as the generalized forward-backward method (M.R. Pino, L. Landesa, J.L. Rodriguez, F. Obelleiro and R. J. Burkholder, IEEE Trans. Antennas Propag., 47, 961-969, 1999) must model the target plus a large portion of the sea surface. This makes the computational domain extremely large, and becomes intractable for 3D targets at radar frequencies. On the other hand, efficient numerical methods for just the rough surface scattering are well-developed, such as the canonical grid method (J. T. Johnson, IEEE Trans. Antennas Propag., 46, 297-302, 1998) and simple physical optics. Likewise, efficient numerical solutions for the scattering by large 3D targets are also available, such as the multi-level fast multipole method (J. M. Song, C. C. Lu and W. C. Chew, IEEE Trans. Antennas Propag., 45, 1488-1493, 1997). It is therefore of interest to decouple the rough surface from the target so that each region may be dealt with separately.

The approach used here is based on a reciprocity formulation for computing the electromagnetic scattering from a target on a rough surface. This approach has been used previously for targets *above* a rough surface (T. Chiu and K. Sarabandi, IEEE Trans. Antennas Propag., 47, 902-913, 1999), and for jet engines inside long inlet ducts (P. H. Pathak and R. J. Burkholder, IEEE Trans. Microwave Theory Techniques, 41, 702-707, 1993). The target backscattered electric field $\vec{E}^s(\vec{r})$ at an arbitrary point $\vec{r}$ is given by an integral over the outer surface $\bar{S}_T$ of the target as

$$\vec{E}^s(\vec{r}) \bullet \hat{p}^i = \int_{S_T} \left[\vec{E}^s(\vec{r}') \times \vec{H}^i(\vec{r}') - \vec{E}^i(\vec{r}') \times \vec{H}^s(\vec{r}') \right] \bullet \hat{n} dS'$$

where $\vec{E}^s(\vec{r}'), \vec{H}^s(\vec{r}')$ are the target-scattered electric and magnetic fields on $\bar{S}_T$. $\vec{E}^i(\vec{r}'), \vec{H}^i(\vec{r}')$ are the incident electric and magnetic fields on $\bar{S}_T$ due to a dipole test source $\hat{p}^i$ at $\vec{r}$ with the *target absent,* and are found using a rough surface scattering code. $\vec{E}^s(\vec{r}'), \vec{H}^s(\vec{r}')$ are found by illuminating the target with the incident fields $\vec{E}^i(\vec{r}'), \vec{H}^i(\vec{r}')$ and solving the *local* scattering problem of the target in the presence of the rough surface. This paper will discuss ways to solve the local scattering problem approximately without considering the entire rough surface. Numerical results will be presented which compare the accuracy of the decoupled approach with the full surface/target model.

Fast and Exact Method for Calculating Bistatic Scattering from Periodic Rough Surfaces

Dayalan Kasilingam
University of Massachusetts Dartmouth
North Dartmouth, MA 02747

Even though in the past, scattering calculations have focussed on the backscatter component, in recent years there has been an increased interest in calculating bistatic scattering from targets and natural surfaces. Methods for bistatic calculations have followed the techniques used for backscatter calculations, where a single incidence and scattering direction are identified and the scattering components are calculated in these directions. However, ideally bistatic scattering calculations should calculate the bistatic scattering components in all possible scattering directions.

For periodic surfaces, the scattering components can be calculated exactly since the solution involves a discrete set of scattering modes known as Floquet modes. However, this set includes an infinite set of evanescent modes, which do not carry any power but are necessary to match the boundary conditions at the periodic surface. In practice, the series of evanescent fields is truncated at a point beyond which the contributions from these modes are negligibly small. The number of evanescent modes varies according to the roughness of the surface. For calculations of scattering from slightly rough to moderately rough surfaces, the number of evanescent modes may be small. However, for more complicated surfaces, a large number of such modes may have to be included. Furthermore, due to their exponential dependence, the computation of evanescent modes and their projections are generally tedious and may result in significant computational errors due to the large fluctuation in their values.

In this paper, a technique, which eliminates the need to compute the evanescent modes, is presented. The evanescent modes are not simply substituted out, but instead they are factored out of the calculations by projecting the boundary conditions onto a subspace, which is orthogonal to all the evanescent modes. The method is exact and generates results, which are consistent with more established methods. Results from this method are compared with results from those from other methods and found to be similar. Since the number of propagating modes is finite, the computation speed is significantly faster. In addition, the elimination of the fast-changing, evanescent modes also improves the accuracy of this method. For lossless media, it is shown that the scattering components can be related to the incident components through a unitary linear transformation. This unitary transformation defines a model that provides the bistatic scattering components in terms of all possible incident scattering components. Several examples of bistatic scattering from ocean and terrain like surfaces are presented.

Application of Optimization Methods for Modeling of Nonlinear Electromagnetic Wave Interaction with Random Discrete Media

V.G. Spitsyn, Y.R. Tsoy, I.V. Fedotov
Department of Computer Engineering, Tomsk Polytechnic University,
84, Sovetskaya street, Tomsk, 634034, Russia,
Tel: +7 3822 418912, Fax: +7 3822 419149,
E-mail: spitsyn@ce.cctpu.edu.ru

The electromagnetic wave nonlinear propagation in the absorbing media, including of random discrete inhomogeneities, is explored. The media is contained of semitransparent object in a view of sphere, cylinder and parallelepiped. There is supposed that the typical sizes of objects more large than the length of electromagnetic wave. In this paper we consider the model of electromagnetic signal multiple interaction with discrete inhomogeneities chaotically disposed in the media.

The results of solving the problem of nonlinear electromagnetic wave interaction with stratified random discrete media are presented in paper (V.G. Spitsyn, *IEEE AP-S International Symposium*, 4, 398-401, 2003). Method of Monte-Carlo is used for solve this task in indicated publication. However, for the realization of numerical experiments it is necessary a very large time of computation (V.G. Spitsyn, *Modeling of radiowave scattering on the ionospheric plasma disturbances, created of space vehicle*, Tomsk: Publishing House "STT", 2002). That is why we explored the possibility of application the optimization methods for solve this problem.

There is constructed the artificial neural network, which described the state of random discrete media. The determination of neural network topology is realized on the base application of genetic algorithm (Y.R. Tsoy, *Proc. of 7-th Korea – Russia International Symposium on Science and Technology*, 3, 181-187, 2003). In the process of modeling of nonlinear electromagnetic signal propagation across the neural network is occur the changing of parameters and topology of neural network. In the result of calculation we received the distribution of wave absorption coefficient in media and the distribution of energy scattering and absorbing signal into media in dependence of time interaction.

Magnetic Resonant Imaging RF Coil Analysis and Design

Xin Xie and George W. Pan
Arizona State University
Tempe, AZ 85287

Magnetic resonant imaging (MRI) has many advantages over the X-ray, ultrasonic and other images. The resolution and signal to noise ratio of the MRI are superior, because in the MRI no inverse scattering is involved. The FR coil of the MRI plays an essential

role in the quality of the images. When commercial software is employed to analyze the RF coil, the slow convergence and high computational cost may be unacceptable. In the paper we present a technique that analyzes the RF performance of the coils in a simple manner, yet with high accuracy. We computes the desired 2nd resonant frequency of the harmonically rotating fields (referred to as the B1) in terms of the configuration, geometry and material properties. We then evaluate the uniformity of the magnetic flux density with the field of view (FOV) and the display the vector fields, Finally, we present the way to optimize the system design the provides the maximum B1 under certain constrains.

FDTD Analysis of Several Broadband Antennas Close to Human Tissues

Qingsheng Han* (qhan3@po-box.mcgill.ca)
Milica Popović (poppy@ece.mcgill.ca)

Department of Electrical and Computer Engineering, McGill University
Montréal, Québec, Canada H3A 2A7

Microwave radiation has so far shown promise for noninvasive imaging (detection) and treatment in medicine, from cancer detection to hyperthermia. Pulsed microwave probing has been used or suggested for a range of biomedical applications. A key element in this methodology is a suitably designed antenna structure, either as a single element or in an array configuration.

In this work, we present a comparative study of several broadband antennas reported in the literature. These include resistively loaded dipole, bowtie and conical antennas, folded unipole antenna and the slotline-bowtie hybrid. Each one of these structures is modeled and numerically tested using the SEMCAD FDTD-simulation software, which allows us to incorporate detailed models of the human body in the simulation. These SEMCAD models include more than a hundred different distinguished tissue types.

The testing procedure involves antenna simulation within a series of geometries and source excitations of interest. For example, the behavior of each antenna is evaluated for several possible locations (close to the head, adjacent to the human breast, in the mid-thigh section). In addition, various pulse widths and shapes, as well as continuous waveforms, are used for source excitations. Further, it is known that the impedance and characteristics of an antenna lying in the vicinity of the air-substrate interface exhibits large variations with the distance of the antenna from the interface. Therefore, the distance of antenna from the human body is also taken as a parameter in our numerical studies. Finally, in studies where the particular human anatomy allows, each antenna element is examined for its suitability for an antenna array.

The modeling outputs used as measures (in various combinations of the above-mentioned parameters) for this comparative study include transmitting and receiving antenna characteristics and the distribution of power deposited in the nearby tissues (SAR).

Finite Element Modeling of a Radio-Frequency Phased Array Designed for Hyperthermia Cancer Treatments in the Intact Breast

Sandra Soto-Cabán[†], Leo Kempel[†], Thaddeus V. Samulski[‡], and Robert J. McGough[†]
[†]Department of Electrical and Computer Engineering, Michigan State University
[‡]Department of Radiation Oncology, Duke University Medical Center

Abstract

Hyperthermia is defined as the therapeutic use of temperatures above 41°C, where the goal of this therapy is to deposit heat in cancerous tissues. Heat can inactivate cells, cause tumor regression, and enhance the action of many anticancer drugs, all of which are desirable for cancer therapy. Recent success in the hyperthermia clinic has accelerated the development of technology of electromagnetic applicators. The purpose of this work is to develop electromagnetic hyperthermia applicators to treat the intact breast in patients with locally advanced breast cancer (LABC). To achieve this goal, the effects of a three-dimensional arrangement of antennas and frequency on temperature distributions and power deposition that can be achieved in regional hyperthermia using an electromagnetic phased array are investigated. The antennas are end-loaded dipoles, and all calculations are performed using the finite element method. After the mesh is defined, the electric field is computed for each antenna and then superposed. This applicator is tested using a simulated breast phantom. To model this phantom, the thermal and electromagnetic properties of normal breast tissue and tumor are applied to a geometry model in FEMLAB. This model is placed inside the applicator, which is a tank filled with deionized water, and then power deposition responses generated are evaluated for the RF phased array prototype. Results of simulated power depositions in a 3-D breast model containing a tumor and normal tissue will be presented for a 4-channel RF array prototype. These results, which predict power depositions with the finite element method, will impact future array designs and treatment strategies for LABC patients.

FDTD Analysis of a Gigahertz TEM Cell for Ultrawideband Pulse Exposure Studies of Biological Specimens

Zhen Ji, Susan C. Hagness, John H. Booske
Department of Electrical and Computer Engineering
University of Wisconsin-Madison, 1415 Engineering Drive, Madison, WI 53706

Satnam Mathur
McKesson BioServices, Brooks City-Base, TX 78235

Martin Meltz
Department of Radiation Oncology
University of Texas Health Science Center, San Antonio, TX 78229.

A Gigahertz TEM (GTEM) cell has been designed and adopted for ultrawideband (UWB) baseband electromagnetic pulse (EMP) exposure studies of biological specimens. The objective of recent experiments is to examine cellular and molecular responses occurring after exposure of mammalian cells to high average peak power EMPs (~ 1 ns pulse width). In these experiments, the GTEM cell is loaded with T-25 flasks containing cells suspended in culture media. Important information about the spatial uniformity and temporal transients of electromagnetic fields within the media in the flasks is very difficult to obtain experimentally. Finite-difference time-domain (FDTD) simulations are regarded as a practical means of acquiring the required dosimetry information.

The objective of this study is to obtain transient dosimetry information in a GTEM cell loaded with T-25 flasks containing cell culture media. The first phase of this study has focused on developing a realistic three-dimensional FDTD model of the unloaded GTEM cell and validating the simulation results by comparison with experimental measurements of the electric field pulses at several points within the GTEM cell. The experimentally generated waveform is approximated in the FDTD simulations using a double exponential pulse with a width of ~ 1 ns. The time-domain vertical electric fields are recorded at several sampling points along the horizontal floor of the empty GTEM cell. Experimental waveforms were measured at these same locations using an asymptotic conical dipole D-dot sensor. The FDTD-computed waveforms agree well with the experimental measurements. The second phase of this study involves computational studies of the GTEM cell loaded with T-25 flasks. Here, FDTD simulations are conducted to evaluate field distributions in space and time, as well as SAR distributions, inside the cell culture medium. In this talk, we will highlight the key results of these dosimetry studies.

Error Estimates of Stepped Waveguide Material Characterization Measurements

Sean Dorey[†], Michael Havrilla[*†] and William Baker[#†]
Department of Electrical and Computer Engineering
[#]Department of Mathematics and Statistics
Air Force Institute of Technology
WPAFB, OH 45433

Dennis Nyquist and Edward Rothwell
Department of Electrical and Computer Engineering
Michigan State University
East Lansing, MI 48824

Rectangular waveguide material characterization measurements using a reduced-aperture sample holder have recently been introduced in order to alleviate sample-size fabrication difficulties for low-frequency applications. This modal analysis based technique has now been expanded to accommodate multi-layered sample environments in order to support large flimsy materials or allow for samples that do not completely fill the longitudinal extent of the holder. In addition, since uncertainties in test sample thickness and placement are predominantly encountered in material characterization measurements, a differential error analysis is performed to determine associated error bounds.

A wave transmission matrix approach was employed to model the multi-layered sample holder region (R.E. Collin, *Field Theory of Guided Waves*, IEEE Press, 1991). The complex field amplitudes of the first layer are related to those of the Nth layer through the cascaded product of individual 2×2 matrices that describe the incident and reflected waves in each layer. The differential error analysis on the material parameters is based upon a Taylor series expansion about the nominal test sample thickness ℓ_o and placement p_o. For example, the associated error bound for the real part of the permittivity ε' is given by

$$\Delta \varepsilon'_{true} = \varepsilon'\left(\ell_o + \Delta \ell, p_o + \Delta p\right) - \varepsilon'\left(\ell_o, p_o\right) \approx \frac{\partial \varepsilon'\left(\ell_o, p_o\right)}{\partial \ell} \Delta \ell + \frac{\partial \varepsilon'\left(\ell_o, p_o\right)}{\partial p} \Delta p = \Delta \varepsilon'_\ell + \Delta \varepsilon'_p = \Delta \varepsilon'$$

where the derivatives are computed numerically and the Triangle Inequality is used to obtain an approximation to the worst case error bound $\left|\Delta \varepsilon'\right| \leq \left|\Delta \varepsilon'_\ell\right| + \left|\Delta \varepsilon'_p\right|$.

Experimental results for a magnetic absorbing material that doesn't completely fill the longitudinal dimension of the sample holder will be presented to verify the wave transmission matrix methodology. It will also be demonstrated that the deviations between ideal full-aperture and reduced-aperture measurements are readily explained by the uncertainties in test sample thickness and placement.

[†]   The views of the co-authors expressed in this article do not reflect the official policy of the U.S. Air Force, Department of Defense, or the U.S. Government.

Eliminating signal processing artifacts due to FFT in the analysis of broadband signal using the Matrix Pencil method

Santana Burintramart, Tapan K. Sarkar
Department of Electrical Engineering & Computer Science
121 Link Hall Syracuse University
Syracuse, New York 13244-1240
Phone: 315-443-3775 Fax: 315-443-4441
Email: sburintr@syr.edu, tksarkar@mailbox.syr.edu

In this paper, we introduce the Matrix Pencil (MP) method for the purpose of frequency domain analysis. Based on Harmonic modeling, any signal can be expressed in the form of sum of complex exponentials. It has been shown that the MP method can estimate both amplitudes and frequencies of the signal in noise (Y. Hua and T. K. Sarkar, Matrix pencil method for estimating parameters for exponentially damped/undamped sinusoids in noise, 1990). When the signal is corrupted by noise, signal and noise spaces can be separated via the Singular Value Decomposition (SVD). By setting enough number of dominant frequencies, i.e. number of largest singular values, we can get similar result as when using the Fast Fourier Transform (FFT). One aspect of the MP method is that there is no limitation of spectral sampling interval which is limited by the length of the sampled signal in the FFT. Therefore, close frequency components can be estimated with less number of samples.

We analyzed sample signals using the MP method with window size of 400 samples, and compared the results with the FFT with 1921 samples using measured data. The results were similar for both cases except that the MP method gave the more accurate frequency information than the FFT. However, since the number of estimated frequencies in the MP method is proportional to the window length, the results from the MP method showed less number of data than the other. We also applied the small length window to the data, and observed only some important frequency of the signal. It turns out that resonant frequencies could be estimated although the window length is smaller than the signal waveforms. Therefore, it is possible to reveal some information about the signal with a limited number of samples.

The Matrix Pencil method is an alternative tool for high accuracy spectrum analysis and it can also be used to estimate the resonant frequencies of targets of interest using very few samples of the signal.

Remote Microwave Measurement System for Pipeline Integrity Monitoring

Satish Vellakkinar[1]*, Thomas X. Wu[1],
Mitch Auerbach[2], Curt Lochman[2] and Larry Mertens[2]
[1]University of Central Florida, Orlando, FL 32816
[2]EMTEL Corp, Melbourne, FL 32940

Pipelines are generally safe modes of transportation and are used to transport bulk of natural gas and hazardous liquids. Breaches in these pipelines pose a high risk to the lives and property of individuals and also generate hundreds of millions of dollar loss of the products carried in these pipelines. The federal government (Department of Transportation) and federal Office of Pipeline Safety (OPS) enforces on implementing an effective monitoring system that can save lives, millions of dollars a year in mishap losses, pipeline failure and vandalism, and losses due to potential terrorist activities. In current pipeline monitoring systems, there is a significant delay in identification and location of breach and all these processes involve high cost. Also no acceptable automated notification system has been designed, which in turn increases delay in notification and place significant burden on the resources of local public safety agencies. These objectives demonstrate the need to develop a real time monitoring system that can detect and locate a pipeline breach and thereby identify the geographic region of the hazard generated.

In this paper, we propose a remote microwave measurement system for pipeline integrity monitoring. The system uses the pipe interior as a microwave transmission line (waveguide) and transmitters/receivers (transceivers) are used to monitor the pipe continuity. This system will detect small changes in signal transmission related to pipe wall penetrations/ruptures; after a breach is detected, the system applies time-domain reflectometry techniques (similar to radar imaging) to determine the relative location of obstruction or breaches in the pipeline. Upon detection of failure, it geo-locates the breach and provides telecommunications capabilities to notify and mobilize the response team within minutes of the event. An important attribute of this system is that the measurement will not disturb the gas medium being transported. Also the mechanical design of the transceivers will allow "hot installation" in a fully operational pipeline without the need to shut down. This will increase the potential application to existing (operating) pipelines without the need to shut down the gas and in turn has high application value.

Effect of Inner Ground Plane on the Isolation between Tx and Rx Band in SAW Duplexer Package

Hao Dong[*], Thomas X. Wu, University of Central Florida, Orlando, FL 32826
Kamran S. Cheema, Benjamin P. Abbott, SAWTEK, Inc., Apopka, FL 32703

SAW duplexers are very important components in the analog or digital mobile phone system. A duplexer has three ports - the receiver output, the transmitter input and the antenna ports (T. Makkonen, S. Kondratiev, V. P. Plessky, T. Thorvaldsson, J. Koskela, J. V. Knuuttila and M. M. Salonaa, IEEE Trans. Ultrason., Ferroelect., Freq. Contr., 48, 3, 652-665, 2001). Most critical electrical requirements for a duplexer are very low loss in the transmitter and receiver filter paths and high isolation between them. The insertion loss for the receiver band sets the noise figure and degrades the sensitivity of the receiver. On the other hand, the insertion loss of the transmitter band has direct impact on the battery life of the radio.

In this paper, we discuss the effect of inner ground plane on the isolation between Tx and Rx band in SAW duplexer package. Good isolation is achieved by reducing the coupling between transmitter and receiver channels. For the KPCS duplexer package, the chip is mounted on the inner ground plane which is a big metal piece. If we cut the center part of the inner ground plane, part of the fields above the inner ground plane will be absorbed by dielectric material. Then the isolation can be improved. Through the analysis of the field distribution, we cut different shapes on the inner ground plane to investigate the effect on the isolation improvement. Finally, we find cutting "x" shape from the center of inner ground plane can give us the best isolation. Fig. 1 shows the inner view of the package with the modified inner ground plane. The isolation can be improved from 1.73 to 1.76 GHz at Tx band and 6.3 dB improvement is achieved at 1.75 GHz as shown in Fig. 2. At the same time, the performance in passband can keep the same.

Fig. 1. Inner view of the package with the modified inner ground plane.
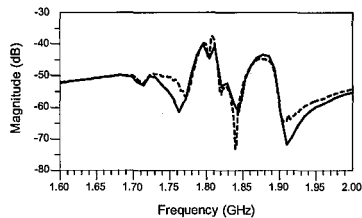
Fig. 2. Isolation between Tx and Rx band. The solid line shows the new result with modified inner ground plane. The dashed line shows the result without cut.

Accurate Modeling and Design of Printed Circuit Testing Board for SAW Duplexer Measurement

Hao Dong[1*], Thomas X. Wu[1], Kamran S. Cheema[2], Benjamin P. Abbott[2]
1 University of Central Florida, Orlando, FL 32826
2 SAWTEK, Inc., Apopka, FL 32703

The electrical properties of SAW duplexer largely depend on electromagnetic effects of chip layout, bonding structures and package. But with smaller size, higher frequencies and increased performance requirements, the printed circuit testing board (PCTB) has significant impact on the measurement of electrical characteristics of the duplexer (F. M. Pitschi, J. E. Kiwitt, K. Ch. Wagner, H. Bilzer, P. Schuh and W. Menzel, 2003 IEEE Ultrasonics Symposium, 401-406, 2003). For SAW duplexers, a key specification is the rejection which has to reach 60 dB levels. Therefore, the analysis and design of the PCTB become more important.

In this paper, we discuss accurate modeling and design of the PCTB for SAW duplexer. The full-wave analysis is used to model the PCTB. The port definition and boundary setup are discussed. The comparison between simulation and measurement results is shown to prove the validity of our model. Based on this model, we investigate the PCTB substrate material, layer stack and exemplify the impact of PCTB on the measurement of electrical characteristics of the SAW duplexer. In order to reduce the impedance among the metal layers and reduce the coupling among the feeding transmission lines, periodic vias are made in the PCTB. The effects of plating vias and solid vias are compared. The position and number of the vias are investigated to minimize the reflections, losses and cross-talk. Fig. 1 shows the measurement setup for SAW duplexer on the PCTB. In this structure, the plating vias are used to reduce the impedance and cross-talk. This empty PCTB has excellent isolation among three ports.

Transmitter Port

Receiver Port

Antenna Port
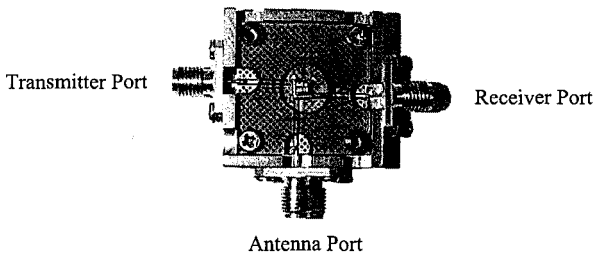
Fig. 1. Measurement setup for SAW duplexer on the printed circuit testing board.

Analytical Modeling of Planar Coil Inductor on a Ground Plane Using a Segmentation Technique

Marie Yvanoff and Jayanti Venkataraman, Rochester Institute of Technology, NY.

The inductor has become a critical component in RF circuits. The prediction of its behavior over a broad range of frequencies is very important. Analyzing and modeling the inductance introduces many difficulties. At present, it has been done by full wave solvers and approximate quasistatic analysis, each with its own advantages and limitations. However, there is still a critical need for a simple closed form expression for the design of an inductor that includes ground plane and material parameters.

In this work, a segmentation method is used that is based on dividing the geometry of the inductor into rectangles and combining the characteristics of the segmented elements by an interface network that includes spacing, line width, dielectric characteristic and ground plane. By this technique, simple expressions have been developed that require a very short computational time. As an example, a 2-turn inductor shown in figure1a has been segmented. The segments are connected via interconnecting ports that are different from the excitation ports 1 and 2 (fig1b), using an interfacing network (fig1c). The Z-matrices (Z_1, Z_2.... Z_7) corresponding to the individual segments are computed with the ground/power plane model (G. Lei, et al. *"Wave model solution to the Ground/Power Plane Noise Problem"* IEEE, April 1995).

The resulting Z matrices are transformed to S-matrices in order to combine the segments through the interface network. The resulting S matrix of order of 2 x 2 is converted to the Z matrix using eq. (1):

$$[Z] = ([U] - [S])^{-1} (Z_0[U] + Z_0[S])$$ (1)

At port1, the input impedance with port 2 terminated by Z_L is: $Z_{in} = Z_{11} - \dfrac{Z_{12}Z_{21}}{Z_{22} + Z_L}$ (2)

The reactance of the inductor (fig1a: $\varepsilon_r = 4$, $d_{substrate} = 5\mu m$, $\sigma = inf$, s = 2mm, w=2mm, a=b=20mm)) and the corresponding S11 and S12 as a function of frequency are shown in fig2a and b and have been compared to full wave solvers. Comparison of theoretical and measured results will be done for a wide range of inductors at different frequencies. Based on these results, the validity of the elements of the Z-matrices and the interface network will be investigated for different spacing and coupling effects.
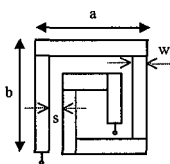
Fig1a: 2 turn planar Inductor
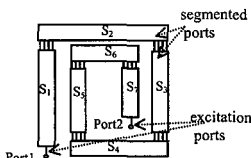
Fig1b: segment division
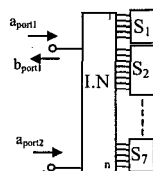
Fig1c: Interface Network
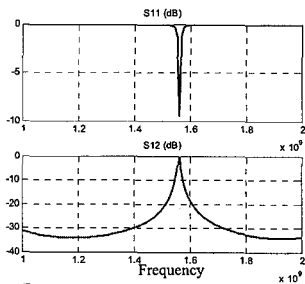
Fig2a: S_{11}(dB) and S_{12}(dB)
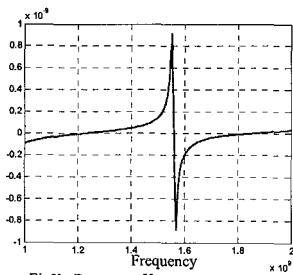
Fig2b: Reactance X_L

Capacitive-Inductive-Capacitive Configurations in a Strip Line for Multi-Layered BPF Applications

Yasushi Horii

Kansai University, 2-1-1 Ryozenji Takatsuki, Osaka 569-1095, JAPAN

Phone & Fax: +81-726-90-2476, E-mail: horii@res.kutc.kansai-u.ac.jp

In recent years, multi-layered fabrication techniques have been advanced drastically with the progress of low temperature co-fired ceramic (LTCC) technology, and various kinds of high performance devices have been developed and miniaturized. In such a movement, this paper proposes a novel multi-layered band pass filter having two small capacitive-inductive-capacitive configurations in a strip line substrate (CIC-BPF).

Fig.1 shows geometry of the CIC-BPF, which includes two CIC-layers and an I/O-layer. Each CIC-layer is composed of two $12 \times 4 \, mm^2$ capacitive patches and a 0.5mm meander-like inductive line so as to work as a resonant element. In the I/O layer, a parasitic element with $7 \times 1 \, mm^2$ is added to control frequencies of transmission zeros. Relative permittivity of all substrates is $\varepsilon_r = 2.62$.

Scattering characteristic of the CIC-BPF, calculated by the FDTD method, is presented in Fig.2 (a). Comparing with a non-parasitic model by black ink, the CIC-BPF with a parasitic element shows narrower passband characteristic of BW$_{-3dB}$= 10.5% and clear transmission zeros at 0.60GHz and 1.61GHz across the passband. Experimental result of the handmade prototype model fabricated on a Rexolite2200 substrate is also presented in Fig.2 (b). Though unacceptable errors are observed in experiments due to the tolerance occurred in the handmade process, the concept of the CIC-BPF can be validated. This filter configuration is suitable for developing a new type of LTCC BPFs in the shielded form.

(a) Theoretical results by FDTD
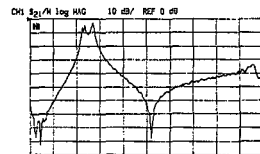
(b) Experimental results (0-5GHz)

Fig.2   Scattering characteristics.

Fig.1   Geometry of a CIC-BPF.

FDTD Simulation of Scattering from Objects with Double-Negative Material Characteristics

J.F. Ma, Wenhua Yu, T. Su and R. Mittra
Electromagnetic Communication Laboratory, 319 EE East
The Pennsylvania State University, University Park, PA 16802
Email: rajmittra@ieee.org

With appropriate modifications, the FDTD can handle both the electric and magnetic types of dispersive media. It has also been used to study double negative materials (DNG) [R. Luebbers, APS/URSI 2003], where waves propagating across an air-DNG interface and radiating within a DNG shell have been investigated. In this paper we extend the FDTD analysis to the simulation of scattering from objects with DNG property, and present some preliminary results for the problem of EM scattering from canonical objects filled with DNG.

We consider a dielectric sphere for our example, and begin by computing the backscattering RCS of a dielectric sphere with a dispersive permittivity and constant permeability. We then compare the results to that derived by using the analytical formula, and see from Figure 1 that the agreement is good. Next, we repeat the problem for the case of a constant permittivity and dispersive permeability and again the results are found to agree well (see Fig.2). In the two cases simulated above, a single pole-pair Lorentz model (with different parameters) is assumed for the dispersive nature. The real part of the permittivity becomes negative in the frequency range of 26 to 38 GHz, while the real part of the permeability goes negative between 26 and 34 GHz. When the both permittivity and permeability are dispersive, the material becomes a DNG in the frequency range where the real parts of both the permittivity and permeability are negative. Figure 3 shows that the FDTD simulation results for the backscattering RCS of a doubly-dispersive dielectric sphere *vs.* frequency, along with the analytical result for the same. The sphere becomes DNG in the frequency range of 26 to 34 GHz. Caution must be exercised in choosing the correct sign of the wave number in the DNG range when computing the analytical result, as has been pointed out previously in the literature. We found that same care should also be used in choosing the sign of the wave number for frequencies close to the DNG region; otherwise the imaginary part of wave number might be positive and, hence, the result would be non-physical. We note from Fig. 3 that the RCS does not exhibit an abrupt change in the DNG range, and the simulated results agree well with the analytical one.
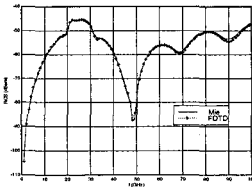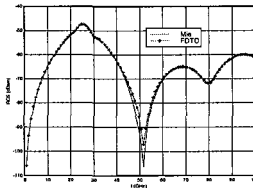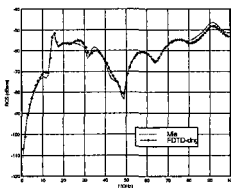
| Fig. 1 | Fig. 2 | Fig. 3 |

Fig. 1 Dispersive permittivity sphere with $\mu_r=1.0$ and sigma=0.0. Lorentz parameters are: ε inf=2.5, ε s=6.0, w=25 Ghz, δ=0.1 w

Fig. 2 Dispersive permeability sphere with ε_r=1.0 and sigma=0.0. Lorentz parameters are: $\mu\_$inf=1.5, $\mu\_$s=3.0, w=25 Ghz, δ =0.1 w

Fig. 3 Doube dispersive sphere. Lorentz model parameters: $\varepsilon\_$inf=1.5, $\varepsilon\_$s=3.0, w_1=25 GHz, δ_1=0.1w_1, $\mu\_$inf=2.5, $\mu\_$s=6.0, w_2=25 GHz, δ_2=0.1w_2

Modeling High Contrast Metamaterials with Variable Higher Order Basis Functions

B. C. Usner*, K. Sertel, J. L. Volakis
ElectroScience Laboratory, Department of Electrical Engineering
The Ohio State Univ., 1320 Kinnear Rd., Columbus, OH 43212.

Current work on antenna miniaturization suggests that high contrast composites can lead to miniature and often broadband designs (Kiziltas et. al., IEEE 2003 Ant. Prop. Int. Symp., vol.1, pp.485-488). However, accurate modeling of high contrast composites poses significant computational difficulties (Jin and Volakis, IEEE MTT-T, vol. 37, pp. 1641-1645, 1989). In general, the presence of $|\epsilon_r|$ acts as an error amplifier. That is, to achieve a field solution accuracy δ, the corresponding accuracy of the numerical method must be $\delta/|\epsilon_r|$. Thus, for large values of $|\epsilon_r|$, accurate geometric modeling along with increased field resolution is necessary.

Typically, to increase field resolution within high contrast regions one increased mesh density. However, this approach is not well suited for integration with design algorithms where many different material configurations must be considered. For example, refining the mesh globally can unnecessarily increase the total number of unknowns needed for an accurate solution. Additionally, local regridding around high contrast regions require new meshes for different material configurations making numerical design methods intractable. To avoid regridding, in this paper we propose high order basis functions whose order can be adjusted for higher accuracy. Specifically, hierarchical basis functions are analyzed to allow for dynamic upgrading of the order depending on accuracy. Traditionally, hierarchical basis functions have been avoided due to their tendency to cause ill-conditioning of the system matrix (Volakis et. al., *Finite Element Method for Electromagnetics*, IEEE Press, 1998, p.62). However, recently introduced hierarchical basis functions (Jørgensen et. al., IEEE 2002 Ant. Prop. Int. Symp., vol. 4, pp. 618-621) produce well conditioned system matrices even for expansion orders of ten or more. These basis functions were also shown to be very efficient even for a volume integral equation for the scattering from inhomogeneous dielectric objects (Kim et. al., IV Int. Conf. on Ant. Theory and Tech., vol. 1, pp. 113-116, 2003).

This work generalizes these hierarchical basis functions for volume integral equation formulations to study high contrast composites (Sertel et. al., IEEE 2003 Ant. Prop. Int. Symp., vol. 3, pp. 2-5). The advantage of this approach is that both dielectric and magnetic materials can be modeled using only a single vector field unknown within each volume element. The use of both curl-conforming and divergence-conforming basis functions will be examined for the representation of the electric field intensity. Our analysis will be also compared with standard volumetric techniques (both FE-BI and VIE) employing linear expansion functions. Numerical results will be given for the scattering from composite targets containing high contrast ratios, as well as the extension of this method to compute antenna gain and impedance properties in the presence of sophisticated material designs.

377

Computing Bulk Effective Permittivity
From Thin Film Simulations

*Keith W. Whites** and *John Preheim*
Department of Electrical and Computer Engineering
South Dakota School of Mines and Technology
501 East Saint Joseph Street
Rapid City, SD 57701-3995
(whites@sdsmt.edu)

There are many techniques available for computing the quasi-static effective permittivity, ε_{eff}, of a composite material formed by periodically loading a host material with electrically small inclusions. For particles of separable shape, it is possible to employ T-matrix methods and obtain accurate ε_{eff} values at essentially any realizable volume fraction. Results for two-phase metallic spheres are available in the literature (R. C. McPhedran and D. R. McKenzie, *Proc. R. Soc. Lond.*, A. 359, 45-63, 1978), as well as for multi-phase cylinders (F. Wu and K. W. Whites, *Electromagn.*, 21, 97-114, 2001) and spheres (K. W. Whites, *J. Appl. Phys.*, 88, 1962-1970, 2000).

In the case of complex-shaped inclusions (i.e., those that have a non-separable shape), it is also possible to obtain accurate values for ε_{eff}, though often at a much higher computational expense. These methods include integral equation solutions for cylindrical particles (B. Sareni, *et al.*, *IEEE Trans. Magn.*, 33, 1580-1583, 1997), as well as three dimensional particles (K. W. Whites and F. Wu, *IEEE Trans. Microwave Theory Tech.*, 50, 1723-1729, 2002)

There are two assumptions common to all of these techniques. The first is that space is completely filled by the periodic placement of particles. The second is that an excitation is provided to produce a uniform effective polarization density throughout this space.

While these are fairly banal assumptions, they are conditions not usually available in commercial computational electromagnetics packages. Such software has become extremely powerful in the simulation of EM scattering by complex-shaped objects in complicated environments. It would be advantageous to apply these tools in the computation of quasi-static effective permittivity for artificial electromagnetic materials.

In this paper, we will describe a technique we have used to compute the quasi-static ε_{eff} for electrically-thin films of periodically located particles with potentially complex shape. From the uniform plane wave scattering by these thin films, we have been able to accurately extract the bulk quasi-static ε_{eff} from films that may only be 10 particles thick.

As an example, a lattice of metallic "cone-needles" as shown in the figure was simulated in *Microwave Studio* from CST, Inc. This is a commercially available simulation package that uses the finite integration technique. At a volume fraction of only 12%, $\varepsilon_{r,\text{eff}} = 13.9$ along the particle axis, which compares to only $\varepsilon_{r,\text{eff}} = 1.4$ for conducting spheres at a similar volume fraction. This approach has been validated to less than 1% difference in ε_{eff} for lattices of metallic spheres and cubes using results from the references listed earlier.

Averaged Transition Conditions for Electromagnetic Fields at a Uniform Periodic Distribution of Small Scatters

Mohamed A. Mohamed*
Edward F. Kuester
Dejan Filipovic
Department of Electrical and Computer Engineering
University of Colorado
425 UCB, Boulder, CO 80309-0425
email: Mohamed.mohamed@colorado.edu
kuester@schof.colorado.edu

Christopher L. Holloway
National Institute of Standards and Technology
Electromagnetics Division
U.S. Department of Commerce, Boulder Laboratories
325 Broadway, Boulder, CO 80305

Melinda Piket-May
Department of Electrical and Computer Engineering
University of Colorado
425 UCB, Boulder, CO 80309-0425

A *metafilm,* the two-dimensional equivalent of a metamaterial, is a distribution of electrically small scatterers in a surface. In a previous work of the authors, generalized sheet transition conditions (GSTCs) for the average electromagnetic fields across a random metafilm characterized by electric and magnetic polarizability densities were derived. The GSTCs are expected to have wide application to the design and analysis of antennas, reflectors and other devices where controllable scatterers are used to form a ``smart'' surface. In this work the GSTCs for a uniform periodic distribution of scatterers is derived. A comparison between the plane wave transmission and reflection coefficients of random and uniform scatterer distributions in the metafilm in the limit of small scatterer separation is presented. In addition, the dependence of reflection and transmission coefficients on incidence angle will be examined using an implementation of the GSTCs in the finite element method.

Wave Propagation through Chiral Periodic Structure with Arbitrary Shape

Xiaomin Yang* and Thomas X. Wu
Department of Electrical and Computer Engineering
University of Central Florida
Orlando, FL 32816

Attention has been focused on electromagnetic chirality (D. L. Jaggard, A. R. Mickelson, and C. H. Papas, *Appl. Phys.*, 1979, vol. 18), and its potential applications to microwave, millimeter wave and optical wave devices. In this paper, we investigate wave propagation through chiral periodic structure with arbitrary shape. The structure is composed of a chiral layer with dielectric constant ε and chirality parameter κ as shown in Fig. 1. The upper air-chiral boundary is arbitrarily curved, while the lower boundary is flat.

Although perturbation theory and coupled-mode theory have been used to analyze chiral periodic structure (K. M. Flood and D. L. Jaggard, *IEEE Journal of Quantum Electronics*, 1994, vol. 30, pp. 339–345), those are approximate methods and can only be used for low frequency applications. In our analysis, we use rigorous mode-matching method to solve the problem. Staircase approximation is introduced to change the curved structure to a multilayer structure. The field solutions in the uniform air regions and unbounded air-chiral periodic array have been derived. Mode-matching method is used at the boundaries to calculate the scattering characteristics. Numerical results are displayed to explain the underlying physical properties of the chiral periodic structure. We have investigated and explained Wood's anomalies at high frequencies by the excitation of leaky waves guided along the periodic layer. The influence of frequency, chirality parameter, incident angle, curve shape and period are discussed. We have also found the chiral periodic structure can be used as both a frequency selective device and a mode conversion device.
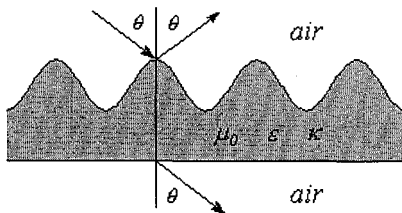
Fig. 1. A chiral periodic structure.

Scattering of a Plane Wave by Two Strongly Coalescing Perfectly Conducting Spheres

Robert H. MacPhie* and **Cintia Man**
Department of Electrical and Computer Engineering
University of Waterloo, Waterloo, ON N2L 3G1 Canada
E-mail: r.macphie@ece.uwaterloo.ca

Almost a century ago Mie obtained the solution for the scattering of a plane electromagnetic wave by a sphere (*Ann. Physik*, 25, p.377, 1908). He made use of potential functions leading directly to the spherical multipole fields $\vec{M}_{mn}^{(3)}(r,\theta,\Phi)$ and $\vec{N}_{mn}^{(3)}(r,\theta,\Phi)$ scattered by the sphere. More recently, Bruning and Lo solved the problem of plane wave scattering by two separated spheres (IEEE Trans. AP-19, p.378, 1971) by using two sets of multipole fields scattered from each sphere.

In this paper we consider two strongly coalescing spheres of equal radius a with center to center spacing of d<a as shown in the diagram below. However, instead of using two sets of scattered multipole fields originating at the centers o and o' of spheres A and B respectively, we consider only multipole fields $\vec{N}_{mn}^{(3)}$ and $M_{mn}^{(3)}$ from sphere A.

The plane wave is expanded as a sum of multipole fields $\vec{N}_{mn}^{(1)}$ and $\vec{M}_{mn}^{(1)}$. We require that the total tangential E-field vanish on the partial spherical surfaces of both sphere A and B. To express the multipole fields from sphere A in the coordinates of sphere B we use the Translation-Addition Theorem (*Stratton, Electromagnetic Theory*, p.563, 1941). Then Galerkin's Method leads to a set of linear equations for the scattered field amplitudes. Unlike the cases of single or separated spheres, the multipole field products, when integrated over the two partial spheres are *not orthogonal*. However, we have obtained closed form expressions for the integrals which are valid for any separation d. Numerical results will be presented for various sphere sizes and separations.

Author Index